PROCEEDINGS

VOLUME 2

PERMAFROST

Sixth International Conference

PERMAFROST

Sixth International Conference

PROCEEDINGS (Vol. 2)

July 5–9, 1993

Beijing China

Organized by

Lanzhou Institute of Glaciology & Geocryology,
Chinese Academy of Sciences & Chinese Society of
Glaciology and Geocryology

South China University of Technology Press

[粤]新登字 12 号

Sixth International Conference Proceedings on Permafrost (Vol. 2)

Published by South China University of Technology Press

(Wushan Guangzhou China)

First Published 1993

ISBN 7-5623-0484-X / P • 1

PERMAFROST

Sixth International Conference

PROCEEDINGS (Vol. 2)

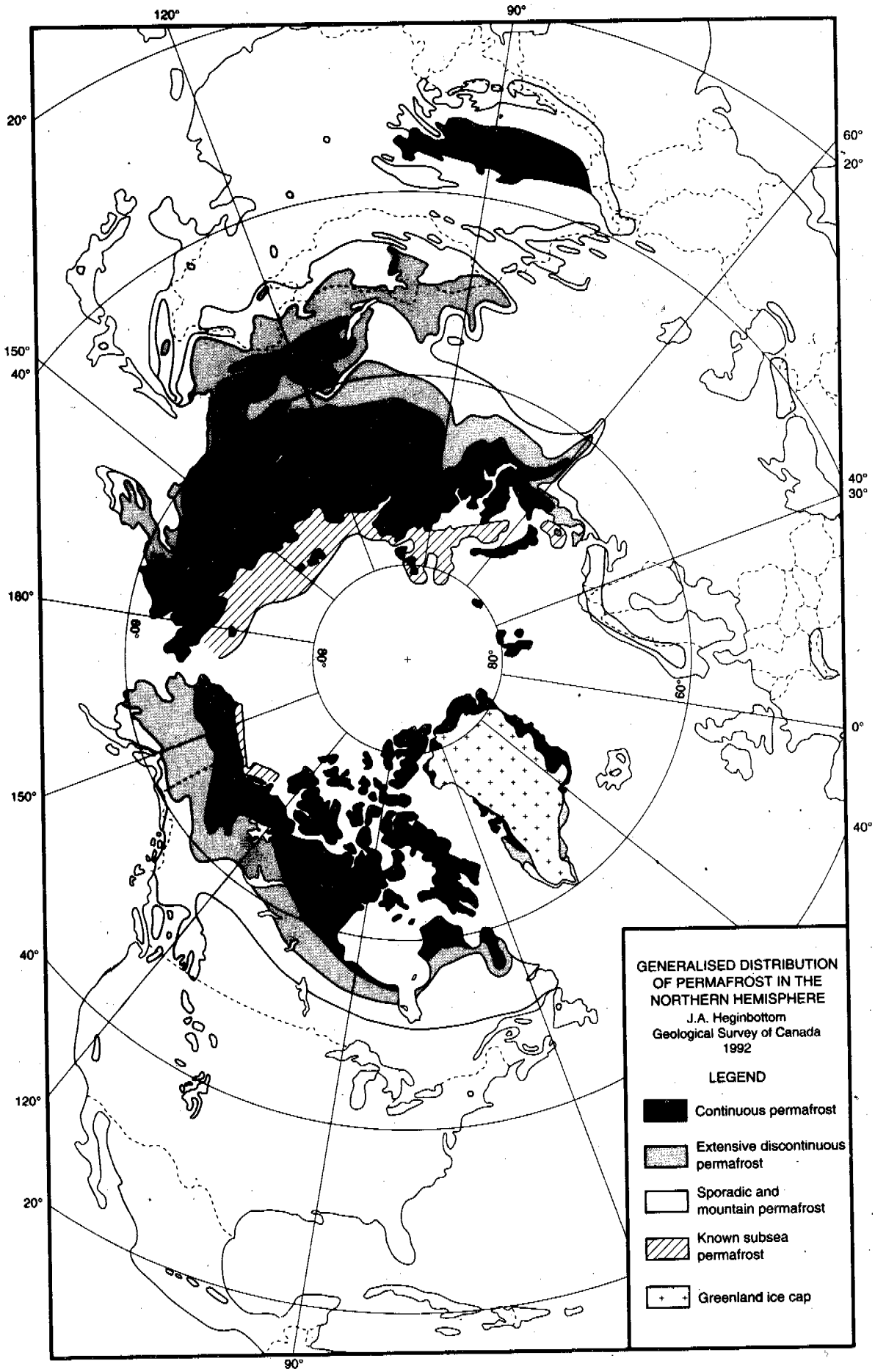
120°
90°
20°
60°
20°
150°
40°
40°
30°
180°
80°
80°
80°
60°
0°
150°
40°
40°
120°
20°
90°
GENERALISED DISTRIBUTION OF PERMAFROST IN THE NORTHERN HEMISPHERE
J.A. Heginbottom
Geological Survey of Canada
1992
LEGEND
Continuous permafrost
Extensive discontinuous permafrost
Sporadic and mountain permafrost
Known subsea permafrost
Greenland ice cap

PREFACE

About one-fifth of the land area of the earth is underlain by perennially frozen ground, or permafrost. It affects many human activities, causing unique problems in the environment, ecosystem, resource development and constructions in cold regions. Since permafrost is a thermal condition, it is very sensitive to changes in climate. Global warming could result in permafrost degradation, causing resultant ecological and socioeconomic consequences. Thus, permafrost has become more and more important in the development of polar and high altitude regions which occupy key positions in the global system.

It is necessary to give scientists and engineers an opportunity to meet regularly in order to discuss the state of the art of science and technology in their fields, and to gain the impetus for further work, as well as to compare permafrost conditions with other regions of the world, particularly regions where only seasonally frozen soils currently exist. The International Conferences on Permafrost are organized to serve this purpose.

The First International Conference on Permafrost was therefore held in the United States at Purdue University, in 1963; the Second in Yakutsk, Siberia, 1973; the Third in Edmonton, Canada, 1978; the Fourth in Fairbanks, Alaska, 1983; and the Fifth in Trondheim, Norway, 1988.

The Sixth International Conference on Permafrost (VI ICOP) was co-sponsored by several national scientific and technical organizations, and was held under the auspices of the Chinese Society of Glaciology and Geocryology (CSGG), which is in the Adhering National Body of the International Permafrost Association (IPA), and was organized by the Lanzhou Institute of Glaciology and Geocryology (LIGG), Chinese Academy of Sciences, with the collaboration of the State Key Laboratory of Frozen Soil Engineering, LIGG. The support and the guidance of the International Permafrost Association were extremely important for us in preparation for the conference.

The VI ICOP was successfully held on 5-9 July 1993 at Beijing, China. About 274 participants (including 26 accompanyings) from 21 countries attended this conference. Among them, 27 and 22 attendants participated in the field trips from Beijing to Lhasa and from Beijing to Tianshan Mountain, respectively.

The eighth IPA council meeting was held during this conference on 5 July 1993, from 1950 to 2145, at which new IPA officers were elected and appointed. They are: President, Cheng Guodong (China); Vice President, Hugh M. French (Canada); Vice President, Nikolai N. Romanowskii (Russia), and Secretary General, Jerry Brown (USA).

A total of 189 contributed papers are included in first volume of the proceedings which contains almost all the papers accepted for presentation at the paper sessions. A total number of 98 papers, reports and abstracts are included in this second volume of the proceedings, among which one is the reviewed oral presentation paper writen by G.C. Lewis et al, 9 are invited papers presented at the special sessions, 77 are poster papers, 5 are poster abstracts. The poster papers submitted by Chinese authors and Mongulian authors are reviewed. Many scientific and engineering disciplines were represented, including physics, chemistry and mechanics of frozen soil, geophysics, periglacial geomorphology, soil science, climatology, hydrology, ecology, civil and mechanical engineering. The high quality of the papers was the result of hard work by the authors, as well as from the assistance given by the Editorial Committee of the International Permafrost Association, and by the numerous reviewers in the member countries.

Finally, the Chinese Organizing Committee wishes to acknowledge all of you that have participated in the preparation for this conference: the authors of the papers, the reviewers, the sponsors, the publisher, and the staff of many institutions that have been working to make it a successful conference.

Cheng Guodong
Chairman
Chinese Organizing Committee
Sixth International
Conference on Permafrost

CONTRIBUTING SPONSORS

The Financial Support to the Sixth International Conference on Permafrost is mainly contributed by the following organizations.

Governmental

Commission of National Natural Science Foundation of China;
Chinese Academy of Sciences;
Geography Society of China;
South-South Cooperation Fellowship Program, Academia Sinica;
China International Centre for Economic and Technical Exchanges, Ministry of Foreign Economic Relations and Trade.

Nongovernmental

The First Highway Survey and Design Institute, Ministry of Communication;
Cold Regions Development and Research Society of China;
Central Coal Mining Research Institute, Ministry of Coal Mining of China;
Heilongjiang Provincial Institute of Water Conservancy Science;
The First Survey and Design Instittue, Ministry of Railway of China;
Heilongjiang Provincial Institute of Cold Region Construction Science;
Heilongjiang Provincial Institute of Communication Science;
Northwest Institute of Railway Science, Ministry of Railway of China;
Gansu Provincial Institute of Water Conservancy Science;
Northeast Survey and Design Instittue, Ministry of Water Conservancy;
Mining Industry University of China;
Inner Monggulia Institute of Water Conservancy Science;
Jilin Provincial Institute of Water Conservancy Science;
Heilongjiang Provincial Institute of Low Temp. Construction;
International Science Foundation.

CHINESE HONORARY COMMITTEE

Chairman:	Zhou Guangzhao	President of Chinese Academy of Sciences, Academician.
Vice-Chairmen:	Sun Honglie	President of Natural Resources Expedition Commission of China, Academician.
	Liu Dongsheng	President of International Union for Quaternary Research, Academician.
	Sun Shu	Vice-President of the National Natural Science Foundation of China, Academician.
	Zhu Lilan	Vice-President of the State Science and Technology Commission of China, Academician.
	Liu Shu	Professor, the State Science and Technology Association of China.

Members: Li Jiejun, Li Yusheng, Wang Sijing, Zheng Du, Xu Shaoxing

CONSULTATIVE COMMITTEE

Chairman:	Shi Yafeng	Academician
Vice-Chairmen:	Dai Moan	Vice-Governor of Heilongjiang Province.
	Yang Shengfu	Director of Engineering Administration, Department of the Ministry of Communications of China.
	Zhang Xiangong	Professor, Geology University of China.

Members: Zhu Xuan, Dai Dingzong, Xu Ronglie, Ouyang Ziyuan, Xue Shiying, Weng Shida, Zhang Jiazhen, Zhao Chunian, Cui Zijiu

ORGANIZING COMMITTEE

Chairman: Cheng Guodong

Vice-Chairmen: Wu Ziwang, Zhou Youwu, Yu Xiang, Ge Qihua, Zhang Jie

Secretary-General: Zhu Yuanlin

Associate Secretary-Generals: Xu Xiaozu, Chen Xiaobai, Tong Boliang, Huang Yizhi, Qiu Guoqing, Tong Changjiang, Gu Zhongwei

Members: Wu Jingming, Yu Qun, Liu Hongxu, Huang Xiaoming, Jia Jianhua, Zhu Qiang, Dai Huiming, Xie Yingqi, Xu Bomong, Lu Guowei

Overseas Members: J. Brown, H.M. French, N.A. Grave

Review Process

The review of abstracts and manuscripts for this pre-Conference publication was conducted under the supervision of the Chinese Organizing Committee and the IPA Editorial Committee. Approximately 450 abstracts were received from 24 countries. It was necessary to limit the number of papers from Russia and China. These countries were asked to invite a more limited number of appropriate papers. A review form was agreed to and each paper received two or more reviews. Some papers were rejected; in other cases the authors simply did not submit manuscripts. Individuals without papers were encouraged to submit posters and have their abstracts published in a post-Conference volume. In order to save time and to employ native languages in the reviews, all Chinese and Mongolian papers were reviewed in China and all Russian papers were reviewed in Russia, employing the standard review form. All Russian and Chinese reviewed papers were available in English in August 1992 when members of the Editorial Committee met in Washington, D.C., during the IPA Council meeting. The papers and review forms were examined and discussed at that time, and members of the IPA Council were asked to assist with additional reviews.

Review of the 100 non-Chinese or -Russian papers involved reviewers from many of the IPA member countries. This review process was conducted by the Chair, IPA Editorial Committee, in consultation with members of the Committee. Below is a list of all individuals who provided these reviews. The IPA Editorial Committee and the Chinese Organizing Committee express their appreciation to all those who devoted their valuable time and expertise to this process. Deserving particular thanks for their assistance in selecting reviewers and following up with many of them are Alan Heginbottom, Geological Survey of Canada; Nikolai Grave and Valery Volgina, Russian Academy of Sciences; Eugene Marvin, Cold Regions Research and Engineering Laboratory, representing the American Society of Civil Engineers; and John Zarling, University of Alaska, representing the American Society of Mechanical Engineers. The Cold Regions Research and Engineering Laboratory is gratefully acknowledged for furnishing instructions, samples and layout sheets for preparation of final camera copy for the proceedings volumes. Members of the IPA Editorial Committee are:

Jerry Brown, Chair, USA
H.M. French, Canada
N.A. Grave, Russia
Cheng Guodong, China
L. King, Germany
E.A. Koster, The Netherlands
T.L. Péwé, Ex Officio, IPA Executive Committee

Reviewers

H. Jonas Akerman, University of Lund, Lund, Sweden
Donald Albert, Cold Regions Research and Engineering Laboratory, Hanover, New Hampshire, USA
Bernard Alkire, Michigan Technological Institute, Houghton, Michigan, USA
Duwayne Anderson, Texas A&M University, College Station, Texas, USA
Ronald Atkins, West Lebanon, New Hampshire, USA
Abdul Aziz, Gonzaga University, Spokane, Washington, USA
T.H.W. Baker, National Research Council of Canada, Ottawa, Ontario, Canada
Richard Berg, Cold Regions Research and Engineering Laboratory, Hanover, New Hampshire, USA
Patrick Black, Cold Regions Research and Engineering Laboratory, Hanover, New Hampshire, USA
George Blaisdell, Cold Regions Research and Engineering Laboratory, Hanover, New Hampshire, USA
Steven Blasco, Geological Survey of Canada, Dartmouth, Nova Scotia, Canada
Jerry Brown, Arlington, Virginia, USA
Margo M. Burgess, Geological Survey of Canada, Ottawa, Ontario, Canada
Chris Burn, Carleton University, Ottawa, Ontario, Canada
Nel Caine, University of Colorado, Boulder, Colorado, USA
L. David Carter, U.S. Geological Survey, Anchorage, Alaska, USA
Edward Chacho, Jr., Cold Regions Research and Engineering Laboratory, Hanover, New Hampshire, USA
Edward Chamberlain, Cold Regions Research and Engineering Laboratory, Hanover, New Hampshire, USA
Ian D. Clark, University of Ottawa, Ottawa, Ontario, Canada
Gary Clow, U.S. Geological Survey, Menlo Park, California, USA
Bill Connor, Alaska Department of Transportation and Public Facilities, Fairbanks, Alaska, USA
Scott Crowther, Crowther Associates, Anchorage, Alaska, USA
Scott Dallimore, Geological Survey of Canada, Ottawa, Ontario, Canada
Larry Dingman, University of New Hampshire, Durham, New Hampshire, USA
Jean-Claude Dionne, Université Laval, Québec City, Québec, Canada
Francesco Dramis, Universita di Camerino, Camerino, Italy
Larry Dyke, Geological Survey of Canada, Ottawa, Ontario, Canada
Robert Eaton, Cold Regions Research and Engineering Laboratory, Hanover, New Hampshire, USA
P.A. Egginton, Geological Survey of Canada, Ottawa, Ontario, Canada

David Esch, Alaska Department of Transportation and Public Facilities, Juneau, Alaska, USA
K.R. Everett, Ohio State University, Columbus, Ohio, USA
Oscar Ferrians, U.S. Geological Survey, Anchorage, Alaska, USA
Kaare Flaate, Norwegian Road Administration, Oslo, Norway
D.C. Ford, McMaster University, Hamilton, Ontario, Canada
Stephen Forman, Ohio State University, Columbus, Ohio, USA
Hugh M. French, University of Ottawa, Ottawa, Ontario, Canada
Masami Fukuda, Hokkaido University, Sapporo, Japan
John R. Giardino, Texas A&M University, College Station, Texas, USA
Odd Gregersen, Norwegian Geotechnical Institute, Oslo, Norway
George Gryc, U.S. Geological Survey, Menlo Park, California, USA
Wilfried Haeberli, Versuchsanstalt für Wasserbau, Hydrologie und Glaziologie, Zurich, Switzerland
Bernard Hallet, University of Washington, Seattle, Washington, USA
Stuart A. Harris, University of Calgary, Calgary, Alberta, Canada
William D. Harrison, University of Alaska, Fairbanks, Alaska, USA
David G. Harry, Energy, Mines and Resources, Ottawa, Ontario, Canada
Donald W. Hayley, EBA Engineering Consultants, Ltd., Edmonton, Alberta, Canada
Beez Hazen, Northern Engineering and Scientific, Anchorage, Alaska, USA
J. Alan Heginbottom, Geological Survey of Canada, Ottawa, Ontario, Canada
Karen Henry, Cold Regions Research and Engineering Laboratory, Hanover, New Hampshire, USA
Christopher E. Heuer, Exxon Production Research Co., Houston, Texas, USA
Ken Hinkel, University of Cincinnati, Cincinnati, Ohio, USA
Larry Hinzman, University of Alaska, Fairbanks, Alaska, USA
Pieter Hoekstra, Blackhawk Geosciences, Inc., Golden, Colorado, USA
Vincent Janoo, Cold Regions Research and Engineering Laboratory, Hanover, New Hampshire, USA
Thomas Jenkins, Cold Regions Research and Engineering Laboratory, Hanover, New Hampshire, USA
Nils Johansen, University of Alaska, Fairbanks, Alaska, USA
G.H. Johnston, Ottawa, Ontario, Canada
Alan S. Judge, Geological Survey of Canada, Ottawa, Ontario, Canada
Douglas Kane, University of Alaska, Fairbanks, Alaska, USA
B.D. Kay, University of Guelph, Guelph, Ontario, Canada
G. Peter Kershaw, University of Alberta, Edmonton, Alberta, Canada
Stephen Ketcham, Cold Regions Research and Engineering Laboratory, Hanover, New Hampshire, USA
John Kimble, Soil Conservation Service, Lincoln, Nebraska, USA
Lorenz King, Justus Liebig Universitat, Giessen, Germany
Eduard Koster, University of Utrecht, Utrecht, The Netherlands
William B. Krantz, University of Colorado, Boulder, Colorado, USA
Raymond A. Kreig, RA Kreig & Associates, Anchorage, Alaska, USA
Pavel J. Kurfurst, Geological Survey of Canada, Ottawa, Ontario, Canada
Arthur H. Lachenbruch, U.S. Geological Survey, Menlo Park, California, USA
Branko Ladanyi, Université de Montréal, Québec, Canada
J.P. Lautridou, Centre de Géomorphologie, Caen, France
Antoni G. Lewkowicz, Erindale College, University of Toronto, Mississauga, Ontario, Canada
B.H. Luckman, University of Western Ontario, London, Ontario, Canada
Virgil Lunardini, Cold Regions Research and Engineering Laboratory, Hanover, New Hampshire, USA
Philip Marsh, National Hydrology Research Institute, Saskatoon, Saskatchewan, Canada
Terry McFadden, University of Alaska, Fairbanks, Alaska, USA
J.D. McKendrick, University of Alaska, Palmer, Alaska, USA
Brainerd Mears, University of Wyoming, Laramie, Wyoming, USA
Michael Metz, GeoTech Services, Inc., Golden, Colorado, USA
Bruce Molnia, U.S. Geological Survey, Reston, Virginia, USA
Yoshisuke Nakano, Cold Regions Research and Engineering Laboratory, Hanover, New Hampshire, USA
F.E. Nelson, Rutgers University, New Brunswick, New Jersey, USA
J.F. Nixon, Nixon Geotech, Calgary, Alberta, Canada
Walter Oechel, San Diego State University, San Diego, California, USA
Kevin O'Neill, Cold Regions Research and Engineering Laboratory, Hanover, New Hampshire, USA
Thomas Osterkamp, University of Alaska, Fairbanks, Alaska, USA
Samuel I. Outcalt, University of Michigan, Ann Arbor, Michigan, USA
Kim Peterson, University of Alaska, Anchorage, Alaska, USA
Troy L. Péwé, Arizona State University, Tempe, Arizona, USA
J.A. Pilon, Geological Survey of Canada, Ottawa, Ontario, Canada
Wayne Pollard, McGill University, Montréal, Québec, Canada
Vern Rampton, Terrain Analysis and Mapping Services Ltd., Carp, Ontario, Canada
W.R. Rouse, McMaster University, Hamilton, Ontario, Canada
Frank Sayles, Cold Regions Research and Engineering Laboratory, Hanover, New Hampshire, USA
D.C. Sego, University of Alberta, Edmonton, Alberta, Canada
Paul V. Sellmann, Cold Regions Research and Engineering Laboratory, Hanover, New Hampshire, USA
Gaius Shaver, Marine Biological Laboratory, Woods Hole, Massachusetts, USA
Sally Shoop, Cold Regions Research and Engineering Laboratory, Hanover, New Hampshire, USA
Yuri Shur, RA Kreig & Associates, Anchorage, Alaska, USA

Michael Smith, Carleton University, Ottawa, Ontario, Canada
C. Tarnocai, Agriculture Canada, Ottawa, Ontario, Canada
Rupert G. Tart, Jr., Golden Associates, Inc., Anchorage, Alaska, USA
J.C.F. Tedrow, Rutgers University, New Brunswick, New Jersey, USA
Howard Thomas, America North Inc., Anchorage, Alaska, USA
Clement Tremblay, Ministry of Transport, St. Foy, Québec, Canada
Rein Vaikmae, Estonian Academy of Sciences, Tallinn, Estonia
Robert O. Van Everdingen, Arctic Institute of North America, Calgary, Alberta, Canada
Brigitte van Vliet-Lanoe, Centre de Géomorphologie, Caen, France
Theodore Vinson, Oregon State University, Corvallis, Oregon, USA
John Vitek, Oklahoma State University, Stillwater, Oklahoma, USA
Donald A. Walker, INSTAAR, University of Colorado, Boulder, Colorado, USA
James Walters, University of Northern Iowa, Cedar Falls, Iowa, USA
Baolai Wang, University of Ottawa, Ottawa, Ontario, Canada
A. Lincoln Washburn, University of Washington, Seattle, Washington, USA
Kathleen D. White, Cold Regions Research and Engineering Laboratory, Hanover, New Hampshire, USA
Sidney White, Ohio State University, Columbus, Ohio, USA
Peter J. Williams, Carleton University, Ottawa, Ontario, Canada
Ming-Ko Woo, McMaster University, Hamilton, Ontario, Canada
John Zarling, University of Alaska, Fairbanks, Alaska, USA
Bai Chongyuan, LIGG, Chinese Academy of Sciences, China
Chen Xiaobai, LIGG, Chinese Academy of Sciences, China
Cheng Guodong, LIGG, Chinese Academy of Sciences, China
Gu Zhongwei, LIGG, Chinese Academy of Sciences, China
Guo Dongxing, LIGG, Chinese Academy of Sciences, China
Liang Yizhi, LIGG, Chinese Academy of Sciences, China
Kang Ersi, LIGG, Chinese Academy of Sciences, China
Li Guoliang, Northwest Institute of Railway Science, Ministry of Railway, China
Li Shude, LIGG, Chinese Academy of Sciences, China
Liu Tieliang, Northwest Institute of Railway Science, Ministry of Railway, China
Qiu Guoqing, LIGG, Chinese Academy of Sciences, China
Sheng Zhongyan, LIGG, Chinese Academy of Sciences, China
Tong Boliang, LIGG, Chinese Academy of Sciences, China
Tong Changjiang, LIGG, Chinese Academy of Sciences, China
Wu Bangjun, LIGG, Chinese Academy of Sciences, China
Wu Ziwang, LIGG, Chinese Academy of Sciences, China
Xu Xiaozu, LIGG, Chinese Academy of Sciences, China
Zeng Zhonggong, LIGG, Chinese Academy of Sciences, China
Zhang Changqing, LIGG, Chinese Academy of Sciences, China
Zhou Youwu, LIGG, Chinese Academy of Sciences, China
Zhu Qiang, Gansu Provincal Institute of Water Conservancy Science, Ministry of Water Conservancy, China
Zhu Linnan, LIGG, Chinese Academy of Sciences, China
Zhu Yuanlin, LIGG, Chinese Academy of Sciences, China
V.T. Balobaev, Permafrost Institute, Siberian Branch of the Russian Academy of Sciences, Yakutsk, Russia
L.N. Chrustalev, Moscow State University, Moscow, Russia
V.P. Chernjadiev, Institute of Engineering Construction Survey, Moscow, Russia
G.I. Dubikov, Institute of Engineering Construction Survey, Moscow, Russia
A.D. Frolov, Russian Humanities University, Moscow, Russia
B.U. Genadinnik, Institute of Cryosphere of the Siberian Branch of the Russian Academy of Sciences, Tyumen, Russia
N.A. Grave, Russian National Permafrost Committee, Russian Academy of Sciences, Moscow, Russia
S.E. Grechishev, Institute of Hydrogeology and Engineering Geology, Moscow, Russia
I.E. Gurianov, Permafrost Institute, Siberian Branch of the Russian Academy of Sciences, Yakutsk, Russia
I.V. Klimovsky, Permafrost Institute, Siberian Branch of the Russian Academy of Sciences, Yakutsk, Russia
A.A. Mandarov, Permafrost Institute, Siberian Branch of the Russian Academy of Sciences, Yakutsk, Russia
N.G. Moskalenko, Institute of Hydrogeology and Engineering Geology, Moscow, Russia
A.V. Pavlov, Institute of Hydrogeology and Engineering Geology, Moscow, Russia
O.P. Pavlova, Institute of Engineering Construction Survey, Moscow, Russia
N.N. Romanovsky, Moscow State University, Moscow, Russia
G.E. Rosenbaum, Moscow State University, Moscow, Russia
A.V. Sadovsky, Institute of Basements and Underground Constructions, Moscow, Russia
N.V. Tumel, Moscow State University, Moscow, Russia
K.F. Voitkovsky, Moscow State University, Moscow, Russia
S.S. Vyalov, Moscow Engineering Construction Institute, Moscow, Russia
Yu.K. Zaretsky, Institute "Hydroproject," Moscow, Russia

Jerry Brown
Chairman of the
IPA Editorial Committee

Zhu Yuanlin
Secretary-General of the
Chinese Organizing Committee

CONTENTS

OPENING PLENARY SESSION

Tuesday, July 6, 1993

CHENG GUODONG - Respected Dr. Troy Pèwé, President of the International Permafrost Association; respected Madam Deng Nan, Vice President of the State Science and Technology Commission of China; respected Madam Hu Qiheng, Vice President of the Chinese Academy of Sciences; distinguished delegates, distinguished guests, and ladies and gentlemen: Welcome to the formal sessions of the Sixth International Conference on Permafrost. I am Cheng Guodong, Chairman of the Chinese Organizing Committee for the Conference. It gives me great pleasure to announce the formal opening of the Sixth International Conference on Permafrost. This Conference is Organized by the Lanzhou Institute of Glaciology and Geocryology with the collaboration of the State Key Laboratory of Frozen Soil Engineering of the Lanzhou Institute, and the Center for International Scientific Exchange of the Chinese Academy of Sciences, under the auspices of the Chinese Society of Glaciology and Geocryology. The society is the Adhering Body for the International Permafrost Association. On behalf of these institutions, I have the honour of expressing the warmest welcome to all participants of this Conference. Today, I will first introduce the dignitaries at the front table and then say a few words about the Conference. This will be followed by an opening address from the president of the International Permafrost Association.

It is my pleasure to introduce the persons at the front table. At my far right is Professor Zhu Yuanlin, Secretary general of the Conference, and Deputy Director of the State Key Laboratory of Frozen Soil Engineering, Next to Professor Zhu is Mr. Zhang Hengxuan, Vice Chairman of the Cold Regions Development and Research Society of China. Next is Dr. Jerry Brown, an overseas member of the Organizing Committee for this Conference and who contributed a great amount of help during the preparation of this Conference. Next to Dr. Brown is Academician Shi Yafeng, Chairman of the Consultative Committee for the Conference, Honorary President of the Chinese Society of Glaciology and Geocryology, and Honorary Director of the Lanzhou Institute of Glaciology and Geocryology. Next is Dr. Hugh French, the leader of the Canadian Delegation, and Dean of Science at the University of Ottawa. On my immediate right is Madam Hu Qiheng, Vice-President of the Chinese Academy of Sciences. And on my immediate left is Dr. Troy Pèwé, President of the International Permafrost Association. Next to Dr. Pèwé is Madam Deng Nan, Vice President of the State Science and Technology Commission of China. Her attendance is a very exciting event. Next to Madam Deng is Dr. Ross Mackay, Secretary General of the IPA, a leading permafrost researcher and holder of numerous honors. Next to Dr. Mackay is Academician Tu Guangzhi, Member of the Presidium of the Chinese Academy of Sciences, Chief of the Division of Geosciences. Next to Academician Tu is Dr. Lovell, leader of the US Delegation, and the Chairman of the Advisory Committee on Working Groups of the IPA. Next is Dr. Kamensky, leader of the Russian Delegation, and Director of the Permafrost Institute of the Russian Academy of Sciences.

Let me turn now to the Conference. More than 277 research papers and poster papers were submitted, among them about 153 from overseas scientists and engineers involved in geocryology, and 124 from Chinese participants. About 300 frozen ground researchers from 22 countries are attending this Conference. This gives us an opportunity to review the state of our knowledge on the subject. We will be able to benefit from this opportunity to develop a vision of the future for permafrost research and development in the world. I would also like to point out that many papers have been written primarily by young researchers; thus it seems that the Conference will achieve one of its primary objectives.

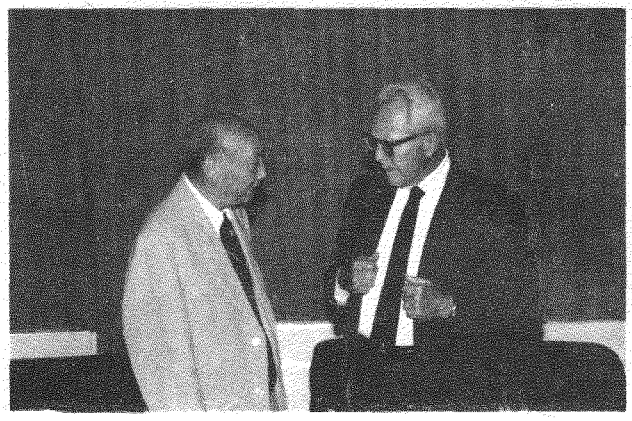

which is to promote a new generation of scientists and engineers interested in geocryology.

In this time we have a many problems with population growth, resource developments and the protection of the environment. Many of our permafrost regions are rich in renewable and non-renewable resources which are required for the benefit of the human race. To develop these resources, we have to continually seek to improve our engineering design and construction techniques and help promote a clean environment. Linked with this is the realization that permafrost science, as the basic research, involving the origin, distribution and nature of permafrost and related fields such as hydrology are essential to sound engineering design and a clean safe environment. At present, considerable attention has been directed to concerns regarding potential changes in permafrost due to human activities and carbon dioxide-induced climate warming. We must remember that the ground is the very foundation on which the ecosystems evolve and human infrastructures are built. Climatic warming will change the permafrost terrain, thus changing the very foundation of the ecosystems and infrastructures. It is, therefore, clear that we are faced with numerous challenges. To meet these challenges, we need not only to work hard, but also to learn through the experiences of others. For these reasons, international conferences and international studies are essential. The International Permafrost Association is thus organized to serve this purpose. Let's now call on Dr. Troy Péwé, President of the International Permafrost Association.

TROY L. PÉWÉ - Thank you Professor Cheng, Madam Deng Nan, Madam Hu Qiheng, distinguished guests, and ladies and gentlemen: The International Permafrost Association is most pleased and honored that the People's Republic of China is hosting the Sixth International Conference on Permafrost. This marks a turning point in the history of IPA. Now each of the founding countries will have hosted an International Permafrost Conference.

Madam Deng Nan, Madam Hu Qiheng, it is my pleasure to thank you for the continuing interest and support that your respective organizations, and your country in general, have given to research and application of permafrost studies, not only in China, but to international cooperation in this field.

On behalf of the IPA, I wish to extend our great appreciation to the Chinese Society of Glaciology and Geocryology and to the Lanzhou Institute of Glaciology and Geocryology under whose auspices and organization this conference is being held.

It has been ten years since the official founding of the International Permafrost Association in 1983 at the Fourth International Conference on Permafrost held at Fairbanks, Alaska. But it has been 20 years since the idea for an international organization was advanced by P.I. Melnikov at the Second International Conference on Permafrost held at Yakutsk, USSR, in 1973.

Our international activities started with the First International Conference on Permafrost held at Purdue University, Lafayette, Indiana, USA, in 1963. It has been my privilege to participate in all of the conferences to date and serve as Vice President of IPA, 1983-1988, and President, 1988-1993. Ross Mackay has been our founding, hard-working, and guiding Secretary General for the pioneering 10 years. Ross and I extend our heartfelt thanks to the other members of the Executive Committees who guided the Association through these early years: P.I. Melnikov, President, 1983-1988; Kaare Flaate, Vice President, 1983-1988; and Cheng Guodong and V.P. Melnikov, Vice Presidents, 1988-1993. For the last five years, personnel of the Standing Committees, Working Groups and National Adhering Bodies have greatly aided in the development of our active organization.

Perhaps it would be well to review progress of the IPA, especially of the last five years. Four of the 20 Adhering Member Countries (Canada, China, USA, USSR) were charter members, and the others joined in the last ten years. Our constitution and bylaws were formalized in 1988 and revised in 1993.

With a firm early foundation, IPA has undergone an extensive maturing and expansion. The Executive Committee and members of the Council have met annually: 1988 (Oslo), 1989 (Yamburg, Siberia, USSR), 1990 (Quebec City), 1991 (Beijing), 1992 (Washington, D.C.) and 1993 (Beijing). The council met in 1990 and 1992. In 1989 IPA was approved as an Affiliated Organization of the International Union of Geological Sciences (IUGS), one of the largest and most active non-governmental scientific organizations in the world.

The establishment and functioning of Standing Committees and Working Groups during the last five years probably has been the most important action of the IPA to date.

The 24-page IPA news bulletin, Frozen Ground, has been well-received worldwide since its initiation in 1990 when it grew from the original IPA newsletter. Publication is the courtesy of

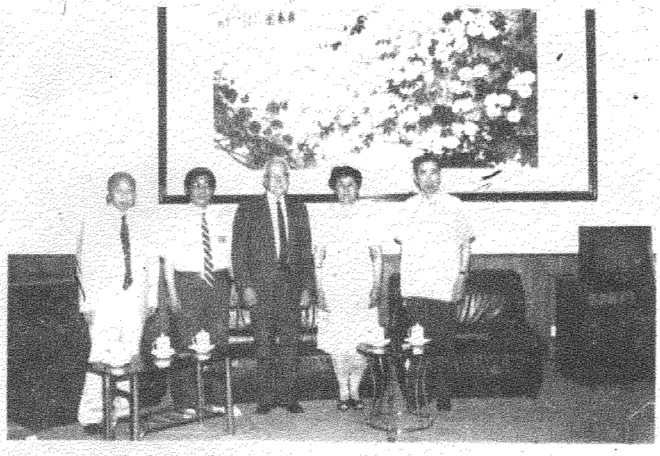

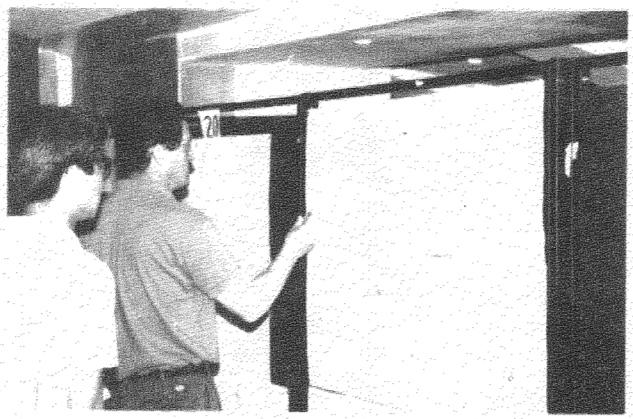

the Cold Regions Research and Engineering Laboratory, Hanover, N.H. USA, and 1600 copies are printed and distributed throughout the world by the adhering members. A permafrost and ground ice map of the Northern Hemisphere is being prepared at a scale of 1:10,000,000 and will be published by the U.S. Geological Survey.

The Working Groups constitute the heart of the "action center". Six groups were organized in July 1988 and one in 1992, and one is in 1993. It is a pleasure to report that the Working Groups have been exceedingly active since their inception with field symposia on various subjects in Switzerland, Russia, United States, Canada, Sweden, Netherlands, France, and others; and publication of symposium results as well as bibliographies and preparation of a multilingual glossary.

The importance of permafrost research in science and engineering is being more widely appreciated because of International Conferences on Permafrost such as this one, as well as activities of our Working Groups, and IPA in general. Past climates can be better understood by a knowledge of the history of frozen ground, its formation and degradation over geologic time; a better understanding of permafrost will permit more successful construction proceduces in polar and mountain areas; even a better understanding of the environment of some of the other planets will be possible because of our current and future work with frozen ground.

In closing, I believe the future for permafrost research looks bright. Best wishes and success, especially to the young scientists and engineers of the world, for continued work in the study of frozen ground.

HU QIHENG - Mr. Chairman, ladies and gentlement, It is a great honour for me to be with you at the Opening Session of this conference. On behalf of the Chinese Academy of Science, I would like to warmly welcome all of you to the Sixth International Conference on Permafrost and to express our thanks to the International Permafrost Association for guidance and support of this Conference.

It is the first time that this Conference is held in China since its first meeting in 1963. I believe that this Conference must be very important for Chinese geocryologists in order to stimulate international exchanges and cooperation, to raise the position of China in the world and to futher develop the permafrost research in China.

Since 1960's, the Chinese scientists have been doing deep and wide investigations on seasonally and permanently frozen ground, especially on the widely-distributed, high altitude permafrost. Meanwhile, they have made great achievements and contributions to the research on frozen soil physics, mechanics and engineering properties and to the design and construction of engineering works in cold regions. With further development of the Western and Northeast China, the study on frozen soil must play more and more important role in the economic development and related construction.

Although we have gained great progress in the research on permafrost, there are still some disparities compared with developed countries. At present, the study on permafrost has been closely related to the global climate change and ecological and environmental conditions. We are happy to enhance scientific exchange and cooperation with the scientists and engineers from various countries and to accelerate the development of permafrost science.

Finally, please accept my best wishes for the success of this grand conference. Thank you for your attention.

TU GUANGZHI - Ladies and gentlement, friends and comrades, It is my great pleasure to extend to you a warm welcome on behalf of the Earth Sciences Division of the Chinese Academy of Sciences. You as scientists and engineers have gathered here from all over the world to attend the Sixth International Conference on Permafrost.

Among the various disciplines of earth sciences, geocryology on the study of permafrost is a relatively new one, but it has made rapid progress in recent years. This could be judged by the number of papers presented at this conference which cover a wide area of research. A casual glance at these papers would reveal the strong interest fowards geocryology from other branches of earth sciences.

As an economic geologist who is engaged in the studies of gold deposits at the present time, I have found that, as is the case in Siberia, Canada and Alaska, the placer gold deposits in China are preferentially located in regions of permafrost. It seems probable that gold accumulates to form placer mainly by chemical or biochemical means. This serves a good example of close ties between geocryology on the one hand and ore exploration and geochemistry on the other.

China is a third world country. We need a thorough development in science and technology. China could offer a good opportunity and a sound background for almost all branches of earth sciences. We welcome earth scientists from all

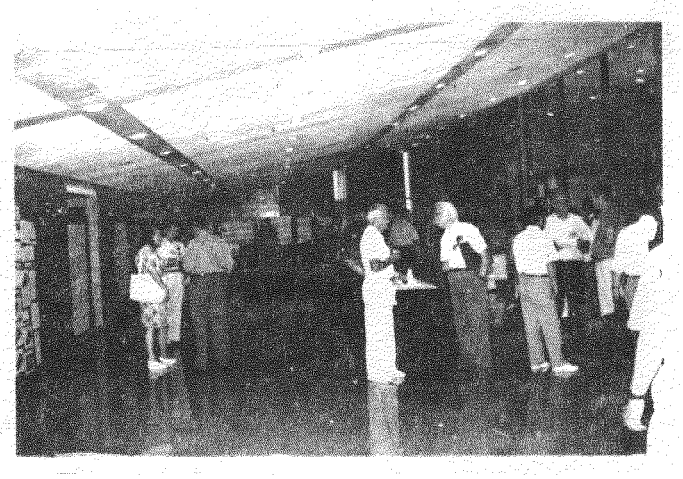

over the world to come to China to exchange opinions, scientific achievements and ideas with us. I do hope our conference would prove to be a successful one and you will enjoy your stay at this conference and in China as well. Thank you.

SHI YAFENG - Ladies and gentlemen, and honoured guests, On behalf of the Chinese Society of Glaciology and Geocryology and the Lanzhou Institute of Glaciology and Geocryology (LIGG), Chiense Academy of Sciences, I would like to welcome you to Beijing and the Sixth International Conference on Permafrost.

I am especially delighted that this conference is being held for the first time in a developing country in Asia.

Since 1978 end the Third International Conference on Permafrost in Edmonton, Canada, the Chinese permafrost community has been actively invalved with the various International Permafrost Conferences and very interested in the advances and developments in geocryology all over the world.

As you all know, ladies and gentlement, China has a long history, but its permafrost research is relatively recent. However China is the third largest permafrost country in the world, with 2 millian km^2 of the teritory underlain by permafrost. The inception and developments of permafrost science in China was closely associated with exchanges of scholars with foreign countries. For example, some of the pioneer permafrost scientists in China were trained in the former Soviet Union. Nowdays, with the increase of international collaboration, Chinese graduate students and visiting scholars are sent abroad to learn more about advanced science and technology. These exchange programmes have, in one way or another, assisted China in keeping pace with the state-of-the-art of the international permafrost and its related sciences. Here, it is, therefore, more appropriate them ever to express my sincere thanks and appreciation to the hosting countries and organizations (institutes and universities), and supervisors of these Chinese scientists.

Permafrost provides opportunities and challenges for both engineers and scientists specializing in cold regions to cope with various construction and geotechnical problems and to reveal the mystery of many periglacial landforms and processes. We hope, that with the increase of international collaboration and exchanges of ideas and data, more and more features and mysteries in geocryology will be uncovered.

I'd also like to say how proud I am of the number of participants from the LIGG. Those of you who will be participanting in one of the two field trips will have the occassion to visit Lanzhou and see first hand the research that is ongoing there.

I am also very pleased to see so many familiar faces and have so many experts from all over the 22 countries of the world gathering here in Beijing to exchange ideas and discuss research results. If the number of participants is any indicator, we should expect a very rewarding and successful conference. Ladies and gentlemen, once again, welcome to China, welcome to Beijing, and welcome to the Sixth International Conference on Permafrost.

C. WILLIAM LOVELL - Thank you, Mr. Chairman. On behalf of the U.S. Committee for the IPA, the U.S. National Academy of Sciences, and the many scientific and engineering specialists for permafrost in the United States, I bring greetings to the attendances of the Sixth International Conference on Permafrost.

I had the pleasure of serving on the Organizing Committee of the very fast ICOP held in 1963 at Purdue University in Lafayette, Indiana, USA. Therefore I can appreciate, in at least a small way, the enormous efforts of the Organizing Committee for the Sixth ICOP, led so ably by Cheng Guodong. The contributions of the Honorary Committee, the Consultative Committee and the governmental and nongovernmental sponsors were also essential.

Some 52 U.S. scientists and engineers have travelled to Beijing to attend the 6th ICOP and to deliver 29 papers. I would like to give special recognitive to may 10 codelegates on the U.S. National Academy of Sciences Delegation. They are: Dr. Bernard Hallet, Deputy Chief Delegate, Dr. Roger G. Barry, Mr. George Gryc, Mr. Rupert G. Tart, Jr., Dr. Chien-Lu Ping, Dr. John P. Zarling, Dr. A.H. Lachenbruch, Dr. Jerry Brown, Dr. Troy L. Pêwé, Ms. Sally A. Shoop.

We all anticipate with great pleasure the technical, cultural and social associations that will result from this conference. And we greatly appreciate the many fine efforts of our Chinese hosts which make all of this possible. Thank you.

HUGH FRENCH - Mr. Chairman, Mr. President, Hu Qiheng, Tu Guangzhi, ladies and gentlemen, On behalf of the National Research Council of Canada, and the Canadian permafrost community,

I bring greetings from Canada, I bring greetings not only from my colleagues here with me in Beijing, but also from numerous colleagues who were unable to attend. Our permafrost community covers a wide range of permafrost science and engineering interests. They exist at the academic, governmental and geotechnical (commercial) levels.

Canada, like China, is a vast country. Unlike China, it only has a population of less than 30 millian. But, like China, it possess significant and extensive areas underlain by permafrost. As such, we have much in common and much to learn from each other as we continue to develop our respective countries, both materially and c·lturally.

Canada was the host of the 3rd International Conference on Permafrost, held in Edmonton in 1978. There was a small delegation from China to that conference - approximately 10 persons. Today, as we can see, Chinese permafrost science has grown and prospered, and it is impressive.

Equally impressive is the amount of organization that must go into running a conference such as this, planning the technical program, arranging the field excursion and local programs, the accommodation and registration, and the banquets and reception is a daunting task. I recognize this and thank you, Mr. Cheng, and your colleagues for the opportunity to benefit from this conference.

Therefore, on behalf of all Canadians present, and numerous others who are unable to be here, I extend my greetings and offer you my best wishes for a most successful and productive conference in an atmosphere of cordiality and friendship.

R.M. KAMENSKY - Mr. Chairman, ladies and gentlemen, dear friends and colleagues, On behalf of the Russian delegation I greet you cordially at the VI International Conference on Permafrost. We are gathered here in Beijing to extend our knowledge of permafrost gained during the past five years and discuss the strategy of further research among international community of permafrost researchers. I am happy to say that during the last years international cooperation has strengthened in studying permafrost. For example, the Permafrost Institute of the Russian Academy of Sciences is conducting joint work with the Japanese scientists. We work in close cooperation with Chinese scientists. Thus, a joint Russian-Chinese expedition worked on the Tien-Shan to study alpine permafrost. It resulted in joint publication printed at the Permafrost Institute. We have brought the copies to Beijing and they are available for purchase. We are conducting research in cooperation with two institutes in Kharbin, China, in the field of permafrost engineering. In Sept. 1993 an international workshop on Protection of Engineering Structures from Frost Heave will be organized jointly with them. We hope that the Conference in Beijing will be successful. We are grateful to the Organizing Committee, our colleagues in the Lanzhou Institute of Glaciology and Geocryology for inviting us to the Conference and for warm hospitality. Thank you.

JERRY BROWN - It is an honor and a pleasure to meet you here today and to have served as an overseas member of the Organizing Committee. On behalf of the many countries and individuals participating in the conference, I extend our collective appreciation to the Chinese Organizing Committee and sponsors for hosting and organizing the VICOP. In addition to those attending the conference in Beijing, there are many individuals who assisted us, but were unable to attend. These include authors and reviewers of papers. In my role as Chairman of the IPA Editoral Committee, I wish to extend special appreciation to the Conference General-Secretary, Professor Zhu Yuanlin and his colleagues for organizing the conference publications. The preconference proceedings volume is a major accomplishment and it will convey the results of the conference to the scientific and engineering communities throughout the world.

Finally, Secretary General Robin Brett of the International Union of geological Sciences, the parent organization of the IPA, has extended his best wishes to Professor Cheng Guodong for a successful conference. I also wish the conference great success and thank the organizers and sponsors in their contributions to the advancement of permafrost science and engineering. Thank you.

ZHANG HENGXUAN - Ladies and Gentlemen, It is a great event in the scientific world of the cold region countries that the remarkable 6th International Conference on Permafrost is opening in Beijing, the capital city of China. On this occasion and on behalf of the Cold Region Development institute of China, I would like to give sincere congratulations to the conference, and warm welcome to the scientists from different parts of the world.

With the advance of cold region development, the study on frozen earth has become more and more important. The International Conference on

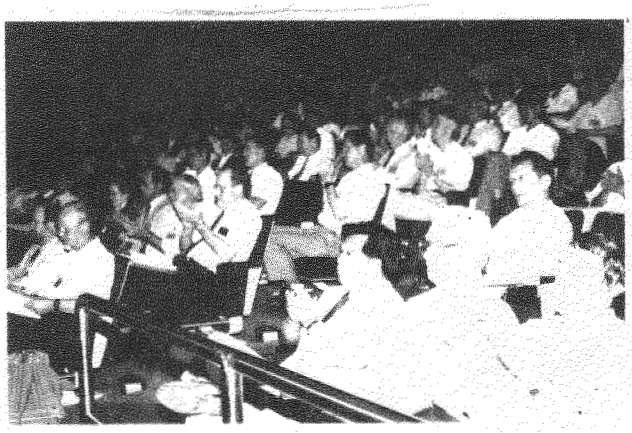

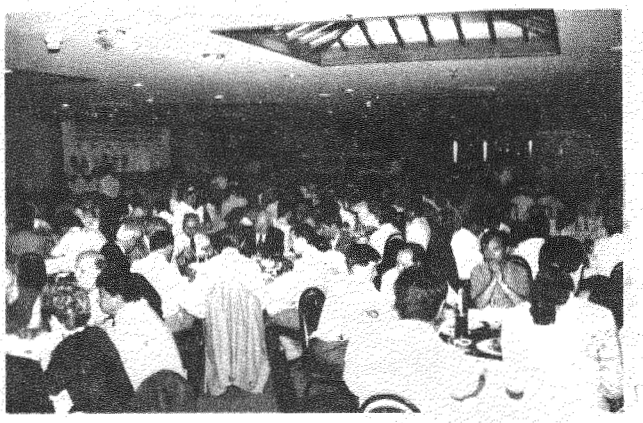

Permafrost, which is held every five years, has provided the scientists and engineers with an opportunity for regular contacts and exchanges of experience, to discuss the current status and the future of research on frozen ground. This indicates that the research and development of frozen ground has opened a new road for the mankind to make use of frozen ground and overcome the damage caused by the frozen earth. I believe that the 6th International Conference on Permafrost will record a new chapter in the world history of frozen ground research.

The Cold Region Development Institute of China is an academic organization which consists of experts, scholars and leading officials. It aims at the research work of cold region development and the promotion of economic and technical cooperation will greatly promote the cooperation will greatly promote the cooperative development of the international cold regions. A major event will be held in January, 1994 in Harbin to celebrate the 10th anniversary of the Ice and Snow Festival and the 20th anniversary of Ice-Lantern Snow. At the same time, we will hold the International Research Conference on the Development of Ice and Snow Culture. The conference will not only activate and enrich the artistic and cultural life of the people in cold regions, but also promote the regional development as well as tourism, trade, economic and technical exchange and cooperation and friendly relations between different parts of the world. Experts and scholars are welcome to come to the meeting.

During the course when the world economy is becoming more and more internationalized, modernized and divided into groups, the development and cooperation between international regions are given more and more attention by many countries and regions. The development of the countries and regions in the cold area is constrained by adverse natural environment, which set many negative conditions for their economic development. We must combine different forces, to convert the adverse conditions into favorable ones. We will do our best to create a comfortable environment and land for the people to live and work. We wish the conference a success. We hope you enjoy your stay in Beijing. Thank you.

ZHU YUANLIN - Dear Chairmen, ladies and gentlemen, I am very glad to be with you here attending the Sixth International Conference on Permafrost. On behalf of the State Key Laboratory of Frozen Soil Engineering, the Lanzhou Institute of Glaciology and Geocryology, Chinese Academy of Sciences, I would like to express a warm welcome to all of you for attending this conference.

Our State Key Laboratory of Frozen Soil Engineering is a new and modern laboratory equipped with various kinds of test equipment and devices and living accommodations. It is one of the best cold regions science laboratories in the world, and is open to the world.

Scientists and engineers, especially young promising researchers are encouraged to apply to our Laboratory Science Foundation and do research work at our Laboratory. We would like to invite you to visit our Laboratory after this conference.

I hope this conference will turn out to be a successful conference. And I wish all of you have a good time during the conference, good time as Beijing and good time in China. Thank you for your attention.

CLOSING PLENARY SESSION

Friday, July 9, 1993

CHENG GUODONG - Ladies and gentlemen. Welcome to the final formal session of the Sixth International Conference on Permafrost. We have been meeting here in Beijing for the past five days to freely exchange ideas and knowledge, discuss joint studies, develop friendship. Now we gathered for a few items of business. I would like to thank all of you, on behalf of the Chinese Organizing Committee for attending the Conference. I am sure you all agree that the conference has been extremely beneficial to all of you.

Now I would first like to call on Professor Albert Pissart to read the necrology.

We will hear now from Professor Troy Pèwè. Under his very capable leadship and guidance, the IPA and continuing development of permafrost science and engineering have been internationally assured. Professor Pèwè was given special recognition by the University of Alaska in 1991, when he receive an honorary degree of Doctor of Science. Such an award is the highest tribute a University can convey to a distinguished individual, and in his case recognized his major contribution to the understanding of Alaska, geology and his international leadership in permafrost research. In addition to the honors bestowed on him by the University, the State of Alaska's legislature gave him an official certificate recognizing his years of dedication to the University of Alaska and its students, as well as his numerous accomplishments associated with permafrost research in Alaska and world wide. It's my pleasure, on behalf of the IPA and the Chinese Organizing Committee to present him a gift in honor of Professor Pèwè for his tremendous contributions to the IPA and permafrost research.

Next, I would like to call on Professor Ross Mackay. As a Secretary General he has made tremendous contributions to the IPA. Besides, he remains our most productive permafrost scientist, and spent more time in the field since his retirement than many will in their entire lives. The award of the 1991 Logan Medal signifies the substance and leadership of his research. His most recent work on thermal contraction cracking provides a remarkable synthesis of detailed field observations and the theory of crack propagation in solids. It is my honor on behalf of the Chinese Organizing Committee to present Professor Mackay a gift in honor of his life time dedication to permafrost research and to the IPA and with our sincere good wishes.

Let me try to explain the meaning of the gift. This is a Chinese character which means longevity. In China, crane also symbolizes longevity, and the old man is a long-lived man. So we wish Prof. Mackay a long, long life.

We will now have a few closing remarks from the leaders of the delegations, we will hear first from Dr. Lovell, representing the US Delegation.

Next, let's call on Professor French, representing the Canadian Delegation.

Out next speaker is Dr. Kamensky, representing the Russian Delegation.

I would like now call on Academician Shi Ya-Feng, representing Chinese Delegation.

Now, we will hear from members of the new IPA Executive Committee. Firstly, I would like to take this opportunity to express my heartfelt gratitude to all of you for the honor you have accorded me, to be the President of the IPA. Science and technology are a kind of wealth created in common by all mankind. They must in

turn serve the needs of all people. We scientists and engineers must join our minds and hands to explore the secrets of science and open new realms of civilization for the common progress of mankind. The IPA should promote this kind of union in the field of Geocryology. To reach this goal we still have a long way to go, and are faced with numerous challenges, which are technologic, scientific and social in nature. But we will do our best to meet the challenges, to further all research in permafrost.

Now I would like to call on Professor Hugh French, the new Vice President of the IPA.

Next, we will hear from Professor Romanovsky, the new Vice President of the IPA.

Next speaker is Dr. Jerry Brown, the new Secretary General of the IPA.

Now let's again call on Professor French.

Thank you Professor French. At this time we should all extend our gratitude to the Government of Canada for the opportunity to organize the Seventh International Conference on Permafrost in Canada in 1998.

I am sure that all of you noticed the banner proclaiming the International Conferences on Permafrost, all six conferences. In addition to the Conferences being proclaimed in four languages, there are the logos of the past six conferences. It is now my duty to pass the banner on the Canada and Professor French, who will be in charge of it until the next conference. I think they will add another logo. Professor French, please accept this banner.

We have now reach the end of the final program of the Sixth International Conference on Permafrost. As Chairman of the Chinese Organizing Committee for the Sixth International Conference on Permafrost, I would like to thank you again for participating in the conference and wish you all a safe and enjoyable journey home.

I now declare the Sixth International Conference on Permafrost closed. Thank you.

ALBERT PISSART - I have a sad task to perform. A number of our friends and colleagues working in the general discipline of permafrost have passed away recently. I refer to the period since the last Permafrost Conference in Trondheim in 1988:

I invite you to rise to hear their names. I would ask you to pause for a moment of reflection to think about these friends and colleagues.

From Russia: Professor A.I. Popov
Moscow State University
Igor A. Nekrasov, E.M. Katasonov
The Permafrost Institute of the Russian Academy of Sciences, Yakutsk
O.N. Tolstikhin
Saint Petersburg University
P.F. Shvetsov
Russian Academy of Sciences, Moscow

From the United States:
William Benninghoff
University of Michigan
James Zumberge
University of Southern California
John Reed
U.S. Geological Survey
Andrew Assur CRREL
Malcolm Mellor CRREL
Richard Goldthwaite
Ohio State University

From Poland: Professor Cseppe
University of Krakow

SHI YAFENG - Dear Mr. Chairman, ladies and gentlemen, As an elder Chinese scientists in this conference, and one of initiatives of Geocryology in China, I would like to make use of the closing ceremony to say few words to express my feelings and ideas.

The International Permafrost Association has a very good spirits of cooperation and democracy. Since the First International Conference on Permafrost held at Lafayette in 1963, and since establishment of International Permafrost Association, these spirits have been developed. Dr. Mackay and Dr. Péwé are the Examples of this spirit. The two famous North America geocryologists who are Secretary General and President, respectively, of International Permafrost Association, are leaving their posts, but their spirits of cooperation and democracy, and unremitting effort for the development of permafrost science are with us forever.

The Sixth International Conference on Permafrost has been successfully held in Beijing, and elected Professor Cheng Guodong as the President of IPA for the next five years. This is a great trust for China and Chinese permafrost workers. I wish to express my sincere thanks to every representatives of this conference. I am very glad to hope that the next five years will be more successful under the cooperation of President Cheng Guodong, Vice-Presidents Hugh French, Nikolai Romanovsky and Secretary General Jerry Brown. I also hope the Seventh International Conference on Permafrost will be successful in Canada in 1998. I hope that Chinese scholars make more efforts for next conference with more accomplishments. Thank you.

JERRY BROWN - Good morning friends and colleagues. Once again I would like to thank the Chinese Organizing Committee for organizing this conference. I believe the conference has been a great success. The goal to bring together scientists and engineers from all over the world to discuss existing and new knowledge has been fulfilled. The three special sessions focused on current problems and concerns. The Data and Information Workshop provides new opportunities to retrieve and exchange information. The paper and poster sessions shed new light on our understanding of geocryology.

The IPA Council met twice during the week. At this time I would like to personally recognize and thank Ross Mackay, IPA Secretary general for the past ten years, for his dedicated service to the IPA and the its Councils. Without his hard work and conscientious efforts the IPA would not be the international organization it is today. The Council was very busy this week discussing accomplishments and plans of the eight working groups. Two new members were admitted to IPA; Spain and the multinational adhering body representing Southern Africa. The new Council passed a resolution calling upon the IPA to become more directly involved with the governmental (IPCC) and non-governmental (IGBP) Global Change activities and programs. The Council also

encouraged our Russian colleagues to consider the establishment of a data subcenter for permafrost and ground ice. We heard plans for the 1998 conference in Canada and encouraged our European colleagues to begin planning for the eighth conference in 2003 in Europe. Over the next five years I will be in contact with many of you and hope to learn of you activities for reporting in Frozen Ground. For those of you going on the post-conference field trips I wish you success and for those of you returning home, have a safe journey. Thank you and I hope to see you all in 1998.

FIELD TRIP A-1 FROM LANZHOU TO LHASA
(JULY 12 - 22, 1993)

Following the VIth International Conference on Permafrost in Beijing, two technical field trips departed for Lanzhou and Urumqi. About 20 members of the conference and ten accompanying Chinese guides and support personnel took part in the post-conference field trip to the Qinghai-Tibet-Plateau, the "Roof of the World". During the six-day bus trip and over 2000 km from Lanzhou to Lhasa (cp. Figure 1), the field trip permitted the participants to observe selected periglacial, glacial and permafrost sites on the plateau. During this short period we gained an impression of the characteristic permafrost and permafrost related phenomena, of the distinctive geoecological and biological zonation of this region as well as of the local people, their living conditions in and adaptions to this unique environment.

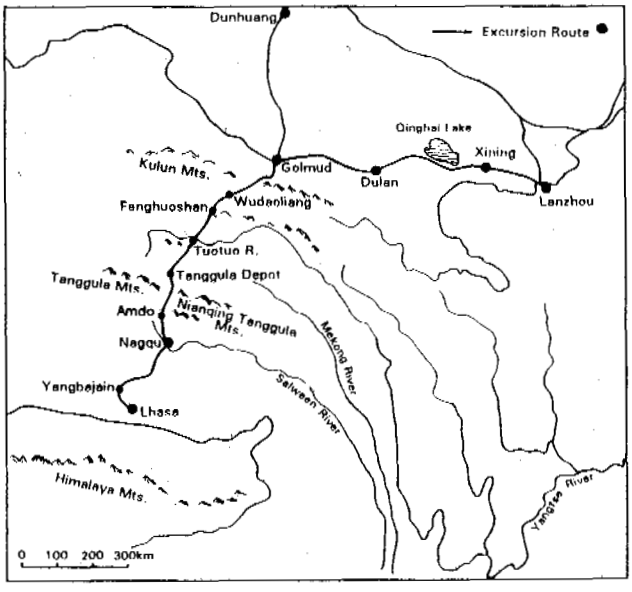

Figure 1: Route map

JULY 10 AND 11: LANZHOU

Local sightseeing and city excursion
Visit to the State Key Laboratory of Frozen Soil Engineering, Lanzhou Institute of Glaciology and Geocryology (Figure 2).
An evening banquet prepared by the staff of LIGG (Figure 3) highlightened the visit.

Figure 2: Group photograph in front of the State Key Laboratory of Frozen Soil Engineering, Lanzhou Institute of Glaciology and Geocryology (by J. Brown)

JULY 12: LANZHOU - QINGHAI LAKE VIA XINING

The route led through an impressive loess-landscape which is characterized by linear down-cuttings. Xining City (2275 m a.s.l.) with about 570.000 people is located in the northeastern part of the Qinghai-Tibet-Plateau. The Qinghai-Tibet-Highway begins at Xining and ends after a distance of 2000 km in Lhasa.
There was a visit and photo stop at the Taer Temple about 30 km southwest of Xining. The Gelupa monastary is one of the most important Lama monastaries in modern China.
After having passed an agriculturaly dominated landscape of extended fields of rape and corn and pastures we arrived at the hotel at the Qinghai Lake (3194 m), China's largest salt water lake.

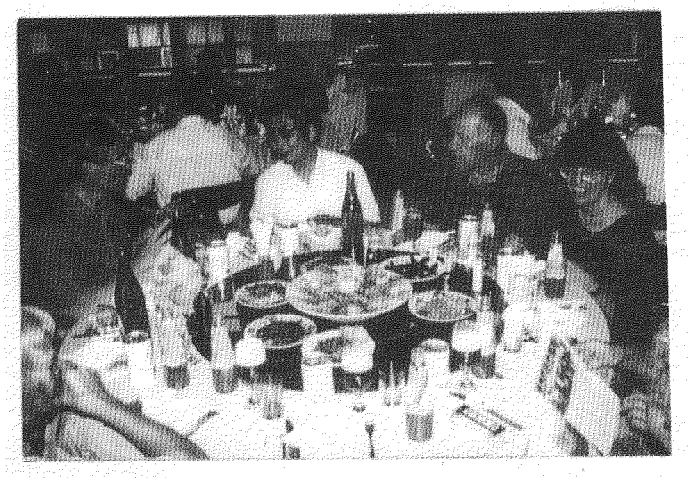

Figure 3: Participants enjoying a banquet in Lanzhou (by E. Schmitt)

JULY 13: QINGHAI LAKE TO DULAN

The route passes through an extended treeless, pasture land located at the northern border of the monsoon region (Figure 4). As a result of the monsoon season rain followed us to the mountain pass (3750 m a.s.l.). Behind the pass, southwest of the Qinghai-Nanzang-Mountains towards Dulan the landscape became drier.

Photo stop at the Chaka Salt Lake which was surrounded by dry, halophile grassland. The Chaka Salt Lake with a total saltreserve of 440 million tons has been mined for 300 years.

Photostop at Zaka, a central town with irrigated cultivation of rape. The landscape in the spur of the Gola mountain chain is similar to high altitudinal deserts. Irrigated agriculture could only be observed at the mouth of valleys originating in desert-like mountains. Longitudinal dunes were characteristic landscape elements.

Overnight at the Dulan Hotel.

Figure 4: Herdsmen in the Qinghai Lake region (by E. Schmitt)

JULY 14, DULAN TO GOLMUD

The third day followed the Qaidam Basin. The landscape varied from mountains, oases along rivers and desert landscape with dunes, salt flats and salt marshes. Towards Golmud the climate became drier and the landscape changed from a half-desert to a full-desert (Figure 5) with a typical desert vegetation cover. The dune landscape is dissected by dry rivervalleys having their origin in the glaciated mountains which border the basin to the south.
Golmud (2800 m a.s.l) is a large industrial oasis town and the administrative centre of the Qinghai Province. The LIGG Permafrost Research Station was visited during the two-day visit.

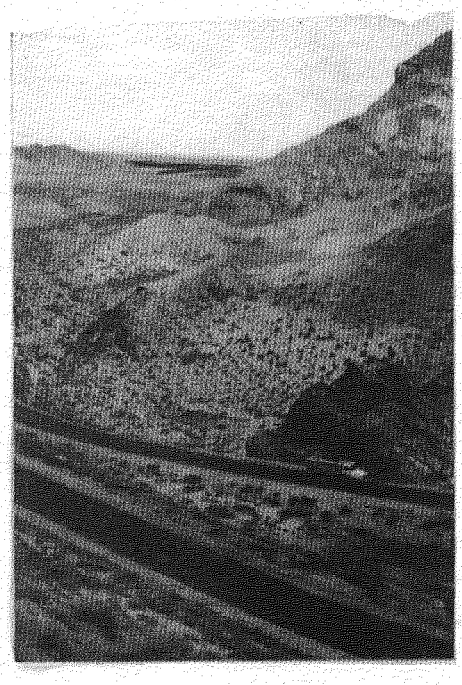

Figure 5: Desert landscape near Golmud (by L. King)

JULY 15: GOLMUD AND ITS SURROUNDINGS

A one-day excursion was made from Golmud to the Qarhan Salt Lake located in the middle east of the Qaidam Basin. The basin is the largest down-fault basin of the Qinghai-Tibet-Plateau covering 5800 km^2. It is the most extensive salt lake of twenty-five found in the basin (Figure 6).

Figure 6: Participants discussing the surficial structure of the Qarhan salt lake playa (by L. King)

JULY 16: GOLMUD TO NACHITAI

The Qinghai-Tibet Highway crosses the Kunlun Mountains, the high plains around the Yangtse River, the Tanggula Range and the plateau basin region of northern Tibet. Permafrost underlies 800 km along the excursion area. On the first stage of the travel, the wide valleys of Golmud River and its tributaries, large dilluvial fans and prominent moraines in the river valleys are observed.

Between 4150 and 4200 m a.s.l., in the upper part of Golmud River Valley and Xidatan Valley, a fault block valley 150 km from Golmud, permafrost is discontinuous with a mean annual ground temperatures of 0.1 to 1.0°C.

The northern lower limit of continuous permafrost was reached at about 4350 m a.s.l.. Permafrost is continuous in a distance of 550 km from 4350 m on the north slope of the Kunlun Mountains southwards to Amdo on the southern slopes of the Tanggula Mountains.

From Xidatan Valley two moraines of the last glaciation are seen at 4400 m and 4300 m on the north-facing slopes of East Kunlun Mountains. An outer end moraine with an extension of about 10 km is developed along the south side of the valley. From the highway can be seen various periglacial phenomena such as rock glaciers above 4900 m a.s.l. to the northwest of the Kunlun Pass, detritus slopes, solifluction slopes at 4520 m a.s.l. and pingos.

A ground temperature observation field of the Lanzhou Institute of Glaciology and Geocryology was visited.

Sand dunes at Xidatan on the valley bottom form a large chain of active crescent sand dunes of local Quaternary deposits. In the 1970s three dunes moved over the old highway at an elevation of 4350 m a.s.l..

Overnight in Nachitai Military Depot at 3550 m a.s.l..

JULY 17: NACHITAI TO WUDAOLIANG

After crossing the Kunlun Mountains Pass (4776 m) in the mid-section of the Eastern Kunlun Mountains the open plateau was reached. Near by the pass a large open-system pingo which developed during the Pleistocene was visited (Figure 7). Recent climatic conditions in the area: mean annual air temperature is below - 5°C, yearly precipitation is at least 280 mm and the winterfrost lasts about 7-8 months.

The descending to 4500 m a.s.l., which is the altitude of most parts of the plateau, the region is characterized by smooth depressions. Damage to the road is mainly caused by the melting of ground ice.

Along the Qingshui River permafrost thickness is 10-50 m. Numerous thermokarst lakes of varying size and form, the largest being several square kilometers, and pingos are present.

The Wudaoliang Basin has permafrost thickness of 30-6o m.

The Hon Xil Permafrost Observation Site is mainly used to study the effects of vegetation on the ground temperature regime and the permafrost formation.

Overnight at the Wudaoliang Military Depot (4700 m a.s.l.).

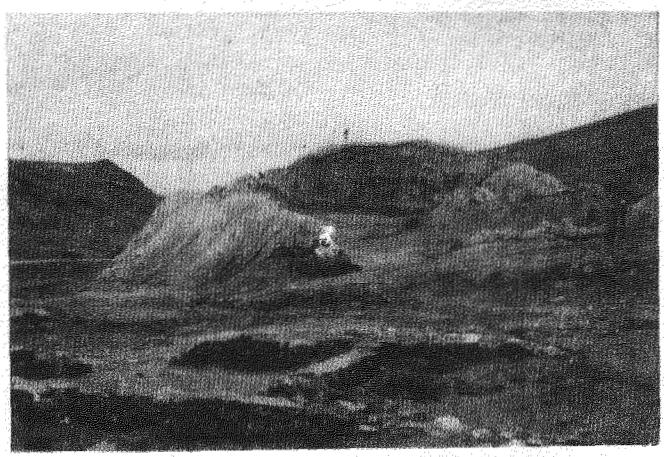

Figure 7: Open-system pingo near Kunlun Mountains Pass, 4776 m (by L. King)

JULY 18: WUDAOLIANG TO TANGGULA MILITARY DEPOT

The mean altitude from Wudaoliang towards the Tanggula Mountains is slightly above 4700 m.

Photo stop at sand erosion slumpings, a special kind of thermoerosion in the wind blown sand deposition area of the plateau. The slumping

consists of loose paleo-windblown deposits such as fine-grained sand, silt and clay. The sparse vegetation consists of traces of pastures. The ice content of the permafrost in these layers was estimated to be 30%, a value questioned by some of the participants as being too low.

Visit to the Fenghuoshan Observation Station (Figure 8), where the most intensive permafrost studies of the Qinghai-Tibet-Plateau are carried out. It is a major test facility and was used by the Northwest Branch of the China Academy of Railway Science for testing embankments and piles in anticipation of a railroad across the Plateau. The station also has ongoing long term temperature records.

Figure 8: The Fenghuoshan Observation Site (by J. Brown)

Visit to an explosive seasonal frost mound in the intersection zone between the NW striking compression torsion fault and the NE striking tension torsion fault in front of Wuli Mountains.

Photostop at the hot springs in the intersection of two faults in the Buqu River Basin at the north slope of Tanggula Mountains. Here in the area of discontinuous permafrost geothermal phenomena like hot springs as well as the presence of river and lake beds cause large thaw areas. Buqu River Valley is a prominent example for such a thaw area.

Overnight at the Tanggula Military Depot (5060 m a.s.l.).

JULY 19: TANGGULA TO NAGQU

Crossing of the Tanggula Mountains Pass. With an altitude of 5231 m a.s.l. the highest point of the Qinghai-Tibet highway was reached (Figure 9). Here the end moraines of the last glaciation could be seen near Basico Lake at the east of the pass.

Figure 9: The excursion group at Tanggula Mountains Pass (5231 m), the journey's highest point (by E. Schmitt)

After crossing Tanggula Pass, which represents the border between Qinghai Province and Tibet, the North Tibetan Plateau was entered. It is open to the south-west monsoon which causes an increase in the annual temperature and precipitation compared with the northern Qinghai-Tibet Plateau. Due to descending altitude the continuous permafrost is gradually replaced by discontinuous, sporadic and island permafrost. The limit between continuous permafrost and island permafrost runs near highway milestone 116, north it is continuous and south it occurs as island permafrost.

Overnight in Nagqu (4507 m a.s.l.) an important city in the eastern part of the plateau basin region of Northern Tibet.

JULY 20: NAGQU TO LHASA

The route led along glaciated mountain ridges, through a shrub and grassland vegetation, forest steppes and a densely populated, rich cultivated landscape which appeared with descending altitude.

Photostop at hot springs of the Gulu geyser area near by a Tibetan settlement in front of the Nianqing Tanggula Mountains. The group received a warm welcome from the local people (Figure 10).

Visit to the Yangbajing hot geothermal area and the terrestrial steam generating electric station about 90 km west of Lhasa.

Descent through the V-shaped Londui Valley to Lhasa. At 4100 m a.s.l. the valley widened and was occupied by cultivated fields of rape, and from 3950 m a.s.l. on with barley fields dominating the landscape. Closer to Lhasa from 3700 m on downwards, they were replaced by corn fields.

Arrived in Lhasa (3658 m a.s.l.), the capital and religious and cultural centre of Tibet, at 6 o'clock p.m.

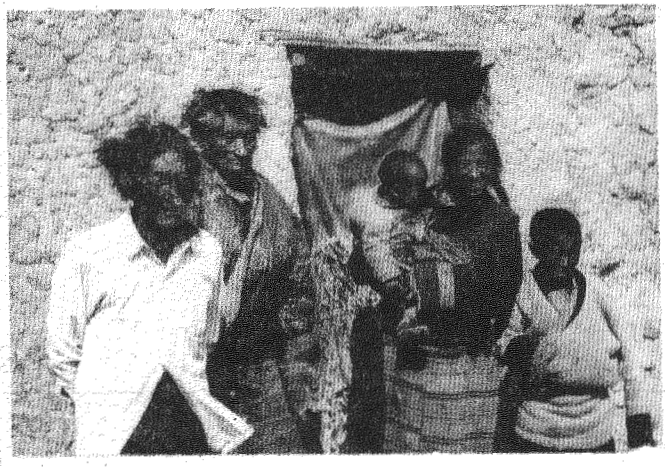

Figure 10: Tibetans welcome the excursion group while visiting hot springs in the Gulu geyser area (by L. King)

JULY 21 AND 22 LHASA:
City excursions to temples, monastaries, local markets etc..

JULY 23: FLIGHT FROM LHASA TO CHENGDU
Most of the group returned to Beijing on July 24. The excursion and the special circumstances under which it took place will certainly be remembered for a long time by all the participants.

REFERENCES:

Liu Tungsheng & Yuan Baoyin (1991): Quaternary Glaciations and Periglaciations in the Qinghai-Xizhang (Tibetan) Plateau. Excursion guide book. International Union for Quaternary Research, XIII International Congress, Beijing, China, 1991.

Guo Dongxin & Zhao Xiufeng, eds (1993): A Guide to the Permafrost and Environment of the Qinghai-Xizang Plateau. Excursion guide book, VIth International Conference on Permafrost, Beijing, China, 1993.

ACKNOWLEDGEMENTS:

Thanks are given to **Lorenz King** for contributions and **Jerry Brown** for the improvement of the english manuscript.

Elisabeth Schmitt
IPA, Chair Editorial Committee

JULY 11: FLIGHT BEIJING - URUMQI

JULY 12: CITY EXCURSION IN URUMQI

Urumqi (1.2 million people of several nationalities) is the capital of Xinjiang Uygur Autonomous Region. It is located on an alluvial fan at the northern foot of Tian Mountains. According to its latitudinal and longitudinal location (about 43° N and 86° E) it has a dry, continental climate. Trees and irrigation furrows follow all roads. The irrigation water source is the Tian Shan. The city is characterized by dense traffic and large industry causes a remarkable air pollution.

Visit to the Xinjiang Museum of Geology and Mineral Products.

JULY 13: URUMQI - TURPAN - URUMQI

Excursion to Turpan in the middle part of the Xinjiang Uygur Autonomous Region. As an intermontane basin in the Tian Shan it is surrounded by Mt. Bogdas in the north, Mt. Karawuquntag in the west, Mt. Jueluotag in the south and Kumtar desert in the southeast. Its lowest point is 155 m m.s.l..

The route was characterized by the transition from steppe to desert and allowed a view to the snowy Bogda Shan (5445 m a.s.l.) during the entire day.

Photostop at the Lake of Chaiwo Pu where salt exploitation and irrigated fields could be observed. In the upper Turpan basin the consequences of recent flooding (road destruction) across the extensive arid plain east of Urumqi (appaerently due to the lack of vegetation) after night rainfall in the surrounding mountains could be observed. On the ride through the stony desert (hammada) green oasis Turpan and an oil exploitation field were passed.

Visit to ancient Bizalik Thousand Buddha Caves on the cliff of Mutuo Valley, 48 km notheast of Turpan City. The sandy soil is covered with ventifacts.

Visit to the ancient city of Gaochang nearby the caves. It was built in the 1st century, destroyed in the 14th century and has been a key point along the ancient silk road.

Visit to the grape Valley, which is an 8-km long and half-kilometer wide oasis rich in water. The 400 hectares of cultivated land include 220 hectares of wine-growing.

Visit to the ancient, but still active Korez irrigation system and the Wudaolin forest belt which is fed by this irrigation system of wells, underground-and surface-channels.

JULY, 14: URUMQI- TIANCHI LAKE - URUMQI

Left Urumqi heading to Tianchi (Heavenly) Lake about 60 km east of Urumqi in the San Gong River Valley on the north slope of Bogda Shan. The route passed steppe and pasture in the foothill zone northeast of Urumqi and irrigation systems on arable land and forests in the Fukong area. The transition from desert to steppe and forest belt (conifers) took place in a horizontal distance of about 30 km.

The visit to Tianchi Lake (1910 m a.s.l) in a mountainous setting provided an opportunity for speculation on alternative mechanisms of formation of the lake (ancient bedrock landslide or moraines). The bluff at the outlet showed unstratified coarse and fine deposits and layered fluvial sediments. The sunny morning allowed a beautiful view to the snowy summit of Bogda Shan while in the afternoon it became cloudy.

JULY, 15: URUMQI - URUMQI RIVER GLACIOLOGICAL STATION - CANGFANGGOU SECTION

Drive to Tian Shan Glaciological Station with several stops en route to inspect and discuss periglacial features. Late Pleistocene alluvial fan sediments of Urumqi River with an alternate bedding of coarse, dark fluvial and fine, light sediments without clear signs of stratification were passed. The question of the origin of the fine sediments (fluvial or eolian) and the genesis of the fan were up for discussion. No signs of periglacial features could be observed.

About 10 km in front of the mountain range Urumqi River terraces could be seen. Two main terraces were clearly distinguished in the distance. The height of these terraces were estimated to be about 50 m. The edges of the loess covered terraces (Figure 1) are maturely dissected due to water erosion.

In the gorge of the upper reach of the Urumqi River (Daxigou River) the Yingxiongqiao hydrolgical and climatological station is located at 1830 m a.s.l.. The observations include water level, temperature, discharge and suspended sediments of the water, precipitation, humidity, air temperature as well as river ice conditions.

At the upper end of the fault basin of Houxia (Rear Gorge) the base camp of Tian Shan Glaciological Station is located (2130 m a.s.l.).

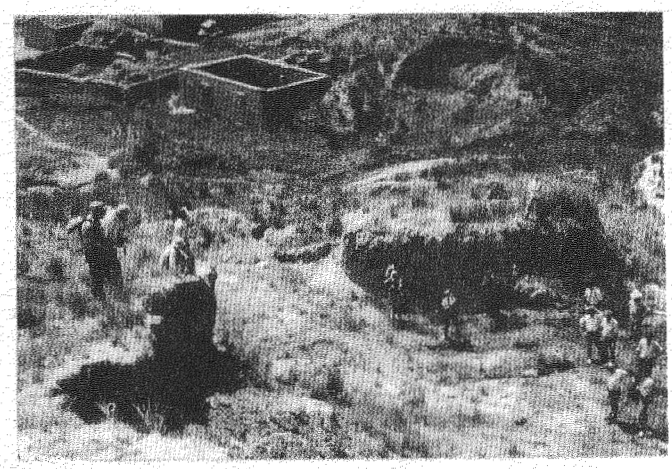

Figure 1: Discussion on the origin and age of the loess cover of one of the Urumqi River terraces (1650 m a.s.l.)

Figure 2: Lunch at the Glaciological Station summer camp (3540 m, a.s.l.): P. Lilley, R. Lehmann, C. Harris and M. Allard (left to right)

JULY 16: GLACIOLOGICAL STATION - SHENGLI DABAN PASS - GLACIOLOGICAL STATION

The highly interesting day was devoted to alpine settings and glaciers in the Urumqi River head waters. The glaciological station summer camp (Figure 2), Glacier No. 1, the precipitous road past Wangfeng Highway Maintenance and ubiquitous glacial and periglacial landforms provoked lively discussions among members of the group.

The gravel road along the upper Urumqi River (Daxigou River) climbed a second gorge and a V-shaped valley and passed Uigur camps. No signs of late-Pleistocene glaciation like U-shaped valleys and Nunataks could be observed. Wood and trees disappeared and an alpine setting with debris slopes characterized the landscape. On north facing slopes above 2900 m high mountain permafrost is present.

Permafrost areas were reached at about 3000 m a.s.l. near Wangfeng Highway Maintenance Squad. Here, clear forms of glaciation as hanging valleys and end moraines of the Wangfeng formation (C^{14} age of 14920 ± 750 years B.P.) were developped. Under periglacial conditions a series of gelifluction steps and tongues were formed.

The road to Shengli Daban pass (4020 m a.s.l.) was built in 1960 on a steep, dangerous debris slope covered with large blocks. Rockfalls are obeserved at many places. Ongoing repairs of the road are necessary. The elevation of the surrounding mountains is about 4300 m a.s.l..

View to retreating Glacier No. 3 on the northern slope of Mt. Karawuquauntag. The lateral moraine contains buried glacier ice. A snow avalanche could be observed on the steep hanging-cirque glacier.

The 20 m depth borehole No. 5, drilled in gneiss bedrock in a sharp turn of the road (3900 m a.s.l.) is the highest borehole in the Chinese Tian Shan. The mean annual ground temperature is -4.9°C and permafrost thickness is estimated to be 230 m. The active layer thickness is 1.75 m in September.

Rock Glacier No. 4 (Figure 3)is located on a north facing slope in front of Glacier No. 3 and cut by the old highway. Since 1960 mean advance of RG4 is 18 cm/year. The rock glacier is not tongue shaped. Patterned ground between RG4 and the moraine of Glacier No. 3 could be observed.

Figure 3: Rock Glacier No.4 (3550 m a.s.l.) cut by the old highway

The glaciological station summer camp (3540 m a.s.l.) is a climatological station with 35 years record starting in 1958; Borehole No. 4, 18 m in depth, was drilled in 1990. The depth of zero annual amplitude is 15 m. Permafrost thickness is estimated to be 100 m.

The frost mound next to a small creek (Figure 4) with an ice core is probably caused by an injection at about 3500 m a.s.l.. Its height is about 1.2 m and it is partly eroded due to thermokarst. Several smaller frost mounds are located in the area.

Figure 4: Frost mound near a small ice cored creek probably caused by injection

A young thermokarst erosion channel (Figure 5) in the ice-rich permafrost (depth about 2 m) on a gentle slope of the valley bottom is caused by road runoff. Clear ice was visible.

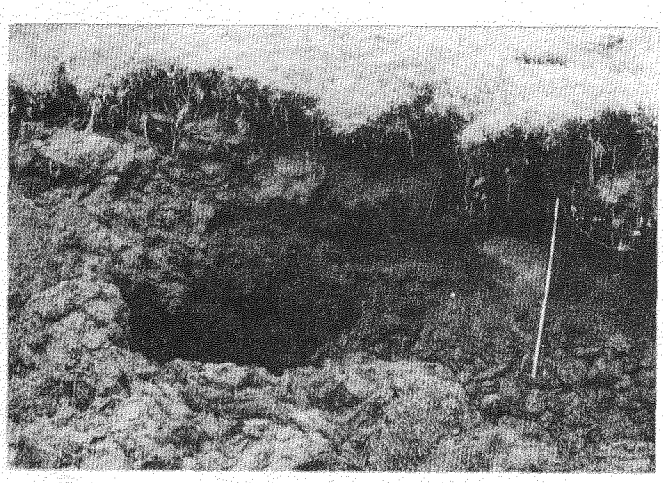

Figure 5: Thermokarst erosion channel in ice-rich permafrost near the Glaciological Station summer camp in the Urumqi River Valley. The scale of the folding rule is 1 m.

Walk along the moraines of the Wangfeng formation. Road cuts show an unstratified till and glaciotectonic thrust sheets. The end moraine of the lower limit is located at about 2900 m a.s.l..

A profile at the Red May Bridge on a terrace about 20 m above Urumqi River shows glacio-fluvial sediments as well as talus and lake deposits.

JULY 17, 1993: GLACIOLOGICAL STATION - GLACIER NO. 1 - URUMQI

The 3.7 km long gravel road from the summer camp to the glacier was built in 1981 mainly by hand and in view of permafrost characteristics. Stone stripes are formed beside the road. Walk down the moraine onto the south branch of the glacier.

Glacier No. 1 (Figure 6) is a small glacier with two branches in north facing cirques. It is retreating, south and north branch are still connected by a very short section but will probably separate in a few years. Mass balance measurements are carried out every four to six weeks since 1959. High ablation and accumulation during summer. During the visit a fresh and wet snow cover on the ice could be observed.

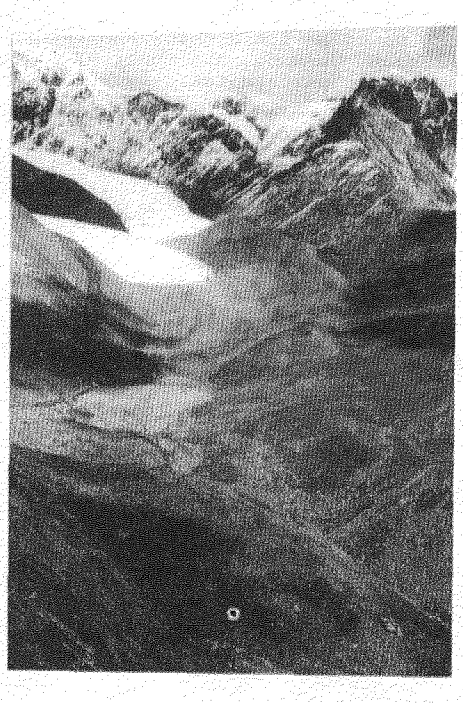

Figure 6: South and north branch of Glacier No. 1. in the background and the active Rock Glacier No. 2 in the foreground.

An empty cirque, sorted circles, stripes and protalus ramparts could be observed in the surroundings of the glacier. The thickness of the active layer is about 1.5 m. No solifluction measurements take place. High mountain vegetation characterizes the landscape.

The active Rock Glacier No. 2 is located next to the glaciological station. The rock glacier is not tongue shaped but very similar to the form of protalus ramparts. It is situated below a steep north facing debris slope. Its active zone is in the middle part of the front slope.

Return to Urumqi.

JULY, 18: FLIGHT FROM URUMQI TO BEIJING.

REFERENCES

Chaohai, L. et al. (1991): Handbook of the Tian Shan Glaciological Station, Lanzhou.

Guoqing, Q., Shije, L., Huijun, J. & Lin, Z. (1993): Guide book of the field trip A-2 of the International Conference on Permafrost. Lanzhou.

ACKNOWLEDGEMENTS: Thanks are given to Jerry Brown for the improvement of the english manuscript.

The report based on field notes and reports by **Rainer Lehmann**, Germany, and **Chuck W. Slaughter**, USA. All photographs are taken by R. Lehmann.

edited by Elisabeth Schmitt,
IPA, Chair Editorial Committee

INTERNATIONAL PERMAFROST ASSOCIATION

STANDING COMMITTEES AND WORKING GROUPS

MEMBERSHIP AND PURPOSE

The following Committees and Working Groups were approved for five years at the IPA Council meeting, July 8, 1993, Beijing, China. Working Groups and Committees are expected to report on progress at Council meetings and regularly in the Frozen Ground News Bulletin. Working Group membership is limited to Chair, Secretary and six full members; exceptions to this limit are made by the Council. Ex Officio members from the IPA Executive Committee and Working Group Chairs may be represented on other Working Groups. There may be an unlimited number of corresponding members on Working Groups and interested individuals should apply to the Working Group Chair.

IPA EXECUTIVE COMMITTEE
Cheng Guodong, President (China)
H.M. French, Vice President (Canada)
N.N. Romanovsky, Vice President (Russia)
Jerry Brown, Secretary General (USA)

ADVISORY COMMITTEE ON WORKING GROUPS
C.W. Lovell, Chair (USA)
W. Haeberli (Switzerland)
S.E. Grechishchev (Russia)
Ex Officio: H.M. French, IPA Executive Committee

FINANCE COMMITTEE
O.J. Ferrians, Jr., Chair (USA)
A. Pissart (Belgium)
Zhu Yuanlin (China)
Ex Officio: J. Brown, IPA Executive Committee

EDITORIAL COMMITTEE
E. Schmitt, Chair (Germany)
N.A. Grave (Russia)
J.A. Heginbottom (Canada)
K. Hall (Southern Africa)
Xu Xiaozu (China)
Ex Officio: J. Brown, IPA Executive Committee

WORKING GROUPS
Mountain Permafrost
Terminology
Global Change and Permafrost
Data and Information
Periglacial Processes and Environments
Cryosols
Foundations
Seasonal Freezing and Thawing of Permafrost Areas

WORKING GROUPS

Mountain Permafrost

Purpose: To improve the exchange of information on, describe the state of knowledge about, and stimulate research activities concerning permafrost at high altitudes and in rugged topography, especially at low latitudes. The objectives of the WG over the next five years are to (1) promote application of computer models to predict permafrost occurrence, (2) organize inter-comparisons of results of modelling and field mapping, (3) coordinate long-term monitoring with regard to warming trends, (4) investigate energy exchanges in the active layer and (5) improve understanding of permafrost creep/rock glacier formation.

W. Haeberli, Chair (Switzerland)
F. Dramis, Secretary (Italy)
S. Harris (Canada)
A. Gorbunov (Kazakhstan)
M.M. Koreisha (Russia)
Ex Officio: Cheng Guodong, IPA Executive Committee

Terminology

Purpose: To develop a set of internationally accepted permafrost terms for engineering and scientific use, with language equivalents. Over the next five years the WG plans to complete development of the multi-language index with the addition of definitions, complete the English-Russian dictionary of over 2000 terms and incorporate the new Chinese-Russian-English glossary into a common index. The Working Group will disseminate and encourage use of such terminology.

R.O. van Everdingen, Chair (Canada)
V. Konishchev, Secretary (Russia)
J. Akerman (Sweden)
A. Corte (Argentina)
F. dramis (Italy)
O.J. Ferrians, Jr. (USA)
J. Karte (Germany)
O. Gregersen (Norway)
J.P. Lautridou (France)
Qiu Guoqing (China)
Ex Officio: N.A. Romanovsky, IPA Executive Committee

Global Change and Permafrost

Purpose: To identify the effects and consequences of global changes in temperature and related phenomena upon the nature of permafrost and its distribution. An annotated bibliography of permafrost and climate change was completed and the special issue of Permafrost and Periglacial Processes on the same topic was published and distributed at the VI COP. Activities over the next five years include preparation of an inventory of existing ground temperature sites, standardization of data collection and archiving in cooperation with the WG on data and information, more direct involvement with global modelling activities, and convening of workshops on related problems. The Working Group is encouraged to interact with other national and international projects groups concerned with global change (e.g. IGBP, IPCC).

F.E. Nelson, Chair (USA)
A. Taylor, Secretary (Canada)
O.A. Anisimov (Russia)
M.K. Gavrilova (Russia)
T.E. Osterkamp (USA)
Ex Officio: Cheng Guodong, IPA Executive Committee
R.G. Barry, WG Data and Information
W. Haeberli, WG Mountain Permafrost

Data and Information

Purpose: To improve and standardize and collection, archiving, documentation and dissemination of permafrost data. Activities over the next five years include a proposed workshop on Data Priorization 1994, continued efforts to assemble and publish permafrost data under the auspices of WDC - B (Boulder, develop a carto-bibliographic data base, and update the permafrost bibliographic compilation. The Working group will collaborate with the WG on Terminology, Global Change and other national and international committees and agencies concerned with relevant data.

R.G. Barry, Chair (USA)
J.A. Heginbottom, Secretary (Canada)
J. Akerman (Sweden)
M.J. Clark (United Kingdom)
Chen Xianzhang (China)
E.S. Melnikov (Russia)
Ex Officio: F.E.Nelson, WG Global Change
R.O.van Everdingen, WG Terminology

Periglacial Processes and Environments

Purpose: (1) To investigate the frequency and magnitude of periglacial processes, especially those occurring within the active layer, (2) to evaluate different methodologies and techniques for process measurements, and (3) to predict the effects of potential climate change on periglacial environments using contemporary data and the stratigraphic record. Over the next five years the WG will conduct several symposium, field trips and prepare a handbook on recommended techniques for investigating periglacial processes. The WG operates jointly with the IGU Commission on Frost Action Environments and its President J.-P. Lautridou, (France) and Secretary C. Harris, (United Kingdom).

A.G. Lewkowize, Chair (Canada)
C. Harris, Secretary (United Kingdom)
J. Akerman (Sweden)
Cui Zhijiu (China)
B. Hallet (USA)
A. Pissart (Belgium)
V. Solomatin (Russia)
V. Vandenberghe (The Netherlands)
Ex Officio: J.P. Lautridou (France), IGU Commission on Frost Action Environments

Cryosols

Purpose: To develop and maintain close working relations between soil and permafrost scientists throughout the bipolar regions, and to develop projects to correlate and/or consolidate the vast amounts of information, maps, and data on soils that are of interest to IPA. Activities over the next five include characterization of soil climates, map the relationship of permafrost and cryosol distribution and participate in several field trips and conferences: soil correlation in Northwestern North America in late July 1993; field trip to Magadan-Kolyma region in summer 1994, attendance at the International Soil Science Society (ISSS) Subcommission on Frozen Soils in 1994, and organization of the Second International Conference on Cryopedology in Syktyvkar in 1996. Coordination and liaison will be provided with the ISSS and other organizations having common interests.

D. Gilichinsky, Chair (Russia)
C.L. Ping, Secretary (USA)
J. Bockheim (USA)
G. Broll (Germany)
Wang Haoqing (China)
B. Jakobsen (Denmark)
G. Mazhitova (Russia)
C. Tamocai (Canada)

Foundations

Purpose: To collect information on the practice of foundation engineering in various permafrost regions of the world and to synthesize guidelines for effective engineering practice. Activities over the next five years include preparation of concise state-of-the-art-reports on such topics as pile foundations and foundation research and conduct seminars and workshops on related topics including a special seminar on foundation failures. The WG encourages monitoring and reporting of the performance of foundations in permafrost and works closely with the WG on Seasonal Freezing and Thawing and national and international engineering and geotechnical organizations and societies including the Canadian Geotechnical Association and the American Society of Civil Engineers.

J.W. Rooney, Chair (USA)
K. Flaate, Secretary (Norway)
R.M. Kamensky (Russia)
L. Krustaley (Russia)
P.J. Kurfurst (Canada)
R.C. Tart, Jr. (USA)
Zhu Yuanlin (China)
Ex Officio: A. Phukan (USA), WG Seasonal Freezing and Thawing

Seasonal Freezing and Thawing of Permafrost Areas

Purpose: To improve the exchange of information on, describe the state of knowledge about, and stimulate research activities concerning frost action in soils and measures to protect against its harmful effects in permafrost areas. The WG will assist in organizing the next symposium on Frost in Geotechnical Engineering in Lulea, Sweden, in March 1997, and work closely with the WG foundations and other WG on problems of common interest. The WG interacts with other national and international groups and organizations (e.g. International Society of Soil Mechanics and Foundation Engineering (ISSMFE) and its Technical Committee on Frost (TC 8); the American Society of Civil Engineers (ASCE) and its Technical Council on Cold Regions Engineering (TCCRE); the International Symposium for Ground Freezing; the International road Federation).

A. Phukan, Chair (USA)
B. Ladanyi, Secretary (Canada)
M. Fukada (Japan)
H.L. Jessberger (Germany)
S. Knutsson (Sweden)
G.Z. Perlstein (Russia)
K. Senneset (Norway)
E. Slunga (Finland)
Ex Officio: J.W. Rooney (USA), WG Foundations

RESOLUTION: INTERNATIONAL PERMAFROST ASSOCIATION

Approved July 8, 1993 at the IPA Council Meeting, Beijing, China

WHEREAS the importance of permafrost is reflected in both international governmental and non-governmental reports and science plans (Intergovernmental Panel on Climate Change (IPCC); IGBP core projects: International Global Atmospheric Chemistry Project (IGAC); Land-Ocean Interactions in the Coastal Zone Project (LOICZ); Biospheric Aspects of the Hydrological Cycle Project (BAHC); and Global Change and Terrestrial Ecosystems Project (GCTE);

WHEREAS the distribution and properties of permafrost are of increasing interest to those concerned with assessing the influence of global climate change on high latitudes and high altitudes;

WHEREAS permafrost is sensitive to climate and contains a memory of past climate changes;

WHEREAS the IPA is concerned with the advancement of knowledge on the formation and degradation of permafrost at regional and global scales;

Be it RESOLVED that the IPA, consisting of 20 adhering national bodies, representing many earth science and engineering disciplines, seek a more active role in the IGBP-core programs by communicating IPA interests and activities to relevant IGBP programs, IPCC assessments, and other programs;

FURTHERMORE the IPA notify other national and international scientific and engineering organizations of its present working groups' plans and activities including the availability in early 1994 of the IPA 1:10,000,000 map of permafrost and ground ice of the Northern Hemisphere;

Finally, be it RESOLVED that relevant IPA working groups give particular attention to global climate change and prepare status and trend reports for the Seventh International Conference on Permafrost, to be held in Canada in August 1998.

Permafrost and Changing Climate*

F.E. Nelson[1], A.H. Lachenbruch[2], M.-k. Woo[3], E.A. Koster[4],
T.E. Osterkamp[5], M.K. Gavrilova[6], Cheng Guodong[7]

[1]Department of Geological Sciences, Cornell University, Ithaca, NY, USA 14853†
Chairman, IPA Working Group on Permafrost and Global Change

[2]U.S. Geological Survey, Menlo Park, CA, USA 94025

[3]Department of Geography, McMaster University, Hamilton, Ontario, Canada, L8S 4K1

[4]Geographical Institute, University of Utrecht
Heidelberglaan 2, 3584 CS, Utrecht, The Netherlands

[5]Geophysical Institute, University of Alaska, Fairbanks, Alaska, USA 99775

[6]Permafrost Institute, Yakutsk, Russia 677018

[7]Lanzhou Institute of Glaciology and Geocryology, Lanzhou, P.R. China 730000

INTRODUCTION

The focus on climate change and its effects on ecosystems and human activities has so intensified in recent years that it is now a central issue in many of the natural and social sciences. Governmental interest and public support for research on this topic has provided the impetus for highly visible and coordinated national research initiatives, and intense debates centered on appropriate responses to the issue permeate public-policy discussions (e.g., Levine *et al.* 1992, Messner *et al.* 1992, Rothman and Chapman 1993, Wirth 1993). Climate change has even provided a tentative, if controversial, basis for intergovernmental cooperation (Houghton *et al.* 1990, von Moltke 1989, Agarwal and Narain 1990). Although permafrost has the potential to be a major element in the fabric of climate-change research, it has to date occupied only a tangential position with respect to both policy discussions and construction of integrative climate-change scenarios. A new resolution, which appears elsewhere in this volume, puts the International Permafrost Association on record as giving permafrost/climate-change interactions high priority (IPA 1993).

Permafrost is a temperature condition of the solid Earth; its existence depends on the local heat balance in cold regions. The widely discussed models for contemporary greenhouse warming generally predict that effects will be greatest in these regions (e.g., Budyko and Izrael 1987, Maxwell and Barrie 1989, Roots 1989; but see Kahl *et al.* 1993, Walsh 1993) and, in general, that they will alter the surface heat balance and the temperature and distribution of permafrost (Nelson and Anisimov 1993, Riseborough and Smith 1993). Relatively rapid changes may occur in the position of the top of permafrost (depth of summer thaw) and in the distribution of warm permafrost near its southern limit; these changes can impact the dynamics of a broad range of surface processes and may release greenhouse gases, currently stored in permafrost, to the atmosphere. Changes in the position of the lower boundary of permafrost will, however, generally be unimportant for hundreds or thousands of years, during which time the downward propagating thermal wave will preserve a lingering record of the climatic event at depth. In the presence of a changing climate, therefore, permafrost can play at least three important roles: 1) as a *recorder* of climate change, 2) as an *agent* of environmental changes that affect ecological and human communities, and 3) as a *facilitator* of further climate change.

*This contribution is based on an invited lecture by A.H. Lachenbruch and presentations by the other authors in a plenary session on "Global Climate Change and Permafrost" at the Sixth International Conference on Permafrost, Beijing, July 6, 1993.

†Permanent address: Department of Geography, Rutgers University, New Brunswick, NJ, USA 08903

PERMAFROST AS A RECORD KEEPER

In cold continuous permafrost, as in other impermeable earth materials, there is little movement of groundwater and heat transfer is almost exclusively by conduction, a process that follows relatively simple mathematical rules. Thus, if a climatic change in the past altered mean annual temperature at the base of the active layer, the change would propagate slowly downward into the permafrost at a rate that can be calculated. In effect, the ground "remembers" the major events in its surface temperature history, and careful temperature measurements made today to depths of a few hundred meters can provide information on the history of local surface temperature during past centuries.

In high latitudes, bodies of water that do not freeze to the bottom in winter generally have mean bottom temperatures near or above 0°C, whereas the mean temperature of the adjacent land surface may be much lower (e.g., -10° to -15°C near the shores of the Arctic Ocean today). Insofar as the solid earth is concerned, the migration of a lake or ocean shoreline therefore leaves a dramatic "climatic change" in its wake: a warming if the shore is advancing on the land or cooling if the shoreline is retreating from the land. Geothermal methods can be applied to temperature measurements in wells on the submerged Arctic continental shelf to interpret the chronology of rapid shoreline transgression in progress on much of the Arctic shoreline today, and of the inundation of the Arctic continental shelf following the last glaciation. Effects of predicted global sea-level rise on low-lying permafrost can be estimated by the same methods (Lachenbruch 1957, Lachenbruch *et al.* 1982, 1988a, Wang 1993).

Additional information about the history of the recent climatic system can be obtained by measuring the temperature, depth, and ice content of existing permafrost and modeling the surface conditions that must have existed to generate the permafrost observed. Where ice content is high and permafrost is deep, as in Prudhoe Bay, Alaska or eastern Siberia, such calculations provide climatic information on timescales approaching 10^5 years, the period of glacial cycles (Balobaev *et al.* 1978, Harrison 1991, Osterkamp and Gosink 1991).

In addition to the information on climate history contained in the present thermal state of permafrost, much can be learned about past surface conditions from the cold-climate geomorphic features and organic materials preserved in buried permafrost (Carter *et al.* 1987, Mackay 1988). Of particular interest are ice-wedge polygons, which form from the percolation of summer meltwater into a network of deep thermal contraction cracks that form during winter in cold brittle permafrost. Evidence on the seasonal growth and deterioration of past generations of ice wedges reveals changes in past surface conditions where these networks of massive ice are preserved in the stratigraphic record (Lachenbruch 1966, Mackay and Matthews 1983).

Climate Signals in Permafrost Temperatures: From Climate to Permafrost

Many important environmental changes associated with climate change in permafrost regions do not occur in permafrost, but rather in the active layer above it. The permafrost generally shares its upper boundary with the base of the active layer (Figure 1), and acts as a "listening post" for temperature changes that occur there. However complex the thermal changes in and above the active layer may be, the only parameter recorded by permafrost is the temperature change that makes its way to the base of the active layer, for practical purposes, the *mean annual* temperature change. It is this quantity, the mean annual temperature at the top of permafrost ($\bar{T}_{pf}$), whose time history is estimated in "climatic" reconstructions from borehole temperature measurements.

Such reconstructions are based on the assumption that, except for the effects of steady heat flow from the earth's interior, a change in mean annual temperature with depth can be caused only by a past change in surface temperature. This will be true where heat transfer is exclusively by conduction with non-changing properties, and where effects of sources and sinks, if they exist, cancel each other over the yearly cycle. Although these conditions are generally satisfied in most cold permafrost, they clearly do not apply in the overlying active layer, snow, and air. In general, therefore, $\bar{T}_{air}$ (mean annual air temperature, Figure 1) will differ from $\bar{T}_{ss}$ (mean annual temperature of the "solid surface"; snow in winter, ground in summer), and $\bar{T}_{ss}$ will differ from $\bar{T}_{pf}$ (mean annual temperature at the top of permafrost, Figure 1), whether or not the climate is changing. Effects above the solid surface are addressed by the radiation balance of climatology, considered briefly below. Between the solid surface and permafrost, the temperature offset ($\bar{T}_{ss}$- $\bar{T}_{pf}$, Figure 1) is determined by the complex dynamics of the snow/active-layer system. Clearly, there are many different

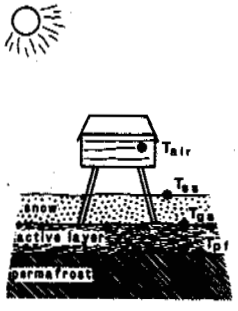

Figure 1. Measurement sites for the differently defined surface temperatures: Tpf at upper surface of permafrost, Tgs at ground surface, Tss at the solid surface of the snow pack when it is present and ground surface when it is not, and Tair in a standard observatory thermometer shelter.

types of surface change, climatic and otherwise, that can produce the same change in permafrost temperature, and some environmentally important thermal changes in the active layer might have little effect on $\bar{T}_{pf}$. It is important, therefore, to maintain a distinction between changing permafrost surface temperature and changing climate.

Simple references to "climatic warming" imply that it can be characterized or defined by an increase in mean annual air temperature near the Earth's surface. Figure 2 is a reminder of the inadequacy of such a definition for predicting environmental effects controlled by the active layer, which is most sensitive to summer temperature. The three cases illustrated in Figure 2 all represent a 4°C mean annual warming (from -9° to -5°C), achieved respectively, with warmer summers, warmer winters, or much warmer winters with somewhat cooler summers. The first might have dramatic effects on surface environments, the third might have little or none. The second is more consistent with predictions from most general circulation models (IPCC Working Group 1990, Maxwell 1992). These relationships can be addressed in an approximate fashion by the ratio of freezing and thawing degree-day sums (Nelson and Outcalt 1987). In all three cases, the warming will generally propagate to permafrost, where it may be detectable for centuries, but a distinction among the three original surface conditions will not be possible.

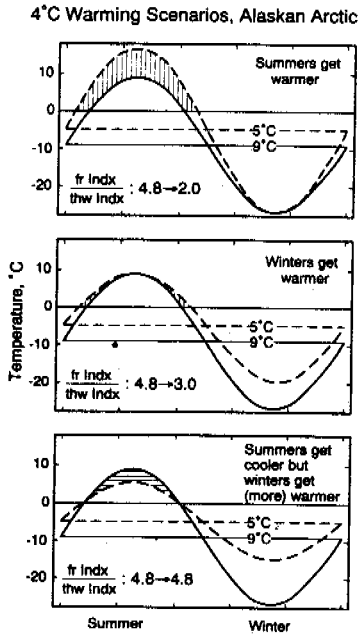

Figure 2. Three scenarios for the same warming (from solid to dashed curves) of mean ground surface temperature ($\bar{T}_{gs}$). Summer conditions that control the environmentally sensitive active layer are quite different for each, as indicated by the ratio of annual freezing degree days to thawing degree days (see Nelson and Outcalt 1987).

Next to the shift in mean air temperature, the most obvious agent to shift $\bar{T}_{pf}$ is winter snow cover, which insulates the ground in winter, causing $\bar{T}_{pf} > \bar{T}_{ss}$ (the "snow offset", e.g., Goodrich 1982, Zhang and Osterkamp 1993); a secular increase in snow cover (a *bona fide* climatic change) can cause a conspicuous warming signal in permafrost. A more subtle $\Delta\bar{T}_{pf}$ signal from the snow can occur with no change in snow cover or mean air temperature if the amplitude of seasonal temperature variation increases; the same snow cover causes more warming because of greater damping in colder winters as the climate becomes more continental (Lachenbruch 1959). This may be the principal cause of the difference in $\bar{T}_{pf}$ from -9°C at Barrow on the Alaskan Arctic coast to -6°C at Umiat, 80 km inland. Both have similar mean air temperatures and snow cover, but Umiat has a more continental climate.

In general, the mean annual temperature will not be the same at different levels between the air/solid interface and the top of permafrost, as explained schematically in Figure 3. For seasonal effects that make it easier for downward heat transfer through the snow and active layer than upward transfer out of them, $\bar{T}_{pf}$ will be greater than $\bar{T}_{ss}$ when the two have reached equilibrium. Examples are infiltration (with possible lateral flow) of summer meltwater and rain, a unidirectional process that advects heat downward, and the "snow offset," which insulates the ground selectively in winter. These are designated Type II processes in Figure 3. Examples of Type I processes, which can cause a steady negative offset of permafrost temperatures, are the change in the active layer from a good thermal conductor when it is frozen in winter to a poorer one that inhibits downward heat flow when thawed in summer. An effect of the same sign is the upward transport of moisture (and dehydration, reducing conductivity) in the active layer to supply surface evaporation

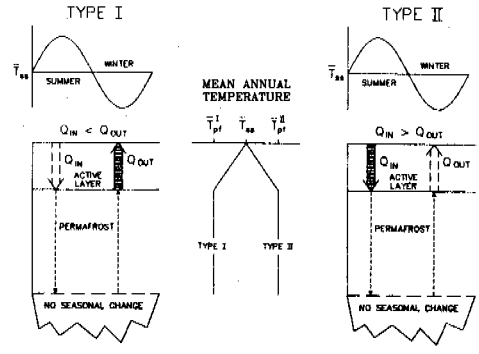

Figure 3. Snow and active-layer processes (Type I) that cause the periodic seasonal influx of heat in summer (Q_{in}) to be less than the seasonal outflow in winter (Q_{out}) generally contribute to a decrease in mean temperature with depth. Those that cause the periodic summer inflow to exceed the periodic winter outflow (Type II) generally contribute to an increase in temperature with depth. Environmentally induced changes in any such snow or active-layer processes are remembered in the permafrost temperature record as changing "climate."

and transpiration; it tends to counteract heat gained by downward conduction in summer. A number of other seasonal processes involving non-conductive transport of sensible and latent heat by migrating moisture, sometimes involving vaporization, condensation, and ice segregation in the active layer have been described (e.g., Nakano and Brown 1972, McGaw *et al.* 1978, Hallet 1978, Mackay 1983, Nelson *et al.* 1985, Outcalt *et al.* 1992). Subtle changes and interactions among the factors that control some of these processes, for example, prolongation of the zero curtain by non-linear interaction of latent heat of soil freeze/thaw and snow cover (Goodrich 1982), could cause a change in heat balance within the active layer that would be remembered by permafrost temperatures as a change in $\bar{T}pf$.

The permafrost surface temperature, $\bar{T}pf$, may be the most important single parameter for the integrated history of environmental conditions. Understanding its full range of implications, however, requires a knowledge of the physics of thermal processes that control it, as well as supplementary information whenever possible. Whether past changes in $\bar{T}pf$ were a direct response to changing climatic parameters, including precipitation and snow cover, or to changing geomorphic conditions, drainage patterns, or the heat and water balance of evolving plant communities, they are a unique source of information that we should attempt to relate to environmental factors, including climate change, land use, and others that will help us to understand the dynamics of changing ecosystems.

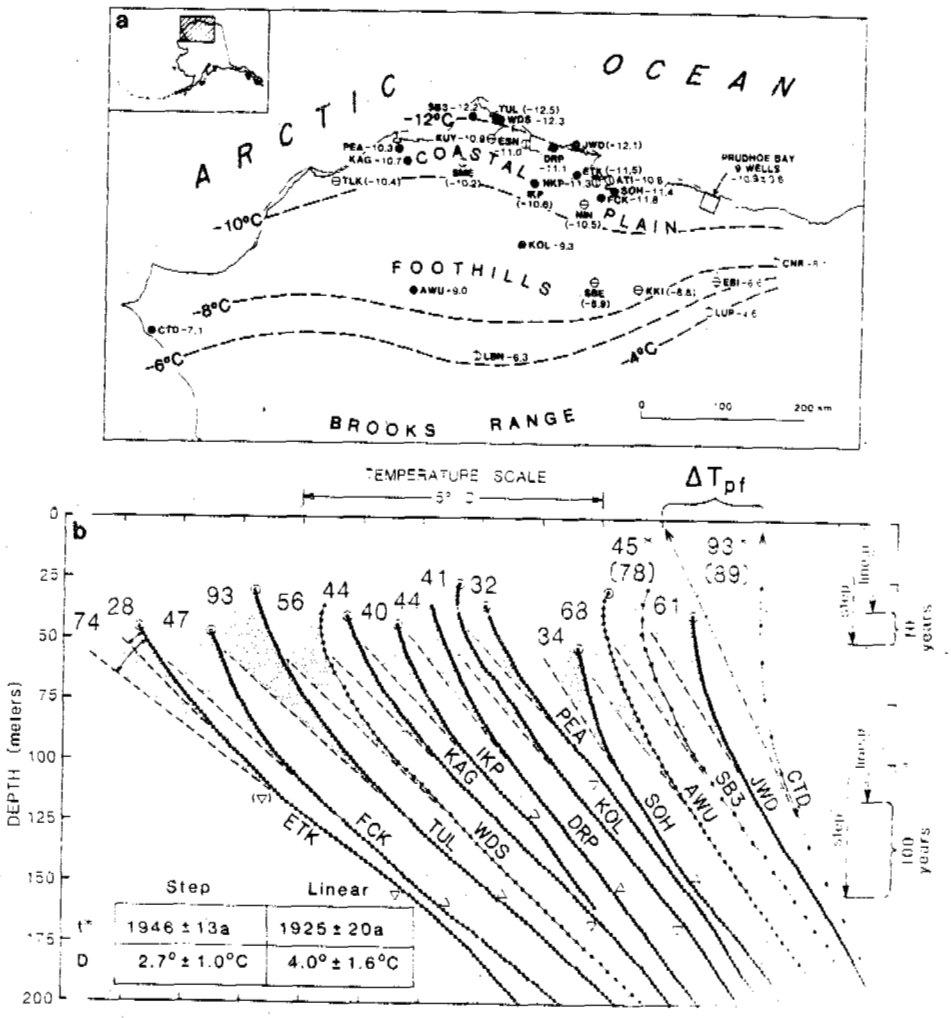

Figure 4. Borehole temperatures in part b are from sites denoted by solid circles in part a. Shaded region for each curve is the recent warming anomaly; numbers by curves denote time in years before 1984 for start-up of best-fitting model of linear warming. Insert in part b summarizes statistics for starting date and total warming for best-fitting step and linear models (after Lachenbruch and Marshall 1986).

The Temperature Signal from Recent Warming Events

Figure 4b shows a group of typical temperature profiles from oil wells on the Alaskan Arctic coastal plain. With few exceptions (see map of Figure 4a), they generally have a linear portion at depth and a curved portion near the surface. The simplest interpretation of the profiles is that the linear portion at depth represents steady heat flux from the Earth's interior (which we measure to be 0.05 to 0.10 W/m^2), and the curved part represents a recent warming event propagating downward (shaded area). The amount of surface warming ($\Delta\bar{T}_{pf}$) is the difference between the temperatures obtained by extrapolating the straight and curved parts to the surface, a few °C in these cases (see curve CTD, Figure 4b). The duration of the warming event, several decades to a century according to simple heat-conduction models, is estimated from the depth of penetration of the anomalous curvature, referenced in the right-hand margin of Figure 4b. Arrows show where the bottom of the anomaly should be 10 or 100 years after the start of a step or linear change in surface temperature.

Figure 5 compares three formal reconstructions of surface temperature history ($\bar{T}_{pf}$) from the anomaly (shaded region) at AWU (Figure 4b). The timing and magnitude of the step and linear functions were determined by the least squares method described by Lachenbruch and Marshall (1986), and the smooth curve (Clow *et al.* 1991) by the method of spectral expansion (Parker 1977, Clow 1992), in which the unknown time history is represented by a series of orthonormal functions. All of the reconstructions fit these data within observational error (± 0.05°C) and there is little basis for preferring one to another. (The resolution can be greatly improved, however, by increasing the measurement precision to the presently feasible ± 0.001°C.) The results show that although these measurements do not resolve details of the surface temperature history, there can be little doubt about the big picture; at AWU and most of the other holes in this 2 x 10^5 km^2 region, there was a marked, but laterally variable increase in temperature at the top of permafrost ($\bar{T}_{pf}$) of a few degrees Celsius during the twentieth century (Lachenbruch and Marshall 1986, Lachenbruch *et al.* 1988a, Clow *et al.* 1991). Some sites show a more recent cooling, believed to be related to engineering disturbance (Lachenbruch and Marshall 1986). A reason for this dramatic and locally variable change has not been found in the limited records of surface temperature or snowfall from the region, and its cause remains unknown.

From Figure 6, it can be seen that heat accumulation in the solid Earth from the unbalanced downward "climatic" flux (c) must be of the same order as the upward geothermal flux (g), which it nullifies to yield near-zero gradients near the surface (Figure 6b). The estimates for the AWU of g ~ 0.06 W/m^2 and c ~ 0.16 W/m^2 (Lachenbruch *et al.* 1988a) are illustrated in Figure 6. It is of interest to compare these modest solid-earth fluxes to the

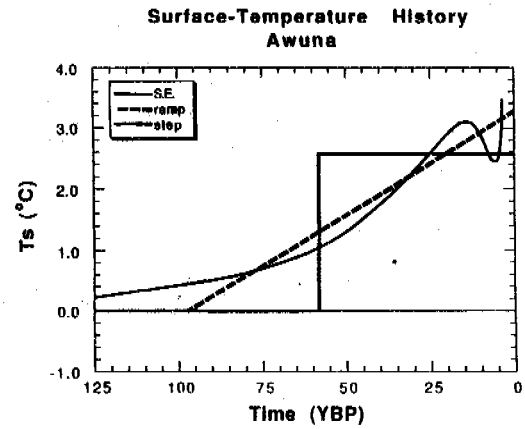

Figure 5. Best-fitting step, ramp, and spectral expansion models for recent warming event at AWU, Figure 4 (after Lachenbruch *et al.* 1988a, Clow *et al.* 1991).

more vigorous activity on the other side of the Earth's surface. The larger "top-side" fluxes drive the ecosystem, and their balance point determines the Earth's surface temperature (Weller and Holmgren 1974). They consist of the incoming and outgoing radiation components and their difference (the net radiation, Figure 6a), which, among other things, is responsible for melting snow and evaporating water, allowing them to return to the sea or the atmosphere to balance both the thermal and hydrologic budgets in preparation for the next annual cycle. The numbers on the arrows (Figure 6a) indicate that these top-side climatic fluxes sum to zero as they should if the climate is not changing. However, from Figure 4 we know that climate is changing; at Awuna about 0.16 W/m^2 more has been going into the Earth than out for a half century or so. As this is just 1/100th of the net radiation (itself a difference of large numbers), we cannot detect it by trying to keep a balance sheet of fluxes at the Earth's surface. Thus, while the unbalanced climate flux (C in Figure 6) is an inconspicuous second-order effect in the climatic system, it is a conspicuous first-order effect that dominates the thermal regime of the upper 100 m in the solid-earth system (Figures 4 and 6b). The solid Earth is a good monitor for changes in the surface energy balance. The downward flowing heat cannot go far in a century because the Earth is a poor conductor; it is all contained in the stippled region (Figure 6b), which represents the complete climatic event from start to finish.

PERMAFROST AS AN AGENT OF ENVIRONMENTAL CHANGE

It is paradoxical that in permafrost regions the portion of the ground that has the greatest influence on surface dynamics is the very portion that is *not* permafrost: the active layer and its vegetation. The permafrost, of course, imparts to the active layer its important characteristics: a base generally at

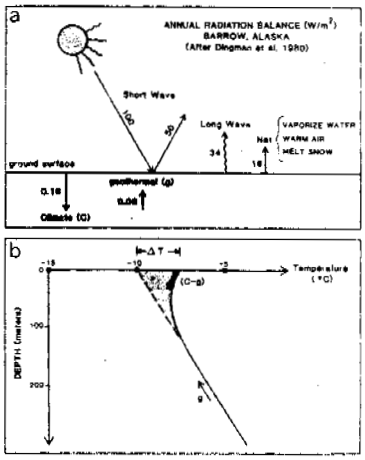

Figure 6. Typical thermal conditions in permafrost regions of the Alaskan Arctic. a. Average annual energy fluxes (W/m^2) above and below the Earth's surface. b. Geothermal regime: g is steady geothermal heat loss, C is heat gain from warming climate, stippled region represents total heat accumulation by the solid earth from warming event.

subfreezing temperature and impermeable to moisture, with conditions generally prohibitive for penetration by roots. Under typical conditions, the active layer is the growth medium for biotic systems and the reservoir for their water and nutrient supply (Gersper *et al.* 1980), the locus of most terrestrial hydrologic activity (Hinzman *et al.* 1991, Kane *et al.* 1992), and a boundary layer across which heat, moisture, and gases are exchanged between the solid earth and atmospheric systems.

With climate warming, (increased mean annual and/or summer temperature), the depth of thaw and settlement of the surface will generally increase (e.g., Kane *et al.* 1991, Nakayama *et al.* 1993, Waelbroeck 1993), but not uniformly; for example, deepening troughs can form over a network of large ice wedges, thereby altering drainage patterns and the distribution of wet and dry habitats. The changed distribution and motion of the soil water can have a dominant effect on the thermal and chemical balance, including the rates of biogeochemical reactions, the productivity of living systems, the decomposition of organic matter, the generation or uptake of CO_2 and CH_4, and other characteristics of the active layer that influence (and are influenced by) the distribution of plant communities (Oechel and Billings 1992, Shaver *et al.* 1992).

Changes in the mechanical and thermal condition of permafrost as its moisture changes state during climate change can cause interacting surface effects (mechanical, thermal, hydrological, and biological), whose major impacts are treated in the following subsections.

Terrain Susceptibility and Implications for Developments

The environmental impacts of permafrost and its growth and deterioration with changing climate depend primarily on the amount and form of the ice it contains; both interstitial ice and massive ice bodies are common. The impacts are almost all manifestations of the dramatic change in strength and heat-transfer properties associated with phase change. Melting of interstitial ice, for example, decreases strength and increases permeability, permitting increased water flow. This, in turn, leads to increased advective heat transfer, and accelerated melting in an unstable progression that can cause collapse of massive ice, soil flowage, and disruption of the landscape.

In warmer permafrost, near the margins of its extent, increasing surface temperature can cause summer thawing to depths too great to refreeze in winter. The resulting taliks can be conduits for groundwater flow and associated convective heat transfer (e.g., Anisimov 1989). The presence of unfrozen water in warm permafrost may be a common occurrence, owing to small amounts of soluble impurities commonly present in groundwater (Osterkamp 1989). This unfrozen water changes the thermal properties of the permafrost, makes them temperature dependent, and creates a distributed latent heat sink throughout the body of permafrost. These factors can result in very complex thermal and hydrologic regimes in marginal permafrost areas and in many areas will cause them to deteriorate rapidly. The latitudinal gradient of mean annual surface temperature near the warm margins of continental permafrost generally ranges from 0.3°-$3.0^{\circ}C$/100 km (Zamolotchikova 1988, Mackay 1975, Anisimov 1989). Thus, in some regions like central Canada and Siberia, climatic warming of a few degrees can subject vast areas to marginal decay. This process, together with the effects of a thickening active layer, will be responsible for prompt (10°-10^{2} years), major impacts on the dynamics of permafrost regions subjected to a warming climate (Stuart 1986, Nelson and Anisimov 1993).

Unlike the slow loss of permafrost by heat conduction from below in continuous permafrost areas, however, the rapid loss of warm discontinuous permafrost is a process that is not well known. There are few published data for such aspects as thawing rates at the permafrost table and base, processes of talik development, time scales for thawing, or the importance of lateral heat flow. In the absence of such empirical data, simulation studies assume great importance. Riseborough (1990) carried out a numerical simulation on the effects of latent heat on the thermal response of the upper 20 m of permafrost. Where unfrozen water is present, he suggested that short-term, near-surface ground temperature trends are not necessarily an

absolute measure of the magnitude and rate of change to the surface thermal regime. Riseborough and Smith (1993) linked the thermal response of permafrost in the Fort Simpson area of Canada's Northwest Territories to a 2x CO_2 warming scenario from the Canadian Climate Centre general circulation model. Randomized weather records, superimposed on the trend provided by the GCM, were used to drive a numerical heat-transfer model that evaluated the thermal response of permafrost over a 140-year period. Results from 121 replications were highly dependent on particular details in the simulated surface climate, and gave a wide range of times for disappearance of the permafrost profile. Interannual climatic variability appears to be an important factor in the evolution of permafrost under an overall warming trend.

Despite our lack of data on thawing permafrost, there is abundant historical evidence for thermokarst development over extensive regions. Evidence for the existence of thermokarst relief at subcontinental scales, in the form of alas complexes, ice-wedge pseudomorphs, truncated wedges, and interpermafrost taliks, has been found across Siberia, and has been related to specific intervals characterized by distinct climatic warming (Baulin *et al.* 1984, Kondratjeva *et al.* 1993). These include the close of the Pleistocene (Baulin and Danilova 1984), the "Holocene Optimum" in Yakutia (Soloviev 1959) and a late Holocene warming 300-2500 years BP in western Siberia (Solomatin 1992).

Some appreciation for the potential impact of climate-induced permafrost degradation in areas of intensive development can be gained through examination of current problems involving ice-rich terrain in Siberia. Although permafrost degradation induced by direct anthropogenic activities such as clear-cutting of forests are not optimal analogs for climate-induced effects, their scale can in some instances allow us to visualize the regional impacts that worst-case climate-change scenarios could eventually have in areas of ice-rich permafrost. Moreover, local- and regional-scale human activities are likely to be superimposed on broader climatic influences, and their effects may therefore be additive.

Regions that contain extensive areas of warm, ice-rich permafrost, as in western Siberia and the Far East, are particularly sensitive to landscape disturbance and increased thaw depths (Vyalov *et al.* 1993). At exploratory drill sites in northern Chukotka, active-layer thickness increased by a factor of two to three in terrain subjected to removal of vegetation cover, compared with adjacent undisturbed areas. The Bykovsky fish-processing plant in Yakutia, which supplied fish to the entire USSR during World War II, is an example of problems that may be encountered in many settlements under a warming climate. The ice content of the ground beneath Bykovsky is as high as 90%, with only 0.6-1.0 m of mineral-soil overburden. Disturbance of the upper 5-15 cm of moss and turf cover has initiated thermokarst processes that will necessitate abandonment of the community within the next ten years (Grigoriev *et al.* 1990).

Climatic warming also has serious implications for the stability of engineered works in mountainous regions (Haeberli 1992, *Haeberli et al.* 1993). Specific examples include the Qinghai-Xizang Highway in Tibet (An *et al.* 1993, Cheng, this volume) and projects described by Ulrich and King (1993) in the Alps.

Hydrology of Permafrost Areas

Several points are noteworthy when considering the hydrological consequences of permafrost thaw.

- Frozen ground has very low hydraulic conductivity (Burt and Williams 1976) and most permafrost materials can be regarded as impervious to storage and transmission of significant quantities of water. Thus, infiltration and percolation is limited (Woo 1986), and groundwater flow is restricted to taliks and seasonally thawed zones (van Everdingen 1987). Thickening of the active layer and formation of new taliks accompanying climatic warming will expand subterranean passageways for storage and circulation of groundwater.
- Permafrost retains varying amounts of water in the form of ground ice, much of which remains in storage for centuries or millennia. Some of this ice will be released to the hydrologic cycle when permafrost degrades, but once melted and drained, this source of water will be depleted.
- Heat and moisture fluxes strongly affect each other. Latent heat is involved in the freezing and thawing processes while the thermal conductivity and capacity of thawed soils differ greatly from those of frozen soils (Farouki 1981, Lunardini 1981). Increased thawing of the permafrost will have hydrologic feedbacks.
- Climatic warming in permafrost regions will likely be accompanied by changes in the precipitation regime. Alterations in the magnitude and timing of precipitation, as well as the form of precipitation (e.g., rain *vs.* snow), will influence the hydrologic rhythm of a region under a changed climate. Climatic change, with its attendant effects on permafrost and vegetation development, will affect all the water balance components, while modifications of several hydrologic elements will have significant feedback on the permafrost.

Precipitation is the major source of water input to permafrost basins. Warmer conditions will shorten the freezing period. At low elevations, snowfall may occur later and snowmelt may be earlier than at present, so that peak melt events may not be as concentrated or as intense. At high elevations, the effect of temperature lapse rate on the freezing altitude will counter some of the effects of temperature increases. Together with increased storminess and orographic influences, conditions may even favor more snowfall at high elevations while rainfall increases in the lower zones. For areas where the ground snow cover does not decrease significantly, the insulating effects on the permafrost may not diminish in the future.

Evaporation in permafrost regions is limited by the long duration of snow and ice cover on the ground and by the low level of energy available during the thawed season. A warming scenario will shorten the snow- and ice-covered period (except perhaps for high altitudes), and provide more heat in summer. Part of this will be due to reduced ground heat flux as the frozen substrate deepens to lessen the ground temperature gradients, and part is due to the higher sensible heat available. Computer simulation (e.g., Kane *et al.* 1991) suggests that higher evaporation will accompany higher summer temperatures. Should climatic change continue, however, the vegetation will likely be different from today, probably at all scales, from the species to the biome level. If the lichens and mosses that tend to be suppressors of evapotranstiration (Rouse *et al.* 1977) are replaced by transpiring plants, evaporative losses will increase. Large-scale hydrologic changes may occur in the extensive wetlands that occupy large tracts of the discontinuous permafrost regions of Eurasia and North America. Enhanced evaporation associated with the projected warming will lower the water table, followed by changes in the peat characteristics as the wetland surfaces become drier (Woo 1992).

Permafrost degradation will thicken the active layer. This should allow greater infiltration and water storage, especially for rain that falls during the thawed period. Thus, there will be more groundwater available to sustain baseflow in the fall, resulting in an extended streamflow season. In terms of runoff responses to basin water input, Slaughter *et al.*'s (1983) study in central Alaska provides a modern analog to what the future pattern may be: small basins with low percentages of permafrost tend to produce smaller ranges of flow conditions, yielding fewer high flows of large magnitude and more discharge during low flow seasons.

Streamflow of most rivers in permafrost areas exhibit a nival regime, which is characterized by high snowmelt runoff in spring, followed by low summer flows that are occasionally raised by rainfall events (Church 1974). In the temperate zone, rain-generated peaks dominate and the seasonal runoff pattern follows a pluvial regime (Woo 1990). As climatic warming occurs, particularly if winter temperature increases are pronounced, the snowmelt peak flow may be similar to or lower than the present, depending on whether snowfall increases or otherwise. Rain-induced flows may be more frequent if rainstorms become prevalent, although higher evaporation and more deeply thawed active layers available for moisture storage may reduce the runoff peaks. The baseflow period will be extended, depending on how much later the winter arrives. In general, the nival regime runoff pattern will weaken for many rivers in the permafrost region, and the pluvial influence upon runoff will intensify for rivers along the margins of the discontinuous permafrost zones.

The impacts of global warming on the hydrologic system are full of time lags; examples include such considerations as uneven storage changes causing variable response time, and whether the changes are steady or involve thresholds (see Woo *et al.* 1992). Other considerations include feedbacks between the hydrological and external systems or among different hydrological elements; "random" signals emanating from climatic variability, chance occurrences of events and phenomena; and human factors, including development in permafrost areas, activities involved in resource extraction, and changes in land use. Our task is to deduce the hydrologic tendencies under climatic change forcing, constrained by uncertainties in the climate model predictions. Given the current limited level of knowledge on permafrost hydrologic and climatic processes, only generalized statements on the impacts, not detailed quantification, should warrant our confidence.

Ecological and Geomorphic Effects

Comprehensive overviews of the very large literature on ecological responses to climatic change are provided by Gates (1993) and Solomon and Shugart (1993). A rich literature also exists on permafrost as an ecological factor, much of it potentially useful in the context of climatic change (e.g., Gill 1975, Lukin and Billings 1983, Morrissey *et al.* 1986, Burn and Friele 1989, Evans *et al.* 1989, Gross *et al.* 1990, Zoltai and Vitt 1990, Lafleur *et al.* 1992, Lavoie *et al.* 1992).

Considerable interest has focused on geographical shifts of the forest-tundra transition as a response to climatic change; a recent publication by Timoney *et al.* (1992) provides a firm basis for monitoring northward migration of the forest tundra in northwestern Canada, as well as for simulation studies. Much effort has already been expended on predicting latitudinal shifts of the boreal and tundra zones (e.g., Solomon 1986, Kauppi and Posch 1988, Monserud *et al.* 1993; also see discussion in Gates 1993 and Solomon and Shugart 1993). Experiments linking vegetational responses to GCM-derived climate scenarios generally predict poleward migration of vegetation classes, and shrinkage of the area occupied by tundra. Simulation experiments by Bonan *et al.* (1992) suggest, however, that important climate feedback mechanisms could be triggered by shifts in the forest-tundra transition, including those accomplished by such anthropogenic activities as extensive deforestation in the boreal zone. Permafrost is an important ecological factor in the arctic and subarctic and should be considered explicitly in future modeling exercises.

Geomorphic responses to climate warming were reviewed in detail by Woo *et al.* (1992). Development of thermokarst phenomena at regional scales is likely to occur, and has important implications for resource management, as well as the other impacts on human activities outlined above.

Potential also exists for widespread slope failure in response to a general climatic warming trend, although relationships are likely to be complex and spatially inhomogeneous. Lewkowicz (1992), for example, presented evidence that rapid *rates* of thaw

penetration into ice-rich subsurface layers may be a more important factor in triggering active-layer detachment slides than is the simple maximum annual depth of thaw. This conclusion again suggests the importance of interannual climatic variability for realistic assessments of the response of permafrost to climatic warming (cf. Riseborough and Smith 1993).

Slaughter and Hartzmann (1993) suggested that degrading pingos in the discontinuous permafrost zone could be used to monitor the onset or progression of climatic warming; palsas and other near-surface, ice-rich landforms in subarctic peatlands may also prove useful in this capacity.

Concerns have been expressed about the effects on coastal permafrost of a greenhouse-induced rise in sea level (e.g., Roots 1989, Barnes 1990, Woo *et al.* 1992). Recent observational and modeling work focused on the response of the Antarctic ice sheet to climatic warming suggests, however, that the ice sheet may receive increased nourishment, and that a large increase in sea level could be delayed substantially (Bentley and Geovinetto 1991, Sugden 1992).

PERMAFROST AS A FACILITATOR OF CLIMATE CHANGE

A very large amount of carbon has been stored in peatlands of the boreal and tundra regions during the Holocene. Much of this carbon is sequestered in permafrost; under conditions of climate warming, general retreat and thinning of permafrost may convert these regions into net sources of carbon (Billings 1987, Oechel *et al.* 1993, but also see Yarie and Van Cleve 1991, Bonan *et al.* 1992, Kolchugina and Vinson 1993), initiating feedback effects and enhanced warming.

Methane in shallow permafrost

A substantial body of literature has accumulated in recent years on methane emissions in northern regions (e.g., Harriss *et al.* 1985, Moore and Knowles 1987, 1990, Whalen and Reeburgh 1988, Moore 1990a, 1990b, Morrissey and Livingston 1992, Torn and Chapin 1993). The intense interest in this subject is motivated by recognition of methane's effectiveness as a greenhouse gas and by its rapidly increasing concentration in the atmosphere (Cicerone and Oremland 1988). Although few data are available, large amounts of CH_4 may be stored in permafrost regions; a widespread increase of thaw depth in response to climatic warming could, in principle, release a substantial proportion of this methane, triggering feedback effects in the atmospheric system.

Although there has been a tremendous upsurge of research on methane in northern regions, details of the methane budget are very poorly known. Great variability has been observed in sampled emission rates (e.g., Morrissey and Livingston 1992) and the few data available on the methane content of permafrost also suggest high variability (Kvenvolden and Lorenson 1993). Moreover, the relationships between methane flux, soil moisture, and soil temperature are poorly known (Vourlitis *et al.* 1993).

Two recent papers attempted to model the release of methane from permafrost, using one-dimensional numerical heat-transfer models driven by GCM-generated climate-change scenarios. Basing their estimates of the methane content of permafrost on data obtained from areas near Fairbanks (Kvenvolden and Lorenson 1993) and Prudhoe Bay (Moraes and Khalil 1993, Rasmussen *et al.* 1993) in Alaska, estimates of the maximum global rates of methane release were, respectively, 25-30 and 5-8 Tg/yr. These results underscore the uncertainty surrounding this topic. Far more data on the methane content of permafrost are necessary before truly reliable estimates can be made. Future modeling efforts involving circumarctic extrapolation should also be based on the large-scale, high-quality map of permafrost distribution scheduled for publication in early 1994 (Brown 1992), rather than one of the many published small-scale depictions, the majority of which are poorly documented (see Nelson 1989, Nelson and Anisimov 1993).

Gas hydrate: a record keeper and agent of climate change

Sediments in cold regions may trap large quantities of natural gas, largely methane, in ice-like crystalline structures containing water molecules and called *gas hydrates* or *clathrates* (Katz *et al.* 1959). They store natural gas efficiently (up to ~150 times as much methane as an equal volume of free gas under standard conditions of temperature and pressure. Gas hydrates are of interest in connection with global climate change as a potential source of atmospheric methane, one of the most important greenhouse gases. They are also of interest as a potential commercial source of energy.

Gas hydrates are stable under special conditions of low temperature and/or high pressure that obtain in only a small, superficial part of the solid earth. The stability field is shown in Figure 7, assuming the common ("hydrostatic") condition, wherein fluid pressure is equal to the weight of a column of water extending to the surface. For the typical Arctic coastal conditions illustrated for Barrow, Alaska ("0 yrs," Figure 7a), methane hydrate is stable between about 200 and 700 m, and permafrost extends downward below a thin active layer to a depth of about 400 m. At Prudhoe Bay, Alaska, the higher conductivity (lower thermal gradient) ice-rich permafrost extends to a depth of 600 m and the hydrate stability field to more than 1 km (Figure 7b). Under steady conditions, hydrates will be stable on the continent only in colder permafrost regions. For the typical steady-state temperature gradient illustrated in Figure 7a, the surface temperature would have to be below about -5°C for the geotherm to intersect the hydrate field.

The principal global-change question about gas hydrate is: will a warming climate destabilize gas hydrates, release methane to the atmosphere, and thereby enhance the warming by its contribution to the greenhouse effect? The geothermal effect of a sudden increase of surface temperature by 10°C is illustrated

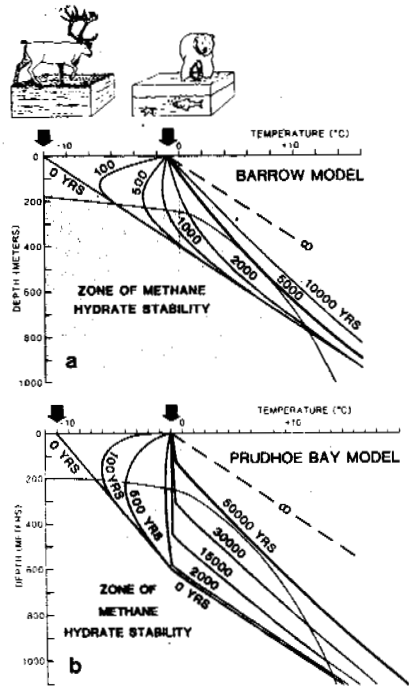

Figure 7. Thermal decay of methane hydrate stability field (shaded) beneath a transgressing Arctic shoreline. Land surface with geotherm typical of Barrow, Alaska (a), or Prudhoe Bay, Alaska (b), is inundated by sea (mean annual bottom temperature, -1°C) at time t= 0 years. Destabilization takes ten times longer at Prudhoe Bay owing to latent heat absorbed by its high ice-content permafrost (Lachenbruch *et al.* 1982, 1988b, 1988c, Lachenbruch and Saltus, unpublished calculations).

in Figure 7a. This is much more severe than predictions of climate models, but it is an accurate representation of the "climate change" that occurs when Arctic seas override the land, a process that must have occurred over millions of square kilometers on the Arctic continental shelf as it was inundated by rising sea level following the last glaciation. Transgression continues today at rates exceeding a meter per year along much of the Arctic coastline (e.g., Carter *et al.* 1987, Mackay 1986). Figure 7a suggests that the effects of a thermal disturbance today would not reach the top of the gas hydrate field at ~200 m for centuries, and for initial conditions typical of Barrow, Alaska today (Lachenbruch *et al.* 1988c), significant methane release could not occur for thousands of years. If, unlike the "Barrow model" in Figure 7a, the permafrost were ice rich as at Prudhoe Bay (Lachenbruch *et al.* 1982, Lachenbruch *et al.* 1988b), the destabilization would take tens of thousands of years (Figure 7b. Although the phase boundaries of gas hydrates vary with composition, fluid pressure, and salinity, these examples serve to illustrate two rather general points:

- Significant amounts of methane will not be released from destabilized methane hydrate in permafrost areas by present-day climate change for a millennium or more.
- Present-day contributions to atmospheric methane from destabilized hydrate should be sought on the Arctic continental shelf, where warming started with inundation thousands of years ago (Lachenbruch *et al.* 1982, 1988b, Kvenvolden 1988, MacDonald 1990, Judge and Majorowicz 1992, Osterkamp and Fei 1993).

INFORMATION ISSUES

Research into the effects of climatic change on permafrost has generated a substantial increase in the number of publications on this topic since the last permafrost conference (Koster and Judge 1994). Although warming trends have consistently been predicted to be most pronounced in the high latitudes (e.g., Roots 1989), the permafrost community has, with only a few exceptions (e.g., Lachenbruch and Marshall 1986), not communicated the importance of its subject as a recorder, facilitator, and agent of climate-induced changes to the larger scientific community, especially in high-impact, integrative media.

Interest in the potential effects of climatic change on permafrost is widespread and increasing; the situation is reflected in the growth of literature on this general topic over the past five years. Reviews have been published recently by Barry (1985), Williams and Smith (1989), Pissart (1990), Street and Melnikov (1990), Vinson and Hayley (1990), Haeberli (1992), Koster (1991, 1993a), Koster and Nieuwenhuijzen (1992), Melnikov and Street (1992), Gavrilova (1993), and Haeberli *et al.*(1993). Several of these publications built upon earlier efforts by McBeath (1984) and French (1986).

Despite worldwide interest in climate change issues and the assumption that northern wetlands and permafrost regions play a vital role in the global climate system, relatively few studies have appeared specifically dealing with these subjects and presenting new data. The *IPCC Scientific Assessment of Global Change* (Houghton *et al.* 1990) reflects this minor attention to climate-permafrost interactions, with only two short paragraphs on high-latitude methane sources (p. 22) and temperature profiles in permafrost (p. 225).

Similarly, permafrost bibliographies produced by Heginbottom and Sinclair (1985) and Brennan (1988, 1993) reveal that, despite a large number of citations, only a limited number of publications explicitly present data on the response of permafrost to former, present, or future climatic changes. A similar conclusion can be drawn from the overview presented in Table 1, which reflects items published through 1992. Studies on "frozen ground properties" (125) and "permafrost engineering" (203), predominantly of North American origin, provide the necessary background for climate change impact analysis, but do not address the subject in depth. Studies on "paleoenvironmental

Table 1. Number of publications according to subject categories (Permafrost Science and Engineering)

Sources:
- IV International Conference on Permafrost, Fairbanks, Alaska, 1983, Proceedings and Final Proceedings (1937 pp)
- V International Conference on Permafrost, Trondheim, Norway, 1988, Proceedings Volumes 1, 2 and 3 (1620 pp)
- V Canadian Permafrost Conference, Québec, Canada, 1990, Proceedings Collection Nordicana No. 54 (424 pp)
- Permafrost and Periglacial Processes, Volumes 1.1-4.2 (1214 pp)

	Fairbanks	Trondheim	Québec	PPP	Total
1. *Frozen ground properties*	52	41	17	15	125
1.1 Permafrost physics (incl. ground thermal conditions)	33	20	8	5	66
1.2 Permafrost chemistry (and mineralogy)	5	8	4	2	19
1.3 Ground ice characteristics (incl. massive ground ice)	3	7	2	5	17
1.4 Permafrost and geophysical surveys	11	6	3	3	23
2 *Permafrost distribution and site characteristics*	63	72	11	37	183
2.1 Areal extent and temporal changes ('climatic change')	11	9	4	6	30
2.2 Active layer processes, snow and soils ('buffer layer' interactions)	6	17	2	-	25
2.3 Land permafrost (site characteristics)	8	13	3	4	28
2.4 Offshore and near-shore permafrost	9	7	1	-	17
2.5 Mountain (alpine) permafrost (incl. rock glaciers and rock streams)	13	18	-	24	55
2.6 Permafrost mapping and remote sensing (incl. planetary permafrost)	16	8	1	3	28
3. *Frozen ground hydrology (soil moisture, surface and ground water)*	26	29	3	4	62
4. *Frozen ground and paleoenvironmental (-climatic) reconstruction (incl. cryostratigraphy and periglacial structures)*	20	10	-	10	40
5. *Periglacial processes (field and laboratory studies) and phenomena*	47	47	9	47	150
5.1 Frost heaving (incl. frost mounds, cryoturbation)	15	17	4	7	43
5.2 Frost sorting (incl. patterned ground)	6	9	1	3	19
5.3 Frost cracking and wedging	6	3	2	2	13
5.4 Frost weathering (incl. karst features, caves)	5	6	-	20	31
5.5 Mass movement and slope processes (incl. wind action)	8	7	2	14	31
5.6 Permafrost degradation and thermokarst (incl. thermo erosional features)	7	5	-	1	13
6. *Permafrost engineering (design and constructions)*	100	86	17	-	203
6.1 Permafrost strength and foundation structures (piles, buildings, bridges)	34	40	11	-	85
6.2 Permafrost and pipelines (oil, gas, water and cables)	22	11	3	-	36
6.3 Permafrost and roads, railways, airfields, dams, canals	26	19	3	-	48
6.4 Permafrost and mining (excavations) and drilling operations	9	13	-	-	22
6.5 Permafrost and gas hydrates	2	1	-	-	3
6.6 Offshore permafrost exploration and constructions	7	2	-	-	9
7 *Permafrost ecosystems and northern wetlands*	17	3	-	2	22
8. *Permafrost and environmental impact (waste disposal, constructions) and protection*	15	5	-	2	22
					807

reconstruction" (40) and on "periglacial processes" (150), largely of European origin, are only marginally of interest in this respect, leaving 183 studies relevant to this discussion in the category "permafrost distribution and site characteristics." Surprisingly few investigations were found on "permafrost *ecosystems and northern wetlands.*"

The *Annotated Bibliography on Permafrost and Climatic Change* (Koster and Judge 1994) selectively summarizes investigations, published between 1960 and 1992, that treat the interrelationships in the atmosphere/buffer layer/permafrost system. The more than 250 entries concern a variety of topics, including former changes in permafrost (analog, cryostratigraphic and cryo-geothermal studies), present interrelationships in the permafrost system (monitoring studies), and future changes (impact assessment and simulation studies). Apart from a fairly large number of abstracts, derived from the *Proceedings* of the previous International Permafrost Conferences, the origin of the relevant publications proved to be highly diversified. Recent review papers by Vandenberghe and Pissart (1993) and Haeberli *et al.* (1993) clearly indicate the past accomplishments and future perspectives of periglacial science in Europe with respect to climate change issues. A weakness common to most summaries of periglacial literature, however, is inadequate coverage of the Russian and Chinese literature, a shortcoming that is also evident in the IPA Working Group's bibliography (Koster and Judge 1994). Table 2 illustrates the topics covered by this literature survey; the numbers appear impressive but most studies underline the uncertainties in assessing the response of permafrost to climate change. Only a few studies (< 10%) "predict" changes due to anticipated climate changes, and these are mainly based on tentative simulation experiments.

Table 2. Number of publications according to subject categories (climate - permafrost interactions, 1980-1992)

Source:
Annotated Bibliography on Permafrost and Climatic Change, IPA Working Group on Present Global Change and Permafrost (1993).

1. *Cryostratigraphy/reconstruction paleotemperatures*	13		
2. *Climatic change and permafrost distribution/sensitivity*	23		
2.1 Spatial (horizontal) changes		17	
2.2 Altitudinal changes/mountain permafrost		6	
3. *Atmosphere - 'buffer layer' - permafrost interactions*	134		
3.1 Microclimatic/meteorologic observations		8	
3.2 Geothermal gradient/regime		42	
3.3 Heat fluxes/radiation balance		21	
3.4 Site characteristics		63	
3.4.1 Snow cover			16
3.4.2 Vegetation			23
3.4.3 Fire/anthropogenic disturbances			12
3.4.4 Soil attributes/hydrology			13
4. *Climate change and permafrost response*	54		
4.1 Thermokarst		10	
4.2 Other geomorphic effects		12	
4.3 Coastal/subsea/offshore permafrost		13	
4.4 Engineering aspects		13	
4.5 Socio-economic consequences		6	
5. *Permafrost ecosystems/greenhouse gases/gas hydrates*	28		
6. *Reviews*	15		
	267		

CONCLUSIONS: AN AGENDA FOR RESEARCH

Climatic warming raises the specter of a very severe and specific set of problems in high-latitude regions. To address these challenges in an effective manner will require coordinated and sustained effort by the permafrost research community. Some of the more prominent issues in need of resolution are outlined below.

Modeling

General circulation models (GCMs) are the primary means currently used to investigate and predict the nature, extent, and distribution of climatic change. GCMs are complex, three-dimensional models of the earth's atmosphere and oceans; because they are extremely consumptive of computing resources they are implemented over very coarse geographical lattices. The internode distances of these models, often several degrees of latitude and longitude, is of profound importance for application of their results to a variety of scientific problems. Issues of scale dependence and the applicability of GCMs to problems involving regional climate are therefore the focus of intensive efforts at present (e.g., Karl *et al.* 1990, Boville 1991, Giorgi and Mearns 1991, Grotch and MacCracken 1991, Gutowski *et al.* 1991, Hewitson and Crane 1992).

With only the few exceptions noted in earlier sections, and in contrast to the efforts of botanists and ecologists (e.g., Solomon 1986, Kauppi and Posch 1988, Thomas and Rowntree 1992), permafrost scientists have not made extensive use of GCM results in their discussions about potential impacts of climate change. Although scale-related problems are substantial, as are others involving the formulation of explicit linkages between GCM results and the transient response of permafrost to climatic change (see discussion in Burn and Smith 1993), general circulation models are the scientific community's primary tools for forecasting climate- change scenarios. As part of the International Permafrost Association's focus on climate-change issues (IPA 1993), high priority should be given to developing linkages between permafrost research and models of climate change, over a hierarchy of geographical scales.

Technological issues

Technology introduced in the commercial market during the last decade has made possible substantial improvements in the feasibility, cost, and scale of field measurement programs in remote cold-climate regions. As in many other areas of science, technological innovations will allow us to expand the scope of our investigations to such an extent that the nature of the questions we ask is fundamentally altered. Introduction of relatively inexpensive battery-powered, computer-controlled measuring and recording systems, for example, has made it possible to obtain high-frequency time series at remote sites, allowing extensive evaluation of local conditions and their variability. Accuracy requirements can be stringent, however, particularly where permafrost temperatures are near 0°C, or in special applications. Some of the less costly instrumentation is not optimally configured for the temporal intervals, sensing resolution, or temperature conditions required for permafrost research. Recent unpublished calculations by Zhang and Osterkamp, for example, suggest that highly accurate determination of *in situ* thermal diffusivity may require accuracy on the order of ±0.01°C in the measurements. Permafrost researchers should communicate their needs and standards to manufacturers clearly and in detail, particularly in the sphere of low-priced instrumentation, which may require only inexpensive modifications to achieve a configuration that can be used effectively and widely.

In the even more demanding application of using the information stored in permafrost as a paleoclimatic signal, to achieve a reliable means of identification, reconstruction, and future monitoring of recent changes in the temperature at the permafrost surface requires that temperatures be monitored with a precision of ~ ±1 milliKelvin (mK). If borehole temperatures can be remeasured over a period of years with millidegree precision, we can overcome major obstacles to the reconstruction of surface temperature posed by steady-state effects of inhomogeneity and three-dimensionality. Commercially available thermistor transducers, metering bridges, and borehole logging cables are adequate to construct systems with a sensitivity of a fraction of a mK. The two principal limitations to attaining the desired precision in the field are: 1) returning to the same measurement depths with adequate precision on relogging, and 2) controlling the random convection of the generally unstable fluid in the borehole. These problems are currently being addressed by a team at the U.S. Geological Survey in Menlo Park.

Remote sensing has become an important tool in many aspects of polar research (e.g., Hall and Martinec 1985, Epp and Matthews 1991); permafrost is no exception. Remote sensing has proven effective for relating vegetation and other terrain conditions to permafrost (e.g., Morrissey *et al.* 1986, Morrissey 1988, Belanger *et al.* 1990, Liang and Gu 1993, Peddle and Franklin 1993). Ground-penetrating radar is extremely useful for delineating permafrost distribution at local scales (Arcone *et al.* 1982, Doolittle *et al.* 1992), and should prove equally effective for monitoring areas with the potential for stability problems under conditions of general warming (Judge *et al.* 1991). As remote-sensing technology evolves, it is likely to increase in importance as a geocryological tool. Enhanced resolution from space-borne sensors, for example, may provide a means for observing large-scale mass movements or the degradation of near-surface permafrost in subarctic peatlands on a circumpolar

basis, rather than at the local or regional scales necessitated by the use of sequential aerial photography (Thie 1974).

Measurement Programs and Data Archives

As important as the contributions of individuals or small groups of investigators may be, maximum advantage can be made of technological advances only if the data derived from them are made available to the larger scientific community. Recent studies suggest strongly that to view climate change as operating primarily at low frequencies is overly simplistic (Bradley and Jones 1992, Stevens 1993; instead, integrated paleoclimatic evidence indicates that climate change operates at a variety of temporal and spatial scales, and that pronounced, regional oscillations take place at the decadal scale. The implications of these findings are profound for studies of permafrost, and underscore the critical need for integration of data, on a global basis.

Despite its importance to a large number of fields in basic and applied science, there has been little consensus about or attempts to achieve a coordinated, international implementation of field measurements of ground temperature. Records are extremely few in many parts of the circumpolar regions and standardization presents a formidable barrier to comparative or integrative studies of existing records. Given the very high levels of interest and concern about the amplification of global warming in the polar regions, it is imperative that an international measurement program be implemented on a global basis. A program of ground-temperature measurements is needed urgently, similar in scope to the ITEX (International Tundra Experiment) effort to monitor and evaluate the effects of climate warming on arctic biota (Molau 1992). A circumpolar network of ground-temperature stations, ideally at or near ITEX locations, will establish critical empirical linkages between air and ground temperature. Moreover, such a network can provide information about the nature, extent, and rate of thaw that will be necessary for realistic regional and global planning activities.

Much of the foregoing discussion centers on climate change, its detection, and the derivation of recent climate history from relatively deep boreholes in thick permafrost. There is an acute need to inventory borehole locations and archive the data from them. This review also draws attention to the shortage of observational data describing permafrost thawing or disappearance, and emphasizes the importance of the active layer for permafrost evolution under a warming climate. Detection and documentation of warming in the upper layers of permafrost, as well as changes in the active layer, are critical to the advancement of our knowledge about climate change itself, as well as the response of permafrost to it. Brennan and Barry's (1989, also see Barry and Brennan 1993) suggestions for programs to collect, standardize, and archive permafrost-related data, on an international basis, must be given high priority if we hope to obtain the background necessary to monitor changes in permafrost areas sensitive to climatic or anthropogenic disturbances. Only with an integrated, global database can adequate understanding be attained about the degradation of permafrost, its effects on geomorphic processes, and its potential to threaten the integrity of man-made structures and facilities.

Acknowledgments

The authors thank Drs. Jerry Brown and Roger Barry for helpful reviews of the manuscript.

REFERENCES

Agarwal, A. and S. Narain (1990). Global Warming in an Unequal World: A Case of Environmental Colonialism. Centre for Science and Environment, New Delhi.

An, W., Z. Wu, Y. Zhu, and A. Judge (1993). Influence of climate change on highway embankment stability and permafrost in the permafrost region of the Qinghai-Xizang Plateau. In Proceedings of the Sixth International Conference on Permafrost, Volume 1, 11-16. South China University of Technology Press, Wushan, Guangzhou, China.

Anisimov, O.A. (1989). Changing climate and permafrost distribution in the Soviet Arctic. Physical Geography 10(3), 285-293.

Arcone, S.A., P.V. Sellmann, and A.J. Delaney (1982). Radar detection of ice wedges in Alaska. CRREL Report 82-43, 15 pp.

Balobaev, V.T., V.N. Devyatkin, and I.M. Kutasov (1978). Contemporary geothermal conditions of the existence and development of permafrost. In Sanger, F.J., (ed.), Proceedings of the Second International Conference on Permafrost, USSR Contribution, 8-12. National Academy of Sciences, Washington, DC.

Barnes, P.W. (1990). Effects of elevated temperatures and rising sea level on arctic coasts. Journal of Cold Regions Engineering 4(1), 21-28.

Barry, R.G. (1985). Cryosphere and Climate Change. U.S. Department of Energy, Office of Energy Research, Office of Basic Energy Research, Washington, D.C., DOE\ER-0235.

Barry, R.G. and A.M. Brennan (1993). Sixth International Conference on Permafrost: Towards a permafrost information system. In Proceedings of the Sixth International Conference on Permafrost, Volume 1, 23-26. South China University of Technology Press, Wushan, Guangzhou, China.

Baulin, V.V. and N.S. Danilova (1984). Dynamics of Late Quaternary permafrost in Siberia. In Velichko, A.A., (ed.), Late Quaternary Environments of the Soviet Union, 69-77. University of Minnesota Press, Minneapolis.

Baulin, V.V., B. Belopukhova, and N.S. Danilova (1984). Holocene permafrost in the USSR. In Velichko, A.A., (ed.), Late Quaternary Environments of the Soviet Union, 87-91. University of Minnesota Press, Minneapolis.

Belanger, J.R., S.R. Dallimore, and P.A. Egginton (1990). Applications of thematic mapper thermal infrared imagery for permafrost and terrain studies, Richards Island, N.W.T. In Proceedings of the Fifth Canadian Permafrost Conference, 231-238. Centre d'etudes nordiques, Université Laval/National Research Council of Canada, Québec.

Bentley, C.R. and M.B. Geiovinetto (1991). Mass balance of Antarctica and sea level change. In Weller, G., C.L. Wilson, and B.A.B. Severin, (eds.), Proceedings, International Conference on the Role of the Polar Regions in Global Change, Volume II, 481-488. Geophysical Institute, University of Alaska, Fairbanks.

Billings, W.D. (1987). Carbon balance of Alaskan tundra and taiga ecosystems: past, present and future. Quaternary Science Reviews 6(2), 165-177.

Bonan, G.B., D. Pollard, and S.L. Thompson (1992). Effects of boreal forest vegetation on global climate. Nature 359, 716-718.

Boville, B.A. (1991). Sensitivity of simulated climate to model resolution. Journal of Climate 4(5), 469-485.

Bradley, R.D. and P.D. Jones (1992). Climate Since A.D. 1500. 679 pp. Routledge, Chapman & Hall, London.

Brennan, A.M. (1988). Permafrost Bibliography Update 1983-1987. Glaciological Data Report GD21. 225 pp. World Data Center A for Glaciology, Boulder, CO.

Brennan, A.M. (1993). Permafrost Bibliography Update 1988-92. Glaciological Data Report GD-26. World Data Center A for Glaciology, Boulder, CO.

Brennan, A.M. and R.G. Barry (1989). Ice Core Update 1980-1989. Permafrost Data Workshop. 127 pp. Glaciological Data Report GD-23, World Data Center for Glaciology, Boulder, CO.

Brown, J. (1992). A circumarctic map of permafrost and ground ice conditions. In Gilichinsky, D.A., (ed.), Proceedings, 1st International Conference on Cryopedology, 15-21. Pushino Research Centre, Pushino, Russia.

Budyko, M.I. and Y.A. Izrael (1987). Anthropogenic Climatic Change. 405 pp. Hydrometeoizdat, Leningrad, in Russian; English edition published by The University of Arizona Press, 1992.

Burn, C.R. and P.A. Friele (1989). Geomorphology, vegetation succession, soil characteristics and permafrost in retrogressive thaw slumps near Mayo, Yukon Territory. Arctic 42(1), 31-40.

Burn, C.R. and M.W. Smith (1993). Issues in Canadian permafrost research. Progress in Physical Geography 17, 156-172.

Burt, T.P. and P.J. Williams (1976). Hydraulic conductivity in frozen soils. Earth Surface Processes 1, 349-360.

Carter, L.D., J.A. Heginbottom, and M.-k. Woo (1987). Arctic lowlands. In Graf, W.L., (ed.), Geomorphic Systems of North America, Centennial Special Volume 2, 583-627. Geological Society of America, Boulder, CO.

Christensen, T.R. (1993). Methane emission from Arctic tundra. Biogeochemistry 21(2), 117-139.

Church, M. (1974). Hydrology and permafrost with reference to northern North America. In Proceedings, Workshop Seminar on Permafrost Hydrology, 7-20. Canadian National Committee, International Hydrological Decade, Ottawa.

Cicerone, R.J. and R.S. Oremland (1988). Biogeochemical aspects of atmospheric methane. Global Biogeochemical Cycles 2(4), 299-327.

Clow, G.D. (1992). The extent of temporal smearing in surface-temperature histories derived from borehole temperature measurements. Global and Planetary Change 6, 81-86.

Clow, G.D., A.H. Lachenbruch, and C.P. McKay (1991). Inversion of borehole temperature data for recent climatic changes: examples from the Alaskan arctic and antarctica. In Weller, G., C.L. Wilson, and B.A.B. Severin, (eds.), Proceedings, International Conference on the Role of the Polar Regions in Global Change, Volume II, 533. Geophysical Institute, University of Alaska, Fairbanks, AK.

Dingman, S.L., R.G. Barry, G. Weller, C. Benson, E.F. LeDrew, and C.W. Goodwin (1980). Climate, snow cover, microclimate, and hydrology. In Brown, J., P.C. Miller, L.L. Tieszen, and F.L. Bunnell, (eds.), An Arctic Ecosystem: the Coastal Tundra at Barrow, Alaska, 30-65. Hutchinson & Ross, Stroudsburg, PA.

Doolittle, J.A., M.A. Hardisky, and S. Black (1992). A ground-penetrating radar study of Goodream Palsas, Newfoundland, Canada. Arctic and Alpine Research 24(2), 173-178.

Epp, H. and S.B. Matthews (eds. 1991). Remote Sensing of Arctic Environments. Arctic 44(Supplement 1), 171 pp.

Evans, B.M., D.A. Walker, C.S. Benson, E.A. Nordstrand, and G.W. Peterson (1989). Spatial interrelationships between terrain, snow distribution and vegetation patterns at an Arctic foothills site in Alaska. Holarctic Ecology 12(3), 270-278.

van Everdingen, R.O. (1987). The importance of permafrost in the hydrological regime. Canadian Bulletin of Fisheries and Aquatic Sciences 215, 243-276.

Farouki, O.T. (1981). Thermal Properties of Soils. CRREL Monograph 81-1, 151 pp. U.S. Army Cold Regions Research and Engineering Laboratory, Hanover, NH.

French, H.M. (1986). Climate Change Impacts in the Canadian Arctic. Proceedings of a Canadian Climate Program Workshop, 3-5 March 1986. 171 pp. Environment Canada, Orillia, Ontario.

Gates, D.M. (1993). Climate Change and its Biological Consequences. 280 pp. Sinauer Associates, Sunderland, MA.

Gavrilova, M.K. (1993). Climate and permafrost. Permafrost and Periglacial Processes 4(2), 99-111.

Gersper, P.L., V. Alexander, S.A. Barkley, R.J. Barsdate, and P.S. Flint (1980). The soils and their nutrients. In Brown, J., P.C. Miller, L.L. Tieszen, and F.L. Bunnell, (eds.), An Arctic Ecosystem: The Coastal Tundra at Barrow, Alaska, 421-432. Dowden, Hutchinson & Ross, Stroudsburg, PA.

Gill, D. (1975). Influence of white spruce on permafrost-table microtopography, Mackenzie River Delta. Canadian Journal of Earth Sciences 12, 263-27?

Giorgi, F. and L.O. Mearns (1991). Approaches to the simulation of regional climate change: a review. Reviews of Geophysics 29(2), 191-216.

Goodrich, L.E. (1982). The influence of snow cover on the ground thermal regime. Canadian Geotechnical Journal 19, 421-432.

Grigoriev, M.N., I.V. Pozdniakov, and V.P. Romanov (1990). Cryogenic processes in ice complex ground caused by man-induced disturbance of the surface. In Ratsionalnoie prirodopolzovanie v kriolitozone, IMZ SO AN SSSR, Yakutsk.

Gross, M.F., M.A. Hardisky, J.A. Doolittle, and V. Klemas (1990). Relationships among depth to frozen soil, soil wetness, and vegetation type and biomass in tundra near Bethal, Alaska, U.S.A. Arctic and Alpine Research 22(3), 275-282.

Grotch, S.L. and M.C. MacCracken (1991). The use of general circulation models to predict regional climatic change. Journal of Climate 4(3), 286-303.

Gutowski, W.J.J., D.S. Gutzler, and W.-C. Wang (1991). Surface energy balances of three general circulation models: implications for simulating regional climate change. Journal of Climate 4(2), 121-134.

Haeberli, W. (1992). Possible effects of climatic change on the evolution of Alpine permafrost. In Boer, M.M. and E.A. Koster, (eds.), Greenhouse-Impact on Cold-Climate Ecosystems and Landscapes. Catena Supplement 22, 23-35. Catena Verlag, Cremlingen-Destedt, Germany.

Haeberli, W., Cheng Guodong, A.P. Gorbunov, and S.A. Harris (1993). Mountain permafrost and climatic change. Permafrost and Periglacial Processes 4(2), 165-174.

Hall, D.K. (1988). Assessment of polar change using satellite technology. Reviews of Geophysics 26(1), 26-39.

Hall, D.K. and J. Martinec (1985). Remote Sensing of Ice and Snow. 189 pp. Chapman and Hall, New York.

Hallet, B. (1978). Solute redistribution in freezing ground. In Proceedings of the Third International Conference on Permafrost, Volume 1, 85-91. National Research Council of Canada, Ottawa.

Harrison, W.D. (1991). Permafrost response to surface temperature change and its implications for the 40,000-year surface history at Prudhoe Bay. Journal of Geophysical Research 96B(2), 683-695.

Harriss, R.C., E. Gorham, D.I. Sebacher, K.B. Bartlett, and P.A. Flebbe (1985). Methane flux from northern peatlands. Nature 315, 652-654.

Heginbottom, J.A. and M.P. Sinclair (1985). Cumulative Index to Permafrost Conference Proceedings (1958-1983). 215 pp. Geological Survey of Canada Open File Report 1135, Ottawa.

Hewitson, B.C. and R.G. Crane (1992). Regional-scale climate prediction from the GISS GCM. Global and Planetary Change 97, 249-267.

Hinzman, L.D., D.L. Kane, R.E. Gieck, and K.R. Everett (1991). Hydrologic and thermal properties of the active layer in the Alaskan Arctic. Cold Regions Science and Technology 19(2), 95-110.

Houghton, J.T., G.J. Jenkins, and J.J. Ephraums (1990). Climate Change. The IPCC Scientific Assessment. 364 pp. Cambridge University Press, Cambridge.

IPA (1993). Resolution on permafrost and global climate change, approved at IPA Council Meeting, July 8, 1993, Beijing, China. Frozen Ground 14, in press.

Judge, A. and J.A. Majorowicz (1992). Geothermal conditions for gas hydrate stability in the Beaufort-Mackenzie area: the global change aspect. Global and Planetary Change 6(2/4), 251-263.

Judge, A.S., C.M. Tucker, J.A. Pilon, and B.J. Moorman (1991). Remote sensing of permafrost by ground-penetrating radar at two airports in Arctic Canada. Arctic 44(Supplement 1), 40-48.

Kahl, J.D., D.J. Charlevoix, N.A. Zaltseva, R.C. Schnell, and M.C. Serreze (1993). Absence of evidence for greenhouse warming over the Arctic Ocean in the past 40 years. Nature 361(6410), 335-337.

Kane, D.L., L.D. Hinzman, and J.P. Zarling (1991). Thermal response of the active layer to climatic warming in a permafrost environment. Cold Regions Science and Technology 19(2), 111-122.

Kane, D.L., L.D. Hinzman, M.-k. Woo, and K.R. Everett (1992). Arctic hydrology and climate change. In Chapin, F.S. III, R.L. Jefferies, J.F. Reynolds, G.R. Shaver, and J. Svoboda, (eds.), Arctic Ecosystems in a Changing Climate: an Ecophysiological Perspective, 35-57. Academic Press, San Diego.

Karl, T.R., W.-C. Wang, M.E. Schlesinger, R.W. Knight, and D. Portman (1990). A method of relating general circulation model simulated climate to the observed local climate. Part I: Seasonal statistics. Journal of Climate 3(10), 1053-1079.

Katz, D.L., D. Cornell, R. Kobayashi, F.H. Poettmann, J.A. Vary, J.R. Elenbass, and C.F. Weinaug (1959). Handbook of Natural Gas Engineering. 802 pp. McGraw-Hill, New York.

Kauppi, P. and M. Posch (1988). A case study of the effects of CO2-induced climatic warming on forest growth and teh forest sector. A. Productivity reactions of northern boreal forests. In Parry, M.L., T.R. Carter, and N.T. Konijn, (eds.), The Impact of Climatic Variations on Agriculture. Volume I. Assessments in Cool Temperate and Cold Regions, 183-195. Kluwer Academic, Dordrecht, The Netherlands.

Kolchugina, T.P. and T.S. Vinson (1993). Climate warming and the carbon cycle in the permafrost zone of the former Soviet Union. Permafrost and Periglacial Processes 4(3), 149-163.

Kondratjeva, K.A., S.F. Khrutzky, and N.N. Romanovsky (1993). Changes in the extent of permafrost in the late Quaternary period in the territory of the former Soviet Union. Permafrost and Periglacial Processes 4(2), 113-129.

Koster, E.A. (1991). Assessment of climate change impact in high-latitude regions. Terra 103, 3-13.

Koster, E.A. (1993a). Global warming and periglacial landscapes. In Roberts, N., (ed.), The Changing Global Environments, 127-149. Boston, Basil Blackwell.

Koster, E.A. (1993b). Introduction--present global change and permafrost, within the framework of the International Geosphere-Biosphere Programme. Permafrost and Periglacial Processes 4(2), 95-98.

Koster, E. and A. Judge (1994). Permafrost and Climatic Change: an Annotated Bibliography. in press pp. World Data Center A for Glaciology, Boulder, CO.

Koster, E.A. and M.E. Nieuwenhuijzen (1992). Permafrost response to climatic change. In Boer, M.M. and E.A. Koster, (eds.), Greenhouse-Impact on Cold-Climate Ecosystems and Landscapes. Catena Supplement 22, 37-58. Catena Verlag, Cremlingen-Destedt, Germany.

Kvenvolden, K.A. (1988). Methane hydrates and global climate. Global Biogeochemical Cycles 2(3), 221-229.

Kvenvolden, K.A. and T.D. Lorenson (1993). Methane in permafrost--preliminary results from coring at Fairbanks, Alaska. Chemosphere 26(1-4), 609-616.

Lachenbruch, A.H. (1957). Thermal effects of the ocean on permafrost. Geological Society of America Bulletin 68, 1515-1530.

Lachenbruch, A.H. (1959): Periodic heat flow in a stratified medium with application to permafrost problems. U.S. Geological Survey Bulletin 1083-A, 36 pp.

Lachenbruch, A.H. (1966). Contraction theory of ice-wedge polygons: a qualitative discussion. In Permafrost International Conference, 63-71. U.S. National Academy of Sciences-National Research Council 1287, Washington, D.C.

Lachenbruch, A.H. and B.V. Marshall (1986). Changing climate: geothermal evidence from permafrost in the Alaskan arctic. Science 234, 689-696.

Lachenbruch, A.H., J.H. Sass, B.V. Marshall, and T.H.J. Moses (1982). Permafrost, heat flow, and the geothermal regime at Prudhoe Bay, Alaska. Journal of Geophysical Research 87(11B), 9301-9316.

Lachenbruch, A.H., T.T. Cladouhos, and R.W. Saltus (1988a). Permafrost temperature and the changing climate. In Senneset, K., (ed.), Proceedings of the Fifth International Conference on Permafrost, Volume 3, 9-17. Tapir Publishers, Trondheim, Norway.

Lachenbruch, A.H., S.P.J. Galanis, and T.H.J. Moses (1988b). A thermal cross section for the permafrost and hydrate stability zones in the Kuparuk and Prudhoe Bay oil fields. U.S. Geological Survey Circular 1016, 48-51.

Lachenbruch, A.H., J.H. Sass, L.A. Lawver, M.C. Brewer, B.V. Marshall, R.J. Munroe, J.P. Kennelly, S.P.J. Galanis, and T.H.J. Moses (1988c). Temperature and depth of permafrost on the Arctic slope of Alaska. In Gryc, G., (ed.), Geology and Exploration of the National Petroleum Reserve in Alaska. U.S. Geological Survey Professional Paper 1399, 645-656.

Lafleur, P.M., W.R. Rouse, and D.W. Carlson (1992). Energy balance differences and hydrologic impacts across the northern treeline. International Journal of Climatology 12(2), 193-203.

Lavoie, C. and S. Payette (1992). Black Spruce growth forms as a record of a changing winter environment at treeline, Québec, Canada. Arctic and Alpine Research 24(1), 40-49.

Levine, M.D., J.A. Sathaye, and P.P. Craig (1992). Strategies for addressing climate change: policy perspectives from around the world. Energy 17(12), 1121-1136.

Lewkowicz, A.G. (1992). Factors influencing the distribution and initiation of active-layer detachment slides on Ellesmere Island, arctic Canada. In Dixon, J.C. and A.D. Abrahams, (eds.), Periglacial Geomorphology, 223-250. Wiley, New York.

Liang, F. and Z. Gu (1993). Application of remote sensing images to the investigations of the changes of permafrost environment in burned forest regions, Da Hinggan Ling, China. In Proceedings of the Sixth International Conference on Permafrost, Volume 1, 388-392. South China University of Technology Press, Wushan, Guangzhou, China.

Luken, J.O. and W.D. Billings (1983). Changes in bryophyte production associated with a thermokarst erosion cycle in a subarctic bog. Lindbergia 9, 163-168.

Lunardini, V.J. (1981). Heat Transfer in Cold Climates. 731 pp. Van Nostrand Reinhold, New York.

MacDonald, G.J. (1990). Role of methane clathrates in past and future climates. Climatic Change 16, 247-291.

Mackay, J.R. (1975). The stability of permafrost and recent climatic change in the Mackenzie Valley, N.W.T. Geological Survey of Canada Paper 75-1, Part B, 173-176.

Mackay, J.R. (1983). Downward water movement into frozen ground, western arctic coast, Canada. Canadian Journal of Earth Sciences 20, 120-134.

Mackay, J.R. (1986). Fifty years (1935 to 1985) of coastal retreat west of Tuktoyaktuk, District of Mackenzie. Geological Survey of Canada Paper 86-1A, 727-735.

Mackay, J.R. (1988). Pingo collapse and paleoclimatic reconstruction. Canadian Journal of Earth Sciences 25(4), 495-511.

Mackay, J.R. and J.V.J. Matthews (1983). Pleistocene ice and sand wedges, Hooper Island, Northwest Territories. Canadian Journal of Earth Sciences 20, 1087-1097.

Maxwell, J.B. (1992). Arctic climate: potential for change under global warming. In Chapin, F.S. III, R.L. Jefferies, J.F. Reynolds, G.R. Shaver, and J. Svoboda, (eds.), Arctic Ecosystems in a Changing Climate: an Ecophysiological Perspective, 11-34. Academic Press, San Diego.

Maxwell, J.B. and L.A. Barrie (1989). Atmospheric and climatic change in the Arctic and Antarctic. Ambio 1, 42-49.

McBeath, J.H. (1984). The Potential Effects of Carbon Dioxide-Induced Climatic Changes in Alaska, Proceedings of a Conference. 208 pp. School of Agriculture and Land Resources Management, University of Alaska, Miscellaneous Publication 83-1, Fairbanks.

McGaw, R.W., S.I. Outcalt, and E. Ng (1978). Thermal properties and regime of wet tundra soils at Barrow, Alaska. In Proceedings of the Third International Conference on Permafrost, Volume 1, 47-53. National Research Council of Canada, Ottawa.

Melnikov, P.I. and R.B. Street (1992). Terrestrial component of the cryosphere. In Tegart, W.J.McG. and G.W. Sheldon, (eds.), Climate Change 1992: the Supplementary Report to the IPCC Impacts Assessment, 94-102. Australian Government Publishing Service, Canberra.

Messner, W., D. Bray, G. Germain, and N. Stehr (1992). Climate change and social order; knowledge for action? Knowledge and Policy 5(4), 82-100.

Molau, U. (1992). ITEX Manual. 9 pp. Man and the Biosphere Program, Goetborg, Sweden.

von Moltke, K. (1989). International agreement to stabilize climate: lessons from the Montreal Protocol. Climatic Change 14, 211-212.

Monserud, R.A., N.M. Tchebakova, and R. Leemans (1993). Global vegetation change predicted by the modified Budyko model. Climatic Change 25(1), 59-83.

Moore, T.R. (1990a). Gas exchanges between peatlands and the atmosphere. Canadian Geographer 34, 86-87.

Moore, T. (1990b). Spatial and temporal variations of methane flux from subarctic/northern boreal fens. Global Biogeochemical Cycles 4(1), 29-46.

Moore, T.R. and R. Knowles (1987). Methane and carbon dioxide evolution from subarctic fens. Canadian Journal of Soil Science 67, 77-81.

Moore, T.R. and R. Knowles (1990). Methane emissions from fen, bog and swamp peatlands, Québec. Biogeochemistry 11, 45-61.

Moraes, F. and M.A.K. Khalil (1993). Permafrost methane content: 2. Modeling theory and results. Chemosphere 26(1-4), 595-607.

Morrissey, L.A. (1988). Predicting the occurrence of permafrost in the Alaskan discontinuous zone with satellite data. In Senneset, K., (ed.), Proceedings of the Fifth International Conference on Permafrost, Volume 1, 213-217. Tapir Publishers, Trondheim, Norway.

Morrissey, L.A. and G.P. Livingston (1992). Methane emissions from Alaska Arctic tundra: an assessment of local spatial variability. Journal of Geophysical Research 97(D15), 16,661-16,670.

Morrissey, L.A., L.L. Strong, and D.H. Card (1986). Mapping permafrost in the boreal forest with thematic mapper satellite data. Photogrammetric Engineering and Remote Sensing 52(9) 1513-1520.

Nakano, Y. and J. Brown (1972). Mathematical modeling and validation of the thermal regimes in tundra soils, Barrow, Alaska. Arctic and Alpine Research 4(1), 19-38.

Nakayama, T., T. Sone, and M. Fukuda (1993). Effects of climatic warming on the active layer. In Proceedings of the Sixth International Conference on Permafrost, Volume 1, 488-493. South China University of Technology Press, Wushan, Guangzhou, China.

Nelson, F.E. (1989). Permafrost in eastern Canada: a review of published maps. Physical Geography 10(3), 233-248.

Nelson, F.E. and O.A. Anisimov (1993). Permafrost zonation in Russia under anthropogenic climatic change. Permafrost and Periglacial Processes 4(3), 137-148.

Nelson, F.E. and S.I. Outcalt (1987). A computational method for prediction and regionalization of permafrost. Arctic and Alpine Research 19(3), 279-288.

Nelson, F.E., S.I. Outcalt, C.W. Goodwin, and K.M. Hinkel (1985). Diurnal thermal regime in a peat-covered palsa, Toolik Lake, Alaska. Arctic 38(4), 310-315.

Oechel, W.C. and W.D. Billings (1992). Effects of global change on the carbon balance of Arctic plants and ecosystems. In Chapin, F.S. III, R.L. Jefferies, J.F. Reynolds, G.R. Shaver, J. Svoboda, and E.W. Chu, (eds.), Arctic Ecosystems in a Changing Climate: an Ecophysiological Perspective, 139-168. Academic Press, San Diego.

Oechel, W.C., S.J. Hastings, G. Vourlitis, M. Jenkins, G. Riechers, and N. Grulke (1993). Recent change of Arctic tundra ecosystems from a net carbon sink to a source. Nature 361, 520-523.

Osterkamp, T.E. (1989). Occurrence and potential importance of saline permafrost in Alaska. In Proceedings of the Workshop on Saline Permafrost,, Winnepeg, Manitoba.

Osterkamp, T.E. and T. Fei (1993). Potential occurrence of permafrost and gas hydrates in the continental shelf near Lonely, Alaska. In Proceedings of the Sixth International Conference on Permafrost, Volume 1, 500-505. South China University of Technology Press, Wushan, Guangzhou, China.

Osterkamp, T.E. and J.P. Gosink (1991). Variations in permafrost thickness in response to changes in paleoclimate. Journal of Geophysical Research 96B(3), 4423-4434.

Outcalt, S.I., K.M. Hinkel, and F.E. Nelson (1992). Spectral signature of coupled flow in the refreezing active layer, northern Alaska. Physical Geography 13(3), 273-284.

Parker, R.L. (1977). Understanding inverse theory. Annual Review of Earth and Planetary Sciences 5, 35-64.

Peddle, D.R. and S.E. Franklin (1993). Classification of permafrost active layer depth from remotely sensed and topographic evidence. Remote Sensing of Environment 44(1), 67-80.

Pissart, A. (1990). Advances in periglacial geomorphology. Zeitschrift für Geomorphologie Supplementband 79, 119-131.

Rasmussen, R.A., M.A.K. Khalil, and F. Moraes (1993). Permafrost methane content: 1. Experimental data from sites in northern Alaska. Chemosphere 26(1-4), 591-594.

Riseborough, D.W. (1990). Soil latent heat as a filter of the climate signal in permafrost. In Proceedings of the Fifth Canadian Permafrost Conference, 199-205. Centre d'etudes nordiques, Université Laval/National Research Council of Canada, Québec.

Riseborough, D.W. and M.W. Smith (1993). Modelling permafrost response to climate change and climate variability. In Lunardinai, V.J. and S.L. Bowen, (eds.), Proceedings, Fourth International Symposium on Thermal Engineering & Science for Cold Regions, 179-187. US Army Cold Regions Research and Engineering Laboratory, Special Report 93-22, Hanover, NH.

Roots, E.F. (1989). Climate change: high latitude regions. Climatic Change 15(1/2), 223-253.

Rothman, D.S. and D. Chapman (1993). A critical analysis of climate change policy research. Contemporary Policy Issues 11(1), 88-98.

Rouse, W.R., P.F. Mills, and R.B. Stewart (1977). Evaporation in high latitudes. Water Resources Research 13, 909-914.

Schmitt, E. (1993). Global climatic change and some possible geomorphological and ecological effects in arctic permafrost environments, Isfjorden and Liefedefjorden, northern Spitsbergen. In Proceedings of the Sixth International Conference on Permafrost, Volume 1, 544-549. South China University of Technology Press, Wushan, Guangzhou, China.

Shaver, G.R., W.D. Billings, F.S. Chapin III, A.E. Giblin, K.J. Nadelhoffer, W.C. Oechel, and E.B. Rastetter (1992). Global change and the carbon balance of Arctic ecosystems. Bioscience 42, 433-441.

Slaughter, C.W. and R.J. Hartzmann (1993). Hydrologic and water quality characteristics of a degrading open-system pingo. In Proceedings of the Sixth International Conference on Permafrost, Volume 1, 574-579. South China University of Technology Press, Wushan, Guangzhou, China.

Slaughter, C.W., J.W. Hilgert, and E.H. Culp (1983). Summer streamflow and sediment yield from discontinuous permafrost headwater catchments. In Proceedings of the Fourth International Conference on Permafrost, Volume 1, 1172-1177. National Academy Press, Washington, DC.

Smith, M.W. and D.W. Riseborough (1983). Permafrost sensitivity to climatic change. In Proceedings of the Fourth International Conference on Permafrost, Volume I, 1178-1183. National Academy Press, Washington, D.C.

Solomatin, V.I. (1992). Geoecologia Severa. 270 pp. Izdatelstvo MGU, Moscow.

Solomon, A.M. (1986). Transient response of forests to CO2-induced climate change: simulation modeling experiments in eastern North America. Oecologia 68, 567-579.

Solomon, A.M. and H.H. Shugart (eds. 1993). Vegetation Dynamics & Global Change. 338 pp. Chapman & Hall, New York.

Soloviev, P.A. (1959). Kriolitozona severnoi chasti Leno-Amginskogo mezhdurechia. 144 pp. Izdatelstvo AN SSSR, Moscow.

Stevens, W.K. (1993). In new data on climate changes, decades, not centuries, count. The New York Times December 7, C4.

Street, R.B. and P.I. Melnikov (1990). Seasonal snow cover, ice and permafrost. In Tegart, W.J.McG., G.W. Sheldon, and D.C. Griffiths, (eds.), Climate Change. The IPCC Impacts Assessment, 7.1-7.33. Australian Government Publishing Service.

Stuart, A. (1986). The development of a spatial permafrost model for northern Canada and its application to scenarios of climate change. KelResearch Corporation, Downsview, Ontario.

Sugden, D. (1992). Global warming: Antarctic ice sheets at risk? Nature 359(6398), 775-776.

Thie, J. (1974). Distribution and thawing of permafrost in the southern part of the discontinuous zone in Manitoba. Arctic 27, 189-200.

Thomas, G. and P.R. Rowntree (1992). The boreal forests and climate. Quarterly Journal of the Royal Meteorology Society 118B(505), 469-497.

Timoney, K.P., G.H. La Roi, S.C. Zoltai, and A.L. Robinson (1992). The high subarctic forest-tundra of northwestern Canada: position, width, and vegetation gradients in relation to climate. Arctic 45(1), 1-9.

Torn, M.S. and F.S. Chapin III (1993). Environmental and biotic controls over methane flux from Arctic tundra. Chemosphere 26(1-4), 357-368.

Ulrich, R. and L. King (1993). Influence of mountain permafrost on construction in the Zugspitze Mountains, Bavarian Alps, Germany. In Proceedings of the Sixth International Conference on Permafrost, Volume 1, 625-630. Proceedings of the Sixth International Conference on Permafrost, Wushan, Guangzhou, China.

Vandenberghe, J. and A. Pissart (1993). Permafrost changes in Europe during the last glacial. Permafrost and Periglacial Processes 4(3), 121-135.

Vinson, T.S. and D.W. Hayley (1990). Global Warming and Climatic Change. Journal of Cold Regions Engineering 4, 73 pp.

Vourlitis, G.L., W.C. Oechel, S.J. Hstings, and M.A. Jenkins (1993). The effect of soil moisture and thaw depth on CH4 flux from wet coastal tundra ecosystems on the North Slope of Alaska. Chemosphere 26(1-4), 329-337.

Vyalov, S.S., A.S. Gerasimov, A.J. Zolotar', and S.M. Fotiev (1993). Ensuring structural stability and durability in permafrost ground areas at global warming of the Earth's climate. In Proceedings of the Sixth International Conference on Permafrost, Volume 1, 955-960. South China University of Technology Press, Wushan, Guangzhou, China.

Waelbroeck, C. (1993). Climate-soil processes in the presence of permafrost: a systems modelling approach. Ecological Modelling 69(3,4), 185-225.

Walsh, J.E. (1993). The elusive Arctic warming. Nature 361(6410), 300-301.

Wang, B. (1993). A numerical simulation of coastal retreat and permafrost conditions, Mackenzie Delta Region, Canada. In Proceedings of the Sixth International Conference on Permafrost, Volume 1, 664-669. South China University of Technology Press, Wushan, Guangzhou, China.

Weller, G. and B. Holmgren (1974). The microclimates of the Arctic tundra. Journal of Applied Meteorology 13, 854-862.

Whalen, S.C. and W.S. Reeburgh (1988). A methane flux time series for tundra environments. Global Biogeochemical Cycles 2, 399-410.

Williams, P.J. and M.W. Smith (1989). The Frozen Earth: Fundamentals of Geocryology. 306 pp. Cambridge University Press, New York.

Wirth, T.E. (1993). Developments in US Policy toward global climate change. US Department of State dispatch 4(22), 399.

Woo, M.-k. (1986). Permafrost hydrology in North America. Atmosphere-Ocean 24, 201-234.

Woo, M.-k. (1990). Consequences of climatic change for hydrology in permafrost zones. Journal of Cold Regions Engineering 4(1), 15-20.

Woo, M.-k. (1992). Impacts of climatic variability and change on Canadian wetlands. Canadian Water Resources Journal 17, 63-69.

Woo, M.-k, A.G. Lewkowicz, and W.R. Rouse (1992). Response of the Canadian permafrost environment to climatic change. Physical Geography 13(4), 287-317.

Yarie, J. and K. Van Cleve (1991). Changes in the source/sink relationships of the Alaskan boreal forest as a result of climatic warming. In Weller, G., C.L. Wilson, and B.A.B. Severin, (eds.), Proceedings, International Conference on the Role of the Polar Regions in Global Change, Volume II 436-439. Geophysical Institute, University of Alaska. Fairbanks, AK.

Zamolotchikova, S.A. (1988). Mean annual temperature of grounds in East Siberia. In Senneset, K., (ed.), Proceedings of the Fifth International Conference on Permafrost, 237-240. Tapir Publishers, Trondheim, Norway.

Zhang, T. and T.E. Osterkamp (1993). Changing climate and permafrost temperatures in the Alaskan Arctic. In Proceedings of the Sixth International Conference on Permafrost, Volume 1, 783-788. South China University of Technology Press, Wushan, Guangzhou, China.

Zoltai, S.C. and D.H. Vitt (1990). Holocene climatic change and the distribution of peatlands in western interior Canada. Quaternary Research 33(2), 231-240.

PRESENT HUMAN INDUCED CLIMATIC CHANGE AND CRYOECOLOGY

Maria K. Gavrilova

Permafrost Institute, Siberian Branch, Russian Academy of Sciences, Yakutsk, 677018, Russia

Permafrost is a consequence of cold climate. But the climate is not constant, it changes continuously. Until recently cryogenic processes were altering under effect of natural climate changability. Man's affect changing microclimate of locality has increased recently. Under large-scale activity it leads to catastrophes. A great danger may be caused by climate warming under atmosphere pollution. It will cause reinforcement of thermokarast phenomena.

INTRODUCTION

Climate of any place undergoes continuous change both short-term and long-term (Gavrilova, 1992 a). At present, man can not affect large-scale climate forming factors such as cosmic, astronomic, geological and others, but can only influence to some extent the geographic factors as the atmosphere transparency and terrain.

Predicted macroclimatic change resulting from human-induced atmospheric pollution and an increase in carbon dioxide content in the atmosphere in the future. Meanwhile, permafrost researchs are concerned about human-induced changes of a lower scale, i.e. meso-, micro- and nanoclimatic changes caused by terrain and surface disturbances.

CLIMATE AND NATURAL CRYOGENIC PHENOMENA

Permafrost is characterized not only by negative temperatures, but the presence of cementing frozen water ranging from microparticles to huge ice bodies as well. sharp temperature fluctuations and phase transitions of water give rise to cryogenic processes such as frost fracturing, frost heaving, ground ice melting, ground subsidence, thermokarst, thermal abrasion, thermal denudation, thermal erosion, solifluction, formation of open and closed taliks and others.

These processes are active under natural conditions, and they are associated with general climatic and other physico-geographical conditions. In recent years, it has been revealed that they follow a cyclic pattern coinciding with short-term (tens to hundreds of years) climate fluctuations. For example, during the years of heavy precipitation the rate of thermal erosion increases, and many new thermokarst lakes form, while during dry years the lakes degrade, taliks freeze below lakes, pingos form actively (Bosikov, 1990). During warmer periods ground water seepage and icing formation occur intensely. Cooling is accompanied by upward development of relief, while warming by downward development (Shpolianskaia, 1992).

Cyclical changes in cryogenic processes occur on a seasonally basis as well. For example, in areas of perennial freezing of ground, landslides are more active in fall (when frozen material have thawed), and in areas of seasonal freezing in spring after snow melting (Rosenbaum, Mudrov and Tumel, 1990). Intensified fracturing takes place from November to March, i.e. when air and surface temperatures are the lowest (Sukhodrovsky, 1969).

MICROCLIMATE AND ANTHROPOGENIC CRYOGENIC PHENOMENA

Under natural conditions the cryogenic processes take place slowly and in a smaller extent, and the rate of recovery is higher. Human activities cause acceleration of cryogenic processes, an increase in the area of adverse impacts, and the permafrost terrain very often loses its ability to recovery. A new geosystem forms, and permafrost may disappear in some areas.

Deforestation accompanying development of the region, removal of vegetation and snow cover, irrigation and drainage improvements cause significant changes in the heat and moisture balances both at the ground surface and in the upper layer of the ground. This can lead to local permafrost degradation or aggradation, especially in the island permafrost zone, for example, in the Baikal-Amur Railway Region.

Investigations on heat balance and microclimate show that deforestation results in intensification of seasonal thawing: in the North it is by a factor of 1.5, in Central Yakutia by a factor of 2, and in southern Siberia soils frozen in winter thaw entirely. In the North removal of the soil cover (as the forest litter) causes an addi-

tional increase under a disturbed surface freeze in winter more intensely. Observations in southern Yakutia show that if the moss and snow covers are removed, the upper soil temperatures are twice as small in winter (Gavrilova, 1977,1973, 1978).

The effects of human activities on permafrost depend on the scale and duration of the impact, as well as the climatic zone, terrain conditions, the nature of the warm and cold seasons, trends in naturally occuring processes. If human–induced and natural processes coincide in time, cryogenic processes intensify, if not, they may be weakened or even damped. On the whole, in cold Yakutia clearing of trees results in a lowering of the upper ground temperatures, while in warmer southern Siberia it causes permafrost to disappear in clear–cut areas.

CATASTROPHIC CONSEQUENCES OF MAN ACTIVITY IN THE CRYOLITHOZONE

In the permafrost areas, detrimental impacts of human activities become evident immediately. Deep impassable ruts and bogs formed along the paved roads in rural areas are the first evidences. If the early settlers of Siberia could simply displace the heaved gates and fences, nowadays, this can not be applied to large blocks of multi–storey buildings in cites and large settlements, requiring urgent maintenance measures.

Well–known Bykovsky fish–processing plant located in Arctic Yakutia, which supplied fish to the entire country during the second world war, will have to be abandoned within 10 years. The ice content of the ground under the Bykovsky settlement is 90%, the ice bodies are up to 10 m wide at the top, the thickness of a covering ground layer is only 0.6 to 1 m, average natural thaw depth is 0.6 m (Grigoriev, et al., 1990). Disturbance of the upper 5 to 15 cm moss and turf cover has initiated cryogenic processes. The rate of shore erosion is up to 10 m / yr.

Warm permafrost is particularly sensitive to landscape disturbance, as in western Siberia and the Far East. At exploratory drill sites in northern Chukotka active layer thickness increases by a factor of 2 to 3 as compared to adjacent undisturbed areas, when vegetational and soil cover are removed, and the thawed zone enlarges around (Kotov and Maslov, 1992). Funnel–shaped hollows form in the mouth of deep oil and gas exploratory boreholes caused by melting of blocks of ground ice.

Big towns generally favor the preservation of permafrost and even strengthen it due to the existence of an insulating "cultural layer" and shadowing effect of buildings. In the city of Yakutsk, at a depth of 10 m the ground temperatures lower to 4 to 5°C below zero during 4 to 5 years, if proper construction and maintenance approaches are used (Popenko et al., 1990).

Problems arise if construction is performed carelessly neglecting standards and codes for placing of foundations, construction materials are of poor quality, maintenance is made incorrectly, foundations are flooded by industrial and domestic waste. In Yakutsk, 40% of large–panel residential buildings require urgent repair measures, and 20% may collapse soon.

Settlements located in the permafrost zone are sources of chemical contamination of the environment (Makarov, 1992). Poor permeability of permafrost, small depth of thaw, low temperatures and other factors facilitate the decay of chemical substances. Concentrated solutions are transported by surface water contaminate huge areas. In some locations weak platic–frozen ground and taliks may develop. Salinized frozen ground erodes the concrete foundations. Contaminated frozen ground becomes an aggressive factor impeding man's activity.

There is increasing concern about construction of linear structures (railwayes, highways, pipelines, power transmission lines, irrigation channels, etc.). The reason is that during construction and maintenance not only the construction sites are disturbed, but adjacent areas as well. In many cases access roads have not been built in advance, and drainage facilities have been made poorly. It has resulted in deeper thawing, ground subsidence, thermal erosion, ground water seepage, icing, paludification and landslides.

for the Baikal–Amur Railway the maintenance costs have already exceeded the construction costs. Zones of thawed ground develop along oil and gas pipelines. In central Yakutia these zones are 0.75 to 1.5 m wide (Popov, 1992). Reclamation channels are highly susceptible, and when they are destroyed, it results in that agricultural lands become unusable because of water erosion of soils. The water in reclamation channels causes melting of ice resulting in depressions and in cave–ins, and water is discharged to the formed depressions. The bed of a channel made for basin irrigation in central Yakutia was designed to be 2 m wide 20 years later it is 10 to 20 m wide (Ugarov, 1992; Chang and Melkozerov, 1992).

Recently, drainage and irrigation improvements have been introduced in agricultural areas of Transbaikal, Yakutia and Chukotka because of dry climates there. These improvements have been applied to 8.5% of agricultural lands in central Yakutia. They have already resulted in gross production of fodder grass 15–18%, potatoes 80%, vegetables 100%. However, improper use of irrigation methods (excessive irrigation in particular) results in paludification, formation of depressions and cave–ins, heaving as the permafrost is impervious to water. One quater of reclaimed lands have already had to be abandoned. Restoration is required through filling of depressions, cutting of mounds and grading. More frequent cycles of irrigation with smaller amount of water have been recommended by the researchers of the Permafrost Institute to prevent water from reaching the ground ice table(Intensifikatsia..., 1988; Gavriliev, 1991). Construction of hydroelectric power plants exerts harmful influences on the environment (Bianov et al., 1992). Water reservoirs must impounded for power plants because the river discharge is not uniform throughout the year. However, forests and meadows are flooded, water quality deteriorates, hydrological and hydrogeological regimes change, earth materials are redeposited. Impounded water warms up the reservoir bed and shores.

The Vilui hydroelectric power plant was the first project on permafrost. The water impoundment lasted 7 years (1967–1973). In the first year the depth of thaw in the water reservoir bed increased to 5 m, in the second year 7 m, in the third year 8.5 m (Kamensky et al., 1973). At present, thickness of the thawed layer is 20 m (Kamensky and Olovin, 1990). Fifteen–year observations (1977–1989) show that the retreat rate of low ice content shores is 1 to 2 m / yr, that of ice–rich shores is 4 to 5 m / yr (Konstantinov, 1992).

The modification of shorelines in the Amguema hydroelectric power plant which is under construction in Chukotka has been

predicted to occur as following : during the first year of operation the upper 1.5 to 2 m layer of unconsolidated rocks will be subjected to thermal erosion, in 2–3 years ground ice will extensively melt, later the water reservoir will enlarge 5% due to thawing of permafrost; finally peat and moss cover will come to the surface that can cause damage to the power plant units(Tishin, 1990).

PREDICTED CLIMATE WARMING AND THERMOKARST

Nowadays mankind is concerned about predicted man–induced global climatic change (warming) related to atmospheric pollution resulting from industrial development. It is predicted that in the middle of the 21st century global air temperatures may rise by 3 ± 1.5°C (Antropogenie izmenenia klimata, 1987). Climatic warming is forecasted to be greater at high latitudes, i.e. in the permafrost zone (5 to 10°C per year) (Gavrilova, 1992 b). It is obvious that the earth surface and upper soil–ground will immediately response to these sharp changes. Cryogenic procesases will develop extensively as they are dependent upon both climatic conditions and local human–induced impacts (Kachurin, 1961; Shur, 1977; Romanovsky, 1977).

Thermokarst development has the following stages: melting of ground ice, formation of a depression, filling with water, thermal and physical impact of water, drainage of a lake, diminishing of a thermokarst feature.

Melting of ice may commence due either climatic warming or local disturbance of an insulating layer (vegetational and soil covers).

Evidences of relict thermokarst relief are found in western and eastern Siberia which developed 10 thousand years ago. It coincided in time with the period of Late Pleistocene temperature maximum. The second phase of intensive thermokarst development (of a smaller extent) took place 5 to 6 thousand years ago in central Yakutia (Yakutian temperature maximum) (Soloviev,1959) and 2.5 to 3 thousand years ago in western Siberia (Late Holocene warming) Geoecologia Severa, 1992). The thermokarst features that can be observed at present in central Yakutia are 200 to 300 years old, and those in western Siberia and Chukotka are 500 to 700 years old (Tomirdiaro, 1972). Although it is believed that during the past 300 to 400 years the climate (air temperatures) has not been changing, secular variations in humidity could have effect.

Thermokarst development depends on all climatic factors: cloud patterns (radiative heating), temperature (general heat background), precipitation (insulating effect of snowcover, water balance constituents), air humidity and winds (evaporation rate) and others (Efimov, 1950; Nemchinov, 1958; Soloviev, 1961).

Precipitation is a very important factor in development of thermokarst features and associated lakes. Precipitation changes on a alasses had less water during the periods of 1890–1900 and 1914 to 1947, while between these two periods they had relatively greater amount of water (Soloviev, 1961). Direct relationship with precipitation is found through meteorological research of precipitation variations (Gavrilova, 1987). Bosikov (1991) gives more detailed chronology of high and low water precipitation data as well.

Chigir (Geologia Severa, 1992) believs that forecasts of change in the cryogeosystem should take into account the combination of secular climatic sequences: warm and humid, warm and dry, cold and humid, cold and dry. The cryogenic processes will develop differently in different periods.

It is predicted that by the middle of the 21st century the amount of precipitation will increase at high latitudes (Antropogenie izmenenia Klimata, 1987).

CONCLUSION

Thus, if global climate does change significantly in future, the cryogenic processes will develop intensely, thermokarst in particular. Thermokarst development will be caused both by macroclimatic and microclimtic changes, i.e. global warming, increase in precipitation amount, and extensive human activities.

REFERENCES

Budyko, M. and Y.Izrael (1987). Antropogenie izmenenia klimata. 407 p. Gidrometeoizdat, Leningrad.

Bianov, G., M.Malyshev and I. Sergeev (1992). Ecological aspects of use of hydroenergy in the permafrost zone: Ratsionalnoie prirodopolzovanie v kriolitozone, 46–50 pp. Nauka, Moscow.

Bosikov, N.(1990). Changability of general humidity in the area and dynamics of cryogenic processes: Ratsioalnoie prirodopolzovanie v kriolitozone, 58 p. IMZ SO AN SSSR, Yakutsk.

Chang, R. and G. Melkozerov (1992). Peculiarities of structure and performance of reclamation channels in Yakutia: Ratsionalnoie prirodopolzovanie v kriolitozone, 86–92 pp. Nauka, Moscow.

Efimov, A.(1950). Development of thermokarst lakes in central Yakutia: Isledovanie Vechnoi Merzloty v Iakutskoi Respublike (Vol.2), 98–114 pp. Izdatelstvo AN SSSR, Moscow.

Gavrilova, M.(1973). Climate of central Yakutia (Klimat Tsentralnoi Iakutii). 2nd edition. 120 p. Knizhnoe izdatelstvo, Yakutsk.

Gavrilova, M. (1978). Climate and Perennial freezing of ground (Klimat i mnogoletnee promerzanie gornykh porod). 214 p. Nauka, Novosibirsk.

Gavrilova, M.(1987). Analysis of changes in natural climatic conditions in Yakutia to the beginning of the next century: Prirodnye uslovia osvaevaemykh regionov Sibiri, 146–159 pp. IMZ SO SSSR, Yakutsk.

Gavrilova, M.(1992 a). Impact of global climatic change on the permafrost zone: Ratsionalnoie prirodopolzovanie v kriolitozone, 4–8 pp. Nauka, Moscow.

Gavrilyev, p. (1991). Reclamation of permafrost areas in Yakutia (Melioratsia merzlotnykh zemel v Iakutii). 182 p. Nauka, Novosibirsk.

Solomatin, V.(1992). Geoecologia Severa (vvedenie v geokrioecologiu) (Northern geoecology. Introduction into geocryecology). 270 p. Izdatelstvo MGU, Moscow.

Grigoriev, M., I.Pozdniakov and V.Romanov (1990). Cryogenic processes in ice complex ground caused by man–induced disturbance of the surface: Ratsionalnoie prirodopolzovanie v kriolitozone, 60 p. IMZ SO RAN, Yakutsk.

Intensifikatsia kormoproizvodstva v zone reki Amgi. Recomendatsii (Intensification of production of fodder in the Amga River area) (1988). 40 p. Knizhnoie izdatelstvo, Yakutsk.

Kachurin, S. (1961). Thermokarst development in the USSR terri-

tory (Termokarst na territorii SSSR). 292 p. Izdatelstvo AN SSSR, Moscow.

Kamensky et al. (1973). Guide. North–western Yakutia (Putevoditel. Severo–Zapadnaia Iakutia). 45 p. IMZ SO AN SSSR , Yakutsk.

Kanmensky, R. and B. Olovin (1990). Changes in climatic and permafrost conditions in the zone of thermal impact from the large water reservoirs in the Far North: Ratsionalnoie prirodopolzovanie v kriolitozone, 20–21 pp. IMZ SO AN SSSR. Yakutsk.

Konstantinov, I.(1992). Shore erosion of the water reservoir of the Vilui hydroelectric power plant: Ratsionalnoie prirodopolzovanie v kriolitozone, 57–63 pp. Nauka, Moscow.

Kotov, A. and V. Maslov (1992). Man–induced changes in the permafrost zone of the Nizhneanadyr depression: Ratsionalnoie prirodopolzovanie v kriolitozone, 159–165 pp. Nauka, Moscow.

Makarov, V.(1992). Ecological–geochemical problems in the permafrost zone in Yakutia: Ratsionalnoie prirodopolzovanie v kriolitozone, 133–139 pp. Nauka, Moscow.

Nemchinov, A.(1958). Cyclical variations of water levels in lakes in central Yakutia: Nauchnie soobshenia Yakutskogo filiala AN SSSR (Vol.1), 30–37 pp. Knizhnoe izdatelstvo, Yakutsk.

Popenko, F., A. Petrov, and S. Petrova (1990). Man–induced impacts on frozen Quaternary deposits in Yakutsk:Ratsionalnoie prirodopolzovanie v kriolitozone, 96 p. IMZ SO AN SSSR, Yakutsk.

Popov, V. (1992). Examination of a gas pipeline laid in the area of ice wedges: Ratsionalnoie prirodopolzovanie v kriolitozone, 102–107 pp. Nauka, Moscow.

Romanovsky, N. (1977).Theory of thermokarst: Vestnik Moskovskogo Universiteta, seria geologia, No.1, 65–71 pp.

Rosenbaum, G, Y. mudrov and N.Tumel (1990). Effect of climatic change on solifluction: Ratsionalnoie prirodopolzovanie v kriolitozone, 12 p. IMZ SO AN SSSR, Yakutsk.

Shpolianskaia, N. (1992). The permafrost zone as an indicator of present climatic change (Western Siberia): Ratsionalnoie priodopolzovanie v kriolitozone, 30–35 pp. Nauka, Moscow.

Shur, Y. (1977). Thermokarst (Thermokarst). 81 p. Nedra, Moscow.

Soloviev, P. (1959). Permafrost in nothern part of the Lene–Amga interfluvial (Kriolitozona severnoi chasti Leno–Amginskogo mezhdurechia). 144 p. Izdatelstvo AN SSSR, Moscow.

Solviev, P. (1961). Cyclical variations of water content in the alass lakes in central Yakutia related to climatic fluctuations: Voprosy geografii Yakutii, 48–54 pp. Knizhnoe izdatelstvo, Yakutsk.

Sukhodrovsky, V.(1969). Present relief formation in central Yakutia: Voprosy geografii Yakutii (Vol.5), 148–159 pp. Knizhnoe izdatelstvo, Yakutsk.

Tishin, M. (1990). Prediction of shoreline modifications in the water reservoir of the Amguema hydroelectric power plant: Ratsionalnoie prirodopolzovanie v kriolitozone. 26 p. IMZ SO AN SSSR, Yakutsk.

Tomirdiaro, S. (1992). Permafrost and development of mountainous and lowland areas (Vechnaia merzlota i osvoenie gornykh stran i nizmennostei). 174 p. Magadan.

Ugarov, I.(1992). Methods of construction of irrigation channels in areas with ground ice occuring close to the surface: Ratsionalnoie prirodopolzovanie v Kriolitozone, 92–94 pp. Nauka, Moscow.

RECENT PERMAFROST DEGRADATION ALONG THE QINGHAI-TIBET HIGHWAY

Cheng Guodong*, Huang Xiaoming** and Kang Xingcheng*

*Lanzhou Institute of Glaciology and Geocryology,
Chinese Academy of Sciences, Lanzhou, China
**Northwest Institute of Chinese Railway Academy
of Sciences, Lanzhou, China

This paper presents some observation results of climatic change and the response of permafrost along the Qinghai-Tibet Highway during the last decades, and discusses a problem about the Qinghai-Tibet Plateau and initiation of climatic change.

Connecting Lhasa and Xining, the respective capitals of the Tibet Autonomous Region and Qinghai Province, the Qinghai-Tibet Highway traverses more than 560 km of high-altitude permafrost. Six meteorological stations are located along the highway; of these, Wudaoliang, Fenghuo Shan, and Tuotuohe are in the area of the plateau underlain by permafrost.

Instrumental records show a coincidence of trends in climatic changes between Xining in western China and those in eastern China and the rest of the globe (Fig.2). The worldwide warming that began in the 1880s reached a maximum in the 1940s (Zhang, 1976; Cheng, 1984). The instrumental records of five meteorological stations along the Qinghai-Tibet Highway show decreasing air temperatures during the 1960s, and a pronounced reversal of this trend in the 1970s. The only exception to this trend was the Wudaoliang station during the early 1980s (Fig.3), although the reasons for this situation are not understood at present.

PERMAFROST DEGRADATION ALONG THE QINGHAI-TIBET HIGHWAY

Evidence of permafrost degradation has been found in areas of both discontinuous and continuous permafrost in the vicinity of the highway. Temperature measurements and drillholes along the highway have demonstrated in many localities that near its lower altitudinal limit permafrost is separated from the active layer by a thawed layer (Wang 1993).

Another line of evidence in the region is a rise in the base of the permafrost. Ground temperature measurements from 1974 to 1989 in a borehole in the northern Jingxian valley at 4530 m shows the permafrost base rose 5 m in 15 years. The mean annual ground temperature at a depth of 20 m increased by 0.2~0.3°C during the same period (Table 2). Moreover, some permafrost bodies have disappeared entirely.

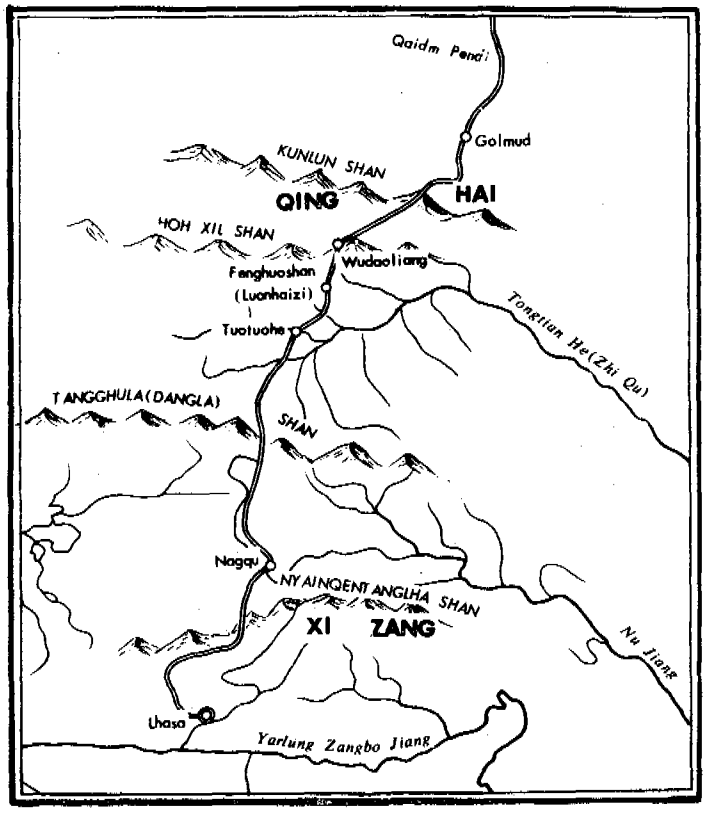

Fig.1 Locations of meteorological stations along the Qinghai-Tibet Highway

Table 1. Elevation of meteorological stations along the Qinghai-Tibet Highway

Station	Golmud	Wudaoliang	Fenghuo Shan	Tuotuohe	Nagqu	Lhasa
Elevation m, a.s.l.	2806	4780	4800	4700	4507	3658

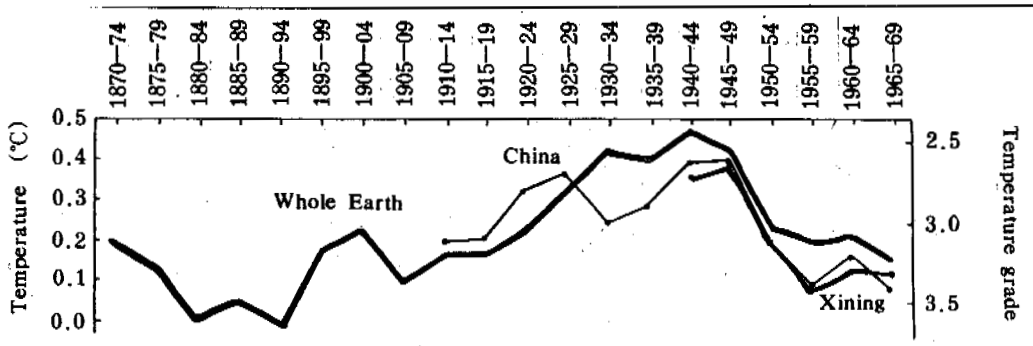

Fig.2 Comparison of average temperature changes since 1870 in the world and in Xining, China
Successive 5-year means expressed as departures from the means for 1880-84 in the whole world and successive 5-year means expressed as temperature grades in China (Modified from Zhang, 1976)

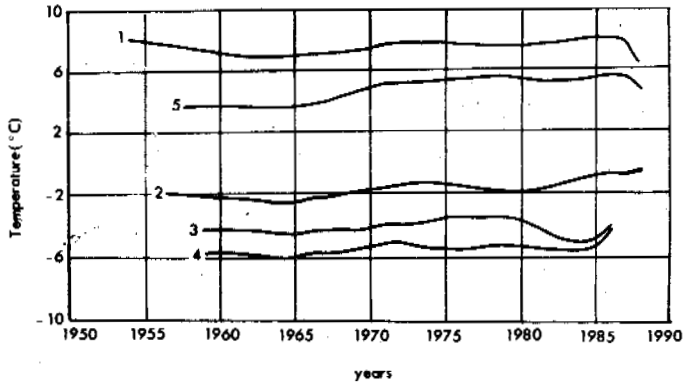

1. Lhasa 2. Nagqu 3. Wudaoliang 4. Tuotuohe 5. Golmud

Fig.3 5-year running mean curves of air temperature on the Qinghai-Tibet Plateau

Table 2. Rising of permafrost base at the north of Jingxian valley

Year	1974	1979	1985	1989
Depth of permafrost base (m)	15	14	12	10

(after Wang)

Ground temperature measurements from 1975 to 1989 in a borehole at 4670 m a.s.l. near Highway Maintenance Squad No.124, for example, illustrate the process of thinning and disappearance of permafrost near its former lower elevational limit (Table 3).

Areas of the Plateau underlain continuously by permafrost have also been affected by degradation. Fenghuo Shan station was established in 1961 by the Northwest Institute of Railways of the Academy of Sciences. Permafrost in this area attains thicknesses of about 100 m. Records from Fenghuo Shan show a warming trend in both air and ground temperatures. Between 1980 and 1992, mean annual temperature at a depth of 15 m increased by 0.2°C, by 0.4°C at 10 m, by 0.8°C at 5 m, and by 0.4°C at a depth of 3 m (Fig.4).

Ground temperature measurements in two other boreholes near Fenghuo Shan also illustrate the warming trend in permafrost in this area. Mean annual temperature at the 15 m level in a borehole on a south-facing slope increased by 0.1°C from 1982 to 1992 (Fig.5). At the corresponding depth is a borehole on a north-facing slope, mean annual temperature increased by a similar amount over a 28 year period (Fig.6).

Table 3. Ground temperature in borehole 124-4 (°C)

Time \ Depth (m)	1	2	3	4	5	6	7	8	11	15	19
79-08-05	0.6	-0.1	-0.3	-0.1	-0.2	-0.2	0	0.2	0.5	0.5	0.8
84-08-07	-0.2	-0.3	-0.3	-0.1	0.1	0.1	0	0.2	0.7	0.8	0.9
89-07-26	0.7	0.1	0.1	0	0.1	0.1	0.2	0.2	0.6	0.8	0.9

(after Wang)

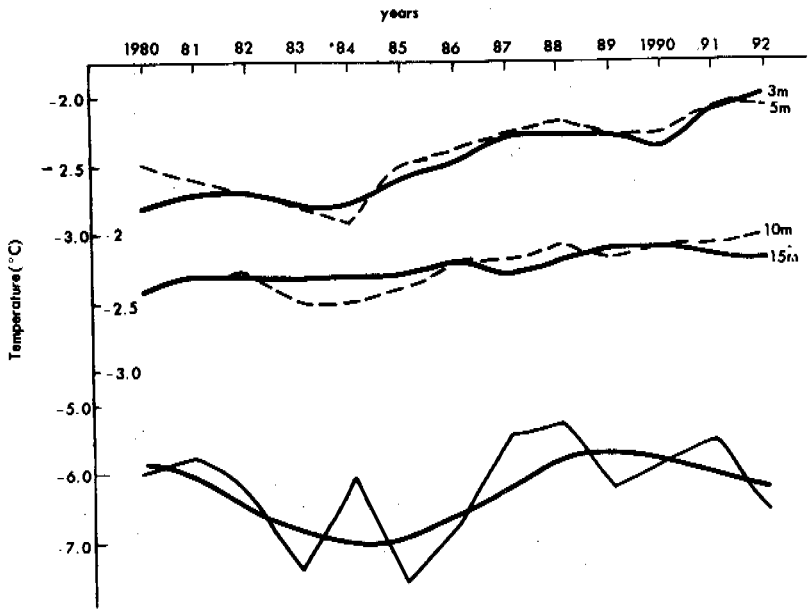

Fig.4 Mean annual air and ground temperatures at Fenghuo Shan Station

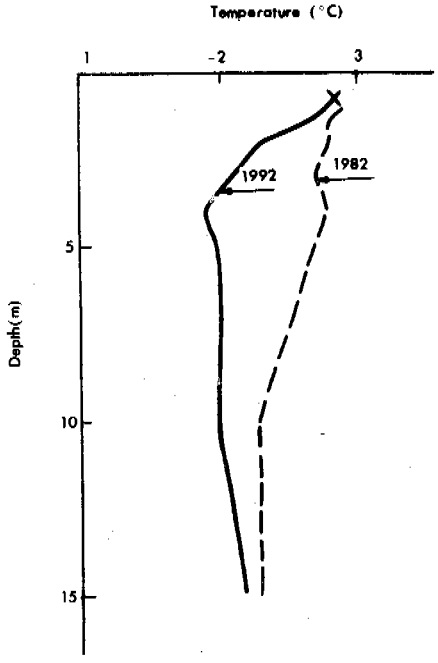

Fig.5 Mean annual ground temperature in 20 m deep borehole at Fenghuo Shan

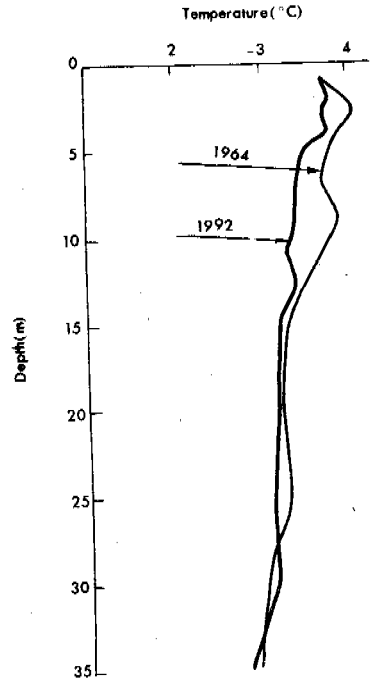

Fig.6 Mean annual ground temperature in 35 m deep borehole at Fenghuo Shan

QINGHAI-TIBET PLATEAU AND INITIATION OF CLIMATIC CHANGE

The warm and cold periods in eastern China, reconstructed for the last 500 years by means of phenology, are comparable to those obtained for the Qilian Mountains through dendroclimatological methods. Based on comparisons between eastern China and the Qilian Mountains (Table 4), the onset of both warm and cold periods averages 15 years earlier in the latter (Zhang et al., 1976, 1981; Cheng, 1984; Tang and Li, 1992).

The air-temperature grade of the Qinghai-Tibet Plateau and the warm-cold periods in the Qilian Mountains have been reconstructed, based on tree-ring data. Comparison between these data sets revealed that the relatively cold and warm periods in Tibet were about 10-40 years, on average about 30 years earlier than those in the Qilian Mountains (Fig.7). Accordingly, it has been suggested that the Qinghai-Tibet Plateau may be an important source region for climatic variations lasting 30-100 years (Tang and Li, 1992).

REFERENCES

Cheng Guodong, (1984) Study of climate change in the permafrost regions of China — A review in Final Proceedings of the 4th International Conference on Permafrost, National Academy Press, Washington, D.C., pp.139-144.

Tang Maocang and Li Cunqiang, (1992) An analysis on the Qinghai-Xizang Plateau as "a distrubing source region" for climatic changes, in Proceedings of the First Symposium on the Qinghai-Xizang Plateau, Science Press, pp.42-48.

Wang Shaoling, (1993) Permafrost changes along the Qinghai-Xizang Highway during the last decades, Arid Land Geography, Vol.16, No.1, pp.1-8.

Zhang Jiacheng et al., (1976) Climatic changes and causes, Science Press, Beijing, pp.288.

Zhang Xiangong, Zhao Qin and Xu Ruizhen, (1981) Tree rings in Qilian Shan and the trend of climatic change in China, in Proceedings of National Conference on Climatic Change, Science Press, Beijing, pp.26-35.

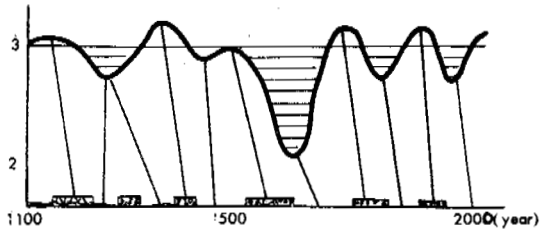

Fig.7 Comparison between the air temperature grade of the Qinghai-Tibet Plateau and the warm-cold periods in Qilian Mountains during the last thousand years (after Tang and Li)
black — warm period;
empty — cold period.

Table 4. Comparison of cold and warm periods between Qilian Mountains and east China

Period	East China (from phenology)	Qilian Mountains (from dendroclimatology)	Difference of median year
Cold	1470-1520 A.D.	1428-1537 A.D.	12
	1620-1720	1622-1740	-12
	1840-1890	1797-1870	31
	After 1945	after 1924	
Warm	1550-1600 A.D.	1538-1621 A.D.	-7
	1720-1830	1741-1796	6
	1916-1945	1871-1923	33

RESEARCH ON PERMAFROST AND PERIGLACIAL PROCESSES IN MOUNTAIN AREAS - STATUS AND PERSPECTIVES

Wilfried Haeberli

Laboratory of Hydraulics, Hydrology and Glaciology (VAW)
Swiss Federal Institute of Technology (ETH), Zurich-Switzerland

INTRODUCTION

During the past decades, intensified human activity together with the sensitive reaction of snow and ice to ongoing and potential future warming trends led to remarkably increased awareness not only concerning the scientific interest, beauty and vulnerability of cold mountain ranges but also with regard to environmental aspects, technical problems and natural hazards encountered in such remote areas. In view of this development, the *International Permafrost Association (IPA)* established a *working group on mountain permafrost* at the Fifth International Conference on Permafrost, held at Trondheim, Norway. Within the framework of this activity and in cooperation with the *IPA working group on periglacial environments*, international workshops were organized at Interlaken, Switzerland, in 1991 and at Calgary, Canada, in 1992. These workshops not only enabled exchange of experience among specialists from various parts of the world but also aimed at assessing the state of knowledge in the field and at formulating research recommendations as well as internationally co-ordinated projects for the future. The following text attempts at drawing the main conclusions from these reflections.

STATUS

A series of situation reports were compiled for the Interlaken workshop. In addition, a review on mountain permafrost and climatic change was written for the *IPA working group on present global change and permafrost* and discussed at the Interlaken workshop. These reports reflect a broad consensus among experts and actively involved scientists about especially important topics concerned. They can be summarized as follows:

Prospecting for mountain permafrost and mapping of associated phenomena (King et al. 1992) requires a combination of techniques to be applied. Direct investigations (drilling, digging), indirect (geophysical) soundings and measurements (seismic refraction, geoelectric resistivity, bottom temperatures of winter snow, or radar), natural indicator phenomena (perennial snow patches, cold springs emerging from snow-free areas, intact rock glaciers, push moraines s.s., specific vegetation patterns etc.) and computer simulations based on empirically calibrated algorithms and digital terrain information using Geographical Information Systems (Keller 1992) are most promising. The time of pure guessing with regard to the presence or absence of mountain permafrost and to its main characteristics (temperature, thickness, ice content) should now have definitely passed. Evidently, a minimum level of sophistication and funding is necessary for adequate research on permafrost and its relation to periglacial processes and phenomena in high mountain areas. The most urgent need concerns detailed quantitative information from core drilling and borehole measurements (cf., for instance, Vonder Mühll and Holub 1992).

The study of the *distribution of mountain permafrost and climate* (Cheng and Dramis 1992) first of all encounters difficult problems with definitions (where is the limit between "mountain" and "lowland" permafrost?) as well as with concepts of zonation or "beltation" (continuous - discontinuous - island - sporadic permafrost). Development of a common terminology would facilitate the discussion about global patterns of mountain permafrost distribution. Consideration of climatic parameters such as mean annual air temperature, freezing and thawing indices or solar radiation (cf., for instance, Hoelzle 1992) has been successful in at least half-quantitatively determining the influence of altitude, latitude and continentality on large-scale occurrence patterns and characteristics of mountain permafrost. However, continued research is needed to understand regional variability in more detail. In particular, the surface energy balance in mountain permafrost areas and active layer processes (especially advective energy fluxes involved with steeply inclined blocky surface layers) up to now essentially remain black boxes in our understanding and striking obstacles to scientific progress.

A considerable variety of field and laboratory investigations is being devoted to *processes and landforms in the periglacial mountain belt as related to seasonally and perennially frozen ground* (Lautridou et al. 1992). One special focus of interest concerns the chain of processes and forms linking mechanical weathering of rock walls, cliff recession, scree formation, and debris

displacement by solifluction, avalanches, debris flows and permafrost creep (cf. also Olyphant 1983). A special meeting held at Caen, France in 1991, devoted to problems of cryogenic weathering and organized under the auspices of the *IGU commission on frost action environments and the IPA working group on periglacial environments* illustrated the advantages of combining laboratory experiments with extensive field measurements and theoretical mödelling (cf., for instance, Matsuoka 1991). The model of crack propagation due to segregation ice growth in water-saturated rocks with interconnected cracks as proposed by Hallet et al. (1991) deserves special attention, especially with regard to the influence of permafrost conditions in bedrock walls. The corresponding effects relating to the continuous presence of ice in cracks at greater depth, the influence of long-term warming trends and the potential destabilization of heavily fissured rock masses in greater volumes remain to be investigated.

Thanks to a growing number of precise field measurements (drilling, geophysics, photogrammetry etc.), *permafrost creep on slopes and rock glacier formation* are now much better understood than a few decades ago (Barsch 1992). Perennial freezing and supersaturation in ice of non-consolidated materials such as talus, till or even anthropogenic deposits induces fundamental changes in their geotechnical properties by reducing internal friction between rock particles and by enabling large-scale stress transmission and cohesive flow behaviour according to the rheology of ice rather than to that of non-consolidated debris. Rock glaciers and push moraines s.s. as the landforms resulting from cumulative straining of perennially frozen sediment bodies are composite products of various interacting and competing processes involved with the build-up and transformation of talus or moraines by various slow and rapid processes. Inherent to the complex origin of such landforms with their manifold transitions and analogues is the fact that definitions and terminologies necessarily remain problematic. Emphasis should therefore rather be on the investigation of the thermal and rheological conditions involved with long-term preservation of ice underneath the surface and the creep mode of ice/rock mixtures (cf., for instance, Vonder Mühll and Haeberli 1990, Wagner 1992). Such an approach also has the potential of improving the paleoclimatic interpretation of relict features of permafrost creep (cf., for instance, Dramis and Kotarba 1992, Sollid and Sørbel 1992).

A great amount of work remains to be done in order to learn more about the complex *relations and interactions between mountain permafrost, glaciers, snow and water* (Harris and Corte 1992). The radical change of permeability at the permafrost table is a vital source of soil moisture in arid regions and greatly speeds up suprapermafrost runoff during snowmelt or liquid precipitation. Soil and active layer texture thereby plays an important role and also heavily influences conductive and advective fluxes of sensible as well as latent heat. The behaviour of intra- and subpermafrost water is best studied using tracer experiments, borehole observations (cf., for instance, Tenthorey 1992, Vonder Mühll 1992) and physico-chemical analyses of water-cycle components. The snow cover as one of these components is linked to mountain permafrost through especially close interactions involving thermal ground insulation during cold periods, reduced snow metamorphosis within and retarded spring runoff from the winter snowpack in permafrost areas as well as intense ground cooling by latent heat, snow emissivity and albedo effects during summer to fall (Keller and Gubler 1993). The relation between permafrost and glaciers is quite well understood in a general way and for static conditions (cryosphere schemes: maritime and continental climatic conditions) but detailed understanding of individual cases requires modelling of complex time-dependent flow and freeze/ thaw dynamics with full glacier/permafrost coupling - a challenge for the 21st century ?

Experience with *construction, environmental problems and natural hazards in periglacial mountain belts* grows but is still far from being adequate (Haeberli 1992). Systematic site investigation and design recommendations are needed for construction on perennially frozen ground of buildings, hydropower and transportation installations or protection work against floods, rockfalls and snow avalanches at high altitudes. Environmental aspects related to permafrost should be more thoroughly studied in connection with the preparation and maintenance of ski runs and the hazards from steep periglacial slopes must be more carefully considered. During the extraordinary floods in the Alps in summer 1987, the periglacial belt produced the largest sediment volumes eroded and displaced by debris flows. It is also noteworthy that the last three major rock fall events in the Alps all seem to have had some - still unexplained - connections with perennial ice in bedrock cracks (Val Pola/Valtellina, Italia 1987; Tschierva/Engadin, Switzerland 1988) or increased hydraulic conductivity in degrading permafrost (Randa/Matter Valley, Switzerland 1991). The thinking process concerning the effects of permafrost growth and degradation on steep slopes and rock walls needs to be intensified. On the Qinghai-Xizang Plateau, highway construction on relatively warm permafrost and the danger of increasing desertification with potential future warming and permafrost degradation are of greatest concern (cf. Guo and Zhao 1993).

The sensitivity of surface and subsurface ice with respect to atmospheric conditions together with the intensity of morphodynamic processes in rugged topography leads to strong *reactions of mountain permafrost to climatic change* (Haeberli et al. 1993a). The focus of interest is with the marked warming periods of the late Pleistocene and the 20th century as a basis for better understanding and realistically anticipating effects of potentially continued if not accelerated future warming due to anthropogenic greenhouse forcing. Combined glacier/permafrost studies have been quite successful in reconstructing regional patterns of

paleotemperature and paleoprecipitation during the late glacial transition from predominantly cold and dry to generally warmer and more humid conditions such as it appears to have been characteristic for many mountain ranges. Backward extrapolation of statistical relations between borehole temperatures in permafrost and meteorological parameters (air temperature, thickness of winter snow etc.) may help with assessing permafrost evolution in relation to 20th century warming and - for cases with supersaturated (low-permeability) permafrost - can be compared with analyses of borehole temperature profiles using heat conduction theory. It should thereby be kept in mind that both, the signals from and the effects on mountain permafrost, are highly relevant to studies of global warming trends, because they reflect 3-dimensional aspects (latitude/longitude/altitude) of cryosphere changes and concern one of the most heavily affected ecosystems on earth.

PERSPECTIVES

Decades of worldwide research in periglacial mountain belts have enabled the present state of knowledge to be developed. This tradition of high mountain research has long been predominantly directed at the most fascinating phenomena and at problems which could be addressed and treated by individuals, small research groups and modest instrumentation. The future potential for fast changes and extreme disequilibria in cold mountain areas, however, is a challenge which more and more requires detailed process studies concerning aspects and questions which have remained nearly untouched until recently. Scientific progress is now especially necessary in the fields of non-steady evolutions of and interactions between various components of the mountain environment like permafrost and snow, glaciers, groundwater or bedrock under conditions of changing surface energy balance. In addition to such process studies, international coordination and cooperation could be envisaged with regard to *mapping, modelling and monitoring* of mountain permafrost in order to reach a more complete view in space and time of present conditions and potential future developments. Corresponding research strategies first of all depend on the scale considered.

An overview at the scale of *hemispheres and continents* can be gained by compiling the existing literature and by applying climatic indices of large-scale permafrost occurrence such as mean annual air temperature in combination with altitude information and a simplified classification of vertical belts. A first step into this direction was made with the extensive discussion and intercomparison of mountain permafrost conditions during the field trips in the Alps and in the Alberta Rocky Mountains as connected to the IPA workshops at Interlaken and Calgary. Previously mentioned differences in relative extent of altitudinal permafrost belts (continuous, discontinuous, sporadic) were recognized to be first of all due to different definitions and terminology. In the Alpine sense of the term, a belt of discontinuous permafrost indeed extends over at least 600 meters and probably even more in the Alberta Rockies. Striking differences in nature, however, for the Alberta Rockies as compared with the Alps concern structural-geologic influences (predominance of bedded sedimentary rocks), the rarity of the meadow belt and the marked overlap between permafrost and forest areas. Attempts are presently being made at compiling a map of circumpolar permafrost distribution for the northern hemisphere, which also contains general information concerning the occurrence of low-latitude mountain permafrost. The three reviews on permafrost in mountain ranges of North America (Harris and Giardino 1993), Europe (King and Åkermann 1993) and Central Asia (Qiu 1993) prepared in connection with the present contribution for the same special session on mountain permafrost and periglacial processes within the framework of the VI International Conference on Permafrost are examples of such compilations. Based on earlier reviews (cf. for instance Cheng 1983, Corte 1988, Fuji and Higuchi 1978, Gorbunov 1978, Harris 1988) and newly available information, it should be possible to reach global coverage at a comparable level within the coming years.

The combination of mapping and modelling techniques should enable considerable progress to be made in the coming years at the scale of *individual mountain ranges and groups of mountains*. Spatial simulation of permafrost conditions by computer (GIS) models making use of digital terrain information should thereby be compared with maps and inventories of indicator phenomena such as intact rock glaciers, long-lasting snow, or suitable vegetation patterns. Concerning rock glaciers as permafrost indicators, not the origin of the ice but the thermal condition for preserving ice in the ground over long periods, i.e. perennially negative ground temperatures, constitute the essential point. Other potential indicator phenomena in permafrost-underlain peatland as well as the Kurums of Asian authors need more detailed investigation. The presently available empirical rules from the Alps for predicting permafrost distribution as a function of topography can only be applied to other mountain areas after transformation of the involved functions (aspect, altitude, snow/avalanche effects) according to large-scale variations in mean air temperature, solar radiation and precipitation regimes (effects of latitude and continentality). Systematic application and field testing of modified model versions for selected mountain ranges could help with adapting and further developing, i.e. generalizing the algorithms, which would then also serve as a key for simulating past and potential future changes as a response to climatic forcing. At the same time, models are to be developed and tested which more closely relate to physical processes, especially to the surface energy balance with its principal influencing parameters: solar radiation, temperature and snow (cf. Hoelzle et al. 1993).

The basis for such improved models is formed by detailed process studies, modelling of transient reactions and long-term monitoring at the scale of *small catchments and selected research sites*. At present, neither the climatic scenarios provided by General Circulation Models (GCMs) nor the present knowledge about mountain permafrost as a function of topography and microclimatic conditions enable any exact regional/local predictions to be made. Long-term measurements of the most important parameters involved (temperature, rheological properties, ice content, hydraulic permeability, frost heave and thaw settlement etc.) are therefore of high priority. The techniques (drilling, borehole observation, photogrammetry, semi-quantitative analysis of infrared aerial photography, runoff measurements etc.) for such long-term monitoring purposes are available today. Corresponding programmes have recently been initiated in some places (Haeberli et al. 1993b) but need internationally co-ordinated support and completion. Results from long-term monitoring - as they become available - can be used to calibrate models of transient response at individual points (for instance, heat conduction, melting and thaw settlement in material with variable ice content, etc.). Calculations for individual points can later be combined with spatial simulations of surface permafrost conditions in order to simulate typical transient effects at depth for extended areas. In a further step, such model simulations must be tested and further developed by applying appropriate sounding methods at characteristic sites indicated by model simulations. They could then hint at especially sensitive areas and help assessing the representativity of monitoring at a restricted number of sites. In fact, our state of knowledge and preparedness with regard to assessing and hopefully mitigating potential effects of realistic warming scenarios essentially depends on the establishment of adequate long-term monitoring programmes.

RECOMMENDATIONS AND ACKNOWLEDGEMENTS

Systematic international coordination and cooperation concerning permarost at high altitudes and in rugged topography should continue with emphasis on modelling, mapping and monitoring, especially in view of potential future warming effects. A concentrated knowledge transfer and inter-comparison project could be carried out in various mountain areas of the world with regard to the application of GIS-models using digital terrain information in combination with field mapping (rock glacier distribution, soil and spring temperatures, BTS soundings etc.) for simulating present-day, past and potential future permarost distribution patterns. In addition, co-ordinated planning of monitoring programmes (photogrammetry, borehole observations, surface energy balance etc.) should be stimulated and the short/long-term stability of supersaturated sediments on slopes (creep/ rock glaciers, thaw/ debris flows) be examined/modelled by applying modern sounding/computer techniques.

Thanks are due to the members of the *IPA working group on mountain permafrost* and to J.P. Lautridou, chairman of the *IPA working group on periglacial environments* as well as to the involved IPA council members for their most valuable and encouraging help and assistance during the first 5 years of working group activity. The members of the *IPA working group on mountain permafrost*, J.P. Lautridou and a number of friends and colleagues at VAW/ETH Zurich reviewd an early draft of the present report.

REFERENCES

Barsch, D. (1992): Permafrost creep and rockglaciers. Permafrost and Periglacial Processes 3, 3, p. 175 - 188.

Cheng, G. (1983): Vertical and horizontal zonation of high-altitude permafrost. Fourth International Conference on Permafrost, Fairbanks, Alaska/USA, Proceedings, p. 136 - 141.

Cheng, G. and Dramis, F. (1992): Distribution of mountain permafrost and climate. Permafrost and Periglacial Processes 3, 2, p. 83 - 91.

Corte, A.E. (1988): Geocryology of the central Andes and rock glaciers. Fifth International Conference on Permafrost, Trondheim, Norway, Proceedings 1, p. 718 - 723.

Dramis, F. and Kotarba, A. (1992): Southern limit of relict rock glaciers, Central Apennines, Italy. Permafrost and Periglacial Processes 3, 3, p. 257 - 260.

Fuji, Y. and Higuchi, K. (1978): Distribution of alpine permafrost in the northern hemisphere and its relation to air temperature. Third International Conference on Permafrost, Edmonton, Canada, Proceedings 1, p. 367 - 371.

Gorbunov, A.P. (1978): Permafrost investigation in high mountain regions. Arctic and Alpine Research 10, 2, p. 283 - 294.

Guo Dongxin and Huang Yizhi (1993): A guide to the permafrost and environment of the Qinghai-Xizang Plateau (field trip Lanzhou - Lhasa; July 11 - 22, 1993). Published by the Organizing Committee of the Sixth International Conference on Permafrost, 56p.

Haeberli, W. (1992): Construction, environmental problems and natural hazards in periglacial mountain belts. Permafrost and Periglacial Processes 3, 2, p. 111 - 124.

Haeberli, W., Cheng, G., Gorbunov, A.P. and Harris, S.A. (1993, a): Mountain permafrost and climatic change. Permafrost and Periglacial Processes 4, 2, p. 165 - 174.

Haeberli, W., Hoelzle, M., Keller, F., Schmid, W., Vonder Mühll, D. and Wagner, S. (1993,b): Monitoring the long-term evolution of mountain permafrost in the Swiss Alps. Sixth International Conference on Permafrost, Beijing, China, Proceedings 1, p. 214 - 219.

Hallet, B, Walder, J.S. and Stubbs, C.W. (1991): Weathering by segregation ice growth in micro cracks at sustained sub-zero temperatures: verification from an experimental study using acoustic emissions. Permafrost and Periglacial Processes 2, 4, p. 283 - 300.

Harris, S.A. (1988): The alpine periglacial zone. In: Clark, M.J. (ed.): Advances in Periglacial Geomorphology, Wiley, Chichester, p. 369 - 413.

Harris, S.A. and Corte, A. E. (1992): Interactions and relations between mountain permafrost, glaciers, snow and water. Permafrost and Periglacial Processes 3, 2, p. 103 - 110.

Harris, S.A. and Giardino, R. (1993): Permafrost in mountain ranges of North America. Sixth International Conference on Permafrost, Beijing, China, Proceedings 2 (present volume).

Hoelzle, M. (1992): Permafrost occurrence from BTS measurements and climatic parameters in the eastern Swiss Alps. Permafrost and Periglacial Processes 3, 2, p. 143 - 147.

Hoelzle, M., Haeberli, W. and Keller, F. (1993): Application of BTS measurements for modelling mountain permafrost distribution. Sixth International Conference on Permafrost, Beijing, China, Proceedings 1, p. 272 - 277.

Keller, F. (1992): Automated mapping of mountain permafrost using the program PERMAKART within the geographical information system ARC/INFO. Permafrost and Periglacial Processes 3, 2, p. 133 - 138.

Keller, F. and Gubler, H.U. (1993): Interaction between snow cover and high mountain permafrost at Murtèl/Corvatsch, Swiss Alps. Sixth International Conference on Permafrost, Beijing, China, Proceedings 1, p. 332 - 337.

King, L., Gorbunov, A. P. and Evin, M. (1992): Prospecting and mapping of mountain permafrost and associated phenomena. Permafrost and Periglacial Processes 3, 2, p. 73 - 81.

King, L. and Åkermann, H.J. (1993): Mountain permafrost in Europe. Sixth International Conference on Permafrost, Beijing, China, Proceedings 2 (present volume).

Lautridou, J.P., Francou, B. and Hall, K. (1992): Present-day periglacial processes and landforms in mountain areas. Permafrost and Periglacial Processes 3, 2, p. 93 - 101.

Matsuoka, N. (1991): A model of the rate of frost shattering: application to field data from Japan, Svalbard and Antarctica. Permafrost and Periglacial Processes 2, 4, p 271 - 281.

Olyphant, G.A. (1983): Computer simulation of rock glacier development under viscous and pseudoplastic flow. Geological Society of America Bulletin 94, p. 499 - 505.

Qiu, G. (1993): Mountain permafrost in central Asia. Sixth International Conference on Permafrost, Beijing, China, Proceedings 2 (present volume).

Sollid, J.L. and Sørbel, L. (1992): Rock glaciers in Svalbard and Norway. Permafrost and Periglacial Processes 3, 3, p. 215 - 220.

Tenthorey, G. (1992): Perennial névés and the hydrology of rock glaciers. Permafrost and Periglacial Processes 3, 3, p. 247 - 252.

Vonder Mühll, D. (1992): Evidence of intrapermafrost groundwater flow beneath an active rock glacier in the Swiss Alps. Permafrost and Periglacial Processes 3, 2, p. 169 - 173.

Vonder Mühll, D. and Haeberli, W. (1990): Thermal characteristics of the permafrost within an active rock glacier (Murtèl/ Corvatsch, Grisons, Swiss Alps). Journal of Glaciology 36, 123, p. 151 - 158.

Vonder Mühll, D. and Holub, P. (1992): Borehole logging in Alpine permafrost, Upper Engadin, Swiss Alps. Permafrost and Periglacial Processes 3, 2, p. 125 - 132.

Wagner, S. (1992): Creep of Alpine permafrost, investigated on the Murtèl rock glacier. Permafrost and Periglacial Processes 3, 2, p. 157 - 162.

PERMAFROST IN THE MOUNTAIN RANGES OF NORTH AMERICA

Stuart A. Harris

Department of Geography, University of Calgary
Calgary, Alberta, Canada T2N 1N4

John R. Giardino
Departments of Geography and Geology
Texas A & M University, College Station, TX 77843, USA

Mountain permafrost extends along the Western Cordillera of North America from the Arctic Ocean south to Mexico. It also occurs along the lower coastal mountains in eastern North America as far south as the Gaspé Peninsula, where warm tropical air and the effect of the Gulf Stream combine to keep the ground warm. Coldest ground temperatures (-10° to -20°C) and thickest permafrost occur in the Queen Elizabeth Islands. Most is post-glacial and the greater permafrost distribution in the western mountains is due to their greater altitude, the proximity to the cold Arctic air masses in winter, cold air drainage, rain shadow effects and chinook winds causing thin winter snow covers on the eastern side of the Cordillera. Climatic warming may be occurring on the Prairies, but the upper mountain slopes are generally not showing warmer air temperatures in this Continental and Subcontinental climate. Instead, it seems likely that major shifts in air mass distribution may be necessary to alter these mountain climates. In the mountains of eastern Canada, there is evidence for degradation of permafrost.

INTRODUCTION

Pioneer work was carried out in Canada by Brown (1967, 1978), in Alaska by Ferrians (1965), and in the contiguous United States by Péwé (1983). The altitudinal distribution in the Eastern Cordillera was described by Harris (1986), and more recently Heginbottom and Dubreuil (1993) have assembled the currently available data for the most recent permafrost and ground ice map for the National Atlas of Canada and for the Circumarctic map of permafrost and ground ice conditions (Brown et al., 1993). This report is based largely on these sources.

DISTRIBUTION

The mountain permafrost areas extend along the eastern and western margins of North America, from the Queen Elizabeth Islands in the north, south to Mexico, where permafrost occurs above about 4500 m (Péwé, 1983; Heine, personal communication, 1993) on the tops of volcanoes. In the north, these areas grade into polar permafrost at low elevations, but in the western sub-Arctic south of the Brooks Range and south-Central Yukon, they become discontinuous to sporadic, and are limited to the higher mountain ranges when mapped at a small scale (e.g., Harris & Brown, 1982; Heginbottom & Dubreuil, 1993; Brown et al., 1993). The tectonically active, young mountains form a broad belt. The lower limits for continuous (>80% of the landscape underlain by permafrost), discontinuous (30-80% underlain by permafrost) and sporadic permafrost (<30%) generally rise southwards along the Eastern Cordillera of Canada and the contiguous United States (Harris, 1986). Because the mountain tops become progressively higher in elevation southwards to the Colorado-New Mexico border, mountain permafrost can be found through a very wide range of latitude and on into Mexico.

Permafrost also occurs in the mountains along the eastern rim of the Arctic Islands and down along these mountains to the Gaspé, where it occurs sporadically on mountain tops under alpine tundra vegetation (Gray & Brown, 1982). It disappears in New England as a result of the influence of the Gulf Stream and tropical air masses from the Caribbean. These mountains are lower and geologically older, but are still quite rugged and tectonically active in various sections.

CHARACTERISTICS

In the Queen Elizabeth Islands, near-surface permafrost temperatures range between -10° and -20°C, and the permafrost is thick. Ground ice contents are highly variable and closely related to the nature of the bedrock. The permafrost is post-glacial in the surficial glacial sediments, but may be relict in older materials, including massive icy beds, some of which may represent buried glacial ice (e.g., Lorrain & Demeur, 1985; French & Harry, 1990) or other surface ice (e.g., snowbanks). Permafrost existence beneath the former ice sheets and basal ice temperatures of -17°C are common today.

In the Eastern Arctic Islands, the mountains contain permafrost with mean annual ground temperatures ranging from -2°C to -12°C beneath the alpine tundra vegetation. Ground ice appears to be of limited extent except in peatlands.

In the Cordilleran of northwestern North America, conditions vary with topography, latitude, proximity to the Arctic air masses and to the Pacific air masses. Along the Arctic coast, mean annual ground temperatures are -4°C to -10°C, but these increase to -1°C to -4°C southwards in central Yukon and in the central Alaska Range. Permafrost occurs only on the eastern side and on the tops of the coastal mountains around the north Pacific Ocean. At Mount Garibaldi (near Vancouver) it is limited to the mountain tops. Ice contents can be high near the Arctic coast and southwards along in the eastern Cordillera through the Yukon Territory, although they are highly variable and generally decrease southwards. Sufficient interstitial ice occurs in sediments on block slopes to generate active rock glaciers as far south as southwestern Alberta, and these can also be found locally on high mountain peaks as far south as Mexico. Apart from these cases, ice contents tend to be less than 10% by volume south of the Yukon Territory.

Mean annual ground temperatures are appreciably warmer along the eastern rim of the Arctic Islands and down to the Gaspé, as a result of the higher snowfalls east of Hudson Bay. Ground ice content is variable, but generally low.

Where the mean annual ground temperatures are above -3°C, there tends to be a marked effect of aspect on permafrost distribution which increases inversely with latitude in Canada. Most of the permafrost is post-glacial because most of the area of present-day mountain permafrost was covered by Late Wisconsin ice. Relict permafrost from colder glacial climates has only been demonstrated on Plateau Mountain, southwest Alberta (Harris & Brown, 1982), which was a nunatak.

CLIMATIC PROCESSES

Mountain permafrost areas exist because the microclimate permits sufficient heat removal from the ground surface for part of the ground to remain below 0°C for more than two consecutive years. Basic climatic factors

favouring its formation include low winter snow cover, high winds removing the snow cover above tree line, proximity to cold Arctic air masses for long periods of time in winter, maritime temperate air masses in summer (not tropical air masses), and cold air drainage. The Canadian Cordillera is characterized by rain shadow areas in the lee of the coastal mountain ranges with chinook winds that remove much of the winter snow cover by ablation. The further east and north the area is, the greater the frequency of cold Arctic air masses in winter. Permafrost occurs in two situations, viz., altitudinal permafrost on the upper slopes of the mountains resulting from the cooler temperatures at higher elevation, and at the foot of mountain ranges because of cold air drainage (e.g., Harris, 1982). The latter process extends southwards at least as far as southwest Alberta, where it has become more prevalent in the last eight years. Heavy snow accumulations on the slopes of mountain ranges facing Pacific coast winds tend to result in a high elevation for the lowest level of permafrost westwards across the Cordillera in British Columbia as the climatic regime changes from subcontinental to maritime.

Further north, cold air drainage and prevalence of cold Arctic air in winter result in far lower ground temperatures at a given elevation, culminating in the conditions on the Queen Elizabeth and Ellesmere Islands, where mean annual air temperature can be as low as -20°C. Summers are short and cool. This is a continental permafrost climate.

Southwards in the Cordillera, permafrost occurs most frequently on the east and north-facing slopes of the highest mountains where snowfall is reduced or the snow cover is removed by high winds. The main occurrences are along the eastern Cordillera, although ice caves can be found in the coastal ranges as far south as northern California.

Along the east coast of North America, the higher precipitation tends to reduce the frequency of permafrost at a given elevation and latitude in spite of the proximity of the mountains to a cold sea current. The occurrences of permafrost end abruptly where the coastal mountains are adjacent to the warm Gulf Stream drift, and where the maritime Tropical air masses penetrate from the Caribbean.

LANDFORMS

In areas not dominated by glaciers, e.g., Ellesmere Island, mountain permafrost regions can be divided into three groups, viz.: those dominated by active rock glaciers, by active block streams and by solifluction/gelifluction landforms. The areas with active block streams are mainly limited to the northeast Yukon Territory, which has a suitable combination of low precipitation and intense winter cold. These landforms are associated with active ice wedges and open system pingos, as well as massive ground ice in the valley floors. Spectacular icings (Lauriol et al., 1991) and seasonal frost mounds (Leffingwell, 1919; van Everdingen, 1978, 1982) may occur at the base of slopes.

From east-central Yukon Territory and the Brooks Range southwards to southwest Alberta and southeast British Columbia, the Cordillera exhibits abundant active rock glaciers. The climate is moist and cold enough to provide the interstitial ice necessary for the formation of near-slope rock glaciers. In the southwest Yukon Territory and Central Alaska, these are associated with open system pingos at the foot of slopes. Eastwards at this latitude, extensive thick peat deposits have formed on the valley floors and exhibit palsas and peat plateaus. Although the pingos are confined to the area north of the 60th parallel, palsas and peat plateaus can also be found in the northern parts of British Columbia and Alberta. Degrading ice wedges occur in south-central Alaska and Yukon, but active ice wedges have been reported from Mayo (Burn, 1990) and certainly occur to the north. Ice caves are present from Old Crow southwards.

South of Kananaskis Lakes in Alberta, the landscape of active rock glaciers is replaced by one with gelifluction and solifluction forms, together with felsenmeer and block slopes, on the lower part of the mountains. Active rock glaciers occur in the moister, cold climates near mountain tops. Patterned ground is common in the block fields, but peaty permafrost landforms are rare. Ice caves are common in areas of thin surficial deposits over limestones, dolomites, or volcanic rocks.

In eastern Canada, rock glacier-dominated mountains are normal, although the shorter time since deglaciation and massive bedrock limits their development in eastern Quebec and Labrador. They are associated with occasional palsas, patterned ground and ice wedges.

EFFECTS OF CLIMATIC CHANGES

From the discussion on climatic processes, it is obvious that any changes in climate may greatly alter the permafrost distribution in the mountains of North America. There is good evidence for permafrost being formed on the higher parts of the Appalachian Mountains since the last glaciation (Clark & Schmidlin, 1992), whereas similar evidence can be found in the Cordillera from Mexico north through New Mexico, Arizona (e.g., Blagbrough & Farkas, 1968; Barsch & Updike, 1971) and Colorado (Giardino, 1983) to Alberta and British Columbia. Thus, in Banff National Park, inactive near-slope rock glaciers can be found along the Bow River valley at an elevation 600 m below the present-day regional permafrost limit. Similar occurrences can be found in Jasper National Park, so there must have been some very profound changes in climate producing a markedly different distribution of mountain permafrost in post-glacial times both in eastern and western North America.

Further north around Fairbanks, Westgate et al. (1990) have shown that permafrost landforms have developed periodically for over 3 Ma B.P. The first dated evidence for cold conditions in British Columbia is 3.5 Ma from Wells-Gray National Park (Hickson & Souther, 1984), which agrees with the evidence from Patagonia (see Corte, 1991). In Central Yukon, periglacial features date to at least 2.5 Ma in non-glacial sediments at Old Crow. Cold conditions first developed on the rising high mountains of the St. Elias Range as early as Miocene times (Armentrout, 1984), but appear to have mainly caused alpine glaciation, although some permafrost conditions may have also been developed in nunataks at high altitudes.

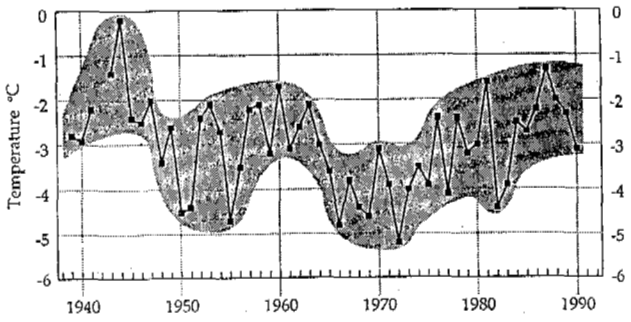

Fig. 1. Variation in mean annual air temperature at Watson Lake between 1939 and 1990 (based on AES, Monthly).

Figure 1 shows that the so-called "climatic change" of the last decade which is regarded as being the result of an increase in carbon dioxide, has not yet produced mean annual air temperatures outside the extremes measured during the last 50 years in central and southern Yukon Territory (Wahl et al., 1987; Harris & Schmidt, 1993). Similarly in southwest Alberta, the only mountain weather station at a permafrost site showing an appreciable rise in mean annual air temperature is Marmot Basin #1 near Jasper. The others show greater variability and frequency of major cold air drainage events, but no major overall change.

In contrast, there is evidence for warming at the few lowland weather stations along the Mackenzie River valley in the Arctic, but data from mountain sites in this area are lacking. This warming trend is also seen in data recorded since 1970 from the Plains region of Alberta. It is quite obvious that if a major change in mean annual air temperature occurred in the mountains, there would be adjustments in the distribution of mountain permafrost, as is occurring presently at Marmot Basin, but it would seem

that the mountain climates of western North America are not reacting to the perceived climatic change inferred from nearby lowland stations. This may mean that whereas major changes could occur in permafrost distribution at lowland sites, the distribution of mountain permafrost may remain largely the same as at present. It seems likely that major shifts in air mass distribution may be needed to alter the subcontinental and continental mountain permafrost climates. The different air masses would generate a new pattern of winds which would produce a different pattern of ocean currents, and together these would have a profound effect on the climate of the coastal mountains.

Along the east coast, the evidence for climatic change in the mountains is lacking, but there is strong evidence for a climatic change that has been occurring in the last few decades in western and central Quebec, where palsas are degrading near the southern limit of permafrost. Features interpreted as ice-wedge casts in post-glacial sediments have been reported from the St. Lawrence Lowlands, so there is evidence for substantial Holocene climatic change in this area as well.

Thus, the occurrence of permafrost appears to be complex, and numerous environmental variables are responsible for controlling its location. Whereas the numerous variables controlling permafrost development are known and understood, the relations between the various variables are problematic at best.

REFERENCES

AES, Monthly. Monthly Record. Environment Canada, Atmospheric Environment Service, Toronto.

Armentrout, J. M. (1984) Recalibration of Miocene molluscan stages and consequent recorrelation of Alaskan formations. Geological Society of America Abstracts with Programs 15(5), 267.

Barsch, D. and R. G. Updike (1971) Periglaziale Formung am Kendick Peak in Nord-Arizona während der letzten Kaltzeit. Geographische Helvetica 3, 99-114.

Blagbrough, J. W. and S. E. Farkas (1968) Rock glaciers in the San Mateo Mountains, south-central New Mexico. American Journal of Science 266, 812-823.

Brown, J., O. J. Ferrians, Jr., J. A. Heginbottom and E. S. Melnikov (1993) Circumarctic map of permafrost and ground ice conditions. Proceedings, 6th International Permafrost Conference, Beijing.

Brown, R. J. E. (1967) Permafrost Map of Canada. National Research Council, Building Research Division, NRC #9767, and Geological Survey of Canada, Map 1246A.

Brown, R. J. E. (1978) Permafrost. Plate 32 in: Hydrological Atlas of Canada, Ottawa. Fisheries and Environment, Canada. 34 Plates.

Burn, C. R. (1990) Implications for palaeoenvironmental reconstruction of Recent ice-wedge development at Mayo, Yukon Territory. Permafrost & Periglacial Processes 1, 3-14.

Clark, G. M. and T. W. Schmidlin (1992) Alpine periglacial landforms of eastern North America: A review. Permafrost & Periglacial Processes 3, 225-230.

Corte, A. E. (1991) Chronostratigraphic correlations of cryogenic and glacigenic episodes in Central Andes with Patagonia. Permafrost & Periglacial Processes 2, 67-70.

Ferrians, O. J., Jr. (1965) Permafrost Map of Alaska. United States Geological Survey Miscellaneous Geological Inventory Map 1-445. Scale 1:2,500,000.

French, H. M. and D. G. Harry (1990) Observations on buried glacier ice and massive segregated ice, Western Arctic Coast, Canada. Permafrost & Periglacial Processes 1, 31-43.

Giardino, J. R. (1983) Movement of ice-cemented rock glaciers by hydrostatic pressure: An example from Mount Mestas, Colorado. Zeitschrift für Geomorphologie 27, 297-310.

Gray, J. T. and R. J. E. Brown (1982) The influence of terrain factors on the distribution of permafrost bodies in the Chic-Choc Mountains, Gaspésie, Quebec. Proceedings, 4th Canadian Permafrost Conference, Calgary, Alberta. National Research Council of Canada, Ottawa, 23-35.

Harris, S. A. (1982) Cold air drainage west of Fort Nelson, British Columbia. Arctic 35, 537-541.

Harris, S. A. (1986) Permafrost distribution, zonation, and stability along the eastern ranges of the Cordillera of North America. Arctic 39, 29-38.

Harris, S. A. and R. J. E. Brown (1982) Permafrost distribution along the Rocky Mountains in Alberta. [Roger J. E. Brown Memorial Volume, H. M. French, Ed.] Proceedings of the Fourth Canadian Permafrost Conference, Calgary, Alberta. National research Council of Canada, Ottawa, 59-67.

Harris, S. A. and I. H. Schmidt (1993) Peat plateaus, km 160-167, Robert Campbell Highway, Yukon Territory. Journal of Paleolimnology. In the Press.

Heginbottom, J. A. and M. A. Dubreuil (1993) A new permafrost and ground ice map for the National Atlas of Canada. Proceedings, 6th International Permafrost Conference, Beijing.

Hickson, C. J. and J. G. Souther (1984) Late Cenozoic volcanic rocks of the Clearwater-Wells Gray area, British Columbia. Canadian Journal of Earth Sciences 21, 267-277.

Lauriol, B., J. Cinq Mars and I. D. Clark (1991) Localisation, genèse et fonte de quelques naleds du Nord du Yukon (Canada). Permafrost & Periglacial Processes 2, 225-236.

Leffingwell, E. de K. (1919) The Canning River region, northern Alaska. United States Geological Survey, Professional paper #109. 251 pp.

Lorrain, R. D. and P. Demeur (1985) Isotopic evidence for relic Pleistocene glacier ice on Victoria Island, Canadian Arctic archipelago. Arctic & Alpine Research 17, 89-98.

Péwé, T. L. (1983) Alpine permafrost in the contiguous United States: A review. Arctic and Alpine Research 15, 145-156.

van Everdingen, R. O. (1978) Frost mounds at Bear Rock, near Fort Norman, Northwest Territories, 1975-1976. Canadian Journal of Earth Sciences 15, 263-276.

van Everdingen, R. O. (1982) Management of groundwater discharge for the solution of icing problems in the Yukon. In: Proceedings of the 4th Canadian Permafrost Conference. H. M. french, Ed., Associate Committee on Geotechnical Research, National Research Council, Ottawa, 212-226.

Wahl, H. E., D. B. Fraser, R. C. Harvey and J. B. Maxwell (1987) Climate of Yukon. Atmospheric Environment Service, Environment Canada, Ottawa. climatological Series #40. 321 pp.

Westgate, J. A., B. A. Stemper and T. L. Péwé (1980). A 3m.y. record of Pliocene-Pleistocene loess in interior Alaska. Geology 18, 858-861.

MOUNTAIN PERMAFROST IN EUROPE

Lorenz King[1] and Jonas Åkerman[2]

[1] Geographical Institute, Justus Liebig University,
D-35390 Giessen, Germany
[2] Department of Physical Geography
University of Lund, S-233 62 Lund, Sweden

Abstract:

In several European countries a good knowledge about the properties and the distribution of mountain permafrost has been a vital factor for the development of these areas. This concerns particularly Svalbard (mining and construction activities), the Fennoscandian mountains and the Alps (traffic and protection measures). The distribution of mountain permafrost in Europe is displayed and the most important permafrost features for these mountain areas are mentioned. Whereas island permafrost is very common in many mountain areas, and sporadic permafrost, too, continuous or discontinuous permafrost is restricted to Svalbard, the Fennoscandian mountains and the Alps.

INTRODUCTION

A "Circumarctic Map of Permafrost and Ground Ice Conditions" at a scale 1:10 million has been recently prepared by different member countries of the International Permafrost Association (IPA) and a first draft map has been presented and discussed at the Sixth International Permafrost Conference in Peking 1993. In addition, the IPA Working Group on Mountain Permafrost prepared a special session with contributions from America, Europe and Asia (Haeberli 1993). This paper is part of these presentations and summarizes the knowledge concerning mountain permafrost in Europe.

Available information shows, that permafrost in Europe exists in:
a) Northern Europe (incl. Iceland, the Svalbard Archipelago and the Fennoscandian Mountains)
b) the Alps and
c) the Pyrénées.

To a smaller extent permafrost is also present in:
d) the Tatry Mountains (Poland, Slovakia),
e) the Carpathian Mountains (Romania),
f) the Abruzzi Mountains (Italy) and
g) Scotland.

Permafrost areas are small in Europe, when compared to the American Cordilleras or to Asia with their large areas of mountain and plateau permafrost. However, the European mountains are relatively densely populated or developed, and a good permafrost knowledge is a vital factor in and for these areas and their development (cp. Haeberli, 1992). Therefore, there is a good knowledge about mountain permafrost distribution and properties in quite a number of European countries. During the IPA sponsored international workshop on "Permafrost and Periglacial Environments in Mountain Areas" in Interlaken, Switzerland, 16-20 September, 1991, much of this knowledge has been presented and discussed together with American and Asian permafrost specialists, and research sites in the Alps have been visited before and after the workshop. Meanwhile, most presentations have been published in three issues of Permafrost and Periglacial Processes (volume 3, 1-3, 1992). The references to these papers form an excellent bibliography on mountain permafrost.

One of the sessions was also devoted to definition and classification of mountain permafrost. It was agreed there, that mountain permafrost is perennially frozen ground in mountain areas. This includes mountains in tropical, moderate and polar areas, and their common feature is a considerable altitudinal difference that produces special morphological forms. It is generally accepted today, that active rockglaciers are the most visible expression of mountain permafrost as creep of thick talus or morainic material. A great number of other geomorpholocical expressions for permafrost exist, too, and will be treated in this paper.

According to the considerable altitudinal differences, the distribution pattern of mountain permafrost is rather a vertical than a horizontal one, with many difficulties involved for its presentation on maps. In a short horizontal distance, permafrost may exist as continuous (90 - 100%), discontinuous (50 - 90 %), sporadic (10 - 50 %) or island (0 - 10%) permafrost.

Although these definitions have been used for the Permafrost Map of the Northern Hemisphere presented at the Sixth International Permafrost Conference in Peking, and have also been adopted by the authors for this paper, it should be realized, that these mentioned terms are also used in a different manner not only in Europe, but also in earlier studies in North America. Thus, e.g. the term "sporadic" is often used for areas with less than 10% occurrence, "patchy discontinuous" for 10 to 50% and so on. The addition of percentage values to these terms certainly is a good approach to definition problems and helps to avoid misunderstandings.

SVALBARD

The Svalbard Archipelago is mainly located between about 74° and 80° northern latitude and belongs to the area of continuous permafrost with a MAAT of about -4°C and lower (Åkerman 1980, 1987, King et al., in prep.). Permafrost thicknesses of about 100 m (along the west coast and the larger fiords) and 250 to 450 m (further inland) have been measured, especially in the existing coal mines (Liestøl 1980, 1986, Landvik et al. 1988). Large parts of Spitsbergen, the main island of the archipelago, are an area of rugged mountainous terrain with only narrow coastal plains.

The central parts of Spitsbergen and the large islands in the east are built by young sedimentary rocks and the mountains are plateaulike and divided by wide glacial valleys. 60% of the archipelago are covered by glaciers.

Ice-wedge polygons are frequent in the valley bottoms of the large wide valleys of central Nordenskjöld Land (Svensson 1976). However their distribution is not clear as they are often mixed up with the even more common and more widely distributed soil wedges. These soil wedges are mistakenly often classified as ice-wedges in maps and inventories, because their surficial appearance might be similar (Åkerman 1980, 1987). Pingos are common and found in the large wide valleys of central Nordenskjöld and Andrée Land and more rarely on Edgeøya and Barentsøya. A majority of the pingos are interpreted as open system pingos (Liestøl 1976) but a few have been classified as closed system pingos (Svensson 1973). Palsa-like frost mounds have been reported from Nordenskjöld Land and Nordaustlandet (Åkerman 1982, Salvigsen 1977). Icings of different origin are common all over the region (Åkerman 1980) and most commonly produced by the winter discharge from subpolar glaciers. An interesting form are icings produced in association with some of the surging glaciers.

Steep rock slopes often produce vast amounts of debris, that form rockglaciers in favoured places. These phenomena of mountain permafrost have been studied by Humlum (1982) and by Sollid and Sørbel (1992), also in cooperations with colleagues from ETH-Zürich (Hoelzle, in prep.). Push moraine formation is often favoured by the existence of permafrost in glaciofluvial or marine sediments in the valley floors. The mechanisms of push moraine formation has been studied by Van der Wateren (1992), Lehmann (1993; cp. also Gripp 1926, Sollid & Sørbel 1988).

Although Greenland belongs to the North American continent, it is also regarded as part of the "Nordic Countries" of Europe for historical reasons, and a large number of permafrost studies have been done by European scientists, especially from Denmark. References are compiled in Åkerman (in prep.).

ICELAND

Iceland experiences a mild and humid oceanic climate. Permafrost is limited to the central highlands above 450 m a.s.l. (Thorarinsson 1951, Schunke 1975). The majority of the permafrost observations in Iceland are connected with the flá-surfaces (Islandic bogs), that are characterised by numerous small ponds alternating with level surfaces of wet ground and by a multitude of large hummocks, called rúst (or dys). These rústs are the equivalent of "palsar" in the Scandinavian terminology and found between 400 m and 800 m a.s.l. Their lower limit corresponds fairly well with the 0°C isotherm. At higher altitudes the palsas (rústs) are larger, higher and more stable. Heights may reach 3 m and diameters up to 30-40 m are common.

Observations of permafrost in terminal moraines, rockglaciers and push moraines have been mentioned by Eyles (1978), Humlum (1985) and Rutten (1951). Permafrost is certainly also present in the glacier-free rockwalls and summits above 800 m a.s.l., but no systematic studies have been done.

FENNOSCANDIA

In Fennoscandia, the traditional opinion until recently was, that permafrost in Fennoscandia, even in the northernmost parts, basically was restricted to the palsa bogs (Fries & Bergström 1910, Hamberg 1905, Rapp & Rudberg 1960, Wramner 1973). However, recent studies made clear, that the extent of permafrost is much more widespread and that the majority of the permafrost areas belong to "mountain permafrost" (Østrem 1964, Svensson 1962b, Rapp & Clark 1971, King 1976, 1982, 1983, 1986, Rapp 1982, King & Seppälä 1987, Åkerman & Malmström 1986, Jeckel 1988, Sollid & Sørbel 1992, Ødegard et al. 1992, cp. also Åkerman, manus.). The distribution of permafrost in Fennoscandia is basically a vertical zonation as follows:

Island permafrost with a high or medium high ice content is common in and around the Fennoscandian mountains and is found from Hardangervidda and Dovre in southern Norway (Sollid & Sørbel 1974) up to the Varanger Peninsula in the north. Within this class permafrost is more or less restricted to organic soils, to bogs and to palsas or palsa-like features (Svensson 1962a, 1986, Åhman 1977, Meier 1985, Seppälä 1988). Annual and short-lived frost blisters are also common, here. Island permafrost is quite often observed at altitudes above 1000 m a.s.l. in the south, and reaches down to sea level altitude in the north. In the southernmost mountains of Hardangervidda (Norway) and Jämtland and Härjedalen (Sweden) it may even be found considerably lower than 1000 m a.s.l. at very selected places, mainly bogs. In Jämtland several sites between 650 and 750 m a.s.l. with palsa-like forms and small permafrost lenses have been reported by Smith (1911) or Lundquist (1962).

Sporadic permafrost occupies the mountain areas above 1.200 m a.s.l. in the south (Jotunheimen) and above 750 m a.s.l. in northern Sweden (Kebnekaise). Further north and inland, and due to increased continentality (cp. King & Seppälä 1987, Malmström 1988), this belt can also be found at lower altitudes of 300 m to 400 m. The strong gradient in continentality from west to east is displayed in Figure 1 (cp. also values in table 1). Icings, often in association with karst drainage in the mountains and with small groundwater springs are quite common in the sporadic permafrost belt. Pingo-like features regarded as transitional forms between palsas and pingos are found in the Abisko, Finnmarksvidda and Rastosjaure areas (Svensson 1969, Lagerbäck & Rohde 1985, Åkerman & Malmström 1986); in the lower levels these forms are often relict.

With increasing altitudes, the sporadic permafrost belt gradually changes into discontinuous permafrost at altitudes of about 1600 m a.s.l. in Jotunheimen, and 1200 m a.s.l. in the Kebnekaise mountains. This permafrost belt shows rockglaciers and ice-cored moraines in the steeper, alpine type mountains (Barsch 1971, Østrem 1964) and pronounced large-scale polygon patterns in the smoother Scandinavian fjell-type mountains (Rapp & Clark 1971, Rapp & Annersten 1969). Rock glaciers may reach down into the sporadic zone, especially in the more continental, eastern mountain areas (Barsch & Treter 1976), where the periglacial areas have quite a considerable vertical extent due to a high glaciation limit and relatively low mean annual air temperatures.

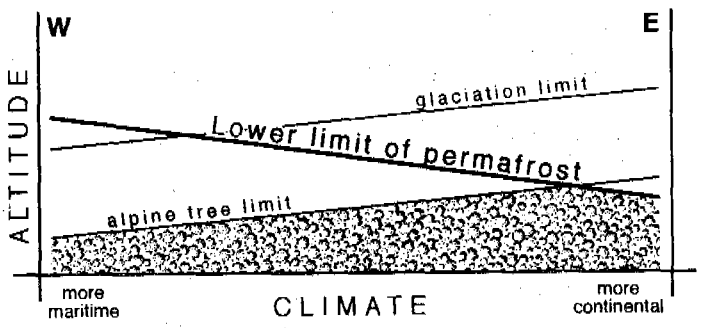

Figure 1: Schematic section across the Scandinavian mountain ranges. From west to east the lower permafrost limits drop considerably and the altitude of the glaciation limit increases. Thus permafrost is mainly found in the eastern (and northern) parts with a more continental climate; the western mountain ranges experience much precipitation and are often glacierized.

The continuous permafrost belt is found above 2060 m in Jotunheimen (Norway) and above 1600 m a.s.l. in northern Sweden (King 1984). It is an area where patterned ground is often as well developed as in many high arctic areas, if slope and sediment cover are favourable. Permafrost thicknesses of about 70 m have been measured even at the relatively low altitude of 1200 m a.s.l. (Ekman 1957) and the thickness of permafrost is estimated to be more than 100 m at about 1500 m a.s.l. and probably even 200 to 300 m in the highest elevations of the Kebnekaise mountain (2400 m a.s.l.) in northern Sweden (King 1984, 1986).

ALPS AND JURA

Research in mountain permafrost has a long tradition in Europe and started mainly in the Alps with the investigation of rockglaciers (Barsch 1978, Haeberli 1985). It is generally agreed today, that active rockglaciers are the most typical phenomena for widespread sporadic or discontinuous mountain permafrost (Barsch 1992). Rockglacier research is still continued in the Swiss, Italian, French and Austrain Alps, and there are a large number of thorougly investigated rockglaciers in all these mentioned countries (cp. Haeberli et al. 1992, Belloni et al. 1993, Evin et al. 1993). Research includes studies of rockglacier movement over a few and up to 25 years, rockglacier drilling and detailed geophysical borehole logging, as well as many geophysical sounding techniques (e.g. Francou et al. 1992, Haeberli et al. 1979, Von der Mühll et al. 1990, 1992). In more recent years, similar studies have also been conducted on Iceland, in the Fennoscandian mountains, as well as on Spitsbergen (cp. references in previous chapters). Freeze/thaw cycles in permafrost areas (e.g. King 1990) and creep of permafrost (Haeberli 1985, Wagner 1992) are other important research topics. Important methodological advances in mountain permafrost research also originated in the Alps: the BTS-method has become an accepted working tool for mapping permafrost very efficiently (e.g. Guglielmin et al. 1993, Hoelzle et al. 1993). Modelling of mountain permafrost distribution and its automated mapping will bring new knowledge and new ideas about permafrost distribution of large areas that have not been investigated detailedly until now (cp. Keller 1992). A methodological review concerning mapping and prospecting of mountain permafrost is given by King et al. (1992). It shows that the Alps represent an important research area for comparative studies in other mountain areas of the world (Cheng et al. 1992, Gorbunov 1978).

In addition to scientific projects (Haeberli 1993), research in mountain permafrost has also been greatly promoted by construction measures. In the Alps, construction includes railways, cable cars, skilifts, restaurants and hotels, communication towers, hydropower installations, high power transmission lines, and protection measures against natural risks. Construction sites can be found in all permafrost belts, from the sporadic to the continuous one (Haeberli 1992). Many bedrock exposures have thus been created and allowed the study of ice-filled bedrock-joints or temperature gradients in tunnels. The scientific permafrost community is very grateful for these engineering activities, and should carefully follow these, wherever possible. Comparable development activities have only started in Northern Europe, Eastern Europe and the Pyrénées, and we will certainly learn much more about mountain permafrost distribution in Europe in the years to come.

In the Alps, permafrost occurs from the southern French and Italian Alps over the central Swiss Alps to the Austrian and German Alps. Predominantely sporadic permafrost with low ice content in bedrock and high ice-content in nonconsolidated sediments exists at altitudes between 2000 m and 2500 m a.s.l. Patchy vegetation and alpine meadows cover these areas and relict and inactive rockglaciers are typical and more numerous than active ones here. Island permafrost extends much further down, to altitudes considerably lower than the treeline in general. The occurrences are limited to special places, as e.g. snow-free rockwalls and slopes exposed to the north, long lasting avalanche deposits and ice-caves in limestone areas. There, the MAAT may be markedly higher than 0°C.

Discontinuous permafrost is common at altitudes above about 2500 m a.s.l. and gradually changes into continuous permafrost at altitudes above 3000 to 3500 m a.s.l. The mean permafrost temperature is -5° to -6°C at Jungfraujoch (3500 m a.s.l., northern Swiss Alps) and about -15°C with maximum permafrost thicknesses expected to exceed 1000 m on Monte Rosa (4,500 m a.s.l., southern Swiss Alps; cp. Haeberli & Funk 1991).

In contrast to the Fennoscandian mountains the Alps have not been shaped by a continental ice-sheet, and flat or rolling mountain landscapes are missing and steep slopes prevail. Due to this geomorphological characteristics of the Alps, the permafrost features so typical for the "Scandinavian fjell" (palsas, pingo-like features, ice-cored moraines, vast large scale polygon patterns) are missing in the Alps or are restricted to a few selected places. Active phenomena of creeping ice-supersaturated sediments from moraines and talus (rockglaciers) dominate instead, and the number of rockglaciers matches the number of glaciers. All forms of solifluction are quite widespread, too.

The Jura mountains are located in France and Switzerland, northwest of the Swiss Alps. For large areas, they consist of parallel folds of mesozoic sediments, often limestone. In the northeast, their continuation reaches to the cuesta-like Alb mountains in Germany. Alltogether, this mountain area is several hundred kilometers long and reaches above 1500 m a.s.l. at many points. Although the MAAT is above freezing point, ice-caves (island permafrost) may be found at many places even at altitudes below 1200 m a.s.l. (Pancza 1992).

OTHER EUROPEAN MOUNTAINS

Besides the main mountain ranges of continental Europe, the Alps and the Scandes, there are a great number of larger and smaller mountain ranges, where permafrost has been proven or where it can be expected, e.g. the Pyrénées, the Carpathians and the Appennine. Table 1 gives the approximate lower limits for island, sporadic and discontinuous mountain permafrost in the mountains of continental Europe.

The lowermost limits for island permafrost include areas of ice caves in karst areas, and the MAAT may therefore reach values considerably above the freezing point there. At the lower limit of sporadic permafrost the MAAT is in the order of -1°C to -1.5°C, and above the altitude of the -3.5°C MAAT discontinuous permafrost (> 50%) can be expected. The maximum altitude of the respective mountain range gives a first idea of the area affected by perennially frozen ground.

In the Pyrénées, geomorphological research has a long tradition, on the French side as well as on the Spanish one and the interest in mountain permafrost research is present, too (cp. Gutierrez et al. 1981). There are more than a dozen active rockglaciers in the Spanish Pyrénées in areas reaching above 2800 m a.s.l. (Agudo et al. 1992, San José et al. 1992, Serrano et al. 1991). According to David Palacios (written communication) the area above 2800 m a.s.l. is regarded as the altitudinal belt of sporadic permafrost (10 - 50 %). In addition to the studies of active permafrost, Chueca (1992) has mapped 170 rockglaciers as relict permafrost forms. The joining of the Spanish national body to the International Mountain Permafrost Association will certainly have a positive effect on more detailed mountain permafrost research in the Pyrénées, where more areas are expected to be underlaid by permafrost according to the existing MAAT of -1.5°C and lower.

In the central part of the Italian Appennine, the Abruzzi mountains, there are three small mountain areas where permafrost can be expected: Gran Sasso, Maiella and Monte Vellino (Dramis & Kotarba 1992).

In the Southern Carpathians, Romania, inactive and active rockglaciers have been reported in altitudes above 2000 m a.s.l. by Urdea (1992). In the Fagaras, the Paring and the Retezat mountain massifs many mountain tops and crests reach altitudes between 2300 and 2500 m a.s.l. and the MAAT at Omu

Table 1: Approximate lower limits for island (0 - 10%), sporadic (10 50%) and discontinuous (> 50%) permafrost in continental Europe. Continuous permafrost exists only in the Alps and in the highest parts of the Scandinavian mountains.

	0 - 10 %	10 - 50%	more than 50 %	Max. Altitude
Fennoscandia				
North / East	400 - 0 m	900 - 300 m	1300 - 700 m	2120 m
South	650 m	1400 - 1000 m	1900 - 1400 m	2470 m
Alps				
- Central, East	1500 m	2500 m	3000 m	4800 m
- South (France)	1750 m	> 2500 m	> 3000 m	3840 m / 4100 m
Jura Mtns.	1150 m	- - - -	- - - -	1720 m
Spain, Pyrénées	2000 m	> 2800 m	- - - -	3400 m
Italy, Abruzzi	2000 m	- - - -	- - - -	2900 m
Yugoslavia	> 2000 m	- - - -	- - - -	2520 m
Albania	> 2000 m	- - - -	- - - -	2760 m
Bulgaria	> 2000 m	- - - -	- - - -	2930 m
Carpathian Mtns.				
- South	2300 m	- - - -	- - - -	2540 m
- East	1900 m	- - - -	- - - -	2060 m
- West (Tatry)	1500 m	2400 m	- - - -	2650 m

(2505 m a.s.l.) is -2.6°C. Here again, a large number of relict rockglaciers exist below about 2000 m a.s.l. and proove former permafrost conditions (Ichim 1978, Urdea 1993).

The mean annual air temperature in the Northern Carpathians, especially in the Tatry mountains (Poland, Slovakia) is lower than -1.5°C, too, and these climatic conditions undoubtedly favour the development of sporadic permafrost. Whereas relict permafrost features have been studied, research on the distribution of active permafrost is still urgently needed (cp. Czudek, 1993).

In Scotland the existence of small permafrost island in the highlands cannot be excluded according to the existing temperatures.

ACKNOWLEDGEMENTS:

Additional contributions for this report came from the following colleagues: Matti Seppälä (northern Finland), Wilfried Haeberli (Switzerland), Michèle Evin (France), Francesco Dramis (Italy), David Palacios (Spain) , Adam Kotarba (Poland) and Petru Urdea (Romania).

REFERENCES:

SVALBARD

Åkerman, H.J. (1980): Studies on Periglacial Geomorphology in West Spitsbergen. PhD thesis. Lunds Universitets Geografiska Inst. Scr. Avh. LXXXIX: 297 pp.

Åkerman, H.J. (1982): Observations of palsas within the continuous permafrost zone in eastern Siberia and in Svalbard. Geografisk Tidsskrift 82: 45-51.

Åkerman, H.J. (1987): Periglacial forms of Svalbard - A review. In: Boardman, J. (ed.): Periglacial Processes and Landforms in Britain and Ireland, Cambridge University Press: 9-25.

Åkerman, H.J. (in prep.): Mountain permafrost in the Nordic countries, a review. - In preparation for Lunds Univ. Naturgeogr. Inst., rapporter och Notiser (1994).

Gripp, K. (1926): Über Frost und Strukturboden auf Spitzbergen. Zeitschr. Gesellsch. f. Erdkunde: 351-354.

Humlum, O. (1982): Rock Glaciers in Northern Spitsbergen: A discussion. Journ. Geol. 90: 214-218.

King L. & M. Volk (in prep.): Glaziologie und Glazialmorphologie des Liefde- und Bockfjordgebietes, Nordspitzbergen. - In preparation for Zeitschrift für Geomorphologie N.F., Suppl.-bd. (1994)

Landvik, J.Y. et al. (1988): Glacial history and permafrost in the Svalbard area. Permafrost, Fifth International Permafrost Conf. Proceedings 1: 194-198, Trondheim.

Lehmann, R. (1993): The Significance of Permafrost in the Formation and Appearance of Push Moraines, Examples of the Canadian Arctic and Spitsbergen. Sixth International Conference on Permafrost, Beijing 1993, Proceedings Vol. 1: 374-379.

Liestøl, O. (1976): Pingos, springs, and permafrost in Spitsbergen, Norsk Polarinstitutt Årbok 1975: 7-29.

Liestøl, O. (1980): Permafrost conditions in Spitsbergen. Frost i Jord 21: 23-28.

Liestøl, O. (1986): Permafrost på Svalbard og på fastlandet. Klimatiske forutsetninger, utbredelse og tykkelse. Fjellsprengningsteknikk, bergmekanikk, geoteknikk. Tapir.

Salvigsen, O. (1977): An observation of palsa-like forms in Nordaustlandet, Svalbard. Norsk Polarinst. Årbok: 364-367.

Sollid, J.L. & L. Sørbel (1988): Influence of temperature conditions in formation of end moraines in Fennoscandia and Svalbard. Boreas 17: 553-558.

Sollid, J.L. & L. Sørbel (1992): Rock glaciers in Svalbard and Norway. Permafrost and Periglacial Processes 3, 3: 215-220.

Svensson, H. (1976): Iskilar som klimatindikator. Svensk Geogr. Årsbok 52: 46-57.

Van der Wateren, D. (1992): Structural Geology and Sedimentology of Push Moraines. Diss., Faculteit der Ruimtelijke Wetenschappen, Univ. van Amsterdam: 230 pp.

ICELAND

Eyles, N. (1978): Rock glaciers in Esjufjöll nunatak area, southeast Iceland. Jökull 28: 53-56.

Humlum, O. (1985): Genesis of an imbricate push moraine, Höfdabrekkujull, Iceland. Journal of Geology 93: 185-195.

Rutten, M.G. (1951): Polygon soils in Iceland. Geologie en Mijnbouw, Mai 1951

Schunke, E. (1975): Die Periglazialerscheinungen Islands in Abhängigkeit von Klima und Substrat. Abh. Akad. Wiss. Göttingen 30: 273 pp.

Thorarinsson, S. (1951): Notes on patterned ground in Iceland, with particular reference to the Icelandic "Fia's". Geogr. Ann. 33: 144-156.

FENNOSCANDIA

Åhman, R. (1977): Palsar i Nordnorge. Medd. Lunds Univ. Geogr. Inst. Scr. Avh. 78: 165 pp.

Åkerman, H.J. & B. Malmström (1986): Permafrost mounds in the Abisko area, Northern Sweden. Geogr. Ann. 68 A, 3: 155-165.

Åkerman, H.J. (in prep.): cp. section on Svalbard

Barsch, D. (1971): Rock glaciers and ice-cored moraines. Geogr. Ann. 53 A, 3-4: 203-206.

Barsch, D. & U. Treter (1976): Zur Verbreitung von Periglazialphänomenen in Rondane/Norwegen. Geogr. Ann. 58 A: 83-93.

Ekman, S. (1957): Die Gewässer des Abisko-Gebietes. Kungl. Vetenskapsakademiens Handlingar 4, e ser. 6, 6: 172 pp.

Fries, T. & E. Bergström (1910): Några iaktagelser öfver palsar och deras förekomst i nordligaste Sverige. Geol. Fören. Förhandl. Stockholm 32: 195-205.

Hamberg, A. (1905): Till frågan om alltid frusen mark i Sverige. Ymer 24: 87-93.

Jeckel, P.P. (1988): Permafrost and its altitudial zonation in N. Lapland. In: Permafrost, Fifth International Permafrost Conference, Proceedings Vol. 1: 170-175.

King, L. (1976): Permafrostuntersuchungen in Tarfala, Schwedisch Lappland, mit Hilfe der Hammerschlagseismik. Z. Gletscherk. u. Glazialgeol. 12, 2: 187-204.

King, L. (1982): Qualitative und quantitative Erfassung von Permafrost in Tarfala (Schwedisch Lappland) und Jotunheimen (Norwegen) mit Hilfe geoelektrischer Sondierungen. Z. Geomorph., Suppl.Bd. 43: 139-160.

King, L. (1983): High mountain permafrost in Scandinavia. In: Permafrost, Fourth International Conference, Proceedings Vol. 1: 612-617, Nat. Acad. Press, Washington, D.C.

King, L. (1984): Permafrost in Skandinavien, Untersuchungsergebnisse aus Lappland, Jotunheimen und Dovre/Rondane. Heidelberger Geogr. Arb.76: 174 pp.

King, L. (1986): Zonation and ecology of high mountain permafrost in Scandinavia. Geogr. Ann. 68 A: 131-139.

King, L. & M. Seppälä (1987): Permafrost thickness and distribution in Finnish Lapland - results of geoelectrical soundings. Polarforschung 57, 3: 127-147.

Lagerbäck, R. & L. Rodhe (1985): Pingos in northernmost Sweden. Geogr. Ann. 67 A, 3-4: 239-245.

Lundquist, J. (1962): Patterned ground and related frost phenomena in Sweden. Sveriges Geologiska Undersökning, Ser. C 55: 101 pp.

Malmström, B. (1988): Occurence of permafrost on the Varanger Peninsula, northernmost Norway. Norsk Geogr. Tidsskr. 42: 239-244.

Meier, K.-D. (1985): Studien zur Verbreitung, Morphologie, Morphodynamik und Ökologie von Palsas auf der Varanger-Halbinsel, Nord-Norwegen. Essener Geographische Arbeiten 10: 114-204.

Ødegård,R. et al. (1992): Ground temperature measurements in mountain permafrost, Jotunheimen, Southern Norway. Permafrost and Periglacial Processes 3: 231-234.

Østrem, G. (1964): Ice-cored moraines in Scandinavia. Geogr. Ann. 46: 282-337.

Rapp, A. (1982): Zonation of permafrost indicators in Swedish Lapland. Geogr. Tidsskrift 82: 37-58.

Rapp, A. & L. Annersten (1969): Permafrost and tundra polygons in northern Sweden. In: Péwé, T. (ed.): The periglacial environment. Montréal, Canada.

Rapp, A. & G.M. Clark (1971): Large nonsorted polygons in Padjelanta National Park, Swedish Lapland. Geogr. Ann. 53 A: 71-85.

Rapp, A. & S. Rudberg (1960): Recent periglacial phenomena in Sweden. Biul. Perigl. 8: 143-154.

Seppälä, M. (1988): Palsas and related forms. In: M.J. Clark (ed.): Advances in Periglacial Geomorphology: 247-278.

Smith, H. (1911): Postglaciala regionförskjutningar i norra Härjedalen och södra Jämtlands fjälltrakter. Geol. Fören. Stockholm Förh. 33: 503-530.

Sollid, J.L. & L. Sørbel (1974): Palsa bogs at Haugtjørnin, Dovrefjell, South Norway. Norsk Geografisk Tidsskrift 28,1: 53-60.

Sollid, J.L. & L. Sørbel (1988): Influence of temperature conditions in formation of end moraines in Fennoscandia and Svalbard. Boreas 17: 553-558.

Sollid, J.L. & L. Sørbel (1992): Rock glaciers in Svalbard and Norway. Permafrost and Periglacial Processes 3, 3: 215-220.

Svensson, H. (1962a): Några iaktagelser från pals områdon. Norsk Geogr. Tidsskrift 18, 5-6: 212-227.

Svensson, H. (1962b): Tundra polygons. Photographic interpretation and field studies in North Norwegian polygon areas. Arb. Norges Geol. Unders 223: 298-327.

Svensson, H. (1969): A type of circular lakes in northernmost Norway. Geogr. Ann. 51 A: 1.12.

Svensson, H. (1986): Some morphoclimatic aspects of periglacial features of northern Scandinavia. Geogr. Ann. 68 A:123-130.

Wramner, P. (1973): Palsmyrar i Taavavuoma, Lapland. Göteborgs Univ. Naturgeogr. Inst. Rapp. 3: 140 pp.

ALPS AND JURA

Barsch, (1978): Active Rock Glaciers as Indicators for Discontinous Alpine Permafrost, an Example from the Swiss Alps. Proceedings of the Third International Conference of Permafrost, July 10-13, 1978, Edmonton, Alberta, Canada. Vol. 1: 349-352, Ottawa.

Barsch, D. (1992): Permafrost creep and rockglaciers. Permafrost and Periglacial Processes 3, 3: 175-188.

Belloni, S., A. Carton, F. Dramis & C. Smiraglia (1993): Distribution of permafrost, glaciers and rock glaciers in the Italian mountains and correlations with climate: an attempt to sythesize. Sixth International Conference on Permafrost, Beijing 1993, Proceedings Vol. 1: 272-277.

Cheng, G. & F. Dramis (1992): Distribution of mountain permafrost and climate. Permafrost and Periglacial Processes 3, 2: 83-91.

Evin, M., D. Fabre, A. Assier & Ch. Guillain (1993): Les glaciers rocheux du Roure. Société hydrotechnique de France, section glaciologie, Grenoble: 6 pp.

Francou, B. & L. Reynaud (1992): 10 years surficial velocities on a rock glacier (Laurichard, French Alps). Permafrost and Periglacial Processes 3, 3: 209-214.

Gorbunov, A. P. (1978): Permafrost investigation in high mountain regions. Arctic and Alpine Research 10, 2: 283-294.

Guglielmin, M. & C. Tellini (1993): First example of permafrost mapping with BTS in the Italian Alps (Livigno, Sondrio, Italy). Acta-Naturalia de l'Ateneo Parmenese 29, NN. 1/2: 39-46.

Haeberli, W. (1985): Creep of mountain permafrost: internal structure and flow of alpine rock glaciers. Mitt. der Versuchsanstalt für Wasserbau, Hydrologie und Glaziologie 77, ETH Zürich: 142 pp.

Haeberli, W. (1992): Construction, environmental problems and natural hazards in periglacial mountain belts. Permafrost and Periglacial Processes 3, 2: 111-124.

Haeberli, W. (1993): Research on permafrost and periglacial processes in mountain areas - status and perspectives. (This volume)

Haeberli, W., M. Evin, G. Tenthorey, H.R. Keusen, M. Hoelzle, F. Keller, D. Vonder Mühll, S. Wagner, M. Pelfini & C. Smiraglia (1992): Permafrost research sites in the Alps: excursions of the International Workshop on Permafrost and Periglacial Environments in Mountain Areas. Periglacial Processes 3, 3: 189-202.

Haeberli, W. & M. Funk (1991): Borehole temperatures at the Colle Gnifetti core-drilling site (Monte Rosa, Swiss Alps): Journal of Glaciology 37, 125: 37-46.

Haeberli, W., L. King & A. Flotron (1979): Surface movements and lichen-cover studies at the active rock glacier near the Grubengletscher, Wallis, Swiss Alps. Arctic and Alpine Res. 11, 4: 421-441.

Hoelzle, M., W. Haeberli & F. Keller (1993): Application of BTS-measurements for modelling mountain permafrost distribution. Sixth International Conference on Permafrost, Beijing 1993, Proceedings Vol. I: 272-277.

Keller, F. (1992): Automated mapping of mountain permafrost using the program PERMAKART within the geographical information system ARC/INFO. Permafrost and Periglacial Processes 3, 2: 133-138.

King, L. (1990): Soil and rock temperatures in discontinuous permafrost: Gornergrat and Unterrothorn, Wallis, Swiss Alps. Permafrost and Periglacial Processes 1,2: 177-188.

King, L., A. P. Gorbunov & M. Evin (1992): Prospecting and mapping of mountain permafrost and associated phenomena. Permafrost and Periglacial Processes 3,2: 73-81.

Pancza, A. (1992): La gélivation des parois rocheuses dans une glacière du Jura Neuchâtelois. Permafrost and Periglacial Processes 3, 2: 49-54.

Vonder Mühll, D. & W. Haeberli (1990): Thermal characteristics of the permafrost within an active rock glacier (Murtèl/Corvatsch, Grisons, Swiss Alps). Journal of Glaciology 36, 123: 151-158.

Vonder Mühll, D. & P. Holub (1992): Borehole logging in Alpine permafrost, Upper Engadin, Swiss Alps. Permafrost and Periglacial Processes 3, 2: 125-132.

Wagner, S. (1992): Creep of Alpine permafrost, investigated on the Murtèl rock glacier. Permafrost and Periglacial Processes 3, 2: 157-162.

OTHER EUROPEAN AREAS

Agudo, C., E. Serrano & E. Martinez de Pison (1989): El glaciar rocoso activo de Los Gemelos en el Macizo de Posets (Pirinéo Aragones): Cuaternario y geomorfología. Vol. 3: 83-91.

Chueca, J. (1992): A statistical analysis of the spatial distribution of rock glaciers, Spanish Central Pyrenees. Permafrost and Periglacial Processes 3, 3: 261-265.

Czudek, T. (1993): Pleistocene Periglacial Structures and Landforms in Western Czechoslovakia. Permafrost and Periglacial Processes 4, 1: 65-76.

Dramis, F. & A. Kotarba (1992): Southern limit of relict rock glaciers, Central Appennines, Italy. Permafrost and Periglacial Processes 3, 3: 257-260.

Gutierrez, M. & J.L. Peña (1981): Los glaciares rocosos y el modelado acompañante en el área de la Bonaigua (Pirinéo de Lérida). Bol. Geol. Minéro 92: 11-20.

Ichim, I. (1978): Preliminary observations on the rock glacier phenomenon in the Romanian Carpathians. Revue Roumaine Géol. Géof. Géogr., Géographie 23, 2: 295-299.

San José, J.J. De, C. Agudo, E. Serrano & F. Silio (1992): Auscultación topografica y fotogrametrica del glaciar rocoso de Las Argualas (Pirinéo Aragones): datos preliminares. In: F. Lopez Bermudez, C. Conesa Garcia & M.A. Romero Diaz (eds.): Estudios de geomorfología en España, actas de la reunion de la II reunion nacional de GEO: 423-431, Murcia.

Serrano, E., E. Martinez de Pison et al. (1991): El glaciar noroccidental del Besiberri (Pirinéo de Lérida). Pirinéos 137: 95-109

Urdea, P. (1992): Rock Glaciers and Periglacial Phenomena in the Southern Carpathians. Permafrost and Periglacial Processes 3, 3: 267-273.

Urdea, P. (1993): Permafrost and Periglacial forms in the Romanian Carpathians. Sixth International Conference on Permafrost, Beijing 1993, Proceedings Vol. 1: 631-637.

STUDIES ON MOUNTAIN PERMAFROST IN ASIA

Qiu Guoqing

Lanzhou Institute of Glaciology and Geocryology
Chinese Academy of Sciences, Lanzhou 73000, China

Asia has the largest permafrost area in the world. The existence of frozen ground and frost action was known long ago, while the systematic investigations on mountain permafrost were carried out since the 50's of this century. The mountain permafrost can be divided into three broad categories, i.e., the permafrost developing in mountains in the continuous belt of the Eurasian continental permafrost zone on a frigid background, the permafrost developing in mountains out side the Eurasian continental permafrost zone on a warm to temperate background and the permafrost in mountains in the discontinuous belt of the Eurasian continental permafrost zone. The distribution of mountain permafrost has a close relation to the climatic variation in three dimensions. Much more work is needed for searching a perfect classification of mountain permafrost.

HISTORY

Asia has the largest permafrost area in the world. The existence of frozen ground and frost action was known long ago. In China, the Book of Rites: Seasons, that was written 2000 years ago, described exactly the seasonal fluctuation of climate and the processes of ground freezing and thawing (Shi et al.,1964); the outstanding Chinese geographer Xu Xiake had reported the existence. Of block field and the difference in frost action between the north- and south-facing slopes in the Mt. Wutaishan of Northern China in 1633 (Xu, 1980). In West Tianshan, frost fissures and frost mounds were first reported by V.I. Roborovsky in 1893; the first information about permafrost in AK-Say basin of Inner Tianshan was given by A.I. Bezsonov in 1913 (Gorbunov,1993). With the exploitation of Siberia since the 19th century, many data and knowledge was obtained and the geocryology became an independent dicipline firstly in Russia in this century.

Since 1950'S, permafrost investigations were undertaken in the Northeast China in the interest of forest exploitation and railroad construction in the Mt. Da-Hinggan Ling region. During the period from 1950'S to 1970'S, comprehensive investigations on natural condition and resource were carried out in West China, many publications, as the results of those expeditions, emphasized the importance of altitudinal zonation and the frost action in mountains. Special permafrost researches were carried out in the Mts. Altai Shan, Qilian Shan, Qinghai-Xizang Plateau of China, the Mts. Zayilisky Alatau, West Tianshan, Inner Tianshan and Pamir of the USSR / CIS, the Mts. Khentei and Khangai of Mongolia since 1960'S. In the past 3 years, a joint expedition in Northern Tianshan was undertaken by the Lanzhou Institute of Glaciology and Geocryology, Academia Sinica and the Permafrost Institute of Siberia Branch of the Russian Academy of Sciences.

On the basis of the previous work, it is possible to review and discuss some aspects of the permafrost studies in mountain areas of Asia.

DISTRIBUTION OF MOUNTAIN PERMAFROST

According to Gorbunov (1988), the mountain permafrost "should include only those perennially frozen soils which occur over 500 m above sea level, and is absent below this level". Cheng and Dramis (1992) suggested that the term "mountain permafrost" is used to include both alpine permafrost and polar mountain permafrost, Which is not conventionally considered as alpine permafrost. In this review, Cheng's concept is used.

Generally, the mountain permafrost can be divided into three broad categories, i.e.,

1. the permafrost developing in mountains in the continuous belt of the Eurasian continental permafrost zone, on a frigid background;

2. the permafrost developing in mountains outside the Eurasian continental permafrost zone, or on a warm to temperate background;

3. the permafrost developing in mountains in the discontinuous belt of the Eurasian continental permafrost zone, this is the transitional type of the first two.

The permafrost in mountains of the northern part of East Siberia is the typical one of the first type. There, the mean annual air temperature ranges from −7.5 to −15 °C or lower, permafrost is present everywhere with a mean annual ground temperature of −3 to −11 °C in plains, depressions and valleys, −7 to −15 °C at mountains (Ershov et al, 1989 a). Such a mountain permafrost developing on an extremely frigid background without a lower limit was named the "Verkhoyangsk type alpine permafrost by Gorbunov (1978). Such kind of mountain permafrost is also seen in the Mt.

Byrranga and Mt. Putorana of the northern part of Central Siberia Plateau.

Outside the Eurasian continental permafrost zone, the development of mountain permafrost depends mainly on the variation of climate in three dimensions. For example, in the Chinese Tianshan, according to the statistics using the data from 17 stations, the dependence of the mean annual air temperature T on the latitude X1, longitude X2 and altitude X3 is known as follows (Qiu, 1993):

$$T = 109.28 - 2.19X1 - 0.024X2 - 0.0051X3 \quad (1)$$

The correlation coefficient R of (1) is 0.9596. The corresponding standard regression coefficients are:

B1 = −0.48 for X1;
B2 = −0.025 for X2;
B3 = −0.93 for X3.

For the vast area from Mt. Qilian Shan to the Mt.Himalaya, according to the statistics by using the data from 78 stations,

$$T = 66.25 - 0.92X1 - 0.14X2 - 0.0056X3 \quad (2)$$

The correlation coefficient R of (2) is 0.9530. The corresponding standard regression coefficients are:

B1 = −0.77 for X1;
B2 = −0.20 for X2;
B3 = −1.12 for X3.

Thus, it could be concluded that in the mountains of West China the mean annual air temperature decreases very obviously from lowland to high mountain, decreases obviously from south to north and slightly decreases from west to east. Such a variation of mean annual air temperature in three dimensions influences in the development of permafrost in high mountains, the cold islands standing on the temperate–warm background in the middle–low latitudes while the lower limit of the discontinuous mountain permafrost ascends southwards (Zhou et al, 1991):

2700–3100 m a.s.l. in Mt.Tianshan;
3500–3900 m a.s.l. in Mt.Qilian Shan;
4150–4200 m a.s.l. at the Xidatang of the Mt. Kunlun Shan;
4600 m a.s.l. on the south side of Mt.Tangula, and
5100–5300 m a.s.l. in the Mt. Himalaya Shan.

Such a latitudinal variation of the lower limit is also seen in the central Asia part of CIS, e.g., it rises from 3200–3700 m a.s.l. in the Mt.Zayilisky Alatau up to 3600–4000 m in Pamir (Gorbunov, 1978).

The lower limit of the mountain permafrost also descends eastwards. For example, along the 43°N latitude, it lies at 3300m a.s.l. in the Balshaya Almatinka Permafrost Station in Kazakhstan, 2900–3250 m a.s.l. in the Chinese Tianshan Glaciological Station (Qiu, 1993),1900–2000 m a.s.l. in the Mt. Changbai Shan (Zhou et al, 1991) and the Northeast Korea (Viktor An, 1993), and down to 1700 m a.s.l. in Hokkaido.

In the Mt.Qilanshan at 37°–40°N, the permafrost lower limit descends from 3900 to 3500 m a.s.l. eastwards; in the Mt.Wutai Shan at 38°N it lies at 2300 m a.s.l. In the Mt. Kunlun Shan at 36°–34°30′N, it descends from 4400–4500 m in the northwest, 4150–4200 m a.s.l. in the middle and 3850–3900 m at the southeast end; in the Mt. Taibai Shan (34°N) in the Shannxi Province, it lies at 3000 m a.s.l.(Zhou et al, 1991). All of these document an eastward descent of the lower limit of mountain permafrost, and this would result from the decrease of air temperature in the same direction.

The permafrost regions in the Mongolian Republic and the Northeast China are in the south part of the Eurasian Continental Permafrost Zone. 63% of the territory of the Mongolian Republic is underlain by permafrost (Lomborichen, 1993), where the lowest and southernmost position of the permafrost islands was considered as both the lower limit of the sporadic permafrost belt and the south limit of the permafrost zone(Joint Soviet–Mongolia Scientific Research Geological Expedition, 1974). Although the continuity of permafrost tends to increase northwards, showing a latitudinal zonation, it is also obvious that the permafrost with higher continuity, lower temperature and a greater thickness occurs in the cold centers or the three mountain systems i.e., the Mt. Mongolian Altay in the southwest, the Mt.Khangai in the west and the Mt.Kentei in the middle part of Northern Mongolia, standing on the background of sporadic island permafrost belt, in other words, the latitudinal zonation and altitudinal zonation are of the same importance in the development of permafrost, while in the other kinds of mountain permafrost region there is not such a wide sporadic permafrost belt. In Northeast China, the south limit of permafrost is also determined according to the southernmost position of permafrost islands(Guo et al, 1981). The west secor of the south limit approximitely coincides with the 0 to −1 °C isotherm, the middle ––0°C, and the east—0 to +1°C. The W–shanped running of the south limit might result from the special terrain with the Mt.Aershan (700–1200m a.s.l.) in the southwest and the Mt.Xiao Hinggan Ling in the southeast and the lower plain in the middle(Guo et al, 1981). The fact that the permafrost increases in continuity and thickness and decreases in temperature shows a latitudinal zonation. The coldest and thickest permafrost occurring in the north is the result of the altitudinal zonation,and the terrain has also effect on it. Although different in terminology, the distribution of permafrost in Northeast China and Mongolia can be compared to each other. The sporadic scarce–island– and island–permafrost belts in Mongolia is corresponding to the island–permafrost belt in Northeast China, the Predominantly continuous belt in Northeast China might correspond to the discontinuous belt, according to there continuity. The mountain permafrost in the Zabaykal region and the southern part of East and Central Siberia is on the background of the discontinuous permafrost belt of the Eurasian Continental Permafrost Zone.

CLASSIFICATION

An important problem in mountain permafrost studies is to provide a perfect principle for the classification related to the distribution of permafrost.

It was suggested that the alpine permafrost be divided into the continuous, discontinuous and sporadic zones like that in the polar and subpolar regions, but the definitions would be somewhat different. If above a certain altitude the permafrost distributes everywhere, then this altitude could be defined as the lower limit of the continuous permafrost; if above a certain altitude only on some sides of the slopes can the permafrost occur, then this altitude could be defined as the lower limit of the discontinuous permafrost; below the discontinuous permafrost zone, only in some localities with a special cryogenic condition can the permafrost occur, then this

kind of permafrost could be defined as the sporadic one (Gorbunov,1978). The permafrost that develops under the thick forest and moss cover and the permafrost that develops in the high-porosity block fields is the typical sporadic permafrost in Mt.Tianshan. This classification is quite simple and useful in permafrost investigation and mapping to distinguish the development condition and distribution characteristics of the cryolithozones. It is questioed that the mounatin mass is cut separately and is discontinuous, the individual summit of the mountain mass rose up to a high absolute altitude with a low mean annual air temperature,say, as low as −10 to −15°C, of course, the summit itself is subject to perennial freezing to a depth of several hundred meters, the temperature in the cryolithozone may be lower than −5 to −10 °C, and all sides of the slopes are underlain by permafrost and could be defined as the continuous permafrost zone;however, on the background of the whole mountain system in middle-low latitudes, the cryolothozone is only a small island occupying. Only several percent of the whole mountain area, in this way the cryolothozone is discontinuous. Thus, there was another suggestion that the permafrost be divided into the stable, less stable, unstable and extremely unstable ones on the basis of their temperature and thickness (Cheng and Wang, 1982). This classification might be more perfect theoretically, however, it needs many data in temperature and thickness obtained from boreholes and other observation sites, so it could only be used in some areas being studied in detail. A perfect classifiction should be available for the planning of engineerings and for the prediction of possible change of environment in the near future, in addition, it should also be simple and clear on the basis of parameters easier to obtain. Much more work is needed for searching a perfect classification of mountain permafrost.

REFERENCE

Cheng Guodong and Wang Shaoling,1982,On the permafrost zonation of the high-altitude permafrost in China. Journal of Glaciology and Geocryology, 4(2),pp.1-17.

Cheng Guodong and F.Dramis, 1992, Distribution of mountain permafrost and climte. Permafrost and Periglacial Processes. 3.2,pp83-91.

Ershov, E.D. et al, 1989 a, Geocryology in USSR (Eastern Siberia),"NEDRA" Press, Moscow. p.515.

Ershov,E.D. et al, 1989 b, Geocryology in USSR(Central Siberia) "NEDRA" Press, Moscow. p.414.

Ershov,E.D. et al, 1989c, Geocryology in USSR (Mountain Regions in Southern USSR)."NEDRA" Press, Moscow. p.359.

Gorbunov, A.P., 1978, Permafrost investigations in high-mountain regions. Arctic and Alpine Research. Vol.10,No.2.pp283-294.

Gorbunov, A.P., 1988, The alpine permafrost zone of the USSR. in:Proceedings of The Fifth International Conference on Permafrost. Vol.1. Tapir Publishers, Trondheim.pp.154-158.

Gorbunov, A.P.,1993, Geocryology of the Tianshan. in:Proceedings of The Sixth International Conference on Permafrost. Vol.2.pp. 1105 -1107 .

Guo Dongxin, Wang Shaoling, Lu Guowei and Dai Jinbo,1981,Division of permafrost regions in the Da and Xiao-Hinggan Ling of Northeast China. Journal of Glaciology and Geocryology, 3(3), pp.1-9.

Joint Soviet-Mongolian Scientific Research Geological Expedition, 1974, Geocryological conditions of the Mongolian People's Republic. "NAUKA" Press, Moscow. p.200.

Lomborichen, R.,1993,Cryogenic processes and phenomean in Mongolia. in : Proceedings of the Sixth International Conference. Vol.1. South China Technology University Press. pp.411-415.

Permafrost Institute of Siberian Branch, Academy of Sciences, USSR, 1974, General Geocryology (Obshaya Merzlotovedenye). Science Press, Beijing. p.318.

Qiu Guoqing, Huang Yizhi and Li Zuofu, 1983, Alpine permafrost in Tianshan, China. in: Proceedings of 4th International Conference on Permafrost. National Academy Press, Washington D.C. pp.1020-1023.

Qiu Guoqing, 1993, Development condition of alpine permafrost in Mt.Tianshan, China. Proceedings of Sixth International Conference on Permafrost, Vol.1. South China Technology University Press. pp.533-538.

Shi Yafeng et al, 1964, Basic characteristics of existing glaciers in China. ACTA Geographica Sinica.30(3). pp.183-208.

Shi Yafeng et al, 1988, Explanation to the map of snow, ice and frozen ground in China (1:4000000). Cartographic Publishing House, Beijing. p.32.

Viktor An, 1993, Permafrost in the north of Korean Penisula. in: Proceedings of the Sixth International Conference on Permafrost, Vol.1. South China Technology University Press.pp.843-845.

Xu Hongzhu, 1981, Xu Xiake's Travels. Acient Literature Publishing House, Shanghai. p.82.

Zhou youwu, Qiu Guoqing and Guo Dongxin, 1991, Quaternary permafrost in China. Quaternary Science Review. Vol.10.pp.511-517.

LINEAR CONSTRUCTION IN COLD REGIONS — PAVED ROADS AND AIRFIELDS

Ted S. Vinson

Professor, Department of Civil Engineering, Oregon State University, Corvallis, OR 97331

The performance of paved roads and airfields in cold regions may be categorized with respect to three modes of distress: (1) distortion and pavement faulting, (2) disintegration, and (3) cracking. By far the most prevalent problem for an asphalt concrete pavement is cracking. Cracking may be traffic/load associated or non-traffic/load associated. Traffic/load associated cracking may be related to fatigue failure and subgrade rutting in an asphalt concrete pavement structure. Low temperature cracking may be caused by two distress mechanisms. First, transverse cracks can extend through the entire pavement structure and into the subgrade. This type of transverse crack is associated primarily with the thermal contraction of soil (in the base, subbase, and/or subgrade) rather than the asphalt concrete surface layer. Second, transverse thermal cracks can occur wholly in the asphalt concrete surface layer. Methodologies presently exist to allow the resistance of an asphalt concrete pavement to fatigue, subgrade rutting, and low temperature cracking to be quantified and easily incorporated in pavement design for the subarctic and arctic.

INTRODUCTION

Roads and airfields located in the arctic and subarctic may be classified into three distinct groups: (1) gravel surfaced, (2) "flexible" — bituminous surfaced, and (3) "rigid" — portland cement concrete (PCC) surfaced. For example, the Alaska Department of Transportation and Public Facilities (Alaska DOTPF) maintains a total centerline network of about 8000 km (5000 mi) of which about 3520 km (2200 mi) are paved. Essentially all of the paved roads are bituminous surfaced (asphalt concrete (AC), bituminous surface treatment, seal coat, etc.). However, in Russia essentially all paved roads in the arctic and subarctic are rigid portland cement concrete (i.e., prefabricated slabs).

Virtually all roads and airfields in the subarctic and arctic were initially constructed of a gravel fill placed directly on the existing vegetation to take advantage of the insulation and latent heat capacity of the surface organic layer (Crory, 1988). The bearing surface was created by adding fines to "bind" the gravel, which was then compacted and graded. The binder material was necessary because the aggregates which were used were not crushed.

Since the number of paved roads and airfields in the subarctic and arctic is not great, their performance and factors which cause distress to asphalt concrete may not be fully appreciated by professionals involved in their design and construction. The purpose of this paper is to provide a review of the performance of paved roads and airfields in the subarctic and arctic and to briefly discuss design methodologies to relate to three major distress modes in an asphalt concrete pavement, namely, fatigue, subgrade rutting, and low temperature cracking.

PERFORMANCE OF PAVED ROADS AND AIRFIELDS IN THE SUBARCTIC AND ARCTIC

Road and airfield pavement performance in cold regions may be categorized with respect to three modes of distress (Vinson et al., 1986): (1) distortion and pavement faulting, (2) disintegration; and (3) cracking. In the discussion that follows, a background of these distress modes together with a limited review of the current state-of-the-art of research and/or practice is presented.

Distortion and Pavement Faulting

Frost heave and thaw degradation in the active layer are primary causes of distortion (movement) and faulting of pavements in the arctic and subarctic. Distortion distress is also associated with buried structures remaining fixed while the surrounding soil heaves or "jacking" out of the ground under successive freeze-thaw cycles.

Frost heave distortion is greatest toward the end of the winter. Evidence of differential movements for asphalt concrete pavements after spring thaw is generally suggested by scrape marks from a snow plow blade. Very often, however, differential movements are not obvious after spring thaw. Remnant evidence of differential movement may be associated with loss of fines beneath a distorted section that results in "lipping" at a crack or the formation of a "birdbath".

The greatest differential movements observed over a one-year period are generally associated with differences in soil frost heave response, for example, a difference in soil response may occur between a backfill material in a culvert trench and the adjacent soil underlying the pavement. If the backfill soil is identical to the adjacent soil underlying the pavement, the differential movements may be reduced, but generally cannot be eliminated if the soil is frost susceptible.

Berg and Johnson (1983) noted that drains, culverts, or utility ducts placed under pavements on frost susceptible subgrades often experience differential heave and should be avoided. They provide guidelines for transition zones for culverts or utilities that must be placed beneath pavements on frost susceptible soils as well as longitudinal and transverse transitions to accommodate interruptions in pavement uniformity.

Rice (1975) succinctly identified the causes of frost heave as the three W's: winter, water, wick (i.e., cold temperatures, access to

water, a frost susceptible soil). It is universally recognized that mitigation of distress related to frost heave involves the elimination of one or more of these factors. Considering the evolutionary history of most roads and airfields it may not be practical to remove frost susceptible soils since they often comprise most of the embankment. Consequently, insulation is experiencing increased use to prevent the advance of the freezing front into the embankment to mitigate frost action (Kestler and Berg, 1989).

A consideration of frost heave suggests the related problem of thaw weakening in the pavement structure. Pavement deterioration under repeated loads is a process of cumulative damage. During spring thaw, the supporting capacity of a pavement surface layer provided by the base, subbase, or subgrade, can be reduced owing to excess pore-water in the supporting layers. Under these conditions damage accumulation for a given traffic volume and load is greatest and can lead to a substantial reduction in overall pavement life (Rutherford and Mahoney, 1986). An example calculation which follows the mechanistic approach to pavement design (Mahoney and Vinson, 1983) suggests the magnitude of the problem at the Nome Airfield (Vinson and Rooney, 1991). Considering the potential for a fatigue failure in the asphalt concrete under three design aircraft loadings at the Nome Airfield, it was demonstrated that 85% of the annual damage occurs in a one month "typical" spring thaw condition.

Adequate drainage provisions can mitigate thaw weakening and damage accumulation in a pavement structure. As thaw progresses from the surface downward the water released can, in general, only drain upwards (since the ground is frozen beneath and lateral redistribution is often not possible owing to slower thawing and/ or less permeable soils in the vicinity of the shoulders). The situation points to the definite need for free draining base and subbase courses and longitudinal drains to remove the thaw water. Impedance of subsurface drainage elements caused by frozen soils must be considered in the design process (Berg and Johnson, 1983).

Distortion distress of pavements in the subarctic and arctic caused by thaw-consolidation of underlying ice-rich permafrost is related to conductive and/or convective heat transport processes. Representative case histories which document this problem have been presented for Nome (Rooney et al., 1988), Kozebue (Esch and Rhode, 1976), and Bethel (McFadden and Seibe, 1986) airfields. It is extremely important when seeking a solution to a permafrost degradation problem to identify the contribution related to conductive versus convective heat transport processes. Permafrost degradation related to conduction may be associated with an inadequate thickness of gravel fill and/or the change in albedo of the surface when it is paved. Traditional solutions for a conduction problem are to increase the thickness of the fill (Hennion and Lobacz, 1973) or insulate the problem area (Esch 1973, 1986; Esch and Rhode, 1976; Rooney et al., 1988). Non-traditional solutions include changing the surface albedo using paint (Fulweider and Aitken, 1963; Berg and Aitken, 1973; Berg and Esch, 1983), the use of thermoprobes (or thermosyphons) (McFadden and Siebe, 1986), prevention of snow acting as an insulation blanket during the winter (Zarling et al., 1988), use of air duct systems (Zarling et al., 1983), and pre-thawing followed by dynamic consolidation (Rooney et al., 1988).

Permafrost degradation related to convective heat transport is associated with ground water flow beneath the airfield or through the embankment. The influence of convection is to cause a positive inflow of heat into the system, thereby slowing down or preventing long-term freeze back or, alternatively, accelerating the depth of thaw. The solution to a convective heat transport problem generally involves the modification of an existing subdrain system and/or the enhancement of subsurface drainage away from the pavement structure embankment.

Rutting distortion can occur in the asphalt concrete surface layer. The mechanistic approach of pavement design presented in a later section of this paper considers rutting related to the accumulation of deformations associated with vertical strain at the top of the subgrade. A discussion of rutting related to the use of low viscosity asphalt cements in cold regions is given by Janoo (1989). He notes that rutting is related primarily to the aggregate in the mix and to a much lesser degree the grade of the asphalt cement. To minimize the potential for rutting, a well-graded angular aggregate (with two or more fracture faces) is recommended. The occasional practice of adding one-half percent to the design asphalt cement content should be avoided as it may contribute substantially to rutting.

Disintegration

Disintegration is the breaking up of a pavement into small, loose particles. Disintegration may be accelerated by freeze-thaw cycles, or traffic loading, especially adjacent to cracks.

In an asphalt concrete pavement, disintegration is generally related to insufficient asphalt cement content in the mix, poor compaction of the mix (which may be related to cold weather construction (Eaton and Berg, 1978)), overheating of the mix, or asphalt stripping. The first three problems can be avoided by carefully following conventional mix design practice and conscientiously supervising the construction of the pavement. The potential for stripping may be overlooked!

Stripping of an asphalt concrete pavement is the loss of adhesion between the asphalt cement and the aggregate. Stripping is due to the action of water or water vapor in the asphalt concrete pavement. Specifically, water gets between the asphalt cement film and the aggregate surface. Since the aggregate surface generally has a greater attraction for water than asphalt, the water is drawn between the asphalt cement and aggregate surface and strips the asphalt away from the aggregate. The rate at which stripping takes place depends on the temperature, type of aggregate, and viscosity and composition of the asphalt (Tyler, 1938). A summary and evaluation of laboratory test procedures used to identify the potential for stripping has been prepared by Terrel and Shute (1989).

Two characteristic types of pavement failures are associated with stripping. If water enters the asphalt cement pavement through the upper surface, raveling of the aggregate occurs. If stripping occurs from the bottom of the pavement upwards, random cracking and potholing is generally not detected until it is too late to prevent.

Concern for stripping suggests that the asphalt concrete should be densely compacted to achieve maximum impermeability. If the pavement has a high voids content, water will enter at the surface and create the potential for stripping. Further, water can enter the pavement through cracks.

Winter snow removal practices can also create potential for stripping. Snow plowed to the sides of a roadway prevents the frozen shoulders from thawing during warmer periods. The frozen shoulders act as a barrier to drainage of free water provided by de-icing salts/solutions or snow/ice thaw associated with the heat absorbing black asphalt pavement.

Cracking

By far the most prevalent airport pavement performance problem is cracking. Cracking may be traffic/load associated or non-traffic/load associated. With respect to roads, both traffic/ load and non-traffic/load associated cracking may exist. With respect to airfield pave-

ments, non-traffic/load associated problems related to changes in temperature in the pavement structure and underlying ground are predominant.

Fatigue of asphalt concrete refers to cracking caused by repeated bending due to traffic. Fatigue related to pavement cracking is often referred to as "alligator cracking." The mechanistic approach to pavement design presented in a later section of this paper considers fatigue cracking related to the accumulation of deformation associated with tensile strains at the bottom of the asphalt concrete surface layer.

Reflection cracks are an expression of the crack pattern in an underlying pavement. They are caused by horizontal and/or vertical movements in the pavement beneath an overlay. Reflection cracks may be observed in both asphalt concrete overlays on old PCC pavements and asphalt concrete pavements. Despite extensive work using techniques such as stress and strain relief interlayers, geotextiles, or reinforcing in the overlay, an economic solution to prevent reflection cracks does not exist. Reflection cracks have been observed within 6 to 12 months after construction of an overlay on a 50 mm asphalt concrete surface that was cold milled to an initial thickness of 12 mm (Vinson et al., 1986). The only way to completely eliminate reflection cracking is to remove the old pavement.

Reflection cracks have been associated with the use of a cement treated base (CTB). Vita et al. (1988) did not find this to be the case at the Bethel, Alaska, Airfield which consists of a CTB underlying an asphalt concrete pavement. CTB reflection cracks did not appear to be a serious problem at Bethel. In fact, the construction and performance of CTB in cold regions has been very successful and it should be considered for more routine use in the future (Vinson et al., 1984).

Two distress mechanisms are believed to cause thermal cracking in the subarctic and arctic (Fromm and Phang, 1972; Esch and Franklin, 1989; Tian and Dai, 1988). First, transverse cracks may be caused by the overall contraction of the entire pavement structure and/or underlying subgrade. This mechanism may cause the crack to extend through the entire pavement structure and into the subgrade. The crack can extend across the pavement surface into the shoulder and be several inches wide. This type of transverse crack is associated primarily with the thermal contraction of soil (in the base, subbase, and/or subgrade) rather than the asphalt concrete surface layer. In fact, they can occur in both paved and unpaved roads and airfields at intervals of 12 to 90 m and depths extending to 2 m (Esch and Franklin, 1989).

Second, low temperature cracking is attributed to tensile stresses induced in the asphalt concrete pavement as the temperature drops to an extremely low temperature. If the pavement is cooled to a low temperature, tensile stresses develop as a result of the pavement's tendency to contract. Friction between the pavement and the base layer resists the contraction. If the tensile stress induced in the pavement equals the strength of the asphalt concrete mixture at that temperature, a microcrack develops at the edge and surface of the pavement. Under repeated temperature cycles or the occurrence of colder temperatures, the crack penetrates the full depth and across the asphalt concrete layer. Tian and Dai (1988) note that it may be possible for a thermal crack to reflect up through the asphalt concrete layer from an underlying stabilized layer if the coefficient of contraction of the stabilized layer is greater than that of the asphalt concrete layer.

The primary pattern of low temperature cracking is transverse to the direction of traffic and is fairly regularly spaced at intervals of 30 to 60 m for new pavements to less than 5 m for older pavements. If the transverse crack spacing is less than the width of the pavement, longitudinal cracking may occur, and a block pattern can develop. The complex pattern of cracking that may be observed in many older pavements is a result of (1) the increase in stiffness (i.e., hardening) of the asphalt cement with age, and (2) the change in the geometry of the pavement slab. On the taxiway at Fairbanks Airfield a 3 m "block pattern" developed on the taxiway associated with longitudinal and transverse thermal cracks (Esch and Franklin, 1988).

Fromm and Phang (1972) noted that the transverse cracks caused by the overall contraction of the pavement structure and subgrade are not as serious as cracks occurring wholly in the asphalt concrete surface layer. Cracks restricted to the asphalt concrete surface layer allow ingress of water which in turn increases the rate of stripping and allows pumping of a fine granular base course. Water entering the crack during the winter may result in the formation of an ice lens below the crack which produces upward lipping at the crack edge. Also, de-icing solutions may also enter the crack and cause localized thawing of the base which, in turn, may result in a depression around the crack. Cedergren and Godfrey (1974) noted that 70% of surface runoff can enter a crack 1 mm wide.

CURRENT PAVEMENT DESIGN PRACTICE FOR TRAFFIC/ LOAD RELATED CRACKING

Corps of Engineers Procedure

Since World War II, the Corps of Engineers has developed pavement design procedures (road and airfield) that can be used to develop structural design requirements. The available design procedures for pavements subject to freezing and thawing in the underlying soils are based on either of two basic concepts:

- Control of surface deformation resulting from frost heave (or thaw).
- Provision of adequate bearing capacity during the most critical climatic period.

Based on the above considerations, three separate design approaches can be used:

- Complete protection method: Sufficient thicknesses of pavement and non-frost susceptible base course are provided to prevent frost penetration into the subgrade.
- Limited subgrade frost penetration method: Sufficient thicknesses of pavement and non-frost susceptible base course are provided to limit subgrade frost penetration to amounts that restrict surface deformation to within acceptable limits.
- Reduced subgrade strength method: The amount of frost heave is neglected and the design is based primarily on the anticipated reduced subgrade strength during the thaw.

Hennion and Lobacz (1973) recommend that seasonal thawing and freezing should be restricted to the pavement (surfacing and non-frost susceptible base course) in continuous permafrost regions. The concept is comparable to the complete protection method wherein the critical factor is the depth of thaw rather than the depth of frost penetration.

Alaska DOTPF Procedure

The Alaska DOTPF (1982) has issued pavement design guidelines based on research begun in 1976. The primary objective was to study the various relationships that controlled the performance of flexible pavements. Approximately 120 pavement sections were selected on the existing state maintained road network for the research program. The results of that study (McHattie et al, 1980) significantly influenced the design procedure.

The Alaska DOTPF design guidelines focus on the fact that increased fines (No. 200 minus material in the unbound layers of a

pavement structure) lead to increased thickness of asphalt concrete surfacing. In those areas of Alaska where asphalt concrete is readily available, increased fines in the underlying layers may be acceptable. However, in remote arctic regions the production of asphalt concrete is expensive and should be minimized. Thus, it is prudent to specify non-frost susceptible (NFS) materials in the underlying layers to the extent possible to minimize the following:

- The requirements for asphalt concrete (if not eliminate its need, altogether);
- The potential for frost heave;
- The potential for other types of pavement distress such as alligator cracking and rutting.

Mechanistic Design Approach

A mechanistic approach to pavement design involves (1) predicting stresses, strains, and deflections in a pavement structure owing to a specified geometry and magnitude of wheel loading conditions, and (2) adjusting the properties and thicknesses of the elements in the pavement structure to insure the predicted stresses, strains, and deflections are within allowable limits. The mechanistic approach provides flexibility in modeling a pavement structure owing to the fact that measured material properties associated with a range of thermal and drainage conditions in the field may be incorporated in the analysis.

In the mechanistic approach calculated strains at critical locations in the pavement structural section are limited to acceptable levels for a specified number of load repetitions (i.e., the design life). Knowledge of strains under design loading conditions at critical locations in a pavement structure allows an estimate of design life to be made or the structural adequacy of the pavement to be assessed. Two conditions are generally employed to define failure of the pavement structure:

- Surface layer fatigue failure. The tensile strain at the bottom of the surface layer cannot exceed the maximum allowable tensile strain for a specified number of load repetitions.
- Subgrade rutting failure. The vertical compressive strain at the top of the subgrade cannot exceed the maximum allowable vertical strain for a specified number of load repetitions.

In the mechanistic approach, the stresses, strains, and deflections in a pavement structure may be predicted using resilient moduli of the materials comprising the structure and multilayer elastic theory. The resilient moduli of the materials comprising the runway pavement structure are determined (1) in the laboratory under repeated load test conditions that simulate traffic loading (Vinson, 1989), or (2) with non-destructive falling weight deflectometer surveys of an existing pavement structure (Vinson et al., 1989, 1991). The stresses, strains, and deflections in a pavement structure may be computed using available computer programs (Hicks, 1982).

Mahoney and Vinson (1983) illustrate the mechanistic design approach for several conceptual pavement structures subjected to representative arctic environmental and loading conditions (specifically Barrow, Alaska). Limiting pavement response parameters included (1) pavement surface deflection (associated with fatigue cracking and/or rutting), (2) horizontal tensile strain at the bottom of an asphalt concrete surface layer (associated with fatigue cracking), (3) vertical compressive stress at the top of rigid board insulation (associated with the design compressive strength of the material), and (4) vertical compressive strain at the top of the subgrade (associated with rutting). Pavement structural sections of various thicknesses of asphalt concrete, base, insulation, and subgrade were considered under three environmental conditions: (1) early winter, (2) late winter, and (3) spring thaw. The design loading condition selected was a fully loaded "DJB" dump truck and 100,000 repetitions in a 20-year design period.

LOW TEMPERATURE CRACKING OF SUBARCTIC AND ARCTIC ROADS AND AIRFIELDS

It is inevitable that low temperature cracking will occur in asphalt concrete pavements constructed in the subarctic or arctic. Esch and Franklin (1988) state that all pavements in Alaska, with the possible exception of those in the south-coastal areas, can be expected to suffer from thermal contraction cracking. Therefore, it is imperative that design engineers involved in establishing the requirements for pavement structures identify an asphalt concrete mixture that will minimize low temperature cracking without compromising other performance characteristics, for example, resistance to rutting.

Three approaches may be employed to identify the low temperature cracking resistance of an asphalt concrete mixture: (1) regression equations, (2) mechanistic prediction, and (3) simulation measurement.

Regression Equations

Based on an analysis of data from 26 airfields in Canada, Haas et al. (1987) established the following regression equation to predict the average transverse crack spacing in a pavement structure:

$$TCRACK = 218 + 1.28\ ACTH + 2.52\ MTEMP + 30\ PVN - 60\ COFX \quad (1)$$

in which,

TCRACK	=	Transverse crack average spacing in meters
MTEMP	=	Minimum temperature recorded on site in °C
PVN	=	McLeod's dimensionless Pen Vis Number
COFX	=	Coefficient of thermal contraction in mm/1000 mm/°C
ACTH	=	Thickness of the asphalt concrete layer in centimeters

The PVN in equation (1) (determined from the penetration at 25°C and the kinematic viscosity at 135°C) is an indicator of temperature susceptibility of the asphalt cement (McLeod, 1987). As the PVN decreases, for a given grade of asphalt, the temperature susceptibility increases. Consequently, as the PVN decreases, the average crack spacing increases. Further, crack spacing increases with pavement age and minimum temperature, but decreases with pavement thickness. These trends are expected based on the observations of other researchers.

Equation (1) may not be applicable to roads and airfields in the subarctic and arctic. The 26 airfields considered were south of the 50° north latitude. Fifteen were "coastal associated" airfields. Approximately half of the observations were made for pavement overlays. Finally, extracted asphalt cement properties were used to develop the regression equation(s).

Mechanistic Prediction

Low temperature cracking occurs in the surface layer when the thermally induced tensile stress (owing to the pavement's tendency to contract with decreasing temperature) equals the tensile strength of the asphalt concrete mixture. The thermally induced tensile stress is generally calculated from a pseudo-elastic beam analysis equation of the following form (Hills and Brien, 1966):

$$\sigma(\dot{T}) = \alpha \sum_{T_o}^{T_f} S(t,T) \cdot \Delta T \qquad (2)$$

in which,

$\sigma(\dot{T})$	=	accumulated thermal stress for a particular cooling rate, $\dot{T}$,
α	=	coefficient of thermal contraction,
T_o, T_f	=	initial and final temperature, respectively,
$S(t,T)$	=	asphalt mix stiffness (modulus), time- and temperature-dependent,
ΔT	=	temperature increment over which $S(t,T)$ is applicable.

The approximate solution suggested by equation (2) may yield reasonable results providing that two input parameters are correctly measured or assumed: (1) the coefficient of thermal concentration, and (2) the asphalt concrete mix stiffness. The tensile strength of the asphalt concrete mixture may be estimated or measured in the laboratory in either direct or indirect tension. In the mechanistic approach the fracture temperature is established by equating the tensile stress calculated from equation (2) with the tensile strength at that temperature.

The determination of both the asphalt concrete mix stiffness and the tensile strength requires that the rate of cooling in the field (and the associated development of tensile stresses and strength) be related to a rate of loading or deformation in the laboratory (or in the case of a creep test, a time after initial loading). To date, a procedure to accomplish this task has not been conclusively demonstrated to the pavement engineering community. Further, in the calculation of thermal stress the thermal contraction coefficient is generally assumed to be 2 to 2.5 $\times$ 10^{-5}/°C. Recent measurements of the thermal contraction of mixes with high voids contents or mixes employing modified asphalt cement suggest this assumption could be in error by a factor of two or three. Further, age conditioning of the specimens for the determination of the mix stiffness or tensile strength has not been considered in the application of this approach. Finally, it has been noted by several researchers that any approach that is fundamentally related to a measurement of the stiffness of the mix will not be acceptable for mixtures which employ modified asphalt cements.

Simulation Measurement

Monismith et al. (1965) were the first to suggest that the thermally induced stress, strength, and temperature at failure could be measured in a laboratory test which simulated conditions to which a pavement slab was subjected in the field. The basic requirement for the test system is that it maintains the test specimen at constant length during cooling. Arand (1987) made a substantial improvement to the test system by inserting a displacement "feedback" loop which insured that the stresses in the specimen would not relax because the specimen length is continuously corrected during the test.

A recent version of this system developed under the Strategic Highway Research Program (SHRP) is presented by Vinson et al. (1993). The thermal stress restrained specimen test (TSRST) system consists of a load frame, screw jack, computer data acquisition and control system, low temperature cabinet, and temperature controller. A beam or cylindrical specimen is mounted in the load frame which is enclosed by the cooling cabinet. The chamber and specimen are cooled with vaporized liquid nitrogen. As the specimen contracts, LVDTs sense the movement and a signal is sent to the computer which in turn causes the screw jack to stretch the specimen back to its original length. This closed-loop process continues as the specimen is cooled and ultimately fails. Measurements of elapsed time, temperature, deformation and tensile load are recorded with the data acquisition system.

Under the SHRP effort over 400 TSRSTs were performed to characterize the thermal cracking resistance of asphalt-aggregate mixtures. Based on the test results, the following conclusions are appropriate:

- TSRST results provide an excellent indication of low temperature cracking resistance of asphalt concrete mixtures. A ranking of low temperature cracking resistance based on TSRST fracture temperature is in excellent agreement with a ranking based on the physical properties of asphalt cements.
- Based on a substantial number of test results, asphalt type, aggregate type, and air voids contents are factors which have a major effect on the low temperature characteristics of asphalt concrete mixtures. Softer asphalt cements and aggregates with a rough surface texture and angular shape provide greater resistance to low temperature cracking of asphalt concrete mixtures. Fracture strength was greater for mixtures with low air voids content.
- The degree of aging has a significant effect on low temperature cracking resistance of mixtures. As the degree of aging of a mixture increases, fracture temperature becomes warmer and fracture strength decreases. The degree of the influence of aging depends on the asphalt type.
- Increasing the amount of asphalt cement in the mixture does not improve the resistance of the mixture to low temperature cracking.
- The TSRST can be used in routine mix evaluation for low temperature cracking resistance of asphalt concrete mixtures.

Vinson et al. (1993) have presented a framework to evaluate the low temperature cracking resistance of road and airfield pavements based on TSRST results.

SUMMARY AND CONCLUSIONS

Professionals involved with the design of pavements in the subarctic and arctic must be concerned with three modes of distress: (1) distortion and pavement faulting, (2) disintegration, and (3) cracking. By far the most prevalent problem for asphalt concrete pavements is cracking, followed by distortion related to differential frost heave. Methodologies presently exist to allow the resistance of an asphalt concrete pavement to fatigue, subgrade rutting, and low temperature cracking to be quantified and easily incorporated in pavement design for the subarctic and arctic.

REFERENCES

Alaska DOTPF (1982) Guide for flexible pavement design and evaluation, Anchorage, AK, and Alaska DOTPF (1993) Preconstruction Manual, Chapter 11-Design.

Arand, W. (1987) Influence of bitumen hardness on the fatigue behavior of asphalt pavements of different thickness due to bearing capacity of subbase, traffic loading, and temperature. Proc., 6th International Conference on Structural Behavior of Asphalt Pavements, University of Michigan.

Berg, R. and T. Johnson (1983) Revised procedure for pavement design under seasonal frost conditions. Special Report 83-27, USACRREL, Hanover, NH.

Berg, R.L. and G.W. Aitken (1973) Some passive methods of controlling geocryological conditions in roadway construction. Proc., North American Contribution, 2nd International Conference on Permafrost, Yatutsk, USSR.

Berg, R.L. and D.C. Esch (1983) Effect of color and texture on the surface temperature of asphalt concrete pavements. Proc., 4th International Conference on Permafrost, Fairbanks, AK.

Cedergren, H.R. and K.A. Godfrey (1974) Water: key cause of pavement failure. Civil Engineering, ASCE.

Crory, F.E. (1988) Airfields in arctic Alaska. Proc., 5th International Conference on Permafrost, Vol. 3, Trondheim, Norway.

Eaton, R.A. and R.L. Berg (1978) Temperature effects in compacting an asphalt concrete overlay. Proc., Cold Regions Specialty Conference, ASCE, Vol. 1, Anchorage, AK.

Esch, D.C. (1973) Control of permafrost degradation beneath a roadway by subgrade insulation. Proc., North American Contribution, 2nd International Conference on Permafrost, Yakutsk, USSR.

Esch, D.C. (1986) Insulation performance beneath roads and airfields in Alaska. Proc., 4th International Conference on Cold Regions Engineering, ASCE, Anchorage, AK.

Esch, D.C. and D. Franklin (1989) Asphalt pavement crack control at Fairbanks International Airfield. Proc., 5th International Conference on Cold Regions Engineering, St. Paul, MN.

Esch, D.C. and J.J. Rhode (1976) Kotzebue Airfield, runway insulation over permafrost. Proc., 2nd International Symposium on Cold Regions Engineering, ASCE.

Fromm, H.J. and W.A. Phang (1972) A study of transverse cracking of bituminous pavements. Proc., AAPT, Vol. 41.

Fulwider, C.W. and G.W. Aitken (1963) Effect of surface color on thaw penetration beneath a pavement in the arctic. Proc., 1st International Conference on the Structural Design of Asphalt Pavements.

Haas, R., F. Meyer, G. Assaf, and H. Lee (1987) A comprehensive study of cold climate airfield pavement cracking. Proc., AAPT, Vol. 56.

Hennion, F.B. and E.F. Lobacz (1973) Corps of Engineers technology related to design of pavements in areas of permafrost. Proc., North American Contribution,2nd International Conference on Permafrost, Yakutsk, USSR.

Hills, J.F. and D. Brien (1966) The fracture of bitumens and asphalt mixes by temperature induced stresses. Proc., AAPT. Vol. 35.

Janoo, V.C. (1989) Use of low viscosity asphalts in cold regions. Proc., 5th International Conference on Cold Regions Engineering, ASCE, St. Paul, MN.

Kestler, M. and R. Berg (1989) Engineering design and construction in permafrost regions: a review. Proc., North American Contribution, 2nd International Conference on Permafrost, Yakutsk, USSR.

Mahoney, J.P. and T.S. Vinson (1983) A mechanistic approach to pavement design in cold regions. Proc., 4th International Conference on Permafrost, Fairbanks, AK.

McFadden, T. and C. Siebe (1986) Stabilization of permafrost subsidence in the airfield runway at Bethel, Alaska. Proc., 4th International Specialty Conference on Cold Regions Engineering, ASCE, Anchorage, AK.

McHattie, R., B. Connor, and D. Esch (1980) Pavement structural evaluation of Alaskan highways. Report No. FHWA-AK-RD-80-1, Alaska DOTPF, Juneau, AK.

McLeod, N.W. (1987) Pen-vis number (PVN) as a measure of paving asphalt temperature susceptibility and its application to pavement design. Proc., Paving in Cold Areas Mini-Workshop, Vol. 1, 147-240.

Monismith, C.L., G.A. Secor, and K.E. Secor (1965) Temperature induced stresses and deformations in asphalt concrete. Proc., AAPT, Vol. 34, 248-285.

Rice, E. (1975) Building in the North. Monograph, The Geophysical Institute, University of Alaska, Fairbanks, AK.

Rooney, J.W., J.F. Nixon, C.H. Riddle, and E.G. Johnson (1988) Airfield runway deformation at Nome, Alaska. Proc., 5th International Conference on Permafrost, Trondheim, Norway.

Rutherford, M. and J.P. Mahoney (1986) A thermal analysis of pavement thawing. Proc., 4th International Conference on Cold Regions Engineering, Anchorage, AK.

Terrel, R.L. and J.W. Shute (1989) Summary report on water sensitivity. Strategic Highway Research Program, National Research Council, SHRP-A/IR-89-1003, Washington, DC.

Tian, D. and H. Dai (1988) Cold cracking of asphalt pavement on highway. Proc., 5th International Conference on Permafrost, Trondheim, Norway.

Tyler, O.R. (1938) Adhesion of bituminous films to aggregates. Purdue University Research Bulletin, No. 62, Vol. 22.

Vinson, T.S. (1989) Fundamentals of resilient modulus testing. Proc., Workshop on Resilient Modulus Testing: State of the Practice, Oregon State University, Corvallis, OR.

Vinson, T.S., D.H. Jung, and J.W. Rooney (1993) Pavement performance and low temperature cracking of subarctic and arctic airfields. Proc., 6th International Conference on Permafrost, Beijing, China.

Vinson, T.S., J.P. Mahoney, and M. Kaminski (1984) Cement stabilization for road construction in Cold Regions. Proc., 3rd International Cold Region Engineering Specialty Conference, ASCE, Edmonton, Alberta, Canada.

Vinson, T.S. and J.W. Rooney (1991) A mechanistic approach to pavement design for Nome Airfield. Proc., 6th International Cold Regions Engineering Specialty Conference, ASCE, Lebanon, NH.

Vinson, T.S., J.W. Rooney, H. Zhou, and N. Coetzee (1991) Tudor Road rehabilitation, Anchorage, Alaska. Proc., Road and Airport Pavement Response Monitoring Systems, ASCE, USACRREL, NH.

Vinson, T.S., H. Zhou, R. Alexander, and R.G. Hicks (1989) Backcalculation of layer moduli and runway overlay design: U.S. Coast Guard Air Station, Kodiak, Alaska. Proc., State of the Art Symposium on Pavement Response Monitoring Systems for Roads and Airfields, USACRREL, NH.

Vinson, T.S., I. Zomerman, R. Berg, and H. Tomita (1986) Survey of airfield pavement distress in cold regions. Proc., 4th International Conference on Cold Regions Engineering, Anchorage AK.

Vita, C.L., J.W. Rooney, and T.S. Vinson (1988) Bethel Airfield, CTB pavement performance analysis. Proc., 5th International Conference on Permafrost.

Zarling, J.P., W.A. Braley, and D.C. Esch (1988) Thaw stabilization of roadway embankments. Proc., 5th International Conference on Permafrost, Vol. 2.

Zarling, J.P., B. Connor, and D.J. Goering (1983) Air duct systems for roadway stabilization over permafrost areas. Proc., 4th International Conference on Permafrost, Fairbanks, AK.

CURRENT DEVELOPMENT ON PREVENTION OF CANAL FROM FROST DAMAGE IN PRC

Chen Xiao-bai

Lanzhou Institute of Glaciology and Geocryology,
Chinese Academy of Sciences, Lanzhou, China

The frost damage condition of canal was very heavy and has been paid much more attention by scientists and engineers in China in last 20 years. The main results conducted *in situ* and *in door* are summarized including frost heave mechanism, classification, water migration and heave distribution along depth, frost heave prediction models and frost heaving force etc. Some anti-heave countermeasures of canal used effectively and widely, such as flexible lining, anti-heave structures, and insulation structures as well, are introduced briefly also.

INTRODUCTION

The annual water discharge in China is the Number 6 in the world and the average for per person is about one fourth of that in the world. The annual amount of water for agriculture using in China is near 88 percentage of total water expended in which the irrigation amount is about 94% of the agricultural one which is almost 82.7% of total amount of water expended in China. However, the utilization coefficient of the irrigation water is only 40 to 50% which means about 42% of the total amount water expended in China was lost during transporting in canal. Comparing with the utilization coefficient of 70 to 80% in the developed countries, about 30 to 50% of water discharge in China was osmosized out off canal because of poor lining. Up to now, the length of lining canal is 10 to 50% of the total in different proviences, for instance, in Xinjiang district there were 23000 km canals with different types of lining which was 10% of the total in 1986; in Xanxi province the length of lining canal was 1009 km in 1988 which was 45% of the total one; In Hunan province there were 8000 km canals with lining which was 19.85% of the total; In Sicuan and Fuje provinces the length of lining canal was 39.37% and 22% of the total one respectively (Jian, 1992).

The seasonally frozen ground is widely distributed to the north of Changjiang River with the half areas of the total in China. The frost depth increases from South to North and from the place with a low elevation to that with a high elevation and with the maximum one of around 3 m. The amount of frost heave is 10 to 30 cm and some over 40 cm. In gerenal, the frost heave will make the canal suffered frost damage as the frost depth is over 50 cm. It is sure that the frost damage to the canal is the main reason causing seepage. According to the statistical data, about half length of canal with concrete lining, 2800 km, was suffered by frost damage in Xinjiang; for the main irrigation network in Xanxi province, the frost crack phenomena were very popular in canal with concrete lining which occurred on the surface of south slope and north slope of the canal with 75.3% and 27% of total area respectively.

The frost damage to the bridge, culvert as well as sluice gate projects was very heavy. Almost all of the timber bridges in Heilongjiang province were suffered frost heave with the maximum frost displacement of 1 to 2 m; In Inner Mongolia district, about 35% of total bridges with different types were in frost damage, and 63% of total culverts were not worked well in which 25% of the total ones suffered very serious frost damage, as about 71% of total sluices were stood frost damage as well.

A large amount seepage of water from canal caused by frost heave made the land at the both sides of canal, 100 to 200 m in wideth, saline-alkalized. For intance, during the thirty years from 50's to 70's, the irrigation area increased to three times in Inner Mongolia while the area saline-alkalized increased to 10 times more than that of before at the first 10 years which was about 73.8% of the total farmming area, and there were about 30% of total farmming area saline-alkalized in Ninxia district.

Since realizing that the frost damage was the main reason causing seepage of canal in the whole regions of North and North-West China with a seasonally frost condition, the water conservancy institutes and colleges in the regions as well as Chinese Academy of Sciences paid more attentions for understanding the mechanism of soil frost heave and finding the more effective ways to prevent the canals and hydraulic structures from frost damage both in door and in situ. Some large observation stations established in Heilongjiang, Gansu, Liaunin, Xanxi, Xinjiang, Inner Mongolia, Shandong, Shanxi and Ninxia Provinces (Autonomous regions)

in which different subjects have been observed such as the frost processes under various types of soil and water conditions, and the regularities on the profiles of water redistribution, frost heave as well as frost heaving forces along the depth. In engineering practice, different anti-heave countermeasurements were conducted with various structures widely including replacing clayey soils with gravel, sand and blown sand with different content of fine grained soils; increasing the density of soils with dynamic consolidation method; strengthening drainage; improving soils with chemical agents; insulating foundation bases by means of effective insulations; anti-heave structures such as arch and curve structures, anchored structures, flexible ones as well as some special structures with large overburden pressure etc. Based on a large amount of data collected from observation stations as mentioned above for years and the wealthy experiences accumulated from practice, a Design Norm for canal was established by The Water Conservancy Ministry of PRC as a professional standard (SL23-91), the other one with a title of Anti-heave Design Norm for Hydraulic structures will be established in not long future by the Ministry. Besides above, according to the local conditions some special detailed rules and regulations for application in engineering practice have been made already by local government. Up to now, it started to the new stage of that the results of frost heave study and experience have been applied to the practical projects in cold regions in China.

NEW RESULTS OF APPLIED STUDY

In the period from 1978 to 1988, because the scientists and engineers have been engaging in understanding the behavors of frost susceptibility of soils during freezing in door and in situ, and in the practice for accumulating the experiences in order to deal with the frost damage problems to the structures in cold regions, some wealthy results could be sumed beriefly as follows:

1. Frost Susceptibility Classification of Base Soils

As well known that the index for evaluating the criteria of frost susceptibility of soils was and is the ratio of frost heave or the rate of frost heave widely. As the variation of frost depth in China from the north to the Changjiang River to the far north is 40 cm to near 300 cm, it is difficult to predict the degree of frost damage to the structure by using the indexes. After analysing large amount of statistical data collected from different regions in China, the regressive results show that the degree of frost damage to the structures depends on the total amount of frost heave. Consequently, the total amount of frost heave has been accepted as an index for evaluating the degree of frost damage of base soils with which the base soils were devided into five classes with the name of Non FH, Weak FH, FH, Heavy FH and Very heavy FH as well which is responsible to the total amount of frost heave of h<2 cm, 2 cm<h=<5 cm, 5 cm<h=<12 cm, 12 cm<h=<22 cm, and h>22 cm respectively (SL23-91).

For the coarse grained sils in the Design Norm, the coarse grained soil contained 6% by weight of fine soil with a size of <0.05 mm is defined as a frost susceptibility soil. However, the author's work indicated (Chen et al, 1988a) that the frost susceptibility of coarse soils depends on not only by the content of fine grained soil by weight but also by the local frost penetration rate,ei.:

$$\eta = f\ (V_f,\ C_d)$$

The formala was illustrated for practical using already (Chen et al, 1988b).

2. A Distribution of Frost Heave along Depth

Based on the observational data in situ, the distribution of FH along depth could be described as: a high FH zone will occur in half down part of frost depth for the condition with a shallow groundwater level; a uniform distribution of FH will appear along depth or a high FH zone occurs in the middle part while groundwater level is not very shallow and not very deep or the drainage condition is very poor; if the ground surface is replaced by sandy gravel cushion, a high FH zone will occur beneath the cushion or nearby groundwater level (Zhu, Q. et al, 1988a). Heilongjiang Provincial Water Conservancy Institute has the similar conclusion. After analysing the data collected from different observation stations, Lionnin Provincial Water Conservancy Institute has sumed various types of FH distribution as shown in Table 1 (LWCI, 1986).

Table 1. A Classification on Distribution of FH along Depth

Class.	G.W.L.*		Soil	G.S.W.**		Clas. FH
	BF	MF		Suf.	Unsuf.	
I	$H_w>H_o$	$H_w>H_o$	Uniform			L/O**** or Uniform
	$H_w>H_o$	$H_w>H_o$	C/S***			
	$H_w<H_o$	$H_w>H_o$	Uniform			
	$H_w<H_o$	$H_w>H_o$	C/S			
	$H_w<H_o$	$H_w<H_o$	Uniform			
	$H_w<H_o$	$H_w<H_o$	C/S			
II	$H_w>H_o$	$H_w<H_c$	C		x	Uniform
	$H_w>H_o$	$H_w<H_o$	C/S		x	
	$H_w<H_o$	$H_w>H_o$	S/C			
	$H_w<H_o$	$H_w<H_o$	S/C			
	$H_w<H_o$	$H_w<H_o$	Uniform			
	$H_w<H_o$	$H_w<H_o$	C/S			
III	$H_w>H_o$	$H_w<H_o$	S			O/L or Uniform
	$H_w>H_o$	$H_w<H_o$	S/C			
	$H_w>H_o$	$H_w<H_o$	C/S	x		
	$H_w<H_o$	$H_w<H_o$	S			
	$H_w<H_o$	$H_w<H_o$	S/C			

*G.W.L.- Groundwater level, $H_w$and H_c-Capilary height; **G.S.W.-Conditions of ground surface water; Suf.-Sufficient, Unsuf.-Unsufficient; ***C-Clayey soil, S-Sandy soil, the left side of/is upper part and the right side of/is down part of frost depth; x-Lake of the term; ****O-Non FH and L-large FH, the mean of/is the same likes above.

3. Determination of Frost Depth

After statistical analysing the data of frost depth with different local conditions collected from 134 meteorological stations in North China for years, a rule of frost depth has been found

by Jiling Provincal Water Conservancy Institute (SL23-91) in which the annual variation coefficient of frost depth C_v will decrease with the increase of frost depth. The standard frost depth could be expressed by freezing index I_o with a function of $H_o=\alpha . I_o^{1/2}$ while $\alpha=2.84 \exp(1.921.10^{-4}.I_o)$. During the calculation of frost depth in practice, some coefficients of frequency model ratio K_f and slope correction K_s as well as groundwater influence K_z are considered as follows:

$$H_d = H_o.K_f.K_s.K_z$$

where, H_d is Design Frost depth and H_o is standard one.

The observational works on an effect of sunshine on the frost depth have been conducted already in Gansu, Xanxi, Ninxia and Shandong districts as well. The results have been applied in the Norm yet in which K_s equals 0.65 to 1.0 for the slope facing sun, 1.0 to 1.2 for the bottom of canal and 1.2 to 1.5 for the slope without sunshine. The groundwater influence coefficient K_z depends on not only GWL but also soil types and is listed in Table 2 (SL23-91).

Table 2. The Value of Groundwater Influence Coefficient K_z

Soil type / G.W.L.	C. & S. with H or M I_1	C. & S. with L I_1	Sand
H_w=>2.0	1.0 -0.95	1.0	1.0
2.0>H_w=>1.5	0.95-0.90	1.0 -0.95	1.0
1.5>H_w=>1.0	0.90-0.84	0.95-0.90	1.0 -0.97
1.0<H_w=>0.5	0.84-0.75	0.90-0.80	0.97-0.94
0.5>H_w=>0	0.75-0.62	0.80-0.70	0.94-0.85

Each signal's mean is shown in Table 4.

Recently years, a theorical frost depth in different conditions with various angles between sunshine ray and ground surface was calculated by means of energe balance method (Gou et al, 1993; Li, 1993).

4. Sufficient Conditions of an Anti-heave Countermeasure by Replacing Clayey Soil with Sandy or Gravel (Chen et al, 1979)

At first, limiting the content of fine grained soil as mentioned above; Secondly, designing a sufficient replacing thickness; and thirdly, having a necessary drainage condition. All of the three is the sufficient conditions of replacing clayey soil with sand or gravel for anti-heave.

Based on the observational data collected in situ, a suitable replacing ratio has been supposed as listed in Table 3 (Zhu, Q.et al, 1988b).

Besides coarse sand and gravel used for cushion meterials, blown sand was and is widely utilized in Gansu and Inner Mongolia districts (Chen et al, 1986; Cheng et al, 1991, Zhu,D. et al, 1986a; Zhau et al, 1986) while a service instruction has been provided by the experimental results in door conducted by the authors (Chen et al, 1986). A detailed service instruction on application of blown sand to canal engineering projects has been established by Inner Mongolia Water Conservancy Institute (IMWCI, 1987).

5. An Effect of Groundwater Level on Frost Heave

Table 3. Replacing Ratio of Anti-heave Cushion of Canal

G.W.L.* (cm)	Soil type	Replacing ratio** ε (%) Up. p.s.	Dow. p.s. & Bot.
$H_w>H_d+250$	Clayey soil with high I_1 & silty soil	50-70	70-80
$H_w>H_d+150$	Clayey soil with middle I_1 & silty soil		
$H_w>H_d+150$	Clayey soil with low I_1 & silty soil	40 -- 50	
H_w < that mentioned above	Clayey soil with high or middle I_1 & silty soil	60-80	80-100
	Clayey soil with low I_1 & silty soil	50-60	60-80

*G.W.L.-Groundwater level, H_w; H_d-Design frost depth; ε** -Percentage of replacing depth to frost depth; Up.p.s.-Upper part of slope; Dow.p.s. & Bot.-Down part of slope & Bottom of canal; I_1-Liquid limit of water content.

A large amount of results collected from observational stations in situ and engineering practices show that there is a critical groundwater level H_{wo}. While H_w=>H_{wo}, the frost heave will be independent on groundwater level. After analysing the statistical data, the value of critical groundwater level H_{wo} was listed in Table 4 (SL23-91).

Table 4. The Value of Critical Groundwater Level

Soil type	C. with H I_1 & S.	C. with M I_1 & S.	C. with L I_1 & S.	Sandy soil
H_{wo}(m)	2.0	1.5	1.0	0.5

C.-Clayey soil; S.-Silty soil; I_1-Liquid limit of water content; H-High; M-Middle; L-Low.

Based on the results collected in situ from Xinjiang, Liaunin, Gansu, Xanxi, Heilongjiang etc, a regression function for expressing the relation between frost heave ratio and groundwater level H_w is as follows:

$$\eta = a \ EXP \ (-b \ H_w)$$

The function has been conducted in door already (Chen et al, 1988c). In order to use the relation conveniently in engineering practices, an apparent frost heave ratio f was recommended which is defined as follows:

$$f=h/(H_f+h)\times 100\% = \eta/(100+\eta) = \alpha_1 EXP(-\beta_1 H_w)$$

After regression of observational results in situ, the value of the constants of α_1 and β_1 is listed in Table 5 (SL23-91).

Table 5. The Value of α_1 and β_1

Soil type	H_w	α_1	β_1
C. with H I_1 & S.	$0=<H_w=<1.0$	40-30	1.25
	$1.0<H_w=<2.5$	27-21	0.85
C. with M I_1 & S.	$0=<H_w=<2.5$	30-19	1.1
C. with L I_1 & S.	$0=<H_w=<1.5$	19-14	1.2

*The constants have to be used the bigger value while I_1 is higher.

While $H_w>H_{wo}+0.5$ m defined as a deep groundwater level, the apparent frost heave ratio f could be expressed by:

$$f = \alpha_2(W - \beta_2 Wp)$$

where, α_2 equals 0.4 to 0.5 while the content of clayey soil varies from 10% to 30% by weight;
β_2 equals 0.7 to 0.9, and the more the content of silt the less the value;
W-the average water content of soil profile by weight along standard frost depth collected at the period of five days early or later while air temperature down to 0°C;
Wp-plastic limit of water content of soil.

6. Frost Heave Prediction Models

The mechanism of frost heave is quite complex which depends on not only soil type but also hydraulic-geological condition and local climate etc. As a result, it is difficult to find an uniform model. Scientists and engineers who work in different regions have had their own experience and data collected by themself and they have their own custom to deal with their own problems they met. Some frost heave prediction models for using in canal engineering are introduced as follows:

1) Gansu models (GSWCI, 1986)--
For heavy silty loam $\eta=60.5\ EXP(-0.0164H_w)$
For sandy loam $\eta=284/H_w + 0.2$
For midium fine sand $\eta=65.2/H_w + 0.15$

2) Xinjiang model (Zhu, D. et al, 1986)--
$\eta=a\ EXP\ (-bH_w)$

where, the constants a and b for different situations were listed in Table 6.

3) Liaunin model (Wang, 1987)--

$$f=\alpha[40.0\ EXP(-1.2H_w) + C.H_w]$$

where, the constant α depends on not only soil type but also frost penetration rate V_f and the decay speed of groundwater level V_{gw1} as well, and is listed in Table 7; the constant C is an average affecting coefficient of surface water supply in the ten days around ground surface freezing, and is listed in Table 8.

4) Comprehensive model (Chen & Wang, 1991)--
For coarse grained soil in open system, frost heave ratio η mainly depends on both the content of fine grained soil by weight with a size of given diameter d, C_d, and frost penetration rate V_f, the function could be expressed by:

$$\eta = B_o\ V_f^{B_1}\ C_d^{B_2}$$

After regression, the constants B_o, B_1, B_2 are listed in Table 9 which depends on the size of fine grained soils.

Table 6. The Value of the Constants a and b for Canal

Location / Soil type	E slope		W slope		Bottom	
	a	b	a	b	a	b
Silty clay	16.64	.0062	16.22	.007	16.90	.0062
Heavy loam	14.71	.0091	13.76	.0099	14.24	.0037
Sandy loam	17.52	.014	13.80	.01	14.58	.010
Sandy soil with gravel	13.37	.014	9.94	.0136	11.70	.011

*E slope or W slope--Slope of canal facing east or west.

Table 7. The Value of α

Soil type	Variation of GWL during freezing	α
Clay & loam I_p=7-20	$V_{gw1}<V_f$	1.1 - 0.7
	$V_{gw1}>V_f$	0.9 - 0.6
Sandy loam I_p=1-7	$V_{gw1}<V_f$	0.7 - 0.5
	$V_{gw1}>V_f$	0.6 - 0.4
Sandy soil I_p<1	$V_{gw1}<V_f$	0.5 - 0.3
	$V_{gw1}>V_f$	0.4 - 0.2

Table 8. The Value of Constant C

Precipitation for* ten days (mm)	0-10	10 - 25	25 - 50	>50
C	0	0.5-1.0	1.0-1.5	1.5-2.0

*nearby starting ground freezing.

Table 9. The Constants of B_o, B_1, B_2 and Correlation Coefficient r

Size diameter d(mm)	B_o	B_1	B_2	r
<0.1	2.6312	-0.9988	0.2480	0.9609
<0.05	2.6870	-0.9988	0.2524	0.9609
<0.005	3.6443	-0.9967	0.3159	0.9616
<0.02	2.9120	-1.0005	0.2703	0.9612
<0.002	3.9485	-0.9961	0.3325	0.9616

For clayey soils with water supply at given groundwater level during freezing, a new model was conducted considering initial water content W(%), initial dry unit weight γ_d(t/m³), frost penetration rate V_f(cm/day), groundwater level H_w(m), plasticity index I_p, and ion content S (mmol/100g soil) as well which could be expressed by:

$$\eta=B_0 W^{B_1}\gamma_d^{B_2}V_f^{B_3}EXP(B_4H_w)EXP(B_5I_p)EXP(B_6S)$$

After curve fitting with 76 groups of experimental data, it could be described as follows:

$$\eta=4.4115\times10^{-5}W^{3.6082}\gamma_d^{4.3459}V_f^{-1.1825}$$
$$EXP(-1.4502H_w)EXP(0.1478I_p)EXP(-0.1225S)$$

While frost heave rate R could be expressed as:

$$R=4.6293\times10^{-6}W^{3.5177}\gamma_d^{4.2673}EXP(-1.6059H_w)$$
$$EXP(0.1637I_p)EXP(-0.1245S)$$

7. Frost Heaving Force

As well knownthat the determination of the value of frost heaving force is very big work which should be observed in situ with large scale and taken many years. Based on the data collected mainly from Heilongjiang Provincial Water Conservancy Institute, Low Temperature Institute and Transportation Institute, a practical value for frost heaving force has been provided. Based on the affecting direction of the force, it could be divided three kinds of frost heaving force: tangential one τ affecting along the lateral surface of foundation; normal one σ affecting the bottom of foundation vertically; horizontal one σ_h affecting the surface of retaining wall horizontally. Table 10, 11 and 12 are listed the values already which can be applied in engineering pratice (SL23-91).

Table 10. The Value of Tangential Frost Heaving Force

Classification	Non FH	Weak FH	FH	Very FH	Very heavy FH
τ (KPa)	30-50	50-80	80-120	120-150	150-200

*For very smooth surface of precast concrete pile, the value should time a coefficient of 0.8; and for the coarse surface of stone pie, the value should time a coefficient of 1.2.

Table 11. The Value of Normal Frost Heaving Force

Area of foundation(m²)	5	10	50	>100
Classification	Standard value σ (KPa)			
Non FH	50-100	30-60	20-50	10-30
Weak FH	100-150	60-100	50-80	30-60
FH	150-210	100-150	80-130	60-100
Very FH	210-290	150-220	130-190	100-150
Very heavy FH	290-390	220-300	190-260	150-210

*The listed value is only available for the slab foundation with a short size of more than 2 m.

Table 12. The Value of Horizontal Frost Heaving Force

Classification	Non FH	Weak FH	FH	Very FH	Very heavy FH
Standard value σ_h (KPa)	<50	50-100	100-150	150-200	200-250

All of the value for frost heaving force has been applied in cold regions in China already.

ANTI-HEAVE COUNTERMEASURES

There are many different anti-heave countermeasures in which some of them were the summarizations of local experience. Here, an outline on some of them used widely in North and Northwest China is briefly summarised.

In order to understand the general benefit of different lining in anti-seepage of canal, a large amount test was conducted in Shanxi and Xanxi proviences etc and the results are listed in Table 13. It is obvious that the flexible film lining is the best one in anti-seepage, and the next is the concrete slab casted in site; the third one is the precast concrete slab. Consequently, the first three linings are widely set up in China nowadays.

1. Flexible lining

Plastic film is the most popular flexible material used very widely as a lining material of canal because it is much effective for anti-seepage with which the total water utilization coefficient of canal could increase 10 to 20% while its cost is 1/5 to 1/12 of that with concrete slab lining. The plastic lining of canal covered by soil as a protection layer has been working for more than 25 years. Besides above, the construction of this kind of lining is very simple, especial it is very convenient in old irrigation network with very shallow groundwater level where the amount of frost heave could be more than 30 cm. Therefore, the plastic film lining develops very quickly, for instance, in Xinjiang district from 1980 to 1985 around 5000 km of canal was lined by plastic film.

Table 13. A Stable Seepage Ratio of Canal with Different Lining under Various Water Depth

L.T. / W.D.(m)	Flexible film	Cast situ conc. slab	Precast conc. slab	Grouted riprap	Without lining
1	1	16.3	23.6	42.7	77.0
2	1	11.0	15.9	41.3	58.3

L.T.-Lining type; W.D.-Water depth; Conc.-Concrete;

Because the stabilization of soil protection layer is a big problem, many scientists and engineers are engaging in it. Based on the experimental results with one of the largest

scale and practical experience in situ, a resonable structure design was proposed by the authors (Chen et al, 1987) with which the slope of soil protection layer upon plastic film will be stable.

2. Anti-heave Structures

1) U shaped canal--Since 1975 the first U shaped canal was set up in Xanxi province (Zhu, Q. et al, 1991) with an optium hydraulic section and saving land 1/2 to 3/4 compared with the tradional ladder shaped canal, and increasing anti-heave capacity as well. In 1983, the U shaped canal built by concrete was set up in Xanxi province for 3600 km and up to now it was finished about 20000 km in China with a biggest discharge of 25.8 m^3/s in irrigation canal. Now the machines for constructing U shaped canal with cast in place or precast concrete with the diameters of 40 cm, 60 cm, 80 cm, 100 cm and 120 cm or more have been used widely in practice.

2) Arch shaped bottom of canal--As well known that the lining corner of canal bottom is easy broken during freezing because of concentrated frost heaving stress. It is shown in practice that the amount of frost heave at the arch shaped bottom is about 1/2 to 1/4 of that at the corner of bottom with a ladder shaped. Consequently, the arch shaped bottom of canal with concrete lining is set up rather popularly in seasonally frost regions in China. The structure with an arch shaped bottom is also used in the tunnel for disappering water head very successful in north-east China with strong frost susceptibility base soil (Wang, S.Y., et al, 1993) which is so called anti-heave structure with an arch shaped.

3) "—" shaped sluice--In norm situation, a sluice will be designed as in optium hydraulic condition with much complex structure. However, this complex structure would not work well in cold region with heavy frost heave because the overburden pressure is so small that could not limit the heave in an allowable one. The "—" shaped sluice with a concentrated load and a buried depth over maximum frost depth was set up firstly in Xijiang district and later in Heilongjiang province which is used widely in north China.

4) Concrete box and geofabric sandwedge retaining well--Some retaining walls were set up by means of concrete box with a space inside which were successful in Heilongjiang province because they were permited to have an allowable displacement during freezing. The sandwedge structures were built up in Inner Mongolia in which local soil was covered by geofabrics and built up one upon another. Since they are very flexibale for dealing with frost heave, so it will be a new anti-heave structure for building retaining wall in future.

3. Insulation Structures

The insulation materials were used beneath concrete lining or foundation, or closed the inside surface of retaining wall for preventing frost penetration into base soil, as a result, the frost heave of insulated base soil will be disappeared or limited. A polystyrene form slab was firstly used beneath concrete lining of canal in Shanxi province by Academy of Water Conservancy, and Shanxi Water Conservancy Institute. It was successful and had a good comprehensive benefit (Jin et al, 1987). Later on, the polystyrene form slab was used beneath the concrete lining of canal slope at the place with water level fluctuation which used to be suffered heavy frost damage in a water transport canal in Shandong province. The thickness of polystyrene form slab is about 1/10 to 1/15 of the design frost depth Hd which depends on the material properties (SL23-91). Besides above, insulation slab is also made of pearlite and mineral wool (Jian, 1992). The total capital expenditure of last two will reduce about 1/3 compared with that of insulated by polystyrene form.

All of that mentioned above is an outline of the current development on the subject for preventing canal from frost damage in China. However, there are lots of problems facing to be solved including technique, capital, adiministration and materials etc. as well.

REFERENCES

Chen, X.B. et al. (1979) On anti-heave measure by replacing clayey soil with gravel. Bulletin of Sciences. No.20, 935-939.

Chen, X.B. et al. (1986) An experimental study on frost susceptibility of wind-blown sands. J. Glaciology & Geocryology, No.3, 233-238.

Chen, X.B. et al. (1987) Saturated-dehydrated consolidation of fill with low density and its application to canal engineering, SCIENTIA SINICA, No.7: A, 779-784.

Chen, X.B. et al. (1988a) Frost susceptibility of sandy gravel during freezing, YANTU GONGCHENG XUEBAO, No.3, 23-29.

Chen, X.B. et al. (1988b) A frost heave model of sandy gravel in open system, Proc. V ICOP, 304-307.

Chen, X.B. & Wang, Y.Q. (1988c) Frost heave prediction model of clayey soils, Cold Regions Sciences and Technology, 15, 233-238.

Chen, X.B. & Wang Y.Q. (1991) A new model of frost heave prediction model for clayey soils, SCIENCE IN CHINA (B), No.10, 1225-1236.

Cheng, M.J. et al. (1991) Some anti-heave countermeasures of canal lining in Inner Mongolia, Technique of seepage pevention, No.2, 107-110.

Design Norm of Anti-heave for Canal Engineering (SL23-91)

Gansu Water Conservancy Inst., (1986) A review on the results of prevention of canal from seepage and frost damage in Gansu province, Technique of seepage prevention of canal, Special Issue (4), 2-5.

Guo, D.X. et al. (1993) On freezing and frost heaving rule of base earth of lined canal of Arbitry slope direction and gradient, Proc. ICOP.

Inner Mongolia Water Conservancy Inst. (1987) An experimental report on prevention of canal from frost damage by using blown sand.

Jian, G. (1992) An outline of current development, problems and suggestions on anti-seepage technique of canal in China, Technique of seepage prevention, No.3, 1-8.

Jin, Y.T. et al. (1987) An experimental study on new material and new structure for preventing canal lining from frost damage.

Li, A.G. et al. (1993) Determination of sunshine and sunshade extent coefficient on canal, Proc. ICOP.

Liaunin Water Conservancy Inst. (1986) On design for prevention of anti-seepage structures from frost damage of canal, Technique of seepage prevention of canal, Special Issue (4), 6-10.

Wang, S.R. (1993) A study on basic types of vertical tunnel for disappering water head and their capacity for anti-heave, Proc. ICOP.
Wang, X.Y. (1987) A study of the relation between frost heave ratio (and apparent one) and groundwater level.
Zhau, B.X. et al. (1986) An experimental results on the prevention of canal from frost heave by using blown sand in open system in Nincheng county, Technique of seepage prevention of canal, Special Issue (4),82-89.
Zhu, D.F. et al. (1986a) A discussion on anti-heave effect of wind-blown sands in irrigation canal, J. Glaciology & Geocryology, No.3, 239-244.
Zhu, D.F. et al. (1986b) An experiment of the effect of soil and water conditions on frost heave of canal with concrete lining, Technique of seepage prevention of canal, Special Issue (4), 123-134.
Zhu, Q. et al. (1988a) On the distribution of frost heave along depth in seasonally frost regions, J. Glaciology & Geocryology, No.1, 1-7.
Zhu, Q. et al. (1988b) Subsoil replacement using sand-gravel for preventing frost heave damage of canal lining, J. Glaciology & Geocryology, No.4, 400-408.
Zhu, Q. et al. (1991) A review on the development of anti-seepage technique of canal with concrete lining in China, Technique of seepage prevention, No.1, 1-7.

A MODEL FOR THE INITIATION OF PATTERNED GROUND OWING TO DIFFERENTIAL SECONDARY FROST HEAVE

G. C. Lewis[†], W. B. Krantz[†], and N. Caine[‡]

[†]Department of Chemical Engineering and Institute of Arctic and Alpine Research
[‡]Department of Geography and Institute of Arctic and Alpine Research
University of Colorado, Boulder, CO 80309-0450, U.S.A.

A mathematical model is developed for patterned ground formation owing to secondary frost heave. The latter is caused by freezing-induced cryostatic suction which draws water upward to form ice lenses. This process is potentially unstable because a local perturbation in the heaving causes an increase in the amount of water drawn upward and in the heat transfer to the ambient which in turn allows for more freezing and localized frost heave. This instability mechanism is explored via a linear stability analysis. The model is capable of explaining the formation and many of the characteristics of earth hummocks and has potential application to other forms of patterned ground.

1 INTRODUCTION

"Patterned ground" refers to surface features distinguished by the segregation of stones, ordered variations in ground cover or color, or regular topography. Since it is a manifestation of self-organization in nature, its formation is a question of fundamental significance.

There are very few predictive models which relate the initiation, development, and characteristic features of patterned ground to climatic parameters. Those developed to date are based on two general formation mechanisms: cracking during cooling of frozen ground; and, Rayleigh free convection induced during thawing. The frost-cracking model of Lachenbruch (1961) considers the patterned cracking which occurs in frozen soils owing to the thermoelastic stresses induced by cooling. It has been successful in predicting the occurrence and characteristic width of large ice-wedge polygons in permafrost. In the Rayleigh free convection model of Krantz and coworkers (Ray *et al.*, 1983, and Krantz *et al.*, 1988), the patterning is induced owing to density-gradient-driven free convection which is initiated in water-saturated soil during thawing. Regularly spaced localized regions of downflow and upflow affect the melting causing the underlying ice front to become corrugated. This in turn causes ground-surface patterning owing to its influence on frost heaving of clasts. This model can explain the geometric characteristics of both subaerial and underwater sorted polygons, nets, and stripes.

This paper presents a new predictive model for patterned ground formation which is based on differential secondary frost heave. This model appears capable of explaining many features of earth hummocks and may be applicable to other patterned ground forms as well.

2 SECONDARY FROST HEAVE MODEL

"Frost heave" refers to the uplifting of the ground surface owing to freezing of water within the soil. Its magnitude exceeds that owing to the expansion of water upon freezing ($\sim$10%) because of the freezing of additional water drawn upward. In primary frost heave, this additional water freezes into a continuous layer of nearly pure ice near the ground surface, whereas in secondary frost heave (SFH), it contributes to forming ice lenses interspersed within the soil. "Differential secondary frost heave" (DSFH) refers to laterally nonuniform frost heave which can be either random or ordered as regularly spaced earth mounds which are a form of patterned ground.

Several models have been developed to describe one-dimensional (*i.e.*, nondifferential) SFH; these may be broadly classified as semiempirical models and first principles models. The former can provide accurate predictions of SFH, but require site-specific measurements. First principles models are based on solutions to the coupled transport, flow, and thermodynamics equations subject to appropriate initial

and boundary conditions. The first model of this type was that of O'Neill and Miller (1985). Further development of this model has been done by Piper *et al.,* (1988), Fowler (1989), Nixon (1991), and Padilla and Villeneuve (1992).

It is useful to review the physics in O'Neill and Miller's model. Inherent in this model is the assumption of a subsurface water supply such that the unfrozen soil is initially saturated. Since most soils are "wet" by unfrozen water rather than ice, freezing will consist of ice "fingers" penetrating downward into the pore spaces. This ice will be separated from the soil particles by a layer of unfrozen water which becomes progressively thinner as freezing continues. When this layer becomes sufficiently thin, the water pressure is reduced so that water can be drawn upward by a mechanism referred to as "cryostatic suction".

Gold (1957) associated the pore-water pressure gradient which causes cryostatic suction with a surface tension force at the ice-water interface. Koopmans and Miller (1966) characterized the ability of a soil to induce cryostatic suction in terms of the function $f \equiv p_i - p_w$, where p_i is the ice pressure and p_w is the unfrozen water pressure. They show that for a given soil type f depends only on the unfrozen water volume fraction W, since this determines the unfrozen water film thickness. The cryostatic suction function is frequently described by the Anderson and Tice (1973) equation given by

$$W = af^b \qquad a > 0; \qquad b < 0 \qquad (1)$$

Values of a and b characteristic of different soils can be obtained from the data found in standard references (Freeze and Cherry, 1979). Very fine soils such as clays exhibit very large capillary suction effects and are characterized by $\mid b \mid \sim 0.5$. Coarse soils such as sands exhibit small capillary suction effects and are characterized by $\mid b \mid \sim 1$. Soils such as silts are intermediate in behavior.

The model of O'Neill and Miller then postulates that during freezing of water-saturated soils, cryostatic suction results in a pressure gradient parallel to the temperature gradient which draws water upward. As more water is drawn upward and frozen, the resulting ice supports progressively more of the load; this load arises from the weight of the overlying soil and any structures on the surface. Eventually the pore water and ice can support the full load, thereby permitting the soil particles to separate. This initiates the formation of an ice lens which increases in thickness as more water is drawn upward and freezes. Ice-lens growth is suppressed by continued freezing within the underlying pores which decreases the hydraulic conductivity of the soil. In time, another ice lens will be initiated which cuts off the water flow to the lens above it. In this manner, the alternating layers of ice lenses and soil are created which constitute SFH. Any resistance offered by the frozen soil to frost heave is not included in the model of O'Neill and Miller. This is because O'Neill and Miller assume that the ice moves through the soil via a thermal regelation mechanism. They invoke a "rigid ice approximation" whereby the ice is assumed to move at a constant velocity. Clearly the deformation of the frozen soil will provide a significant resistance to the DSFH; hence the rigid ice approximation is incompatible with DSFH.

3 DIFFERENTIAL FROST HEAVE MODEL

Fowler and Krantz (1993) have generalized the model of O'Neill and Miller to describe three-dimensional (*i.e.,* differential) SFH. Here we discuss a linear stability analysis of the generalized SFH equations of Fowler and Krantz in order to describe the initiation of patterned DSFH.

Space does not permit a detailed development of the generalized SFH model equations. Considerable simplification in the O'Neill and Miller model was achieved by utilizing the "frozen fringe" approximation suggested by Fowler (1989), which recognizes that most of the freezing and ice lens growth is confined to a thin layer which can be reduced to a mathematical plane at which "jump" boundary conditions apply. Further simplifications include ignoring convective heat transfer, and assuming constant physical properties and quasi-steady-state frost penetration.

Figure 1 shows a cross-section of soil displaying DSFH. The z-coordinate is measured positive upwards from a basal plane located below the depth of maximum freezing at which the temperature, T_b, and water pressure, p_b are known. A subfreezing temperature T_s is specified at the ground surface defined by z_s. The instantaneous frost-penetration depth is defined by z_f, at which the normal freezing temperature T_0 is specified. Upward water permeation can occur below z_f owing to cryostatic suction, but not above z_f owing to the ice lenses. The regularity of the DSFH is characterized by its wave length λ.

In order to generalize the predictions, the describing equations are cast in terms of the following dimensionless variables: $T^* \equiv \frac{T-T_0}{T_0-T_s}$, $p^* \equiv \frac{p}{p_a}$, $t^* \equiv \frac{\kappa C_p (T_0-T_s)t}{d^2 L}$, and $z^* \equiv \frac{z}{d}$, in which p_a is the atmospheric pressure, κ is the thermal diffusivity of the soil, C_p is the heat capacity of the soil, d is the depth to

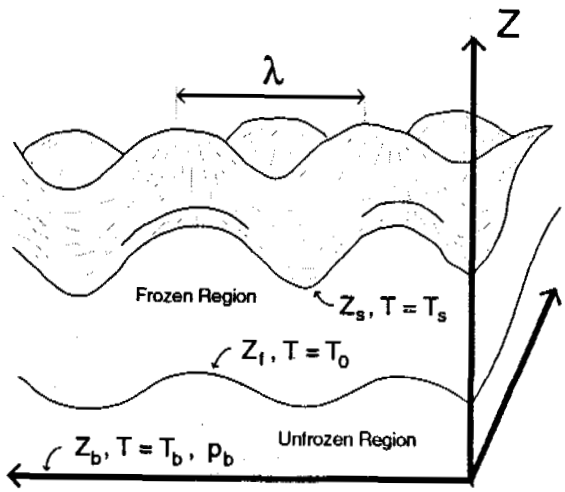

Figure 1: Schematic of patterned differential frost heave.

the basal reference plane from the initial (unheaved) planar ground surface, and L is the latent heat of fusion of water. The characteristic time scale is based on a measure of the time required for frost penetration to the basal plane for which the characteristic velocity is determined from an energy balance across the frozen fringe wherein both conduction and latent heat effects are considered. The resulting dimensionless energy equation is given by

$$\nabla^2 T^* = 0 \qquad 0 < z^* < z_f^{*-}, \qquad z_f^{*+} < z^* < z_s^* \tag{2}$$

where z_f^{*-} and z_f^{*+} denote the negative and positive sides of z_f^*, respectively, to allow for the discontinuity in the temperature gradient across the frozen fringe. The corresponding boundary conditions are given by

$$T^* = -1 \qquad @ \quad z^* = z_s^* \tag{3}$$

$$T^* = 0 \qquad @ \quad z^* = z_f^{*-} \quad \text{and} \quad z^* = z_f^{*+} \tag{4}$$

$$T^* = T_b^* \qquad @ \quad z^* = 0 \tag{5}$$

Two auxiliary conditions are required to determine the frost-penetration and heave velocities, $V_f^* \equiv \frac{V_f dL}{\kappa C_p (T_b - T_s)}$ and $v_s^* \equiv \frac{v_s dL}{\kappa C_p (T_b - T_s)}$, respectively:

$$V_f^* = \frac{dz_f^*}{dt^*} = \frac{1 - (1+\tilde{B})(\phi - W_l) A T'_{f+} - (1+\tilde{B}) T'_{f-}}{\phi + \tilde{B}(\phi - W_l) - A(1+\tilde{B})(\phi - W_l) W_l} \tag{6}$$

$$v_s^* = \frac{dz_s^*}{dt^*} = -A \left[T'_{f+} - W_l V_f^* \right] \tag{7}$$

where T'_{f-} and T'_{f+} denote $\frac{\partial T^*}{\partial n^*}$ evaluated at z_f^{*-} and z_f^{*+}, respectively, and n^* denotes a dimensionless coordinate normal to the freezing front. The dimensionless parameters $\tilde{B}$ and A are defined by

$$\tilde{B} \equiv -B \left\{ \frac{p_b - p_l}{W_l f'_l + \gamma (p_b - p_l) \left(1 - \frac{\rho_i}{\rho_w}\right)} \right\} \tag{8}$$

$$A \equiv \frac{\tilde{B}}{(1+\tilde{B})(1 - \phi + W_l)} \tag{9}$$

$$\text{in which} \quad B \equiv \frac{\gamma \rho_i L^2 K_l}{g k T_0} \tag{10}$$

where p_b is the ground water pore (gauge) pressure at the basal plane, p_l is the water (gauge) pressure immediately beneath the lowest ice lens, g is the gravitational constant, k is the thermal conductivity of the soil, ρ_i and ρ_w are the densities of the ice and unfrozen water, respectively, and $f' \equiv \frac{df^*}{dW}$; the subscript "$l$" denotes evaluation at W_l, the unfrozen water volume fraction beneath the lowest ice lens. This is determined from a force balance at the lowest ice lens:

$$P - p_b = \left[1 - \frac{W_l}{\phi} \right] f_l \tag{11}$$

where P is the load owing to the weight of the overlying soil, ϕ is the porosity of the soil, and f is given by equation 1. Note in equation 11 that we have replaced p_w in the force balance by p_b because of the very large water pressure gradient beneath the lowest ice lens which arises because of the marked dependence of the hydraulic conductivity K on the unfrozen water content of the soil. The quantity K_l is the hydraulic conductivity of the partially frozen soil evaluated at W_l which is assumed to be of the form

$$K_l \equiv K_0 \left[\frac{W_l}{\phi} \right]^\gamma \tag{12}$$

where K_0 and γ are constants characteristic of the particular soil. The driving force for water permeation, $p_b - p_l$, appearing in equation 8 is determined by combining equation 11 with equation 1 for f evaluated at the lowest ice lens at which $p_i = P$ to obtain

$$p_b - p_l = \left[\frac{W_l}{\phi} \right] f_l \tag{13}$$

DSFH is not compatible with the rigid ice approximation used by O'Neill and Miller. In its place we invoke a regelation model suggested by Gilpin (1979) to interrelate the ice motion through the porous media to the normal temperature gradient:

$$v_i^* = -\lambda_G \left[\frac{\partial T^*}{\partial n^*} \right] \tag{14}$$

where v_i^* is the dimensionless ice velocity and λ_G is an empirical constant. The frost-heave velocity defined by equation 7 is assumed to be equal to the ice velocity evaluated at the z_f^{*+}; that is,

$$v_s^* = v_i^* \qquad @ \quad z^* = z_f^{*+} \tag{15}$$

The parameter B defined by equation 10 is proportional to the latent heat content of the permeating water divided by the conductive heat transfer characteristics of the soil; it is characteristic of the soil type: for clay $B \ll 1$; for silt $B \approx 1$; and for sand $B \gg 1$. Equation 6 is the Stefan condition for this moving boundary problem. The derivation of equations 6 and 7 embodies much of the complex physics occurring in the frozen fringe. These equations were obtained by combining equations for the unfrozen water and ice mass balances, energy balance, Darcy permeation flow, Clapeyron relation for the freezing temperature, and overall force balance at the bottom of the lowest ice lens using the formalism for reducing the frozen fringe to a mathematical plane as described by Fowler (1989). The Clapeyron equation is modified to include cryostatic suction effects and is given by

$$T - T_0 = -\left(\frac{T_0}{\rho_i L}\right)\left[\left(1 - \frac{\rho_i}{\rho_w}\right) p_w + f(W)\right] \tag{16}$$

The principal resistance to DSFH is deformation of the overlying frozen soil. Hence, an additional equation is needed to relate the deformation of the frozen soil to the stress acting on it. It is reasonable to assume that the soil remains incompressible, that the frozen region above z_f behaves elastically, and that the elastic strains respond quasi-statically to ice-lens production. A tractable model for small variations in the local heave rate based on thin shell theory (*e.g.*, see Brush and Almroth, 1975) is given by

$$\left[\frac{Eh^3}{9}\right] \nabla^4 w = P \tag{17}$$

where w is the z–deflection of the center of the plate, E is Young's modulus, and h is the thickness of the frozen region.

In order to establish the conditions for which a patterned form of DSFH is possible, it is necessary to solve the above system of equations. We explored this instability mechanism by carrying out a linear stability analysis to determine the conditions required for the initiation of DSFH in the form of ground-surface corrugations having a wave length λ. This analysis can determine the effect of soil type, freezing depth, climatic conditions, *etc.*, on the initiation and characteristic wave length of the patterned DSFH. A more complete development of this analysis is given by Lewis (1993).

The principal results of this linear stability analysis are summarized in Figure 2 for three characteristic soil types: clay (curve *a*); silt (curve *b*); and sand (curve *c*). This figure was prepared assuming that the loading is due only to the weight of the overlying frozen soil and $T_b^* = 0\,^\circ\mathrm{C}$. The modulus of elasticity of the frozen soil was assumed to be $5.0 \times 10^7\ \frac{N}{m^2}$ (Drewry, 1986).

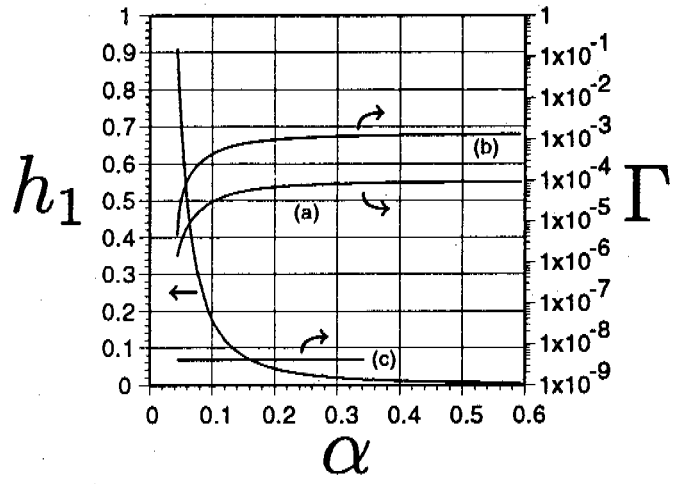

Figure 2: Dimensionless wave number α and growth coefficient Γ as functions of dimensionless frost-penetration depth $\frac{z_s - z_f}{z_s}$ for: (*a*) clay; (*b*) silt; (*c*) sand.

The left ordinate in Figure 2 is the dimensionless freezing front depth $\frac{z_s - z_f}{z_s}$ which is plotted versus the dimensionless wave number α. This figure indicates that for each location of the freezing front there is a preferred unstable wave number, independent of the soil type, which satisfies the linear stability analysis for the coupled heat transfer and permeation described by equations 2–16 and the elasticity constraint given by equation 17.

The right ordinate in Figure 2 is the dimensionless growth coefficient Γ which also is plotted as a function of α. Figure 2 implies that the preferred wave number and its growth coefficient decrease with increasing penetration of the freezing front. These predictions indicate that the one-dimensional SFH process for the specified conditions is unstable such that it will evolve into DSFH characterized by a corrugated heaved ground surface underlain by a corrugated frost-penetration front.

This linear stability analysis predicts that DSFH is theoretically possible in any soil characterized by a cryostatic suction function for which $| b | < 1$. However,

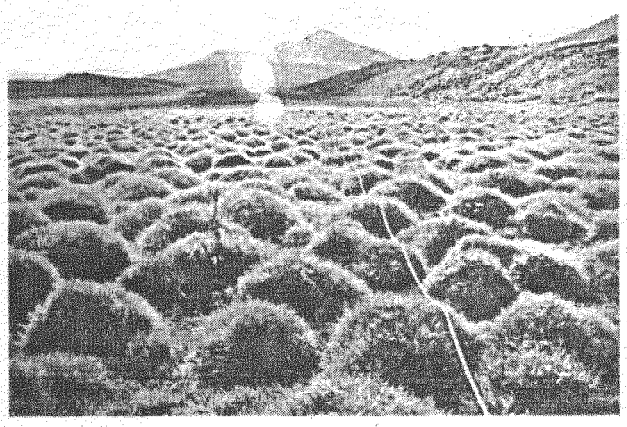

Figure 3: Earth hummocks near Varmahlíd in north central Iceland (authors' photo).

Figure 2 indicates that in general it will be quite insignificant in sands and clays relative to silts owing to the large difference in the growth coefficient Γ for the unstable modes; that is, DSFH will develop quite slowly in sands and clays relative to silts. Note that this analysis predicts that DSFH in any soil can be suppressed by sufficient loading. Moreover, it is suppressed by an increase in the elastic modulus of the frozen soil and by a sufficient increase in the basal plane temperature.

4 APPLICATION TO PATTERNED GROUND

We believe that the regularly patterned DSFH predicted by our model is responsible for the formation of earth hummocks and possibly other forms of patterned ground. Earth hummocks can display striking regularity as shown in Figure 3. In applying this model to patterned ground, we identify the wave length of the DSFH (λ in Figure 1) with the characteristic diameter of the hummocks. For hummocks formed over permafrost, we identify the depth to the basal reference plane, d, with the depth of the active layer.

Tarnocai and Zoltai (1978), who studied earth hummocks in the Canadian arctic, clearly establish that SFH plays a major role in their formation. They report that the moisture in hummocks "...occurred in the form of well-developed vein ice, ice lenses, ice crystals, and massive ice, especially at the permafrost table..." This supports applying the model developed here to earth hummocks since ice-lens formation causes SFH. This model also indicates that the ice lenses will become thicker near the permafrost table because more time is available for ice lens growth when the frost-penetration rate decreases owing to the increased depth.

Tarnocai and Zoltai (1978) also report the internal composition of the hummocks they studied to be fine- to medium-textured materials (clay to silt loam) with a total silt and clay content of 68% or higher. The model predictions indicate that DSFH in general will be significant only in silty soils.

Tarnocai and Zoltai (1978) also report that on level areas hummocks are circular, but on slopes greater than 1% they tend to be elongated downslope. Washburn (1980) reports that striped hummocks can occur on slopes as steep as 15°. These observations also are consistent with the model predictions. Linear stability analysis indicates that the instability which causes one-dimensional SFH to evolve into multidimensional DSFH can be manifest as several different geometric forms. This feature of stability analysis applied to patterned ground forms is discussed in a recent review article (Krantz, 1990). The nonsorted nets observed on level ground correspond to three-dimensional instability modes manifest as interlinked hexagons. Subterranean water flow on sloped terrain will favor two-dimensional instability modes which are manifest as downslope parallel stripes.

Mackay (1977) studied changes in the active layer depth resulting from a forest fire for a permafrost site near Inuvik, NWT; which had displayed hummocks. The short term result of this fire was to cause the hummocks to become inactive and to increase the active layer depth. Pettapiece *et al.* (1978) report that the longer term result of this fire was to cause larger diameter hummocks to become active at this site. The model indicates that an increase in the rate of freezing (*e.g.*, owing to destruction of the ground cover) can cause hummocks to become inactive owing to a decrease in the time available for ice-lens growth. Moreover, Figure 2 indicates that the preferred wave number, α, decreases with increasing frost-penetration depth, $\frac{z_s - z_l}{z_s}$; an increase in the active layer depth then would provide more time for a longer wave length mode to establish the characteristic diameter of the earth hummocks.

The characteristic diameters of hummocks reported by Zoltai *et al.* (1978) and Tarnocai and Zoltai (1978) range from 80 to 200 cm. This is certainly within the range of wave lengths inferred from Figure 2 for the anticipated frost-penetration depths. However, the model cannot predict the observed hummock diameter, since the preferred instability mode changes with increasing instantaneous frost-penetration depth. The reported range of hummock diameters suggests that the

preferred mode impressed on the DSFH is established at shallow frost-penetration depths.

5 CONCLUSIONS

This linear stability analysis of SFH provides the following explanation for the initiation of patterned DSFH. In the absence of significant loading, basal plane temperatures sufficiently above freezing, or highly nondeformable frozen soils, a local perturbation in the frost heave is unstable because it causes a local increase in the water permeation. This additional water is available to cause increased local frost heave because a corrugation in the ground surface and underlying freezing front permit more lateral heat transfer from the soil beneath the peaks to that beneath the troughs. This additional heat transfer is transferred to the ambient air at the surface of the troughs, which is favored by shorter wave length corrugations. However, this is counteracted by deformation of the frozen soil favoring longer wave length modes. The interaction of these two influences results in a preferred wave length for the frost heave, which increases with an increase in the freezing-front penetration owing to the resistance offered by a thicker frozen soil layer.

DSFH is favored in silty soils since they are sufficiently fine-grained to generate adequate capillary suction to draw water upward for ice-lens formation; yet, they have sufficient hydraulic conductivity to permit this permeation to occur at reasonable rates to facilitate ice-lens growth. Clays generate very large capillary suction, but do not have sufficient hydraulic conductivity. Conversely, sands generate negligible capillary suction, but are quite permeable. Hence, patterned ground types which are strongly influenced by SFH tend to form in silty soils.

This model can explain many of the characteristics of earth hummocks and may be able to describe other forms of patterned ground such as sorted stone circles, mud circles, and frost boils. Further development of this model, corroborating it with quantitative studies of hummocks, and applying it to other forms of patterned ground are suggested as areas of further research.

6 ACKNOWLEDGMENTS

The authors acknowledge support from the National Science Foundation (grant DPP-8922548) and the Global Change and Environmental Quality Program and Council on Research and Creative Work at the University of Colorado. One of the authors (WBK) completed a portion of this work as a Guggenheim Fellow and Fulbright Scholar at the Mathematical Institute at Oxford University. The authors express appreciation to Dr. S. C. Zoltai of the Canadian Forestry Service for providing information on his extensive studies of earth hummocks.

7 REFERENCES

1. Anderson, D. M. and Tice, A., (1973). The unfrozen interfacial phase in frozen soil water systems. Ecological Studies Analysis and Synthesis, **4**, 107–124.
2. Brush, D. O. and Almroth, B. O., (1975). Buckling of Bars, Plates, and Shells. McGraw-Hill, Inc., New York, pp. 80 & 88.
3. Drewry, D., (1986). Glacial Geologic Processes. Edward Arnold Pub., London.
4. Fowler, A. C., (1989). Secondary frost heave in freezing soils. SIAM J. Appl. Math., **49**, 991–1008.
5. Fowler, A. C. and Krantz, W. B., (1993). Generalized secondary frost heave model. SIAM J. Appl. Math., in press.
6. Freeze, R. A. and Cherry, I. A., (1979). Groundwater. Prentice–Hall, Englewood Cliffs.
7. Gilpin, R. R., (1979). A model of the "liquid-like" layer between ice and a substrate with applications to wire regelation and particle migration. J. Colloid Interface Sci., **68**, 235–251.
8. Gold, L. W., (1957). A possible force mechanism associated with freezing of water in porous materials. High. Res. Board Bull., **168**, 65–72.
9. Koopmans, R. W. R. and Miller R. D., (1966). Soil freezing and soil water characteristic curves. Soil Sci. Soc. Am. Proc., **30**, 680–685.
10. Krantz, W. B., Gleason, K. J., and Caine, N., (1988). Patterned ground. Sci. Am., **259**(6), 68–76.
11. Krantz, W. B., (1990). Self-organization manifest as patterned ground in recurrently frozen soils. Earth-Sci. Rev., **29**, 117-130.
12. Lachenbruch, A. H., (1961). Depth and spacing of tension cracks. J. Geophys. Res., **66**(12), 4273–4292.
13. Lewis, G. C., (1993). A Predictive Model for Differential Frost Heave and Its Application to Patterned Ground Formation, M.S. thesis, University of Colorado, Boulder.
14. Mackay, J. R., (1977). Changes in the active layer from 1968 to 1976 as a result of the Inuvik fire. Report of Activities, Part B; Geol. Surv. Can., Paper 77-1B, 273–275.
15. Nixon, J. F., (1991). Discrete ice lens theory for frost heave in soils. Can. Geotech. J., **28**, 843–859.
16. O'Neill, K., and Miller, R. D., (1985). Exploration of a rigid ice model of frost heave. Water Resour. Res., **21**, 281–296.
17. Padilla, F. and Villeneuve, J.-P., (1992). Modeling and experimental studies of frost heave including solute effects. Cold Reg. Sci. Technol., **20**, 183–194.
18. Pettapiece, W. W., Tarnocai, E., Zoltai, S. C., and Oswald, E. T., (1978). Guidebook for a Tour of Soil, Vegetation and Permafrost Relationships in the Yukon and the Northwest Territories of Northwestern Canada. International Society of Soil Science, 11th Congress, Edmonton.
19. Piper, D., Holden, J. T., and Jones, R. H., (1988). A mathematical model of frost heave in granular materials. Fifth International Conference on Permafrost Proceedings, ed. K. Senneset, Tapir, Trondheim, pp. 370–376.
20. Ray, R. J., Krantz, W. B., Caine, T. N., and Gunn, R. D., (1983). A model for sorted patterned ground regularity. J. Glaciol., **29**(102), 317–337.
21. Tarnocai, C. and Zoltai, S. C., (1978). Earth hummocks of the Canadian Arctic and Subarctic. Arct. Alp. Res., **10**(3), 581–594.
22. Washburn, A. L., (1980). Geocryology. Wiley, New York, N.Y.
23. Zoltai, S. C., Tarnocai, C., and Pettapiece, W. W., (1978). Age of cryoturbated organic materials in earth hummocks from the Canadian arctic. Third International Conference on Permafrost Proceedings, National Academy Press, Washington, D.C., pp. 325–331.

Initiation of Segregation Freezing Observed in Porous Soft Rock during Melting Process

Satoshi Akagawa,

Institute of Technology, Shimizu Corporation,
Tokyo 135, Japan

Ice lens appearance in freezing soil and porous soft rock varies greatly. This difference is assumed to be governed by the cohesion or tensile strength of the porous materials, such as soils and soft rocks.

In this paper, the author demonstrates the empirical results which show ice lens initiation in a melting frozen porous soft rock where no pore water flow and negative to zero net heat flow at the segregating ice lens is maintained.

The mechanism of the ice lens initiation and growth in melting porous soft rock is discussed in the light of thermodynamics and mechanical properties of the rock.

The discussion supports the assumption with the data demonstrated in this paper ; the tensile strength of freezing porous material may play the role in determining of suction pressure at growing ice surface, and may control ice lens initiation and continuous growing properties.

INTRODUCTION

Ice lens appearance in freezing soil and porous soft rock varies greatly. Comparing the properties in frost heave tests, conducted with constant boundary temperature conditions and an open pore water line system, it may be said that (1) many fine ice lenses are seen in frozen normally-consolidated soils, (2) a reduced number of thin ice lenses are seen in frozen over-consolidated soils, (3) a more reduced number of thick ice lenses are seen in Tertiary soils which have slight measurable tensile strength, and (4) a few dominant thick ice lenses are seen in frozen porous soft rock.

This difference seems to be related to the magnitude of the interaction between soil grains which is measured as the cohesion and/or tensile strength of each material. Low cohesion may cause frequent thin ice lenses and high tensile strength may cause restricted thick ice lenses.

Experimental results mentioned above reveal an assumption that cohesion and/or tensile strength of freezing porous materials affect the properties of ice lensing. In other words, tensile strength may play the same role as super-cooling does at ice lens initiation in freezing soil.

In order to examine the assumption mentioned above, unusual frost heave tests were conducted. The procedure of the frost heave tests was specially arranged to eliminate the super-cooling of pore water which may assist the initiation of ice lenses. For this purpose, frost heave tests in the thawing condition were ntroduced . Theoretically and experimentally it was understood and confirmed that ice lenses may not initiate or grow in thawing conditions (ex Gilpin, 1982). A certain amount of net heat flow at the growing ice surface is required to meet the latent heat budget of ice nucleation (Akagawa, 1990). In macroscopic view, the required net heat flow will never be supplied in melting process.

In this paper, details of the frost heave tests conducted under the thawing conditions are explained with test results, and the process of ice lens initiation in the thawing condition is discussed.

EXPERIMENT

Sample used

Welded tuff with the properties listed in Table-1 was used as the specimen. It has already been confirmed that the tuff frost heaves against its tensile strength of 1.4 MPa in the freezing process (Akagawa et al., 1988), and that its properties which affect frost susceptibility, such as pore structure and/or unfrozen water properties, are similar to those of frost susceptible soils (Akagawa, 1991).

Table-1 Physical and mechanical properties of tuff

	Unfrozen Dry	Unfrozen Saturated (20℃)	Frozen Saturated (-5℃)	Frozen Saturated (-15℃)	Frozen Saturated (-25℃)
Apparent specific gravity	1.40	1.72	-------	------	-------
Porosity(%)	37.9				
Strength(MN/m^2)					
Compressive	14.7	6.6	12.0	18.5	26.2
Tensile	1.6	1.4	1.4	4.4	5.7
Tangent modulus (MN/m^2)	4812	3548	2859	2068	3763
Secant modulus (MN/m^2)	4596	3126	3097	3410	6281
Elastic wave velocity(km/s)	2.45	2.72	3.20	3.67	3.89
Poisson's ratio	0.17	0.28	0.46	0.38	0.42

Apparatus

A triaxial frost heave test cell, shown in Fig.1, which was placed in 2 ℃ chamber was used for this experiment. With this apparatus lateral heat flow and side friction were reduced as much as possible. The boundary temperatures of the specimen were maintained by circulating temperature controlled liquid in pedestals which are seen at both side of the specimen in the figure. The temperature profiles were acquired with temperature readings from platinum temperature transducers placed every 1cm over the specimen. A pore water line was open from the water reservoir to the specimen and the amount of the flow was measured automatically. The expansion of the specimen was measured with a digital deformation transducer which generated one pulse for every 1um deformation.

Procedure

Sample preparation

The trimmed specimen, which had the dimensions of 60mm in diameter and about 90mm in height, was submerged in water under a vacuum condition for more than 3 months. After the installation of the specimen in the triaxial frost heave cell, following almost the same procedure as conventional triaxial compression test, pore water was circulated from the bottom pedestal to the upper pedestal for 24 hours to avoid unfavorable air bubbles. During this period, both pedestals were maintained at a same temperature, +2℃, to equalized the initial specimen temperature.

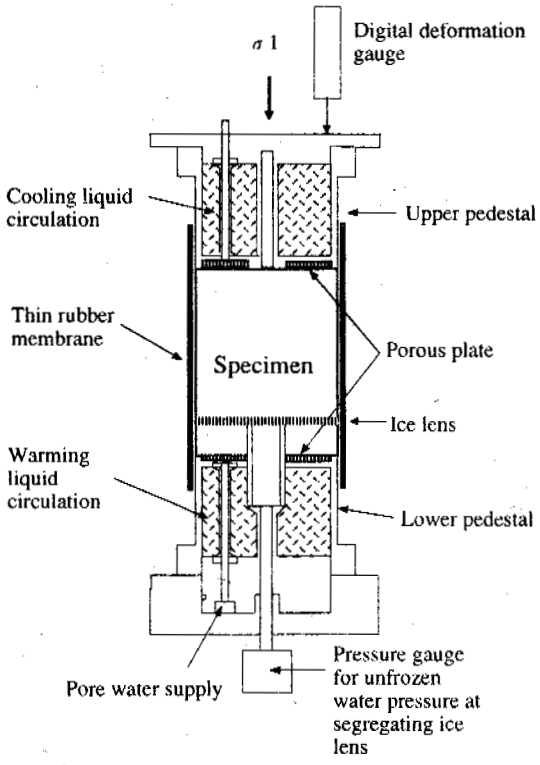

Fig.-1 Triaxial frost heave cell

Test procedure

As for the first step of this experiment, the specimen was frozen from top to bottom uniaxially, controlling the temperatures of the upper and lower pedestals at -15℃ and 0℃ respectively. After the confirmation of negative temperatures over the entire specimen, further lowering of the specimen temperature was conducted by ceasing the temperature control at bottom pedestal. The frozen specimen was cooled down further by heat extraction from the upper pedestal. After it had been he confirmed that the specimen had not expanded, the temperature of the bottom pedestal was increased to the scheduled positive temperature in order to thaw the specimen from the bottom upward. Since this was the very beginning of the experiment, all the test conditions were maintained throughout the experiment.

In order to achieve the above mentioned test procedure, the test conditions, shown in Table - 2, were applied.

Table-2 Test conditions

Test name A

	Freeze up	1st thaw back	2nd thaw back	3rd thaw back
σ 1 (kgf/cm²)	0.095	0.095	0.095	0.095
σ 3 (kgf/cm²)	0	0	0	0
Pw (kgf/cm²)	0	0	0	0
Tc (℃)	-15	-15	-12	-12
Tw (℃)	0 or -2	+3.5	+3.5	+5.55

Test name B

	Freeze up	thaw back
σ 1(kgf/cm²)	0.095	0.095
σ 3(kgf/cm²)	0	0
Pw(kgf/cm²)	0	0
Tc (℃)	-15	-15
Tw (℃)	0 & no cont.	+5.3

Test name C

	Freeze up	thaw back
σ 1(kgf/cm2)	5.62	5.62
σ 3(kgf/cm2)	5.43	5.43
Pw(kgf/cm²)	5.00	5.0 & closed
Tc (℃)	-15	-14.4
Tw (℃)	0 & no cont.	+5.1

TEST RESULTS

The heave and pore water flow curves of Test A to Test C are shown in Fig.2-A-1 to Fig.2-C-1 . Temperature changes in the freezing specimens are also shown in Fig.2-A-2 to Fig.2-C-2 . Temperature profiles at some important periods are shown in Fig.2-A-3 to Fig.2-C-3. These temperature profiles were drawn with temperature data at "a", "b", "c", "d", and "e' in Fig.2-A,B,C-2, and correspond to the following; initial temperature profile, steady temperature profile at first freezing phase, steady temperature profile at second freezing phase, ice lens initiation in first thawing phase, and continuous ice lens growth in thawing phase.

During the first freezing phase, "a" to "b", specimens seemd to expand, however this was not frost heaving but expansion due to the freezing of bulk water and is usually called in-situ freezing. In this phase, pore water was expelled from the specimen which is a typical phenomena

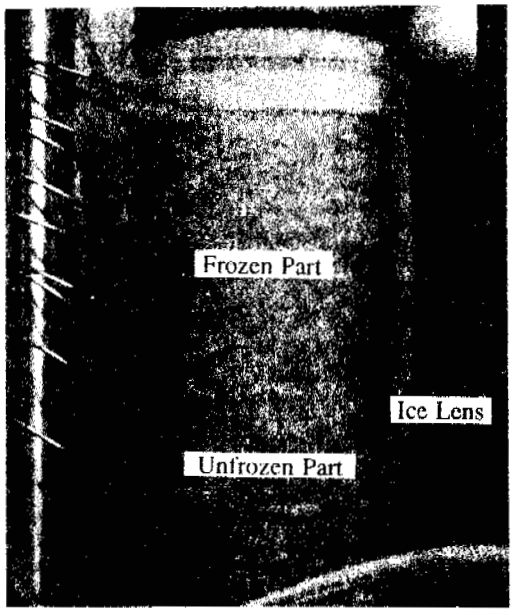

Photo 1 Freezing specimen

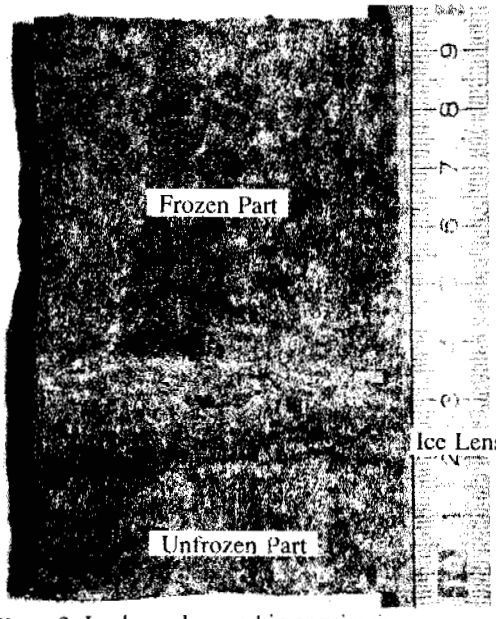

Photo 2 Ice lens observed in specimen

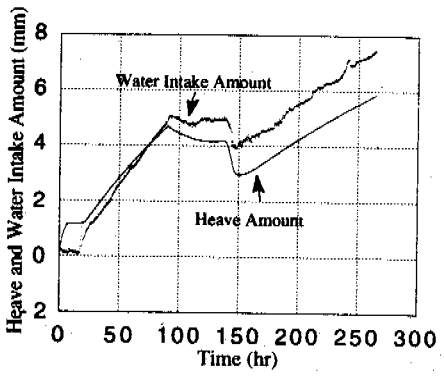

Fig 2-A-1

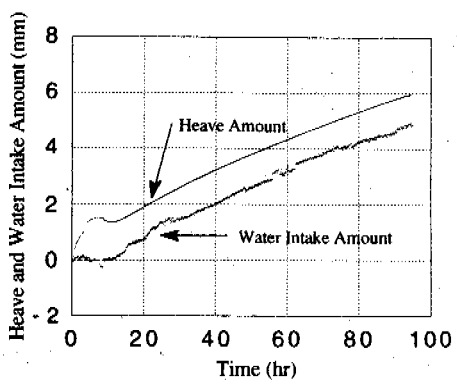

Fig 2-B-1

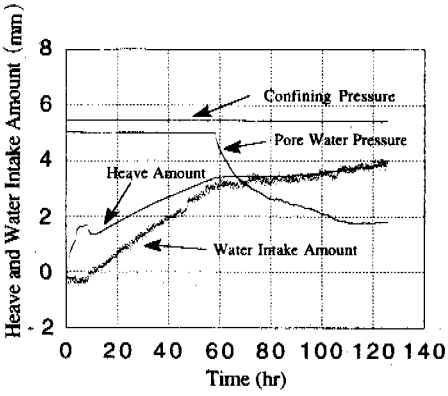

Fig 2-C-1

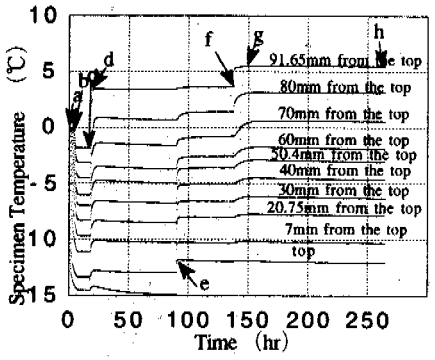

Fig 2-A-2

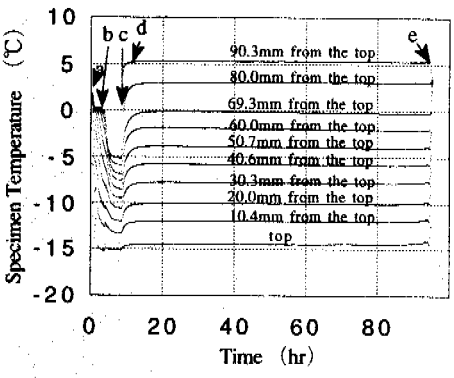

Fig 2-B-2

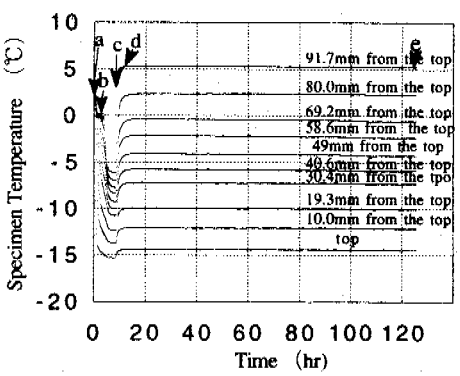

Fig 2-C-2

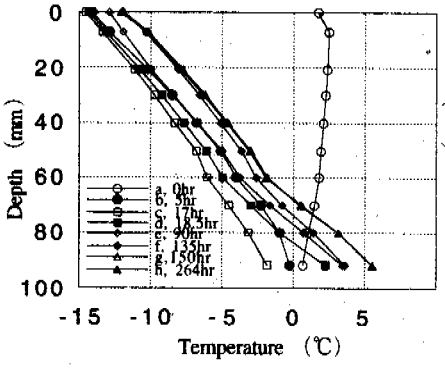

Fig 2-A-3

Fig 2-A Test results of Test-A

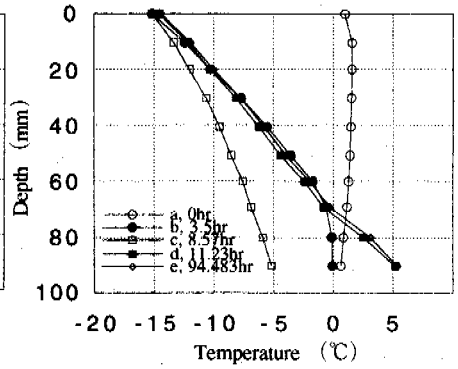

Fig 2-B-3

Fig 2-B Test results of Test-B

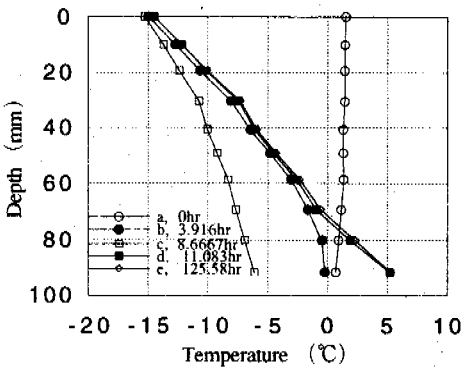

Fig 2-C-3

Fig 2-C Test results of Test-C

of in-situ freezing. At a time "b", the specimen temperature went below zero entirely and then further freezing was accomplished by releasing control of the warming pedestal temperature to avoid super-cooling. This procedure led to the warmest temperature at "c" in Fig.2-A, B, C-2, where the specimen is lower than -4 ℃, as shown in Fig. 2-A, B, C-3. During this period, the expansion was ceased abruptly. Immediately after the period "c", the temperature of the warming pedestal was increased to 4 ℃ in Test A and 5℃ in Tests B and C. A couple of hours later, as the lower part of the specimen became positive in temperature, gradual expansion was started at about the period "d" in Fig.2-A, B, C-2. As time elapsed, the heave rate increased to a rate of about 0.06mm/hr with pore water in-take. These combinations, such as expansion of specimen and pore water in-flow reveals that the frost heaving with ice lens segregation was taking place. Actually, ice lens growth was confirmed through a semi-transparent rubber membrane as shown in Photo-1.

In Test A, further thawing was conducted twice, at the periods "e" and "f". During both thawing phases, reduction of heave amount was seen first and then recovery of heave amount was confirmed as time elapsed. However, the recovery was not very clear in the period "e" to "f", because of the insufficient time length.

After the frost heave tests, specimens were cut in two peices. A typical photo of the ice lenses seen in the Test C specimen is shown in Photo. 2. Due to the high rigidity of the specimen, the distance between the bottom end of the specimen and warmest side of the ice lens did not change over the test durations. Therfore the location of ice lens initiation was measured as this thickness. With these thicknesses and the temperature profiles at "d", "e", "g", and "h", the segregation temperatures, Ts, of ice lenses were observed as shown in Fig.3. These observed Ts values scattered around the formerly observed Ts value, -1.4℃, which was observed in normally conducted frost heave tests.

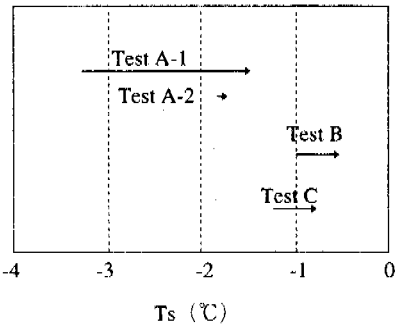

Fig.3 Observed segregation temperature, Ts

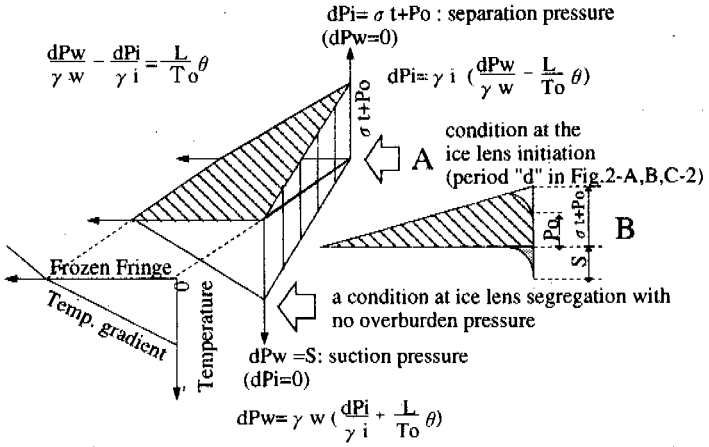

Fig.4 Ice lens initiation scheme with tensile strength

DISCUSSION

Frost heave tests conducted in this work clearly show a possibility of ice lens initiation and growth during the thawing process, although this is only seen with a very slow thaw back process. The test results prompt questions, such as (1)what mechanism may enable ice lens initiation and (2)how is the heat budget for ice lensing maintained.

In the following, a possible understanding of the above questions is discussed.

Since the observed Ts values in this experiment are somewhat similar to what was formerly measured, ice lensing properties observed in the experiment are also similar to usual ice lensing properties (Akagawa, 1988). The observed segregation process of the ice lenses in this experiment is understood to be the usual process. Then thermodynamic condition in frozen fringe at the initiation of ice lensing, the period "d" and "g" in Fig.2-A,B,C-2, is drawn as a triangular section pointed to by an arrow ,"A", in Fig.4. A quasi-equilibrium state was reached because there was no pore water in-flow and available pores in the fringe were filled with ice and unfrozen water. The right most, or highest point of triangle section shows an ice pressure that is almost separating the pore despite its tensile strength, σ t. According to the generalized Clausius-Clapeyron equation, ice pressure developed (dPi) due to the depression of the local equilibrium temperature (dT) is expressed as;

$$dPi = \gamma i \left(\frac{dPw}{\gamma w} - \frac{L}{To} dT \right) \quad (1)$$

where dPw is the suction pressure in unfrozen water, L is volumetric latent heat of fusion, To is the freezing temperature of water in Kelvin at atmospheric pressure, γ is the specific gravity and subscripts w and i refer to water and ice. In this case the temperature should be around -1.4℃. Therefore, dPi should be about 1.55Mpa. Immediately after the pore is enlarged by the separation force exerted by the ice pressure, the ice pressure may drop to the overburden pressure of 9.3kPa. Since this pressure is about 6/1000 of initial dPi, the thermodynamic condition may change to the other side of the 3D drawing, see arrow "C". The triangle shaped section shown by the other arrow represents a relationship governed by generalized Clausius-Clapeyron at dPi=0 as;

$$dPw = \gamma i \left(\frac{dPi}{\gamma i} + \frac{L}{To} dT \right) \quad (2)$$

The thermodynamic condition at the time immediately after ice lens initiation in frozen fringe is shown as a deformed triangle, labled as "B" in Fig.-4, because the thermal field will not change spontaneously. The deformed triangle shows the reduction in ice pressure of σ t and the generation of dPw, i.e. suction force. The relation between σ t and dPw in this case is shown as ;

$$dPw = - \frac{\gamma w}{\gamma i} \sigma t \quad (3)$$

The suction force induced by the tensile strength may be a driving force for flowing pore water from the water reservoir to the segregating ice lens through frozen fringe. As pore water migrates to the segregating ice, the latent heat of ice nucleation may raise the local temperature. If the rise in local temperature is less than the temperature change equivalent to a the pressure change, Pi, from 1.55MPa to 9.3 kPa, i.e. in this case 1.55/1.11 - 0.0093/1.11 = 1.39 (℃e, the suction may continue to function pulling pore water to the growing ice lens. However, although the value of the suction may diminish a certain amount.

In this manner tensile strength may play a role in determiningof suction pressure and therefore control ice lens initiation and the continuous growing that is observed in the thawing condition.

In addition, Eq(3) clearly indicates that if a freezing material has a higher tensile strength, a higher suction force may be expected when the material frost heaves. Therefore it may be said that strong and stable ice lensing occurs more often in freezing porous soft rock compared to usual soil. This tendency may also be expected to the ice lensing properties of Tertiary soils and overconsolidated soils.

CONCLUSIONS

(1) Porous material, i.e. welded tuff, frost heaves while it is thawing under the condition that no super-cooling is available.
(2) The tensile strength of freezing porous material may play the role that super-cooling does at ice lens initiation.
(3) The new ice lens initiation process discussed in this work is favorable to explain the data obtained in this experiment, and the variation of ice lensing properties with respect to change in tensile side strength.

REFERENCES

Akagawa, S., S. Goto, and A.Saito (1988) Segregation freezing observed in welded tuff by open system frost heave test. Proc. 5th Int. Conf. Permafrost, pp1030-1035.

Akagawa, S. (1990) A method for controlling stationary frost heaving. Shimizu Tech. Res. Bull. No.9, pp1-8.

Akagawa, S. (1991) Studies on the process of frost damages to stone remains under cold environments and its preservation method. doctoral thesis submitted to Hokkaido Univ.

Gilpin, R.R. (1982) A frost heave interface condition for use in numerical modelling. Proc. 4th Can. Permafrost Conf., pp459-465.

THE ENSURING AND ECOLOGICAL SAFETY OF THE GAS PIPELINES OPERATING IN THE PERMAFROST ZONE

Vitaly P. Antonov-Druzhinin

ARTTRADEINFO (INGEOTES) Antonov-Druzhinin Private Enterprise,
Novy Urengoy, Tumen Region 626718, Russia

This paper contains data on methodical backgrounds, large-scale experimental research and field test of pipelines in a permafrost zone. It is shown that in the course of the experiment and during the observation of the operating gas pipeline behavior displacements of up to 100 mm were determined. It is desirable that they should be of a seasonally cyclic nature. This can be achieved through the creation of a special temperature condition of gas being transported which prevents the effect of cryogenic heaving on the gas pipeline. The latter effect results in the disturbance of a seasonally cyclic nature of the gas pipeline displacements. It may sometimes lead to vertical pipeline displacements of 300 mm and more. Designed displacements may exceed 2 m per season. The latter phenomena seem to be very dangerous for gas pipelines operation in the permafrost zone.

ANTHROPOGENIC STRUCTURES IN GEOSYSTEMS (LANDSCAPES) OF PERMAFROST ZONE

Problems created by oil and gas fields development in Arctic regions attract much attention in the discussion of interaction of civil and industrial buildings and structures with permafrost.

The investigations carried out must permit us to evaluate changes in natural environment, to single out the anthropogenic component of these changes, to ensure accident-free operation of oil and gas transport units, safety of people, environmental control in the mineral resources production regions of the Arctic.

Consider the spatial-temporal structure of the gas transport geotechnical system as a natural anthropogenic physicogeographical object, taking as an example the "pipeline-environment" system.

These areas and zones are shown (in cross section) in Fig. 1.

The paper submitted to your consideration discusses ecological after-effects of the construction and operation of gas pipelines in a permafrost zone and pertains to zones 2, 3 and 4 (Fig. 1).

The formation of zones 2, 3 and 4 (Fig. 1) is largely determined by natural conditions. Even in case of using identical construction technology these zones have different configuration.

GAS PIPELINING IN PERMAFROST ZONE. EXPERIMENTAL STUDY OF GEOCRYOLOGICAL, ENGINEERING-GEOLOGICAL AND ECOLOGICAL PROBLEMS

The main task of our investigations is to ensure accident-free operation of oil and gas transport units, safety of people. A chilled gas pipelining experiment has been performed on a test site of an operating gas pipeline. In the course of the experiment we have received data on the freezing peculiarities of different soils in the gas pipeline base. The freezing rate was found to be 0.5 to 1.6 mm/hour and that of the pipeline displacement 45-65 mm. Computer simulation of the temperature fields of the soil around the gas pipeline being chilled has been carried out. The simulation results are in good agreement with field test experiments. Classification of permafrost zone geosystems (landscapes) reflecting ecological hazard of natural gas pipelining has been developed.

However, the ecological safety of gas transport system in the permafrost zone is largely determined by its thermodynamics system. Most of all the thermodynamics of the gas transport system depends on the gas pipeline interaction with the surrounding soil, air and water in region 8, zones 9-16 (Fig. 1). Just these processes are discussed in this paper. It is known that the formation of a soil zone exposed to all the year round thermal effect with the "ice-water" phase transition in soil is a process the most typical of the northern gas pipelines in a permafrost zone. This process manifests itself in: 1) the formation of thaw areas beneath the pipelines when gas is transported at a temperature above zero ($t°C>0$)– "warm" gas; 2) the formation of freezing areas during the transportation of gas chilled to a subzero temperature ($t°C<0$)– "cold" gas; 3) the formation of freezing areas within thaw areas with the change-over from "warm" to "cold" gas transportation.

Field Testing

Typical of a permafrost zone of Western Siberia are the following natural

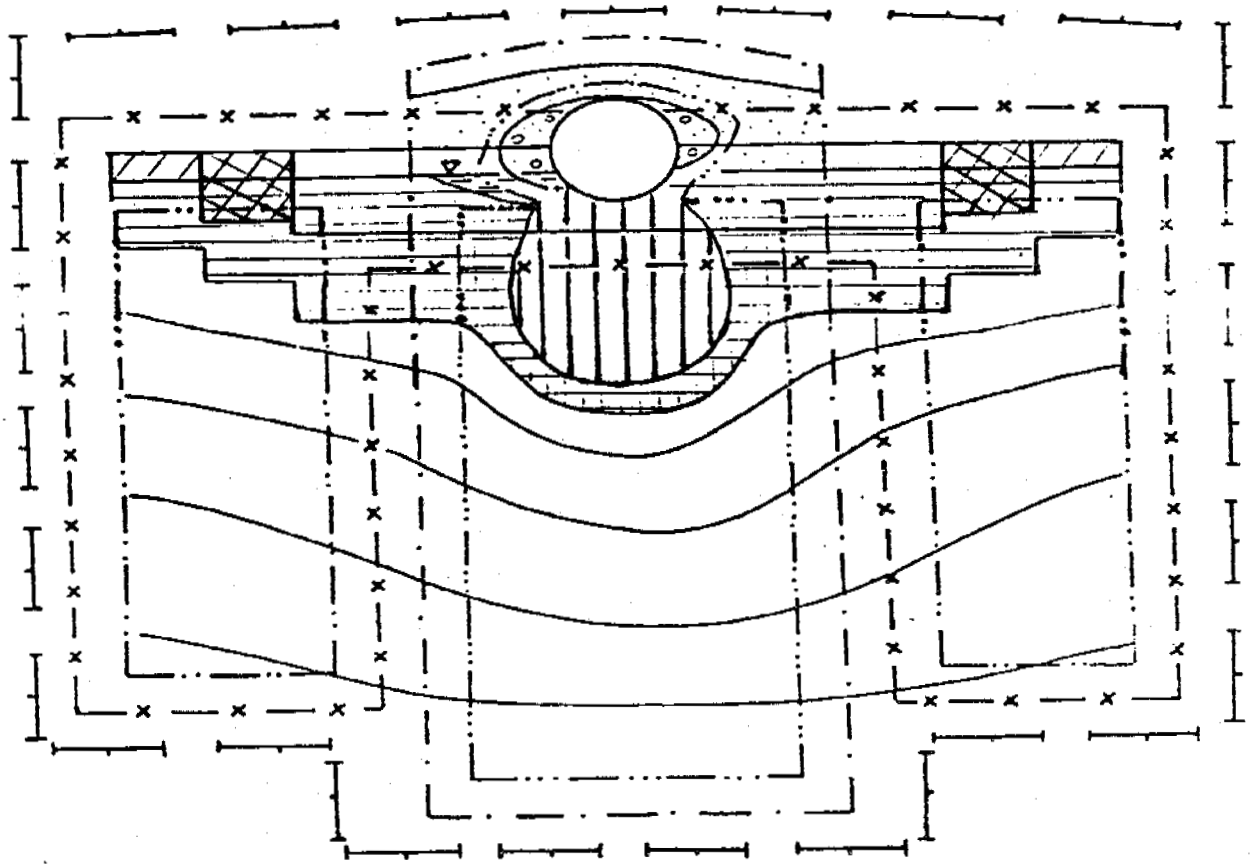

1 - Region of geosystem anthropogenic transformation, which is formed during gas pipeline construction (region exposed to effect of gas pipeline under construction) including: 2 - zone of complete mechanical surface destruction; 3 - zone of partial mechanical surface destruction; 4 - buffering zone; 5 - zones of indirect thermal effect: with "ice-water" phase transition in soil (6), without "ice-water" phase transition in soil (7); 8 - region of geosystem anthropogenic transformation, which is formed during gas pipeline operation (region of operating gas pipeline effect); including: 9 - zone of wind regime change; 10 - zone of surface water flow change; 11 - zone of direct thermal effect, consisting of: 12 - air zone exposed to direct thermal effect; 13 - zone of surface water exposed to direct thermal effect; 14 - rock zone exposed to all the year round thermal effect with "ice-water" phase transition in soil; 15 - rock zone exposed to all the year round thermal effect without "ice-water" phase transition in soil; 16 - rock zone exposed to seasonal direct thermal effect with "ice-water" phase transition; 17 - pipe of the gas pipeline; 18 - soil surface; 19 - boundary of zone exposed to effect of engineering structure resulting from dynamic equilibrium of interrelated subsystems (bergstrich is directed to natural geosystem).

Figure 1. The structure (in cross section) of the gas transport geotechnical system.

geosystems of a landscape stow type: pretundra forests (light forests) growing on unfrozen sands (natural type I) and on permafrost clay loams and sandy loams with mean annul soil temperatures ($t_{av.}$) of about 0 to 1.0°C; tundras on permafrost sandy loams, clay loams and clays with $t_{av.}$ of -3.0 to -3.5°C (natural type II); peat bogs with $t_{av.}$ of -3.0 to -4.0°C and -4.0 to -5.0°C (natural type III: type III-1, free from vein ice; type III-2, containing vein ice); high grass bogs with $t_{av.}$ of -2.0 to +1.0°C (natural type IV).

The main natural peculiarities of the gas pipeline operation in southern forest-tundra were represented in one of our

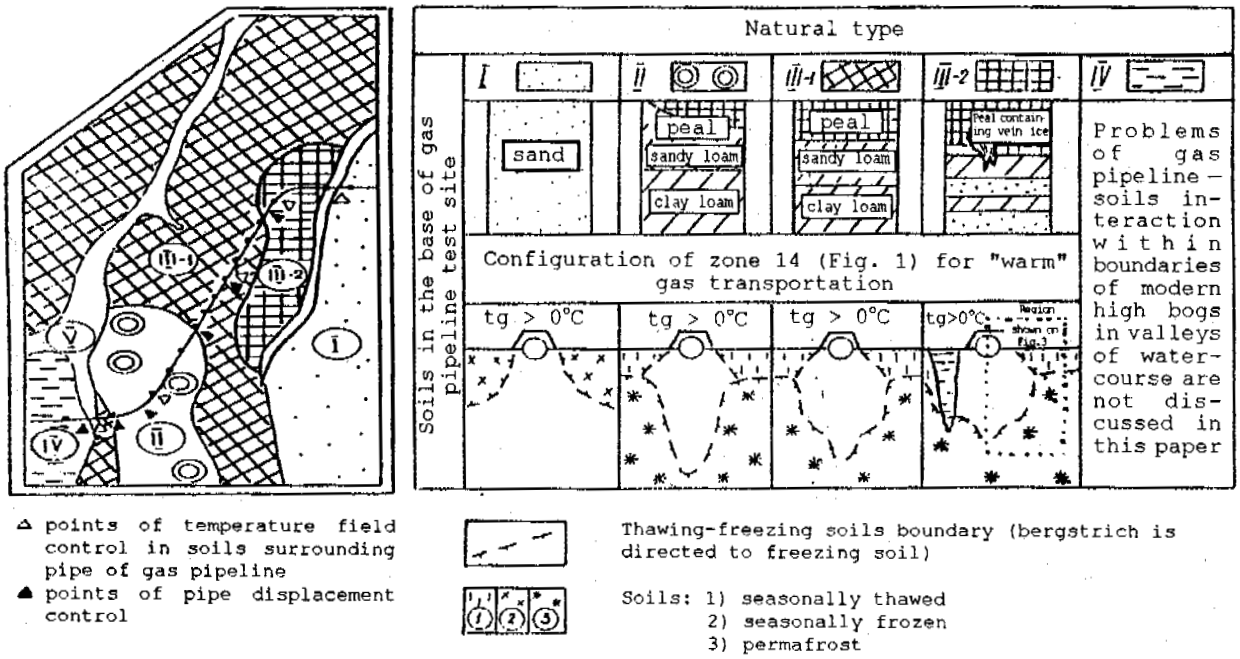

Figure 2. The natural and geotechnical conditions of the gas pipelining test site.

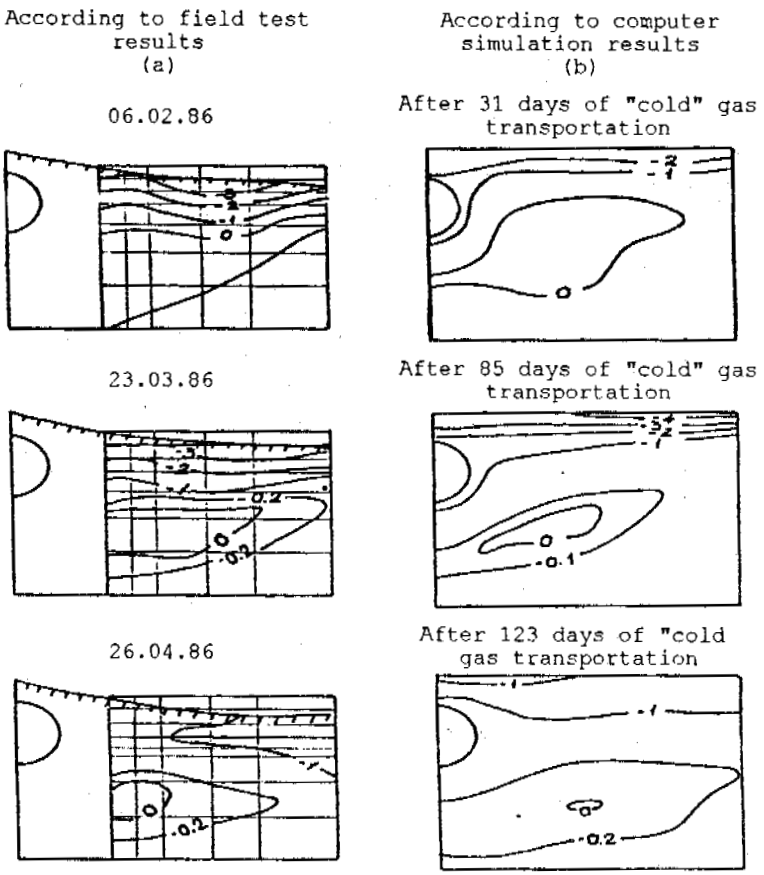

Figure 3. The temperature field in the soil surrounding the gas pipeline.

Table 1. Physical properties of soils in the base of the gas pipeline test site (Fig. 2): (accepted in computer simulation)

Natural type (corresponding to Fig.2)	Calculated type	Lithologic composition	Volume weight of soil skeleton, kg/m	Total moisture content, W	Thermal conductivity, (kg-cal/m-hour °C)		Heat capacity per unit volume (kg-cal/m³ °C)	
					for freezing	for thawing	for freezing	for thawing
I	1*	sand	1600	16	1.75	1.55	480	590
III-2	2	peat, 2.5 m sand	200 1600	200 38	1.15 1.75	0.7 1.55	570 480	900 590
II	3*	sandy loam	1650	30	1.7	1.6	590	835
	4	peat, 1 m sandy loam	200 1650	400 30	1.15 1.7	0.7 1.6	570 590	900 835
III-1	5*	clay loam	1700	32	1.55	1.45	590	835
	6	peat, 1 m clay loam	200 1700	400 32	1.15 1.55	0.7 1.45	570 590	900 835

• the results are duplicated by means of analog computation

experiments which was carried out on a test site of an operating gas pipeline route (Fig. 2). The length of this site is about 2.5 m. According to the program of this experiment the transported gas temperature was changing from positive to negative values. This enabled to observe different types of interaction between the gas pipeline and its soil base.

It was found that during the transportation of gas at low temperatures ($t°<0$) ("cold" gas) the rate of anthropogenic freezing was as follows:

- in coarse and medium coarse sand – 1.6 mm/h (for natural type I)
- in sand-loam soils – 1.6-1.0 mm/h (for natural type II)
- in peaty-mineral soil massif – 0.5 mm/h (for natural type III)
- in water-logged soils and bods – 0.8 mm/h (for natural type IV)

Fig. 3 illustrates the dynamics of the soil temperature field around the gas pipeline during the experimental transportation of "cold" gas in zone 14 (Fig. 1, 2).

Computer Simulation

Following the full-scale field experiment the computer and analog simulation of the temperature field patterns in the soils surrounding the gas pipeline was carried out. The thermophysical characteristics of the soils used in computations are presented in Table I. As an example, we compare the temperature field pattern in the soil surrounding the gas pipeline only for natural type III-2 (calculated type 2). It is characterized by most complex lithologic structure texture of the gas pipeline soil base (a peat layer containing ice veins occurs on sands with inclusion of small layers of clay loams and sandy loams, Fig. 2). The most complex are also the patterns of the zone 14 (Fig. 1, 2) and its temperature field (Fig. 3a). Other natural types are characterized by a similar lithologic texture of a soil base and therefore by a simpler temperature field patterns are in good agreement with measurement data (Fig. 3a, 3b).

Fig. 3 shows the formation and dynamics of an unfrozen ground "bulb" beneath the gas pipeline with change-over from "warm" to "cold" gas transportation. This is a very dangerous phenomenon which may result in the mass and energy redistribution in the gas transporting geotechnical system. The latter may be associated with unforeseen overtension and breakage of pipes followed by unfavorable ecological after effects.

As a result of our investigations we have developed classification of permafrost zone geosystems according to the ecological hazard to the construction and operation of gas pipelines within their boundaries. The most favorable conditions for gas pipelining (for both "warm" and "cold" gas) in the permafrost zone arise in the natural geosystems (landscapes) corresponding to type I. The most unfavorable ecological after-effects may be expected in geosystems corresponding to natural type III-2. Special sufficiently dangerous conditions for the transportations of both "warm" and "cold" gas arise on the watercourse within the bogs (V) but this problem exceeds the framework of this report because of its limited volume.

One of the ways to increase the ecological safety of gas pipelines operation in a permafrost zone is the cryogenic processes' control in zone 2, 14, 16 (Fig. 1). In zones 14 and 16 this is achieved by the transported gas temperature control.

To this effect we have developed a number of mathematical methods including an express-method for determination of the soil thawing and freezing depth within the zone of the direct thermal effect of the gas pipeline.

This method is very convenient for use because it provides reliable information concerning freeze-thaw phenomena of the

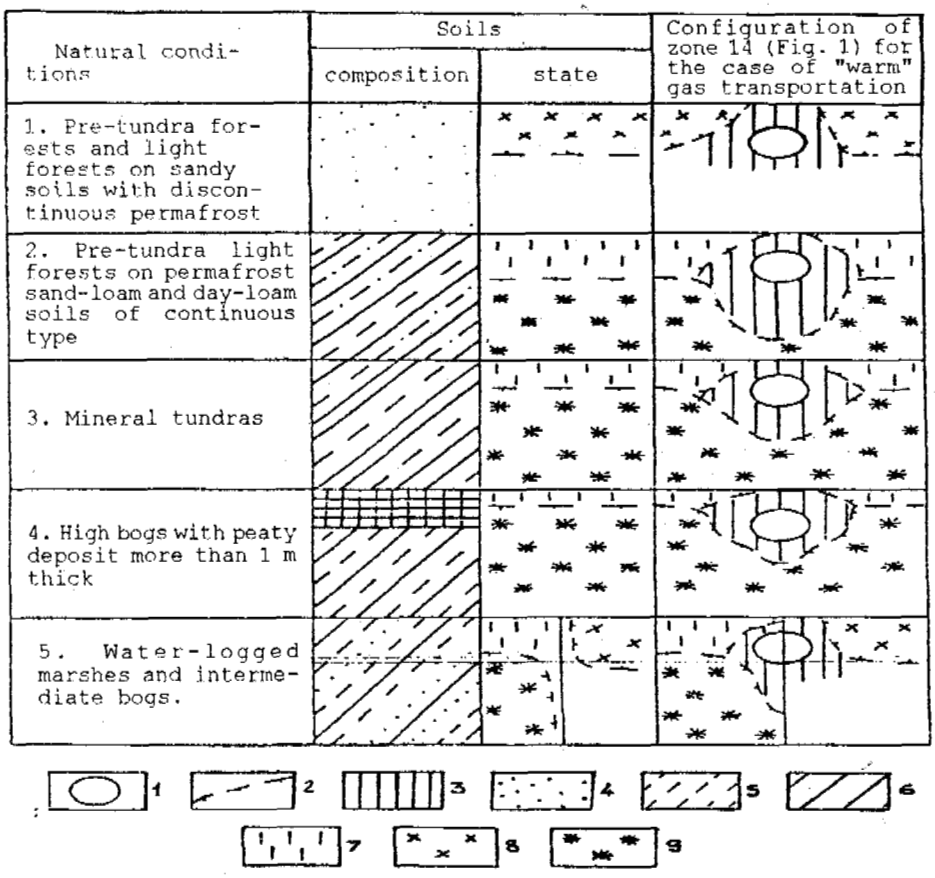

1 – Pipe of the gas pipeline, 2 – thawing-freezing soils boundary (bergstrich is directed to freezing soil), 3 – zone of the all year round thermal effect with water phase transition in the soil; soils composition: 4 – sand, 5 – sandy loam, 6 – clay loam; soils state: 7 – seasonally thawing, seasonally freezing, 9 permafrost.

Figure 4. Heat disturbance of the permafrost surrounding the gas pipeline with "warm" gas.

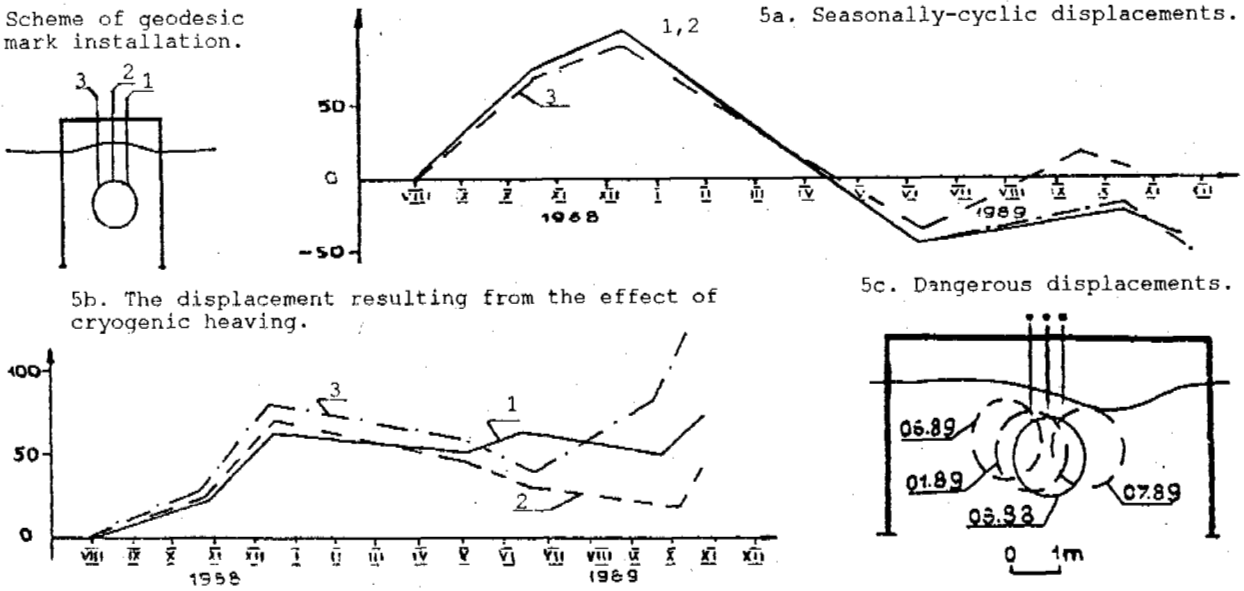

Figure 5. Seasonal displacement of the gas pipeline.

soil surrounding gas pipelines, it is very simple and obvious. Fig. 3 shows a good agreement between the computed and measurement results.

FIELD TEST AND LARGE-SCALE EXPERIMENTAL RESEARCH OF PIPELINES IN PERMAFROST ZONE

Field test and large-scale experimental research of pipelines in permafrost zone under conditions of planes (similar to those of the permafrost zone of Western Siberia) must take into consideration at least five types of gas pipelining natural conditions (Fig. 4).

Field Test

In our approach to field tests of pipelines the object of investigation is not only the gas pipeline as a technical object but the gas pipeline and its natural environment as an integral gas transpiration system. During the observations we study all zones shown in Fig. 1. Such an approach is called engineering-geological monitoring. Under this term we understand observation, data accumulation, prediction of the geotechnical system development as a natural anthropogenic object. The main aim of engineering-geological monitoring is optimization, provision of reliability and ecological safety of the geotechnical system.

At present the service of engineering-geological monitoring is carrying out observations on 75-100 km sites of operating gas pipelines. These are main sites of gas transporting systems of Western Siberia, which are operating under permafrost conditions.

The observation system was designed with account of methodical backgrounds mentioned in the first section of the author's paper. In the process of observation we determined:

1) the thermal field in the soil surrounding gas pipeline; 2) the dynamics of direct thermal effect with "ice-water" phase transition in soil (zone 14, fig. 1); 3) the ground water level beneath the gas pipeline; 4) displacement of gas pipeline and other technical characteristics.

OPTIMIZATION OF GAS TRANSPORTING GEOTECHNICAL SYSTEM IN PERMAFROST ZONE

The brief summary may be presented as follows:

1. The "warm gas" pipelining is unreasonable because it is connected with the permafrost thawing in the pipeline base and the activization of cryogenic processes dangerous for gas pipelines – thermokarst, thermal erosion, ground subsidence etc.

2. The cold gas pipelining is dangerous because of the activization of frost heaving and fracturing of soils and the formation of frozen earth materials beneath the pipelines.

All the above-mentioned testifies to the necessity of developing such a temperature condition of the transported gas which would permit to *control* cryogenic processes in the direct thermal effect zones of gas pipelines (mainly in zones 13, 14, 15, 16 in the region of operating gas pipeline effect 8, Fig. 1).

The temperature condition of the transported gas developed by us permits to prevent dangerous cryogenic processes in these zones. Thereat seasonal gas pipeline displacements become comparable with the extent of seasonally heaving of clay loam in a seasonally nature. As a result, the gas pipeline remains at the elevation mark (Fig. 5a). In case of violation of this condition the forces of cryogenic heaving may affect the gas pipeline. This results in the deviation from a design position (Fig. 5b) and possible dangerous displacements (Fig. 5c).

The data presented are obtained during field nesting of pipelines in the process of engineering-geologial monitoring of the gas transporting systems in the North of Western Siberia. The pipe displacement illustrates in Fig. 5a is determined on the gas pipeline fixed in soil with anchor devices and transporting gas under temperature condition developed by us.

We have presented the methodical backgrounds and the results of large scale experimental research of pipelines in the permafrost zone being carried out by the department of northern geotechnical systems of the trust of Engineering-geological Monitoring and Research. It is worth noting that the development of temperature condition for gas pipelining, which permits to control cryogenic processes, is based on a special permafrost prediction.

Using the computational algorithm we have simulated a problem of finding the monthly average gas temperature which ensures a 0.5 m thaw radius around the pipe all year round.

The simulation results are presented in Fig. 6.

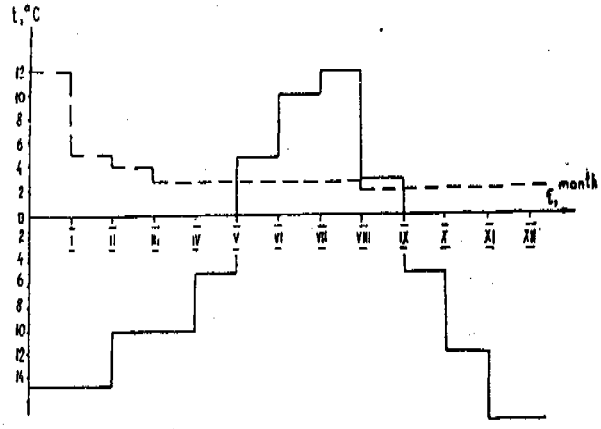

Figure 6. Average monthly gas temperature provide the minimum thaw area (0.5 m) around the gas pipeline.
The first year of operating. The initial soil temperature -7°C.

ENGINEERING AND GEOCRYOLOGICAL STUDIES OF THE CENTRAL PART OF YAMAL PENINSULA CAUSED BY ITS DEVELOPMENT

V.V.Baulin, A.L.Chekhovsky, I.I. Chamanova

PNIIIS, Okrujnol PR. 18, 105058 GSP, Moscow, Russia

The album of different scale engineering geocryological and forecast maps has been drawn up by the PNIIIS to design the projects of extraction, treatment and gas piping. The special features of geocryological conditions of the territory are reflected the occurrence of ice beds and saline frozen soils, slope processes ect. The forecast of geocryological conditions changes is given by means of different technogenic impact upon the environment.

In 1990, Russia began to develop Bovanenkovo gas field situated in the central part of Yamal peninsula (West Siberia).

Engineering and geocryological conditions of the peninsula are complicated and specific. Permafrost that have the annual average temperature from −7°C to −20°C is spread everywhere in the gas field area. Permafrost from the surface and down to the depth of 3–4 m is characterized by high content of ice (0.4–0.6) which decreases to 0.2–0.4 with depth increase. All the sea deposits that occupy 75–80% of the gas field area are salinized. Their salinization changes from 0.1% to 1% and more. Due to this fact frozen clayish soil remain plastic even under low annual temperatures. This makes it more difficult to determine strength and deformation characteristics of salinized frozen soil and significantly diminishes the carrying capacity of pile foundations.

Sloping processes are extremaly dangerous. Depending on the meteorological conditions and the active layer soil composition soil of the slopes at the steepness of 1.5°C can be mobile. When carrying out field studies we observed the whole scale of slope processes from the classic slides to viscous soil flow on the foot of the active layer. Destruction and damage of the vegetative cover facilitates slope processes.

On the territory containing sea deposits massive ice is widely spread. It reaches more than 100 m lengthwise and is 10m and more thicker. Slide 1 shows the map of massive ice spreading in Bivanenkovo gas field. The map is made on the basis of abundent data (over 100 massive ice stripping holes, dozens of outcrops) and computer interpreted aerophotographs, spacephotos and topographic maps. It was found that massive ice properties are connected with numerous diagnostic indicators of its disposition (over 40): age of the topography, its morphology, number of lakes etc.

The reliability of the method applied is 75–80% with massive ice at the depth of 3–5 m and 60–70% with ice at the depth of 5–10 m.

PNIIIS' studies in Bovanenkovo gas field were carried out in three directions: regional engieering and geocryological studies; survey of cryogenic processes and geocryological forecast; studies of salinized frozen soil physical and methanical properties. In the presentation, we are going to dwell on the first two directions.

Regional engeering and geocryological studies were aimed at providing the designers with the survey data at every stage of design work. For this purpose we have worked out map legends and carried out engieering and geocryological mapping in three scales.

A 1:100,000 scale map of ecological and geocryological regionalization contains data on engeering and geocryological conditions in Bovanenkovo gas field area, permafrost resistance to technogenic exposure and on environment– protecting measures (Slide 2). In the process of making the map we have determined every identified engieering and geocryological site's resistance to technogenic damages. The map also provides data on allowable technogenic damages and on recommended complex environment–protecting measures for every engineering and geocryological site. Depending on the potentialities of emergence or activization of cryogenic processes at disbalanced natural conditions resistance of the geological environment to technogenic exposure has been estimated. we have identified three categories of engineering and geocryological sites–resistant, relative resistant, and irresistant ones.

Complex of environment–protecting measures that are suggested for every engineering and geocryological site give information on vegetation removal possibilities; recommended filling height; critical quantity of snow accumulation; filling slopes reinforcement; and surface drainage.

Engineering and geocryological regionalization maps by construction conditions at the scale of 1:25,000 make it possible to estimate the complexity and approximate cost of construction works in every engineering and geocryological site (Slide 3). In the process of regionalizing such factors as slope angles, presence of massive ice

and cryopegs, soil salinity, its temperature and ice content in it, as well as percentage of cryogenic damages and formations in the unit, and flood zone size are taken into consideration.

According to the estimation of various combinations of the above–mentioned geocryological factors several complexity levels for construction sites were graded.

Finally, we have marked 3 levels of construction sites complexity– the least complex, relative complex, and complex sites. To the least compleax sites we attribute plain terrace surfaces and hasureys formed by soils with low ice content; gentle slopes and back flood lands are related to the second group; the most steep slopes formed by soils with high ice content and river bed–side flood zones are related to the third group.

Maps on engineering and geocryological conditions and regionalization by allowable technogenic load at the scale of 1:5,000 are made for the southern part of Bovanenkovo gas field. Primary construction sites are concentrated here (Slide 4). Scenarios of geocryological condition's damages are worked out for every identified engieering and geocryological district and for 7 main construction types. For every type of construction technology within engieering and geocryological districts we have suggested design decisions that provide engieering construction stability.

To observe requirement of preserving the natural geocryological conditions and constructions stability it is necessary to take various measures aimed at regulating ground temperature and depending on the construction type. First, these are various types of refrigerating facilities (ventilated basements and foundations, cooling tubes, thermopiles, heat insulating fillings). Besides, it is very important to install efficient water–conducting systems, belt–formed frozen fillings for preventing slidings etc.

In addtion to the general engieering and geocryological maps and the general ecological and geocryological maps there were developed legends for special geocryological maps and a gas field area mapping by certain permafrost characteristics and cryogenic processes development were carried out.

On the special map of salinized frozen soil and cryopegs at the scale of 1:25,000 there were distinguished three types of salinization – a chloride, a sulphate, and a hydrocarbonate type, with heavy dominating of the first type (Slide 5). Soil salinization in certain cases exceeds 1%. On flood lands and slope terraces, upper parts of sections to the depth of 2–10 m are formed by unsalinized and low–salinized soils that have formed under continent conditions. Below them there occur salinized sea deposits. On the surface, salinized permafrost soils are deposited only within the surfaces of sea terraces that are not affected by denudation.

There were determined mechanisms of cryopeg forming and wide–spread occurence in the salinized frozen and cooled soil. It was found that cryopegs occur at absolute marks from +20 m to –200 m within all the geomorphological levels but the most lenses are deposited at the 5–40 m depths in flood land.

Cryopegs have formed in the course of the Pleistocene and the Holocene, they keep on forming at present as well. the map shows two types of cryopegs, their mineralization, temperature, and brine pressure in lenses. Cryopegs of the first type are deposited at depths from 4 m to 10 m and are dynamic, their lenses are thin and different in horizontal dimension. The existence of the lenses and their mineralization are closely connected with short–period temperature variations in the upper part of permafrost. Cryopegs of the second type are deposited at the depth of 10–40 m and deaper, they are characterized by quasi–stationary condition and considerable pressure. Lenses are up to several meters thick, they reach 300m in extent, and cryopeg properties are less dependent on the surface conditions.

On slide 6 you can see the map of permafrost thickness in Bovanenkovo gas field at the 1:200,000 scale. The map presents the thickness of the negative temperature soil layer containing ice and the depth of the zero isotherm. It was verified that the thickness of permafrost grows with the geomorphological level age increase.

Within the third sea terrace, the thickness if permafrost containing ice makes up 200–225 m, the zero isotherm goes at the depth of 325 m. For flood land the figures are 150–175 m and 250–275 m respectively.

Slide 7 presents the thermokarst forecast map. It gives information on the process dynamics under different types of the surface damages (vegetative cover destruction and cutting away ground of different thickness) with today's climate and the forecast global climate warming.

Technogenic damages of different scale can lead to reversable and irreversable changes of the initial geocryological situation. In the gas field area one can identify three groups of sites according to a potential risk of thermokarst development. The most risky are gentle slopes with massive ice close to the surface– here one can see the connection of thermokarst development with thermal erosion and creeping processes. the map is built on the data of field observations and computer model testing.

To finish the presentation we would like to show the map of technogenic damage in Bovanenkovo gas field area at the scale of 1:25,000.

A forecast of changes in the geocryological situation in terms of the identified types of technogenic damages is also given at the map. The damages are classified by three indicators. A geocryological changes forecast for 10 types of damages is made for the periods of 3–5 years and 20–25 years. 13–14% of the gas field area under development is affected by technogenic damages. The principle conclusion is that the today's level of technogenic exposure has caused the development of separate (not numerous) local seats of the intensified cryogenic processes. Both field observations and forecast indicate that within the boundaries of the most of the damaged sites there goes a gradual recovery of the initial geocryological conditions. This process passes ahead of the ecological situation recovery because the primary vegetation communities are being replaced by the secondary vegetation.

The studies in Bovanenkovo gas field were carried out by the large group of PNIIIS' explorers as well as by specialists from other research institutes (MGU, Foundamentproyect, VSEGINGEO). The authors of the report are very thankful for them for the fruitful and highly professional work without which the presentation would not be possible.

METHODS OF LARGE SCALE ECOLOGICAL AND GEOCRYOLOGICAL CLASSIFICATION OF THE NORTHERN PART OF WESTERN SIBERIA

A.L. Chehovsky, I.I. Shamanova

Industrial and Research Institute for Engineering Investigations of Construction, Moscow, Russia

On the basis of many years of complex engineering geocryological and ecological investigations in the northern region of Western Siberia new methods of large scale ecological and geocryological classification including general recommendations on possible engineering disturbances to nature have been developed.

Ecological and geocryological classification has been made on the basis of estimation of territorial difference of landscape and geocryological conditions and forecast calculations on the changing of geocryological and landscape conditions under engineering disturbances to nature.

Ecological protection of developing territories requires preservation and minimum impact to natural landscape and engineering geocryological conditions and also provides safe design for engineering structures. While undertaking ecological and geocryological territory classification and mapping, it is necessary to provide stability of buildings and structures with minimum engineering interference into nature. On the basis of many years of complex engineering geocrylogical and ecological investigations in the northern region of Western Siberia (Yamal Peninsula), our Institute has developed new methods of large scale ecological and geocryological classification including general recommendations on possible engineering disturbances to nature.

Ecological and geocryological classification has been made on the basis of estimation of territorial difference of landscape and geocryological conditions and forecast calculations on the changing of geocryological and landscape conditions under engineering disturbances to nature. The final stage was the development of recommendations on providing for stability of engineering structures and prevention of the development of dangerous cryogenic processes.

The diagram of natural division is based on indications determining the main peculiarities of engineering geocryological conditions. The peculiarities of the given region are geomorphology, meso and micro relief, slope of the surface, drainage, vegetation, surface sediment composition. The stated types of natural micro-regions are complex indicators of geocryological conditions. The type designs of natural micro-regions are made in accordance with construction development conditions. The determining parameters for type designs of engineering and cryological situations are:

1) average annual temperature of permafrost;
2) ice content of upper layers of permafrost;
3) presence and depth of monomineral ice beds;
4) presence and depth of saline soil and *cryopegs*;
5) surface slope.

Taking into consideration these parameters three types of engineer-geological regions (EGR) have been distinguished.

EGR I: Flat terrace surfaces with slopes less than 1.5 and permafrost characterized by the temperature from -5°C to -8°C. The deposits of upper permafrost zones are icy till 3-4 m. Ice bed deposits are found as a rule below 10 m. The soils are saline along the entire geological section.

EGR II: Terrace slopes and lake depressions with surface slopes more than 1.5 and characteristic permafrost temperature from -1°C to -6°C. The deposits of upper permafrost layers are characterized by high ice contents. The depth of sheet ice occurs below 2 m. The soils are saline along the entire geological section. The cryopeg zones are found at various depths and in some places they are having hydrostatic pressure.

EGR III: River flood plains with lake depressions and surface slopes less than 1.5 and permafrost characterizing by the temperature from -1°C to -4°C. The deposits of upper zones are high ice content. Sheet ice deposits are possible below 10 metres. The soils possess salinity below 4-5 m depth. Cryopegs with hydrostatic pressure occur below 6-8 m.

EGR I is most suitable for construction. Low average annual temperature of rocks, the absence of sheet ice below 10 m depth creates favourable conditions for foundation of engineering structures even with the presence of salinity soils.

EGR II is less suitable for construction since considerable surface slope determines the development of dangerous slope processes, soil's salinity over the entire section, high ice content of soils with sheet ice and a wide temperature interval of permafrost. The complex of negative factors presents considerable difficulties for construction and engineering exploitation.

EGR III occupies an intermediate position between the EGR I and EGR II. The difficulty of erecting engineering structures is connected with relatively high permafrost temperature, presence of cryopegs with hydrostatic pressure and at the

low plain flood lands with flooding of the surface. The absence of salinity soils to the depth 4-5 metres and sheet ice to the depth 10 metres are favourable factors for construction.

Nature protecting measures include a number of activities providing structural stability of soil under the foundations according to principle I (preserving soil in permafrost condition). The most characteristic four types of engineering structures considered are:

I) apartment buildings and industrial structures;

II) gas pipeline (gas transportation with subzero average annual temperature is being planned);

III) embankments of linear structures;

IY) above-ground pipelines on piles.

For each type of structures the maximum possible changes of geocryological conditions (depth of seasonal thawing, average annual temperature of permafrost) and engineering loads (types of engineering disturbances) are given here which may cause the changes in tolerance limits of engineering geocryological conditions. The increase of soil foundation temperature and active layer thickness even in areas most suitable for building construction areas of EGR I, is not permitted for apartment and industrial buildings. This can be explained by the fact that soils are saline and the rise permafrost temperature to -4°C and more will transform soils from solid into plastic frozen state.

The increase of active layer thickness may lead to the formation of impoundments under buildings and structures, thawing of soils and loss of structural stability. At the sites with average annual temperature of permafrost higher than -4°C (EGR II, III), it is necessary to diminich the foundation soil temperature to its transformation into solid frozen state. To prevent the sliding of solids on the slopes (EGR II) it's necessary to decrease the thickness of the active layer.

Under construction and maintenance of structures for types II and III the necessary temperature conditions of foundation soils are provided by the structure of the building itself (road and railway embankments) or by accepted temperature maintenance behaviour (gas pipelines with subzero temperature of gas).

For the structures of type IY - above ground pipelines on piles, the sites with saline soils with temperature higher than -4°C (EGR II) are unfavourable. Such sites need to diminish the foundation soils temperature for 3 - -4°C and keep the temperature condition of soils during the operational period with the use of seasonal cooling devices. At the sites of EGR III with annual average temperature of permafrost higher than - 4°C, the additional decreasing of soil temperature is not needed since 4-5 m depth the soils are not saline and are in solid permafrost state.

The above mentioned requirements of geocryological character are reached by fulfilling number of engineering practices directed to the regulating temperature behaviour of foundation soils and which depends on the type of engineering sites and geocryological situation at the construction site. The main methods of the soil temperature preserving are the providing of vented space under a building and placing ofcooling pipes and channels in foundations of structures. The choice of the method is based on the thermal engineering calculations for specific sites.

The construction of underground pipelines with subzero annual gas temperature and embankments of linear structures do not need special actions for the regulation of temperature of foundation soils.

From the point of view of dangerous engineering geological processes on the territories close to engineering structures, the most complex activities are needed for EGR II. Active layer slides, which are widely spread on slopes in natural conditions, may become more active under construction development of the area. To prevent the development of this process it is recommended to make earth fills of 1.2-1.5 m of height at the construction sites and adjacent territory, to form a good water overflow, to construct a permafrost barrier. Within the limits of EGR II and EGR III, the main activity is directed to prevent the increasing or decreasing of permafrost temperature. The main problem here is to provide free drainage of ground water at the construction sites, organization of drainage structures, maximum limitation of transport across the tundra in summer. EGR III requires also the prevention of formation of snow drifts.

The set of activities providing stability of engineering structures and preventing the development of engineering geological processes in different engineering-geocryological regions are given in a special table in the map's explanation. These are connected with the scheme of natural micro-regions by common figure indexes of nature protection activities.

The map, made on the basis of the given methodology contain the information necessary for optimal location of specific engineering sites, development of nature protection activities and rational use of geological environment. They serve as a cartographic basis of engineering geocryological monitoring.

EXPERIMENTAL STUDIES ON ICE SEGREGATION AND THE MODES OF FROST HEAVING

Chen Ruijie[1] and Kaoru Horiguchi[2]

[1]State Key Laboratory of Frozen Soil Engineering, Lanzhou Institute of Glaciology and Geocryology, Chinese Academy of Sciences, China
[2]Institute of Low Temperature Science, Hokkaido University, Sapporo, Japan

Frost heave rate of freezing soils has been paid close attention to, and numerous theoretical and experimental studies have been done since the beginning of research on freezing soils in cold regions. The temperature gradient across the warm side of the ice lens has long been considered as the driving force of water flow, and the existance of a frozen fringe has been thought of as a definiteness and used as a basis for further research. Some experiments were carried out in which ice lens grew without temperature gradient in the soil. The comparison between ice intrusion temperature and equilibrium temperature indicated that the frost heaving occurred under general conditions (loose soil in natural field) usually is primary heaving.

INTRODUCTION

Since Miller's putting forward the concept of frozen fringe, it has been accepted and used widely, and most of ice segregation processes have been dealed with on the basis of the theory of secondary heaving. The existence of frozen fringe in frost heave process be seldom suspected, though it has hardly been observed up to now. And the temperature gradient in the frozen fringe has been considered as the driving force of water flow toward the ice lens.

Frozen fringe is a thin zone of frozen soil from the growth edge of the ice lens to 0°C isotherm, according to Miller's theory (1978), Konrad and Morgenstern (1980) got a theoretical consideration for one — dimensional frost heave without externally applied load, which was that the water intake flux is proportional to the temperature gradient in the frozen fringe. As early as 1974, however, Vignes carried out a model experiment by using glass tube and confirmed that frost heave rate is a function of the ice-water meniscus temperature and is independent of the temperature gradient of the unfrozen part along the capillary. Besides, Ishizaki,et al., (1985), performed frost heave experiments and obtained a linear relationship between water intake rate and the warm side temperature of the ice lens. Ozawa, et al., (1980), used micropore filter in the experiments and had the ice grow on it, and also obtained the same results with Ishizaki (1985), although the experiments are different in form. Horiguchi (1992) analyzed the frost heaving process theoretically, wrote out the water and heat flow equations during ice segregation, and obtained the linear dependence of water intake rate on segregation temperature.

So far, however, most of the researchers thought that water intake in the forming of ice lens necessarily results from the temperature gradient in the frozen fringe. Hence, we carried out an experiment in which the temperature of the soil sample keeps homogeneous in ice segregation process. More over, it becomes probable to make clear the occurrence of the modes of frost heaving by comparing ice intrusion temperature and equilibrium temperature.

EXPERIMENTS AND ANALYSIS

The apparatus used in the experiments is diagrammed in Fig.1, the soil sample used is Fujino Mori clay, its grain size distribution is showed in the paper about ice intrusion temperature.

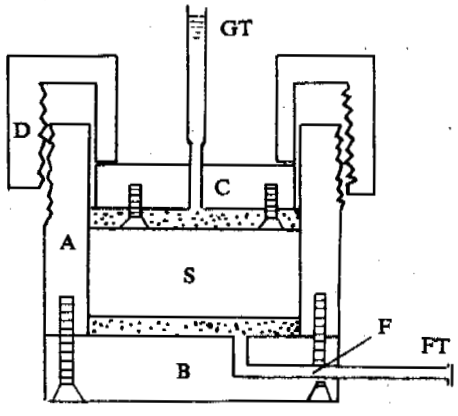

Fig.1 Apparatus

The experimental procedure was similar to that of the ice intrusion experiment except that the screw lid not be used here. After seeding at the bottom tube, ice advanced to the bottom of the soil sample, and ice lens formed here. The water level in tube GT was observed decreasing gradually.

Fig.2 and Fig.3 are the diagrammatic sketch of the experiments.

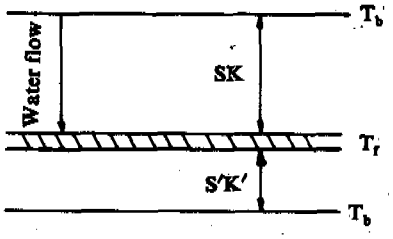

Fig.2 Diagrammatic sketch of the ice segregation in the experiment

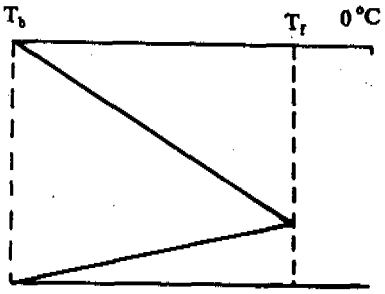

Fig.3 Temperature condition of the experiment
T_b — buth temperature;
T_f — warm side temperature of the ice lens, that is, ice segregation temperature.

Because of releasing of latent heat in forming of the ice lens, ice segregation temperature T_f probably be slightly higher than the surrounding temperature T_b. It indicated that the temperature gradient on the side of water supply is in reverse to that of the so called frozen fringe. If though the latent heat released is not enough to make temperature T_f higher than T_b, T_f is equal to T_b at least. Then no temperature gradient exists in the side of water supply. Now, measuring ice segregation temperature T_f accurately is still a difficult problem. But in a word, temperature gradient and frozen fringe are not always necessary in the forming of ice lens.

Fig.4 is a sketch map about the modes of frost heaving achieved by comparing ice intrusion temperature with equilibrium temperature, according to the definition of ice intrusion temperature in the paper (see this proceedings). When the ice intrusion temperature θ_i of a given soil is lower than the equilibrium temperature θ_e which comes from Clausius-Clapyrom equation, ice can not intrude forwards to form pore ice in the growth side of the ice lens. The frost heaving then be primary heaving, and no frozen fringe exists. Otherwise, the ice can intrude forwards in the growth side of the ice lens to form pore ice, frozen fringe, if the ice intrusion temperature θ_i of the soil is higher than the equilibrium temperature θ_e. And the frost heaving then be secondary heaving.

T_f and T_c is the ice segregation temperature and cold side temperature of the soil respectively.

Fig.5 is the relationship between ice intrusion temperature and confined pressure, the potted line drawn up comes from Clausius-Clapyrom equation. The curve represents change of ice intrusion temperature of silt or clay with

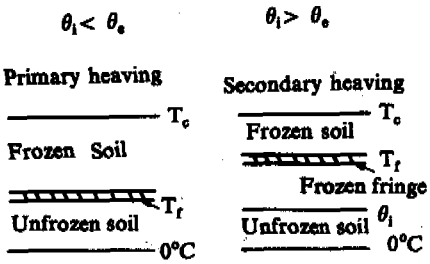

Fig.4 Analysis of the modes of frost heaving

confined pressure (see this proceedings, Chen, et al.).

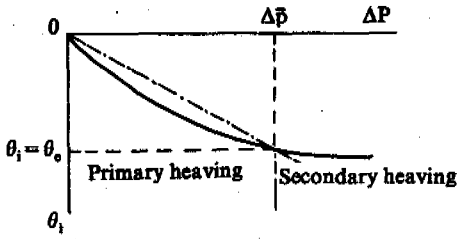

Fig.5 Analysis of the modes of frost heaving

For a given soil, if the confined pressure ΔP reaches a critical value $\Delta\bar{p}$, the ice intrusion temperature θ_i of it will be equal to the equilibrium temperature θ_e. If $\Delta P < \Delta\bar{p}$, then $\theta_i < \theta_e$, the heaving will be primary heaving. In contrast, the heaving will be secondary heaving.

CONTROLLING FACTORS OF FROST HEAVE RATE

Horiguchi (1992) obtained the theoretical result about water intake rate on the basis of Darcy's law:

$$J_m = -\frac{\bar{K} L}{\bar{V}_w g T_o S}(T_f - T_f^o) \qquad (1)$$

where T_f and T_f^o is ice segregation temperature and equilibrium temperature respectively. $\bar{K}$, L, $\bar{V}_w$, S represents apparent hydraulic conductivity, latent heat of ice melting, specific volume of water and distance of water migration respectively. It means that water intake rate is dependent on the ice segregation temperature, or the depression of freezing temperature, $(T_f - T_f^o)$. And it is supported by the experiments by Ishizaki, et al., (1985), It is possible and rational to conclude that the driving force for water flow is the depression of freezing temperature for general conditions.

According to the relationship between heat flow (latent heat) and water flow, we get follows for our experiments (see Fig.2):

$$\begin{aligned} J_m &= -\frac{1}{L}\iint_S k \frac{\partial T}{\partial n} da \\ &= \frac{1}{L}\left(\frac{k}{s} + \frac{k'}{s'}\right)(T_f - T_b) \\ &= B(T_f - T_b) \end{aligned} \qquad (2)$$

where k and a are thermal conductivity, area of integration respectively, B is a parameter relating to the thermal conductivity of the case.

From equations (1) and (2), we get ice

segregation temperature:

$$T_f = \frac{A}{A+B} T_b + \frac{A}{A+B} T_f^\circ \qquad (3)$$

then, from equation (1), we get:

$$J_m = -\frac{AB}{A+B} (T_b - T_f^\circ)$$

Comparing constants A and B which represents thermal and hydraulic condition of the system respectively, we get three kinds of situations as follows:

1) $B >> A$

$$\frac{A}{A+B} \equiv m << 1$$

$$T_f = mT_b + (1-m) T_f^\circ \simeq T_f^\circ \qquad (T_f < T_f^\circ)$$

$$J_m = -A(1-m)(T_b - T_f^\circ) \simeq -A(T_b - T_f^\circ)$$

It indicates that water intake rate is controlled by thermal condition of the system (Ozawa, 1989).

2) $B << A$

$$\frac{B}{A+B} \equiv n << 1$$

$$T_f = (1-n) T_b + nT_f^\circ$$

$$= T_b + n(T_f^\circ - T_b) \simeq T_b \qquad (T_f > T_b)$$

$$J_m = -B(1-n)(T_b - T_f^\circ) \simeq -B(T_b - T_f^\circ)$$

It indicates that water intake rate J_m is controlled by hydraulic condition of the system (Ishizaki, 1985).

3) $A \simeq B$

$$T_f \simeq \frac{1}{2} (T_b + T_f^\circ)$$

$$J_m \simeq -\frac{A}{2} (T_b - T_f^\circ)$$

CONCLUSION

Frost heave rate is not always dependent on temperature gradient on the warm side of the ice lens, and the driving force for water flow is originated from the depression of freezing temperature, but not temperature gradient. In other wards, frozen fringe does not exist constantly in process of ice segregation, the frost heaving due to the forming of warmest ice lens of silt or clay occurred in natural field usually be not secondary but primary heaving because of the relatively low load pressure. For the ice segregation not unidirectional freezing, it becomes possible to estimate the value of ice segregation temperature and which of thermal and hydraulic condition is the dominant factor for water intake, i.e. for frost heaving.

REFERENCES

Edlefsen, N.E. and Anderson, A.B.C. (1943) Thermodynamics of soil moisture. Hilgardia, 15:31-298.

Forland, K.S., Forland, T. and Ratkje, S.K. (1988) Frost heave. Proc. 5th Int. Conf. on Permafrost, Trondheim, Norway, P.344-348.

Horiguchi, K. (1987) An osmotic model for soil freezing. Cold Reg. Sci. and Tech. 14:13-22.

Horiguchi, K. (1991) Transport equations during ice segregation in a dispersed medium. J. Colloid Interface Sci., 144;297-298.

Horiguchi, K. and Miller, R.D. (1983) Hydraulic conductivity functions of frozen materials. Proc. 4th Int. Conf. on Permafrost, Nat. Acad. Sci., Washington, D.C., 504-508.

Ishizaki, T. (1985) Experimental study of final ice lens growth in partially frozen saturated soil. Forth International Symposium on Ground Freezing.

Konrad, J.M. and Morgenstern, N.R. (1980) A mechanistic theory of ice lens formation in fine-grained soils. Can. Geotech. J., 17: 473-486.

Kuroda, T., and Lacmann, R. (1982) J. Cryst. Growth 56, 189.

Miller, R.D. (1978) In "Proc. 3rd Int. Conf. Permafrost" Vol.1, p.707, National Research Council of Canada, Ottawa.

Miller, R.D. (1980) Freezing phenomena in soils (Chapter 11), Applications of Soil Physics (Ed. Hillel, D.).

Ozawa, H. (1989) Segregated ice growth on a microporous filler. Journal of colloid and Interface Science, Vol.132, No.1.

Vignes, M., and Dijkema, K.M. (1974) J. Colloid Interface Sci. 49, 165.

The Relationship between Ice Intrusion Temperature and Confined pressure

Chen Ruijie[1] and Kaoru Horiguchi[2]

[1] State Key Laboratory of Frozen Soil Engineering, Lan Zhou Institute of Glaciology and Geocryology ,Chinese Academy of Sciences
[2] Institute of Low Temperature Science,Hokkaido University,Sapporo,Japan

Ice intrusion temperature is a temperature near and below 0℃ at which the freezing of pore water can advance continuously with no water migration, and unfrozen water content and hydraulic conductivity of the soil decrease sharply at it. The experiments indicated that ice intrusion temperature decreases with increase of the confined pressure, that is, there are different ice intrusion temperature for different pore size because of different degree of compression.

INTRODUCTION

In cold regions, the downward freezing of soil surface, when winter coming, usually is not due to ice nucleation with occurrance of supercooling, but due to ice intrusion. Therefore, ice intrusion temperture is a temperature which differs from the stable freezing temperature after supercooling process and its dependece on confined pressure is significant for study on the process of ice segregation, especially on the modes of frost heaving. The freezing of free water can advance at about 0℃ as well known. The freezing of pore water, however, advance only at a temperature below 0℃, according to the pore size because of adsorption. For a given soil, different pore size responds to different confined pressure. The relationship between ice intrusion temperature and confined pressure was obtained through ice seeding at the bottom of the soil.

APPARATUS AND MATERIALS

The apparatus used is diagrammed in Fig.1, brass cylinder A is connected with bottom plate B in which there is a bore hole F, 2 mm in diameter, connected with a rubber tube FT. There is also a bore hole in the center of the top plate C, which is connected with a rubber tube GT. Lid D can be screwed down along the cylinder to prevent plate C from moving upward. It means that soil sample S, can be confined in the cylinder with certain pore size.

The materials used in the experiments are Corundum A (3—7 μm), Corundum B (24 μm), Fujino Mori clay C, Alluvial clay D and Manaitabashi clay E. Fig.2 and Fig.3 is the diagramm of particle size of Corundum A and B respectively. Fig.4 is the grain size distribution of all materials used.

ICE INTRUSION EXPERIMENTS

A cold liquid buth was used and controlled at a temperature near and below 0℃ , and its temperature was measured by standard thermometer.

A little water was put inside the cylinder holder first and the rubber tube FT was stopped up by a stopper to assure that no air bubble exist in bore hole F. An air–free porous plate N1 was then put on the bottom plate in the cylinder holder and adequate amount of slurry of the soil sample was put on the porous plate. Afterwards ,the top plate N2 was pushed into the holder and the excess water moved up into the tube GT. O ring was used for sealing up the holder. Certain amount of load was used on the top plate C to compress the sample for enough long time until the water level in tube GT did not move. Then the lid D was screwed down to fix top plate C, and the load was taken away.

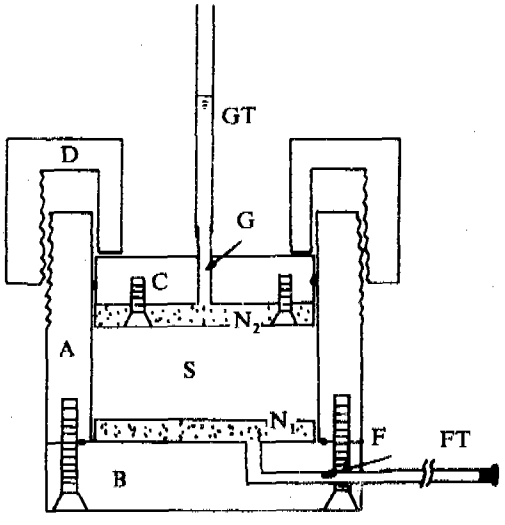

Fig.1 Apparatus

The apparatus prepared was immersed in the cold liquid buth which was controlled at −0.1℃. A small length of tube GT was left outside of the buth so that the water level in it could be observed. Tube FT was then seeded by putting it in liquid nitrogen after about 24 hours. The temperature of the cold liquid buth was lowered by −0.1℃ step by step, and it was observed that the water level in tube GT marched a great deal abruptly at certain temperature. It indicated that the seeding ice had intruded into the soil, that is, ice intrusion occurred. The temperature showed by the standard thermometer is the ice intrusion temperature of this soil under given confined pressure.

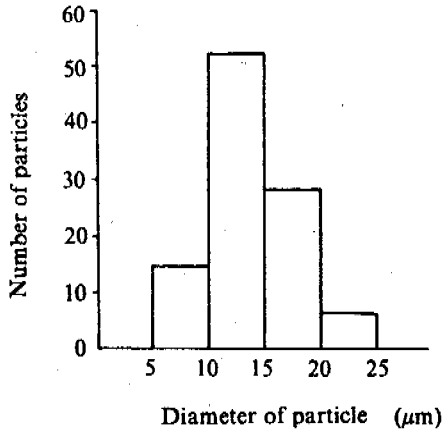

Fig.2 Particle size distribution

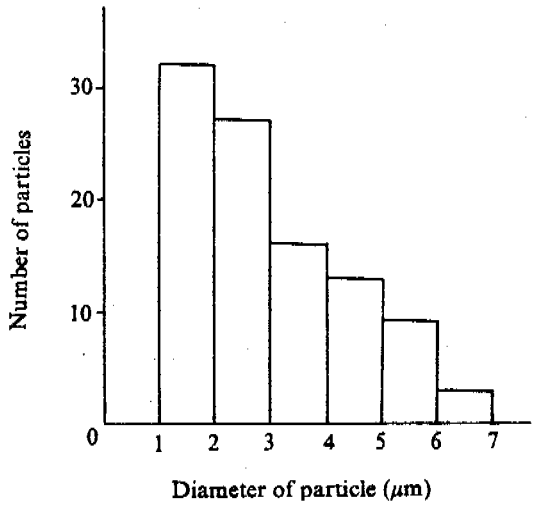

Fig.3 Particle size distribution

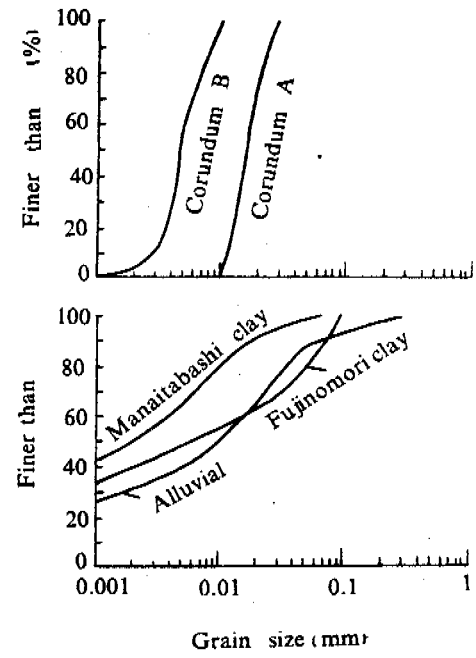

Fig.4 Grain size distribution

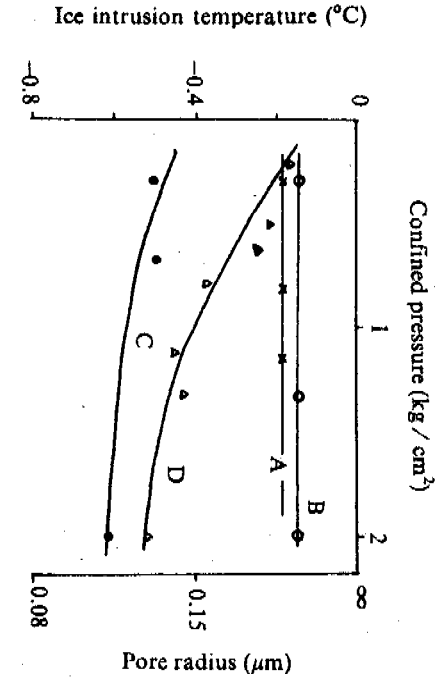

Fig.5 Relationship between ice intrusion Temperature and confined pressure

RESULTS AND DISCUSSION

The experimental results of the relationship between ice intrussion temperature and confined pressure of the materials were showed in Fig.5 Curve A, B, C, D, and E represents Corundum A (3—7 μm), Corundum B (3—7 μm), FujinoMori clay, Alluvial clay and Manaitabashi clay respectively. It can be found that for fine soil, such as FujinoMori clay and Alluvial clay, the ice intrusion temperature decreases with increase of the confined pressure. The ice intrusion temperature of corse particles, such as Corundum, almost keeps constant with increase of confined pressure, that of Manaitabashi clay, however, shows relatively low value compared with other samples, because of its fineness, though there is only one point obtained.

Assuming that the freezing frant at each pore shows a hemispherical meniscus, there will be a depress of the freezing point. This depress corresponds to ice intrusion temperature. The right hand axis in Fig.5 is pore radius calculated from the following equation which comes from the Clausius–clapyron equation and Laplace equation:

$$r_m = -\frac{2T_0\,\sigma}{\rho_i L\,\theta_i}$$

in which r_m, and $\theta_i$respresents pore radius and ice intrusion temperature, respectively. T_0, ρ_i, and L respresents melting point of ice, density of ice and latent heat of melting ice, respectively.

It can be found that the pore radius decreases with increase of confined pressure for fine soil. That is, ice intrusion temperature of fine soil decreases with decrease of pore radius. The two kinds of corse particles, i.e, Corundum A and B, keeps constant because it is almost incompressible and its pore radius keeps almost unchange with change of confined pressure.

REFERENCES

Kaoru Horiguchi 1989 Short Report: Relationship between Confined Pressure of a Sample and Ice Intrusion Temperature. Low temperature Science,Ser.A,48.

PRELIMINARY TESTS OF HEAVE AND SETTLEMENT OF SOILS UNDERGOING ONE CYCLE OF FREEZE-THAW IN CLOSED SYSTEM ON A SMALL CENTRIFUGE

Xiangsheng Chen[1], A. N. Schofield[2] and C. C. Smith[3]

[1]Central Coal Mining Research Institute (CCMRI), Beijing, CHINA
[2]Department of Engineering, University of Cambridge, Cambridge, UK
[3]Department of Civil & Structural Engineering, University of Sheffield, UK

Over the last few decades, geotechnical centrifuge modelling has become increasingly accepted as a valid technique for accurately representing full scale prototype behaviour of geotechnical problems in temperate climates in small scale models subjected to high accelerations. The potential exists for it to be applied to certain cold regions ('unconventional') problems with equal benefit. This paper presents preliminary results of some frost heave and thaw induced settlement tests undertaken on a small centrifuge. The tests involved simulations of heave and settlement of sand, silt, kaolin, and china clay undergoing one cycle of freeze/thaw in a closed system. The results of modelling of models of heave and settlement for both sand and china clay at different g-levels indicate that the centrifuge scaling of both these processes is self-consistent with scaling factors for time and displacement of N^2 and N, respectively, where the g-level is N times of that of the earth's gravity. Different g-levels were not observed to have major influence on the patterns of both forst heave and thaw induced settlement of soils in a closed system, although they seems to have a very slight suppression on heave.

INTRODUCTION

Frost heave and thaw induced settlement of soils are among two of the most investigated topics in cold regions engineering research, much of it driven by development in the polar areas. Many researchers have published data of experiements related to the two problems *e.g.* Miller (1980), Anderson *et. al.* (1978), Nixon & Ladanyi (1978), most of which focus upon laboratory tests, rather than in situ experiments, due to the lengthy, cost and time involved with in-situ testing. Many of the difficulties of conducting full scale field tests may be solved by the modelling of prototype structures in the laboratory using geotechnical centrifuge techniques in which many prototype time-dependent processes can be accelerated by testing a small scale model in an enhanced gravity field (Schofield, 1980). There has been increasing interest in modelling cold regions events in the centrifuge over the last decade; Palmer *et. al.* (1985) describe the potential for the centrifuge to model underwater permafrost and sea ice. Experimental work involving the thaw induced settlement of pipelines has been reported by Smith (1991). Schofield & Smith (1993) describe the potentials and limitations for modelling cold regions problems on the centrifuge.

To date very little work has been done on the centrifuge modelling of frost heave and there remains several aspects of the modelling of frost heave, thaw induced settlement, and a combination of the two which have not completely been understood, particularly the influences of differing g-levels on both heave and settlement and on the patterns or displacement characteristics of soils. Some results of preliminary centrifuge modelling experiments at the Geotechnical Centrifuge Centre of Cambridge University Engineering Department addressing these matters are presented in this paper as well as the results of tests involving the long term heave and settlement of soils undergoing one cycle of freeze-thaw in closed system.

EQUIPMENT, INSTRUMENTATION AND PREPARATION

The machine used for the experiments at Geotechnical Centrifuge Centre of Cambridge University Engineering Department is a small commercially available table-top centrifuge adapted for soil mechanics modelling. It is used with two pairs of counterbalancing 750ml windshielded swinging alloy buckets (Fig. 1.) of internal dimension ϕ 98mm × 122mm and a special slipring stack providing up to 16 multiplexed data channels. At the maximum rotational speed of 383rad/s the acceleration of the base of each bucket at 200mm radius is 3000g. Microprocessor control permits

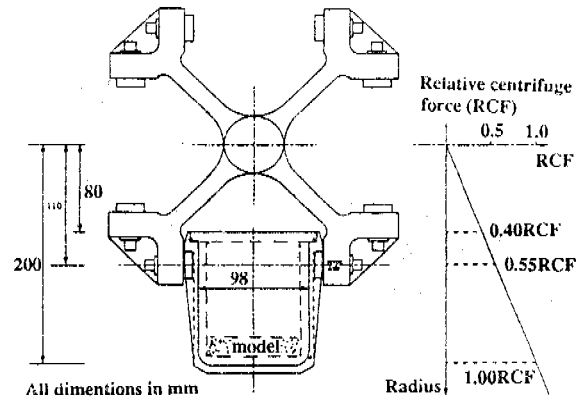

Fig.1. Centrifuge modelling system layout

the adjustment and control of the temperature in the centrifuge chamber within the range of −10°C to +30°C.

A pair of centrifuge buckets contain a counterbalancing pair of identical soil models. These are either placed within custom-made liners (ϕ 82mm × 105mm) which contain soil models (Model A: ϕ 82mm × 30mm, refer to the following) or inner nylon containers (Model B: ϕ 50mm × 20mm and Model C: ϕ 25mm × 10mm, refer to the following), in which soil models are then put.

In these preliminary tests, the freezing generated by cold air in the centrifuge chamber was controlled as far as possible to start from one end (top surface) of the soil model and then to progress to the other end (bottom). Thermistors were employed to measure temperatures on the soil model surface during testing, and a LVDT was installed on each of the model buckets, and used to measure surface displacements (frost heave and thaw induced settlement) of each soil model at the same time.

Computer logging and real time plotting of data made it straightforward both to determine the peak level of frost heave (LVDTs' readings)/temperatures (thermistors' readings) on the basis of which it was determined when defreeze should start (in general, 1 hour

or so after the peak appeared).

In order to minimize the influence of the LVDT's weight (<2g) as far as possible, different sizes of very thin perforated plastic plates were put between spindle end and the surface of soil model. The stress caused by both the spindle and the plate on model surface was kept below 0.063 kN/m^2 for all three kinds of Models. It was not expected that this small magnitude of stress would have a significant influence on the free displacements of soil model.

Each soil model was cylinder with its diameters larger than its heights. Model B (ϕ 50mm × 20mm) and Model C (ϕ 25mm × 10mm) were mainly used, although a larger diameter of Model A (ϕ 82mm × 30mm) was used at the beginning. The heights of 10mm, 20mm and 30mm chosen were mainly based on the available radius of the used small centrifuge. Generally speaking, the ratio of model height to the effective centrifuge ratational radius is recommendated less than or equal to one tenth in order to keep test results to a necessary accurary (Schofield (1980)). Those models with their heights <20mm have a larger ratio $\leq$ 16%.

Four different types of soils were used in the tests: kaolin, china clay, silt and sand. The following is the average of water content W and that of unit weight γ for each kind of soils. Kaolin: $W = 0.70$, $\gamma = 15.30 - 15.99kN/m^3$; china clay: $W = 0.93$, $\gamma = 13.83 - 14.32kN/m^3$; silt: $W = 0.36$, $\gamma = 18.74 \sim 19.52kN/m^3$; and sand: $W = 0.32$, $\gamma = 17.66 \sim 18.25kN/m^3$.

TEST PROCEDURE

For each test, two identical soil models were made up, loaded and tested in opposing centrifuge buckets. This ensured balance would be maintained at all times no matter how the models deformed and also gave a measure of the repeatability of the experiments.

Kaolin, china clay and silt were loaded into model containers as a slurry, while sand was loaded in saturated state under vacuum. Each soil model was then consolidated in the centrifuge before freeze test began. The duration of consolidation differed depending on the types of soils, for example about 10 years (prototype equivalent) for sand in the modelling of models test, and 15 years or so for the china clay in its modelling of models. Upon stopping the machine, the surfeit of water found on the surfaces of soil models was carefully sucked out by using a syringe. The kaoline and clay tended to consolidate with a curved surface due to the radial acceleration field (Fig 2.) and these surfaces were cut level. The temperature within the centrifuge chamber was initialised to around $+10°C$. The LVDT spindles and perforated plastic plates were then placed on the soil surface, and thermistors installed (through one of holes on the plate). Next, all models and transducers were put into the centrifuge when the temperature in the chamber reached $10°C$. The machine was set running and data was logged either manually or by computer. A particular prototype freezing rate was chosen and applied to the model using a scaling factor time of N^2 where N is the model scale, and a model acceleration of Ng was selected. Freezing then took place down to a temperature $-15°C$ for freezing. When the frost peak was observed for one hour then thaw settlement was initiated by raising the surface temperature at the correctly scaled prototype rate up to a temperature of $+18°C$. On completion of the tests, each model was weighed and moisture content taken.

All tests were carried out in a closed system. A series of modelling of models were conducted for each type of soils in order to confirm the validity of centrfuge modelling of frost heave and thaw induced settlement of soils.

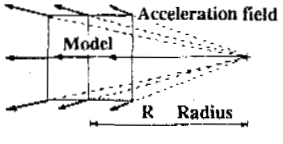

Fig.2. Centrifuge generated radial gravity in soil model (after J-F. Corte)

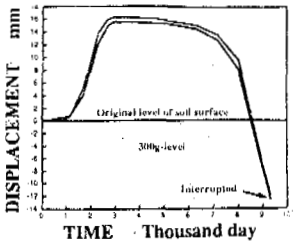

Fig.3. Heave and settlement of prototype kaoline (2m)

RESULTS AND DISCUSSION

Fig.4 (showing thermocouple readings) and Fig.5 show the results of modelling of models tests for prototype china clay and prototype sand undergoing one cycle of freeze-thaw in closed system, respectively, with time scaling factor N^2 and displacement one N. For each test two displacement curves were obtained from the pair of identical soil models in the counterbalanced buckets. From Fig.4 and Fig.5, it can be seen that these two curves are very similar for the same soil models in one flight, which indicates conditions at the two buckets are almost the same and gave confidence in test repeatability. Compared with each other at two different g-levels, it is obvious that the results of modelling of models are very close and the patterns of the displacement curves at the two different g-levels

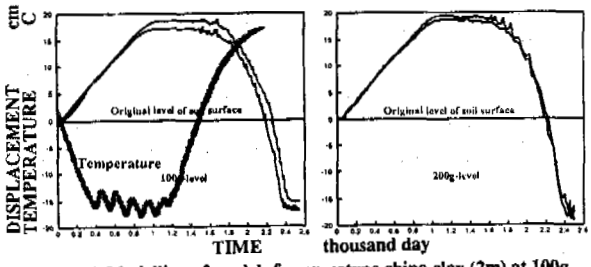

Fig.4. Modelling of models for prototype china clay (2m) at 100g and 200g levels

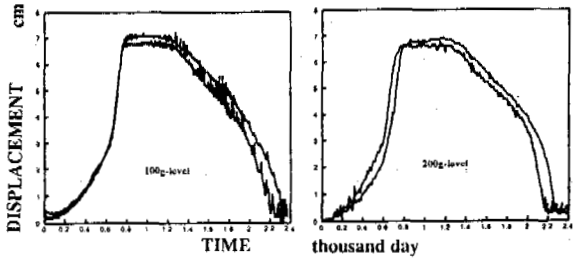

Fig.5. Modelling of models for prototype sand (2m) at 100g and 200g levels

are almost the same for the same soil. These facts indicate that centrifuge modelling of frost heave and thaw induced settlement of soils is feasible if careful attention is paid to controlling the conditions and model preparation. One can also find from the figures that frost heave of china clay is much larger (nearly 1.5 times) than that of sand with the same thickness (2m), which can be mainly attributed to the larger water content (0.93) in the former than that (0.32) in the latter.

It is very interesting to observe in these tests that thaw induced settlement of sand are different from that of china clay. Settlement of sand is almost equal to its heave, while that of china clay (slurry before freezing) is near to twice its frost heave, and as might be expected resulted in a significant body of water on the surface of the china clay models on completion of the tests. A similar finding can be seen in kaolin (Fig.3). This fact indicates that freezing exerts a desiccating effect on clay to some extent similar to that found in freeze/thaw treatment of organic sewer sludge.

On comparing Fig.4 with Fig.5, it is seen that frost heave ratio (frost heave amount to original soil thickness) of sand is less than that of china clay for the same dimension (thick 2m) significantly, and that the heave rate for sand changes from a slow to a sharp increase and takes about 790 days (prototype equivalent) to reach its heave peak, on the other hand, the latter (1.83mm/day or so) increases almost constantly except during the very initial stage, and its duration of heave is little longer-about 975 days. For the thaw induced settlement patterns, sand differs from china clay. The rate of the former changes from slow to very fast, while the latter decreases gradually. The duration of settling, however, is very close though that of sand is slightly shorter (880 days for sand and 910 days for china clay).

Edge friction between soil model side and model container side with silicone grease did not appear to have an obvious influence on frost heave results. This can be seen from Fig.6 and Fig.7 which show heave and settlement of sand at the same g-level but with different thickness (2.8m and 2.4m in prototype). The heave ratio for both is very close (3.40 % for the former and 3.39 % for the latter).

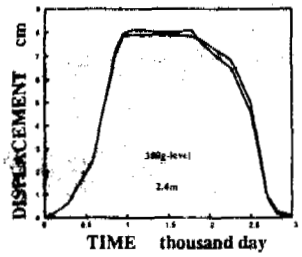

Fig.6. Heave and settlement of prototype sand (2.4m)

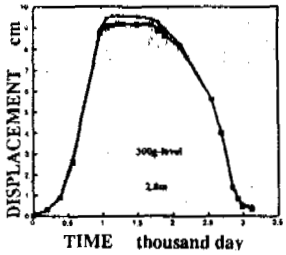

Fig.7. Heave and settlement of prototype sand (2.8

On comparing frost heave of the same soil at different g-levels, it can be seen that the heave ratio slightly decreases with increase of g-level. For example, the heave ratios of china clay are 9 % and 8.4 % at 100g-level and 200g-level, respectively, (from Fig.4.). The same trend can be found for sand in Fig.5, Fig.6 and Fig.7, and for silt in Fig.8 and 9. This fact indicates that g-level may has some suppressing effects on frost heave, that is, the greater the g-level, the slightly less the frost heave in closed system. However it may be possible to attribute this to the radially varying g-field of the centrifuge, which may be significant particularly in this small centrifuge. Tests undertaken in larger machine may be less affected.

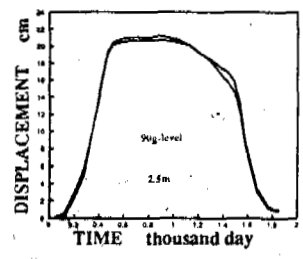

Fig.8. Heave and settlement of prototype silt (2.5m)

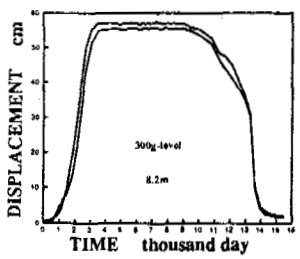

Fig.9. Heave and settlement of prototype silt (8.2m)

Silt undergoes the largest magnitude of frost heave, as shown in Fig.8 and Fig.9. In the former the frost heave ratio reaches 6.8 % and in the latter that is near to 7 %, almost close to that of china clay in which, however, water content (0.93) is larger than that (0.36) in silt.

To freeze a prototype equivalent silt layer of thickness 8.2m needs more than 9 years at a temperature $-15°C$, to defreeze it, however, lasts about more than 13 years if temperature on the soil surface increases from $-15°C$ to $+18°C$ in approximately one year and is then kept constant. To freeze silt of thickness 2.5m needs 1.5 years at a temperature $-15°C$, on ther other hand, to defreeze it lasts almost 2 years, according to the centrifuge modelling of protoype soil. One can find the freezing and thawing time for prototype china clay and sand in Fig.4, Fig.5, Fig.6 and Fig.7.

The results indicate that g-level does not appear to have obvious influence on patterns of frost heave and thaw induced settlement of the same soil, as shown in Fig.8 and 9; in Fig.4; in Fig.5, 6 and 7.

It should be noted that the frost heave ratio for tested soils seems larger for a closed system when their water contents are taken into account. The frost heave of soil in closed system is mainly attributed to its water content. If it is assumed to be purely due to the expansion of water as it forms ice then the expected heave ratio is: $\frac{wG_s \times 0.09}{1+wG_s}$. In these tests, however, the heave ratio of silt reaches 7% (expected 4.4%) with water content 0.36; that of china clay is about 9% (expected 6.4%) with water content 0.93; that of kaolin gets 6% (expected 5.8%) with water content 0.7; and that of sand is proximately 3.4% (expected 4.1%) with water content 0.32. The researi are not clear and should be further investigated.

CONCLUSIONS

From the above some preliminary conclusions can be presented.

a). It appears possible to model frost heave and thaw induced settlement of prototype soils accurately in small centrifuge, and thus by extrapolation in large centrifuge, with time scaling as N^2 and displacement (heave, settlement) as N. This certainly warrants further investigation and if substansiated will demonstrate the centrifuge to be a useful tool for the investigation of prototype frost heave and thaw induced settlement problems in shortened time scales.

b). An increasing g-level appears to have some suppression effect on frost heave of soils, i.e. frost heave decreases very slightly with increase of g-level. However this may be due to the limitations of the g-field in the small centrifuge used and needs further investigation.

c). The g-level does not appears to have an obvious influence on patterns of frost heave and thaw induced settlement.

d). Edge friction between soil model side and model container side does not appears to have an significant effect on frost heave when container sides are well greased.

e). The frost heave ratios of tested soils in closed system seem larger than would be expected from calculations based on the water content alone.

f). A small centrifuge of the type used has been shown to have a very useful capability for performing initial investigations to test the feasibility of certain concepts relatively quickly and at a low cost. The results show that further work on larger (more expensive) machine is worthwhile in this field.

ACKNOWLEDGEMENTS

The authors would like to thank the staff of the Geotechnical Centrifuge Centre of Cambridge University Engineering Department and ANS & A for their kind help, especially Dr. R Phillips, N Baker. The first author wishes to express his sincere gratitude to his supervisor Professor A N Schofield for his very valuable advice and kindness, and to Dr. M D Bolton for his much appreciated help and nomination of the first auther a Fellow Commonership in Churchill College Cambridge which offered him the post for 1992/93 with accommodation, facilities and etc. And finally, the first author is very grateful to Sir Y K Pao Foundation (Hong Kong), the Chinese Government and the British Council for their financial aids.

REFERENCES

Anderson, D M, and Penner, E (1978) Physical and thermal properties of frozen ground (pp37-102); in: Geotechnical engineering for cold regions.

Ketcham, S A (1990) Application of centrifuge testing to cold regions geotechnical studies (internal Report of USACRREL).

Miller, R D (1980) Freezing phenomena in soils (pp254-299); in: In applications of soil physics.

Nixon, J and Ladanyi, B (1978) Thaw consolidation (pp164-215); in: Geotechnical engineering for cold regions.

Palmer, A C, Schofield, A N, Vinson, T S and Wadhams,P (1985) Centrifuge modelling of underwater permafrost and sea ice; Proc 4th Int. Offshore Mechanics and Arctic Enfineering Symposium. Texas, Vol. II, (pp65-69).

Schofield, A N (1980) Cambridge geotechnical centrifuge operations; Twentieth Rankine Lecture, Geotechnique. (pp227-263).

Schofield, A N and Smith, C C (1993/4) Cold Regions Engineering in: Geotechnical centrifuge technology. ed. N. Taylor

Smith. C C (1991) Thaw induced settlement of pipeline in centrifuge model tests; Ph.D. dissertation of Cambridge University.

Vinson, T S and Palmer, A C (1988) Physical model study of artic pipline settlement; Proc 5th Int. Conf. Permafrost. Trondheim. Vol.2, (pp1324-1329).

FROST SUSCEPTIBILITY OF POWDERED CALCIUM CARBONATE

Chen Xiao-bai[1], Corte A.E[2], Wang Ya-qing[1] and Shen Yu[1]

[1]Lanzhou Inst. of Glaciology & Geocryology, Academia Sinica, Lanzhou, China
[2]Regional Investigation Centre of Sciences & Technology, Mendoza, Argentina

Frost susceptibility tests of a powdered calcium carbonate (PCC), collected from the Andes Mts near Mendoza, Argentina, were conducted both in closed and open systems. Experimental results show that an ice segregation and consequently an ice lens and strong frost heave could occur in PCC while rich in moisture. The freezing point T_f(°C) of PCC mainly depends on the moisture W (%) with a function of $T_f=-5199.62\ W^{-3.274}$. The frost heave rate of PCC R (mm/day) in a closed system increases with its water content W(%) intensively while W>17%. In an open system, the frost heave ratio η(%) decreases sharply with the frost penetration rate V_f(cm/day), and its regression equation is $\eta=4.495\ V_f^{-1.109}$. As a result, the frost susceptibility of PCC is very similar to that of clayey soils. After moisture was controlled or mixed with a special agent, the PCC could be very light or not frost susceptible and then could be used as a material in subgrades or base of buildings.

INTRODUCTION

Powdered calcium carbonate is rich in cold and arid areas, such as in the Padagonia regions and Andes Mountains in Argentina, as well as in Taishan Mountains area of China. Up to now, a lot of ancient buildings or structures in China remain unchanged because of stabilized bases mixed with powdered lime. At present, the lime stabilizer is widely used as an anti-heave cushions in China.

The purpose of this paper is to determine the frost susceptibility of PCC collected from the Andes Mts near Mendoza, Argentina and to find a way of using it as a construction material.

EXPERIMENT CONDITIONS

The samples of PCC collected from the Andes Mts near Mendoza, Argentina were less than 1 mm in size. The freezing point was determined by the supercooling method with various water content. For the frost susceptibility test, the samples with a given density and moisture were put in plexiglass cells, 11 cm in diameter and 2 cm in height. A thin grease layer and a membrane were set up between the surface of the cells and samples in order to reduce the friction resistance. The cells were surrounded by insulation. The multi-stages of temperature at the surface and the bottom of the samples were controlled by cycle refrigerator baths with a sensitivity of ±0.02°C and an accuracy of ±0.1°C. The temperature and the displacement of samples were determined by thermocouples and displacement gauges and were collected by HP 3054-S Automatic Data Acquisition and Control System. For an open system, the distilled water was supplied from the sample bottom towards the frost front from a special reservoir with a constant water level. After testing, the samples were cut into pieces for observation of ice segregation and measurement of the moisture profiles along the depth.

EXPERIMENT RESULTS AND ANALYSES

Freezing Point

The experiment results showed that the freezing point only depends on the moisture. Fig.1 illustrates the relation curves of the powered calcium carbonate. After regression, the curve function can be expressed by:

$$T_f=-5199.62\ W^{-3.274},\quad r=.943 \qquad (1)$$

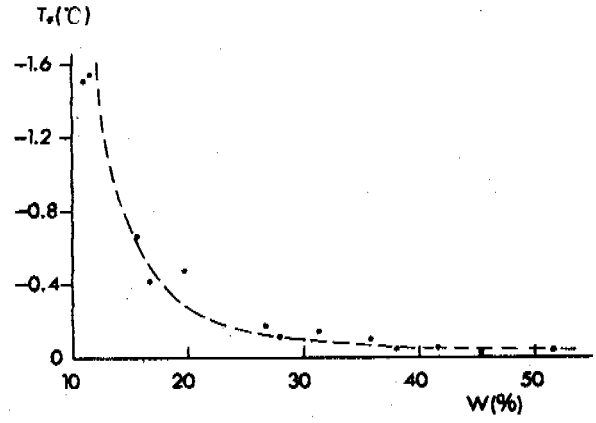

Fig.1 Freezing point of PCC vs water content
in where, T_f — freezing point of PCC, °C;
W — water content of samples, %;
r — correlation coefficient.

Frost Susceptibility

The results of 5 groups of frost susceptibility tests for the PCC with different water content and almost the same density, as well as same boundary temperature, are listed in Table 1. In which, sample CC-1 is in an open system. The

Table 1. The results of frost susceptibility tests on powdered $CaCO_3$ under different water conditions

No.	t (hrs)	Yd (g/cm³)	W (%)	T_f (°C)	h (mm)	Q (ml)	R (mm/day)	System
CC-1	126	1.62	25.51	-.13	22.58	109.6	4.35	open
CC-2	78	1.62	25.76	-.13	10.11		3.11	closed
CC-3	98	1.63	19.80	-.30	7.03		1.72	closed
CC-4	78	1.62	15.15	-.71	0.27		0.08	closed
CC-5	94	1.59	17.97	-.41	1.06		0.27	closed

*t — elapsed time; h — frost heave; Q — water intake.

frost heave and water intake processes are shown in Fig.2. It is obvious that the increase of heave is respondent to water intake.

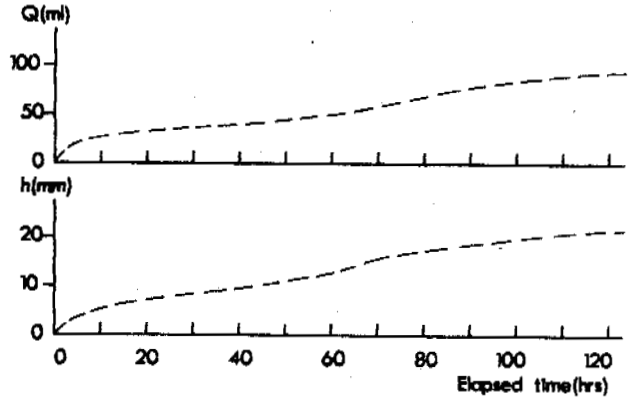

Fig.2 The frost heave and water intake processes of Sample CC-1

Fig.3 and 4 illustrate the temperature isothermal lines and heave processes. It is shown that the heave will reduce with the decrease of moisture in a closed system.

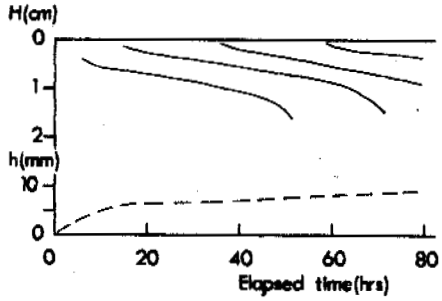

Fig.3 The temperature isothermal line and frost heave process of Sample CC-2

Fig.5 is the frost action profiles of Sample CC-1, CC-2, CC-3 and CC-4 after freezing, respectively. In which a large amount of ice lenses occurred in Sample CC-1, 1 to 2 mm in thickness and 1 to 2 mm in interval, because of water supply during freezing (see Photo), frost heave occurred as well. For Sample CC-2 with an initial water content of 25.76%, a small pingo developed in the top of ice lenses, 0.2 to 0.5 mm in thickness and 0.3 to 0.5 mm in

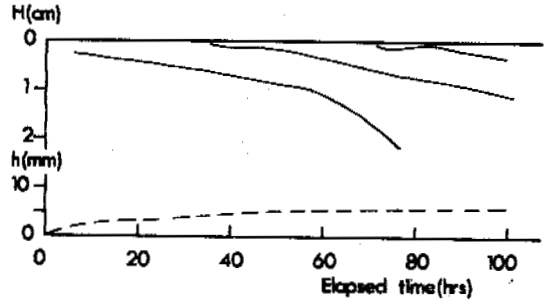

Fig.4 The temperature isothermal line and frost heave process of Sample CC-3

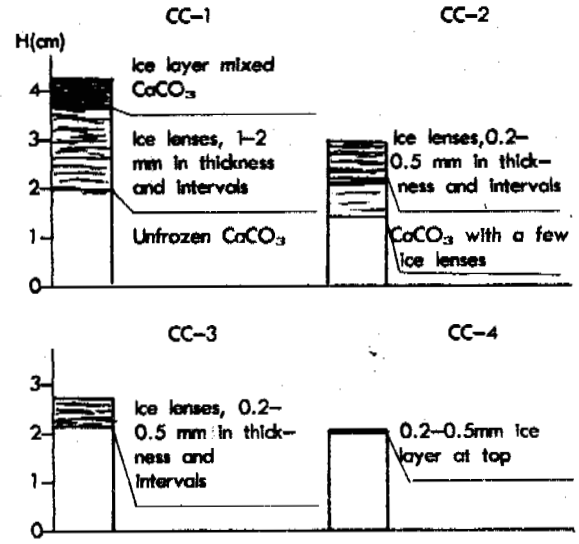

Fig.5 Frost action profiles of Sample CC-1, CC-2, CC-3, CC-4

interval. For Sample CC-3 with an initial moisture content of 19.80%, a fine ice crystal developed in the centre of the top and a few ice lenses under the crystal. For Sample CC-4 with an initial water content of 15.15%, there was only a thin ice layer 0.2 to 0.5 mm in thickness, which covered the upper surface. The water redistribution profiles of Sample CC-1, CC-2, CC-3 and CC-4 are illustrated in Fig.6.

Photo: Ice lenses occurred in Sample CC-1

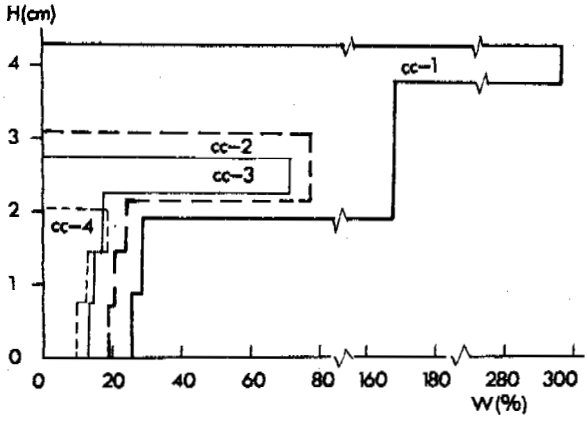

Fig.6 Water redistribution profiles of samples after freezing

From Table 1 we also know that the frost heave rate of PCC in a closed system increases with the moisture intensively while W>16% as shown in Fig.7 which will be useful for controlling frost heave by using limited water content.

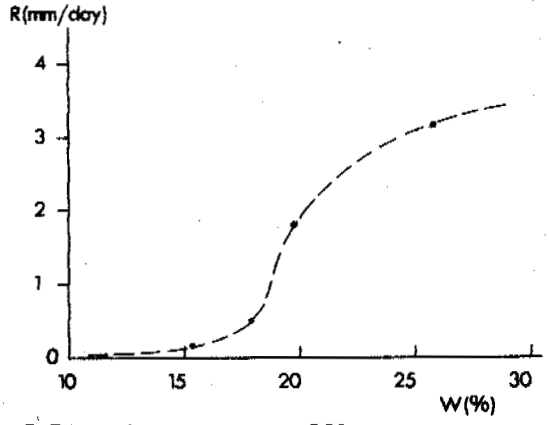

Fig.7 Frost heave rate of PCC vs water content in a closed system

For Sample CC-1 in an open system, the frost heave ratio decreases sharply with the increase of the frost penetration rate as shown in Fig.8 and the regression equation is as follows:

$$\eta=4.495\ V_f^{-1.019},\ r=0.4955 \qquad (2)$$

in where, η — frost heave ratio, %;
V_f — frost penetration rate, cm/day;
Eq.(2) is very similar to that of the authors' earlier works (Chen and Wang, 1983, 1987, 1988).

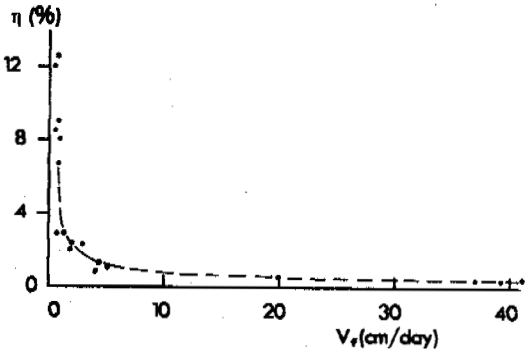

Fig.8 Frost heave ratio vs penetration rate of PCC in an open system

Application of An Anti-heave Agent

As mentioned above, the powdered calcium carbonate is frost susceptible while the moisture is large enough. In order to use the PCC as a material for subgrades or bases, besides controlling the water content, a special anti-heave agent could be used for reducing the frost susceptibility. As an example, if the PCC is mixed with a given content of a special agent with a lower cost, the freezing point might drop to -11.37°C. Consequently, this kind of anti-heave agent is powerful for changing the powdered calcium carbonate with strong frost susceptibility into a very light or non-frost susceptible material.

PRELIMINARY CONCLUSIONS

1. The powdered calcium carbonate collected from the Andes Mts, Argentina is frost susceptible, and a large amount of ice lenses will occur forming pingoes when it is rich in moisture;
2. After controlling the moisture or when mixed with a special anti-heave agent, the powdered calcium carbonate could be very light or non-frost susceptible and then might be used as a material in subgrades or bases of buildings.

REFERENCES

Chen, X.B., Wang, Y.Q. et al., (1983) Influence of penetration rate, surcharge stress and groundwater table on frost heave, Proceedings of VI ICOP, 131-135.

Chen, X.B., Wang, Y.Q. et al., (1987) Ice segregation and frost susceptibility of sandy gravel, Bulletin of sciences, 32(23): 1812-1815.

Chen, X.B., Wang, Y.Q. et al., (1988) Frost heave model of sandy gravel in open system, Proceedings of V ICOP, 304-307.

Comparison of Two Ground Temperature Measurement Techniques at an Interior Alaskan Permafrost Site

Charles M. Collins, Richard K. Haugen, and Timothy O. Horrigan

US Army Cold Regions Research and Engineering Laboratory
Hanover, New Hampshire 03755-1290

Two temperature measurement systems, a string of Chinese-fabricated mercury thermometers and a thermistor assembly, were installed in adjacent boreholes drilled in fine-grained, perennially frozen silt. The Chinese thermometers were provided by the Chinese Academy of Railway Sciences, Lanzhou. The thermometers read to 0.1 °C, and were supplied with correction tables also to 0.1 °C. The thermometers were assembled into a linear string to replicate, as closely as possible, the thermometer strings that are commonly used in China for monitoring ground temperatures. The sensors were installed at the Caribou-Poker Creeks Research Watershed in interior Alaska (65° 10' latitude, 147° 30' longitude). The thermometers were placed at the surface and at -0.6, -1.2, -2.1, -3.0, -4.5, -6.0, -9.0, and -10.0 m, with insulating spacers placed between each thermometer. The cable was suspended in air in a 5-cm-diameter casing installed in a 10-m-deep borehole. The thermometers were pulled from the hole periodically to obtain the temperature readings. The thermistor cable consisted of an assembly of YSI 4407 glass bead thermistors placed at the surface and at -0.3, -0.6, -0.9,-1.2, -1.5, -2.1, -3.0, -4.5, -6.0, -9.0, and -10.0 m. The assembly was inserted in a similar 5-cm-diameter casing installed in a 10-m borehole located 30 cm from the thermometer string. The pipe containing the thermistors was filled with silicon fluid and capped. The cable was extended some distance from the pipe to avoid surface disturbance. Simultaneous measurements were made on the thermometer string and the thermistor assembly over three years. The thermistor string remained undisturbed within the silicon fluid environment. The thermometer string, suspended in air with the insulating spacers, was removed each time a series of readings was made.

For statistical analysis, we grouped these depths into three zones: the upper 1.2 m, the middle range from 2.1 m down to 4.5 m, and the lower from 6.0 m down to 10.0 m. During the summer months of 1988 and 1989 (Fig. 1), the thermometers yielded higher readings (as much as 1.5 °C higher). Conversely, during the winter months, the thermometer readings were lower. The pattern of seasonal differences was not evident during the final year of the test evaluation (1990). In the middle zone (2.1 m through 4.5 m), the pattern was similar, warmer during the warmer months, and slightly cooler during the cooler months. The warmest period of the year at this zone occurs during the late fall. The thermometer readings for this middle zone are skewed upwards only during the warmer period (during the summer and fall) and not during the winter cooling period. Below 6.0 m (Fig. 3), the two time-series for the lower zone were almost parallel to each other. The thermometer readings were higher than the thermistor readings by an average of 0.17 °C, suggesting that the calibration of the thermometers was higher than that of the thermistors. (The average differential between thermometer and thermistor readings was 0.17 and 0.18 °C in the top and middle zones.) Figure 4 shows the time series of the differences between the thermometer and thermistor readings. The upper and middle zones show seasonal patterns of difference for most of the record; the lower zone is stable in this regard.

We attribute the minor differences in measured values between the two sensor types to an apparent difference of about 0.17°C in calibration between the two sensors, and a possible influence of ambient air temperature on the mercury thermom-

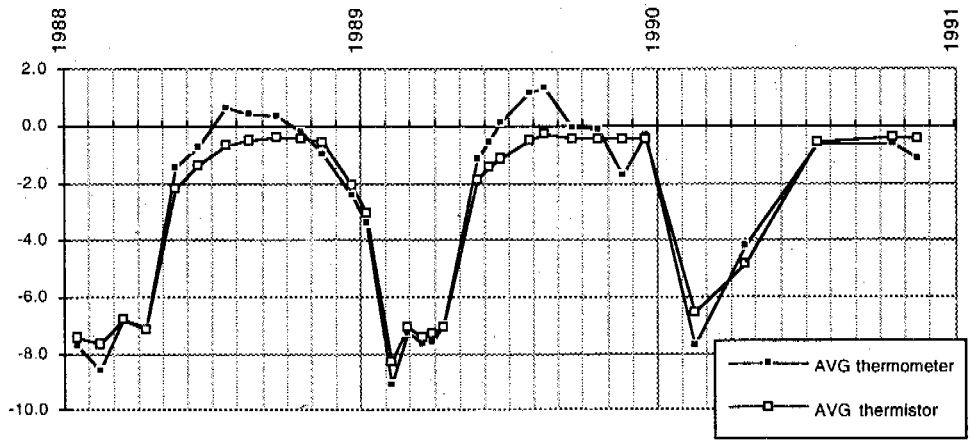

Figure 1. Average temperatures (°C), top 1.2 m, thermometer & thermistor methods.

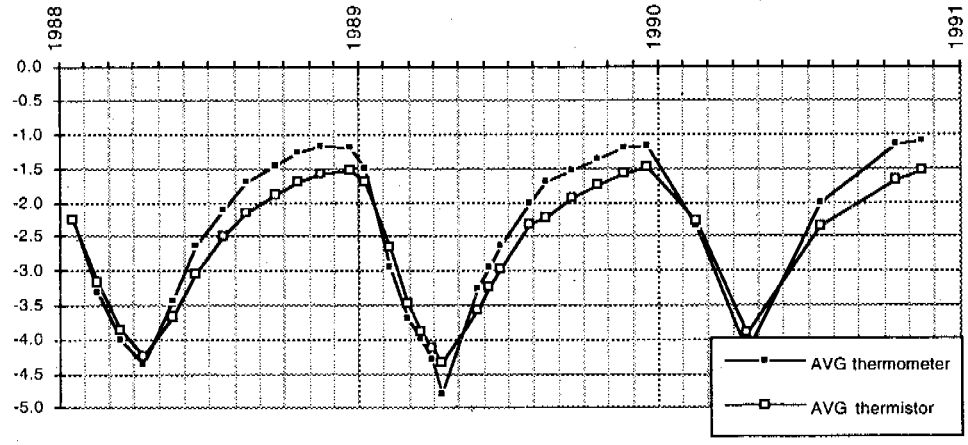

Figure 2. Average temperatures (°C), 2.1 through 4.5 m, thermometer & thermistor methods.

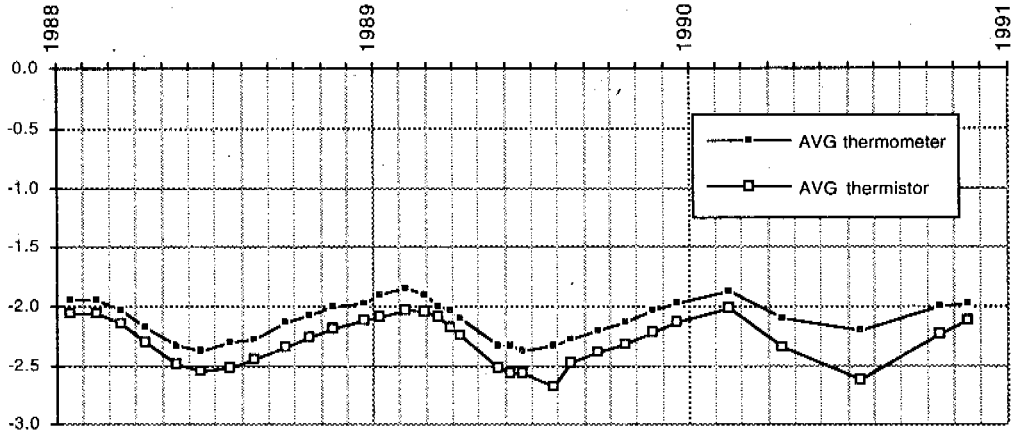

Figure 3. Average temperatures (°C), below 6.0 m, thermometer & thermistor methods.

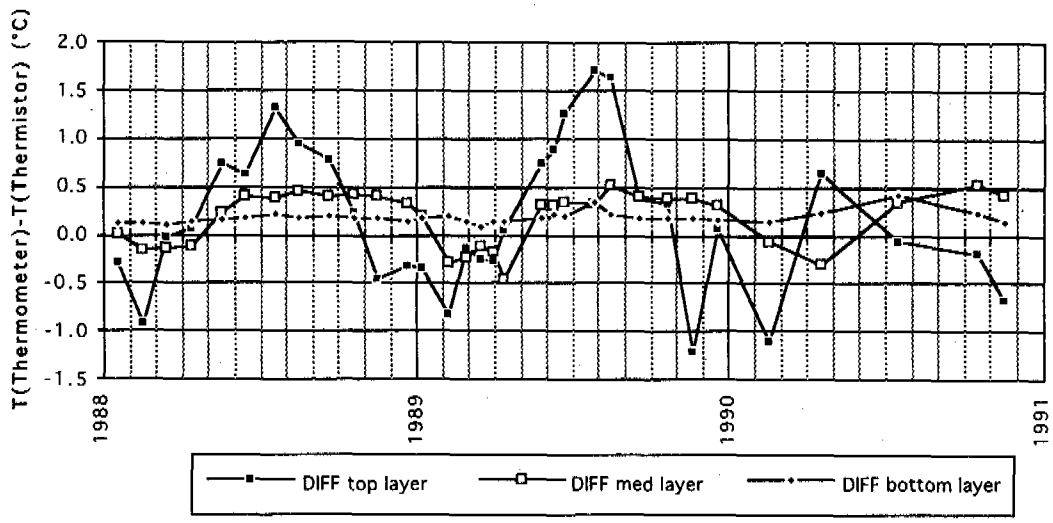

Figure 4. Difference between thermometer and thermistor readings.

eters at the time of reading. Average annual ground temperatures calculated based on the thermometers and the thermistors were within 0.01°C for all levels if the apparent calibration difference is taken into account. We conclude therefore that only minor differences exist between the two types of ground temperature measurements. Our Chinese colleague, Ding Jingkang, has obtained a similar set of data at the Fenghuoshan Permafrost Research Station on the Qunghai Xizang Plateau.

PRELIMINARY STUDY ON THE FREEZING POINT IN SOIL

Cui Guangxin and Li Yi

Mining and Technology University, China

It is presented that the freezing point affected the depth of the freezing wall of a freezing shaft due to the differences of depth, water content and load in mining engineering. The study method and some results are introduced.

THE RELATION BETWEEN ARTIFICIAL FREEZING SHAFT AND FREEZING POINT OF LOADING SOIL

There are many mining mountains where the mines are covered by the Quaternary surface soil with great depth in northeastern, northern, eastern and central regions in China.

It is requisite to build mines well using the method of the freezing shaft in these areas. There have been more than 300 freezing shafts since the first shaft was built in Kailuan mine, Hebei province, in 1955. The sum of the length of all the wells is more than 48000 meters. The maximum freezing depth is 415 m. Artificial freezing shafts have contributed much to the Chinese-coal industry.

The method of the freezing shaft is to cool the ground around the well to a closed circle pipe (freezing wall) before digging the shell of the well so that it can bear ground pressure and keep the shell of the well from the ground water. Under the protection of the freezing wall, the shell of the well can be dug and lined.

The formation of the freezing wall is represented in Figure 1.

$$\frac{\partial t_n}{\partial \tau} = a_n \left(\frac{\partial^2 t_n}{\partial r^2} + \frac{1}{r}\frac{\partial t_n}{\partial r}\right) \tag{1}$$

$$\lambda_2 \frac{\partial t_2}{\partial r}\Big|_{r=\xi} - \lambda_1 \frac{\partial t_1}{\partial r}\Big|_{r=\xi} = B\frac{d\xi}{d\tau} \tag{2}$$

$$\theta(Ro,\tau)=t_y \tag{3}$$

$$\theta(\xi,\tau)=t_D \tag{4}$$

$$\theta(\infty,\tau)=t_o \tag{5}$$

$$\theta(r,o)=t_o \tag{6}$$

where, t_n--temperature; n=1,2 mark of unfrozen and frozen zone respectively; a_n--thermal conductivity; r--coodinate radius; τ--time; λ_1,λ_2--heat conductivity of unfrozen and frozen soil, respectively; ξ--the coordinate of the frozen wall; B--latent heat, θ--temperature function; Ro--coordinate of freezing tube; t_y--temperature of cooling source; t_o--preliminary temperature of soil; t_D--freezing point.

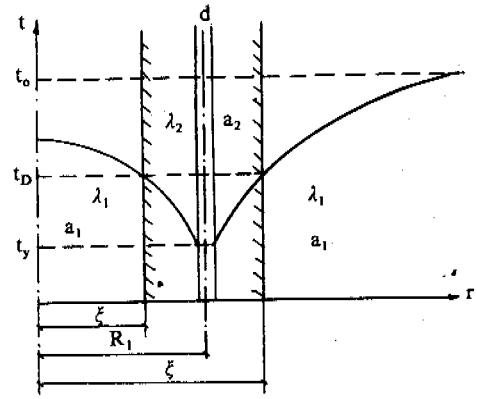

Fig.1 Temperature field along the freezing wall

The strength and stability of the freezing wall are very important for engineering. The thickness of the freezing wall is determined on the basis of strength and stability. So far in design and construction, the zero degree line is defined as the boundary of the freezing wall, that is t_D=0°C. Both in tests and engineering practice it was proved that when there is overburden P, the freezing point of surface soil is lower than 0°C and not a constant, $t_D=f(p,w,s)$. However the function has not been obtained, the thickness of the freezing wall in design is not

equal to that in field. For example, the designed thickness of the freezing wall according to 0°C line is 7 m, while the boundary is along -2°C line, so that the thickness in field is only 5.6 m. It's dangerous to engineering. Designers and technologists had to make them by decreasing the boundary temperature lower than 0°C. It's urgent and a requirement to obtain the function of $t_0=f(P,w,s)$ in the design and construction of freezing shafts.

INTRODUCTION

The study of freezing point under overburden began in the USSR in the 1960s, and it began in the 1970s in China.

In recent years, the freezing point of soil was determined by the temperature increasing due to released latent heat from the curve of temperature vs. time obtained by thermalmeter during soil freezing. But this method is not adaptive to when the temperature is not increasing. So this method has great locality and error.

Liu Zongchao (1987) proposed a criterion of determining the freezing point using volt change during soil freezing, and experimental research was studied for the range of 4 MPa in an open system and the range of 10 MPa in a closed system. This method is simple, and volt change is obvious. However, it needs the premise that volt change is unique. It was regretted that the volt change around the freezing point was not unique, so that some mistaken determination was made.

Freezing point can be determined according to the difference of resistivity between the frozen zone and unfrozen zone. Gu Zhongwei (1982) showed that resistivity of soil depended on water content, salt content and soil properties. The author and assistants propose an identification method to determine the freezing point under overburden using the mutation of resistivity during soil freezing, and the freezing point finder is provided. He Ping (1990) tested the freezing point for different soils and proved that there existed an obvious mutation of resistivity during soil freezing under low overburden.

RESEARCH OF FREEZING POINT UNDER OVERBURDEN

Because it is required to determine the freezing point under overburden in production (i.e. freezing shaft), we proposed a decision scheme of the freezing point in the range of 8 KPa of overburden for clay, sandy clay, clayey sand and sand using the change of restivity change during freezing.

Figure 2 shows the test system. It is composed of a test cell, temperature sensor, fluid-pressure cell and freezing tube. The sensor observed the frost line and temperature. In saturated soil, pressure transfer exists, so that pressure is applied by injecting high pressure liquid through a pressure hole. Liquid pressure is controlled by a pressure-sensor and pressure-control system. Liquid pressure in the fluid pressure cell is transferred to the sample through a soft tubor membrane so as not to mix liquid with the sample.

It is important to determine the frost line during the test. Although it has proved that resistivity changed obviously during soil freezing, the relation between the spot of resistivity mutation and freezing point of soil has not been identified by the test.

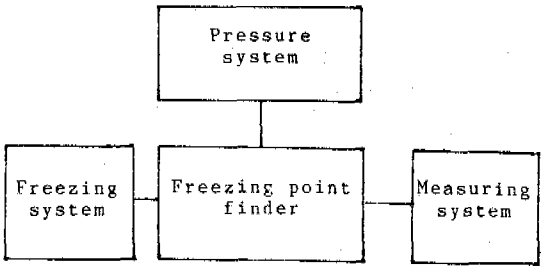

Fig.2 Test system freezing point finder is shown in Fig.3

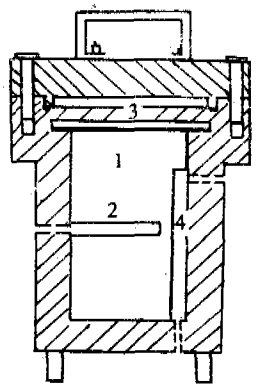

Fig.3 Freezing point finder

The objective of the project is:

1. Find the relation between resistivity change and frost line during soil freezing.
2. Correct the freezing point finder with unclear magnetic resonance.

PRIMARY RESULTS OF THE LAW OF RESISTIVITY CHANGE DURING FREEZING

Clay and sand are saturated and loaded in the test. The sensor with the freezing point finder is composed of thermalcouples and electrodes to measure resistance. Thermalcouples are located between two electrodes. The frozen liquid is NaCl solution (-2°C).

Fig.4 shows the processes of temperature and resistance in saturated sand. Where, line 1 is the curve of temperature vs. time, and line 2 is the curve of resistance vs. time. The temperature becomes obviously steady from 10 to 70 minutes, and the freezing point can be easily determined. Before freezing, the change of resistance is steady, after freezing, it increases rapidly. It is interesting that the distinct increase of resistance occurs at 60 minutes, which corresponds to the later period (not the beginning) of the temperature. It is indicated that the micro-phase change begins at 10 minutes. The ice forms on a large scale at 60 minutes and this results from a rapid increase of resistance. Fig.5 shows the relation between temperature and resistivity. There exists a point of inflection E that corresponds to the freezing point (point A in Fig.4). Fig.6 is the amplified inflected point from Fig.5. H corresponds to super-cooling temperature. At this moment, the resistance does not have an

acute change, soil is unfrozen. The temperature at the inflected point is -0.06°C, that is the freezing point.

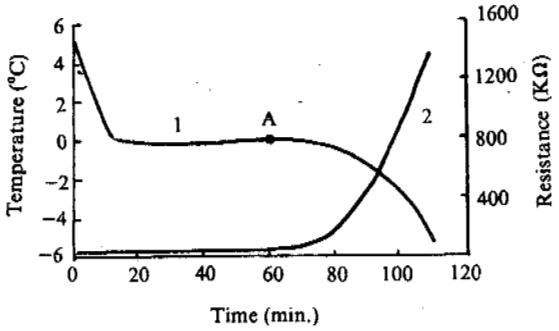

Fig.4 Process of temperature and resistance in saturated sand

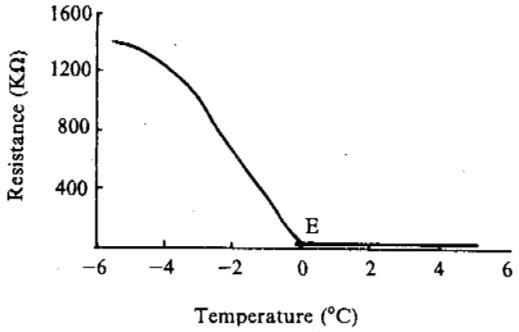

Fig.5 The relation between resistance and temperature in saturated sand

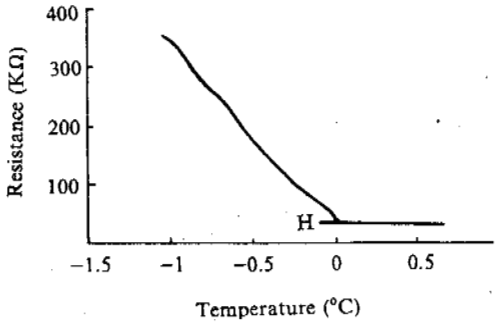

Fig.6 Magnified figure of the point of inflection

The processes of temperature and resistance of saturated soil are shown in Fig.7. The tendency for clay is similar to that for sand except that the stable period of sand is more clear than that of clay. The freezing point of clay is -0.02°C.

The problem to determine the freezing point under overburden is in the process, some conslusions will be published afterwards.

So far, the research states:

1. The change of resistivity of soil reflects the state of freezing/thawing of soil.

2. The inflected point in the curve of resistivity vs. temperature has an intimate concern with the freezing process.

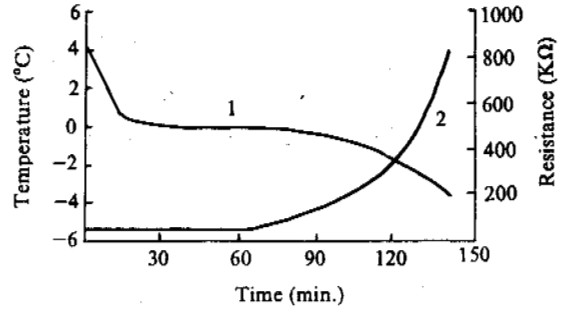

Fig.7 The process of resistance and temperature in saturated clay

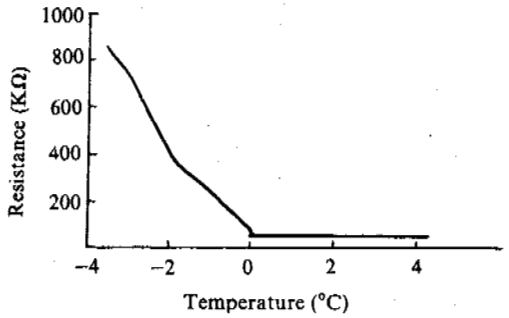

Fig.8 The relation between resistance and temperature in saturated clay

3. Although the sharp change of resistance is certain during soil freezing, a sensor with high sensitivity is required to measure the sharp change of resistance.

4. The polarization of the electrode and soil must be considered while designing the measuring system. When electic pulse is used to measure the resistance, capacity effect is not neglected.

5. Measuring resistance of soil with low voltage can reduce the effect of polarization. When the voltage is lower than 1 volt, the effect of electric potential is considerable.

REFERENCES

Liu Zongchao, (1987) Freezing of Solution and Freezing Thawing Electric Potential, Journal of Glaciology and Geocryology, 9(4), 535-562.

Gu Zhongwei, Wang Shujuan, et al., (1982) Testing Research of Electric Conductivity of Freezing Soil. Proceedings of National Conference on Glaciology and Geocryology (selection) (Geocryology), p.102-109.

He Ping, (1990) The Properties and Applications of Resistance During Soil Freezing, Journal of Glaciology and Geocryology, 12(4), p.265-370.

CACULATION OF MAXIMUM THAWED DEPTH OF PERMAFROST UNDER THE BLACK-COLOUR PAVEMENT BASED ON GEOTHERMAL GRADIENT

Cui Jianheng and Yao Cuiqin

The First Survey and Design Institute of Highway,
The Ministry of Communications, Xian, China

From the engineering state of roads, geological conditions, present research situation and accumulated information in the permafrost area of Qinghai-Xizang, the paper, evading the difficult problem of the thermophysical process of seasonally frozen-thawed layer, directly considers the thermophysical process of frozen-thawed boundary and uses the geothermal gradient caused by various factors(air temperature, terrain, height above sea level, geographical latitude, ground surface condition, soil type, thermophysical property and the effect of water), presents a method to calculate the maximum possible thawed depth of premafrost in a certain period.

INTRODUCTION

On the Qinghai-Xizang plateau, the amount of heat absorbed by black colour road surface is in larger proportion to that absorbed by ground surface. Asphalt pavement restrains the evaporation of heat, in addition, the effects of permeation and convection of water have very large influences on the seasonally thawed depth. when precipitation permeates into soil, its heat and the radiation heat of soil will be taken to the thawed boundary. It is difficult to describe the complex thermophysical process by using a thermophysical equation. But the geothermal gradient effected by various factors can be found by the observation of ground temperature.

If the thermal flow along the road direction is neglected, the temperature accumulated under black road is expressed by a two dimensional field(Ding Dewen,1983):

$$T(x,h) = f(T_1, T_2, X, h)$$

The horizontal and vertical heat flows caused by geothermal gradients ($\partial T / \partial X$ and $\partial T / \partial h$) make up the total heat flow of soil:

$$\varphi = \iint_{\Sigma} \lambda_x \frac{\partial T}{\partial x} dxdy + \lambda_h \frac{\partial T}{\partial h} dxdy$$

the relation of vertical heat flow to total heat flow is defined as the side radiation coefficient,

$$K_m = \frac{\iint_{\Sigma} \lambda_h \frac{\partial T}{\partial x} dxdy}{\iint_{\Sigma} \lambda_x \frac{\partial T}{\partial x} dxdy + \lambda_h \frac{\partial T}{\partial x} dxdy}$$

when the boundary condition of the temperature field is defined, the side radiation condition will certainly be in dynamic equilibrium and the relation of vertical heat flow to total heat flow will be constant.

The paper only discusses the relationship of maximum seasonally thawed depth and the vertical geothermal gradient.

HEAT EXCHANGE ON THE FROZEN-THAWED BOUNDARY

The heat exchange on the frozen-thawed boundary obeys the law of energy conservation and exchange. For the frozen-thawed boundaty, the heat equilibrium condition must be obeyed, it can be expressed by the Stafen equation:

$$\lambda_T \frac{dt_T(\xi,\tau)}{dh} - \lambda_m \frac{dt_m(\xi,\tau)}{dh} = Q_\varphi \frac{d\xi(\tau)}{d\tau} \tag{1}$$

where, λ_T and λ_m are heat conductivity of upper and lower layers for phase change boundaty, $t_T$and $t_m$are soil temperature of upper and lower layers, ξ is the thawed depth.

$Q_\varphi = L\ W\ T_d$, is the consumption heat amount per unit volume during freezing or thawing, L is phase change latent heat of ice, W is natural water content, $T_d$is dry density of soil.

The left portion of the equation is the difference of heat amount getting in and out the boundary, the right portion of the equation means that the phase change boundary moves at the rate of $d\xi / d\tau$ because the heat amount absorbed by the boundary is consumed by soil during thawying or freezing. Equation (1) is also expressed as:

$$q_T - q_m = Q_\varphi \xi' \tag{2}$$

or

$$\lambda_T g_T - \lambda_m g_m = Q_\varphi \xi' \tag{3}$$

where, q_T and q_m are the heat amounts and g_T and g_m are the

geothermal gradient at upper and lower phase change boundary. ξ is the moving rate of the boundary.

If $q_m = q_T$, $\xi = 0$, the boundary does not move. If the heat flow of every point is constant, the upper limit is in the steady state. If the upper limit descends, it certainly absorbs heat from the frozen-thawed boundary. The main condition of the upper limit descending is that annual average heat flow decreases jumping from the upper layer of soil to the lower layer. The dynamic state of the upper limit can be judged by the annual average geothermal gradient of the upper and lower layer of soil at the upper limit boundary, because a different geothermal gradient is corresponding to different heat flow. It has:

$$\frac{q_m}{q_T} = \frac{\lambda_m \cdot g_m}{\lambda_T \cdot g_T} \tag{4}$$

If $g_T > (\lambda_m / \lambda_T) g_m$, it is shown that the upper limit will descend. If the annual average heat current of the upper layer soil is equal to that of the lower, the upper limit is in the steady state. The geothermal gradient at $g_T = (\lambda_m / \lambda_T) g_m$ is regarded as the critical gradient of upper limit movement. If the thermophysical parameters of permafrost do not change, the moving rate of the boundary may be expressed as the function of geothermal gradient (g_T):

$$\xi' = f(g_T) = \frac{\lambda_T g_T - \lambda_m g_m}{Q_\varphi} \tag{5}$$

If $\xi' = 0$, g_T is the critical gradient at which the table starts moving. If the gradient is constant, the moving rate is an inverse measurement of the water amount ($w \cdot T_d$) of frozen soil.

The above discussion is for the uniform medium, but the actual soil layer is not uniform.

VERAGE STEADY TRANSFER HEAT PROCESS

The idea of effective annual average temperature will be introduced here. The purpose is that a uniform soil layre, in which the heat conductivity is equivalent to the actual one, is used to express the actual soil layer.

If the state is steady and effective annual average temperature does not change, because of no inner heat source, the average heat flow is constant, an average steady temperature field is formed and the annual average transfer heat amount is constant. Because the heat exchange between the ground surface and atmospheric layer changes periodically, the heat exchange between the annual temperature change layer and the bottom of the layer is relatively steady. Therefore heat exchange between the annual change layer and outside is steady certainly in an annual period. The algebraical sum of heat amount Q_T absorbed by the ground surface in an annual period with evaporation heat Qm equal to the heat quantity ($q_c t_o$) absorbed into the layer under the annual change layer. The annual average heat flow in ground is:

$$q_c = q = \lambda \frac{t_c - t_o}{h_c} \tag{6}$$

where, q_c is the heat flow entering into the lower boundary of the annual change layer, λ is equivalent heat conductivity, t_c is permafrost temperature, t_o is effective annual average temperature of ground surface, h_c is the annual average depth of ground temperature. Therefore, the soil layer with different heat conductivity can be replaced by a uniform soil layer with equivalent heat conductivity:

$$\frac{h_c}{\lambda} = \frac{h_1}{\lambda_1} + \frac{h_2 - h_1}{\lambda_2} + \cdots + \frac{h_c - h_{i-1}}{\lambda_i} \tag{7}$$

where h_i is the depth of the lower boundary and λ_i is the heat conductivity of the soil layer of number i, respectively.

It is shown that the heat exchange between the annual average steady active layer and the bottom of the layer is not certainly equal to zero. The annual average temperature of frozen soil is not equal to the one of ground surface and is also not equal to the annual average air temperature.

For a large continuous permafrost area, black road surface is only a limited boundary condition, the heat transmitted from the system to permafrost is not enough to change the heat state of permafrost. The temperature field under black road may come to an equilibrium state in the boundary condition for a period. The equilibrium is dynanic, a steady artificial upper limit may be formed under the large area continuous black road surface of permafrost, the equlibrium is corresponding to the climate and environment conditions for a period. The formation of a steady upper limit under the black road surface is essentially the equilibrium question of excessive absorbing heat of black surface and heat current in ground. In an average steady state, the average heat current passing through the permafrost upper limit in a annual period is:

$$\lambda_T \frac{t_T - t_c}{h_T} = \lambda_m \frac{t_c - t_T}{h_c - h_T} \tag{8}$$

where, t_T is effective annual average temperature at the steady permafrost table, h_T is the effective depth of a steady permafrost table. Therefore the critical geothermal gradient can be obtained in the average steady equilibrium state:

$$g_o = \frac{t_T - t_o}{h_T} = \frac{\lambda_m}{\lambda_T} \cdot \frac{t_c - t_T}{h_c - h_T} \tag{9}$$

The observation data of ground temperature shows that the annual average temperature at 0.5m under the black road surface is a plus. It is shown that seasonally thawed depth is more than the frozen depth for black road surface in the average steady equilibrium state. Therefore the unfrozen layer exists certainly between permafrost and the seasonally frozen soil layer. The annual average temperature at the upper limit is zero. The equation (9) may be written as :

$$g_o = \frac{-t_o}{h_T} = \frac{\lambda_m}{\lambda_T} \cdot \frac{t_c}{h_c - h_T} \tag{10}$$

The above discussion is only for a one dimensional heat conduction problem. But, in ground there is heat convection from wat-

er as well as heat conduction, the temperature field is not one dimensional. Therefore the relationship of the average vertical ground temperature gradient and maximum thawed depth depends on ground temperature. The critical average vertical geothermal gradient (g_o) is determined by observed ground temperature.

DATA ANALYSIS

The data was observed every ten days in the period of plus temperature. Observation interval is 0.5m in depth. Because road surface temperature is influenced very largely by the periodic air temperature of daytime, the deviation of the data is large. But the ground temperature at 0.5m depth is influenced very little by air temperature of daytime, and for artificial road, the boundary conditions are similar in each of the road sections. The thermophysical conditions at the depth of 0.5m may be defined as the upper boundary condition in the research system. In addition, the change of ground temperature in a year is periodic, average ground temperature in a plus temperature period is a constant proportion to the one year period, and thawing happens in a plus temperature period. The unfrozen layer exists in the average steady equilibrium state. When a seasonally frozen layer exist, the heat cannot be transimitted into the unfrozen layer. After the seasonally frozen layer thaws, the permafrost layer can absorbed the heat from the upper layer. Therefore, the train of thought to look for the relationship of average ground temperature at 0.5m in plus temperature periods and maximun thawed depth of permafrost does not change the substance of the problem.

Table 1 shows the observation data of ground temperature and calculation results of 6 observation points in different heights above sea level and latitude from 1985 to 1990. Where Te is the average temperature from June to October at 0.5m depth, g_T is called the calculated average geothermal gradient, is the ratio of the average temperature difference between at 0.5m depth and at maximum thawed depth from June to October to the seasonally thawed depth. The thawed depth is the depth where the temperature is −0.1°C. Figure 1 shows the relationship of thawed depth h of every observation point year by year and calculated average geothermal gradient (g_T). The line, passing through the points where g_T are smaller and $\triangle h_T$ are larger, is in unfavourable conditions. The intersecting point of the straight line with g_T axis is the critical calculated gradient (g_o). Under the unfavourable condition, the relationship of g_o and $\triangle h_T$ is:

$$\triangle h_T = A(g_T - g_o) \tag{11}$$

where, A is the change rate of $\triangle h_T$ with g_T. At a constant heat flow condition, the influencing factors on A are the frozen soil type and heat quantity (Q_φ) consumed during ice thawing. It is shown as equation (9) that the critical gradient of ground temperature is the ratio of equivalent heat conductivity of the upper layer soil to lower layer soil at the table and times of average gradient of ground temperature in the annual change layer. when the heat conductivity is constant, g_o is related to $(t_T - t_c) / (h_c - h_T)$. Generally speaking, the temperature (t_c) of frozen soil and the annual change depth (h_c) is related to the height above sea level and latitude. By converting natural soil of every observation point into gravel ($\lambda_o = 2.56$

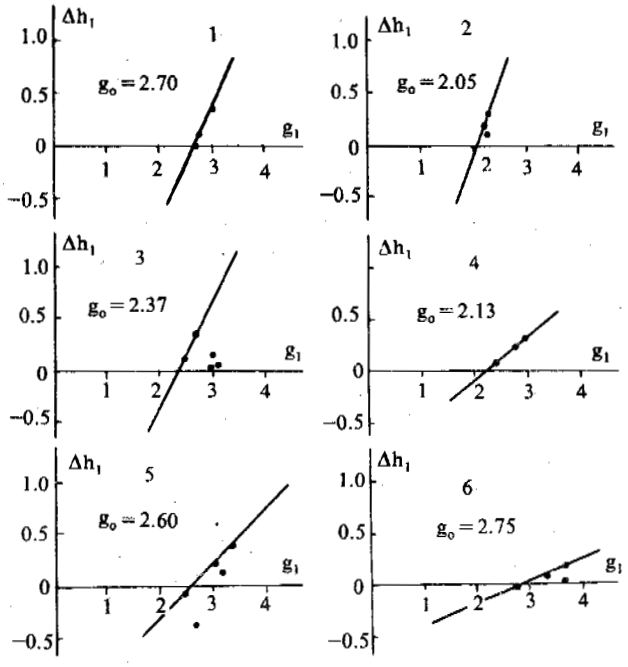

Fig.1 h vs. g

w / m °C), the relationship (see table 2) of g_o' and height (Hs) above ses level and latitude (L) is:

$$g'_o = g_o \cdot K = 0.001618H_s + 0.0022L - 6.06 \tag{12}$$

where, K is converting coefficient of soil layer ($K = \lambda_1 / \lambda_o$), the regression coefficient is 0.94.

From the definition of calculation gradient of ground temperature, the actual maximum thawed depth of calculation points at a constant condition can be obtained:

$$h_o = \frac{T_e}{g_o} + 0.5 = K \cdot \frac{T_e}{g_o} + 0.5 \tag{13}$$

where, Te is the average temperature at 0.5m depth from June to October(°C).

It is confirmed by observation information that the g also exists under natural ground surface. The natural upper limit is thought as the average steady equilibrium limit of permafrost (see Table 3, Fig.2, Fig.3). the relationship of the geothermal gradient under natural ground surface and seasonally thawed depth can be the reference of black colour pavement.

CONCLUSION

The theory of average steady heat transfer processes are introduced to research the relationships of steady table and the gradient of average ground temperature by means of the uniform soil layre replacing the natrual soil layer with different conductivity.

The vertical portion quantity of geothermal gradient measured

Table 1. The observation information of ground temperature

No.	Year	Te (℃)	T_T (℃)	h_T (m)	g_T (℃/m)	Δh_T (m)	No.	Year	Te (℃)	T_T (℃)	h_T (m)	g_T (℃/m)	Δh_T (m)
1#	85			3.50			4#	85			3.88		
	86	7.6	-0.8	3.58	2.80	0.08		86	8.8	-0.5	4.10	2.75	0.22
	87	8.8	-0.6	3.95	3.05	0.37		87	10.2	-0.3	4.40	2.92	0.40
	88	8.9	-0.6	3.95	2.75	0		88	9.6	0	4.50	2.46	0.10
2#	86			4.60			5#	85			4.25		
	87	9.4	0	4.90	2.30	0.30		86	9.1	-0.7	3.90	2.62	-0.35
	88	9.8	0	5.00	2.23	0.10		87	11.1	-0.5	4.30	3.41	0.40
	89	8.9	0	4.90	1.98	-0.1		88	11.5	-0.4	4.45	3.14	0.15
	90	9.7	0	5.15	2.20	0.25		89	9.4	-0.4	4.40	2.48	-0.05
3#	85			3.70				90	11.6	-0.5	4.63	3.10	0.23
	86	9.2	-0.5	3.86	3.03	0.16	6#	85			2.95		
	87	9.9	-0.6	3.92	3.12	0.06		86	6.8	-1.30	3.05	3.30	0.10
	88	9.7	-0.6	3.95	3.01	0.03		87	8.1	-1.0	3.10	3.57	0.05
	89	8.4	-0.5	4.10	2.58	0.15		88	8.3	-0.9	3.30	3.54	0.20
	90	9.3	-0.5	4.45	2.72	0.35		89	7.1	-0.6	3.30	2.75	0

Note: g_T is calculated by using $g_T = T_e - T_T / h_T - 0.5$. T_e and T_T are the mean ground temperatures at 0.5 m and the permafrost table from June to October, h_T is the depth of the permafrost table last year.

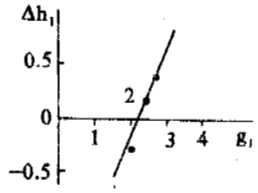

Fig.2 H vs. g (natural ground surface in the north of Xieshui river)

may be considered (the actual gradient of ground temperature is influenced by heat conduction, heat convection, et al.) by means of the statistical method of pure theroy which is used to develop the research of heat conduction, it is in accord with the actual situation.

The method given in the paper can be used to calculate the maximum thawed depth not only for the pavement in large areas of permafrost but also for the natural ground surface and engineering. The method may be as used as a train of thought for continuing research.

ACKNOWLEDGEMENTS

Table 2. The deta of g'_o, H_s and L

No.	Hs (m)	L (°)	λ (W/m°C)	g_o (°C/m)	g'_o (°C/m)
1	4749	35.67	1.65	2.70	1.74
2	4615	35.28	1.80	2.05	1.44
3	4740	35.18	1.66	2.37	1.54
4	4579	35.36	1.78	2.13	1.48
5	4750	34.77	1.70	2.60	1.73
6	4950	34.72	1.92	2.75	2.06

Table 3. The temperature information of the natural ground surface in the west of Xiesui river

year	Te (°C)	Tr (°C)	h_r (m)	g_r (°C/m)	Δh_r (m)
85			2.5		
86	4.10	−0.5	2.5	2.30	0
87	4.40	−0.5	2.67	2.45	0.17
88	4.40	−0.5	2.67	2.26	0
89	3.9	−0.4	2.38	1.98	−0.29
90	5.0	−0.1	2.75	2.71	0.37

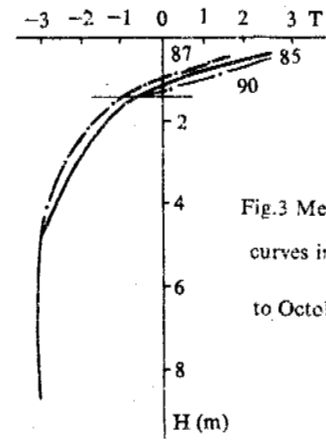

Fig.3 Mean ground temperature curves in Kekexili from June to October in 1985,1987,1989

The authors would like to thank very sincerely Professors Yu Wenxue and Wu Jingming for the valuable help given.

REFERENCES

Ding Dewen, 1983, A New Theory on Temperature and Heat Regime in the Annual Average Depth of Ground Temperature. Proceeding of Second National Conference on Permafrost.

Ding Dewen, 1983, Determination of Characteristic Value of Temperature Field in Annual Average Depth of Ground Temperature. Proceeding of Second National Conference on Permafrost.

OBSERVATION ON PERIGLACIAL MASS MOVEMENT IN THE HEAD AREA OF URUMQI RIVER AND LAERDONG PASS, TIANSHAN MOUNTAINS

Cui Zhijiu[1], Xiong Heigang[2] and Liu Gengnian[1]

[1]Department of Geography, Peking University
[2]Department of Geography, Xingjiang University

Observation of the movement rate and forms of talus, rock glacier, active layer and gelifluction in the periglacial environment in Tianshan Mountains have been conducted since 1986. The talus, which is strongly developed between 3300 and 3900 meters above sea level, is supplied by snow-avalanche, rock fall and alluvial forms. The down-slope moving rate of surface gravel on talus is 0.82-10.4 cm/yr, the mean value is 3.15 cm/yr; and the mean rate of the front line of the talus is 2.22 cm/yr. The rock glaciers evolved from talus and have the shape of lobate, and are distributed at 3300-3950 meters a.s.l. Front movement rate is 0.96-49 cm/yr, mean rate is 21 cm/yr. The active layer is at 3460-3540 meters, with a slope dip angle of 10°-17° and slope orientation of 90-170°, and it creeps down slope with a mean surface rate of 1.13 cm/yr. A large amount of gelifluction lobates are distributed at the north-ward slope near Laerdong Pass with an altitude of 2800-2900 meters, mean surface rate of 13.9 cm/yr and front rate of 2.76 cm/yr.

CLIMATIC CONDITIONS

Based on the data from Daxigou Meteorological Station at 3545 meters in the head area of Urumqi River, where the annual mean temperature is -5.34°C and annual mean precipitation is 430 mm, the times of temperature oscillation around 0°C are 130. The Hydrographic Station at 3805 meters in the empty cirque at the head of Urumqi River shows an annual mean temperature of -7.5°C, and an annual precipitation of 380-460 mm (1987-1989). Annual mean temperature is -2.6°C and precipitation is 830-840 mm (deduced from data of Snow Avalanche Observation Station).

TALUS

Talus is one of the most common alpine features, and ranges widely from the piedmont to the divide and is distributed mainly in an alpine periglacial environment with greater size, density and activity. In periglacial areas, strong freeze and thaw actions favour the breaking of bedrock and the abrupt valley side by glaciation offers a favourable relief for talus formation. Talus appears greatly at 3600-3950 meters above sea level.

Observation was made to measure surface gravel movement and baseline movement of talus in 1986-1991 (Xiong Heigang, et al, 1992), for the results see Table 1. Talus-1, located beneath Glacier 5, consists of till from Glacier 5 and weathering debris from the upper slope. Talus-2 is located at the trough base to the right of Glacier 5 and mainly consists of frost weathering debris from the upper slope. Talus-3 and Talus-4 are located at the back and left side of the empty cirque. The observation started in June, 1986 and continued until August, 1991. Talus-5 and Talus-6 are located at the western side of the empty cirque, Talus-7 is located at the riegel of the empty cirque, Talus-8 and Talus-9 are located at the trough of Glacier 4. The surface gravel movement of the upper, middle and lower lines was taken to show the different movement rates at the talus. Iron poles were used as the datum point to determine the base line movement of the talus. The results are shown in Table 1. Mean movement rate of the surface gravel is 0.82-10.4 cm/yr, total mean rate is 3.15 cm/yr; the mean rate of the upper line is 2.9 cm/yr, middle line is 3.6 cm/yr, lower line is 3.0 cm/yr. Velocity of talus base line is 0.26-5.78 cm/yr, total mean rate is 2.22 cm/yr.

BLOCK SLOPE

Zhu Cheng** arranged a block slope measuring site at 3990 meters, with bedrock slope angle of 27°, slope aspect of 110°, slope length of 275 meters, debris width of 5.5 meters, debris slope angle of 34°, and debris slope length of 69 meters. Lithology is quartz schist. Remeasurement was made in 1990 and it shows a 30-80 cm displacement among 13 points, the mean displacement is 38.46 cm and mean rate of surface gravel on the block slope is 7.69 cm/yr.

The processes of surface gravel on talus are very complex (Washburn, 1979), they can be rolling, sliding, creeping and subsiding, etc. The movement is sporadic. The measurement may only represent the condition in a limited period. For example, surface gravel mean rate of 2.5 cm/yr and maximum rate of 5.8 cm/yr was measured by Rampton (1974) at 25° slope talus in Yukon

*The research was supported by NSFC and Tianshan Glacial Observation Station

**Zhu Cheng, 1990, comparison of periglacial process among Tianshan Mountains, Western Antarctica and Andes, Ph.D. thesis, Peking University, 171 pp.

Table 1. Altitude, form and movement rate of the talus (Talus 1-4 in 1986-1991, Talus 5-9 in 1990-1991)

Number	Altitude a.s.l. meter	Slope aspect degree	Slope length of the talus meter	Middle width of the talus meter	Slope angle of the talus degree	Height of the supply area meter	Slope angle of supply area degree	Rate of surface gravel cm yr^{-1}	Rate of base line cm yr^{-1}
Talus-1	3700	35°	270	115	25°-30°	450	45°-55°	2.5 1.8 1.2	0.26
Talus-2	3700	40°	90	65	30°-35°	450	60°-75°	6.6 10.4 8.4	4.18
Talus-3	3950	135°	175	110	25°-32°	375	45°-60°	0.8 0.9 0.82	1.52
Talus-4	3900	230°	210	95	25°-32°	350	50°-70°	1.68 1.25 1.49	1.82
Talus-5	3900	75°	45	40	28°	560	41°	-	1.4
Talus-6	3920	80°	65	60	30°	610	40°	-	1.03
Talus-7	3840	230°	70	35	27°	355	39°	-	0.88
Talus-8	3640	265°	130	17	28°	520	32°	-	3.1
Talus-9	3680	265°	180	35	28°	720	34.5°	-	5.78

Territory, Canada. Rate of 6.6-111.0 cm/yr on 25° slope talus was measured by Gardner (1973) in Lake Louise, Canada. The rate is 1-450 cm/yr in Chambeyton, French Alps (Michard, 1950). The rate is 0-22 cm/yr on 14°-38.4° talus slope in Lapland (Rapp, 1960). It is suggested that the rate of surface gravel on talus is in the scale of several centimeters, the extreme scale can be several meters per year. The activity and the size of the talus are related to topography, climate, lithology and geological structure.

ROCK GLACIER

The rock glaciers in the head of Urumqi River, mostly lobate-shaped and a few tongue-shaped, are distributed at 3300-3950 meters a.s.l. on the northward slope (Schatter Seite). Most of the rock glaciers are evolved from talus, known as talus rock glacier; a few from moraine, known as glacial rock glacier (Barsch, 1969; Corte, 1987). Form, composition, velocity and structure type have been measured since 1986 (Cui and Zhu, 1989; Zhu, 1989), the results are show in Table 2. RG-1 is tongue-shaped with a ratio of length and width of 1.6; the others are lobate-shaped with a ratio of length and width of 0.2-0.58. The direction of movement is mainly northward, RG-5 is westward and RG-6 is southward. Moving rate of the rock glaciers is 0.96-49 cm/yr, mean rate is 21 cm/yr. The rate of rock glaciers in the Alps is 7-500 cm/yr, mostly 140 cm/yr (Vietoris, 1972; Barsh, 1969; 1975; Chaix, 1943). The rock glaciers in Alberta Park of Canada move down slope by 0.3-0.8 cm/yr (Osborn, 1975). The rate of rock glaciers in Alaska Range is 36-69 cm/yr (Wahrfaftig, 1959). The rate of rock glaciers in Front Range, Colorado and Galena Creek is 2-15 cm/yr and 32-217 (mean 133) cm/yr (White, 1971; Potter, 1969). The rate of rock glaciers in a maritime environment is up to 1 meter or more, whereas in a continental environment the rate is several centimeters.

ACTIVE LAYER

There are long distance telephone wires, which were built in 1979, that have inclined down slope by a slowly active layer creeping since then, passing through the head of Urumqi River. The amount of displacement represents the down slope creep of the active layer, so the surface creeping rate of the active layer can be deduced. The dip angle of 77 wire poles were measured and the slope features were considered at an altitude of 3460-3540 meters. It is assured that the creep of the active layer and the incline of the wire poles are simultaneous and equally-quantitative, the surface creeps quickly and the pole end is nearly inactive. The distance between two poles is 25 meters and the underground part of the poles is 1.5 meters. The surface creep distance:

$$S=h*\sin\alpha/\sin(90°-\alpha/2)$$

where: S displacement distance since (1979 (cm)
α 90° minus dip angle
h 150 cm

The mean moving rate of the active layer surface

$$R=S/12 \qquad R: cm/yr$$

The results are shown in Table 3.

The first part A of 25 poles, striking 245° with slope direction of 170° and slope angle of 10°-15°, creeps down-slope by 0.22-24 cm/yr and the mean rate is 1.0 cm/yr. The pole A-2 was loosened until it crept down-slope 28.8 cm, since 1979, with a mean creep rate of 2.4 cm/yr. The second part B of 29 poles, striking 240° with slope direction of 150° and slope angle of 11°-17°, creeps down-slope 0.22-2.4 cm/yr and the mean rate is 1.11 cm/yr. The pole B-1 at the block stream creeps 2.4 cm/yr and is the most active. The third of 23 poles, striking 215° with slope direction of 90°-140° and slope

Table 2. Form and movement rate of the rock glaciers

Number	Length meter	Width meters	Thickness meters	Altitude of rock glacier terminal meter a.s.l.	Moving direction	Front slope angle degree	Rate cm yr^{-1}
RG-1	100	62		3350	44°	35°	0.96
RG-2	70	120		3600	352°	60°	11.23
RG-3	60	150	83.9	3500	305°	41°	45.0
RG-4	27	101	27	3950	352°	35°	15.5
RG-5	55	130	100.5	3500	280°	41°	49.0
RG-6	20	100.5	41.5	3900	200	32°	6.2

Table 3. Creep rate of the active layer at the head of Urumqi River deduced from inclined wire poles

No.	Dip angle of the pole	Total movement at surface cm	Mean rate cm yr^{-}	Slope feature
A-1	88	5.24	0.44	Part A, Strike
A-2	79	28.80	2.40	245°, slope
A-3	86	10.47	0.87	aspect 170°,
A-4	84	15.71	1.31	A1-12 dry grass
A-5	87	7.85	0.65	land, slope
A-6	86	10.47	0.87	angle 10°,
A-7	88	5.24	0.44	
A-8	82	20.95	1.75	A8 at block
A-9	83	18.33	1.53	stream.
A-10	85	13.09	1.09	
A-11	85	13.09	1.09	
A-12	84	15.71	1.31	
A-13	87	7.85	0.65	A13-19, Wet grass
A-14	85	13.09	1.09	land, slope angle
A-15	90	0	0	11°, A15, 16, 17
A-16	89	2.62	0.22	were supported by
A-17	80	0	0	wire.
A-18	85	13.09	1.09	
A-19	85	13.09	1.09	
A-20	84	15.71	1.31	A20-25, Dry grass
A-21	83	18.33	1.53	land, slope angle
A-22	85	13.09	1.09	11°, A20, 21 at
A-23	85	13.09	1.09	block stream
A-24	82	20.95	1.75	slope 15°.
A-25	88	5.24	0.44	
B-1	79	28.80	2.40	Part B, Strike
B-2	81	23.56	1.96	240°, slope
B-3	86	10.47	0.87	aspect 150°,
B-4	87	7.85	0.65	B1-12, Wet grass
B-5	86	10.47	0.87	land, slope 11°,
B-6	89	2.62	0.22	B1, B2 at block
B-7	87	7.85	0.65	stream, B6, 8
B-8	88	5.24	0.44	supported, B11
B-9	85	13.09	1.09	at thermal-
B-10	87	7.85	0.65	slump.
B-11	85	13.09	1.09	
B-12	88	5.24	0.44	
B-13	87	7.85	0.65	B13-24, Dry,
B-14	88	5.24	0.44	grass land
B-15	84	15.71	1.31	slope 14°,
B-16	82	20.95	1.75	B16, 17 at stream
B-17	82	20.95	1.75	
B-18	88	5.24	2.44	B18 supported
B-19	86	10.47	0.87	
B-20	86	10.47	0.87	
B-21	86	10.47	0.87	
B-22	86	10.47	0.87	
B-23	86	10.47	0.87	
B-24	86	10.47	0.87	
B-25	80	26.18	2.18	B25-29 Wet
B-26	81	23.56	1.96	grass land,
B-27	79	28.80	2.04	slope 15°-17°,
B-28	83	18.33	1.53	B25 at stream,
B-29	85	13.09	1.09	B29 at block stream.
C-1	89	2.62	0.22	Part C, Strike
C-2	88	5.24	0.44	215°, slope
C-3	80	10.47	0.87	aspect 90°-140°
C-4	87	7.85	0.65	C1-13 Wet grass
C-5	81	23.56	1.96	land, C1, 4, 8,
C-6	86	10.47	0.87	12, 16 supported,
C-7	84	15.71	1.31	C5 at block
C-8	89	2.62	0.22	stream, C9 at
C-9	84	15.71	1.31	thermal-karst
C-10	84	15.71	1.31	depression,
C-11	83	18.33	1.53	C13 at block
C-12	87	7.85	0.65	stream, C14-23
C-13	83	18.33	1.53	Dry grass land,
C-14	84	15.71	1.31	slope aspect
C-15	83	18.33	1.53	90°, slope 14°.
C-16	86	10.47	0.87	
C-17	86	10.47	0.87	
C-18	86	10.47	0.87	
C-19	86	10.47	0.87	
C-20	86	10.47	0.87	
C-21	86	10.47	0.87	
C-22	86	10.47	0.87	
C-23	86	10.47	0.87	

angle of 12°, creeps down-slope 0.22-1.96 cm/yr and the mean rate is 0.99 cm/yr. The pole C-5 at the block stream creeps 1.96 cm/yr and is the most active. The total mean creep rate of the surface of the active layer is 1.13 cm/yr. The sorted stripe ground at 1900 meters in Northwest B.C., Canada, creeps 15-33 cm/yr (Makey, 1974), which is greater than that in Tianshan. The down slope creep rate by freezing and thawing and gelifluction is mostly around 0.1-12 cm/yr and the mean is 2.5 cm/yr (Washburn, 1979, Table 6.2). The movement of the active layer is influenced by climate, slope direction and angle, ground-water content, landforms and composition.

GELIFLUCTION

Measurement and sampling were made to study the gelifluction near Laerdong Pass (43°10'N, 84°20'E; 2888 meters a.s.l.) in August 1990 and remeasurement was made in August 1991. grain-size and water content of a pitting at one gelifluction lobate were measured according to the stratification, the result are shown in Table 5. The form of the gelifluction is shown in Table 4. The surface moving rate of the gelifluction is in Table 6 and the front moving rate is shown in Table 7.

The form of the gelifluction in this area is lobate shaped. The ratio of length to width is 0.33~0.95 for most of the gelifluction, and the mean ratio is 0.59, only TLG-4 is tongue shaped with a length to width ratio of 1.51. The height in the middle front of the gelifluctions is 1.55~2.55 meters and mean height is 1.86 meters. The slope angle of the top surface is 10°-30° and mean slope angle is 20°. The front slope is 48°-70° and mean is 59°. The ground surface slope in front of the gelifluction is 12°-31° and the mean is 20°. Vein-ice 0.5-1.0 mm was found at the depth of 106 cm as pitting. grain size analysis shows the mean content of sand, silt, and clay are 41%, 41% and 18% respectively. Water content ranges from 9.74% to 75.21% with a mean of 31%. The water content is an inverse ratio to sand content and direct ratio to clay proportion. Hard plastic tubes of 120 cm were inserted into the gelifluction in August 1990 and their, angles were remeasured in August 1991 (for results see Table 6). Rate of the gelifluction surface is 6.28~16.8 cm/yr and mean rate is 13.9 cm/yr. Wood bars were stuck in the front of the gelifluction to determine the front movement rate in August 1990 and remeasured in August 1991 (for results see Table 7). The minus values of the eastern side at TLG-3 show movement of the ground in front of the gelifluction is greater than that of the front of the gelifluction. The mean rate of the gelifluction front relative to the ground is 2.76 cm/yr with a maximum of 12.5 cm/yr. The moving rate of gelifluction varies in different environments with the range of 0.5~10.0 cm/yr (Dyke, 1981; Egginton, 1985; French, 1974; Mackey, 1981). In Laerdong Pass, the greater movement is suggested to result from the greater slope gradient, precipitation and ground water.

CONCLUSION

The talus, which strongly develops at 3600-

Table 4. Forms of the gelifluction at Laerdong Pass (measured on August 8, 1990).

Number	Gelifluction Length	Width	Height	Slope aspect		Gelifluction Slope angle	Front angle	Ground surface angle	Altitude a.s.l.
		meter							meter
TLG-1	18.3	25.7	2.5	15°	West	19°	59°	23°	
					Middle	10°	52°	20°	2890
					East	175°	54°	24°	
TLG-2	8.55	17.5	1.55	15°	West	7°	48°	31°	
					Middle	29°	54.5°	12°	2890
					East	22°	58°	14°	
TLG-3	28.4	30.0	2.0	13°	West	25°	65°	22°	
					Middle	27°	61°	17.5°	2895
					East	20°	70°	21°	
TLG-4	15.7	10.4	1.65	17°		16°	60°	20.5°	2900
TLG-5	6.5	20.0	1.67	13°		22°	61°	13°	2890
TLG-6	7.0	15.0	1.8	15°		30°	65°	25°	2885

Table 5. Composition and water content of gelifluction

Number	Stratum depth cm	Stratum thickness cm	Composition (%) Sand	Silt	Clay	Water content
TLG-A	0 - 9	9	—	—	—	75.21
TLG-B	15 - 20	5	45.88	42.30	16.61	16.61
TLG-C	20 - 33	13	39.31	42.30	18.39	37.12
TLG-D	33 - 45	12	27.08	50.61	22.31	33.46
TLG-E	45 - 65	20	62.12	29.24	8.64	9.98
TLG-F	65 - 77	12	67.40	25.20	7.40	9.74
TLG-G	77 -101	24	23.11	51.67	25.22	11.12
TLG-H	101 -125	24	22.35	51.87	25.78	35.49

Table 6. Rate of top surface movement of the gelifluction at Laerdong Pass

Number	Primary dip angle of the tube (Aug. 1990)	The dip angle of the next year (Aug. 1991)	Length of the tube underground cm	Moving rate cm yr^{-1}
TLG-1	85°	77°	120	16.8
TLG-2	84°	77°	120	14.7
TLG-3	85°	82°	120	6.28
TLG-4	85°	78°	120	15.0
TLG-5	85°	77°	120	16.8

Table 7. Front moving rate of the gelifluction at Laerdong Pass (in 8,8, 1990-24,8, 1991)

Number	Western side cm	Middle cm	Eastern side cm
TLG-1	1.1	7.0	1.0
TLG-2	0.5	0.7	-0.5
TLG-3	2.0	-2.0	0
TLG-4	-	1.75	-
TLG-5	-	1.0	-
TLG-6	-	12.5	-

3950 meters above sea level in the head of Urumqi River, shows a surface gravel moving rate of 0.82-10.4 cm/yr and a mean rate of 3.15 cm/yr, a base line creeping rate of 0.26-5.78 cm/yr and a mean of 2.22 cm/yr.

The block slope, which develops on the slope angle of 34° and slope orientation of 110° at 3900 meters a.s.l. in the head of Urumqi River, shows surface gravel moving rate of 7.69 cm/yr.

The lobate-shaped rock glaciers, which develop at 3300-3950 meters a.s.l. in the head of Urumqi River, move down slope 0.96-49 cm/yr and the mean rate is 21 cm/yr.

The active layer, which is measured on the slope gradient of 10°-17° and slope orientation of 90°-170° at 3460-3540 meters a.s.l. in the head of Urumqi River, creeps down slope with a surface mean rate of 1.13 cm/yr.

The lobate-shaped gelifluctions, which develop on the slope angle of 20° and slope orientation northward at 2885-2900 meters a.s.l. near Laerdong Pass, snows the surface movement mean rate is 13.9 cm/yr and front rate is 2.76 cm/yr.

REFERENCES

Barsh, D., (1969) Studien und Messungen an Blockgletschern in Macun, Unterengadin, Ieitschrift fur Geomorphologie, Suppl. Bd., 8, pp 11-30.

Barsh, D. and Hell, G., (1975) Photogrammetrische Bewegungsmessungen am Blockgletscher Murtel 1, Oberengadin, Schweizer Alpen: Ieitscher Gletscherkunde, U. Glazialgeologie 2(2), pp 111-142.

Chaix, A., (1943) Les couless de blocs du Parc National Suissei Le Globe, Memoires 82, pp 121-128.

Corte, A.E., (1987) Rock glacier taxonomy, in ROCK GLACIERS ed. Giardino, Shroder and Vitck, Allen & Unwin, Boston, pp 27-39.

Cui, Zhijiu and Zhu Cheng, (1989) The Structural Type of Temperature and Mechanism of Movement of Rock Glacier at the Head of Urumqi River, Tianshan Mountains, Chinese Science Bulletin, Vol.34, No.15, pp 1286-1291.

Dyke, A.S., (1981) Late Holocene solifluction rates and radio-carbon soil ages, central Canadian Arctic, Geological Survey of Canada, Paper 81-1C, pp 17-22.

Egginton, P.A. and French, H.M., (1985) Solifluction and related processes, eastern Banks Island, N.W.T., Canadian Journal of Earth Science, 22, pp 1671-1678.

French, H.M., (1974) Mass wasting at Sachs Harbour, Banks Island, N.W.T., Canada, Arctic and Alpine Research 6, pp 71-78.

Gardner, J.S., (1973) The nature of talus shift on alpine talus slope, in Research in Polar Geomorphology, ed. Fahey and Thompson, 206pp.

Mackey, J.R. and Mathews, W.H., (1974) Movement of Sorted Stripes, the Cinder Cone, Garibaldi Park, B.C., Canada: Arctic and Alpine Research 6, pp 347-359.

Mackey, J.R., (1981) Active layer slope movement in a continuous permafrost environment, Garry Island, N.W.T., Canada Canadian Journal of Earth Sciences 18, pp 1666-1680.

Michard, J.,(1950) Emploi de marques dans l'etude des mouvements du sol: Rev. Geomorphologuie dynamique 1. pp 180-189.

Osborn, G.D., (1975) Avancing rock glaciers in the Lake Louise area, Banff National Fark, Alberia, Canadian Journal of Earth Science 12, pp 1060-1062.

Potter, N.J., (1969) Rock glaciers and mass-wastage in the Galena Creek area, northern Absaroka Mountains, Univ. Minnesota Ph.D. thesis, 150 pp.

Rampton, V.N. and J.B. Dugal, (1974) Quaternary stratigraphy and geomorphic processes on the Arctic Costal plain and adjancent areas, Demarcation Point, Yukon Territory, to Malloch Hill, D.M., Canada, Geol. Survey Paper 74-1, Part A, p 283.

Rapp, A., (1960) Recent development of mountains slopes in Karkeragge and surroundings, N. Scandinavia: Geografiska Annaler 42(2-3), pp 65-200.

Vietoris, L., (1972) Uder den Blockgletscher des Ausseren Hochebenkars: Zeitschr, Gletscherkunde und Glazialgeologie 8(1-2), pp 169-188.

Wahrhaftig, C. and A. Cox, (1959) Rock glaciers in the Alaska Range: Geol. Soc. America Bull. 70, pp 383-436.

Washburn, A.L., (1979) Geocryology, Edward Arnold, pp 230-231.

White, S.E., (1971) Rock glacier studies in the Colorado Range, 1967-1968: Arctic and Alpine Research 3, pp 43-64.

Xiong Heigang and Liu Gengnian, (1992) Measurement and consideration on talus in Tianshan Mountains. Geomorphological processes and environment management conference paper collection, in press.

Zhu Cheng, (1989) The characteristics of the surface movement of the lobate shape rock glacier from the Debris fabric, Tianshan, China, Journal of Glaciology & Geocryology, Vol.11, No.1, pp 82-88.

LONG-TERM SHEAR STRENGTH OF FROST-THAW TRANSIT ZONE

Ding Jingkang[1], Xu Xueyan[2] and Lou Anjing[1]

State Key Laboratory of Frozen Soil Engineering, LIGG, AS, China
[1]Northeast Institute Chinese Academy of Railway Sciences
[2]Harbin Building Engineering Institute

The frost-thaw transit zone is a complicated soil zone with a certain thickness, a beginning freezing temperature, frozen and thawed soil existing together, obvious rheological characteristics and a long term shear strength. The long term shear strength equation is obtained by using several groups of relaxation curves of the shear strength in the frost-thaw transit zone. The ability to resist shear stress is mainly due to the cohesive strength and the inner grind angle being quite small. The long term shear strength is about one-sixth, long term cohesive strength is about one-fifteenth and the long term internal friction angle is about one-twelfth when compared with their different instant values.

INTRODUCTION

The thaw of permafrost in foundations results in the strength of foundation soil decreasing greatly. So the stability of foundations is a problem that should be considered above all when buildings are designed according to the principle of allowing the permafrost foundations to thaw. The strength of melting soil is small and the temperature of the soil layer with a certain thickness near the thawing front maintains the beginning to freeze temperature. The soil zone is high in water content and temperature and is the transit zone of melted and frozen soil and is naturally a weak layer in the foundation of frozen soil. It is significant in the design of slope foundations in permafrost regions and in investigating the mechanical properties of the transit zone (S. Goto and K. Minegisgi, 1988; B.J.A. Stukert and L.J. Mahar, 1983).

The frozen soil in the transit zone have obviously rehological properties. This kind of transit zone, with melted soil in low temperature and frozen soil of high temperature commonly existing, is a more complex zone of soil corresponding to the melted and frozen soil. To understand the characteristics of the transit zone and to provide a basis for building design on slopes in permafrost regions, research was carried out on the long term shear strength of the frost-thaw transit zone, and the results are presented as follows.

TESTING METHODS

Using different shear load with the same vertical load, a set of shear creep curves can be obtained. Then, the long term strength equation and long term strength can be obtained and calculated with different vertical loads. Meanwhile, the long term strength curves and long term value C, ϕ in the soil of the frost-thaw transit zone can be obtained.

Apparatus being used in the shear strength test is a large scale, sheet creep apparatus. Test specimens were subclay taken from the Fenhuo Mountain region of the Qingzhang Plateau. The particle composition is that >0.05 mm takes up 37.7 percent, 0.05-0.005 mm takes up 47.7 percent, <0.005 mm takes up 14.9 percent. The physical properties of the test specimen are shown in Table 1.

Table 1. Physical properties of the test specimen

W(%)	W_L	W_P	I_P	Temperature of beginning to freeze (°C)
23.4	28.6	16.1	12.5	-0.1

The specimen used in the test was remolded soil, with the density being controlled by the design demand of the earth filled foundation, r=19.9 KN/m^3, r_d=16 KN/m^3. The specimen was a cylinder 9.5 cm in height and 11.28 cm in diameter. The finished specimen was placed into a low temperature cabinet to freeze for 24 hours. For the purpose of controlling the positions of the frost-thaw transit zone, two pieces of thermoelectric cell were put into the shear zone of the specimen.

The test of long term shear strength is a shear test with constant load, consolidation and drainage. The test procedures were as follows:

1) Forming and Controlling the Frost-thaw Transit Zone

2) Adding Vertical Load

When the temperature of the shear zone is -1.5°C, half of the vertical load is added and when temperature of the shear zone is -1.0°C, the whole vertical load is added.

3) Consolidation Time: 2.5 Hours

4) Shear

After the specimen is consolidated, the test can begin. During the shear process the temperature in the frost-thaw transit zone and shear load is kept stable.

5) Failure Criterion

When shear displacement reaches 30 mm, namely 27 percent of the specimen diameter, we define it as the limited failure.

6) Grade of Added Load

For the long term shear strength, the grade of added load is shown in Table 2.

Table 2. Grade of added load (N)

Vertical \ Horizontal	2800	2500	2300	2100	1900	1700	1500	1300
4000	✓	✓	✓	✓	✓	✓	✓	
3000		✓	✓	✓	✓	✓	✓	
2000				✓	✓	✓	✓	✓

The grade of vertical load is 4000, 3000 and 2000 N in the test of consolidation and quick shear for the frost-thaw transit zone and melted soil.

TEST RESULTS

1. The relationship between shear displacement and time. Under the action of applied load, the shear deformation obviously has the rheologic characteristics in the frost-thaw transit zone. When shear stress does not change, shear strain increases with time. When the stress is smaller than a certain value, shear strain appears as a characteristic of attenuation. When the stress is over a certain value, shear strain shows the characteristic of non-attenuation as shown in Fig.1, 2, and 3.

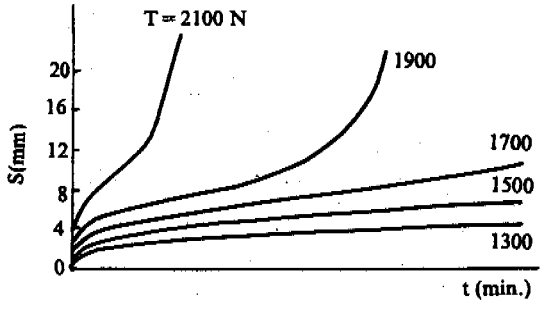

Fig.1 Relationship curver between shear displacement and time when vertical load is P=2400N.

Figures 1, 2 and 3 show that the curves of shear deformation in the frost-thaw transit zone are teh typical creep curves of frozen soil.

Under action of the vertical and horizontal load in each grade, the shear deformation of frost-thaw transit zone has the characteristics of creep deformation. This indicates that the soil in the frost-thaw transit zone mainly has the characteristics of frozen soil.

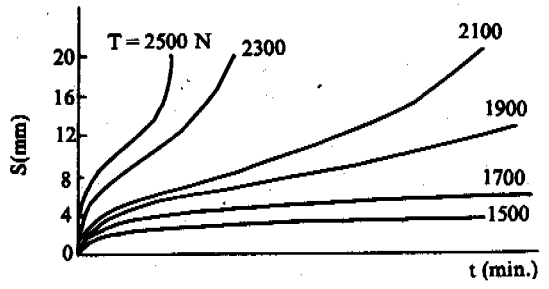

Fig.2 Relationship curver between shear displacement and time when vertical load is P=3400N

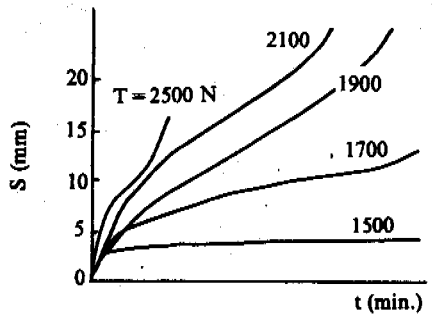

Fig.3 Relationship curver between shear displacement and time when vertical load is P=4000N

Fig.4 shows that the strength of the frost-thaw transit zone is located between the melted and frozen soil, its cohesive strength is larger and internal friction angle is smaller when compared with melted soil, and its cohesive strength is smaller and internal friction angle is larger when compared with frozen soil, as shown in Table 3. This sufficiently indicates the transit properties of the soil in the zone. Testing temperature of the frozen soil below the transit zone is about -2.5°C (the temperature at the beginning of freezing is -0.1°C).

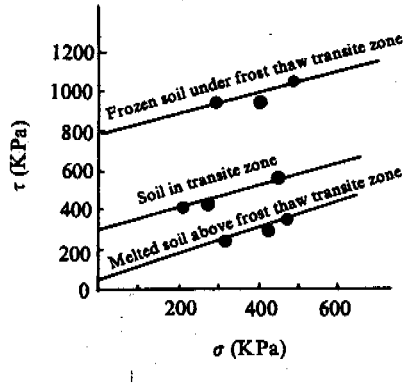

Fig.4 Comparesion of shear strength

2. Long term shear strength of soil in the frost-thaw transit zone. As shown in the former, the soil in the frost-thaw transit zone chiefly

Table 3. Instantaneous value C, ϕ of tested soil

Type of specimen	C(KPa)	ϕ
Frozen soil under frost-thaw transit zone	780	26
Frost-thaw transit zone	300	29
Melted soil above frost-thaw transit zone	47	32

has the characteristics of frozen soil and thus exists as a long term strength.

Fig.5 shows a set of relaxation curves of shear strength in the soil frost-thaw transit zone obtained by Fig.1, 2, and 3.

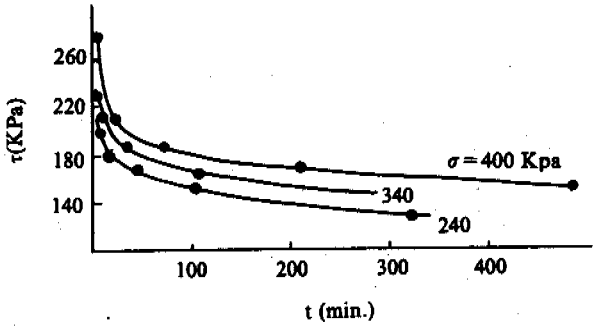

Fig.5 Relaxation curves of shear strength

From Fig.5 it can be seen that the curves with different vertical load are similar. Therefore the long term strength of the soil in the frost-thaw transit zone can be expressed with the same equation with different parameters, that is:

$$\tau = \frac{B}{\lg At}$$

Where A, B — parameters determined by the test, which the unit of A is 1/minute, B is KPa, t — time, minute, τ — shear strength, KPa.

To obtain A and B, the curve of lgt-1/t is drawn, as shown in Fig.6, where the slope of lines is 1/B. The calculated value is exhibited in Table 4. The long term strength of t=50 and 100 years are shown in Table 5.

Table 4. Parameters of the equation for long term strength

Vertical load (N)	A	B
4000	295	800
3400	586	800
2400	2216	800

Drawing curve of σ-T with the value in Table 5, long term value C, ϕ of the frost-thaw transit zone can be obtained, as shown in Table 6.

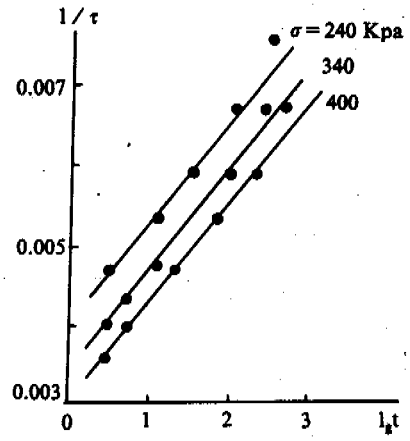

Fig.6 Lgt--1/τ curve

Table 5. Long term shear strength of frost-thaw transit zone

Vertical stress (KPa)	50 years	100 years
400	80.9	78.5
340	78.5	76.3
240	74.3	72.3

Table 6. Long term value of C, ϕ in the frost-thaw transit zone

Limit of year	C(KPa)	ϕ
50	64	2.4
100	62	2.4

From Table 6, we can notice that the cohesive strength decreases with the increase of time, but value of ϕ does not vary basically and is very small.

3. Comparison of long term shear strength with instantaneous shear strength in the frost-thaw transit zone.

According to the boundary conditions of the test for long term shear strength, an instantaneous shear test is carried out in the frost-thaw transit zone. The speed of added load is controlled by time, that is the specimen is sheared with the time of 40 to 60 seconds.

Figure 7 shows the comparison of long term shear strength with instantaneous shear strength in the frost-thaw transit zone. From Fig.7, it can be understood that the long term shear strength is much smaller than the instantaneous shear strength, with the former being one-sixth of the latter. For the values of C and ϕ, the value of C of the former is approximately one-fifth of the latter, the value of ϕ of the former is about one-twelfth of the latter. The long term and instantaneous value of C and in the frost-thaw transit zone are listed in Table 7.

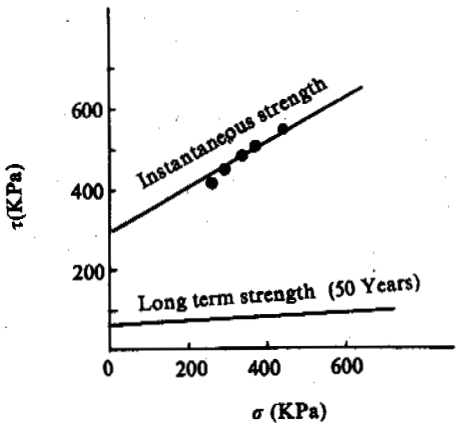

Fig.7 Comparison of shear strength

Table 7. Comparison of value C and ϕ in the frost-thaw transit zone

Time	C(KPa)	ϕ
Long (50 years)	64	2.4
Instantaneous time (1 minute)	300	29.0

4. Temperature variance of the shear zone during the shear process. It was found by the test that the temperature of the soil in the shear zone increases. This indicates that the work done by the exterior force, except for the shear deformation, partly converts into heat. The conversion of energy results in a larger affect on the mechanical characteristics of the soil in the frost-thaw transit zone and frozen soil in high temperature. In Table 8 lists the variance of temperature of the center and the border of the specimen in the fast shear test.

Table 8. Variance of soil temperature during the process of fast shearing (C)

Type of specimen	Position		Remain
	Center	Boundary	
Frozen soil under transit zone	0.345	0.254	The values in this table all are average
The soil in frost thaw transit zone	0.166	0	
Melted soil above frost thaw transit zone	0.110	0.102	

From Table 8 it can be seen that during the process of fast shearing the variance of soil temperature is the largest in frozen soil, second in the transit zone and smallest in the melted soil. It also can be understood from Table 8 that the variance of soil temperature in the center is larger than in the border. This is because more heat in the border of the shear zone is lost. During the process of shearing, the environment temperature is controlled at -2°C and heat produced by shearing radiated through the shear box. Naturally the loss of heat at the border is more and the increase of temperature is smaller. The rise of soil temperature in the shear zone has a certain relation with the appearance of the peak strength of shear stress, in which the temperature of soil rises only after a certain amount of displacement is produced. In frozen soil, in general, when shear displacement reaches 9 percent of the specimens diameter, the temperature of the soil will increase, but in melted soil and soil in the transit zone this value is 6 percent. Following closely with the rise of soil temperature, the peak value of shear stress appears. After that the temperature of soil increases continuously, but the shear stress decreases gradually until the specimen is sheared.

CONCLUSIONS

1. In clay, the soil in the frost-thaw transit zone is a mixture of frozen soil at 0°C and melted soil with obvious rheological characteristics, and its long term shear strength can be calculated with the equation of long term strength presented in this thesis.
2. In clay, the ability of resisting shear stress of the soil in the frost transit zone is mainly composed of cohesive strength since the internal friction angle is very small.
3. In the frost-thaw transit zone its instantaneous shear strength is larger than the shear strength of melted soil. When the stability is calculated for the slope in permafrost areas, the indexs C and ϕ should be determined according to the length of time that load will be added.

REFERENCES

B.J.A. Stukert and L.J. Mahar, (1983) Proceedings, 4th International Conference on Permafrost.
S. Goto and K. Minegisgi, (1988) Direct shear test at a frozen/unfrozen interface, Proceedings, 5th International Symposium on Ground Freezing.

THE COMPRESSING PROPERTIES AND SALT HEAVING MECHANISM STUDY OF SULPHATE SALTY SOIL

Fei Xueliang[1,2] Li Bin[2]

[1]The State Key Laboratory of Frozen Soil Engineering
LIGG, Chinese Academy of Sciences, China
[2]Xian Highway and Transportation University,Xian,China

In the paper, a set of salt heaving laws of sulphate salty soil which is made by adding 3% Na_2SO_4 in Xian-loess in different dry density is obtained through simulated test. It demonstrates that when the temperature is decresed from +25°C to −15°C and the initial water content is certain, the relation between the salt heaving value of sulphate salty soil and initial dry density presents a type of parabolic. It also exists a minimum value interval. In this test condition, this interval is within the range of 1.80g / cm^3 when water content is the best one of the heavier compaction standard test. It is quite important to discover the interval for saline soil areas of highway engineering. In addition, the analysis of test result reveals the mechanism of salt heaving in sulphate salty soil under different initial dry density. It shows why sulphate salty soil heaving ratio changes with the initial dry density.

INTRODUCTION

There is a large area of sulphate salty soil in China. In these areas, there are some peculiarity in highway engineering. First, when sulphate salty soil meets water, its strength is degraded fast and occurs deformation easily when vehicles go through. Secondly, sulphate salty soil can create salt heaving when temperature lowering. It leads to the dry density of the base and subgrade degrading and strength reducing. The parts of salt heaving influence highway's using quality greatly. These two main drawbacks decrease usable years of highway and cause much loss in finance.

The purpose of this study is, by simulated test in laboratory, to obtain the relation of salt heaving ratio to initial dry density (expreeed with r_d) of sulphate salty soil subgrade, then proposing a range of initial dry density for engineering. In the proposed range, the salt heaving can be prevented from creating. And by analyzing test result, the salt heaving mechanism has been concluded why salt heaving changes when initial dry density changes.

TEST METHOD AND MAIN PARAMETERS

Test Method

Sulphate salty soil samples used are made by adding 3% Na_2SO_4 in Xian-loess, in order to obtain the salt heaving value and salt heaving laws of sulphate salty soil in quantity when freezing. Formed temperature of the samples is +20°C; formed method is based on Highway Civil Engineering Test Rules (JTJ051-85 of China). Basic test plan is showed below.

Main Parameters of Soil

Main parameters of soil are showed below.

Test Conditions

There is a insulating material which is 15 cm in thick around the model. Freezing of sample is controlled by Program Temperature Controller and Cooling Bath, freezing rate is 0.5°C / hour. Temperature range is from +25°C to −15°C.

Size of sample is 8 cm in height and 10 cm in diameter. Temperature and deformation of sample are detected by thermal-couples and displacement sensors. All data is collected by Data Taker.

Table 1 Test design table

dry density / water content	1.2	1.4	1.6	1.7	1.8	1.89	1.94
10%	✓	✓		✓			
13.5%	✓	✓	✓	✓			
15.5%	✓	✓	✓	✓	✓	✓	✓
17%	✓	✓		✓	✓		

Note: ✓ is indicated which sample is tested in freezing; unit of dry density is g / cm^3.

TEST RESULT AND ANALYSIS

Result

By simulated test, S-T curves (salt heaving value changing with temperature) which deformation is changed while cooling are obtained; as shown in Fig.1,2,3,4.

Tab.3 is the final salt heaving value taken from Fig.1,2,3,4, under every water content and initial dry density.

Table 2. Soil's main parameters

index / soil type	gravity (g/cm^3)	liquid limit(%)	plastic limit(%)	plasticity of index	max.dry density (g/cm^3)	best water content (%)
plain soil	2.647	36.7	18.2	18.5	1.89	14.24
sulphate salty soil		33.86	15.65	18.21	1.89	15.5

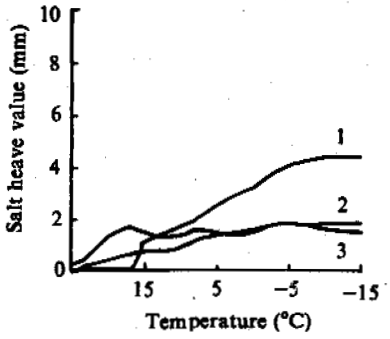

Fig.1 Salt heaving value vs. temperature (initial water content is 10%) (initial dry density (g/cm^3) is: 1—1.3, 2—1.65, 3—1.5)

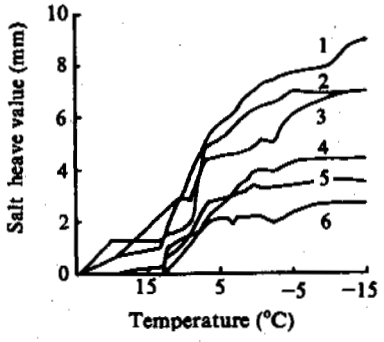

Fig.3 Salt heaving value vs. temperature (initial water content is 15.5%) (initial dry density (g/cm^3) is: 1—1.89, 2—1.54, 3—1.2, 4—1.6, 5—1.7 6—1.8)

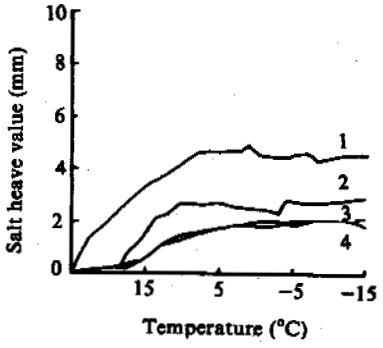

Fig.2 Salt heaving value vs. temperature (initial water content is 13.5%) (initial dry density (g/cm^3) is: 1—1.7, 2—1.2, 3—1.4, 4—1.6)

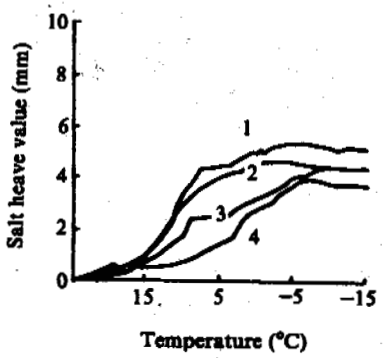

Fig.4 Salt heaving value vs. temperature (initial water content is 17.0%) (initial dry density (g/cm^3) is: 1—1.2, 2—1.4, 3—1.87. 4—1.7)

Table 3. Final salt heaving value (mm)

water content / dry density	10%	13.5%	15.5%	17%
1.2		2.982	7.088	5.1096
1.3	4.378 *			
1.4		2.156	5.6	4.3336
1.5	1.51 *			
1.6		1.87	4.5334	
1.65	1.842 *			
1.7		4.363	3.5865	3.588
1.8			2.7398	
1.87				4.3474 *
1.89			8.933	
1.94			7.044	

* : initial dry density (g / cm^3) of samples has been adjusted.

According to S–T curves (Fig.1,2,3,4), one could know that: no matter which initial water content and initial dry density is chosen, the salt heaving increases constantly while cooling. From inspecting of all the curves, one can discover that salt heaving is increasing quickly in range of from +15°C to −5°C, increasing slow in range of from +25°C to +15°C and −5°C to −15°C. Especially, when temperature is in range of from −5°C to −15°C, salt heaving in many samples increases a little or does not increase.

From Fig.5 one can see: under same initial water content, with initial dry density increasing, salt heaving ratio decreases when initial dry density does not surpass a certain point and increases when initial dry density is over that point.

Mechanism Analysis of Salt Heaving

During cooling, expending of sulphate salty soil is mainly depended on crystallizing of $Na_2SO_4 \cdot 10H_2O$. Its crystallizing equation is :

$$Na_2SO_4 + 10H_2O = Na_2SO_4 \cdot 10H_2O \qquad (1)$$

After crystallizing, Na_2SO_4 becomes $Na_2SO_4 \cdot 10H_2O$, and value of $Na_2SO_4 \cdot 10H_2O$ is 3.1 times over that of Na_2SO_4; sometimes $Na_2SO_4 \cdot 10H_2O$ crystal in soil can cause more expansion, which is depended on the position that crystal lies among soil grains.

Solubility of Na_2SO_4 is affected greatly by temperature. When cooling (higher than −5°C), lot of Na_2SO_4 becomes $Na_2SO_4 \cdot 10H_2O$ and separates from solution existed among soil grains. Salt heaving of samples increases faster in the S–T curve when temperature is between +25°C and −5°C. And the temperature range where

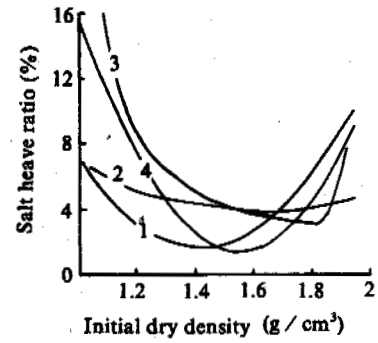

Fig.5 Salt heaving ratio vs. initial dry density
(initial water content (%) is: 1—10.0, 2—13.5, 3—15.5, 4—17.0)

salt heaving increases fastest is between +15°C and −5°C. It is because that $Na_2SO_4 \cdot 10H_2O$ fills into gaps among soil grains or makes soil grains displace when temperature is higher than +15°C and causes samples expanding when temperature is lower than that value.

It should be pointed that: during cooling, as temperature of sample being negative (<−6°C), ice crystal will occur and it will have the volume of water in soil increased 9%. In addtion, the concentration of solution in soil will increase with ice crystal crystallizing, and leads to a little $Na_2SO_4 \cdot 10H_2O$ crystallizing. But the amount of water that could become ice crystal is a little, so a little amount of $Na_2SO_4 \cdot 10H_2O$ will be crystallized out. Thus, $Na_2SO_4 \cdot 10H_2O$ and ice crystal cause volume of sample incresing smaller.

The principle of sulphate salty soil which salt heaving ratio changes with initial dry density altering under a certain initial water content is discussed below.

1). As initial dry density is in smaller range (<critical point), salt heaving ratio decreased gradually with increasing of initial dry density. This is because that: with increasing of initial dry density, compaction of soil increases also, so do restraint conditions in soil (such as friction, cohension, long distance force and short distance force etc.). They resist the heaving actio of $Na_2SO_4 \cdot 10H_2O$ in a certain degree.

On the other hand, distance between soil grains is shorter than before with increasing of compaction and solution existed in adjacent becomes smaller. Thus $Na_2SO_4 \cdot 10H_2O$ crystall (Photograph 1) transfers from adjacent to pore. This leads to salt heaving occuring in adjacent less and less with increasing of compaction of soil.

From above, one can conclude that when initial dry density is in the smaller range, large part of solution in soil is being adjacent, thus crystallizing takes place there too. The crystal gets distance between soil grains increased and makes the structure net of soil grains grow fast. Sample bulking quickly is its macroscopic manifestation.

2). When r_d being the range of critical value, an amount of solution in pore merely fills the pore only after crystallizing (Photograph 2). In addition, interaction between soil grains is rather great.

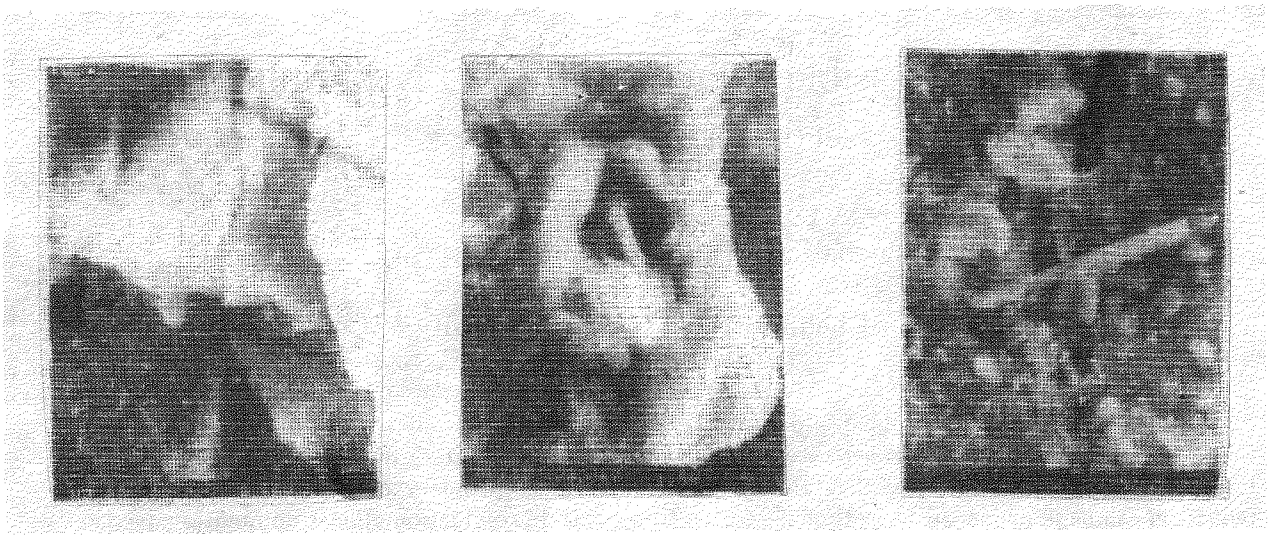

Photo. 1. Test condition is :$r_d = 1.6g/cm^3$, magnified 1500 times

Photo. 2. Test condition is : $r_d = 1.8g/cm^3$, magnified 6500 times

Photo. 3. Test condition is : $r_d = 1.89g/cm^3$, magnified 4000 times

It brings about solution in adjacent little or a little and crystallizing is the same. At the same time, interaction between soil grains restrains salt heaving also. Therefore salt heaving value is smaller then.

3). When r_d over than critical range, no matter whether pores are filled up by solution or not, Na_2SO_4 crystal crstallizes from solution in pore first with lowering of temperature. If pores are not full of solution, crystallizing of crystal will make it fill up soon. Then crystal crystallizes continuously and causes the volume of crystal as well as solution increasing incessantly. Since pores are filled up, increasing of volume will cause pores bulk and lead to occuring salt heaving of sample.

After crystal crystallizing from solution in pore, crystal begins to crystallize from solution combined weeker to soil grains and adjacent (then distance of soil grains has been expanded) with further cooling. Its principle of salt heaving is similar to that of above. It should be noticed that a part of crystal makes progress from pore to adjacent following farther cooling (Photograph 3). It intensifies degree of salt heaving. Though r_d is very large and more interactions between soil grain then, these forces can not resist the action of salt heaving force and result in salt heaving ratio rising. If pores in soil have been filled up before cooling, its salt heaving principle is similar to above, the different is crosses the process that crystal needs to fill pore up.

CONCLUSION

In simulating test, salt heaving value versus temperature in frozen proceeding, S–T curves show that the quickest increasing salt heaving value range of sulphate salty soil is from +15°C to −5°C. Salt heaving ratio will be a little when temperature is higher or lower than that range. As temperature is lower than −5°C, especially, salt heaving almostly does not be occured. Total bulk of ice volume which is crystallized by water and Na_2SO_4 crystal caused by rising concentration because of ice crystallizing in the lower temperature is very small.

As the other advantages, water content,salt content and cooling rate is same, the relatio between initial dry density and the final salt heaving ratio of samples is approximately parabolic, with a minimum salt heaving ratio interval. For sulphate salty soil made by adding 3% Na_2SO_4 in Xian–loess, the lowest value is in the range of $1.80g/cm^3$ of initial dry density when water content is the best water content (this dry density is about 95% of the best dry density).

By analysis of test results, the mechanism of salt heaving has been revealed, that shows why salt heaving ratio of sulphate salty soil changes with initial dry density changing. When r_d is smaller than critical value, principle of salt heaving reducing with the increasing of r_d is that: position of solution in soil changes, from adjacent to pore, and so does the crystallizing, thus bulk action of crystal in soil is reduced. The increasing restraint force in soil restrains this action again. As a result, salt heaving ratio decreases with increasing of r_d in macroscopic. As r_d being critical value range, generally, crystal crystallizes in pore only, it is little or a little crystal crystallizing in adjacent, and restraint force is bigger than. So salt heaving ratio becomes smaller. When r_d is over that range, most part of pore is filled up with the solution, the principle of salt heaving changes a lot with the decreasing of temperature. Crystal occurs in pore first, it makes the pore bulk and part of solution in pore transfers to adjacent. Further cooling will get the crystal crystallized in adjacent, volume of sample bulks again. A part of crystal in pore, at the same time, goes ahead to adjacent, salt heaving value increased once more. These cause salt heaving ratio increasing greatly with adding of r_d.

ACKNOWLEDGEMENT

The author wish to express his appreciation for the financial support of the State Key Laboratory of Frozen Soil Engineering, LIGG AS, China. Thanks also given to the staffis of the State Key Laboratory of Frozen Soil Engineering for their help.

A computationally feasible reduction of the O'Neill-Miller model of secondary frost heave

A.C. Fowler and C.G. Noon
Mathematical Institute, Oxford University
W.B. Krantz
Department of Chemical Engineering, University of Colorado

Following previous work by Holden and co-workers, we have carried out an asymptotic reduction for the O'Neill-Miller model of frost heave, which is a quantitatively accurate representation of the original model, but which only involves the solution of two first order ordinary differential equations. This reduction can be made on the basis that the frozen fringe is thin, conduction of heat dominates advection of heat, and (importantly) the permeability of the frozen fringe is strongly sensitive to the water content. Solutions of the reduced model give predictions of heave versus time and of time of formation and thickness of discrete ice lenses, which agree with O'Neill and Miller's numerical results. Furthermore, the results can be interpreted in accord with the idea that clays heave large loads, but slowly; silts heave small loads, but fast; while sands may not heave at all. An explicit heaving rate parameter can be determined, whose size depends on the soil type through its permeability, characteristic suction, and on the applied load. The method of reduction can be applied to generalised versions of the O'Neill/Miller model, and in particular we have carried out similar analyses in respect of compressible soils, saline soils, and we have also initiated work on the extension of the model to allow for differential frost heave.

1 BACKGROUND

Frost heaving occurs when moist soil, particularly clay or silt, is frozen from the surface downwards (fig. 1). It is manifested by an upward heaving of the surface, which is due not so much to the expansion of water on freezing as to an upwards suction of the subsurface groundwater towards the freezing front. This suction is thought to be due to various effects which contribute to capillary-like forces; these include surface tension between ice and water phases, a chemical potential due to an electrical double layer on clay particles, and disjoining pressure effects due to short range forces in thin water films. A general description of frost heaving is given in the article by Miller (1980).

As the water is drawn upwards to the freezing front, it forms a series of discrete ice lenses in the soil. It is the formation and growth of these ice lenses which causes the heaving at the surface, which can be substantial. Frost heave is a natural phenomenon which occurs in most northerly regions. It is responsible for widespread damage to roads and pavements (even in England, where the construction of the M1 in 1959 was interrupted by heave of the road surface), since in the subsequent thawing, the melting of the ice lenses severely weakens the soil structure (thus facilitating the development of potholes in roads, for example).

Frost heave is also associated with various kinds of *patterned ground formation* in permafrost regions, such as sorted stone circles and soil hummocks, although the precise relationship is not clear. Descriptions of patterned ground are given by Washburn (1980) and Williams and Smith (1989).

The early development of observational, experimental and empirical accounts of frost heave is due to Taber (1929, 1930) and Beskow (1935). In the post-war period, there was a substantial development of physico-chemical theories, and a central figure in this development is R.D. Miller who, in collaboration with numerous colleagues and students (Koopmans and Miller 1966, Miller 1972, Romkens and Miller 1973, Snyder and Miller 1985), developed a consistent account of frost heave based on a number of different physical concepts. This account is outlined below. Reviews of this and other work have been given by O'Neill (1983) and Black (1991).

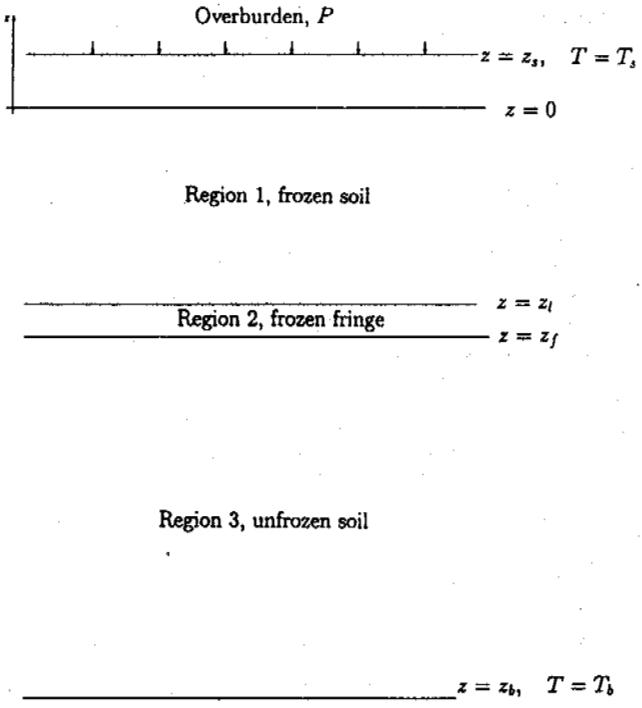

Figure 1: Schematic picture of a heaving soil

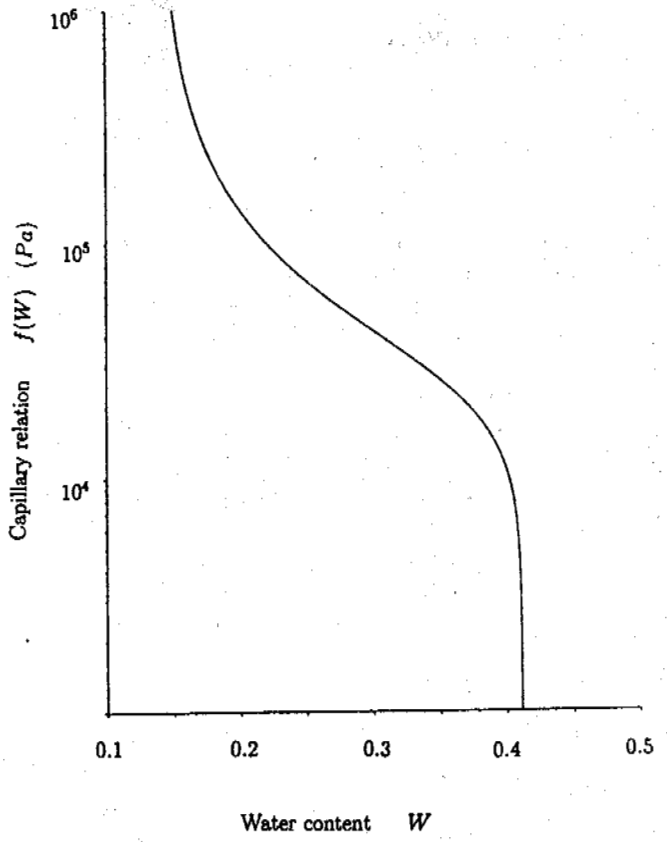

Figure 2: Capillary relation $f(W)$

2 THE MILLER MODEL

Miller (1972) distinguishes between primary heave and secondary heave. In the latter, a thin partially frozen fringe of ice exists below the lowest ice lens. This region of soil contains both pore ice and pore water, and is considered to be in thermodynamic equilibrium. Moreover, the freezing temperature T_f within the fringe is given by a generalisation of the Clapeyron relation, such that T_f is related to the pore pressure exerted by each of the ice and water phases; this relation can be theoretically derived (Loch 1978).

In allowing separate ice and water pressures p_i and p_w, a constitutive relation between them must be prescribed. Miller (1980) takes this in the form $p_i - p_w = f(W)$, where W is the volumetric water fraction in the fringe (fig. 2). As mentioned, this can be ascribed to surface tension as well as other effects, although the physical interpretation of what this means for ice-water re-distribution is less clear. In fact, Miller's 'rigid ice' concept assumes that the pore ice is rigidly connected to the lowest ice lens, and in order for heave to take place due to water freezing on to the lowest lens, this requires the rigid ice to move past the equally 'rigid' (i.e. undeformable, in the model) soil particles.

This is accomplished by the process of thermal regelation, which causes soil particles to move through ice due to an imposed temperature gradient by a melting-refreezing process. Again, this phenomenon has been experimentally observed (Romkens and Miller 1980).

The last feature of Miller's model is a criterion for ice lens formation. This is considered analogous to the formation of cracks in unsaturated soils, and is due to the effective pressure transmitted between soil grains becoming zero. At this point, the soil loses its integrity, and water can push in to form a lens. It is found that lens formation occurs *within* the fringe, and thus the model can explain the formation of a sequence of discrete lenses.

These four concepts (generalised Clapeyron equation, capillary suction, thermal regelation, lens initiation) are central to the Miller model, and are not without their detractors. However, they form the basis for the most conceptually advanced frost heave model, and provide a coherent basis for the study of frost heave.

3 MATHEMATICAL FORMULATION

The Miller model was implemented mathematically by O'Neill and Milller (1982,1985). They treat the frozen, unfrozen and partially frozen fringe as three separate continua, and formulate conservation laws of heat and mass transport in each region. Because of the fine spatial and temporal scale of the model, it is, as Black (1991) says, "hardly ready for use on practical problems. Computational difficulties are unusually formidable ...". Both for this reason, and also because, notwithstanding its complexity, the Miller model is conceptually too *simple* (it considers soil to be rigid and saturated, pore water to be chemically pure, and is essentially limited to one-dimensional heaving), O'Neill and Miller's formulation needs simplification. The way to do this lies in making judicious approximations, which simplify the model without surrendering accuracy. Initial work by Holden (1983), Holden *et al.* (1985) and Piper *et al.* (1988) has been extended by Fowler (1989) and more recently Fowler and Krantz (1993), using four basic approximations: heat transport by advection is small, gravitational effects are small, the frozen fringe is thin (due to the fact that the freezing temperature variation in the Clapeyron relation is small), and the permeability variation with water fraction is large (specifically $k \propto W^\gamma$, with γ (≈ 9) (O'Neill and Miller 1985) being large).

These four approximations allow one to reduce the calculation of frost heave in the O'Neill/Miller model to that of solving two simple first order differential equations for the freezing front position and the soil surface elevation. We now detail the effect of these simplifications.

Firstly, the fringe is thin compared to the length of the soil column, and is consequently seen as a surface by the rest of the soil. Secondly, convective transport of heat is small compared with the conductive flux (i.e. the Peclet number, $Pe \ll 1$). The energy equations outside the fringe then reduce to

$$\nabla^2 T = 0 \tag{1}$$

in $z_s > z > z_f$ and $z_f > z > z_b$ with boundary conditions $T = T_s$ on $z = z_s$, $T = T_0$ on $z = z_f$ and $T = T_b$ on $z = z_b$. The solution to this equation in one dimension is then

$$T = T_s + \frac{z_s - z}{z_s - z_f}(T_0 - T_s) \tag{2}$$

in $z_s > z > z_f$ and

$$T = T_0 + \frac{z_f - z}{z_f - z_b}(T_b - T_0) \tag{3}$$

in $z_f > z > z_s$.

Using these expressions to evaluate the temperature gradient on each side of the fringe, the fringe equations may be solved to determine the locations of the moving boundaries z_s and z_f. This can be done using the fact that the effects of gravity are negligible, and the exponent in the permeability function is large. This fact gives rise to a boundary layer below the lowest ice lens in which the water pressure changes rapidly. Asymptotic methods applied to Darcy's equation lead to a uniformly valid expression for the water pressure as a function of water content. On the formation of a new lens, water content within the boundary layer relaxes rapidly to a steady state and so the water pressure can be considered to be quasi-static.

The remaining differential equations in the fringe express conservation of mass and energy. The small Peclet number and thin fringe allow these equations to be written as a set of algebraic equations for variables evaluated at each side of the fringe. Using the forms found for the temperature and pressure profiles and also the remaining fringe relations, it is possible to reduce these algebraic equations to the two (dimensional) ordinary differential equations

$$\dot{z}_f = -\frac{A}{z_s - z_f} + \frac{B}{z_f - z_b}, \tag{4}$$

$$\dot{z}_s = \alpha\left(\frac{\nu}{z_s - z_f} + W_l \dot{z}_f\right), \tag{5}$$

where A, B, ν and α are constants determined in terms of the parameters of the problem by complicated formulae (see Fowler and Krantz (1993) for details).

4 RESULTS

It is simple to solve the equations (4) and (5) numerically (they can in fact also be solved analytically), and fig. 3 shows a typical sequence of results (Fowler and Noon 1993) for a range of overburden pressures. This sequence compares favourably with a similar figure of O'Neill and Miller's (1985). It is also possible to calculate lens spacing and thickness, and these also vary quantitatively as one might expect.

The form of equation (5) identifies a dimensionless heaving parameter α. This depends in a very complicated way on the applied overburden effective pressure N and the soil type, principally through the

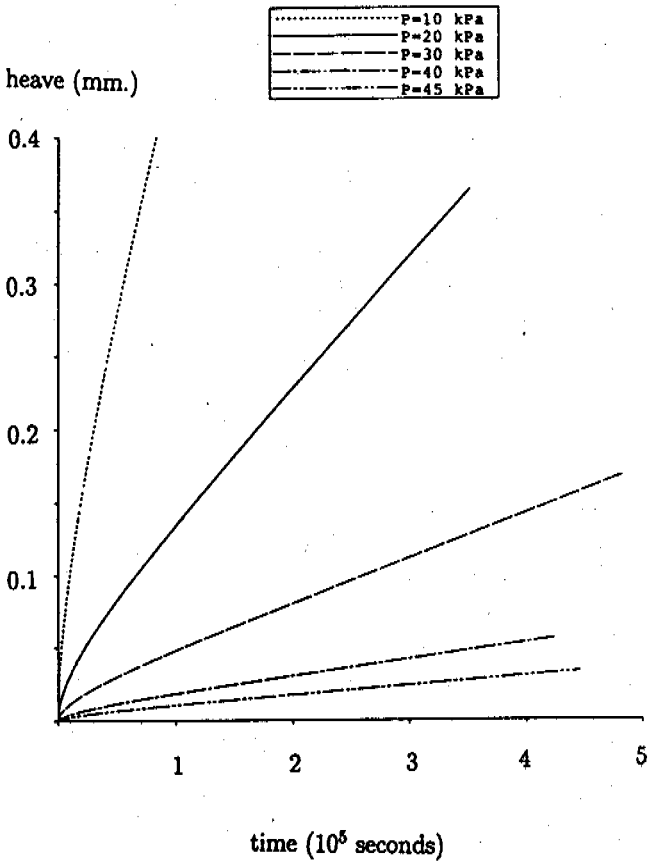

Figure 3: Heave against time for different overburdens

permeability and the characteristic function $f(W)$ in fig. 2. α is proportional to (saturated) permeability, which explains (obviously) why clays should heave more slowly than silts.

The dependence of α on load N is more complicated. Firstly, since N is an effective pressure, zero load corresponds to a positive value of $N = N_0 = p_a - p_\infty$, where p_a is atmospheric pressure, and p_∞ is the far field groundwater pressure. In fig. 4, we plot the variation of α with N for values $N \sim O(1)$ bar, for a characteristic relation $f \propto (1-S)^p/S^q$, where S is the saturation, and $p = 0.3$, $q = 0.3$. This choice of p and q gives a steeply increasing suction as S is reduced, and may be appropriate for finer soils. Depending on the size of N_0, we see that heave decreases more or less exponentially with increasing load, but is maintained for arbitrarily large load. Fig. 5, on the other hand, shows α versus N for $p = 0.3$, $q = 0.1$, the lower value corresponding to lower suctions at low S, and thus a coarser soil. Here there is an asymptote at a finite value of $N = N_c$, beyond which heaving in this mode does not occur, since no lens formation is possible. On the basis of fig. 5, it is possible to understand the absence of heave in sands, on the basis that $N_0 > N_c$, while if $N_0 < N_c$, then one expects heave to occur, but not for arbitrarily large loads. These observations are qualitatively similar to reported heaving characteristics, but further quantitative validatory work is necessary.

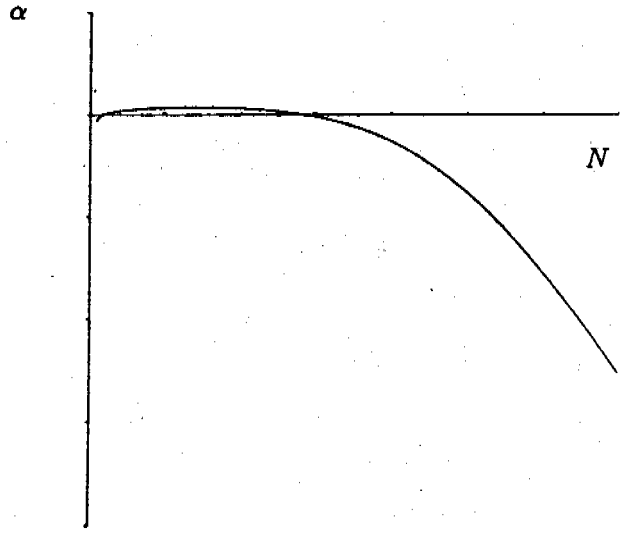

Figure 4: Heave parameter α versus effective overburden N (log-linear scale), clay-type soil

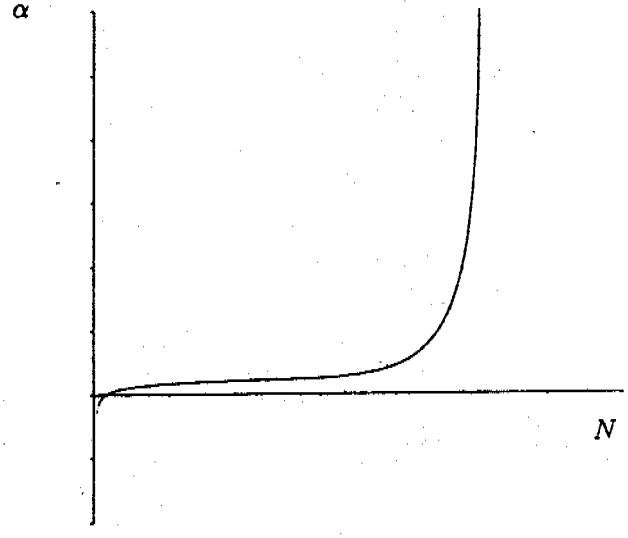

Figure 5: Heave parameter α versus effective overburden N (log-linear scale), sand/silt soil

5 CONCLUSIONS

O'Neill and Miller's model was grid locked because its extraordinary numerical complexity did not allow the possibility of making any realistic extensions to it. In particular, it is conceptually wrong, insofar as the assumption that the ice lens velocity $\mathbf{v}_i$ is spatially constant is (generally) inadmissible for a three-dimensional process. Our previous work not only renders the model tractable, it allows the possibility of extensions by adding new physics to the simplified model, and thus obtaining generalisations of this simple model. As an example, frost heave of saline soils leads to a similar reduction as for pure pore water, the difference lying in that the coefficients in the resulting equations are more complicated.

The application of the model simplifications outlined here to saline and compressible soils is outlined in the thesis by Noon (1993), and further developments to include unsaturated soils, as well as three-dimensional modelling of differential frost heave, are in progress.

6 REFERENCES

1. Beskow, G. 1935 Soil freezing and frost heaving with special application to roads and railroads. Swed. Geol. Soc. C, no. 375, Year Book No.3. Reprinted in Black and Hardenberg (1991).
2. Black, P.B. 1991 Historical perspective of frost heave research. In Black and Hardenberg (1991), pp.3-7.
3. Black, P.B. and M.J. Hardenberg 1991 Historical perspectives in frost heave research. The early works of S. Taber and G. Beskow. CRREL special report 91-23. Hanover, NH.
4. Fowler, A.C. 1989 Secondary frost heave in freezing soils. SIAM J. Appl. Math. **49**, 991-1008.
5. Fowler, A.C. and W.B. Krantz 1993 Generalized secondary frost heave model. SIAM J. Appl. Math., submitted.
6. Fowler, A.C. and C.G. Noon 1993 A simplified numerical solution of the Miller model of secondary frost heave. Cold Reg. Sci. Technol., in press.
7. Holden, J.T. 1983 Approximate solutions for Miller's theory of secondary heave. Proc. Fourth Int. Conf. Permafrost, Fairbanks, Alaska, pp.498-503.
8. Holden, J.T., Piper, D. and R.H. Jones 1985 Some developments of a rigid ice model of frost heave. Proc. Fourth Int. Symp. on Ground Freezing, Sapporo, Japan, pp.93-99.
9. Koopmans, R.W.R. and R.D. Miller 1966 Soil freezing and soil-water characteristic curves. Soil Sci. Soc. Am. Proc. **30**, 680-695.
10. Loch, J.P.G. 1978 Thermodynamic equilibrium between ice and water in porous media. Soil Sci. **126**, 77-80.
11. Miller, R.D. 1972 Freezing and heaving of saturated and unsaturated soils. High. Res. Rec. **393**, 1-11.
12. Miller, R.D. 1980 Freezing phenomena in soils. In *Applications of soil physics*, ed. D. Hillel, Academic, pp.254-299.
13. Noon, C.G. 1993 Mathematical modelling of secondary frost heave. D.Phil. thesis, Oxford University, in preparation.
14. O'Neill, K. 1983 The physics of mathematical frost heave models: a review. Cold Reg. Sci. Technol. **6**, 275-291.
15. O'Neill, K. and R.D. Miller 1982 Numerical solutions for a rigid ice model of secondary frost heave. Water Resour. Res. **21**, 281-296.
16. O'Neill, K. and R.D. Miller 1985 Exploration of a rigid ice model of frost heave. Water Resour. Res. **21**, 281-296.
17. Piper, D., J.T. Holden and R.H. Jones 1988 A mathematical model of frost heave in granular materials. Proc. Fifth Int. Conf. Permafrost, pp.370-376.
18. Romkens, M.J.M. and R.D. Miller 1973 Migration of mineral particles in ice with a temperature gradient. J. Coll. Interface Sci. **42**, 103-111.
19. Snyder, V.A. and R.D. Miller 1985 Tensile strength of unsaturated soils. Soil Sci. Soc. Amer. Proc. **49**, 58-65.
20. Taber, S. 1929 Frost heaving. J. Geol. **37**, 428-461.
21. Taber, S. 1930 The mechanics of frost heaving. J. Geol. **38**, 303-317.
22. Washburn, A.L. 1980 Geocryology: a survey of periglacial processes and environments. John Wiley, New York.
23. Williams, P.J. and M.W. Smith 1989 The frozen earth. CUP, Cambridge.

GEOCRYOLOGY IN MT. TIANSHAN

A.P.Gorbunov

Kazakhstan Alpine Permafrost Laboratory of The Permafrost
Institute of Siberian Branch, Russian Academy of Sciences

The total area of permafrost region in Tianshan is 180–200 thousands Km^2, which the masses of cryolithozone — 90–100 thousands Km^2 in total area and 16 thousands Km^3 in total volume. Usually, the alpine permafrost is located above 2700–3300 m a.s.l., but in some special cases it can occur at 2000 m a.s.l. or lower. The lower limit of continuous permafrost lies at 3500–3700 m a.s.l.; there might not be frozen ground under some large glaciers.

The permafrost in Tianshan started forming no later than Pliocene. The rock glaciers are common seen in Tianshan and can be divided into two categories: the near–glacier and the near–slope area.The former are transformed from moraine material and the latter–from talus or rock–avalanche bodies.

Tianshan, as an unitary geocryological region, occupies the area in 40–46°N. latitude and 67–95°E. longitude. The mountain regions, distributing in the temperate zone, elongate along the boundary between the temperate and subtropic zones. This determines some of the characteristics of the geocryological region.

The major ridges and ranges that constitute this mountain system are: Junggar Alatan, Borohoro, Yirengabirtag, Bogdashan, Karliktag, Kaliktan, Kakshaaltoo, Maigatag, Fergan, Talas and their offshoots. Some scientists considered the Mt. Junggar Alatan as an independent mountain, but, geocryologically, it should be included into the Tianshan system.

The first information of the cryogenic phenomena in Eastern (Middle) Tianshan occurred in the paper written by V.I. Roborovski, who visited the Youldos Basin in 1893. He decribed the frost cracks and frost mounds. The first information of permafrost in Tianshan was reparted by the pedologist A.I. Bezsonov, who visited the AK–Sai Basin in Inner Tianshan in 1913. However, the systematic and purposeful research on permafrost and other cryogenic phenomena in Tianshan started only at 50's and 60's of this century.

Nowadays, the area of permafrost regions estimated by us is 180–200 thousands Km^2, while the masses of cryotithozone – about 90–100 thousands Km^2 in total area and no less than 16 thousands Km^3 in total volume. The following pattern could be seen in Tianshan: the permafrost area is 10 times of the modern glaciers (about 18 thousands Km^2) and two times of the total area of masses of cryolithozone. This pattern is very localized, it depends on the height of mountain and climatic factors dependent upon the geographical position of the region.

If the volumetric ice content is 1% of the whole cryolithozone, then the total volume of ground ice (excluding the buried glacial ice) in cryolithozone should be 160 Km^3.

The permafrost zone could be divided into three subzones, i.e., the island (extremely unstable), discontinuous (unstable) and continuous (stable) ones.

The altitudinal limit of permafrost distribution, dependent upon the geographical latitude, local climate and lithological characteristics (thickness of snow cover, composition of loose sediments, etc), might be at 2500–3600 m a.s.l. with a negative mean annual air temperature and above the upper limit of forest belt. However, under a special microclimatic condition, for example under the cover of coniferous trees, the small permafrost masses could be formed under a positive mean annual air temperature, even down to the altitude of about 2000m. Such kind of permafrost masses were fount in Northern Tianshan, Inner Tianshan and Eastern Tianshan, down to the latitude of 42°N. Thus, the Tianshan might be the southmost mountain systemin the Northern Hamisphere that the permafrost could be found in forest zone. This should be a noticeable problem in forestry.

The lower limit of the continuous or stable permafrost subzone varice from 3500 to 3700 m a.s.l., there might not be permafrost under the large glaciers, even at a considerable high absolute elevation. Comparing the altitudinal position of snowline and the lower limit of continuous permafrost in Tianshan, some important conclusions could be made:

The distance between snow line and the lower limit of continuous permafrost was named the continentality index of permafrost subzone (Gorbunov,1976). Later, S.A. Harris suggested the continentality as the characteristic index, made it clearly in definition and used it to evaluate the geocryological condition in the mountains of Northern America (Oral communication). In the paper , it is called the index of geocryological zone (AA).

The above indices determine the cryogenic state of the ended moraine of modern glacier.

The index in Western Tianshan shows that many ended moraines are in the discontinuous and island permafrost subzones.

Table 1. Index of geocryological zone in Tianshan

No.	Region	AA (Km)
1	Western Tianshan	0–0.1
2	Inner Tianshan	0.4–1.5
3	Northern Tianshan	0.3–0.4
4	Eastern Tianshan	0.4–1.5
5	Junggar Alatan	0.2–0.5

Thus, it could be said that the moraines might be completely or partially in an unfrozen state. The formative condition of glacial mud flow there would considerably differ from that moraines bound by permafrost. Such a condition is dominant in most parts of the Northern Tianshan, Inner Tianshan, Eastern Tianshan and The Mt. Junggar Alatan. In these regions, the large glaciers run down to the discontinuous or island permafrost zones, the ended moraines might be unfrozen or only a small part of the ended moraines could be subject to the perennially freezing. So, these moraines are distineguished in their poor stability and worse preservation in comparison with those moraines bound by permafrost. The frozen and unfrozen moraines also differ significantly from each other in the internal structure. The former is characteried by the existence of intermoraine cavities filled with the considerable amount of melt water. Their burst is usually the origin of the great glacial mud flow.

There is another point to be noticed. On the surface of the frozen moraine, the condition is far more favourable to take forming, because practically no water could infiltrate through the frozen loose–block sediments, this is quite different from the unfrozen moraine.

Geocryological data in Tainshan should that, at a same latitude, the elevation of lower limit of the continuous permafrost didn't change significantly from place to place. The snowline, however, displaces very obviously with the position of the mountain ranges. Even at a same geographical latitude in Tianshan, the snowline varies from 3500 to 5000 m, while the lower limit of continuous permafrost subzone — only within 3500–3700 m a.s.l., because the snowline is sensitive to the total amount and regime of atmosphere precipitation, while the limit of the permafrost subzone is mainly dependent upon the thermal condition changing little from the periphery of Western Tianshan to the Inner Tianshan or the Eastern Tianshan.

The law decribed above doesn't deny the influence of precipitation on the thermal regime of ground.

The thing is that, at a high elevation (higher than 3500–3700 m), the atmosphere precipitation will reduce in winter, and the strong and constant wind will form the discontinuous and compacted snow cover that could not protect the ground from freezing practically.

By the island permafrost subzone, the situation is different at the altitudinal range from the region with little snow to the region with heavy snow the geographical environment changes significantly. This is because of that in the region with heavy snow the permafrost could not form under a thick and continuous snow cover, while in the region with little snow, the absence or thinness of snow cover could promote the perennial freezing of soils. At such an altitude, the wind has no a determinant effect on snow cover as seen at high elevation, so that it can carry out its effect of protecting the soil against cold. All of these result in the occurrence of permafrost masses down to the elevation as low as 1800 m a.s.l. in the region with little snow, while in the region with heavy snow, there would be no permafrost even at 2700–2800 m. The peculiarity of landform will aggravate the difference of geocryological condition in different altitude. Below 3500–3700 m in Tianshan, there are many intermount depressions characterized by the plain landform. There, the calm weather is dominant in winter, where the snow cover, if it is formed, will not be distroyed by wind. At the sections in mountain valleys with a hardly flowing cold air (Urumqi river valley in the area of the Chinese Tianshan Glaciological Station) or in the depressions of Sysumir, Arpin, AK–can, Great and Small Uldous, the anormal cold winter could be encounter. At those depressions with continuous and thick snow cover, permafrost is absent, even at an elevation as high as 3000 m, but at the places without thick and continuous snow cover, the frozen ground could be seen at relatively low altitude.

In the intermount depressions higher than 3500 m, because they are inside the mountain area (Chatir–Kelskaya, Kek–Ala–Chan, Kym–Terskyi Sirt), the trifling snow cover has nc any influence on the altitudinal position of the lower limit of the continuous permafrost subzone, even at the plain condition.

There is another circumstance that forms the distinctive features of perennial frost in the lower and upper geocryological subzones of Tianshan i.e. the alpine landforms dominant in the continuous permafrost subzone.

Since the predominance of steep bedrock slope, the snow cover has no effect of protecting the ground against cold.

All of these, as mentioned above, also determine the stability of the boundary of the continuous permafrost subzone and the unstability of the boundary of the lower geocryological subzones.

Thermal measurement in Tianshan demonstrated that the seasonal fluctuation of ground temperature could penetrate down to a depth of 20–30 m in bedrock. The minimum value of temperature was recorded to be −4.9°C in bedrock (4200m a.s.l., 42°N latitude) and −6.5°C in moraine (4050 m, 42°N latitude). The maximum value of thickness of cryolithozone was observed to be 270 m (4160m a.s.l., 42°N latitude).

The permafrost in Tianshan started forming no later than Pliocene, before the first occurrence of mountain glacier. During the period of Pliocene, Pleistocene and Holocene, the permafrost area became larger, especially in the ice ages of Quaternary. In Late Pleistocene, the lower limit of permafrost extended down to the hillfoot of Northern Tianshan at about 1000 m a.s.l. Unlike the Mt. Alps, there is no any recorded unquestionable case to prove the degradation of permafrost in Tianshan nowadays.

Special attention should be paid to rock glaciers. According to their origin and position, the rock glaciers can be divided into two types, i.e., the near–slope ones and the near–glacier ones. According to their age and dynamics, rock glaciers can be divided into active, inactive and ancient ones. The active rock glaciers in Tianshan are no less than 4000 in number , or rather than 4000 far more.

The near–slope rock glaciers are transformed from talus and rock – avalanche bodies near the slope feet, the near –glacier rock glaciers — mainly from the moraine materal. The formation of the

near–slope glacier is less dependent upon the evolution of glacier, and the latter, however, –– directly upon the ice advance and retreat. When ice advance, it could be completely or partially destroyed. Thus, under the other conditions being equal in those places where the glaciers distinguish themself in high mobility the near–glacier rock glaciers will be seen less than that in those places where the glaciers are more stable. This should be noticed when the rock glaciers are used as the paleogeographical indicator.

THE FREEZING AND FROST HEAVE REGULARITIES OF BASE SOIL FOR ARBITRARY SLOPE DIRECTION AND GRADIENT

Guo Dianxiang, Wei Zhengfeng and Ma Yijun

Institute of Hydraulics, Shan Dong Province

After calculating the solar radiation energy for arbitrary slope direction and gradient and analyzing the effect of udnerground water table on freezing depth, relationships of frost and frost heave with mean annual temperature, solar radiation energy and underground water table are set up. Mathematical models for predicting freezing depth and frost heave of base soil are established for arbitrary slope direction and gradient. The calculation is checked by using observed data of the temperature, freezing depth and frost heave of the base soil.

I. CALCULATION OF DAILY SOLAR RADIATION FOR ARBITRARY SLOPE DIRECTION AND GRADIENT

In unit time, the solar energy flux projecting on unit area is defined as the solar radiation intensity (S_i, the unit is W/m^2). The plane perpendicular to the solar-ray has the maximum radiation intensity, but, the plane parallel to the solar-ray has the minimum radiation intensity. The solar radiation intensity of horizontal ground is directly proportional to the sinus of the solar height (h). Considering the distance between the sun and the earth and the influence of atmospheric transparence, the solar radiation intensity reaching the ground is:

$$S_i = \frac{S}{\rho^2} P_m \sinh \qquad (1-1)$$

Where S is solar constant, about 1326 W/m^2; ρ is vector radius of the earth, in January, ρ^2 is about 0.97; P_m is atmospheric transparence; h is solar height.

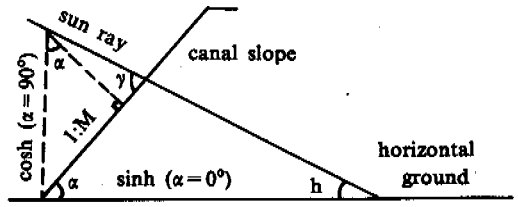

Fig.1 Calculated figure of the solar radiation intensity of canal slope

When the slope angle of a canal bed is α, from the triangular relation of Figure 1, we know that the angle γ between the solar ray and canal slope can be written as γ=h + α. Therefore, when the slope direction is perpendicular to the solar ray, the radiation intensity of the canal slope can be written as:

$$S_N = \frac{S}{\rho^2} P_m \sin\gamma = \frac{S}{\rho^2} P_m \sin(h+\alpha) = \frac{S}{\rho^2} P_m (\sinh\cos\alpha + \cosh\sin\alpha) \qquad (1-2)$$

The solar radiation intensity for an arbitrary slope can be divided into the vertical and horizontal quantity. The vertical quantity of solar radiation doesn't depend on any direction, its projection on arbitrary gradient slope equals $\frac{S}{\rho^2} P_m \sinh\cos\alpha$. The horizontal quantity of solar radiation has to do with the varying solar azimuth (y), therefore, it has the strict slope directionality, and the projection of the horizontal quantity on arbitrary gradient slope equals $\frac{S}{\rho^2} P_m \cosh\sin\alpha\cos(y-\beta)$. At any time, on a different gradient slope, the solar radiation intensity can be expressed as follows:

$$S_{\beta,\alpha} = \frac{S}{\rho^2} P_m(\sin\gamma) = \frac{S}{\rho^2} P_m[\sinh\cos\alpha+\cosh\sin\alpha\cos(y-\beta)] \qquad (1-3)$$

where: y is the arbitrary solar height on arbitrary gradient slope:

$$\sinh = \sin\phi\sin\delta + \cos\phi\cos\delta\cos\omega \qquad (1-4)$$

$$\sin y = \frac{\cos\delta\cos\omega}{\cosh} \qquad (1-5)$$

$$\cos y = \frac{\cos\delta\sin\phi\cos\omega-\cos\phi\sin\delta}{\cosh} \qquad (1-6)$$

Where β is slope direction angle, it equals zero in the north, clockwise rotation is 360°C; y, ω are respectively solar azimuth and hour angle, at high noon, all of them are zero, in the afternoon positive, in the morning negative; α is gradient angle; φ is latitude; δ is equatorial latitude, when the sun is to the south of

the equator, δ is negative, to the north, it is positive.

Putting (1-4), (1-5), (1-6) into (1-3) we can obtain:

$$S_{\beta,\alpha} = \frac{S}{\rho^2} P_m \sin y$$
$$= \frac{S}{\rho^2} P_m[\sin\phi\sin\delta\cos\alpha - \cos\phi\sin\delta\sin\alpha\cos\beta$$
$$+\cos\phi\cos\delta\cos\alpha\cos\omega + \sin\phi\cos\delta\sin\alpha\cos\beta\cos\omega$$
$$+\cos\delta\sin\alpha\sin\beta\sin\omega] \quad (1-7)$$

From sunrise (ω_1) to sunset (ω_2), we integrate (1-7), this is daily solar radiation:

$$\Sigma_d S_{\beta,\alpha} = \frac{180}{\pi}\frac{S}{\rho^2} P_m \int_{\omega_1}^{\omega_2} \sin y\,d\omega$$
$$= \frac{180}{\pi}\frac{S}{\rho^2} P_m \int_{\omega_1}^{\omega_2} (\sin\phi\sin\delta\cos\alpha$$
$$-\cos\phi\sin\delta\sin\alpha\cos\beta + \cos\phi\cos\delta\cos\alpha\cos\omega$$
$$+\sin\phi\cos\delta\sin\alpha\cos\beta\cos\omega + \cos\delta\sin\alpha\sin\beta\sin\omega)d\omega \quad (1-8)$$

Where ω_1, ω_2 are sunrise and sunset hour angles. The calculation method of sunrise and sunset hour angle is the following: in the formula (1-7), let siny=0, we can obtain:

$$\sin\phi\sin\delta\cos\alpha - \cos\phi\sin\delta\sin\alpha\cos\beta + \cos\phi\cos\delta\cos\alpha\cos\omega$$
$$+\sin\phi\cos\delta\sin\alpha\cos\beta\cos\omega + \cos\phi\sin\delta\sin\alpha\sin\omega = 0$$

We solve for ω, these are sunrise and sunset hour angle. The calculation expression is:

$$\omega_1,\omega_2 = \pm\left(\sin^{-1}\frac{C_3}{\sqrt{C_1^2+C_2^2}} - \sin^{-1}\frac{C_1}{\sqrt{C_1^2+C_2^2}}\right) \quad (1-9)$$

where:

$$C_1 = \cos\phi\cos\delta\cos\alpha + \sin\phi\cos\delta\sin\alpha\cos\beta \quad (1-10)$$

$$C_2 = \cos\delta\sin\alpha\sin\beta \quad (1-11)$$

$$C_3 = \cos\phi\sin\delta\sin\alpha\cos\beta - \sin\phi\sin\delta\cos\alpha \quad (1-12)$$

where ϕ,δ,β are known numbers, α is the shaded angle of a point on the canal slope, it is divided into the leaveslope angle α and the sunslope shaded angle α'. The sunslope shaded angle α' is under the influence of the deserted soil height of the canal top on the opposite shore, canal bottom width, and slope point, we can calculate it with the following formula:

$$\text{slope bottom: } \alpha' = +g^{-1}\left(\frac{1}{M+N}\right) \quad (1-13)$$

$$\text{slope middle: } \alpha' = +g^{-1}\left(\frac{1}{3M+2N}\right) \quad (1-14)$$

the leaveslope shaded angle equals the canal gradient angle, that is:

$$\alpha = +g^{-1}\left(\frac{1}{M}\right) \quad (1-15)$$

where M is side slope coefficient, N is the bottom width.

When we calculate the sunrise and sunset hour angle for different gradient and slope with the formula (1-9), at first, we should determine whether the sunrise (or sunset) of the slope is the leaveslope shaded angle (α) or the sunslope shaded angle (α'). If we put α=0 into the formula (1-8), we can obtain the daily solar radiation of horizontal ground:

$$\Sigma_d S_o = \frac{180}{\pi}\frac{S}{\rho^2} P_m \int_{\omega_1}^{\omega_2} (\sin\phi\sin\delta + \cos\phi\cos\delta\cos\omega)d\omega$$
$$= \frac{180}{\pi}\frac{S}{\rho^2} P_m \int_{\omega_1}^{\omega_2} \sinh d\omega \quad (1-16)$$

On the horizontal ground, the sunrise and sunset hour angle can be calculated as follows:

$$\omega_{01},\omega_{02} = \pm\cos^{-1}(-tg\phi tg\delta) \quad (1-17)$$

The solar radiations of the arbitrary slope direction and gradient and horizontal ground have a relation as follows:

$$K_t = \frac{\Sigma_d S_{\beta,\alpha}}{\Sigma_d S_o} = \frac{\int_{\omega_1}^{\omega_2} \sin y\,d\omega}{\int_{\omega_{01}}^{\omega_{02}} \sinh d\omega} \quad (1-18)$$

Result are listed in Table 1.

II. CALCULATION OF FROZEN SOIL DEPTH FOR ARBITRARY POSITION ON THE SLOPE OF ARBITRARY SLOPE DIRECTION AND GRADIENT

1. Calculation of Geothermal Difference on the Slope of Different Slope Direction and Gradient

The formula [2] between the heat flux from solar radiation ground heat interchange is as follows:

$$S_o = \lambda_s \frac{Te-Td}{h_e} = B(Te-Td) \quad (2-1)$$

Where T_e is the earth's surface atmospheric temperature (regarded as ground surface temperature); T_d is the ground surface temperature without solar radiation; B is ground heat emission coefficient; λ_s is coefficient of thermal conductivity of soil body; h_e--viscous layer thickness. (T_e-T_d) is the increase of ground temperature on the horizontal plane under the solar radiation, that is $(T_e-T_d)=\Delta t_o$. From the formula (2-1), we can write:

$$\Delta t_o = \frac{S_o}{B} \quad (2-2)$$

The calculation formula of the increase of ground temperature for arbitrary slope direction and gradient can be written as follows:

$$\Delta t_\beta = K_t G \frac{S_o}{B} \quad (2-3)$$

Where G is the rate of ground heat absorption; G=1-q (q is reflection ratio), other symbols are the same as above.

In winter, the relation between the canal bed temperature and slope direction is very obvious, the negative temperature area is approximately symmetrical with the distribution of slope direction. On the north slope, the duration of negative temperature is the longest, and the negative number is the largest. Central to the north slope, the distribution of negative temperature on the two side slopes are symmetrical. With the rotation of slope direction, the freezing time is lagged, the thawing time is advanced. On the south slope, the negative temperature is the highest, the duration of negative temperature is the shortest. The temperature difference of 5 cm deep soil layer is 4 to 5°C, the temperature difference of 20 cm deep soil layer is 2.5 to 3.0°C.

Table 1. The ratio K_t of lining canal slope and horizontal ground in seasonally frozen ground regions

Latitude	Gradient \ Slope direction	S	SE(SW)	E(W)	NE(NW)	N
N37°	α=90°	1.550	0.914	0.403	0.068	0
	45°	1.841	1.336	0.777	0.247	0
	33.7°	1.732	1.360	0.849	0.366	0.019
	26.6°	1.627	1.329	0.890	0.468	0.180
	21.8°	1.540	1.296	0.916	0.550	0.318
N40°	α=90°	1.678	0.974	0.411	0.063	0
	45°	1.955	1.422	0.779	0.218	0
	33.7°	1.825	1.408	0.849	0.328	0
	26.6°	1.704	1.370	0.888	0.429	0.113
	21.8°	1.606	1.332	0.914	0.512	0.254
N43°	α=90°	1.824	1.035	0.420	0.058	0
	45°	2.080	1.483	0.781	0.189	0
	33.7°	1.929	1.460	0.848	0.288	0
	26.6°	1.792	1.416	0.886	0.386	0.046
	21.8°	1.682	1.372	0.911	0.470	0.182
N46°	α=90°	1.936	1.039	0.427	0.052	0
	45°	2.213	1.546	0.783	0.161	0
	33.7°	2.045	1.517	0.847	0.246	0
	26.6°	1.892	1.466	0.884	0.338	0
	21.8°	1.768	1.417	0.908	0.422	0.104

Remark: To calculate the sunslope shaded angle (α') according to the ratio 3:1 of the canal bottom width and canal depth.

2. Negative Temperature Index Calculation for Arbitrary Slope

In China on the study of canal base soil freezing, according to the Stefan formula, many researchers provided that the relation between frozen soil depth (Z) and negative temperature index (F) can be written as follows:

$$Z = E\sqrt{F} \qquad (2-4)$$

but, because it is difficult to solve the negative temperature index of arbitrary slope direction and gradient, and the formula can't be directly used to calculate the frozen soil depth of arbitrary slope direction and gradient, thus, we regard the negative temperature index as a constant. According to the practically observed data of frozen soil, we inversely solve a series of canal trend coefficients, canal bed position coefficients, etc., thus, we calculate the frozen soil depth for different slope direction and gradient plane (Table 2), but, the computing work is very complex, and the theoretical evidence is not complete.

According to the regression analysis of geothermal materials, we know that geothermal annual change regulation can be approximately described with the sinusoid. The axis of the sinusoid is the annual mean ground temperature (T_e), the half of the difference between the highest and lowest of the curve is the geothermal amplitude (A). Fig.2 is the regressed geothermal change procedure line of the slope, the shaded area is the accumulating value of mean daily negative temperature, therefore we intergrate the shaded area from τ_1 to τ_2 and we can obtain the negative temperature index.

The slopes under the solar radiation, in winter, the ground temperature of the slope increases Δt, the negative temperature index of the slope will decrease. Therefore, we integrate

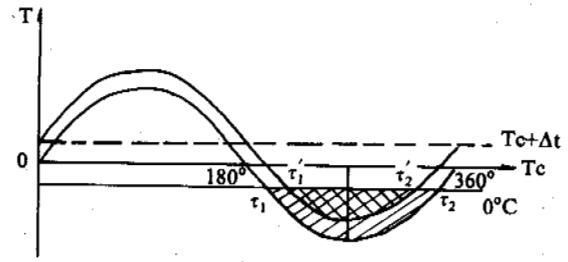

Fig.2 Calculated diagram of the negative temperature index

the ghosted shaded area from τ_1' to τ_2', and can obtain the negative temperature index of the slope under the solar radiation. For arbitrary slope direction and gradient, the general expression of the geothermal annual change is as follows:

$$T_\beta = (T_e + \Delta t_\beta) + A \sin\tau \qquad (2-5)$$

After being integrated we can obtain:

$$F_{\beta_1} = \frac{180}{\pi} \int_{\tau_1}^{\tau_2} [(T_e + \Delta t_\beta) + A\sin\tau] d\tau \qquad (2-6)$$

where:

$$\tau_1 = \pi + \frac{\pi}{180} \sin^{-1}\left(\frac{T_e + \Delta t_\beta}{A}\right)$$

$$\tau_2 = 2\pi + \frac{\pi}{180} \sin^{-1}\left(\frac{T_e + \Delta t_\beta}{A}\right) \qquad (2-7)$$

τ_j is conversion coefficient of days and degrees, 365/360=1.01, we can consider that one day equals one year.

Table 2. The comparison of the measured and computed frozen ground depths for different slope directions

Position	Freezing depth(cm)	Slope direction	Horizontal plane	N	NE (NW)	E (W)	SE (SW)	S
Ying Chang in Nin Xia	Slope middle	Calcu-lated	0.80	1.06	0.96	0.84	0.69	0.57
	Slope bottom	Calcu-lated	0.71	0.94	0.86	0.74	0.61	0.50
	K_z		1.00	1.32	1.20	1.05	0.86	0.71
Frosheaving field Lubei in Shangdong	Slope middle	Calcu-lated	0.35	0.62	0.53	0.39	0.23	0.09
		Meas-ured	0.36	0.61	0.47-0.51	0.31	0.15-0.20	0.10-0.08
	K_z		1.00	1.76	1.51	1.13	0.67	0.26

3. Correction Coefficient of Ground Freezing Depth Considering the Sunshine Factor

The relational expression between the freezing depth of arbitrary slope direction and gradient plane and horizontal ground can be written as:

$$K_\tau = \frac{Z_\beta}{Z_\circ} = \frac{E\sqrt{F_\tau}}{F\sqrt{F_\circ}} = \frac{\overline{F_\beta}}{F_\circ} \qquad (2\text{-}8)$$

Where Z_β is frozen soil depth of arbitrary slope direction and gradient plane; $Z_\circ$ is frozen soil depth of horizontal ground; F_β is negative temperature index of arbitrary slope direction and gradient plane; $F_\circ$ is negative temperature index of horizontal ground.

K_τ changes with the value of $\frac{A}{T_e+\Delta t_\beta}$, when $\frac{A}{T_e+\Delta t_\beta}=1$, there is no frozen ground; $\frac{A}{T_e+\Delta t_\beta}>1$, the slope yields the negative temperature index, because of the different values of Δt_β, it causes the difference of slope directionality, with the increase of $\frac{A}{T_e+\Delta t_\beta}$, the difference of slope directionality gets small. In the high latitude regions where solar radiation intensity is smaller, the difference of slope directionality of K_τ is very small, but, on the south edge of seasonally frozen ground regions, the difference of the slope directionality K_τ is larger. When the frozen ground depth of the horizontal ground is known, we can calculate the frozen ground depth of arbitrary slope direction and gradient plane with the values of K_τ, under the conditions of the same soil properties and buried depth of ground water.

4. To Determine the Influence Coefficient of the Buried Depth of Ground Water on the Frozen Ground Depth

To the freezing depth of the base soil of canal bed, not only is there the difference of slope directionality on the same height, but also there is the difference of the up-down position in the same section. The research for years about frozen ground shows, under the conditions of the same soil properties and negative temperature, the freezing depth is mainly under the influence of the water content of soil. The general regulation is: the more shallow the buried depth of underground water, the more the bottom moisture will migrate upwards, the phase transition heat which the moisture yielded resists the development of the freezing front. The freezing rate is smaller than that of the soil layer with a low water content. In fact, the deeper the buried depth of ground water, the more the freezing depth of the soil body is deep, and the more shallow the underground water table, the more the freezing depth of the soil body is shallow. The influence range (L) of underground water on the freezing depth is the sum of the capillary elevation height (h_m) and freezing depth (z) of soil body, that is:

$$L \leq h_m + z \qquad (2\text{-}9)$$

When L>h+z, the freezing depth isn't under the influence of underground water table, so K_d=1. According to the material of the frost heaving test of Zhang Ye, Gansu Province, within the range of L≤h_m+z, with the decrease of the distance between the underground water table and the freezing depth, the influence of the buried depth of underground water on the freezing increases. The influence coefficient of the buried depth of underground water on the freezing depth is K_d:

$$\frac{1}{K_d} = 0.96 + 0.65e^{-D} \quad \text{(clay and silt of high and middle liquid limit)} \qquad (2\text{-}10)$$

$$\frac{1}{K_d} = 0.94 + 0.5e^{-D} \quad \text{(clay and silt of low liquid limit)}$$

For the above reasons, the freezing depth of arbitrary point on arbitrary slope direction and gradient plane can be calculated as follows:

$$Z_\beta = K_\tau K_d Z \qquad (2\text{-}11)$$

Where Z is the freezing depth of horizontal ground around the canal; K_τ is correction coefficient considering the conditions of the sunshine of different slope direction and gradient; K_d is the influence coefficient of the buried depth of underground water on the freezing depth.

III. FROST HEAVING PREDICTION OF ARBITRARY SLOPE DIRECTION AND GRADIENT PLANE

According to the frost heave mechanism, the three main factors causing the frost heaving are

the soil properties, soil moisture (it stands for the influence of underground water table), and the negative temperature idnex. According to the research achievements on canal frost heaving for years in China, the expression of the calculation about frost heaving is:

$$\Delta h_\beta = y.Z_\beta \qquad (3\text{-}1)$$

Where Z_β is frozen ground depth on the arbitrary slope direction and gradient plane under the condition of the arbitrary buried depth of underground water, it can be calculated according to the formula (2-11); y is the mean frost heaving strength of soil (%).

The relationship between the mean frost heaving strength and water content of soil can be calculated as follows:

1. For shallow buried underground water, the capillary elevation height reaches the frozen ground layer, the water content is larger, and the complimental source is full. The main factor affecting on y is the buried depth of underground water, that is:

$$y = a_1 e^{-b_1 D} \qquad (3\text{-}2)$$

Now we put the tested values of a, b into Table 3.

2. To deep buried underground water, the capillary elevation height can't reach the frozen layer, there is no compliment of the underground water. So the relation between y and the water content before freezing is close, that is:

$$y = a_2(W - b_2 W_p) \qquad (3\text{-}3)$$

where W is the mean water content (%) in the range of the freezing depth before freezing; W_p is the plastic water content (%); a_2, b_2 are coefficients, solved in accordance with the tested materials for years.

IV. CONCLUSIONS

1. The annual mean ground temperature (T_e) and the annual geothermal amplitude (A) determined the negative temperature index in this region. The increased ground temperature Δt_β with the daily radiation is an important factor causing the differences of the negative temperature index.

2. The buried depth of underground water and capillary properties of soil are the important factors yielding the differences of frozen ground depths and frost heaves in the vertical direction.

3. The annual mean ground temperature (T_e), the annual geothermal amplitude (A), the temperature difference of slope direction (Δt_β), and the buried depth of underground water (D) are four basic factors on the freezing of the base soil and the prediction of calculation of the frost heaving.

REFERENCES

Yao Zhensheng, (19) The principle of climatology, The Press of Sciences.

Zhu Bofang, et al., (19) Temperature stress and control of hydraulic engineering concrete structure, The Hydraulic and Electric Press.

Pan Shouwen, (19) The theoretical basic and application of small climatic investigation, The Meteorological Press.

Central Meteorological Bureau, (19) The climatic atlas of China, The Press of Map.

Table 3. The statistic list of the tested values of a_1, b_1 in our country

District / Coefficient	Gansu	Liaonin	Heilongjiang	Xinjiang	Shangdong
a_1	40.0 (silty soil) 14.3 (sandy soil)	37.0 18.5	27.0 20.0	16.9 (silty clay) 14.24 (soil) 14.58 (sandy soil)	46.39 (sandy soil)
b_1	1.25 (silty soil) 1.47 (sandy soil)	1.2 1.4	0.85 0.5	0.62 (silty clay) 0.37 (soil) 1.0 (sandy soil)	0.963 (sandy soil)

PERIGLACIAL PERIOD AND PLEISTOCENE NATURAL ENVIRONMENT OF WESTERN MOUNTAINS OF BEIJING

Guo Xudong
(Institute of Geology, Academia Sinica,Beijing 100029)

Several fossil periglacial phenomena found on the Western Mountains of Beijing enabled us to divide the Pleistocene periglacial period into 6 epochs in the area. During the periglacial epochs the surface temperature was lower than that at present by 12-15°C; precipitation in winter was higher than that at present; depth of permafrost reached -3- -20m or more; and the natural environment was a savanna or tundra. The southern boundary of the periglacial area extended to 38°N.

I. Introduction

During the last years research on the Quaternary periglacial phenomena has been rising to a new level in the world. The scope and depth of the research increased significantly. Intensive research of various recent periglacial processes in polar and sub-polar regions and in some high-latitude regions has promoted the Quaternary periglacial research (Kaisser,1969. Pewe,1975, Washburn,1979) Many scientists have compared the environment of formation of the Pleistocene periglacial phenomena with that of formation of the recent periglacial phenomena of similar activity, estimated the paleoclimatic conditions, and reconstructed the ancient natural environments (Washburn, 1980; Brack,1976, Mears,1981) Since 1976 when periglacial involutions and congelifolds were found in China and the perigalcial climate was suggested, the problem has attracted the attention of scientists, then the research works on the periglacial processes and periglacial epochs in northern China were successively reported (Guo Xudong,1984; Liu Tungsheng et al ,1987. Guo Xudong,1988. Sun Jianzhong,1981)

II Discovery of Fossil Periglacial Phenomena

The Western Mountains are situated in the western and northern parts of the Beijing Plain, i e in a transition zone between Taihang Mountains and Yanshan Mountains The trend of the mountains is approximately northeast The highest peak of the Western Mountains, Dongling Mountain, is at an elevation of 2 303 m and the second peak, Baihuashan Mountain, at 1 991 m, most of the other mountains are lower mounts and hills at elevation lower than 1 000 m The main streams in the area are Yongdinghe River and its tributaries. Qingshuihe River, etc Quaternary deposits are mostly distributed on both banks of river valleys and in intermontane basins. The deposits are mainly loess and loess-like soil, and less alluvial-colluvial sand-gravels .The fossil periglacial phenomena found by us are mostly developed in late Pleistocene Malan loess and middle Pleistocene Lishi loess These periglacial phenomena are ice (soil) wedges, ice (sand) wedges, periglacial involutions, congelifolds, congeliturbations, etc.

(1) Ice (soil) wedges: They are well preserved in Zhaitang Village (i.e. Dongzhaitang) and on a platform by a hill east of Qiansangyu Brickfield

Lithologically a layer of secondary Malan loess and yellowish-brown loess-like soil intercalating with sand-gravel layer are exposed on the profile. The sand and gravel are mostly angular and composed basically of debris after weathering of diabase on the hills It indicates that this layer of loess is indigenous deposits. Its geomorphic position corresponds to the second-step terrace on the Qingshuihe River A large ice (soil) wedge was found on the profile Hole of the wedge was filled with sand and soil and formed a soil wedge (Fig.1) The ice wedge is 1.06m wide at its top and

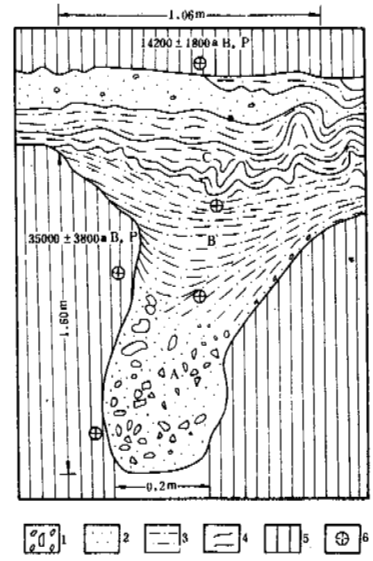

Fig.1. Profile across a fossil ice (soil) wedge east of Qiansangyu
1. Sand-gravel; 2. Coarse-grained sands; 3. Sandy soil; 4. Periglacial involution, 5. Malan loess, 6. Site for sampling.

0.2m wide at its bottom in an U-shape, extending to a depth of 1.60 m. The fillings in the ice wedge represent coarse-grained sand-gravel in its lower part (A), fine-grained sand-soil in middle part with inclined bedding (B), and fine-grained sand-soil in upper part with apparent involution bedding (C). It indicates that the ice wedge after its melting was filled with congeliturbattion materials from slope of hill.

(2) Ice (sand) wedges: The fossil periglacial phenomena are well developed and preserved on the Western mountains at Qiansangyu. A field observation in 1977 indicated that the Malan loess west of Qainsangyu Brickfield contains a brownish-red fossil soil layer in its upper part and a sand-gravel layer about 2m thick in its middle part. 4 groups of juxtaposited different-size fossil ice (sand) wedges were found at the bottom of the sand-gravel layer. The depth of frost cracking of the ice (sand) wedges is usually 0.5-1.0 m. This profile was destroyed by diging soil for brick making.

(3) Periglacial involutions: A profile exhibiting the periglacial involution is found at a loess excavation pit north of Zhaitang Brick Factory. An evident periglacial involution was found in the Lishi loess at eastern side of the profile (Fig.2). It can be seen in Fig.2 that the cryogenic periglacial process caused the homogeneous water-saturated loess with horizontal bedding to be strong bent and deformed, exhibiting well structural form of periglacial involution. On the left top of Fig.2, an ice (soil) wedge about 1m long was found. It deeply indents into a periglacial involution. It indicates that the first cold-frost climatic event was followed immediately by a next more severely cold climatic event.

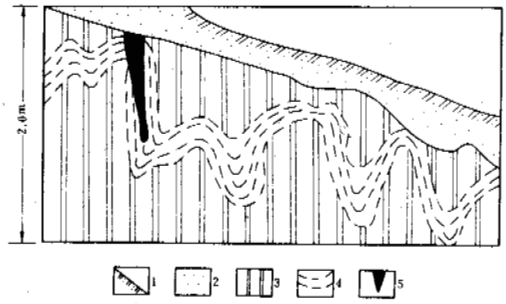

Fig.2. Profile across periglacial involutions in Lishi loess at Zhaitang.

1. Colluvium with sandy soil. 2. Sandy loess. 3. Lishi loess. 4. Periglacial involution. 5. Ice (soil) wedge.

(4) Congelifolds: They resulted from congelation and deformation of soil layer in the Pleistocene periglacial area under the severe cold climate. During our field investigation the congelifolds were found in Lishi loess at middle-lower part of a loess profile east of Yanchi Railway Station. As it is shown in the figure that the homogeneous, more compact loess layer has undergone sharp bending and deformation due to multiple congelations, and became loose in structure characteristic of periglaciation of the loess.

(5) Congeliturbate: A profile across the congeliturbate is located at the site by the highway about one kilometer north of Guanting Forest Center on the northern foot of the Western Mountains. Lower part of the profile consists of Pliocene red clay and middle-lower part of a layer of lithologically mixed loess-like deposits with wave relief and slightly curve bedding, which occur in a sharply unconformable contact with Pliocene red clay. The occurrence of gravel layer and thin layering of the loess-like soil are imbricate in descending order, and gravels are angular. It indicates that this layer of deposits was transported at a small distance and is neither normal fluvium or usual colluvium, but is a congeliturbate characteristic of mudflow terrace. It might be formed as a result of the downward slow creeping of active layer of permafrost or seasonally frost soil during their melting.

III Geologic Time of Formation of the Fossil Periglacial Phenomena

1. Geochronology and Stratigraphical Correlation

On the Zhaitang profile the periglacial involution and ice (soil)wedge that we found are located just at the bottom of Malan loess to the upper part of Lishi loess. Thus we infer their formation time must be the late stage of the Middle Pleistocene. A litho-stratigraphical correlation indicates that the stratigraphic positions of the ice (soil) wedge and ice (sand) wedge swarm at both eastern and western sides of the Qiansangyu Brickfield are the upper and lower parts of the Malan loess, and hence their formation time is the early and late stages of Late Pleistocene. The congelifold system in the Lishi loess at Yanchi is located in the middle and lower parts of the whole profile and hence its formation time is the early-middle stage of Middle Pleistocene. The congeliturbation found at Guanting Forest Center is inferred to be synchronous with the Shizhuang Formation of early Pleistocene from its contact with underlying Pliocene red clay and higher geomorphic position of the fourth-step terrace on Yongdinghe River at which it was found.

2. Paleomagnetic dating

In order to determine geologic age for formation of the fossil periglacial phenomena on two profiles at Yanchi and Guanting Forest Center, we have collected 24 specimens for paleomagnetic dating. All the specimens were demagnetized at an alternative field with a peak of 250 Oe, their magnetic parameters were determined on an English rotational magnetometer and the data were processed and mapped on a computer. The obtained results together with the above-described stratigraphic positions and age data of the fossil periglacial phenomena are shown in Fig.3. It can be seen in Fig. 3

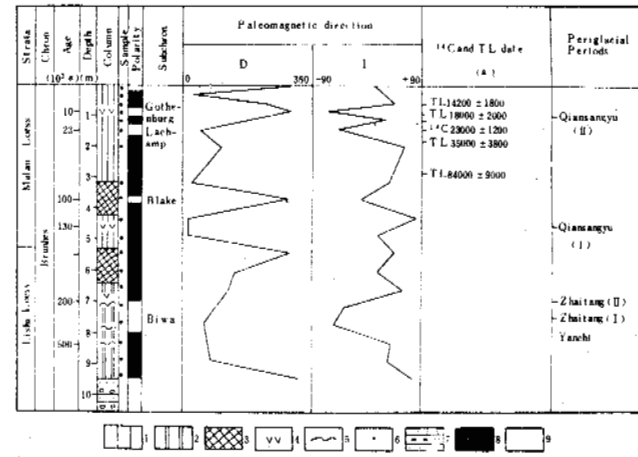

Fig.3. Magneto-stratigraphic column along the Yanchi loess profile and divided periglacial epochs on the Western Mountains of Beijing.

1. Malan loess. 2. Lishi loess. 3. Fossil soil. 4. Fossil ice wedge. 5. Periglacial involution and congelifold. 6. Site for sampling. 7. Sand-gravel layer. 8. Positive polarity. 9. Negative polarity.

that the paleomagnetic polarity column on the whole loess profile at Yanchi is basically positive. Therefore it is of Brunhes positive polarity epoch. The magnetic inclination (I) is usually about 50°, and declination (D) is about 350° in maximum. On the background

of overall positive polarity there are 4 polarity reversal events, their magnetic inclination is negative and significantly varies. They represent 3 reverse polarity events, namely Gothenburg event about 10 000a B.P. Lachamp event of 23 000a B.P. Black event of 0.10 Ma B.P. and Biwa event of 0.2-0.50 Ma B.P. respectively. The middle-upper part of the profile at Guanting Forest Center shows its negative polarity and only the lower part shows positive polarity. It indicates that the polarity column along the whole profile is just at the bottom of Matsuyama reverse polarity epoch, and its threshold age value is 2.43 Ma B.P. the early Pleistocene.

3. Thermoluminescent dating

The thermoluminescent age of Malan loess at Zhaitang was reported by Lu Yanchou et al.(1987). We had determined thermoluminescent age of fossil ice wedges found on the Qiansangyu profile. The samples were collected from filling materials in ice wedges, loess in which the ice wedges are found, and its overlying loess (see Fig.1). The result shows that filling materials from ice wedges are mostly debris of diabass,thus no age value was determined. The age of loess in which ice wedge was found is 35 000±3 800 a B.P. The age of bottom of loess overlying on the ice wedges is 14 200±1 800 a B.P. It is inferred from these data that the formation time of these ice wedges is a very severe cold climate stage after 35 000 a B.P. and before 14 200 a B.P. and may correspond to the time of lowest world sea level in a prevailing stage of the last glacial period, i.e. 18 200 a B.P.

IV. A Preliminary division of Periglacial period

A preliminary division of the periglacial period on the Western Mountains of Beijing is shown in Fig.3. 6-7 periglacial epochs can be divided in the area including those at Guanting Forest Center. They are described in ascending order as follows:

(1) Guanting periglacial epoch: It is represented by the congeliturbation at Guanting Forest Center and is a reflection of the Early Quaternary periglacial cold climate. Its age corresponds to the bottom of Matsuyama reversal, i.e. 2.43 Ma B.P.

(2) Yanchi perigalcial epoch: It is represented by the congelifold on Yanchi profile. The loess deposits have undergone sharp bending and deformation under the periglacial cold climate. Its age corresponds to Biwa event (I), about 0.5 Ma B.P. But the overlying loess has undergone the congelation. The loose texture of the soil layer may represent another cold climate event.

(3) Zhaitang periglacial epoch (I): It is represented by the larger periglacial involution below the second layer of fossil soil on Zhaitang profile and its age corresponds to Biwa event (I), about 0.3 Ma B.P.

(4) Zhaitang periglacial epoch (II): It is represented by the fossil ice (soil) wedge indenting into the above-mentioned periglacial involution and its age corresponds to Biwa event (II), about 0.2 Ma B.P.

(5) Qiansangyu periglacial epoch (I): It is represented by the fossil ice (sand) wedge swarm at the bottom of the gravel layer below a fossil soil layer in the Malan loess on a profile west of Qiansangyu Brickfield. The periglacial climate was more severely cold than that in the previous four epochs. Its age corresponds to Black event, about 0.13 Ma B.P.

(6) Qiansangyu periglacial epoch (II): It is represented by a larger fossil ice (soil) wedge on the profile east of Qiansangyu Brickfield. The ice (soil) wedge was filled obviously with the congeliturbation materials after its formation, which is the best evidence for the warming of periglacial cold climate. Its age corresponds to Gothenburg event inferred to be 18 200 a B.P. representing the most cold periglacial climate in the area.

V. Natural Environment in the Pleistocene

1. Estimation of Paleotemperature

It is usually considered that the depth of ice wedges or sand wedges is an indicator for the degree of cold and frost periglacial climate and the width of ice wedges is an indicator for the frequency of cold and frost periglacial climate. The depth of ice wedges in Malan and Lishi loesses at Qiansangyu (41°N, 115°8'E) and Zhaitang (39°8'N, 115°4'E) is 1.0-1.6 m and width of them is 1.06 m. The temperature at the time of their formation at Qiansangyu and Zhaitang must be lower than the present-day 10°C by 16-18°C, as calculated from the temperature of -6- -8°C of the isotherm indicator for the southern boundary of recently active ice wedges in Alaska of North America suggested by Pewé (1966). But Washburn (1980) suggested that the temperature of -6- -8°C is taken as a standard for comparison to be too low and temperature of -5°C may be a more reliable upper limit at the formation time of ice wedges. We suggest that the temperature during the time of the ice wedge formation at Qiansangyu and Zhaitang may taken to be lower than that at present by 15°C, as the standard taken to be -5°C.

In regard to the temperature condition during the formation time of the periglacial involutions and congelifolds, it was rarely discussed up to now. But some scientists suggested that the temperature during the formation time of chaotic periglacial involutions and pingos was -2°C. For example, the prevailing epoch of the Weichsel glacial period in Netherlands (52-53°N) of North Europe was inferred to be -2°C from the data of chaotic periglacial involutions and pingos, that is lower than that at present by 15°C, and is considered as a southern boundary of permafrost (Washburn,1979). If we take the temperature of -2°C as a temperature standard during the formation time of periglacial involutions and congelifolds, than the temperature during the formation time of periglacial involutions and congelifolds at Zhaitang and Yenchi may be lower than that at present by 12°C. It can seen that the Western Mountains of Bejing and the southern foot of Yanshan Mountains (38°N) can be the southern boundary of Pleistocene permafrost or of periglacial area in eastern China.

2. Estimation of Permafrost Depth

The observed meteorological data from Zhaitang Meteorological Station indicate that the mean temperature in Zhaitang area during the last 10 years is 10.1°C, lower than that in the plain area by 1.4°C and down to -19°C in minimum. The average depth of permafrost is 0.76 m and reaches 0.96 m in maximum. If during the Pleistocene perigalcial period the temperature at Zhaitang dropped down to -5°C, lower than that at present by 15°C, than the depth of permafrost at that time must be similar to that at present in the northern area of Da Hingga Range and reached 20 m or more (Xie Youyu,1981). If the temperature during the periglacial period dropped down to -2°C, than the depth of permafrost may be likened to that at present in the northern area of Songliao Plain, reaching 3-10 m below the surface (Guo Dongxin et al.,1981).

3. Estimation of Precipitation

A certain moisture of soil layers, like the temperature, is one of the necessary preconditions for congelifraction and other plastic deformation of the soil layers. Was the precipitation during Pleistocene periglacial period higher or lower than that at recent time? An annual mean precipitation in the last ten years in Zhaitang area is 451.9mm and 598.8mm in maximum. 80-70% of this precipitation is concentrated in June,August and September and as snow in winter, that is rare solid precipitation. Therefore, the soil layer is usually more moist in summer and more dry in winter. Under this climatic condition recently no congelation can occur in

the soil layer and no ice wedges can be found. In the melting season from the late spring to early summer only a small-scale congelation and frost heaving on road surface, can be found in the area where local lowlands, higher groundwater table and higher moisture in soil layer are present. As shown in Fig.1, the textural and structural flows and plastic deformation of the filling materials indicate that soil layer could undergo larger frost-cracking in the periglacial period and larger congelation, deformation and congeliturbation during melting seasons. It suggests that the moisture of the soil layer was higher than that at present. For this reason, the soil layer could be water-saturated and could undergo plastic creep. It follows that the climate at the beginning of the periglacial period was comparatively dry and cold, but in the middle and late epochs of the periglacial period the climate could become more cold and humid, under which the precipitation might be higher than the present-day 452mm, especially solid precipitation in winter was much higher than that at present.

4. Fossil Vegetation

The sporo-pollen composition and species in the filling materials from periglacial ice wedges at Qiansangyu are similar to those in inter-periglacial Malan loess at Moshikou (Guo Xudong et al.,1981) and Zhaitang (Yan Fuhua et al.,1986). The main flora is *Artemisia* and *Chenopodiaceae*, less *Compositae*, *Humulus*, *Selaginella* and *Ephedra*. Among the woody plants *Pinus* and individual *Aries* are found. The sporo-pollens in the loess around the ice wedges are approximately the same as in their filling materials, mainly *Artemisia*, *Chenopodiaceae* and *Selaginella* and individual *Pinus*. It indicates that the vegetation did not significantly vary from the periglacial period to the inter-periglacial period.

In general, from a viewpoint of ecologic environment, the above-described plants are tolerant of dry and cold climate. It indicates that during that time the surface plants were sparse under the more dry and cold climate and windy winter. The natural features were similar to those of a savanna steppe landscape. But the structural deformation of filling materials in the ice wedges shows that the climate in middle and late epochs of the periglacial period was more cold and humid. Therefore, the savanna might be in a tundra environment.

References

Lu Yenchuo et al.,1987, Thermoluminescent dating of coarse-grained quartz from Malan loess. Kexue Tongbao, Journal of Sciences, (1),47-50 (in Chinese).

Yan Fuhua, Ye Yongying, and Liu Yuexia, 1986, Sporo-pollen analysis of loess at East Zaitang of Beijing. Quaternary Research in China, 7(1),39-43 (in Chinese with English abstract).

Guo Dongxin,Li Zuofu,1981, Historic evolution and formation time of permafrost in northeastern China since late Pleistocene. Glaciology and Geocryology, 3(4) (in Chinese).

Guo Xudong et al., 1981, Possibility of Quaternary glaciation in Western Mountain area of Beijing from "glacial traces" at Moshikou. Glaciology and Geocryology, 3(2),63-66 (in Chinese).

Guo Xudong,1984, A preliminary study on Quaternary climate in China. Glaciology and Geocryology, 6(1), 49-60 (in Chinese).

Guo Xudong, 1988, A discussion on Quaternary glacial climate and environment in China. Scientia Geographica Sinica, 8(2),114-126(in Chinese with English abstract).

Xie Youyu, 1981, Periglacial geomorphology of Northeast China and its zonation. Glaciology and Geocryology, 3(4),17-23 (in Chinese).

Brack R.F.,1976, Periglacial features indicative of permafrost: ice and soil wedges. Quaternary Research, 6(1),3-26.

Kaisser, K.,1969, The climate of Europe during the Quaternary Ice Age. Quaternary Geology and Climate, NAS,1-12.

Liu Tangsheng, Guo Xudong, 1987, The periglacial phenomena on loess plateau, China. Loess and periglacial Phenomena, edited by Marton Pecsi and Huth M.French, Academia Kiado,Pudapest, 141-149.

Mears B.,1981, Periglacial wedges and the late Pleistocene environment of Wyoming's intermontane basin. Quaternary Research, 15(2),171-195.

Péwé,T.L., 1966, Ice wedges in Alaska-Classification, distribution and climatic significance. in: Permafrost International Conference Proc., Natl. Acad. Sci., Natl. Res. Counc. Publ., 1287, 76-81.

Péwé,T.L.,1975, Quaternary geology of Alaska. U.S.G.S. Prof.Pap., 835,145.

Washburn,A.L., 1979, Geocryology, a survey of periglacial processes and environments, 313-318.

Washburn,A.L.,1980, Permafrost features as evidence of climatic change. Earth-Science Review, 15(4), 317-393.

THE PHYSICS OF LIQUID WATER IN FROZEN POWDERS AND SOILS

Haiying FU, J. G. DASH, and L. WILEN,
Department of Physics,
and **B. HALLET,**
Department of Geological Sciences and Quaternary Research Center,
Unersity of Washington, Seattle, WA 98195, U.S.A.

We have studied the dependence of the unfrozen water content of porous media at subfreezing temperatures on the mineralogy, size and surface properties of particles. A series of well characterized monodisperse powders and natural soils were examined by a variety of techniques, including neutron diffraction, quasi-elastic neutron scattering, time domain reflectometry and mercury porosimetry[1] [2][3][4]. The melting process and, hence the amount of unfrozen water remaining unfrozen in porous media at subfreezing temperatures, are governed by surface melting, curvature effects, and impurity effects. Current theoretical treatments of these effects are consistent with experimental results.

INTRODUCTION

It is widely recognized that the persistence of water in the liquid form in porous media as temperatures drop below $0°C$ underlies many important natural phenomena involving freezing, including frost heaving[5][6] and frost weathering[7] [8]. It is also related to a diversity of other processes ranging from ice particle sintering to cloud electrification[9][10]. The amount of unfrozen water in frozen soils and rocks has been well documented, but there is no consensus as to its causes.

Through an interdisciplinary research program we examine the properties of unfrozen water in porous media using of modern experimental techniques and new theoretical developments in condensed matter physics[11]. We relate the persistence of unfrozen water at sub-zero temperatures to the tendency for ice to premelt at the contact with foreign substrates below its bulk melting point and for the freezing point to be lowered due to interfacial curvature and solute effects. The current study focuses on how much ice melts at the contact of a substrate and how this melting depends on the properties of the substrate.

EXPERIMENTS

To ensure maximum experimental sensitivity, fine powders are used as substrates in order to have a large contact area with ice. Powders of spherical particles are used for a concise theoretical treatment. We use time domain reflectometry(TDR) to measure the water fraction in such frozen ice/powder mixtures. TDR employs an electromagnetic wave (EM) pulse and measures the dielectric constant of a medium by analyzing the reflected EM pulse against the incident pulse. The technique provides a sensitive indicator of minute quantities of water because the dielectric constants of water and ice differ greatly at the observing frequency.

We tested monosized spherical powders of various sizes and diverse composition ranging from polystyrene to silica beads. The measured unfrozen water content was found to be consistent with a theory[12] accounting for surface melting, and the effects of curvature and solutes (Figures 1 and 2; the apparent discrepancy in Figure 2 below 1° from melting point is due to the fact that the beads are porous). Despite the wide range of surface properties of these powders, we found no detectable variation of the unfrozen water content with surface property.

Powders consisting of irregularly shaped particles were also tested, including some natural soils. The similarities in nonwetting behavior of ice and mercury on most known materials make it possible to employ mercury porosimetry(MP) to characterize the melting behavior of ice in the porous media[3]. The volume of mercury vapor is equated to that of water and the pressure P of the mercury is related to the temperature $\Delta T = T_m - T$ of ice by

$$\Delta T = P\frac{T_m}{\rho_s q_m}\xi = 5.404 \times 10^{-8} P \frac{°K}{N/m^2},$$

where T_m is the melting point, ρ_s and q_m the density and fusion heat of ice at T_m and ξ the surface energy ratio of ice-water to mercury-vapor. The unfrozen water contents deduced from mercury porosimetry are in close accord with direct TDR measurements for a diversity of artificial powders[3]. For samples such as natural soils, mercury porosimetry and TDR yield similar results, provided apparent impurity effects are taken into account (Figure 3). In a freezing ice/powder mixture, impurities are expelled into the unfrozen water as relatively pure ice crystal form giving rise to significant melting point depression even for pore waters that are initially very dilute.

The temperature dependence of the unfrozen water content for diverse porous substances agrees quantitatively with descriptions of both curvature effects and surface melting, a phenomenon common to many types of solids, and an actively studied topic in condensed matter physics[11]. A simple practical model has been developed to determine the amount of unfrozen water based on measurements of pore size distribution and simple theoretical estimates of Van der Walls interactions affecting the water, which are insensitive to the porous media composition and mineralogy[3]. In addition, novel experiments are currently under way to determine water transport rates over a wide temperature range in single films between ice and foreign surfaces, to provide detailed data for comparison with theory.

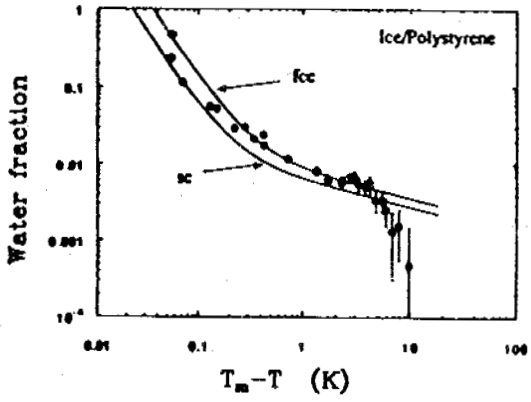

Figure 1. Water fraction in frozen mixture of water/polystyrene beads($5\mu m$ in radius): o: TDR; —: theoretical calculations[11].

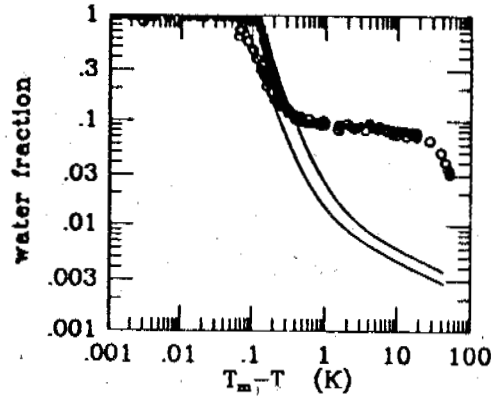

Figure 2. Water fraction in frozen mixture of water/quartz beads ($1.35\mu m$ in radius): o: TDR; •: deduced from MP; —: theoretical calculations[11].

REFERENCES

1 Gay, J.-M., Suzanne, J., Dash, J.G. and Fu, Haiying (1992) J. Cryst. Growth 123, 33.
2 Maruyama, M., Bienfait, M., Dash, J.G. and Coddens, G. (1992) J. Cryst. Growth 118, 33.
3 Fu, Haiying and Dash, J.G. (1993) J. Colloidal interf. Sci., 159, 343.
4 Fu, Haiying (1993) PhD Thesis, University of Washington, Seattle.
5 Anderson, D.M. and Morgenstern, N.R. (1973) in Permafrost, Proc. 2nd Int. Conf., Natl. Acad. Sci., Wash. D.C., pp.257–288.
6 Dash, J.G. (1992) Conf. on Quantum Fluids and Solids, Penn State U., June.
7 Walder, J. and Hallet, B. (1985) Geo. Soc. Am. Bull. 96, 336.
8 Hallet, B., Walder, J.S. and Stubbs, C.W. (1991) Perma. Perigla. Proc., 2, 283.
9 Gilpin, R.R. (1980) J. Colloid Surf. Sci. 77(2), 435.
10 Baker, M.B. and Dash, J.G. (1989) J. Cryst. Growth, 97, 770.
11 Dash, J.G. (1989) Contemp. Physics 30, 89.
12 Cahn, J.W., Dash, J.G. and Fu, Haiying (1992) J. Cryst. Growth, 123, 101.

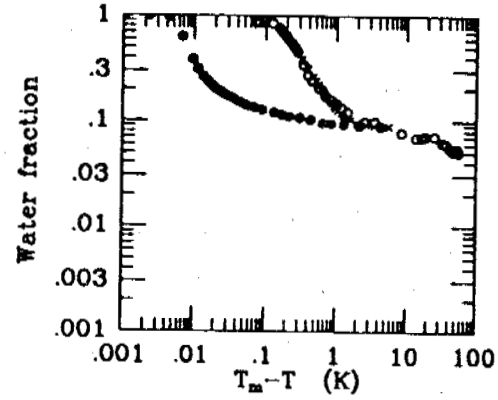

Figure 3. Water fraction in frozen mixture of water/Fairbanks silt: o: TDR; •: deduced from MP; -x-: deduced from MP with impurity correction[3].

A STUDY OF THE THERMAL STATE IN THE PERMAFROST AT THE SEJONG STATION, ANTARCTICA

Uk Han and H.C. Jung

Dept. of Env. Sci., Korea Military Academy, Seoul, Korea 139-799

Borehole temperature measurements at Sejong station were made by geothermal datalogger which was designed by the investigator. During December 31, 1991 - February 1, 1992 six temperature data (at the depth of 28cm, 8cm, -12cm, -32cm, -52cm, and -70cm) were obtained by resistive sensors of CR10 and SM716 every one minute. Fast Fourier Transformation was made on seven temperature data including surface air temperature of meteorological center at Sejong Base every thirty minutes. Profiles of surface and subsurface temperature variations represent freezing, thawing, and heat transfer mechanism at the boundary between active layer and permafrost table. The thermal diffusivities are determined by the Angstrom method, using underground temperatures. The thermal conductivities of the drilled cores and outcrops are measured by the transient method. The thermal diffusivity and conductivity measurements of rock and soil samples give a significant signal on the inferred climatic temperature of the past millenium at Sejong Base by the inversion technique with well-documented meteorological data. The geothermal data in ice-bearing permafrost at Sejong scientific station are interpreted in terms of the temperature history on a time scale of 2,000 years. Two theories are developed: a "forward" theory to calculate the response of ice-bearing permafrost to a surface temperature disturbance, and an "inverse" theory to calculate parameters characterizing the surface temperature history from suitable measurements in the permafrost.

INTRODUCTION

The construction of the King Sejong scientific station at King George Island, Antarctica, has provided an unprecedented opportunity for the study of the subsurface thermal regime in an area of thin, ice-bearing permafrost as shown in Figure 1.

Korean Antarctic Research station, King Sejong Base is located near the southern shore of Marian Cove which is one of the tributary basins of Maxwell Bay. Barton Peninsula is free of snow during austral summer and the exposed area is estimated to 15km^2. At the coast, raised beachs and moraines are developed 5 or 7 m above sea level. The raised beaches of Fildes Peninsula whose height is less than 20 m are known to be formed in Holocene. So all the raised beaches around King Sejong station are considered to be formed in Holocene(Yang and Jeon, 1990).

Han(1991) and Lachenbruch et al.(1982) analyzed the data to obtain the characteristics of the global warming during the last century and an estimate of the equilibrium heat flow. Harrison(1991) studied surface temperature change and its implications for the 40,000-year surface temperature history at Prudhoe Bay, Alaska.

The meteorological data are collected from December 31, 1991 to February 1, 1992 at King Sejong station. The near station level pressure was recorded as 989.8 mb during the period of observation. The annual mean air temperature was -2.0 ℃ and the mean wind speed was 8.0 m/s. Predominant wind direction was northerly and the mean relative humidity was 85 %. In 1991, a lowest temperature of -24.4 ℃ was measured at the 5th of August and the greatest gust of 46.6 m/s was observed on the 11th of September.

In King George Island, 95 % of land surface is covered by glaciers and snow all the year round. The thickness of the glaciers is estimated 100 m. They move slowly and creep over their own bed. In general, sea surface is frozen frequently in the cold season. The thickness of sea-ice reaches 25 - 30 cm.

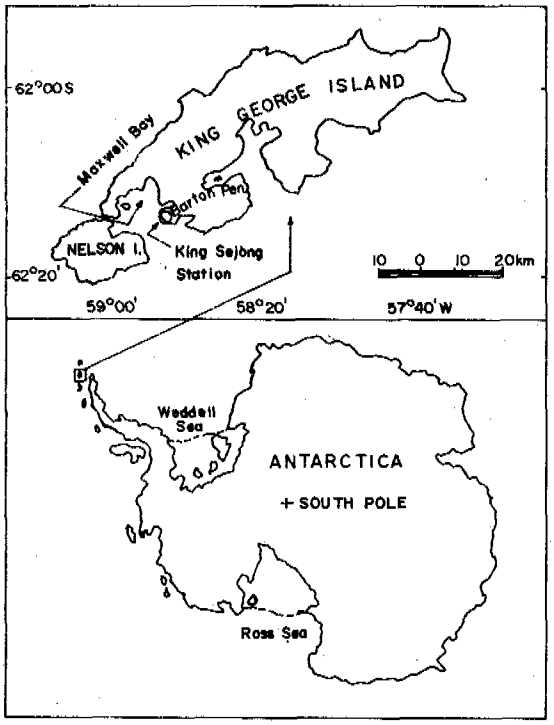

Figure 1. Location of the Korean Antarctic Research station at King Sejong Base.

Temperature measurements from one hole at Sejong station were made by geothermal datalogger which was designed by the investigator and Campbell Scientific Inc. Thermal properties from core samples were measured. Six temperature data at the depth of 28 cm, 8 cm, -12 cm, -32 cm, -52 cm, and -70 cm were obtained by resistive sensors of CR10 and SM716 during every one minute. The subsurface temperatures which were relatively free of the disturbance from drilling are shown in Figure 2.

The thermal diffusivities were determined by the Angstrom method using ground temperature data and laboratory measurements. The thermal diffusivity at the depth of 52 cm are calculated as shown in Figure 3. The thermal conductivities from drilled samples and outcrops were measured by the quick thermal conductivity method. The typical values of rocks are used to calculate the response of the permafrost to surface temperature disturbance.

Fast Fourier Transformation was made on seven temperature measurements including surface air temperature of meteorological center at Sejong station during every thirty minutes. Profiles of temperature variation represent freezing, thawing, and heat transfer at the boundary between the active layer and permafrost table.

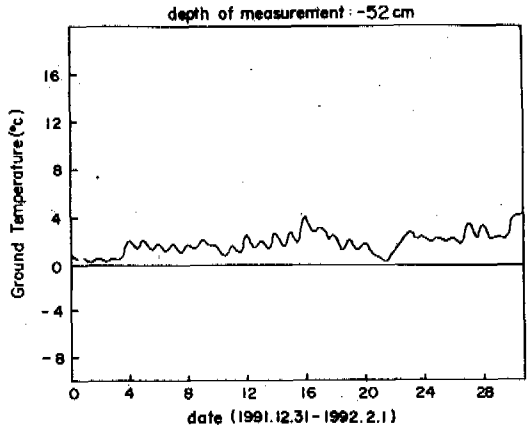

Figure 2. Subsurface temperature variations at depth with 52 cm.

The time constant controlling the response of the Sejong station permafrost thickness to a surface temperature change is of the order of 8,000 years. The results indicate the evidence of a complex climate history in King George Island, Antarctica. The tentative conclusion drawn from geomorphic and geothermal measurements can be reconciled.

This study is devoted to the development of a forward theory of the response of the permafrost to a surface temperature changes, and the development of an inverse theory for the estimation of thermal parameters characterizing climate history.

FORWARD PROBLEM

Since the permafrost at Sejong Base is close to being in equilibrium with the surface temperature, it is adequate to use a simple analytic approximation (Harrison, 1991).

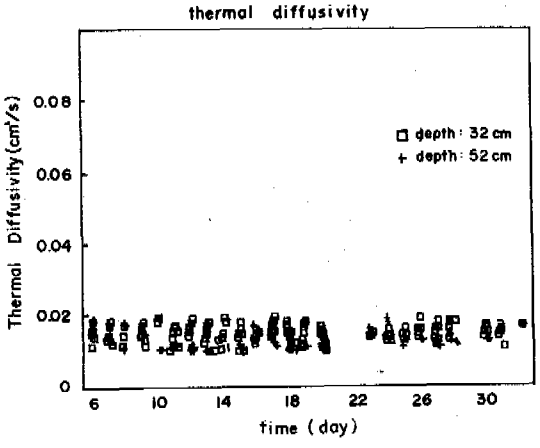

Figure 3. Thermal diffusivity by Angstrom method.

. We assume that the heat transport is purely conductive and that the thermal conductivity is constant except for a discontinuity at the base of the permafrost.

In forward theory, we find the response of the permafrost to a surface temperature T_0 of the form

$$T_0 = T_m(1+\theta_0 f_\theta(t)) \qquad (1)$$

where T_m is the mean surface temperature, θ_0 is a small nondimensional parameter characterizing the amplitude of the time-dependent surface disturbance, and $f_\theta(t)$ is the generalized periodic function

$$f_\theta(t) = \sum_{n=-\infty}^{\infty} c_n e^{in\omega t} \qquad (2)$$

where the C_n are Fourier coefficients, the n are integer, and ω is the angular frequency of the disturbance. If $\theta_0 = 0$, the equilibrium permafrost thickness L_m is determined by

$$k_2 \nabla T_m = -\frac{k_1 T_m}{L_m} \qquad (3)$$

where k_1, k_2 are the thermal conductivities of the permafrost and of the material beneath it, and $k_2 \nabla T_m$ is the equilibrium geothermal heat flow.

For a small θ_0, the permafrost thickness L and the temperature gradient ∇T immediately beneath the base of the permafrost behave as follows:

$$L = L_m(1+\theta_0 f_\eta(t)) \qquad (4)$$

$$\frac{\partial T(L^+)}{\partial z} = \nabla T = \nabla T_m(1+\theta_0 f_\mu(t)) \qquad (5)$$

where L_m, ∇T_m are mean values, and

$$f_\eta(t) = \sum_{n=-\infty}^{\infty} c_n \eta^n e^{in\omega t} \qquad (6)$$

$$f_\mu(t) = \sum_{n=-\infty}^{\infty} c_n \mu^n e^{in\omega t} \qquad (7)$$

η^n, μ^n are nondimensional parameters characterizing the thickness response and the temperature gradient response, respectively.

$$\eta^n = \left[\cosh\{\sqrt{n\omega t_2}(1+i)\} + \frac{\sqrt{n\omega t_2} + n\omega t_3 \frac{1+i}{2}}{\sqrt{n\omega t_1}} \sinh\{\sqrt{n\omega t_1}(1+i)\}\right]^{-1} \qquad (8)$$

$$\mu^n = \sqrt{n\omega t_2}(1+i)\eta^n \qquad (9)$$

where

$$t_1 = \frac{L_m^2}{2\alpha_1} \qquad (10)$$

$$t_2 = \frac{L_m^2}{2\alpha_2} \qquad (11)$$

$$t_3 = \frac{L_m^2 l}{k_1(-T_m)} \qquad (12)$$

α_1 and α_2 are the thermal diffusivities of the permafrost and of the material beneath it, and l is the latent heat per unit volume of the permafrost.

θ_0 is real, but η^n, μ^n are complex because the thickness response and the temperature gradient response are not in phase with the surface temperature disturbance.

We examine the response of the permafrost at Sejong Base to the simple harmonic surface temperature perturbation and calculate the dependence of the response on frequency. The numerical values used are summarized in Table 1. The results are in Figure 4. In the case of the Sejong Base, the characteristic frequency ω_c, at which the gradient response parameter goes through a broad resonance, has the value 5.46×10^{-4} yr^{-1}. For $\omega \ll \omega_c$, the permafrost remains almost in equilibrium with the changing surface temperature.

We also calculate the permafrost responses for the simple harmonic surface temperature distrubance with angular frequency $\omega = 7.85 \times 10^{-4}$ yr^{-1}(the 8,000 year period). The thickness and gradient amplitudes are 0.54 and 0.1, respectively. In addition, the thickness and gradient are phase shifted: they lag the surface temperature by 1,150 yrs and 150 yrs.

INVERSE PROBLEM

If we assume the disturbance function $f_\theta(t)$, then the inverse problem is to solve the equations (1), (3),

Table 1. Input

Parameter	Value	
k_1	1.0	W m^{-1}K^{-1}
k_2	2.0	W m^{-1}K^{-1}
α_1	52.0	m^{2}yr^{-1}
α_2	22.0	m^{2}yr^{-1}
l	1.2×10^8	Jm^{-3}
$T_0^{(p)}$	-2.0	K
$L^{(p)}$	30.0	m
$\nabla T^{(p)}$	30.0	Ckm^{-1}
t_1	8.7	years
t_2	20.5	years
t_3	1712.3	years

k_1, k_2 and α_1, α_2 represent thermal conductivities and thermal diffusivities of the permafrost and of the material beneath it. Volumetric latent heat l, surface temperature $T_0^{(p)}$, the permafrost thickness $L^{(p)}$ and the temperature gradient beneath the permafrost $\nabla T^{(p)}$ are listed. t_1, t_2 and t_3 are time constants controlling the response of the permafrost.

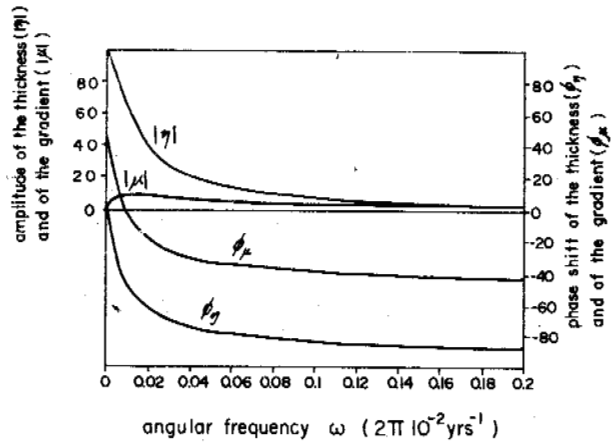

Figure 4. Frequency response of the permafrost thickness and of the temperature gradient beneath the permafrost for a simple harmonic surface temperature perturbation.

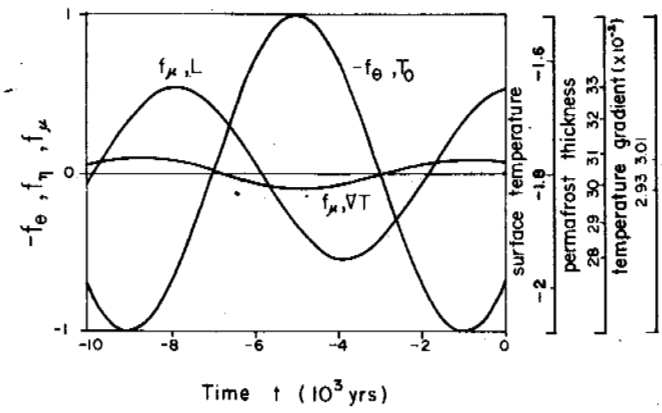

Figure 5. Profiles of the responses of the permafrost thickness and the temperature gradient for the simple harmonic temperature perturbation function with a period of 8,000 years.

(4), (5) for θ_0 and T_m, which are the parameters characterizing the surface temperature history, at t=0.

After some manipulations, one obtains

$$\theta_0 = \frac{\lambda - 1}{f_\theta^{(p)} - \lambda\left(f_\eta^{(p)} + f_\mu^{(p)}\right)} \qquad (12)$$

where λ is defined by

$$\lambda = -\frac{k_1}{k_2}\frac{T_0^{(p)}}{L^{(p)}\nabla T^{(p)}} \qquad (13)$$

λ is disequilibrium parameter. If the permafrost is in equilibrium, then $\lambda = 1$.

Since $\theta_0 \ll 1$, equation (13) is accurate only if $\lambda \simeq 1$.

When θ_0 has been determined, T_m, L_m, ∇T_m are found, therefore, we can determine the permafrost temperature history.

In the case of the Sejong Base, we could determine the temperature histories for the simple harmonic and the sawtooth disturbances. The results are in Figure 5 and Figure 6, respectively.

If

$$f_\theta^{(p)} = f_\eta^{(p)} + f_\mu^{(p)}, \qquad (14)$$

θ_0, and the surface temperature history, are indeterminate. But we have $f_\theta^{(p)} = 0.707$, $f_\eta^{(p)} = 0.533$, $f_\mu^{(p)} = 0.077$ for the simple harmonic disturbance and $f_\theta^{(p)} = -0.738$, $f_\eta^{(p)} = 0.313$, $f_\mu^{(p)} = 0.063$ for the sawtooth function.

The duration of the memory of the permafrost can be expressed in terms of t_3, the time required for the permafrost thickness to adjust to surface temperature disturbance. In the case of the Sejong Base, we emphasize the 2,000-year average temperature. The

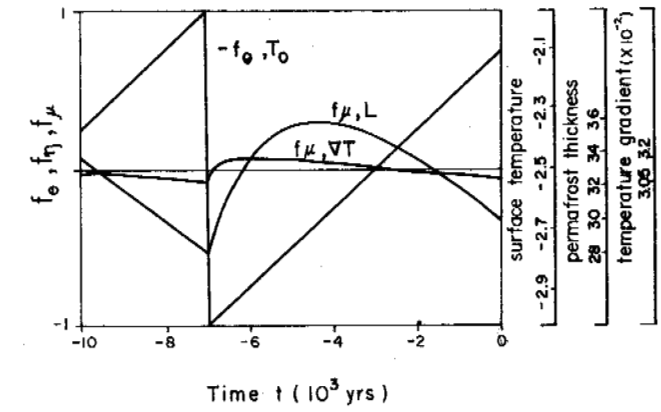

Figure 6. Profiles of the responses of the permafrost thickness and the temperature gradient for the sawtooth temperature perturbation function with a period of 8,000 years.

2,000-year average temperatures are -2.05 ℃, -2.13 ℃ for the simple harmonic and the sawtooth disturbance, respectively.

SUMMARY AND DISCUSSIONS

This study is to analyze the geothermal data and surface temperature at Sejong Base on a 8,000-year time scale. Two theories are developed, a forward problem for calculating the response characteristics of permafrost to surface temperature perturbation, and an inverse problem for estimating parameters

characterizing the surface temperature and thermal history from the permafrost.

The effects on the permafrost response of the three time constants t_1, t_2, and t_3 are calculated, and control the rate of permafrost response to the surface temperature perturbations. The time constant $t_1 \simeq 8$ years is a measure of the temperature within the permafrost to adjust to surface temperature change. The time constant $t_2 \simeq 20$ years is a measure of the time required for the temperature beneath the permafrost to adjust to the position change of the base of the permafrost. Two constants characterize the effects of the sensible heat within and beneath the permafrost. The time constant $t_3 \simeq 1{,}712$ years is a measure of the time required for the permafrost thickness to adjust to surface temperature perturbations. The third constant characterizes the effects of latent heat at the base of the permafrost.

Although there are three time constants (t_1, t_2, t_3), the duration of the memory of the permafrost can be represented in t_3, 1,712 years. The information that can be estimated depends on the form and the phase relative to the present time. Therefore it is important to consider the uncertainty. This uncertainty increases with increasing time into the past. The permafrost remembers best what has happened in the last 1,712 years. In our analyses it seems desirable to emphasize the surface temperature history over the last 2,000 years.

The sawtooth and the simple harmonic oscillation with a 8,000-year period are used to a reasonable approximation to these data. We determined the temperature history for the sawtooth. The memory by the permafrost is the subsurface temperature beneath the active layer. The comparison of the periodic sawtooth and the simple harmonic is an example of how the choice of f_s affects the results.

The present thermal regime at Sejong Base puts constraints on the subsurface temperature over the last 2,000 years. On this time scale there has been very small change and the subsurface temperature over the period was roughly the same. The 0.1 ℃ warming of the past century is calculated.

REFERENCES

Han, U. (1991) Global warming from borehole temperature evidence. J. Kor. Earth Sci. Soc. 12, 93-99.

Harrison, W. D. (1991) Permafrost response to surface temperature change and its implications for the 40,000-year surface temperature history at Prudhoe Bay, Alaska. J. Geophys. Res. 96, 683-695.

Lachenbruch, A.H., H.H. Sass, B.V. Marshall, and T.H. Moses, Jr. (1982) Permafrost, heat flow, and geothermal regime at Prudhoe Bay, Alaska. J. Geophys. Res. 87, 9301-9316.

Yang, J.S. and D.S. Jeon (1990) A study for environmental impacts assessment on natural environment in the new construction area around the Korean Antarctic station. Kor. J. Polar Res. 1, 25-34.

TWO–DIMENSIONAL STEFAN PROBLEM AROUND A COOLED BURIED CYLINDER

H. Haoulani A.M. Cames–pintaux and J. Aguirre–puente

Laboratoire d'aerothermique du C.N.R.S
4 ter, route des Gardes, 92190 –Meudon, France

A two–dimensional finite element numerical method using the enthalpy as thermal variable is used to treat the Stefan problem around a shallow cylinder placed at a finite depth in the ground.

Systematric calculations for a certain number of specific cases conduct to:

the knowledge of the thermal behaviour of shallow buried pipes; a particular study of sensitiveness of the thermal systems to the pricipal parameters as boundary conditions and geometrical and thermophysical characteristics; a proposed empirical model, based in rigorous calculations to predict the evolution of the freezing or thawing front.

The investigation on the heat transfer phenomena in soils with change of phase leads to either a simple method to easily predict the movement of the first line around a buried pipe or a rigorous numerical calculation.

INTRODUCTION

The "LABORATOIRE d'AEROTHERMIQUE DU C.N.R.S" has conducted studies on cooled buried cavities and pipes. This group has developed several numerical models to solve phase change problems allowing the determination of the thermal regime in freezing or thawing grounds.

Two relevant models have been used in many geotechnical problems. They make possible the determination, as function of time, of the progression of the interface seperating the frozen and unfrozen zones, and the thermal field within the domain.

In this paper, we focus our attention on shallow buried pipes.

Axi–symmetrical Model

An axi–symmetrical, one–dimensional model with phase change was developed by Cames–pintaux et al. This model, adapted to cylindrical coordinates, allows to locate the front by solving the Neuman equation on the interface accompanied by the equations of heat diffusion.

For the case of deep buried pipes, the position of the ground surface does not seem to have a significant influence upon the general evolution of the thermal process. Thus, the Stefan problem can be investigated in an axi–symmetrical domain.

In order to solve the problems encountered in the case of shallow buried cavities, the axi–symmetrical model presents some limitations. The use of a two–dimensional model then becomes necessary. The minimal depth at which the problem may be treated with the axi–symmetrical scheme needs to be defined.

Enthalpy Model

A finite element enthalpy method, developed by Cames–pintaux and Lamba, was used to solved the phase change heat transfer problem by considering either a discontinuous surface or a transition area, seperating the frozen and unfrozen zones.

This model has particularly contributed:

to the study of the thermal behaviour of the ground around cylindrical cavities for cryogenic storage,

to the determination of the domain where the axi–symmetrical model may be accurately used to describe or predict the thermal regime.

APPLICATION OF THE TWO–DIMENSIONAL MODEL

Theoretical Aspect

Enthalpy formulation are well adapted to the treatment of problems where the change of phase occurs.

Two mathematical changes of variable combined with the enthalpy formulation are used in finite element enthalpy method proposed by Cames–pintaux and Lamba. This two–dimensional approah was exploited to solve enthalpy equations for different geometry's of the domain under different boundary conditions and for different thermophysical characteristics of soil.

Geometry of the domain

A cylindrical cavity with a radius R_0 and at buried depth R', is considered. In every case presented in this paper, R_0 is equal to 0.1 m.

The symmetry condition reduces calculations to only a half of the system Figure 1. Γ_1 is the plane of symmetry, Γ_2 the cylindrical surface of the cavity and Γ_3 the surface of the ground and the other judiciously chosen limits of the domain. d is the width of the domain always chosen equal to $40 \times R_0$.

Boundary Conditions

The heat flux is null on $\Gamma_1 (\delta\Theta / \delta n = 0)$, the temperature in the cavity Γ_2 is $\Theta = \Theta_{ps}$ and the temperature at the surface and at the other boundary Γ_3 is $\Theta = \Theta_{surf}$.

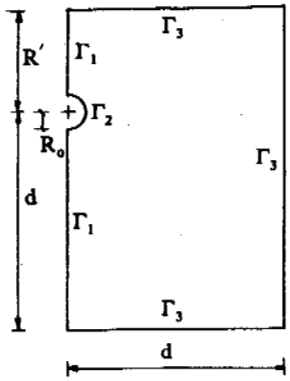

Fig. 1. Underground cavity scheme.

The following numerical values of temperatures have been chosen to be studied:

$$\Theta_{ps} = -9.6℃, -15℃, \text{or } -20℃ \text{ and } \Theta_{surf} = +6.2℃$$

These temperatures are suddenly imposed at t = 0.

It is assumed that the initial distribution of temperature Θ_0 within the system is linear (Figure 2).

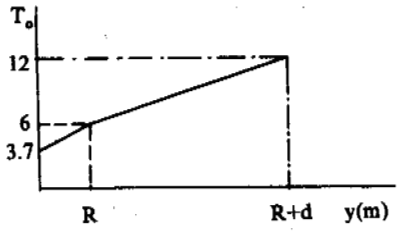

Fig. 2. Temperature distribution at t = 0.

Thermophysical Characteristics of the Ground

To study the effect of the thermophysical properties, particularly thermal diffusivity a and latent heat L, we have used geotechnical data employed in previous papers. The chosen thermophysical characteristics correspond to extreme values of those considered as probable in a group of soils presented by Sawada and Ohno. These values are given in table 1.

table 1

Domain	frozen clay		unfrozen clay	
	a_1	a_2	a_1	a_2
heat capacity $cx10^3$ $(J.Kg^{-1}.K^{-1})$	$c_s = 0.686$	$c_s = 0.978$	$c_l = 1.254$	$c_2 = 1.291$
k thermal conductivity $(W.m^{-1}.K^{-1})$	$k_s = 0.554$	$k_s = 3.400$	$k_l = 0.236$	$k_l = 2.000$

The variation of density corresponding to the transformation water / ice is neglected. Thus: $\mu_s = \mu_l = 2.01x10^3 kg.cm^{-3}$. Calculations have been made for four hypothetical soils defined by combining the two extreme values of diffusivity a and two extreme values of the latent heat L.

Table 2 shows the four soils characterised by the product axL.

Table 2

a * L $(J.m^{-1}.s^{-1})$	latent heat $L_1 = 0.595x10^8$ $(J.m^{-3})$	latent heat $L_2 = 1.973x10^8$ $(J.m^{-3})$
thermal diffusivity $a_1 = 0.401x10^{-6}$ $(m^2.s^{-1})$	23.86	79.12
thermal diffusivity $a_2 = 1.729x10^{-6}$ $(m^2.s^{-1})$	102.87	341.13

RESULTS

These geometrical and thermophysical characteristics were used to solve the Stefan problem by the finite element enthalpy method. For the four soils, the buried depth R' = 1.10 m and the temperature in the cavity $\Theta_{ps} = -15℃$ are considered . For the four soils, the evolution of the upper vertical and lower vertical frost lines are represented respectively on Figure 3 and Figure 4.

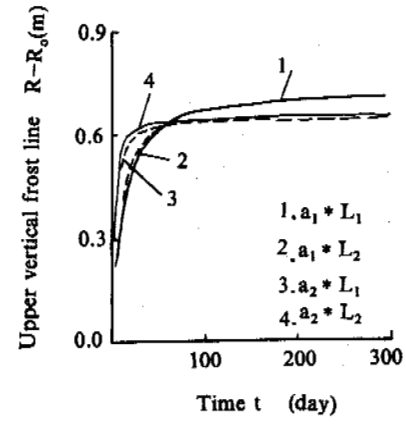

fig. 3. Frost front progression along the upper vertical plane of symetry.

In previous papers, we have studied the thermal behaviour around a cooled urban pipe but only with help of the axi–symmetrical one–dimensinal model.

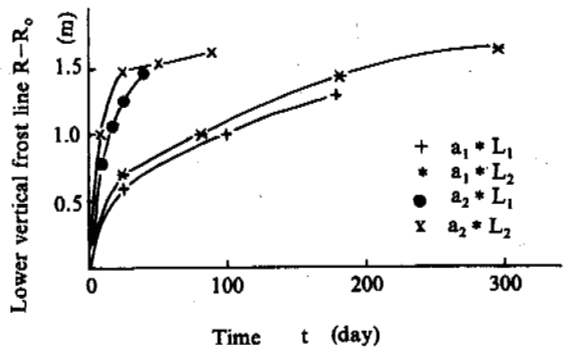

fig. 4. Frost front progression along the lower vertical plane of symetry.

To numerically study the Stefan problem around a buried pipe with an one–dimensional scheme, it is necessary to make a fictitious radious R*(Fig. 5). R*delimits the domain and the same boundary limits are utilized on $\Gamma_2$for the temperature $T_{p/s}$in the pipe and on $\Gamma_3$for the temperature T_{surf}at the surface of soil. The influence on R* and $\Theta_{p/s}$position were studied for the four soil (Fig. 6).

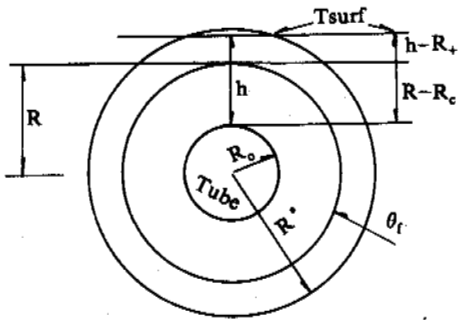

fig. 5 Axi–symmetrical buried pipe.

The two–dimensional and one–dimensional numerical simulations have shown the influence of the principal parameters on the thermal behaviour around the pipe during the freeze / thaw cycle.

1). Incidence of the pipe depth R′:

For a given temperature in the cavity $\Theta_{ps}$and for a given time t, it is noted that the upper vertical frozen zone thickness increases when the pipe depth R′ increases.

2). Variation of the temperature Θ_{ps}within the cavity:

For a given buried depth R′, it is interesting to remark that the upper vertical freezing front movement increases when the temperature Θ_{ps}in the cavity decreases. Nevertheless, a limit value is imposed by the boundary conditions at the qround surface.

3). Effects of the thermal properties a and L.

* Effect of thermal diffusivity a:

The establishment or absence of establishment of steady–state is directly conditioned by the diffusivity a. Thus,the permanent state is rapidly reached in media (a2,L1) and(a2,L2)presenting a high diffusivity.

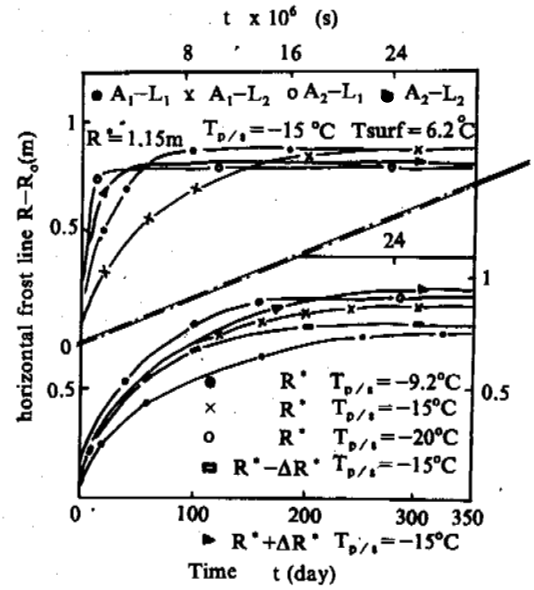

Fig. 6 Incidence of the "R*Θ_{ps}" couple on the frost line position upon vertical axis as a function of time.

* Influence of latent heat L:

The influence of latent heat L on the freezing front behaviour takes place only for transient portion of solution.

This influence is negligible for materials with a high thermal diffusivity, at every time t, but important for materials with a Iow thermal diffusivity a,during the transient portion of the problem.

PRACTICAL METHOD

The use of an elaborate two–dimensional model to solve the numerical problems for shallow buried pipe implies expensive calculations.It is interesting to have a simple model to quickly predict the interface behaviour during a time period T.

The interpretation of results leads to empirical expressions and graphs permitting a valuable synthesis of the results in the exploited domain.

The results are presented as dimensionless variables with regard to curve of frost line obtained for:

$(T)_r = 300$ days (referenced time),

$(\Theta)_r = -15$℃ (referenced temperature within the cavity),

$(R)_r = 1.10$ m (referenced cavity depth),

(a_1, L_1) (referenced soil).

Variation of Pipe Buried Depth R′

The referenced value $A_r$is chosen equal to 0.71 m.

For a given values of $\Theta_{ps}$and T_i, we can predict about the table 3 the upward freezing front location with the help of equation (1):

$$A(R)(\Theta_{ps},T_i)_r = -(R)(\Theta_{ps},T_i)_r A_r \qquad (1)$$

where α(R) can be calculated by a linear interpotation function:

$$\alpha(R)(\Theta_{ps},T_t)_r = (0.9286.R+0.0714) \qquad (2)$$

for $1.05\ m < R' < 1.25\ m$

Table 3. Movement of the upper vertical freezing front (A) as a function of the temperature in the cavity

R′ (m)	1.05	1.10	1.15	1.25
$R = R'/(R)r$	0.954	1.0	1.045	1.136
$A = (R'-Ro)_{up.vert.}$	0.67	0.71	0.73	0.79
$\alpha = A/Ar$	0.944	1.0	1.028	1.113

Variation of the Temperature Θ_{ps} within the Cavity

In the same way, about the values given in table 4 we can predict the frost front location, on the upper vertical plane, as function of dimensionless temperature Θ in the cavity:

$$A(\Theta)(R',T_t)_r = \beta(\Theta)(R',T_t)_r.A_r \qquad (3)$$

we chose for $\beta(\Theta)$ an interpotation function as a quadratic polynomial:

$$\beta(\Theta)(R',T_t)_r = (-0.3648\Theta^2+1.0613\Theta+0.3035) \qquad (4)$$

Table 4. Evolution of the upper vertical freezing front (A) as a function of the cavity depth.

Θ_{ps}(℃)	−9.2	−15	−20
$\Theta = \Theta_{ps}/(\Theta)r$	0.613	1.0	1.333
$A = (R'-Ro)_{up.vert}$	0.58	0.71	0.76
$\beta = A/Ar$	0.817	1.0	1.070

CONCLUSION

The investigation on the heat transfer phenomena in soils with change of phase leads to either a simple method to easily predict the movement of the frost line around a buried pipe or a rigorous numerical calculation.

REFERENCE

Cames–pintaux,A.M., Nguyen–lamba, M., Aguirre–puente, J., 1986. Numerical two dimensional study of thermal behaviour around a cylindrical cooled underground cavity. Domain of validity of axi–symmetrical scheme. Cold Reg. Scie. Technology. 12, 105–114.

Cames–pintaux, A.M., Aguirre–puente, J., 1988. Frost line behaviour around a cooled cavity. 5th International Conference on Permafrost.

Cames–pintaux, A.M., Giat, A.M., Aguirre–puente, J., 1983. Introduction de nouvelles geometries et conditions aux limites dans la methode de Goodrich pour le changement de phase. 16th Congres International du Froid. Tome 2. 595–602.

Cames–pintaux, A.M., Nguyen–lamba, M, 1986. Finite element enthalpy method for discrete phase change. Numerical Heat Transfer 9, 403–417.

Sawada, S., Ohno, T., 1985. Laboratory studies of thermal conductivity of clay, silt and sand in frozen and unfrozen states. 4th International Symp. on Ground Freezing. 2, 53–58.

NOTATION

A	upper vertical frost line position
a	thermal diffusivity
c(Θ)	specific heat
k(Θ)	thermal conductivity
L	latent heat per unit volume
R′	burial cavity axis
R	dimensionless form of R′
R_o	radius of the cavity
$R'-R_o$	burial depth
t	time
T_t	duration of the study
T_e	dimensionless form of T_t
T_o	initial temperature
Θ	dimensionless temperature in the cavity
Θ_f	freezing temperature
Θps	pipe/soil interface temperature
Θsurf	soil surface temperature
μ(Θ)	density
α, β, σ	different dimensionless form of A

Other subscripts

l	liquid
s	solid
r	reference

PERMAFROST MAPPING USING GRASS

Richard K. Haugen, Nancy H. Greeley and Charles M. Collins

U.S.Army Corps of Engineers, Cold Regions Research and Engineering Laboratory, 72 Lyme Road, Hanover, NH 03755–1290

Knowledge of the spatial occurrence of permafrost is critical for hydrologic and engineering purposes. The site for our study is the Caribou–Poker Creeks Research Watershed, a 37–square–mile area near Fairbanks, Alaska. The monitoring of air, surface and subsurface ground temperatures since 1986 in this discontinuous permafrost upland taiga environment has provided ground truth data for proximal permafrost and non–permafrost underlain terrain. In our initial analysis, we found a significant correlation ($r^2 = 0.68$) between observed mean annual surface temperature and calculated equivalent latitude for each of the seven drill hole sites. Equivalent latitude is a theoretical index of direct solar radiation incident on a surface, which serves as a measure of thermal energy received at that point. The use of a GIS to provide a spatial distribution for the equivalent latitude index was an obvious next step in mapping permafrost. Arc–Info DLG files of elevation, soil and vegetation developed previously were translated and imported into GRASS.An equivalent latitude map was developed in GRASS using the equivalent latitude algorithm and an algorithm derived from the observed variations of mean annual air temperature with elevation within the watershed. Further development of our permafrost mapping approach will include the location of all temperature recording sites with a global positioning system (GPS) for entry into the GIS and the refining of mapping algorithms to reflect differing surface energy balance regimes within the soil and vegetation mapping units.

MAP DEVELOPMENT AND GIS PROCESSES USED

The data used in this project was translated from an Arc–Info database of the Caribou–Poker Creek Research Watershed developed under the supervision of Leslie Morrisey for NASA. The data was translated into a GRASS4.0 geographic information system database on a SUN Sparcstation 330 system. The data resolution is 30 meters. The projection used is universal transvers mercator.

The translated elevation map was used as input to create slope and aspect maps using the GRASS r.slope.aspect command. There appeared to be a few places where slope and aspect data were aberrant. These are visible in our final maps as small horizontal linear patterns. An attempt was made to smooth the linear data by using GRASS's smoothing filters, however we felt that the results were not worth the loss of data that occurred throughout the rest of the map after the filtering process.

To create the equivalent latitude map we input the following equation into GRASS's r.mapcalc command:

equivalent latitude = $\sin^{-1}$(sin(slope) * cos(aspect) * cos(actual latitude)+cos(slope) * sin(actual latitude).

GRASS's r.mapcalc command didn't have a sin function, so the derivative equation was used:

```
equivlat = atan((sin(@slope.rec) * cos(@aspect.values) *
cos(65.18288))+cos(@slope.rec) * sin(65.18288)) /
(sqrt(1–exp((sin(@slope.rec * cos(@aspect.values) *
cos(65.18288))+cos(@slope.rec) * sin(65.18288)),2)))
```

The r.mapcalc command processed this formula for each 30 meter data cell of our study area and output a map of the results for each data cell, an equivalent latitude map. The "@"–sign is required in GRASS to enable the use of the category value instead of the category number in each of the map layers used.

To create the mean annual surface temperature (MAST) map, a regression equation was developed using elevation, equivalent latitude and temperature data from data sites in the study area. R.mapcalc was run using this equation:

mast_actual = 21.704–0.003 * elevation–0.29 * equivlat.

Temperatures of inversion zones were then added to the MAST map using the GRASS command r.infer to extract the inversion zones from elevation and slope maps. Pocket inversion zones at elevations from 250–599 meters were assigned a MAST of –2.0°C and other inversion zones from 195–249 meters were assigned a MAST of –4.0°C.

Decision–making rules were developed that would define areas with underlying permafrost. We then used these rules in a script file with GRASS's r.infer command to create the permafrost map layer. The following is the inference rules table script file used to create a map predicting permafrost according to the predicted MAST map, elevation, slope and equivalent latitude:

```
IFMAP mast_plus104–10
    THENMAPHYP9(mast permafrost zone)
IFMAP elevation 195–249
    THENMAPHYP 10–4.6(inversion zone)
IFMAP elevation 250–599
    ANDIFMAP slope.rec0–5
    THENMAPHYP 11(pocket inversion zone)
IFMAP equivlat 67–90
    THENMAPHYP 12 (permafrost).
```

GRASS evaluates each data cell of the map layers named in this table (MAST, elevation, slope and equivalent latitude) and creates a new map layer in which the cell is placed into a category

according to the "rules" of the table. In this case cells which fall into the following categories would be put into the permafrost category in the new map layer: MAST categories from −6°C to 0°C, elevation categories from 195–249 meters, elevation categories above 67°north latitude. (Notice that the category numbers into which these cells were placed were originally 9 through 10. These were later reclassified into category 2 while every other data cell in the new map was reclassified into category 1).

The predicted MAST and predicted permafrost maps shown in this study have areas of solid black coloration which are not defined in the legends. These are actually areas in which the patterns are so dense that the area outlines or patterns create the black effect.

FUTURE RESEARCH

Although the Caribou–Poker Research Watershed has been extensively studied by many researchers since it was first designated as a research area in the early 1970's, this study is the first systematic, longterm attempt to measure ground temperatures within the watershed with the objective of defining permafrost distribution relationships. The sites selected for ground temperature monitoring in Caribou–Poker Creeks Research Watershed were selected to sample a wide diversity of atmospheric, vegetative, and geologic characteristics, all of which influence ground temperature patterns and therefore the distribution of permafrost. The ground temperature information from this study combined with detailed information on site characteristics will permit the analysis of the complex distribution of permafrost in the watershed. The equipment needed to continually record air temperatures and near–surface ground temperatures at each of the borehole sites is expensive, and only recently have we been able to begin acquiring and installing this instrumentation. Three four channel data loggers were installed at three sites(T–1, K–25, and K–20A) in 1990. They are recording air temperature, temperature at two levels in the organic layer, and at the organic / mineral soil interface. In August 1991 a 12 channel logger with senors ranging from +150 cm above the mineral / organic soil interface to −140 cm below this surface, was installed at a valley bottom site near T–1A. These instruments, together with additional sensors designed to measure other components of the surface energy flux which will be installed as funding permits, will provide a more comprehensive analysis of permafrost distribution within the watershed.

Future plans also include a deep (100 to 200 m) bore hole in the valley bottom of Poker Creek is planned for the future. The intent is to penetrate the bottom of the permafrost in this area. The

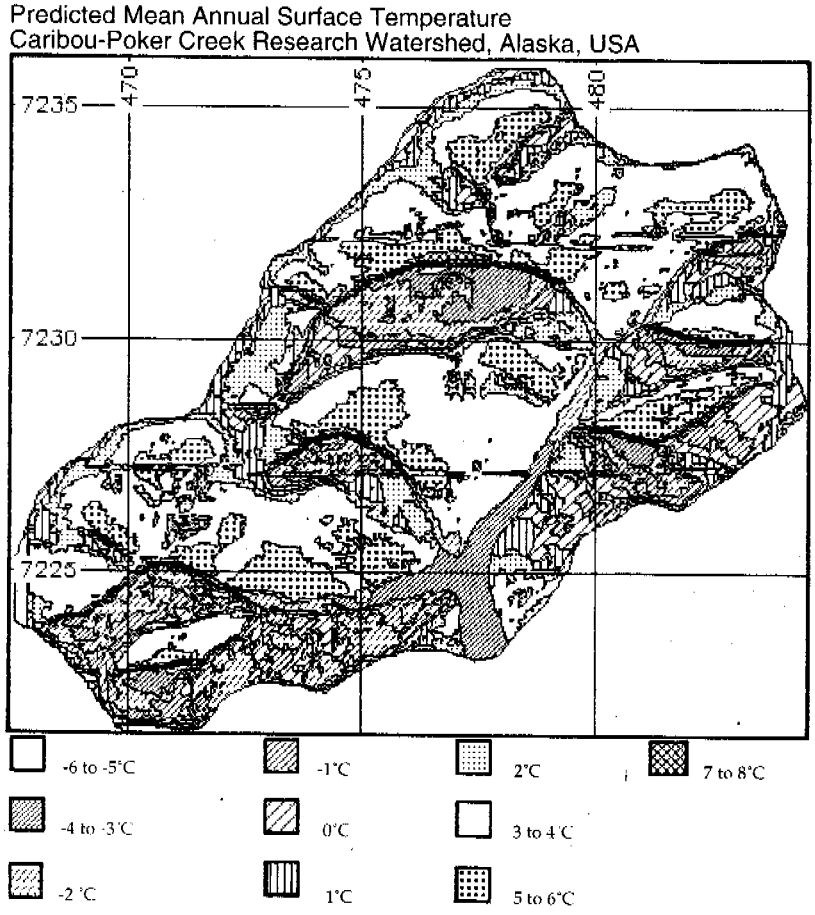

borehole will be equipped with a multi-channel datalogger to continually record ground temperatures and complete surface energy budget instrumentation..

The spatial delineation of permafrost / non-permafrost boundaries will require a complex model which includes the terrain, vegetation, and energy balance components projected to a fine-mesh grid over the watershed. We plan to do this utilizing Geographic Infromation System (GIS) technology. The initial attempts will be done utilizing the more detailed air and surface temperature information obtained beginning in 1990, together with the subsurface temperature data which have been acquired beginning in 1986.

REFERENCES

Bilello, M A(1974) Air masses, fronts and winter precipitation in central alaska. U.S. Army Cold Regions Research and Engineering Laboratory, Research Report 319.

Brown, R.J.E. and T.L.Pewe (1973). Distribution of permafrost in North America and its relation to the environment; a review. Proceedings, Second International Conference on Permafrost,pp.71-100.

Collins,C.M., R.K.Haugen,and R.A.Kreig (1988) Natural ground temperatures in upland bedrock terrain, Interior Alaska. Proceedings, Fifth International Conference on Permafrost, Trondheim, Norway, p56-60.

Dingman, s.L. and Koutz F.R. (1974) Relations among vegetation, permafrost, and potential insolation in Central Alaska. Arctic and Alpine Research.(6),1,37-42.

Haugen, R.K. and J.Brown (1978) Climate and dendroclimatic indices in the discontinuous permafrost zone of the central Alaskan uplands. Proceedings Second International Conference on Permafrost, pp 392-398.

Haugen, R.K., C.W. Slaughter, K.E.Howe, and S.L.Dingman (1982) Hydrology and climatology of the Caribou-Poker Creeks Research Watershed, Alaska, CRREL Report 82-26.

Haugen, R.K., S.I.Outcalt and J.C. Harle, (1983) Relationships between estimated mean annual air and permafrost temperatures in north-central Alaska.Proceedings, Fourth International Conference on Permafrost,pp.462-467.

Jorgenson, M.T., C.W.Slaughter, and L.A. Viereck (1984) Reconnaissance survey of vegetation and terrain relationships in the Poker-Caribou Creeks Watershed, Central Alaska. Unpublished report and map. Institute of Northern Forestry, U.S.Forest Service, Fairbanks, Alaska, 99701. On file at INF.

Koutz, F.R. and C.W. Slaughter (1972) Geologic setting of the Caribou-Poker Creeks Research Watershed, Interior Alaska. Unpublished memo, CRREL.

Morrissey,L.A., L.L.Strong and D.H.Card (1986) Mapping Permafrost in the Boreal forest with Thematic Mapper satellite data. Photogrammetric Engineering and Remote Sensing. V.52, p.1513-1520.

Rieger, S., C.E. Furbush, D.B. Schoephorster, H.Summerfield, and L.C. Gieger (1972) Soils of the Caribou-Poker Creeks Research Watershed, Alaska.CRREL Technical Report 236.

Viereck, L.A., C.T.Dyrness, and A.R. Batten (1982), the 1982

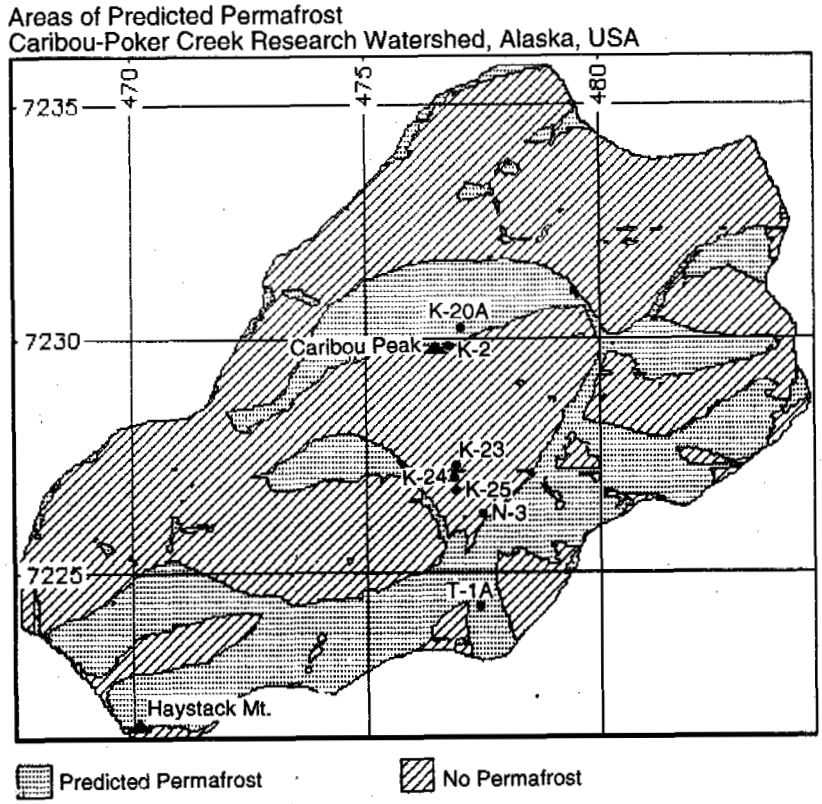

Revision of Preliminary Classification for Vegetation of Alaska. Unpublished report. Institute of Northern Forestry, U.S. Forest Service, Fairbanks, Alaska. 72 pp. On file at INF.

Viereck, L.A., C.T. Dyrness, and A.R. Batten (1986) The 1986 Revision of Alaska Vegetation Classification. Unpublished report. Institute of Northern Forestry, U.S. Forest Service, Fairbanks, Alaska.141 pp. On file at INF.

Vogel, T.C. and C.W. Slaughter (1972) A preliminary vegetation map of Caribou–Poker Creeks Research Watershed, interior Alaska. CREEL Technical Note(unpublished).

Wahrhaftig, c.(1965) Physiographic Divisions of Alaska. U.S. Geological Survey Professional Paper 482.

CIRCUMARCTIC MAP OF PERMAFROST AND GROUND ICE CONDITIONS

J.A. Heginbottom[1], J. Brown[2], E.S. Melnikov[3], and O.J. Ferrians Jr.[4],
[1]Geological Survey of Canada, Ottawa, Canada,
[2]Chairman, IPA Editorial Committee, Arlington, VA.
[3]Institute for Hydrogeology and Engineering Geology (VSEGINGEO), Moscow,
[4]U.S. Geological Survey, Anchorage, AK,

The International Permafrost Association undertook to compile and publish this circumarctic permafrost map, in response to a recognized need for a single, unified international map to depict the distribution and properties of permafrost in the Northern Hemisphere at a scale that would be useful to both permafrost and non-permafrost specialists concerned with global climatic change, resource development in polar regions, and protection of the environment. The map shows the estimated permafrost extent by percent area (90-100%, 50-90%, 10-50%, <10%, and no permafrost present); an estimate of relative abundance of ice in the upper 20 metres as percent volume (>20%, 10-20%, <10%, and 0% or nil); relative abundance of ice wedges, massive ice bodies and pingos; ranges of permafrost temperatures (C) and thicknesses (metres), and the location of subsea and relict permafrost, and cryopegs or unfrozen layers. The map is accompanied by eight cross sections of the permafrost region, illustrating the thickness and nature of permafrost. An accompanying report discusses the regional variations in permafrost attributes and the confidence levels at which they are presented..

INTRODUCTION

In 1990, the International Permafrost Association (IPA) recognized the need for a single, unified international map to depict the distribution and properties of permafrost in the Northern Hemisphere at a scale that would be useful to both permafrost and non-permafrost specialists concerned with global climatic change, resource development and protection of the environment, such as the Intergovernmental Panel on Climate Change, and the United Nations Environment Program. To address this concern, the IPA, at its Council meeting of June 1990 in Quebec City, Canada, approved the compilation and publication of a circumarctic permafrost map. It was agreed to produce the map for the Sixth International Conference on Permafrost, and also that other national and international scientific and engineering organizations would be notified of the project and their cooperation and participation invited. The project, which was coordinated by the IPA Editorial Committee, consisted of five major steps: (1) legend development, (2) initial compilation for North America and Russia by the authors, (3) additional input by national experts for China, other Asian countries and the Nordic and European countries, (4) review and revision, and (5) final cartographic preparation and printing. The United States Geological Survey agreed to support the development of the map by providing cartographic, printing and publishing services, as part of the Circum-Pacific Geological Map project.

The map presents the most significant permafrost or geocryological conditions, namely areal distribution, thickness, temperature, and ground ice characteristics. Deep-lying (relict) and subsea permafrost are also represented.

HISTORY AND CLASSES OF PERMAFROST MAPS

This brief review of permafrost mapping is based on the paper by Heginbottom (1984). According to Nikiforoff (1928) and Baranov (1959), the earliest known map depicting permafrost was prepared by G. Vil'd of Siberia; it was published in 1882 and shows the southern boundary of the "everfrozen region". The earliest map known for North America is credited to Andre in 1913 by Baranov (1959), but unfortunately the reference is not cited and the original work has not been identified. Since these early efforts, over 150 different maps of permafrost and related phenomena have been compiled aw published. Heginbottom (1984) grouped these maps into four categories:

1) Miniature maps of the world, the northern polar regions, or the northern hemisphere continents showing the distribution of permafrost as known at the time of their compilation. These maps range in scale from about 1:30,000,000 to about 1:50,000,000. Examples include maps by Black (1954) and Péwé (1983).

2) National maps showing the distribution of permafrost for the politically defined areas. Scale and level of detail vary widely according to the size of the area covered. These maps can be grouped according to size as single page maps, typically at scales of between 1:50,000,000 and 1:10,000,000, and atlas or wall maps on larger sheets, at scales of between 1:10,000,000 and 1:2,500,000. Examples of the first subclass are Rapp and Annersten's map (1969) of discontinuous permafrost in Sweden; and Ershov's compilations (1988, 1989) for the former Soviet Union. Examples of maps in the latter subclass include Brown's map (1978) of Canada, the map of China by Shi and Mi (1988), Ferrians' map (1965) of Alaska, the maps of the USSR and North America by Popov et al. (1985, 1990), and a new map of permafrost and ground ice in Canada (Heginbottom and Dubreuil, in prep.).

3) Regional and local maps of permafrost or ground ice conditions or related features, which are available for many areas and at a variety of scales. Examples of these maps include Melnikov's map (1966) of Yakutia, Péwé's map (1982) of the Fairbanks area of Alaska, maps of West Siberia by Baulin (1982), and of the Qinghai-Xizang Highway by Tong et al. (1982), and Heginbottom and Radburn's map (1992) of north-western Canada.

4) Maps of various areas showing the former extent of permafrost or the distribution of features indicative of the former occurrence of permafrost conditions such as Kaiser's map of western and central Europe published in Washburn (1990).

Maps can also be grouped by their contents or legend, the most common showing the extent and distribution of 'climatic permafrost', as defined by climatic conditions and usually divided into the

continuous and discontinuous zones (e.g. Brown, 1973). Some maps in this group show areas of alpine or mountain permafrost (e.g. Brown, 1967; Gorbunov, 1978) and subsea permafrost (Mackay, 1972; Péwé, 1983). A second set of maps show specific attributes such as thickness and temperature of permafrost (Judge, 1973; Ershov, 1989) and the distribution of geomorphic features indicative of the occurrence of ground ice, of frozen ground, or of the former extent of frozen ground (Popov et al., 1966), including pingos (Hughes, 1969), ice-wedge polygons or ice wedges (Shumskiy and Vtyurin, 1966), and ice-wedge casts (Williams, 1969). A third group of maps relates permafrost conditions to environ-mental conditions including temperature (Crawford and Johnston, 1971), extent of glaciation (Hughes, 1973), and geology, hydrology or vegetation (e.g. Ferrians, 1965; Fotiev, 1978; Bliss, 1979). Complex maps contain environmental, permafrost and ground ice information. Such maps have more often been prepared in the former Soviet Union (e.g. Baranov, 1956, 1965, 1982; Kudryavtsev et al., 1978; Melnikov, 1966; Fotiev et al., 1978; Vtyurin, 1978; and Ershov, 1989).

PRINCIPLES AND METHODS OF COMPILATION

A major problem in the compilation of maps of complex natural phenomena over very large areas is the variation in the level and accuracy of the available data and information. The principles and methods used in compiling this circumarctic map recognize and accommodate this difficulty. The variations encountered relate both to disparities in the level of field observations, and to variations in environmental and geological factors which control the distribution and attributes of the permafrost and ground ice.

The mapping strategy originally proposed was to delineate landscape units, employing a common physiographic classification of the Northern Hemisphere, and to assign legend attributes in each identifiable unit. This approach was not feasible, however, since no physiographic map of the northern regions of the earth, at the desired scale and level of detail, was readily available and it was beyond the scope of this project to prepare one. It was decided therefore to use existing physiographic or landscape maps in each of the three major national permafrost regions (Russia, Alaska, and Canada). In preparing this map no attempt was made to conduct new field studies and every attempt has been made to use all readily available published and unpublished information.

Map units in Alaska are based on the 1965 map "Physiographic Divisions of Alaska" (Wahrhaftig 1965) and contain information being used to revise the 1:2,500,000 map of Alaska (Ferrians 1965). The Canadian contribution utilizes the 1967 map "Physiographic Regions of Canada" (Bostock, 1970) as a base map and contains much of the information presented on the new permafrost and ground ice map prepared for the 5th edition of the National Atlas of Canada, (Heginbottom and Dubreuil, 1993, in prep.). Russian map units are derived from the geosystems or landscape approach described by Melnikov (1988), in which natural geosystems are delineated according to common relief, vegetation, soil and soil-forming materials and climate. Units for China and Mongolia are based on recompilations of the maps by Shi and Mi (1988) and from Sodnom and Yanshin (1990), respectively. Existing information for the Nordic countries, Greenland, and other mountainous regions of Europe and Asia were modified and compiled from numerous published and unpublished sources, with the assistance of regional specialists, as listed in Table 1.

A preliminary legend was agreed to by the principal authors in Anchorage, Alaska, in September 1991 and revised by the same authors in Ottawa, Canada, in April 1992. The map scale of 1:10,000,000 was selected so that all regions of permafrost occurrence in the Northern Hemisphere could appear on a single, map sheet. The map extends southward to 20°N latitude and includes mountain or high altitude permafrost conditions in Tibet, Scandinavia and central Europe, the Cordillera of North America and mountainous regions of southwestern, central and eastern Asia. A Lambert Polar Azimuthal Equal Area map projection, centred on the north pole, was selected for the map, so that regions of similar latitude would have comparable areas. This feature of the projection was considered important for global change considerations related to potential changes in areal extent of permafrost and ground ice distribution and volumes. A base map was computer generated by the U.S. Geological Survey, Reston, Virginia, USA, using existing World Data Bank II data bases for coastlines, drainage, the latitude and longitude grid, and international boundaries. Glaciers and ice caps for North America, including Greenland, are based on digitized files from Canadian sources. Bathymetry was handscribed after Perry and Fleming (1986).

Although not currently available in digitized form, it is hoped to have the map attributes available in a digital form in the near future. The Canadian contribution was prepared from computerised data bases (Heginbottom and Dubreuil, 1993).

MAP DESIGN AND THEMATIC CONTENT

The map is a comprehensive summary of permafrost and ground ice conditions in the northern circumpolar region. The basic map units are described in terms of the extent of permafrost, the quantity of ground ice, and the relative abundance of larger bodies of ground ice: pingos, ice wedges and bodies of massive ice. Note that no distinction is made between massive ice of intrasedimental origin (Mackay and Dallimore, 1992) and massive ice resulting from the burial of ice formed at the ground surface, such as buried glacier or river ice. Information on permafrost thickness and ground temperatures is given for selected localities across the region.

Permafrost Extent

The general distribution of permafrost and ground ice is divided first into two broad classes, based on regional elevation, physiography and surface geology. Group 1 comprises areas of lowlands, highlands and intra- and inter-montane depressions characterized by thick overburden, wherein ground ice is expected to be generally fairly extensive. The second group covers areas of mountains, highlands, and plateaus characterized by thin overburden and exposed bedrock, where generally lesser amounts of ground ice are expected to occur. For the purposes of this map compilation, thick overburden is defined as being greater than 5 to 10m.

The estimated extent of permafrost in each map unit is presented in four classes, based on the percentage of the ground that is underlain by permafrost (continuous, 90-100%; discontinuous, 50-90%; sporadic, 10-50%; and isolated patches of permafrost, 0-10%). Areas generally free of permafrost are also indicated. For areas of physiographic class 1, the colour scheme uses tones of purple for continuous permafrost, blue for discontinuous permafrost, green for sporadic permafrost and yellow for areas where permafrost occurs in isolated patches. For areas of physiographic class 2, the colour scheme uses tones of brown for continuous permafrost, orange for discontinuous permafrost, gold for sporadic permafrost and yellow for areas where permafrost occurs in isolated patches.

Areas of subsea and relict permafrost, based on both direct and extrapolated measurements, are shown by stippling. The 100 and 200m submarine contours are shown to indicate possible occurrence of subsea permafrost on the continental shelves of the Arctic Basin. For Russia, map units known to contain cryopegs (layers of unfrozen ground with high salt content), are mapped beneath land areas.

Ground Ice

The relative abundance of ground ice in each map unit is presented in the form of qualitative estimates of the percentage of ice in the upper 10 to 20m of the ground. These estimates include

Table 1: Regional Contributors to the Project

Region	Contributors
Russia, Mongolia	G.F. Gravis, L.A. Konchenko, and L.N. Kritzuk, Committee of Geology; and K.A. Kondrat'eva and S.F. Khrusky, Faculty of Geology, Moscow State University, Russia.
Greenland, North Atlantic Islands, Fenno-Scandia	H.J. Åkerman, University of Lund, Sweden, and Matti Seppälä, University of Helsinki, Finland.
Central Europe	W. Haeberli, Swiss Federal Institute of Technology, Zurich, Switzerland, and L. King, Justus-Liebig University, Giessen, Germany
Southern Europe	F. Dramis, University of Camerino, and C. Smiraglia, University of Milano, Italy.
Rumania	A. Kotarba, Polish Academy of Sciences, Krakow, Poland.
Mountains of Central and Southwestern Asia	A.P. Gorbunov, Alma-Alta, Kazakhstan.
China	Guo Dongxin and Qiu Guoqing, Lanzhou Institute of Glaciology and Geocryology, Lanzhou, China.

the volume of segregation ice, injection ice and reticulate ice. Three classes are used for ground ice content (high, >20%; medium, 10-20%; and low, <10%) in areas in physiographic class 1, that is for areas of generally thick overburden. For areas of generally thin overburden (physiographic class 2), only two classes of ground ice are mapped, medium to high (>10%) and low (<10%), due in part to paucity of data.

Gradations in the map colours reflect these distributions, with shades of each colour denoting map units with more ground ice and tints indicating map units with less ground ice.

The distribution and relative frequency of known occurrences of large identifiable underground ice bodies are treated separately and shown by symbols. Ice bodies included in this manner comprise the ice cores of perennial frost mounds, especially pingos; ice wedges; and bodies of massive ice, generally tabular in shape. A simple, three step scale of "abundant, sparse, and absent' is used. Surface ice features, including ice caps, glaciers and very large icings, are shown by patterns and symbols.

Ground Temperature and Permafrost Thickness

Values and ranges of mean annual ground temperatures (Celsius) and permafrost thicknesses (metres) are shown for selected localities across the mapped area. These are based either on measured values or extrapolated observations. The placement of the values in the map unit generally corresponds to the geographic location of the measurements.

Landscape Classification

For Russia, six principle morphogenetic landscape groups are identified: lowland plains, high plains, intra- and inter-montane depressions, plateaus or flat highlands, ridges, and mountains. Overall, for the Russian portion of the map, 19 morphogenetic types of landscapes are identified including, 15 within the first three groups, where accumulative sediments of different origins are well developed. No landscape units are shown within the categories of plateaus and mountains. Erosional or denudational landscape categories have four types.

Major lithological classes present in the upper 10 to 20m of the ground are divided into unlithified and lithified material; the former including peat, clay and silt, sand, and coarse clastic deposits or debris and the latter comprising soluble rocks (eg: limestone or dolomite), insoluble rocks and undifferentiated rocks.

Transects of the Permafrost Region

Eight north-south oriented transects of the permafrost region are shown as insets to the map. The transects illustrate the major characteristics of the permafrost body and its ground ice conditions on a hemispheric basis, and in an idealized but representative manner.

Alaska: The 1280-km long trans-Alaska pipeline route provides extremely useful data from a series of shallow borehole extending from Prudhoe Bay in the north to Valdez at the southern terminus of the pipeline. Additional data from deeper holes has been used, where it is available – mainly in the vicinity of Prudhoe Bay.

Mackenzie Valley: The various Mackenzie Valley pipeline and highway routes, both proposed and constructed, have provided a vast data base for mapping permafrost. These data have been used in compiling this transect. Deeper boreholes, in the Beaufort Sea and Mackenzie Delta areas were also relied on.

Central Canada and Arctic Islands: In the Arctic Islands, the transect is based on data from numerous boreholes drilled for hydrocarbon exploration. On the northern mainland, it is based on data from the few mineral exploration boreholes which have been drilled, along with a limited number of shallow geotechnical borings.

Eastern Canada: This transect is based on limited data from borcholes drilled at a few sites for mineral exploration and production purposes.

European Russia: The transect has been compiled from data from a number of mineral exploration holes.

West Siberia: Many borcholes have been drilled for purposes of hydrocarbon exploration throughout West Siberia. This transect is based on data from these borings, supplemented with data from deep geophysical soundings.

East Siberia: The transect is based on data from boreholes drilled for hydrocarbon exploration, mineral exploration (especially for diamonds) and geological structural research on the Siberian Platform.

Qinghai-Xizang (Tibet) Plateau: This transect is based on research carried out along the line of the highway from Golmud, Qinghai Province, to Lhasa, Xizang Province.

Boundaries, Legend and Sources

Boundaries of permafrost and ground ice map units are shown by a solid line where they are well defined and follow a physiographic unit boundary. Where unit boundaries are gradational or are estimated, a dashed line is used. The approximate position of the northern limit of trees (compiled from several National Geographic Society maps) is shown, since this major change in vegetation has

important implications for ground temperatures and other ecological parameters.

The explanation of the conventions of the map, the colour scheme and the symbols is given in the map legend. A subsidiary legend provides information on the landscape units used for the Russian sector of the map. The principle sources relied on in the compilation of the map are listed.

REGIONAL DISTRIBUTION OF PERMAFROST AND GROUND ICE CONDITIONS

For the first time, a permafrost map of the entire circumarctic region has been compiled using a common legend, so that permafrost and ground ice conditions can be accurately evaluated, thus enabling regional and global comparisons to be made. The distribution and characteristics of permafrost and ground ice are briefly described in the accompanying report, according to major regions of the Northern Hemisphere (Table 2).

The map illustrates how the regional distribution of permafrost and the nature and extent of ground ice within the permafrost region of the northern hemisphere vary not only with latitude and altitude, but also in response to differences in climate, topography, bedrock geology and surficial geology. Quaternary history, with alternating episodes of glaciation and deglaciation, and phases of marine and lacustrine submergence and emergence of the land, also had profound effect on the nature and distribution of both permafrost and ground ice.

Table 2. Regions Used for Descriptions of Permafrost and Ground Ice Conditions

North America
Canada (7 regions)
USA – Alaska (3 regions)
Conterminous USA
Mexico
Sub-Sea Permafrost
North Atlantic
Greenland
Iceland
Svalbard
Fenno-Scandia
Asia
Russia (8 regions)
Mongolia
Korea and Japan
Central Asia
Southwest Asia
Central and Alpine Euorpe

CONCLUSIONS

In preparing this new map, conclusions were drawn about our current knowledge on the distribution of permafrost and ground ice in the Northern Hemisphere and some future information needs. The present map differs from earlier maps of permafrost, first, because it provides information for the whole of the northern circum-polar region and, therefore, for effectively all of the northern hemisphere permafrost region. Secondarily, the map shows for the first time, information on the distribution and nature of ground ice in a systematic manner. All this information is presented in relation to landscape or physiographic units, which should facilitate its use in other, global, hemispheric or regional studies of the interaction between the lithosphere, the cryosphere and other environmental parameters.

As has long been known, there is considerable variability in the quantity, distribution and reliability of basic data on permafrost and ground ice. Compilation of the map has made this particularly apparent to the authors. While these variations reflect real differences in geocryological conditions, they are mainly the result of the different amount of research undertaken in different regions, differences in accessibility, natural exposures, resource development activity, and different national philosophies in the conduct of national surveys of natural phenomena.

Plans to make the map and data available in digital form are being developed.

ACKNOWLEDGEMENTS

Many individuals and organizations have contributed personnel and other resources to the compilation of this map. Several individuals deserve special recognition for their thoughtful involvement early in the project, including, in particular, Ray Kreig and Yuri Shur, Kreig Associates, Anchorage, Alaska; Vladimir Solomatin, Moscow State University; Stanislav Grechishchev, VSEGINGEO, Moscow; and F.E. Nelson, Rutgers University, USA. The assistance and support of J. Akerman, W. Haeberli and L. King in obtaining data has been especially helpful. Notwithstanding the valuable input from those named, plus many others, the presentation of the information and mapping approach utilised are, the sole responsibility of the authors.

REFERENCES

Baranov, I. Ya., ed. 1956. Geocryological map of the USSR. Main Department for Geodesy and Cartography (GUGK), Moscow, scale 1:10,000,000 (Russian).

Baranov, I. Ya. 1959. Geographical distribution of seasonally frozen ground and permafrost. National Research Council of Canada, Technical Translation No.1121, Ottawa.

Baranov, I. Ya., ed. 1965. Principles of geocryological zonation of the permafrost region. Nauka, Moscow, 152 pp. (Russian).

Baranov, I. Ya. 1982. Geocryological map of the USSR. Main Department for Geodesy and Cartography (GUGK), Moscow, scale 1:7,500,000.

Baulin., V.V., ed. 1982. Map of geocryological regions of the West Siberian Plain, USSR Ministry of Geology, VSEGINGEO, scale 1:1,500,000, 4 sheets (Russian).

Black, R.F. 1954. Permafrost -- a review. Bulletin of the Geological Society of America, Vol. 65, pp. 839-856.

Bliss, L.C. 1979. Vegetation and revegetation within permafrost terrain. in Proceedings of the Third International Conference on Permafrost. National Research Council of Canada, Ottawa, Vol. 2, pp. 31-50.

Bostock, H.S. 1970. Physiographic regions of Canada. Geological Survey of Canada, Map 1254A, scale 1:5,000,000.

Brown, R.J.E. 1967. Permafrost in Canada. National Research Council of Canada, Publication 9769, and Geological Survey of Canada, Map 1246A, Ottawa, scale 1:7,603,200.

Brown, R.J.E. 1973. Permafrost. National Atlas of Canada. Department of Energy, Mines and Resources, Ottawa, Plate 11-12, scale 1:15,000,000.

Brown, R.J.E. 1978. Permafrost = Pergélisol [Canada]. Hydrological Atlas of Canada, Department of Fisheries and the Environment, Ottawa, Plate 32, scale 1:10,000,000.

Crawford, C.B., and G.H. Johnston. 1971. Construction on permafrost. Canadian Geotechnical Journal, Vol. 8, pp. 236-251.

Ershov, E.D., ed. 1988,1989. Geocryology of the USSR. Nauka, Moscow, 5 volumes (Russian).

Ferrians ,O.J., Jr. 1965. Permafrost map of Alaska. U.S. Geological Survey, Miscellaneous Geologic Investigations, Map I-445, scale 1:2,500,000.

Fotiev, S.M. 1978. Effect of long-term cryometamorphism of earth materials on the formation of ground water. in Proceedings of the Third International Conference on Permafrost, National Research Council of Canada, Ottawa, Vol. 1, pp. 181-187.

Fotiev, S.M., N.S. Danilova, and N.S. Shevleva. 1978. Zonal and regional characteristics of permafrost in central Siberia. in Permafrost -- The USSR Contribution to the Second International Conference, National Academy of Sciences, Washington, D.C., pp. 104-110.

Gorbunov, A.P. 1978. Permafrost investigations in high-mountain regions. Arctic and Alpine Research, Vol. 10, pp. 283-294.

Heginbottom, J.A. 1984. The mapping of permafrost. Canadian Geographer, Vol. XXVIII, pp. 78-83.

Heginbottom, J.A., and L.K. Radburn. 1992. Permafrost and ground ice conditions of Northwestern Canada. Geological Survey of Canada, Map 1691A, scale 1:1,000,000.

Heginbottom, J.A., and M-A. Dubreuil. 1993. A new permafrost and ground ice map for the National Atlas of Canada. in Proceedings, Sixth International Conference on Permafrost, Beijing, vol. 1, pp. 255-260.

Heginbottom, J.A., and M-A. Dubreuil. (in prep.) Canada -- Permafrost. National Atlas of Canada, 5th edition, scale 1:7,500,000, Plate 2.1 (MCR 4177).

Hughes, O.L. 1969. Distribution of open system pingos in central Yukon Territory with respect to glacial limits. Geological Survey of Canada, Ottawa, Paper 69-34, 8 pp.

Hughes, T. 1973. Glacial permafrost and Pleistocene ice ages. in Permafrost -- the North American Contribution to the Second International Conference, National Academy of Sciences, Washington, D.C., pp. 213-223.

Judge, A.S. 1973. Deep temperature observations in the Canadian north. in Permafrost -- the North American Contribution to the Second International Conference, National Academy of Sciences, Washington, D.C., pp. 35-40.

Kudryavtsev, V.A., K.A. Kondrat'eva, and A.G. Gavrilov. 1978. Geocryological map of the USSR. General Permafrost Studies; Materials for the Third International Conference on Permafrost. Nauka, Novosibirsk, scale 1:2,500,000 (Russian).

Mackay, J.R. 1972. The world of underground ice. Annals of the Association of American Geographers, Vol. 62, pp. 1-22.

Mackay, J.R. and S.R. Dallimore. 1992. Massive ice of the Tuktoyaktuk area, western Arctic coast, Canada. Canadian Journal of Earth Sciences, Vol. 29, pp. 1235-1249.

Melnikov, E.S. 1988. Natural geosystems of the plain cryolithozones. in Permafrost, Fifth International Conference, Proceedings. Tapir Publishers, Trondheim, Norway, vol. 1, pp. 208-212.

Melnikov, P.I. 1966. Geocryological map, Yakustkoi A.S.S.R. Akademia Nauk SSSR, Moscow, scale 1:5,000,000 (Russian).

Nikiforoff, C. 1928. The perpetually frozen subsoil of Siberia. Soil Science, Vol. 26, pp. 61-81.

Perry, R.K., and H.S. Fleming. 1986. Bathymetry of the Arctic Ocean. Geological Society of America, Boulder, scale 1:4,704,075.

Péwé, T.L. 1982. Geologic hazards of the Fairbanks area. Alaska Division of Geological and Geophysical Surveys, Fairbanks, Special Report 15, 109 pp.

Péwé, T.L. 1983. Alpine permafrost in the contiguous United States: a review. Arctic and Alpine Research, Vol. 15, pp. 145-156.

Popov, A.I., S.P. Kachurin, and N.A. Grave. 1966. Features of the development of frozen geomorphology in northern Eurasia. in Proceedings -- Permafrost International Conference, National Academy of Sciences, Washington, D.C., NRC Publication 1287, pp. 481-487.

Popov, A.I., et al. 1985. Map of cryolithology of the USSR. Faculty of Geography, M.V. Lomonosov University, Moscow, scale 1:4,000,000, 4 sheets (Russian).

Popov, A. I., et al. 1990. Cryolithological map of North America. Faculty of Geography, M.V. Lomonosov University, Moscow, scale 1:6,000,000, 4 sheets (Russian).

Rapp, A., and L. Annersten. 1969. Permafrost and tundra polygons in northern Sweden. in The Periglacial Environment, T.L. Péwé, ed., McGill-Queen's University Press, Montreal, pp. 65-91.

Shumskiy, P.A, and B.I. Vtyurin. 1966. Underground ice. in Proceedings -- Permafrost International Conference, National Academy of Sciences, Washington, D.C. NRC Publication 1287, pp. 108-113.

Shi Yafeng and Mi Disheng, eds. 1988. Map of snow, ice and frozen ground in China. Lanzhou Institute of Glaciology and Geo-cryology, Academia Sinica, scale 1:4,000,000, 2 sheets.

Sodnom, N., and A.L. Yanshin, eds. 1990. Geocryology and Geocryological zonation. National Atlas of Mongolia, GUGK, Ulan Bator/Moscow, Plates 40 and 41, scale 1:4,500,000, 1:12,000,000.

Tong Boliang, et al. 1982. Map of permafrost along the Qinghai-Xizan Highway. Lanzhou Institute of Glaciology and Geocryology, Academia Sinica, scale 1:600,000 (Chinese).

Vtyurin, B.I. 1975. Ground ice of the USSR. Nauka, Moscow (Russian).

Wahrhaftig, C. 1965. Physiographic divisions of Alaska. U.S. Geological Survey, Professional Paper 482, 52 pp.

Washburn, A.L. 1980. Geocryology. John Wiley and Sons, Halstead Press, New York.

Williams, R.B.G. 1969. Permafrost and temperature conditions in England during the last glacial period. in The Periglacial Environment., T.L. Péwé, ed., McGill-Queen's University Press, Montreal, pp. 399-410.

Permafrost Studies in Greenland

Henrik Mai [1] and Thorkild Thomsen [2]

[1] Arctic Consultant Group,
Sortemosevej 2 DK 3450 Allerød Denmark
[2] Greenland Power Company
Pilestræde 52 P.O.Box 2128 DK 1015 Copenhagen K Denmark

Data collected for mainly hydro-power purposes since the late seventies have been used for a new permafrost map of south-west Greenland and to permafrost related studies to hydraulic studies.

Mean yearly air- and rocktemperature have been calculated. A linear regression of airtemperature have been established for an overall temperature profile on the westcoast. Rocktemperature have been used in measured depth.

The drawn permafrost map have been drawn with a limit to discountinous permafrost with airtemperature -0,5 to -0,1°C, and continous permafrost with airtemperature -4 to -5°C.

A study of hydraulics structures in permafrost at the location of Pakitsup Aku. is presented with respect of temperature in rock and water surroundings of water filled tunnels

INTRODUCTION

The long-term energy political intention are to base a major part of the energy supply system in Greenland on hydropower. This objective have resulted in considerable hydrological and constructionally investigations also in the field of permafrost.

The investigations started in the end of the seventies and had for the time being a culmination in the middle of the eighties. Data collected since that periode are the basis for detailed temperature and permafrost studies.

PERMAFROST IN GREENLAND

As discontinous permafrost occur in terrain with a mean air temperature of less than about -0,5°C, it is obvious that it plays a significant role in the terrestrial portion of the hydrological cycle.

The precipitation and the radiation energy balance are importent controlling aspect of the arctic hydrological/permafrost regime. It has influence on the supply of energy to evaporation and through its supply of heat to the ground that is tantamount to spreading of the arctic layer.

Because of the tilt of the axis of rotation of the Earth in high latitudes solar energy is received at a low angle, so the net energy on each square meter is relative much less than in the tropics. At latitudes higher than 66,7°N (the Arctic circle) no direct energy is received at all from the sun for at least part of the year, at the same time heat is radiated from the surface perpendicularly into space.

As a result, there is a strong net loss of energy from high latitudes. This loss must be made by transport of heat from low latitudes through ocean current and atmospheric circulation.

These factors make the regional climate of polar areas very dependent on

- transport of heat from low latitudes
- the heat trapping effect of clouds and greenhouse gases

Change in global energy balance or circulation which have an effect on these mechanisms of heat delivery or heat loss, can thus have an exaggerated effect on the climate and environment of high latitude regions.

The various parameters will be documented in the following:

Temperature.

Available temperature data are shown in tabel 1. The stations with temperature values in different depth are locations with rocktemperature thermisters. The calculated yearly mean temperature are not time consistent for all stations but the shortest time period is 5 years.

The inland stations along the westcoast with airtemperature censors (40 stations) are plot with yearly average temperature against northern latitude, figur 1. The databasis are not for all stations consistent in time.

The regression curve for airtemperature with height along the west-coast "AIRcor" curve is iterated found with a correlation coefficient of 0.91. The resulted temperature gradient (average lapse rate) is 0.6°C/100 m.

LOCATION	TIMESERIE (month,year)	TEMP.DEPTH (m)	VALUE (°C)	M.A.S.L
A Nanortalik	08.61 - 07.80	air	+1.7	
B Qaqortoq	01.61 - 09.88	air	+0.7	
C Narsaq	01.58 - 12.69	air	+1.3	
D 60°57'N,45°58'W	07.81 - 09.92	air	-1.6	520
		1.0	+0.7	
		4.0	+1.1	
E Narsarsuaq	12.60 - 09.88	air	+1.1	
F 61°21'N,45°22'W	09.79 - 05.92	air	-4.0	680
		0.5	-1.8	
		1.5	-1.8	
		3.0	-1.7	
		4.0	-1.9	
G Paamiut	12.57 - 12.81	air	-0.5	
H 62°13'N,49°13'W	08.81 - 01.91	air	-2.4	320
		1.0	-0.1	
		4.0	+0.1	
I 62°13'N,49°17'W	07.84 - 03.90	air	-2.5	500
		0.5	-0.8	
		1.5	-0.3	
		3.0	-0.4	
J 63°15'N,50°21'W	07.85 - 07.92	air	-6.5	465
		1.0	+0.3	
		3.0	+0.5	
K Kangerluarsoruseq	01.62 - 08.73	air	-1.0	
L 64°01'N,50°06'W	07.81 - 07.89	air	-4.9	260
		0.5	-3.5	
		1.0	-3.9	
M Nuuk	01.59 - 04.89	air	-1.3	
N 65°09'N,50°09'W	07.85 - 05.91	air	-6.8	450
		1.0	-4.2	
		3.0	-3.0	
O 66°18'N,51°13'W	08.79 - 08.92	air	-9.4	735
		0.5	-6.2	
		1.5	-5.4	
		3.0	-6.1	
		4.0	-6.9	
P Maniitsoq	12.60 - 06.84	air	-1.6	
Q Sisimiut	12.60 - 12.91	air	-3.9	
R Kangerlussuaq	01.74 - 97.84	air	-5.9	
S 67°10'N,53°16'W	08.79 - 08.92	air	-5.4	100
		0.5	-2.2	
		1.5	-1.9	
		3.0	-1.9	
		4.0	-2.2	
T Aasiaat	12.57 - 07.84	air	-4.8	
U 68°43'N,50°50'W	08.84 - 08.91	air	-7.6	140
		1.0	-3.8	
		3.0	-3.5	
V Qasigiannguit	01.62 - 07.80	air	-3.5	
W Ilulissat	01.61 - 06.86	air	-3.9	
X Qeqertarsuaq	12.61 - 06.80	air	-3.6	
Y 69°29'N,50°12'W	08.85 - 08.92	air	-7.1	233
		1.0	-4.0	
		3.0	-4.0	
Z 69°27'N,50°23'W	08.85 - 08.92	air	-6.4	300
		0.5	-3.3	
		1.5	-4.4	
		3.0	-4.5	

Tabel 1 Data basis for permafrost map on figur 3.

Data from Denmark Meteological Institute and Greenland Home Rule Hydro-climatological database by Greenland Fieldinvestigations.

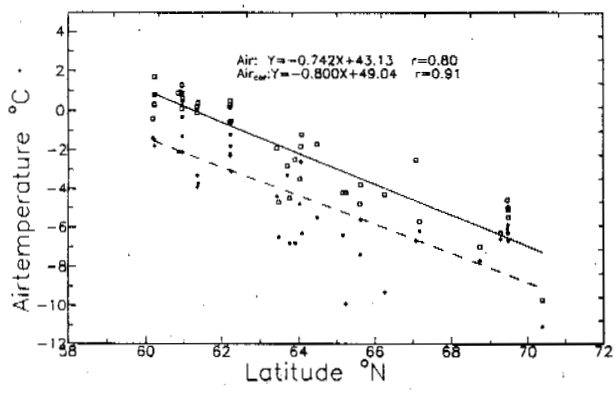

Figur 1. Airtemperature regressioncurve for inland stations in West-Greenland.

Precipitation.

The present precipitation conditions have for Greenland as whole been presented by Ohmura and Reeh (1991), se figur 2.

Alltogether, 251 pits and cores have been used to calculate the distribution of the annual accumulation on the ice sheet. The precipitation data at coastal sites were collected at 35 meteorological station.

The main features of the precipitation distribution are a strong longitudinal gradient exist in southern Greenland, south of 65°N on the west and south of 70°N on the east coast, Ohmura and Reeh (1991)

The mean annual precipitation for all of Greenland is 340 mm w.eq. The mean accumulation on the Greenland ice sheet is estimated at 310 mm w.eq.

For more detailed local variability on the west coast it is nessary to establish a more accurate map taking into account the dominant south-north and west-east precipitation gradient.

Radiation balance.

Measurement of components of the radiation balance equation for the arctic area are only found to a limited extent, Prowse and Ommanney ed.(1990) and Thomsen (1991).

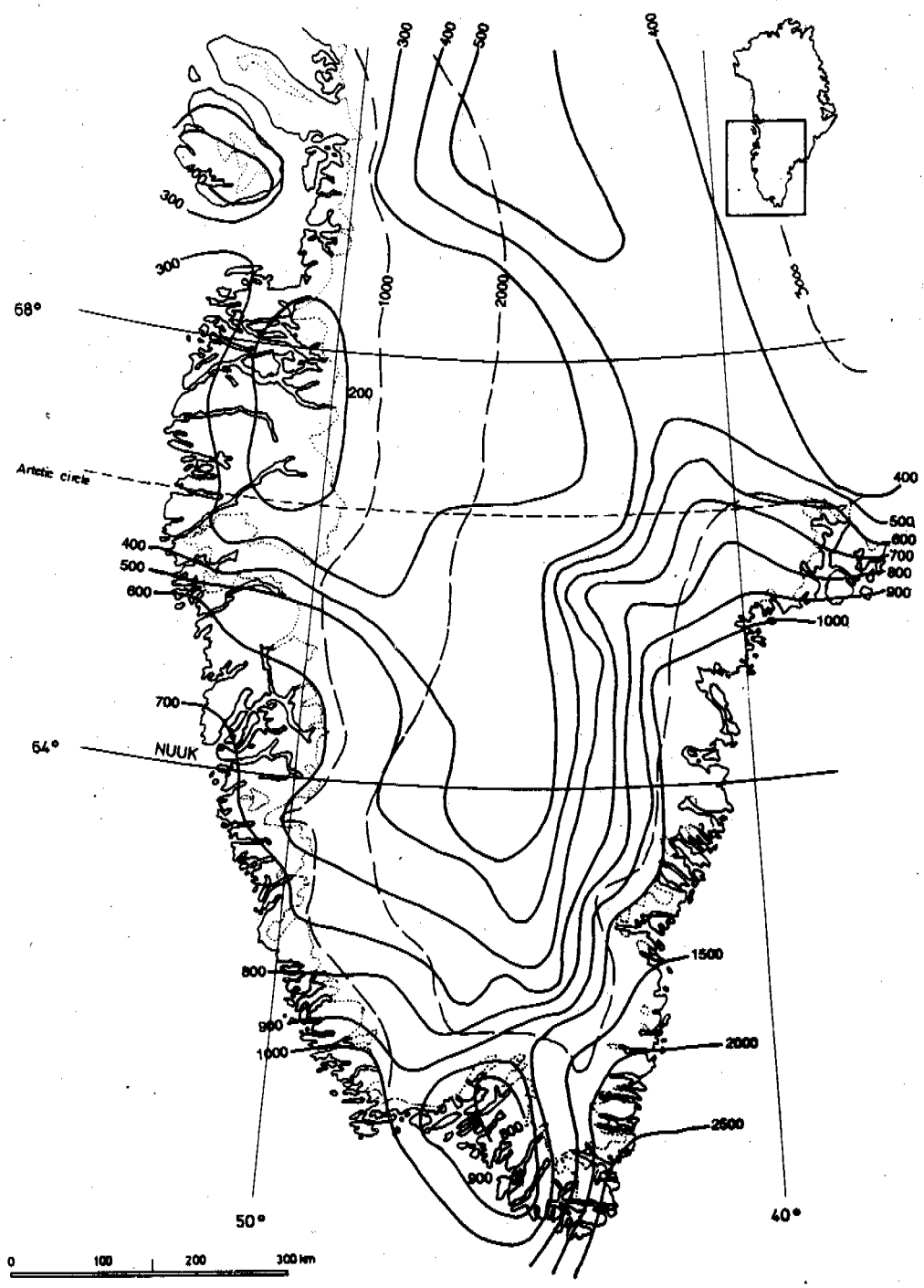

Figur 2. Yearly total precipitation in mm, after Ohmura and Reeh (1991).

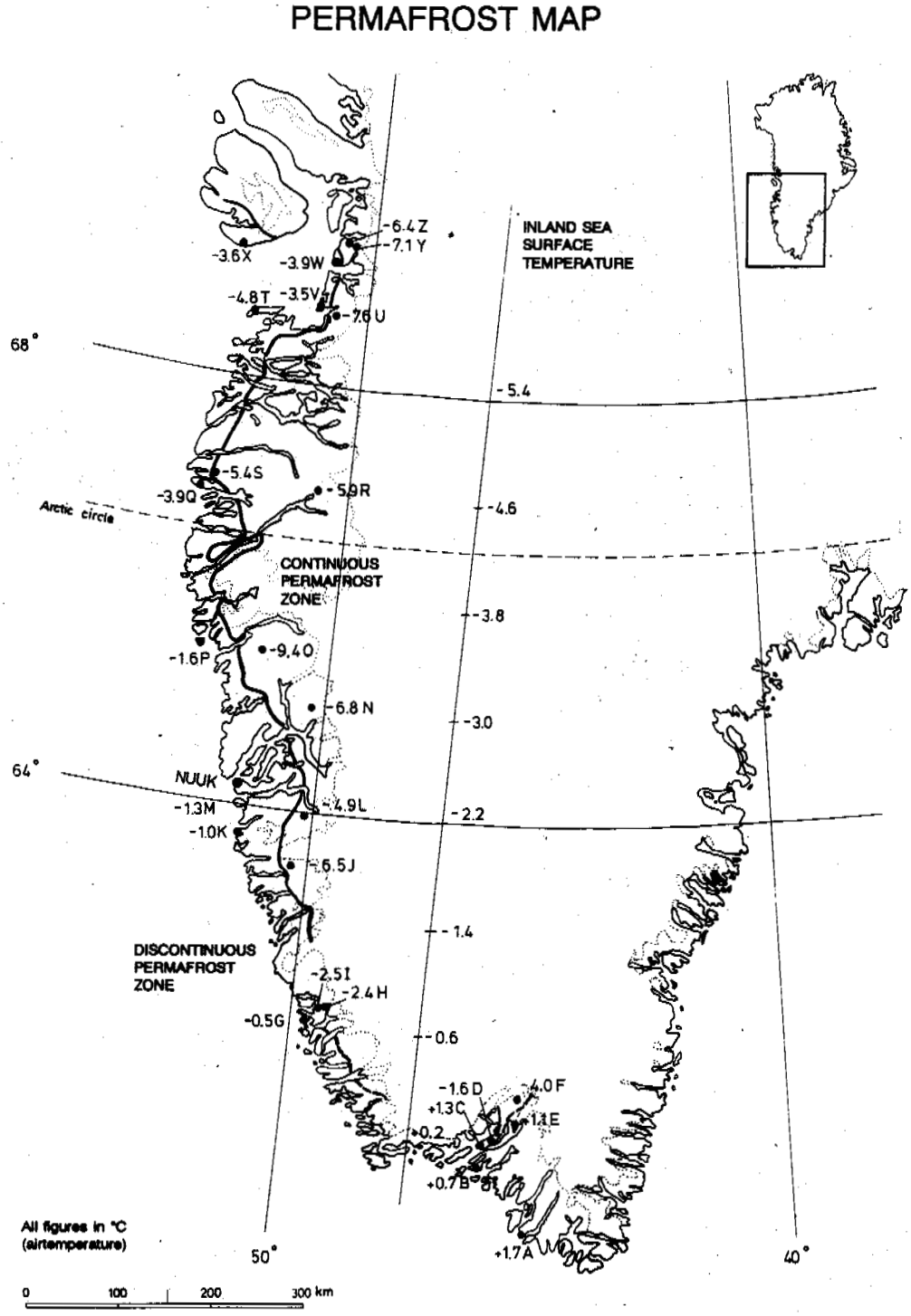

Figur 3. Permafrost distribution in West-Greenland

PERMAFROST DISTRIBUTION

On the basis of the shown temperature and precipitation distribution and also a great deal of subjective knowledge of hydrological information a permafrost map have been drawn, as shown on figur 3.

Besides the contour of temperature parameters, there are shown a calculated inland airtemperature at sea-surface based on the temperature/latitudes correlation on figur 1.

The shown permafrost boundaries are drawn with a limit to discontinous permafrost with airtemperature -0.5 to -1.0°C and to continous permafrost with airtemperature -4 to -5°C.

PERMAFROST RELATED TO HYDRAULICS STRUCTURES

A study of hydraulics structures in permafrost have been carried out on the existing knowledge from temperature and constructionally investigations. Any hydraulic structure in permafrost area is based on knowledge of the initial temperature conditions in the surrounding rock prior to establishment of the structure.

Scarce data requires drastic assumptions to be made. In recent years, finite element and finite difference models have been used to investigate temperature distribution resulting from freeze-thaw cycles in rock and steady state and transient solutions have been derived for stratified rock/soils, Irmen Christensen and Mai ('88).

For the purpose of having waterfilled tunnels in permafrost detailed studies have been carried out to investigate temperature conditions in water-rock interface both in an arctic lake and in a tunnel for hydro-power plant, Mai (1987 - a) and Mai ed. (1993 - first draft).

Scheme for a hydro-power plant in permafrozen rock have made it necessary to study the thermal regime around the water tunnels and in the water body in the reservoir. The studie have been carried out at the basin Paakitsup Akuliarusersua (69°29'N,50°18'W), figur 4.

The hydrological regime is dominated by ablation water from the Icecap. The lakes in the area 187 and 233 (the level above sea) will effect the temperature in the surrounding rock and give the initial conditions for resulting temperature development in the water-tunnels.

The lakes have a relative stabilized temperaturecondition, and will never go below 0°C. Compared to the average airtemperature at the location about -6 to -7°C this will be a much warmer body. The lakes are characterize as "arctic lakes", where temperature never get over +4°C, see figur 5.

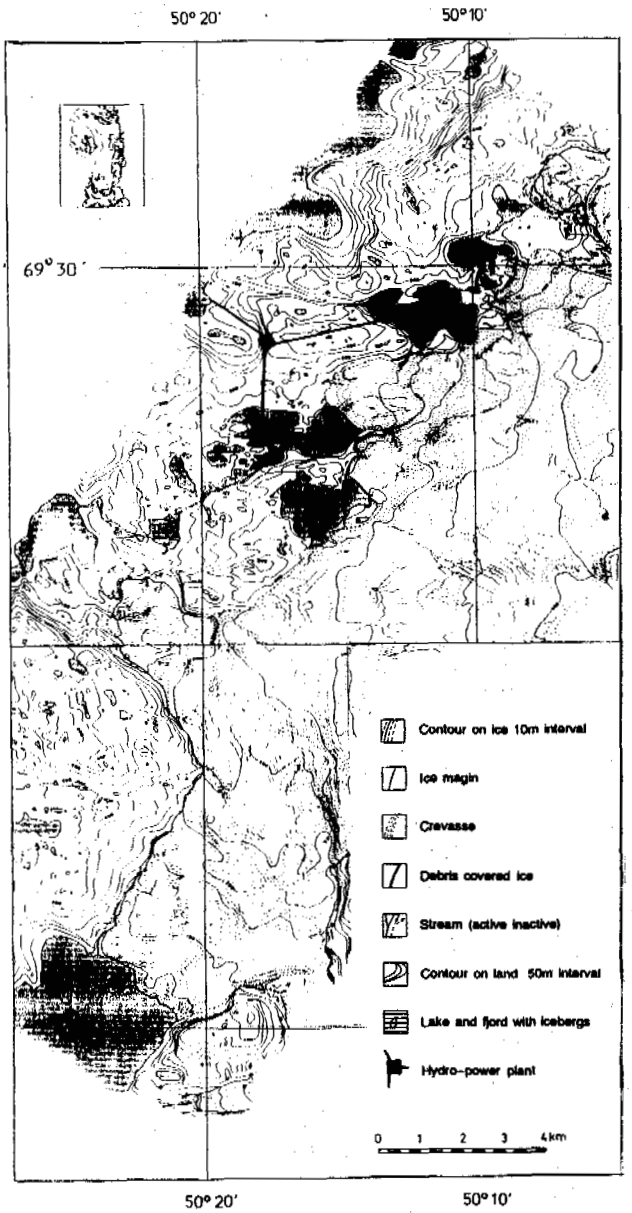

Figur 4. Drainage basin at Paakitsup Akuliarusersua, after H.Thomsen, Geological Survey of Greenland

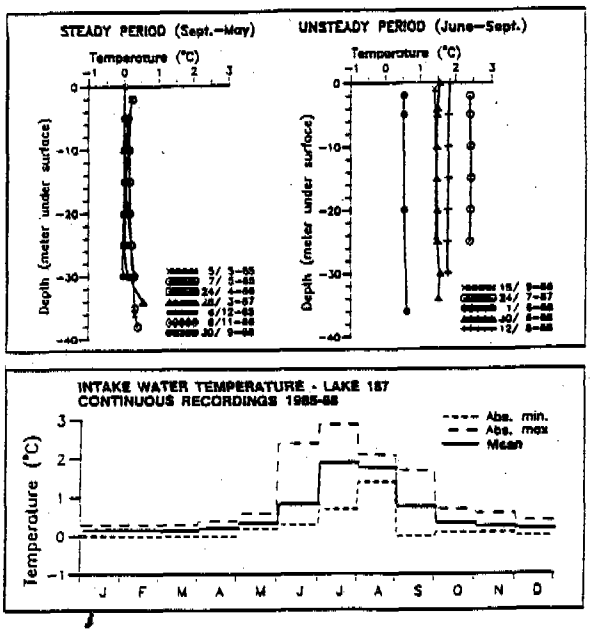

Figur 5. Lake temperature profile in the arctic lake 187 at Paakitsup Aku.

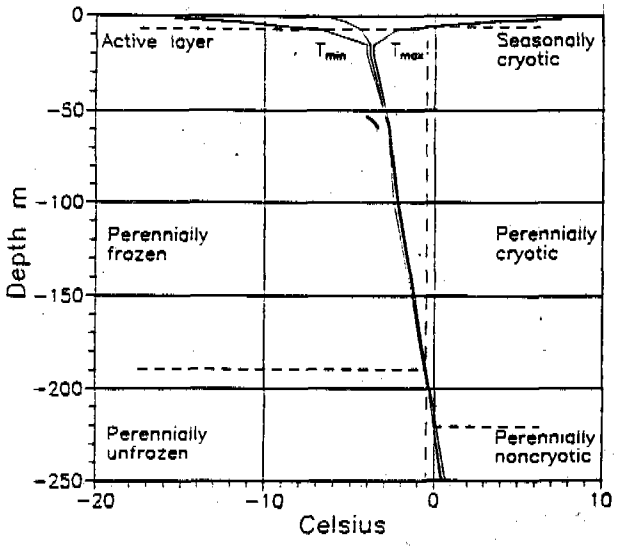

Figur 6. Rocktemperature gradient at Paakitsup Aku, surface level 237 m. above sea.

Fresh water have its maksimum density at +4°C, which means that the warmest water always will remain in bottom and the coldest water in the top. Lake 187 separates a little from lake 233 due to the glacier goes direct into the water in lake 187. This means that lake 187 in general are colder than lake 233.

In lake 187 the summertemperature in the surface will be around 1,5 to 1,8°C., and in lake 233 around 3 to 4°C. In winter temperaure drop at the surface to 0°C, but still a little warmer in lake 233.

The bottomwater in the lakes reflects the summertemperature and can be 1 to 3°C warmer than the surface temperature. Together with temperature profile measurements in the lakes intensive temperature measurements in the rock have taken place.

On one location situated 237 m above sea level temperature has been measured until 250 m below surface. Rocktemperature measure at the station is shown on figur 6. The gradient is calculated to 0,0167°C/m (1°C/60m).

With the known temperature and rock condition the hydro-power scheme was chosen with a lower level headrace as shown on figur 7 to get as little impact on rocktemperature below 0°C as possible.

With the topographic information and the temperature condition in the water and rock a dynamic model was runned to simulate the temperature field close to the tunnel, with the power plant in operation. The model should also be able to describe possible of ice in the water conduct during discontinous operation Mai (1987 - b) and Mai ed. (1993).

The tailrace of the power-plant terminates with a submerged outlet in the fiord.

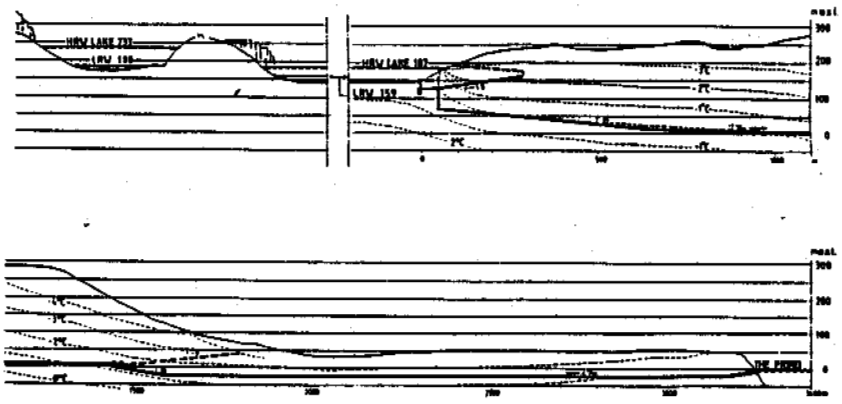

Figur 7. Hydro-power scheme at Paakitsup Akua, with low level headrace.

REFERENCES.

Irmen Christensen, M. and Mai, H. (1988):
Subsurface temperature predicitation for hydropower developments. The 7th Northern Research Basin symposium/work shop. Ilulissat, June 1988.

Mai, H.(1987 - a):
Hydropower tunnels in Permafrost, Conf. Underground Hydropower Plants Oslo, june 1987.

Mai, H., Stigebrandt, A. and Bergander, B. (1987 - b):
Submerged outlet into a fiord from a powerstation in Greenland. Conf. Hydro power in Cold Climates, Trondheim, july 1987.

Mai, H. ed. (1993) - draft:
Permafrost studies for Hydro-Power Permafrostgruppen: Arctic Consultant Group,LIC-Consult and VBB-VIAK.

Prowse, T.D. and Ommanney, C.S.L. ed. (1990):
Northern Hydrology Canadian Perspective, NHRI Science Report No. 1. Environment Canada.

Thomsen, T. (1991):
Arctic Hydrology in Greenland - Permafrost hydrology and data technology. Arctic Hydrology - present and future tasks. Seminar Longyear byen Svalbard. Norwegien National Committee for Hydrology. Report No. 23 - Oslo 1991.

SNOW AND PERMAFROST IN THE TIAN SHAN MOUNTAINS

Hu Ruji and Ma Hong

Xinjiang Institute of Geography, Chinese Academy of Sciences, Urumqi 830011, China

The existence of snow and permafrost is a result of a cold climate in high latitudes and high mountain areas, and they affect on the economic and social developments directly.In the Tian Shan mountains, the seasonal snow cover within the permafrost zone plays an important role in controlling the growth and thaw of unstable permafrost, and it's distribution exhibits almost a same pattern in areal extent with that of permafrost. Snow and permafrost are interdependent, co-existence, and play a positive role in balancing the ecological environment in the mountain areas.

INTRODUCTION

Snow and permafrost are extensively distributed in the Tian Shan mountains. As for snow, reliable records were kept in literature as early as 1,200 yeras ago. Since late the 1950's, the Chinese Academy of Sciences has organized many integrated surveys, investigations, and fixed-position observations of snow and permafrost in the Tian Shan mountains and has achieved a lot of important scientific achievments.

DISTRIBUTION OF PERMAFROST IN THE TIAN SHAN MOUNTAINS

It can be seen from Fig.1, the distribution of permafrost in the Tian Shan mountains shows almost a same pattern with the distribution of snow cover. The lower permafrost limit in shady slopes is generally lower than that in sunny slopes, i.e. about 2,700 m in shady slopes and 3,100 m in sunny slopes, with a difference of 400 m in altitude. The lower limit of permanent snow is about 3,600 m a.s.l. in shady slopes and 4,400 m in sunny slopes, the difference in altitude is about 800m. The altitude differences between the lower limits of permanent snow and permafrost varies greatly from one location to another, with a distance ranging from 870 to 1250m. These suggest that altitude is a dominant factor controlling the distribution of snow and permafrost in the Tian Shan Mountains.

The area of permafrost is approximated at 6.3× 10 Km (Qiu Guoqing ,1983), while the area of permanent snow cover is only 1 × 10 Km (Hu Ruji, 1989). The large difference in coverage area between them indicates a more dependence of existence of permanent-snow upon the raising altitude.

Seasonal frozen soils are also widely distributed in the Tian Shan mountains, and they are almost totally covered by snow cover during the winters. The existence of them affects on landscape and ecological environment of the area significantly, and this effect is

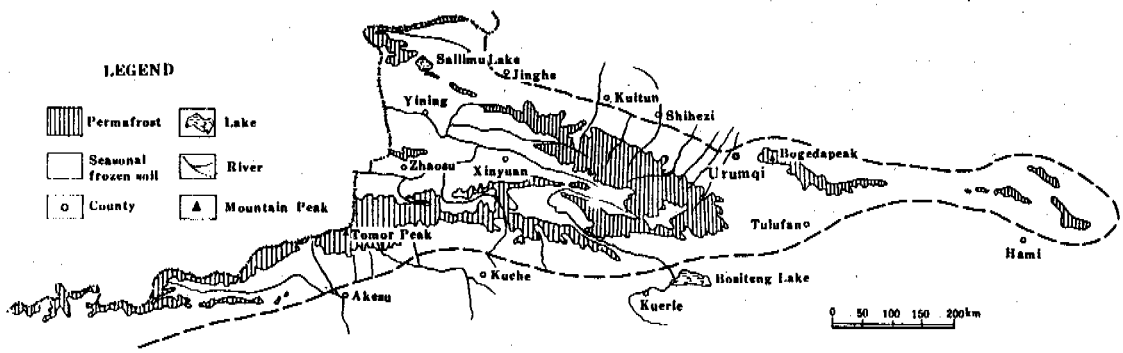

Fig.1 Distribution of permafrost in the Chinese Tian Shan mountains

largely determined by the intensity of interaction between snow cover and the seasonal frozen soils.

DISTRIBUTION OF PERMAFROST WITH VARYING LATITUDE AND LONGITUDE

The distribution of permafrost and snow cover in the Tian Shan mountains exhibit an identical trend along the latitude and longitude directions. The higher the latitude is, the lower the lower permafrost limit. Moreover, the descending magnitude of the lower limit for each degree of latitude increment increased with increasing latitude.

SEASONAL SNOW WITHIN THE PERMAFROST ZONE IN THE TIAN SHAN MOUNTAINS

The ground temperatures near the lower permafrost limit are usually higher and permafrost layers are shallow with a depth no deeper than 20 m. It was recorded that the depths of active layers have been increased to 3.5 m due to increased meltwater from snow and precipitation in the mountain areas (Qiu Guoqing and others, 1983).

Between the lower permafrost limit and stable permafrost areas, an unstable permafrost zone existed. The depth of permafrost in this zone varies greatly, depending on the integrated effects of external conditions, especially the effects snow cover and snowfall events. In the west part of the Tian Shan mountains, the depth of permafrost will increase 50 m with an increasing altitude per 100 m, and in the east part of Tian Shan mounatins, that will increase only 20 m with each 100 m increase in altitude. In addition, several geomorphological landscapes formed due to the interactions between snow and permafrost in this unstable permafrost zone. The typical landscapes are as follows:

Table 1. Lower permafrost limits in different areas of the Tian Shan mountains(from Qiu Guoqing)

Regions	Location		Altitudes of lower permafrost limits (m a.s.l.)					Altitudes of snow line (m a.s.l.)		Altitude differences between lower permafrost limits and snow lines(m)
	East. Long.	North. Lat.	North. slopes	Semi-N slopes	E or W. slopes	Semi-S slopes	South. slopes	North. slopes	South. slopes	
Misocrgou	94° 15′	44° 00′			2950				4200	1250
Kuixan col	86° 63′	42° 56′	2700				3100	3900	4100	1100
Headwater of Urumqi River	87° 00′	43° 07′	2900				3250	3800	4200	925
Motuosala	80° 08′	42° 48′	3250				3390			
Haxilegeng	84° 27′	43° 46′			2920	3050		3600		870
Qiongtailan	80° 18′	41° 54′				3350			4300	870
Tulasu	80° 16′	42° 04′	3000			3250		4000		920
Keqishievbax	80° 10′	41° 42′		3000		3100			4100	950

Qiu Guoqing and others (1983) proposed an empirical equation for calculating the lower permafrost limit in the Tian Shan mountains:

$$H = 11089.5 - 10.6x - 171.2y \qquad (1)$$

where, H is the altitude of lower permafrost limit (m a.s.l.),x is the east longitude, y is the north latitude.

From this equation, the lower permafrost limit will decrese 171.2 m for each degree of latitude increment, and decrease 10.6 m for each degree of longitude increment towards the east. Therefore, the lower permafrost limit shows a pattern of being higher in west and south parts, and lower in east and north parts of the Tian Shan mountains.

The snow cover is extremely uneven in the Tian Shan mountains. From Fig.2, for example, a snow depth of 70 cm occurs in the Yili River basin in the west part of the Tian Shan mountains, While in east part, a snow cover with such depth can only be found in the top of the Haerlike mountain, the difference in altitude between east and west ends of snow depth contour can be as large as 2,200 m, while the altitude difference between the lower permafrost limit in the east and west parts of the Tian Shan mountains is only about 220 m.

Mountain Terraces

The snow erosion landforms are widely distributed in unstable permafrost zones in the Tian Shan mountains. Snow erosion depressions are also commonly observed in this area. The mountain terraces are usually steps of 1 to 5 meters wide and the surface materials differ from one location to another. This landform often stretches into the stable permafrost zone. Professor Qiu Guoqing had once observed the multi-stage mountain terrace in the upper reaches of Alaxigongjing Valley in the Tian Shan mountains.

Mudflow and Mudflow Terraces

Mudflow action zones are usually dispersed below the

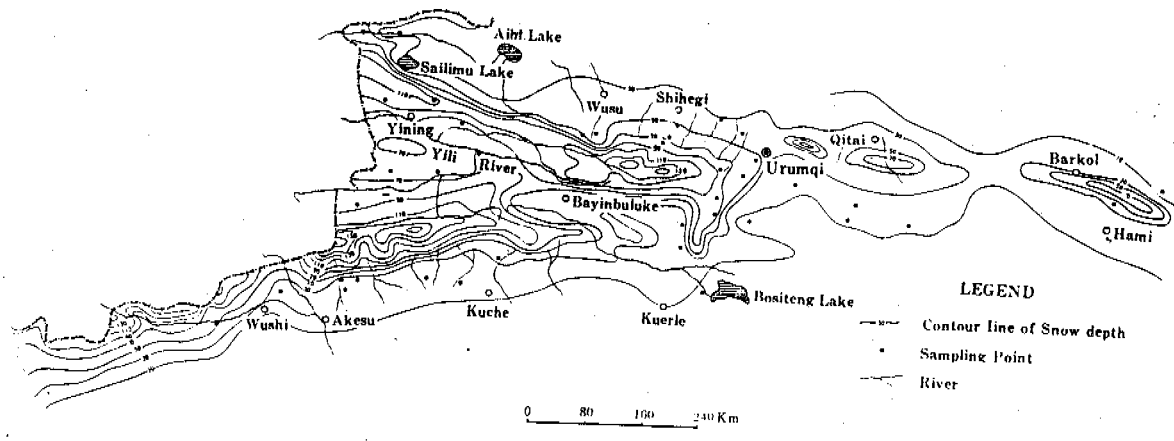

Fig.2 Distribution of snow covers in the Chinese Tian Shan mountains

frost–weathering and scattered gravel slopes. Under the action of repeated thaw–freeze cycles, the meltwater from snow can accumulate above the permafrost layer, the mud stated saturated soil thus leads to mud sliding and forms a variety of micro–geomorphological landscapes, such as, mudflow tongue, and mudflow terrace etc. These geomorphological landscapes are widely distributed within the unstable permafrost zones, especialy in east slopes of Hateerdegen and Xile mountains, south slopes of Yuximolegai mountain and east slopes of Aiken mountain pass.

Thaw depressions are also formed in this area and can be obviously observed. Thaw depression mainly occurs in the area where the ice content of permafrost is relatively high, and especially in areas with deep layers of under ground water, especially in the areas near the Kuixian and Haxilegen mountain pass.

Stone Stripes, Stone Circles,and Block Streams

Stone stripes, stone circles, and block streams are also common in the unstable permafrost zone, and they are the results of integrated actions of frost–heaving of seasonal frost soils, mudflow actions and the erosion of water flow in this area.

In addition, the widely distributed marshes, lakes,and frost–heaving dunes are typical landscapes in this area. Influenced by atmospheric circulation, precipitation in this area is much reduced during the winters, as compared with that during the summers. Moreover, the inversion layer during the winters leads to a further reduction of precipitation in this area, in some years, the ground in this area was only covered by shallow snow covers, or even without any snow deposited at the ground surface. However, strong winds may redistribute the snow and result in frequent drifting–snow hazards to mountain roads. On the other hand, with large amounts of snow accumulated in low–lying areas,and when summer begins, the meltwater from snow may be blocked by impermeable layers of permafrost and, thus, form the typical lake–marsh landscapes.

The depths of snow cover in stable permafrost zones are usually much thicker and can be as deep as several meters. In the Tian Shan mountains, snowfall in this permafrost zone mainly occurs during the summers. Influenced by local topography,avalanches are common in this area,and exhibiting a alpine avalanche landscape–ecological zone during the summers.

THE SNOW COVER WITHIN THE AREAS OF SEASONAL FROZEN SOILS

The snow distribution in the areas of seasonal frozen soil varies with altitude and changing climate conditions and thus follows a typical vertical zonality of landscape in the mountain areas. From Fig.3, a vertical zonality of mountain ecological landscape exists in the Tian Shan mountains. The lower permafrost limit in the mountain areas of the Tian Shan mountains is generally above the forest zone. In the south slopes of the Tian Shan mountains, the forest belts are discontinuously distributed, and the lower permafrost limit thus lies in the meadow gravel zone of high mountains.

Influences by an inversion layer, the deepest snow cover usually occur in the mid–mountain zone of the Tian Shan mountains. The maximum snow depth recorded at the Tian Shan Snow and Avalanche (TSAR) Station was 150 cm (February 15,1985). The existence of snow has a positive effect on the ecological cycles. Moreover, because snow will modify the process of energy exchanges between atmosphere,snow cover, and ground, it plays an important role in determing the growth and thaw of seasonal frozen soils.

It can be seen from Fig 4, the depths of seasonal frozen soils are much reduced due to the deep snow covers in the mid–mountain zone of the Tian Shan mountains. The depths of seasonal frozen soils in this area are in general no more than 80 cm. In addition, the maximum depth of frozen soil lags the lowest air temperature by 20–30 days, and usually occurs in mid–March due to the effects of snow cover. As the season progresses and snowmelt starts, the frozen soil begins it is thawing from both the upper and lower boundaries. This phenomenon is typical of the thawing process of seasonal frozen soils in the western Tian Shan mountains.

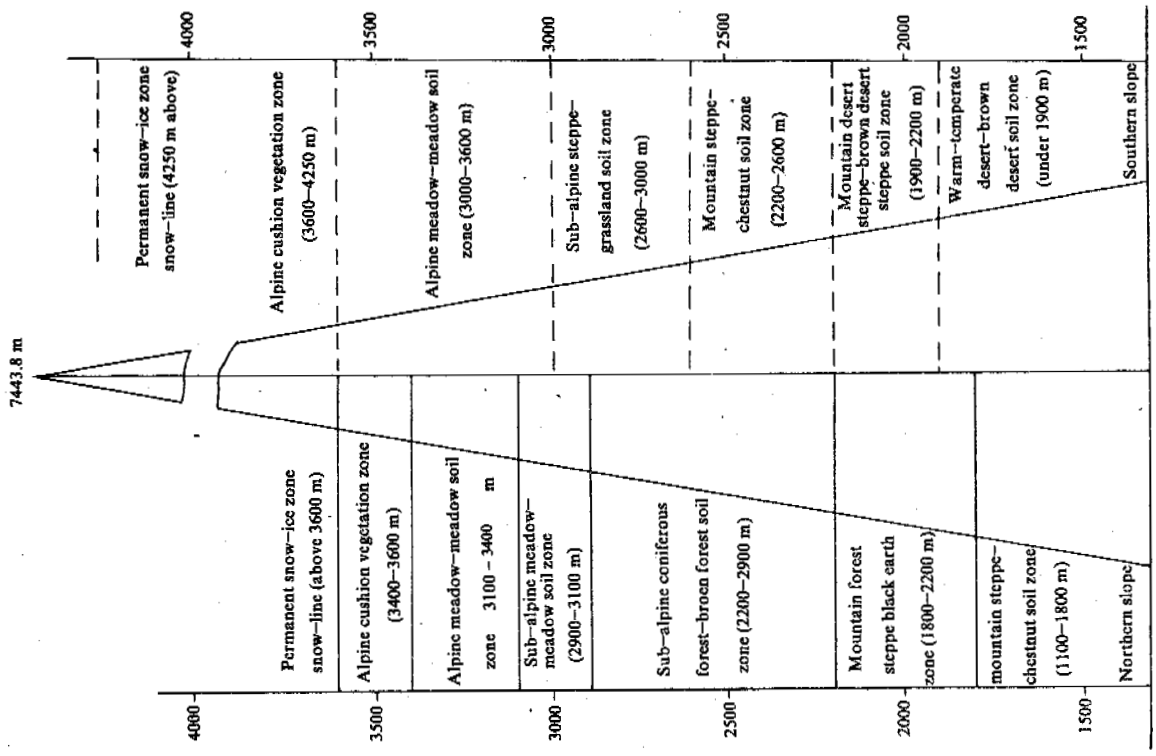

Fig.3 The vertical natural belts of Tianshan mountains northern and southern slope in China

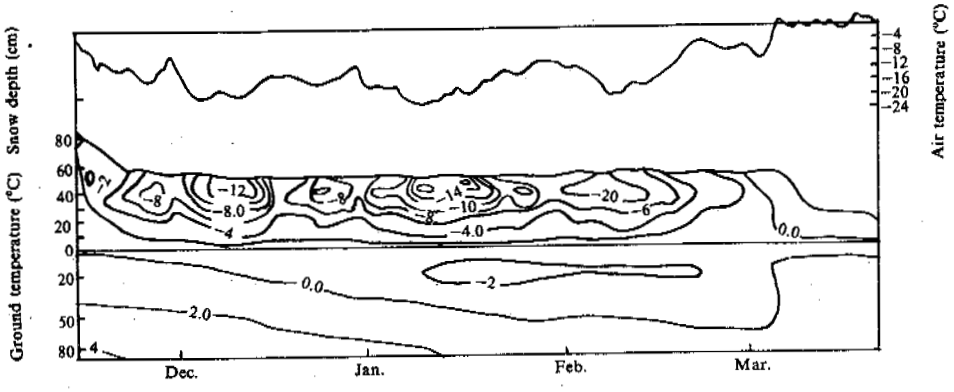

Fig.4 Air,snow and ground temperatures measured at the TSAR Station during the winter of 1983/84 (from Zhang Zhizhong)

REFERENCES

Qiu Guoqing and Huang Yizhi (1983) Basic Characteristics of Permafrost in The Tian Shan, China. In Proceedings of Second Symposium on Permafrost.Lanzhou, Gansu People's Publishing House p.22

Hu Ruji and Jiang Fenqing (1989) Avalanche and it's control in the Tian Shan Mountains, China. Beijing, People's Communucation Publishing House, P.14.

FROST-ACTION DESIGN AND APPLICATIONS OF ENLARGED TYPE PILE FOUNDATION BRIDGE IN WATERLOGGED AREA OF SONGYOUNG

Huang Junheng[1], Xu Zhenghai[2], Ge Huanyou[3] and Zuo Li[4]

[1]Commission for Urban & Rural Construction of Qingdao Municipality, China
[2]People's Government of Heilongjiang Province, China
[3]Water Resources Bureau of Bayan County, Heilongjiang
[4]Water Resources Department of Heilongjiang Province

The principle of self-anchorage by frost heave reaction force were used to design and construct the 15 enlarged type pile foundation bridges in the heavily frozen soil area of Heilongjiang Province. The buried depth of the pile foundation was reduced to 1.8-2.0 meters. Which should have been 12-18 meters according to the normal rules. The 10 years operational utilization shows that the construction is in good condition and no phenomena of frost heave occurred. In addition. The frost heave force for the pile foundation was measured for the first time in this country with reinforcement stress meters laid in splitted seams. After the measurement has been carried out for 3 years. i.e. 2 frozen cycles, the relative error between the measured values and the designed values for the maximum unit frost heave force lies in the range of 4.4-12.5%.

INTRODUCTION

Since 1982 we have used the principle of self-anchorage by frost heave reaction force for preventing frost heave occurrence, and constructed 15 enlarged type pile foundation bridges with reinforced concrete. The buried depth of the pile foundation is 1.8-2.0 meters. Our aim is to conduct the frost-action design of the enlarged pile foundation on a quantitative basis, which needs to use the in-situ measured conventional data in frozen soil and to follow the theory of anti-frost-action: obtain the frost heave reaction force quantitatively; calculate the size of caves on the enlarged foundation necessary for bearing the reaction force, determine the reasonable buried depth of pile foundation, and check over the strength of anti-frost-damage structure required for the enlarged pile foundation.

FROST HEAVE REACTION AND PRINCIPLE OF SELF-ANCHORAGE OF PILE FOUNDATION

The frost heave reaction force is a reaction force produced by the frost heave stress or shear force. It acts on the lower laying soil and thus produces this extra foundation reaction force (see Fig.1).

If the pile is to be built as an enlarged foundation, i.e., a foundation with an anchored sheet at depth Z, to make the eaves bear the reaction force, it will result in a better stability to resist the effect of frost heave on the pile foundation.

FROST-ACTION DESIGN OF ENLARGED TYPE PILE FOUNDATION

Structure Configuration and Basis for Size Selection

a) The buried depth of eaves of enlarged foundation should be chosen to be close to or equal to the maximum frozen depth of soil as far as possible in order to retrain from stress attenuation in the course of transfer of frost heave reaction force in the thawed soil layer.

b) The eaves length l determines the bearing proportion of the frost heave reaction force. It should be as small as possible on condition that the eaves can meet the requirement for the stability of anti-frost-heave.

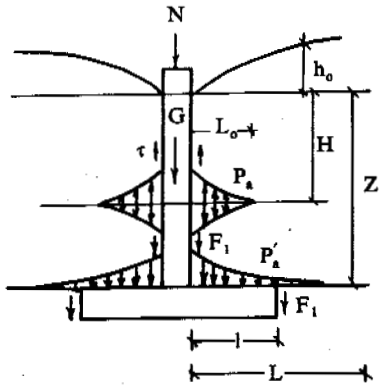

Fig.1 Forces and their distributions acting on a pile

H — frozen depth;
h_0 — frost heave amount on the ground surface;
Z — buried depth of anchored sheet;
l — length of eaves;
τ — tangential frost heave force;
N — upper load;
L_0 — distribution scope of τ;
Pa — frost heave reaction force;
G — weight of pile;
F_1,F_2 — frost heave frictional force;
F_t — soil weight on eaves;
L — distribution scope of reaction force.

3) The enlarged type pile foundation shall meet the requirements for the load-bearing capability and the stability of pile.

We chose Yongchangdong Bridge and Yongchangxi Bridge as the experimental works. The upper parts of these two bridges are made of reinforced hollow flat slabs and their lower parts are enlarged type pile foundations. The eaves are made of reinforced concrete base slabs with dimensions of 2.0x2.0x0.6 and 1.8x1.8x0.6 meters respectively for the two bridges, the diameter of pile is 0.5 meter and the buried depths of foundations are 2.0 and 1.8 m respectively.

Computation of Anti-Frost-Heave Stability

a) Criterion of stability

$$F_a + N + G + F + P_t \geq \Sigma\tau \qquad (1)$$

b) Frost heave shear force

$$\Sigma\tau = \pi DH[\tau]$$

where D — diameter of pile, and
$[\tau]$ — unit frost heave shear force, referring to Table 1.

The distance h from the acting point of the resultant force to the top surface of the enlarged foundation can be calculated as follows:

$h = z - \frac{H_m}{3}$ for the type of frost heave which is bigger at the upper part and none at the lower part, or

$h = z - \frac{H_m}{2}$ for other types,

where H_m is the maximum frozen depth of soil.

c) Frost heave reaction force

According to the recommendation by Heilongjiang Institute of Hydraulic Engineering, the frost heave reaction force can be obtained by using the formula:

$$P_a = \frac{\pi l^2 \Sigma\tau}{h^3}(0.5h - 0.31) \qquad (2)$$

when $1 \leq h$ and $h = z - \frac{H}{2}$

d) Computation examples

The stability of anti-frost-heave

$$K = (P_a + N + G_1 + F + P_t + G_2)/\Sigma\tau$$

ANTI-FROST-ACTION EFFECT OF CASE HISTORY

A. The Number of Enlarged Type Pile Foundation Bridges Built in the Waterlogged Area of Songyong Totals 15 (see Table 3)

B. Tangential F.H. Force Measurement at Yongchang Experimental Bridges

a. Layout of instruments

3 sets of reinforcement stress meters Model KL-20 manufactured in Nanjing were buried respectively in the midpiles of Yongchang Experimental Bridges (see Fig.3). The reinforcement stress meters were welded to the force-bearing reinforced bars of the pile column on a level of 1.8 m above the ground and the reinforced concrete column was blocked with an iron plate to ensure that the reinforced bars were solely acted on by the force during frost heaving of the pile. Variations of resistances and resistance ratios were measured with a proportional bridge for hydraulic engineering use and the values of tangential frost heave force were calculated.

b. Measurement results

(i) Tangential frost heave force (Fig.2,3 and 4). Accomparison between the calculated frost heave shear forces and their measured values is given in Table 4.

The error of unit frost heave shear force lies between 4.4% to 12.5%, which is within the permissible range of errors; while the error of maximum frost heave force ranges from 3.3% to 29.2%. The reason for this bigger error is that the magnitude of frost heave shear force is also dependent on the frozen force between the pile column and its neighbouring soil. At the end of November, the frozen depth is below 50 mm, and the unit frost heave shear force will reach its maximum, moreover, the frozen surface will experience a distruction process; after

Table 1. Design reference values of unit frost heave shear force in kg/cm² (from Heilongjiang Institute of Hydraulic Engineering)

Class of frost heave	Weak frost heave	Medium frost heave	Strong frost heave		
			Grade 1	Grade 2	Grade 3
Frost heave ratio %	1.0-3.5	3.5-6.0	6.0-10	10 - 15	15 - 20
Unit frost heave shear force	0.3-0.5	0.5-0.8	0.8-1.2	1.2-1.6	1.6-2.0

Table 2. Computing results for the stability of anti-frost-heave

η(%)	[τ] kg/cm²	Στ (ton)	P_a (ton)	K	Conclusion
7	0.9	25.4	10.97	1.83	steady
10	1.2	33.9	14.66	1.48	steady
13.3	1.4	40	18.56	1.36	steady

Table 3. Statistics of enlarged type pile foundation bridges built in waterlogged area of Songyong

Name of Bridge	Location	Time of completion	Span	Buried depth (m)	Pile foundation			Remarks
					Diameter of pile (m)	Enlarged foundation slab (m)	Thickness of base slab (m)	
Yongchangdong Bridge	Yongchang Brigade	July, 82	2x6	2.0	0.5	2x2	0.6	
Yongchangxi Bridge	Yongchang Brigade	Aug., 83	2x6	1.8	0.5	1.8x1.8	0.5	5 same bridges
Sanmenwang Bridge	Sanmen-wangjia	Aug., 83	2x6	1.8	0.5	1.8x1.8	0.6	
Qiyi Bridge	Qiyiqiao	Aug., 84	1x6	1.8	0.5	2x2	0.6	8 same bridges

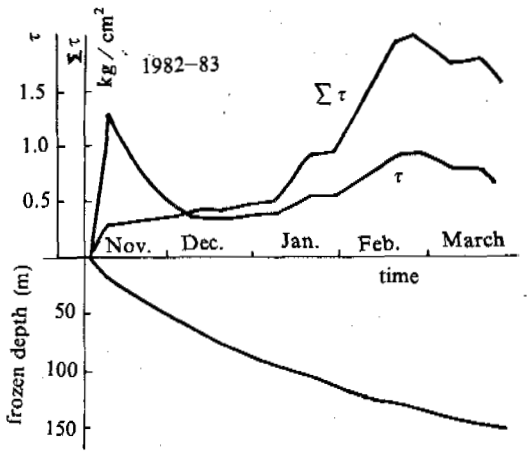

Fig.2 Observed results of tangential frost heave force for Yongchangdong Bridge in 1982-83

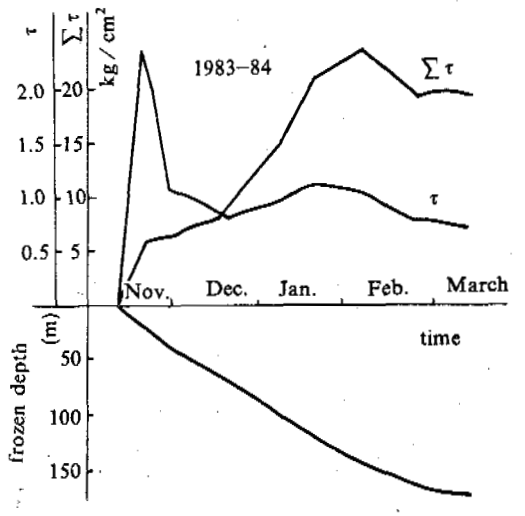

Fig.3 Observed results of tangential frost heave force for Yongchangdong Bridge in 1983-84

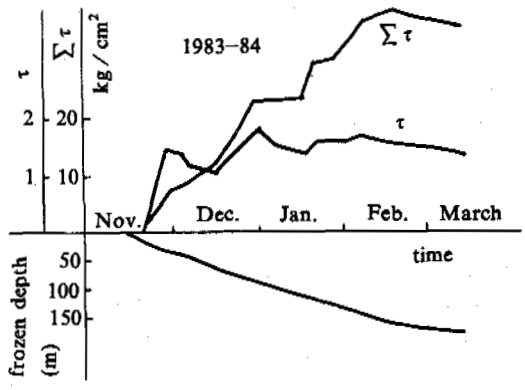

Fig.4 Observed results of tangential frost heave force for Yongchangxi Bridge in 1983-84

that, the frost heave shear force tends to be smaller than the theoretical calculated value, therefore, the measured frost heave shear force is smaller than the calculated value. The stronger the frost heaving of the foundation soil is, the closer will be the calculated value of shear force to its measured value.

(ii) Deformation observations (see Fig.5). Two measuring points (3) and (4) (see Fig.5) were set on their mid-piles at Gongchangdong Bridge and Yongchangxi Bridge. The measured results obtained in the two freezing and thawing cycles between 1982-1984 indicated that the deformation of the mid-piles due to frost heave was less than 1 centimeter, no phenomenon of frost heaving on the bridge surface occurred during the process of frost heave, and the operation of the whole works was in good condition, thus achieving the aim of anti-frost-heave for these works.

CONCLUSIONS

A) The operational practice of these works for 10 years has demonstrated that the enlarged type pile foundation, on which the frost heave reaction force is used to improve the stability of anti-frost-heave, is an excellent structural

Table 4. Comparison between calculated and measured frost heave values

Name			Frost heave ratio (%)	Tangential frost heave force (ton)	Unit tangential frost heave force (kg/cm^2)
Yongchangdong Bridge	1982-1983	Designed	7	25.4	0.9
		Measured	7	20	0.94
		Error (%)		21.3	4.4
	1983-1984	Designed	10	33.9	1.2
		Measured	10	24	1.05
		Error (%)		29.2	12.5
Yongchangxi Bridge	1983-1984	Designed	13.3	40	1.4
		Measured	13.3	38.7	1.55
		Error (%)		3.3	10.7

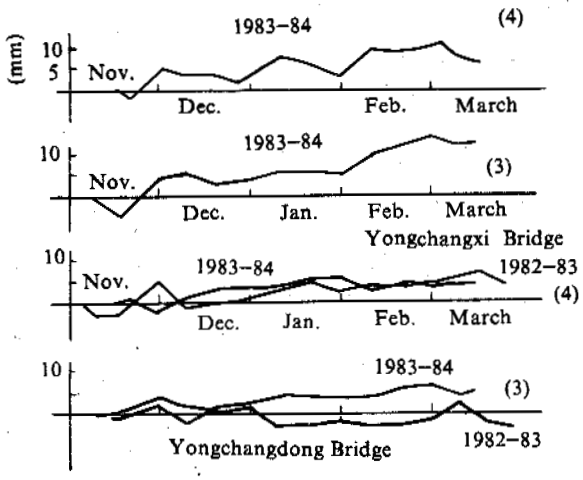

Fig.5 Observed results of deformation on Yongchangdong Bridge

configuration for anti-frost-heaving in the strong frost heaving soil area. It has many advantages, such as simple structure, shallow buried depth, ease of construction and lower work load. Therefore, it is suitable to be spread into wide use in the pile and wall structures of medium and small drainage works.

B) Tongchang Experimental Bridges are the result of an attempt to make the frost-action design using frozen soil theory on a quantitative basis. Through the in-situ observations, a better understanding of frost heave properties in the said area was reached and the values of tangential frost heave shear force and frost heave reaction force might be quantitatively calculated. The values of unit frost heave shear force, measured in the experiment on prototype works during the 2 freezing and thawing cycles of the consecutive three years, are very close to their corresponding theoretical designed values. The error ranges from 4.4% to 12.5%. Owing to this higher accuracy, the frost-action design of enlarged type pile foundation on a quantitative basis can be put into practical use.

THE SHALLOW COVER DESIGN AND CONSTRUCTION TECHNOLOGY OF BUILDING FOUNDATIONS IN DAQING REGION

Jiang Hongju Cheng Enyuan

Daqing Academy of Oilfield Design, China

The perennial observations show that Daqing soil has different frost heave properties from freezing shrink to very strong frost heave. Because of differential heave and thaw collapse in foundation soil, the oilfield building structures are destroyed and the engineering quality is heavily influenced. So, foundations in saesonally frozen ground regions, shallow buried building foundations, and frost damage prevention techniques were studied. Meanwhile, the results obtained from research are applied directly to the engineering design and construction. The results were very good.

THE SHALLOW BURIED FOUNDATION OF BUILDINGS AND DESIGNS FOR PREVENTING FROST DAMAGE

The Design of Shallow Buried Foundations of Buildings

Because of the different properties of frost heave on the basement soil this will result in the deformation of external wall of the building during freezing. During thawing the difference in melting time and velocity of the basement soil under the external wall bottom, the wall produces uneven settlement deformation. If the tangential stress or tensil stress of external wall which caused by the two kinds of action is bigger than the limit of material strength, cracking and deformation would emerge in the wall body. In order to guarentee the normal operation of the building structure, the following work was done:

The correct determination of the frost heave grade of basement soil

For the frost heave grade of basement soil applied in design, two main factors should be considered. One was the frost heave grade in investigation. The other was the change of the frost heave grade of basement soil produced in the building construction or usage.

The frost heave grade of basement soil in researched years was provided by Chinese design standards of building basements and foundations (GBJ7–89). The best way of determination was on the basis of locally observed results.

However, if the frost heave grade of basement soil determined by the method mentioned above was considered as the design basis, two problems would appear:

First, the annual air temperature and precipitation in the area is random. If the year of observation and investigation was arid with high temperatures and a low frozen depth, the frost heave grade of the soil is lower. On the other hand, if the year has heavy rains and low temperatures the grade could be improved.

Second, if the original ground level was decreased during the process of construction, or since the other buildings affected drainage of the ground water, or the buildings were constructed in regions of low temperatures and water weren't drained properly, this results in rise of content of the basement soil and rise of the underwater level, the property of frost heave in the soil would increase. When determining the applied frost heave grade in engineering design, we think that if only one of the two factors mentioned above exist, the frost heave grades of three kinds of soil which are initially determined as non–frost heave soil, less frost heave soil and frost heave soil should rise respectively. The reason is that the critical values of the frost heave ratio in the three kinds of frost heave grades are on the low side)i.e. the average frost heave ratio of non–frost heave basement soil was $\eta <= 1\%$. The average frost heave ratio of less frost heave basement soil was $1\% < \eta <= 3.5\%$, the average frost heave ratio of frost heave basement soil was $3.5\% < \eta <= 6\%$. Meanwhile, because the water content of basement soil will increase and the underground water level will rise and it will be easier to go beyond the critical value of the frost heave ratio of the original basement soil, the initial frost heave grade of the determination will be changed. However, because the critical values of the average frost heave ratio of two kinds of basement soils in strong and stronger frost heave are all high (I.E. strong frost heave is $6\% < \eta <= 12\%$, stronger frost heave is $\eta > 12\%$), it is more difficult to exceed the initial frost heave grade of determination. According to observation of many years, we think it is proper to increse one grade.

The determination of buried depth of building construction

When the buried depth of foundations is determined in the deep seasonal frozen regions, some main factors should be considered:

The quality and amount of load acting on the basement soil.

The geologic structure of basement soil, the physical and mechanical index of soil, the hydrological engineering and geological state. As well as considering the homogenitity and stability of the shallow layer soil.

The size of the building, the important degrees, grades and states of use, with or without a basement, and the foundation types, etc.

The conditions of various diskes, hollows and holes, as well as the cross-pipes under the building foundation and the structural conditions.

The buried depth of foundations neighboring the building.

The condition of frost heave and thaw settlement of basement soil, etc.

The six main factors listed above show: it is one of six elements that seasonal frozen soil influences the buried depth of foundations but it isn't only the elements. Through research and practice it can reach purpose of reliability and safety, if the buried depth of building foundation is above the freezing depth of soil. The methods can be divided into two stages: the first stage was before 1980, under satisfying the conditions of the strength and stability of basement soil, the buried depth of the building foundation was determined between 0.8 and 1.4 m from no frost heave to strong frost heave according to classification of the frost heave grade of the basement soil and characteristics of the building. However, some important building foundations should be deepened. After 1980, through tests and research of various elements for several years, a more rational calculating method was obtained to consider the minimum buried depth of building foundations in frost soils (Jiang Hongju, 1988). After the minimum buried depth of the building foundation was determined by this method and considering the influence of other elements, the suitable adjustments (total or partial deepening) were considered as design values. Through experiments and observation for several years, we think that the building cracks were not produced by tangential frost heave force and caused by an uneven frozen soil layer under the foundation.

During the thawing stage of foundation soil, due to the different directions of the wall body and the different irradiating degree from the sun, as well as the different thinkness of the frozen soil layers and different deformations of frost heave, different thawing times and velocities of the frozen soil layers under the foundation would occur. This resulted in an unequal subsidence and bending deformation of the wall body. The deformation in the two wings of the wall body was the most obvious and caused cracking when the deformation exceeded the allowable deformation value.

The analysis stated above was proved by a large amount of observations and testing of local practical engineerings. The influence of tangential frost heave force couldn't be considered on the three kinds of soils(no, weak and normal frost heave). With soil of strong or very strong frost heave, prevention measures should be considered for safety against the tangential frost heave force of the foundation sidewall in the range of 3 meters from the convex corners of the exterior wall (Fig.1) The tangential frost heave force needn't be removed at a range of total frost depth in unheated buildings and the prevention measures against tangential frost heave should be only considered at half the depth of the outdoor ground.

Prevention measures for frost heave damage in building foundations

The effective and economical methods in Daqing region were introduced as follows:

The foundation depth of an unheated building was determined according to the method mentioned in sectioned above. But with the heat building, whether one or multiple stories, was deepened by 20–30 cm in the corners and convex corners. The deepened length was prolonged 3–4 m (especially at the convex corners on the basis of the coner point). Non-frost heave replacement material could be used in the deepened parts.

For the basement soil of heated buildings with strong and very strong frost heave, the deepened length at the corner points (convex coners) was prolonged 3 m in the direction of the length and width. Non-frost heave replacement material was used at the exterior wall of the foundation. In unheated buildings, nonfrost heave replacement material was used at the coner points and internal and external walls of the foundation. The replaced depth was half of the foundation buried depth along the foundation. On the other hand, the foundation could be made with a ladder-shaped cross section with a slope degree of 1:7 (see Fig.2) in order to eliminate tangential frost heave force.

The apron slope of the wall root should be done properly and it would prevent side wall of the foundation or bottom soil from being permeated by excess water. So as to reduce the action of frost heave and thaw settlement of soil.

The foundation wasn't designed on the first storey balcony of the building and the balcony floor was used in the beam structure.

Under condition of shallow foundation determined by methods of this paper, for safety resons, the concrete periphery beam should be added on the top of the foundation and the upper part of the wall body. The reinforcement of the periphery beam should be along the longitude is needed to increase the diameter of the reinforcement within the convex walls of building and the two ends of the longitudinal walls from 10 meters. The reinforcement of other parts were done with the basis being reinforcement of other parts were done with the basis being reinforcement bars of the structure in order to improve the ability of preventing against freezing-thawing deformation of the wall body.

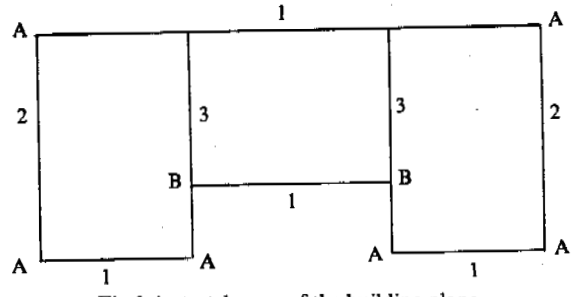

Fig.1 A stretch map of the building plane

Note: A–convex corner, B–concave corner, 1–longtitudinal wall, 2, gable, 3–internal wall.

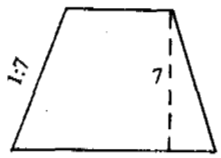

Fig.2 A sectional drawing of trapezoidal foundation

Table 1. The thickness of the allowable remaining frozen soil layer beneath the foundation during spring–thawing

The frost heave grade of basement soil	No frost heave	Weak frost heave	Frost heave	Strong frost heave	Stronger frost heave
The thickness of remaining frozen soil layer (cm)	limit–less	70	50	30	15

The foundation of outer steps of the building should be separated from the foundation of the wall body. The soil under doorway steps should be replaced with non–frost heave material and the depth should be equal to the buried depth of the wall foundation.

The designed temperature of the ends at the corners should be raised properly.

The Design of Frost Damage Prevention in The Field of Construction

In order to not add or reduce the grade of frost heave in the field of construction, the drainage design in the field of construction was important. The following issues should be payed close attention to:

In order to have a good verticle design at the site, the ground should have a proper slope degree which allows rainwater or water seepage from pipes or taps to be drained away quickly so as not to permeate into the ground. Or a blind ditch should be planned using the materials of coarse sand and gravel, etc., at a depth of 0.5–0.7 m to drain ground water.

The comprehensive drainage system for domestic sewage, industrial polluted water and atmospheric precepitation should be considered and linked with the urban drainage system. Meanwhile, drainage measures such as a cable, centrally heated dike and various other pipes and dikes, and a cutting well should be implemented. Water can't be allowed to permeate into the structures to prevent against frost damages.

A BRIEF INTRODUCTION OF CONSTRUCTION AND TECHNOLOGY IN SEASONAL FROST SOIL REGIONS

On the basis of the climatic features and the freezing–thawing procedure on basement soils in Daqin region, the construction stage of engineering could be divided into three stages: spring–thawing, summer and winter. The summer construction was the normal construction, but in winter it was contrary. Measures used during spring–thawing construction (from March 11–20 to June 11–20) will be mainly introduced.

The landform, land vegetation, cave , etc. have effects on the freezing state of basement soil. The grade of frost heave of basement soils, freezing depth and important physical and mechanical parameters of frozen soil (Which were the water content, dry density, thaw settlement factor and thaw compression factor, etc.) should be surveyed and the calculation of thaw settlement should be done.

The bench mark of measuring the site altitude couldn't be acted by the frost heave. The design should use the height of sea level (altitude) and couldn't use a relative height.

Because the natural ground was not even, if frozen soil layers remained under the bottom of the basic trench when the depth of the basic trench was dug to the designed altitude, the allowable remained thickness of frozen soil should be determined in accordance with the table 1. If the basement soil of one building has different grades of frost heave, the thickness of the frozen soil layer would be adjusted in various parts and make the amount of thaw settlement as equal as possible. The total amount of subsidence would be restricted to the range of 10–15 mm.

When the construction field had a complicated landform and more caves or a large area of moved buildings, and there was a frozen soil and warm soil areas and a great difference of frozen depth under the new building, all of the frozen soil should be removed to assure the safety.

If the building had a large volume and the grade of the frozen soil layer under the bottom of the basic trench was also high, the remaining frozen soil can be exposed thoroughly by the method of a thaw trench and the construction could begin when the conditions allowed.

Because of the thawing of the frozen soil layer during process of construction, the water content in the soil was large and a larger subsidence could appear. So to ensure the safety the following points should be payed close attention to:

a), When constructing the foundation, each part should be constructed simultaneously so as to avoid unequal subsidence.

b), For preventing constructing water from flowing into the basic trench of frozen soil, when the foundation was constructed, the quality should be ckecked and the soil of the side wall should be filled into each layer.

c),When concrete was poured, we should avoid the concrete to be poured on the frozen soil layer the measures of maintaining the temperature should be done well in order to prevent the concrete from freezing.

d), Air temperature during March 11–20 drops sharply, so the measures of maintaining the temperature should be done well during process of the construction mortar and hardening.

REFERENCES

Jiang Hongju and Cheng Enyuan, 1988, A method for calculating the minimum buried depth of building foundations, V ICOP Permafrost Proceedings, Vol.2, p1253–1255.

THE PREVENTION AND TREATMENT OF FROST DAMAGE ON BUILDINGS AND CANALS IN PERMAFROST REGIONS

Jiao Tianbao

Yitulihe Branch of Harbin Railway Brueau,Heilongjiang,China

In forest regions of permafrost,the frost damage of buildings and canals is caused by bigger water contents of soils,lower bearing capacity and air temperature,uneven frost heave and thawing settlement etc.This paper introduces mainly how to protect and utlize the bearing capacity of frozen soils, remove underground water,strengthen the whole strength of construction and coldproof and heatproof property etc.to prevent and treat frost damage.

INTRODUCTION

Da Xinggan Ling forest regions located from 119°40′to 127°00′E and 46°30′to 53°21′N are permafrost regions where mean annual air temperature is about −4°C. In these regions,the buildings and canal are often subjected to frost damage in varying degree.So,in this paper,we put forward some measurements of preventing and treating frost damage.

THE PREVENTION AND TREATMENT OF FROST DAMAGE ON BUILDINGS

The Base of Chassis Connected with Buildings of Filling Instead of Digging and The Prevention and Treatment of Frost Damage of The Old Wooden Buildings.

Since the wooden buildings are fairly convenient in forest regions,so this is a main subject to study, prevent and treat the frost damage. The main advantage of new wooden buildings are:

The smaller weight and pressure and the well−adaptability

From structure drawing,we can obtain that the pressure under chassis is only 0.098MPa. When transfered to original ground surface through pad, this pressure becomes to 0.02MPa, and to the bottom of suffered pressure layer,it is 0.04MPa, which only equals to minimum allowable bearing capacity of silt which has maximum water contents. So,this type of building can be built everywhere.For old wooden building which need digging base to lay chassis and bury pillars,it can not be built in regions of silt and poor−geological condition etc.(Fig.1 and Fig.2).

The well−heatproof and radiative property

a). The heatproof property is good,so,this type of building can save the heating fuel. Since the total practical transmitting heat resistance of pad R_o(1.6m²h °C / Kcal) is bigger than the necessary total transmitting heat resistance R_m (1.4m²h °C / Kcal),So its heatproof property completely satisfies with requirement of ground surface.

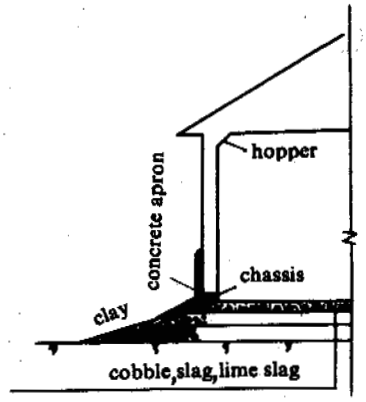

Fig.1 The sectional drawing of house connected with chassis

Compared with the ground surface of red brick or yellow clay,the ground surface of lime slag may reduce the heat−loss 61.5Kcal / m²h. So,for one year (heating 7 months),the house (30m²) can save coal 2.1 T.

b). Protecting original geological conditions are preventing thawing settlement and frost heave. Namely protecting soil conditions of common heating buildings in the ranges of the thawing plate of ± 20% span not to change.

In aspect of absorbing heat: Since the absorbing heat paramet-

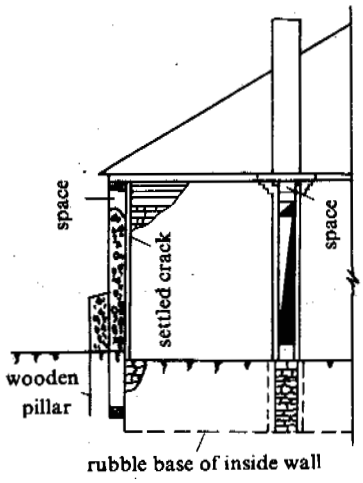

Fig.2 The sectional drawing of old wooden house

er of lime ground (0.29) is smaller than that of brick ground (0.7) ,So,the thawing settlement can be reduced 4.13m.

In aspect of heat conduction: Since the heat conductivity of pad is smaller than that of clay ground surface,So,the thawing settlement can be reduced 1.98m.

In aspect of heat diffusion: Since we lay the apron slope protection of 3m in every sides of building,which increases the radiative volume of pad,the thawing settlement also can be reduced 0.85m.

For old wooden buildings,the buried depth of wall pillar is only situated in place of maximum frost heave force.The tangent frost heave force of a pillar is about 8.4 T,and the normal frost heave force is 18 T. So,the join forces (26.4T) is much bigger than the pressure of a pillar(2.2T). In addition,according to local climatic conditions, for average 3m frost depth, the amount of repeated frost heave and thawing settlement is about 18 cm, and, for 7m thawing layer inside house,the minimum amount of settlement is 20cm over,So,the difference of 38cm between freezing and thawing can cause serious damage of buildings.

The well-entirety can prevent uneven frost heave and thawing settlement of buildings.

According to theoretical calculation, the padcan prevent completely frost heave and thawing settlement of frozen ground layer under buildings. Even some uneven frost heave and thawing settlement, the loose pebble layer can be adjusted,and the floor of reinforced concrete and the chassis connected with buildings can also be balanced. Since the chassis of inside and outside wall are connected together and do not produce relative displacement, so, the frost damage of buildings will not occur.

For old wooden buildings, since different conductivity of inside and outside wall,the inside wall is often produced crackle and damage.So, we design a settled crack with felt to inlay two triangular strip of outside wall,this method can prevent damage of buildings.

The lower cost and convenient construction

Since slag and sawdust are fairly universal in forest regions,and the base filling instead of digging is not limited by conditions,so,the cost of this type of building is lower, and the construction is also fairly convenient.But it is difficult for the old wooden building.

The foot of wall do not produce damage and form frost,and the inside house is dry and do not produce seepage.

We design a hopper of 45° on top of wall.The hopper may not only increase thickness of coldproof layer but make coldproof materials fill into space of wall at any time so that it can avoid disadvantages of ventilation in winter also.For the old wooden building,we also use this method to improve its disadvantages.

The action of eaves, dado, apron and pad are that they may either keep room drying and foot of wall not breaking etc. or prevent thawing settlement of ground surface and forming frost of outside wall etc.. But they are just serious disadvantage of old buildings.

The method by which frost damage of building can be prevented throuth filling instead of digging is only suitable for wooden buildings but also for brick buildings.

The Base of Plug-in Pile of Reinforced Concrete of Protecting Original Vegetation.

In the ice-rich zone ofswamp and tussock hummocks, there are humus soil, silt and layered ice under most of ground surface water,so,the common built method of digging groove and lining base is difficult to construct and prevent frost damage. From 1980's, according to < <Design Standard and Criteria of Base and Foundation in Permafrost Regions, in USSR > > in 1977,we design the turret pile of 30cm corner radius.Meanwhile,we still lay tussock hummocks or slag of 45cm thickness on orignial ground surface(Fig.3) to prevent damage of vrgetation. The buildings which we adapt this methodto build arealwaysgood through perennial use.

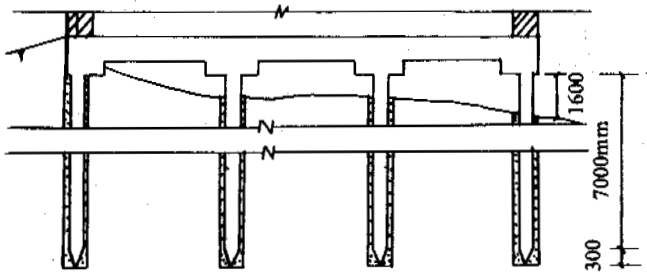

Fig.3 Ventilated and insulated base with reinforced concrete plug-in piles and whole circle beam

Concrete Cone-section Mound Base for Advoiding Frost Heave and Reducing Compressive Pressure.

In permafrost area, Tussock hummocks grow prosperly on slope, and surface water is found everywhere, while clayey frozen ground is found under tussock hummocks. It is impossible to use ideal reinforced concrete plug-in pile base, and it is uneconomical and can not avoid frost damage to use general strip base.So, a cone-section mound base with linking circle beam is selected in a new school building. Good effects are obtained, and the main causes are as follows:

Cement apron with long eaves, high doda and asphalt grouting cracks can protect not only rain water from permeating into base but also apron from cracking due to cohesion with wall during seasonal frost heaving and thawing settlement.

Raising the the ground surface by 0.45m, the heating would not affect the thawing depth.Half filling and half digging not only reduced loss and digging soil, but also was used to intersect upper slope water and to remove ground water.

Two circle beams increased the whole rigidity. and this canprevent the influence of uneven freeze-thaw on building.

Grains beside the bottom of beam can fill the soil settlement and prevent cold air from flowing into room from the bottom of the circle beam.

The air layer between floor arrise can prevent either the heat inside room from transfering to increase thawing depth, or floor and beam from decaying during air flowing.It is more important that when uneven frost heave occurs beneath circle beams, the grains below beams squeeze up cement apron outwards and push toward air layer so as to prevent circle beam from damage.

Base boundary, blind canal and seepage well are filled with grains, and no water and damage on base boundary occured.

Using elliptic cone-section mound concrete base is more economical than using strip base.The tangent and normal frost heaving force between ground and flanks of base could be cleminated because of the smooth surface and the shape of the elliptic base, meanwhile,the normal frost heaving force and compressive pressure on the bottom of base was reduced.(Fig,4)

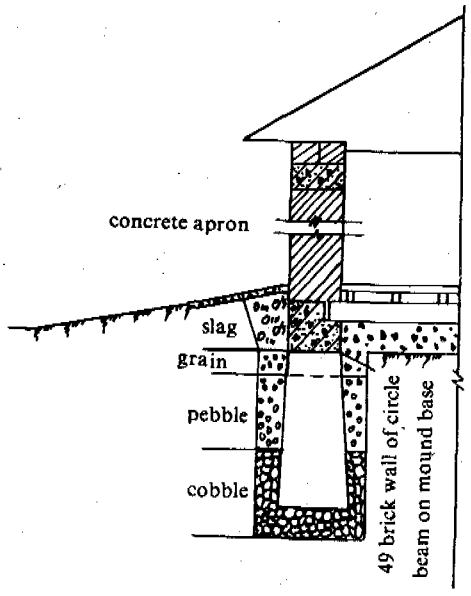

Fig.4 Profile of house with double-circle cone-section mound base

Complete Prevention and Treatment of Frost Damage on Old Buildings.

A forest bureau built a four-floor living building including a closed balcony and a brick-concrete structure in 1985. Cracks appeared due to settlement in summer of 1986.By the begining of 1988, more than ten large cracks showed on the south wall from the bottom of the wall to the arrise of the room. Doors and windows passing toward balcony were compressed to be damaged by crushed bricks. The widthes of some large cracks are more than 50mm. Although most of the widthes of the cracks on inside wall were less than 20cm, but dense cracks caused an unsafty state.

The building was originally desingned as a 2.55m high rubble base-top with a 150 reinforced concrete circle beam(40cm width, 40cm height), 14 reinforcing bars of Φ 12mm, and 2.95m deep base. However, during construction, a reinforced concrete circle beam with 49cm width and 90cm height was set up on a rubble base-top whose height was only 0.7m, and22 reinforcing bars of Φ 14mm were installed.The depth of the base is 1.6-1.7m, which is just in the range of the maximum frost heaving within 2m from ground surface. There was not measurementto prevent cooling, drainage, and refilled inside the room.A closed storage warming room was formed around heater pipe under floor. and this rapide the rate and depth of thawing of underground frozen layer inside the room. In addition, three 30-50mm soil-ice layers existed within the 2 m of the base-bottom, which caused heavy thawing settlement and cracks on the outside walls. The soil around base boundary. which was wetted by rain in autumn, resulted in frost heave in winter.Therefore. about 20cm of seasonal frost heave and settlement occured yearly, which caused vertical cracks on the outside walls. On the other hand, the horizental normal frost heaving force on the flanks of base reached to 10T / m^2, unfilled soil inside room could not support resistence. This resulted in horizental cracks on the outside walls. In later construction, it was found that many parts of under the outside circle beams were hanged in air owing to thawing settlemeht of soil,and the meximum hanged depth at both sides of southwest corner was up to 2-3m.

Combining investigation with local hydrogeological condition, the following treatments are suggested:

Avoiding frost heaving force around base boundary.

In order to prevent rain water from permeating into base to cause frost heaving force, besides raising ground surface and adding concrete apron with grouting asphalt cracks: dry slag, sandy grain, pebble and cobble are filled in order from the depth of 0-0.3m to the bottom of base. This treatment play a role of cold prevention and insulation so as to reduce the frost force on the flank of base. At the same time, underground water is permitted to permeat into blind canal to flow to hidden well.There is no water in

the dry base boundary,so there is not any frost damage.

Avoiding the thawing settlement of base bottom.

Firstly, heaters under floor are moved floor,so the heat source releasing down iseleminated. Secondly, insulated felts, asphalt felts and new floor are paved. Water on floor are not allowed premeating down to wet thebelow insulated materials, and the heat in room can not conduct down. In order to prevent floor from decaying and releasing residual heat down to floor, a few vantilating holes are built in addition to retain a air layer of 25cm beneath floor. A sawdust layer of 30cm with lime is paved on the top of filled dry slag to insulate heat and prevent thawing. By use of these measurements, the frozen layer does not settle and crack does not appear on the inside wall.

Repairing crushed brick walls.

The crushed brick walls are commonly rebuilt. Large cracks are firstly mended using high level cement mortar.After the grouting water is dry, crackse, whose widths are more than 5mm, are grouted into mixed glass–cement mortar,and small cracks of less than 5 mm are compressed into water glass. Some small cracks on walls and ceilings are smoothed with dilute cement mortar.After doors and windows are painted,the building looks like a new one.

The measurements for preventing frost heave, drainage, insulation, and preventing thawing settlement are carried out well during construction. Since the project was finished in 1989,the building has been worked well.

THE PREVENTION AND TREATMENT OF FROST DAMAGE ON CANALS

The common buried depth of local canals is 3.3m, which lies between the minimum frost depth(2.9m) and maximum frost depth(3.5m).Although the damage of seasonal frozen layer is avoided within the depth, the menace of permafrost layer of 2.5m still exists. Therefore, the shallow buried insulated pipeline is used.This kind of pipeline is made mainly by: packing polystyrene of 7cm thickness around the pipeline of Φ 150mm; packing asphalt felts and placing it on the wooden block (one cach pipe) with the size of 12cm width,20cm height and 70cm length; covering reinforced concrete semicircle pipe with the size of 1m diameter and 7cm thickness;and paving slag of 0.5m thickness and clay of 0.2m thickness(Fig,5). The 600m length pipeline,which was built according to the above method, has been running well for six years, especially in rock layer zone. This confirmed that these measurements are effective. The better methods are:(1) Replacing the connection of screw of flange plate with specific hoop, the construction would be rapidly carried out, and the tenacity to resist the uneven freezing and thawing could be strengthened.(2) Replacing alphalt felt and iron line with plastic film and nylon rope to pack polystyrene, cost could be reduced, and tenacity could be strengthened.(3)Replacing reinforced concrete semicircle pipe with reinforced concrete pipe of 0.6m diameter, construction becomes easier, and the rigidity is sterngthened when vehicles pass above the canal. A layer of 15 cm thickness (more than common ground surface frost heave 147mm, and slight less than the average thawing settlement of base)of slag is filled on the bottom and the flanks of base. This can adjust uneven frost heave and thawing settlement. The clay layer of 0.3m thickness is slight higher than ground surface. This not only prevents the top of pipeline from breaking out by behicles but also makes the drainage easy. (4) Hanging the pipeline on the wall of reinforced concrete pipe,a good air layer is maintained and penetration of ground water is avoided..

The feature of this kind of pipeline facilitates the constructing

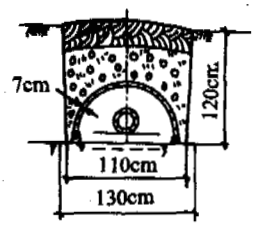

Fig.5 Cross–section of buried shallow pipeline

and repair of pipeline besides preventing frost damage.

In swamp zone with tussock hummocks, is the reinforced concrete pipeline is changed into the shape of groove, and placed on the pad of refilled grains of 0.3m thickness, and if slag is paved according to thermal requirement, and rainproof layer of clay is covered, the pipeline would be more effective.

REFERENCE

Design Standard and Criteria of Base and Foundation in Permafrost Regions, in USSR.Moscow. The House of Architecture, 1977.Translated by Northwest Institute of Chiese Academy of Railway Sciences.

Proceedings of Architectural Design(1–3).Beijing Institute of Industrial Construction, Architecture Engineering Ministry. The House of Chinese Arehitecture Industry(1973–1978).

DETERMINATION METHOD FOR THE COEFFICIENT OF THE DEGREE OF SUNSHINE AND SUNSHADE ON CANALS

Li Anguo and Chen Qinghua

Northwest Hydrotechnical Science Research Institute,
Yangling, Shaanxi, China

The coefficient (K_1) of sunshine and sunshade extent is a basic parameter for predicting frost penetration in engineering design. In order to get an accurate value for the coefficient tallying with the actual case, the total radiation on each part of the canal section and level ground in a freezing period (ΣQ_α and ΣQ) are determined respectively based on geographic latitude, elevation of the canal, local topographic conditions, trend of the canal and shape of the section. Then the coefficient on each part of the section may be determined by

$$K_d = [1 - \frac{(\Sigma Q_{\alpha\beta} - \Sigma Q) \cdot a_s}{F_o \cdot \beta}]^{\frac{1}{2}}$$

INTRODUCTION

The coefficient K_d of the degree of sunshine and sunshade is a basic parameter in forecasting the engineering-design frozen depth (Profession Standard of Water Conservancy and Electricity in P.R. China, 1991). At present an experimental method is used to obtain the value, which is rather limited and is too rough. It has been proved in practice that the degree of sunshine and sunshade in each engineering site varies not only with geographic latitude, sea level height and topographic conditions at the engineering site but also greatly with different engineering patterns. Therefore, according to the above factors and the strike of the canal and the shape of the cross section, etc., the climatology method is used to calculate respectively the total radiant amount of the sun on each part of the canal and horizontal ground in the frozen period and the increment of accumulating temperature on each part of the canal corresponding to the horizontal ground. The calculated formula of the value K_d can be obtained and the K_d can be determined accurately.

1. Determination of the Time of Sunrise and Sunset on Slope

Let $-\omega_H$ and $+\omega_H$ be the time angles of sunrise and sunset under the conditions of no terrain sheltering and at the height H above sea level. $h_{\beta\alpha}$ and $S_{\beta\alpha}$ are the height and radiant flux of the sun on the slope with slope direction β, gradiant α. When there is no other sheltering, the necessary and sufficient conditions for the sun to shine onto the slope are:

$$-\omega_H \leq \omega \leq +\omega_H \tag{1}$$

$$S_{\beta\alpha} \geq 0 \ (\text{or } h_{\beta\alpha} \geq 0) \tag{2}$$

where ω is the time angle of the sun.

Using the astronomical formula, the following can be deduced:

$$\omega_H = \cos^{-1}(-\tan\phi\tan\delta - 0.0177\sqrt{H}\sec\phi\sec\delta) \tag{3}$$

$$S_{\beta\alpha} = I(u\sin\delta + v\cos\delta\cos\omega + s\sin\beta\sin\alpha\cos\delta\sin\omega) \tag{4}$$

where, ϕ — geographic latitude;
δ — the sun longitude;
H — height above sea level (kilometer);
I — the radiative strength of the sun 1.94×10^{-2} Kcal/cm^2.min.

$$u = \sin\phi\cos\alpha - \cos\phi\sin\alpha\cos\beta$$
$$v = \cos\phi\cos\alpha + \sin\phi\sin\alpha\cos\beta \tag{5}$$

Since the necessary condition of sunshine is $S_{\beta\alpha} \geq 0$, then obviously the time angle ω_s with $S_{\beta\alpha} = 0$ is the critical angle when $S_{\beta\alpha}$ turns from the negative to the positive or turns oppositely.

Let the right side of (4) be equal to zero, the expressed equation of the critical time angle ω_s can be obtained as follows:

$$\omega_s = \cos^{-1}\left[\frac{-uv\tan\delta \pm \sin\beta\sin\alpha\sqrt{1-u^2(1+\tan^2\delta)}}{1-u^2}\right]$$
$$\omega_s = \sin^{-1}\left[\frac{-u\sin\beta\sin\alpha\tan\delta \mp v\sqrt{1-u^2(1+\tan^2\delta)}}{1-u^2}\right] \tag{6}$$

From the first part of (6) the two absolute values of the ω_s can be determined, and the symbols for the second half can be given. Supposing that the two values of ω_s are ω_{s1} and ω_{s2} separately, and $\omega_{s2} > \omega_{s1}$, since $S_{\beta\alpha} \geq 0$ is necessary for the slope surface to be exposed to the sun, we can easily see that the time angle ω_1 of sunrise and ω_2 of sunset on the slope should satisfy the following conditions:

If $\omega_{s1} \leq \omega \leq \omega_{s2}$, $S_{\beta\alpha} \geq 0$, then $\omega_1 \geq \omega_{s1}$, $\omega_1 \leq \omega_{s2}$;

If $\omega < \omega_{s1}$, $\omega > \omega_{s2}$, $S_{\beta\alpha} > 0$, then $\omega_1 \leq \omega_{s1}$, $\omega_1 \geq \omega_{s2}$.

At the same time, since it would be possible for slope surface to be exposed to the sun only when $|\omega| \leq |\omega_H|$, ω_1, ω_2 should also satisfy the following condition:

$$\omega_1 \geq -|\omega_H|, \omega_2 \leq +|\omega_H|.$$

2. Determination of the Time of Sunrise and Sunset on Each Part of the Canal

As shown in Fig.1, choosing a free point A on the trapezoid canal with the strike being γ, width of the bottom being B, depth of the canal being H_o, gradient of the sideslope being α, if the heights of both canal banks a, b do not vary greatly and the canal is very long, point A is sheltered from the sunlight by the canal and is equal to that of the two imaginary slope surfaces A_a and A_b. The gradients of them are respectively equal to the elevation angle α_a, observed from point A to the bank top in the direction of the perpindicular bank a (that is, the maximum angle of sheltering from bank a to point A or the maximum angle of sheltering on the horizon made by point A), and the elevation angle α_b, observed from point A to the bank top in the direction perpendicular to bank b. Therefore, the time angle ω_{A1} of sunrise at pont A should be equal to the later of the two imagined slope surfaces A_a and A_b, and the time angle ω_{A2} should be equal to the first of the two. In two other conditions, such as the very long canal in U shape and arc shape and the canal on the edge of the plateau, a method similar to the one mentioned above can also be used to determine the time angle of sunrise and sunset or the amount of sunshine in every day.

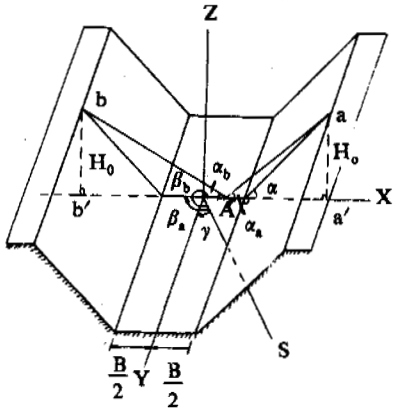

Fig.1 Sketch of the canal and related parameters (see text for details)

In Fig.1, the coordinates of points a, b, and A are: $a(X_a, Z_a)=a(B/2+H_0/\tan\alpha, H_0)$, $b(X_b, Z_b)=b(-B/2-H_0/\tan\alpha, H_0)$ and $A(X_A, Z_A)$, respectively. The gradients of slope A_a and A_b are separately $\alpha_a=(Z_a-Z_A)/(X_a-X_A)$ and $\alpha_b=(Z_b-Z_A)/(X_A-X_b)$. The azimuths of slope A_a and A_b are $\beta_a=\gamma+90°$ and $\beta_b=\gamma-90°$.

Time angles of sunrise and sunset ω_{a1}, ω_{a2} on slope A_a, ω_{b2} and b on slope A_b, can be calculated by the rule described in the first part of this paper by substituting the given data into the relative equations, and then, according to the possible condition that point A could be exposed to the sun.

$$\omega_{A1} = \max(\omega_{a1}, \omega_{b1})$$
$$\omega_{A2} = \min(\omega_{a2}, \omega_{b2}) \qquad (7)$$

The time angles of sunrise and sunset can be obtained at point A.

3. Calculation of the Total radiant Amount Directly Reaching Each Part of the Canal

The daily total radiant amount of the sun on each part of the canal and horizontal ground (corresponding to the condition that the atmosphere is completely transparent or there are no obstructions on the earth) can be calculated with the following:

on each part of canal (Fu Baopu, 1983):

$$W_{\beta\alpha o} = \frac{I_o \tau}{2\pi R^2}[u\sin\delta(\omega_2-\omega_1)+v\cos\delta(\sin\omega_2-\sin\omega_1) - \sin\beta\sin\alpha\cos\delta(\cos\omega_2-\cos\omega_1)] \qquad (8)$$

on horizontal ground:

$$W_o = \frac{I_o \tau}{\pi R^2}[\omega_H \sin\phi\sin\delta+\cos\phi\cos\delta\sin\omega_H] \qquad (9)$$

where, $W_{\beta\alpha o}$, W_o — total daily radiant amount of the sun on each part of the canal and horizontal ground.

I_o — constant of the sun, 1.94×10^{-2} Kcal/cm².min.

R — distance between the sun and ground with the sun-ground average distance as the unit.

τ — the length of time in a day (=24×60 minutes).

ω_1, ω_2 — time angles of sunrise and sunset on each part of the canal determined by the method described in the second part of this paper.

the meaning of the other signs is similar to those in the previously equations.

In any period of time, the total astronomical radiant amount is the sum of total daily astronomical radiant amount in this period.

The radiant amount directly reaching the horizontal ground can be calculated by the experience formula (Gua Guodong and Lu Yurong, 1982).

$$S_o = a + b.Q_o.S_1 \qquad (10)$$

where, S_o — total monthly radiant amount directly reaching horizontal ground, unit (Kcal/cm².month).

Q_o — total monthly astronomical radiant amount on horizontal ground, unit (Kcal/cm².month).

S_1 — average daily sunshine ratio in a month.

a, b are coefficients related to the transparency state of the atmosphere, which can be consulted from Fig.2 (Gao Guodong and Lu Yurong, 1982).

From (10) the following can be obtained:

$$S_o/Q_o = a/Q_o + b.S_1 = f \qquad (11)$$

where f is the function of atmosphere transparency on horizontal ground.

With the research of Fu Baopu, 1983, it can be known that in the range of our country, the function of atmosphere transparency above a

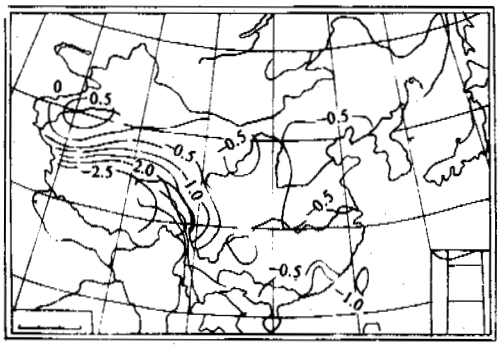

Fig.2(a) Distribution graph of coefficient a in calculting formula of direct radiation in winter (Kcal/cm²)

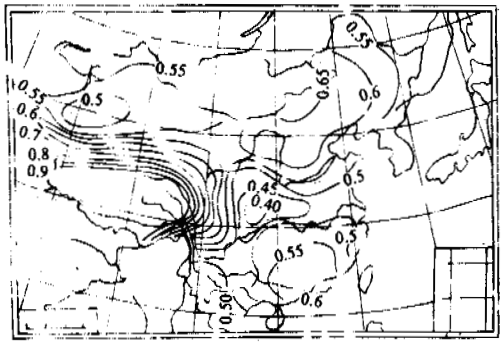

Fig.2(b) Distribution graph of coefficient b in calculting formula of direct radiation in winter (Kcal/cm²)

canal could be expressed by the function f of atmosphere transparency on horizontal ground, that is:

$$\frac{S'_{\beta\alpha}}{Q_{\beta\alpha o}} = \frac{S_o}{Q_o} = f.$$

So, the radiant amount directly reaching each part of the canal can be calculated with the following equation:

$$S'_{\beta\alpha} = f.Q_{\beta\alpha o} = (a/Q_o + b.S_1)Q_{\beta\alpha o} \qquad (12)$$

where, $S'_{\beta\alpha}$ — total monthly amount of radiation directly reaching each part of the canal, unit. (Kcal/cm².month).

$Q_{\beta\alpha o}$ — total monthly amount of astronomical radiation on each part of the canal, unit. (Kcal/cm².month).

4. Calculation of the Total Scattered Radiant Amount on Each Part of the Canal

The scattered radiant amount on the horizontal ground can be calculated with the experience formula of Gao Guodong and Lu Yurong, 1982.

$$D_o = a_1 + b_1.Q_o.n \qquad (13)$$

where, D_o — the total monthly amount of scattered radiation on horizontal ground, unit. (Kcal/cm².month).

Q_o — total monthly amount of astronomical radiation on horizontal ground, unit. (Kcal/cm².month).

n — average total cloud amount in a month.

a_1, b_1 are the coefficients indicating the transparency degree of the atmosphere, which can be found from Fig.3 (Gao Guodong and Lu Yurong, 1982).

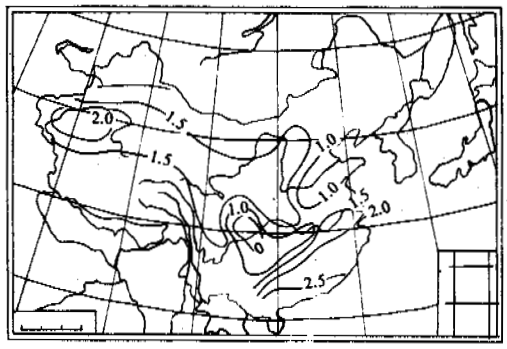

Fig.3(a) Distribution graph of coefficient a_1 in calculting formula of scattering radiation in winter (Kcal/cm²)

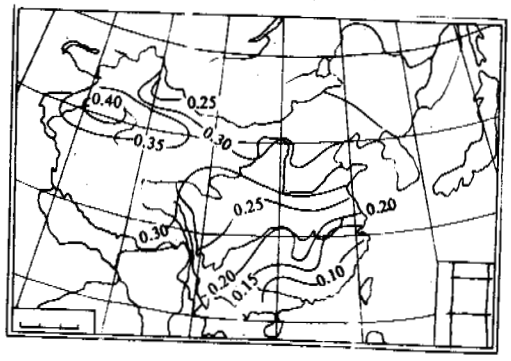

Fig.3(b) Distribution graph of coefficient b_1 in calculting formula of scattering radiation in winter (Kcal/cm²)

Using f' as the transparency degree of the atmosphere, (13) can be changed into:

$$D_o = f'.Q_o = (\frac{a_1}{Q_o} + b_1 n).Q_o \qquad (14)$$

Supposing that the scattering and the radiation are similar in all directions, the calculating formula of scattered radiation flux, by Fu Baopu, 1983, can be referred to.

$$\overline{D}_{\beta\alpha} = \frac{\overline{D}_o}{2}\left[(\cos\alpha_a + \cos\alpha_b)\cos\alpha - (\sin\alpha_a - \sin\alpha_b)\sin\alpha\right] \qquad (15)$$

where, $\overline{D}_{\beta\alpha}$ — the density of the average daily flux of scattered radiation on slope surface, unit. (cal/cm².min).

$\overline{D}_o$ — the density of the average daily flux of scattered radiation on horizontal site, unit. (cal/cm².min).

α — gradient of slope surface.

α_a, α_b are the maximum angles of sheltered area respectively from ridges a, b to the studied point.

The flux formula of scattered radiation at each part of the canal can be written in the form of:

$$\bar{D}_{\beta\alpha i}\begin{cases}=\bar{D}_o\dfrac{1+\cos(\alpha_a+\alpha_b)}{2} & \text{(slope surface of canal)}\\ =\bar{D}_o\dfrac{\cos\alpha_a+\cos\alpha_b}{2} & \text{(bottom of canal)}\end{cases}\qquad(16)$$

where, $\bar{D}_{\beta\alpha i}$ — the density of average flux of scattered radiation on any part of the canal, unit. (cal/cm².min).

α_a, α_b — maximum angles of sheltered area separately from the canal banks a, b to a certain degree.

If considering the model different in all directions, referring to the method put forward by many scholars, that the models are different in all directions is used to calculate the scattered radiation amount on slope surface and are an improvement to the models that are similar in all directions, and approximately using the corrected value given by Li Zhangqing and Weng Duming:

$$A(h_o,\alpha,n,\beta)=\frac{35.1}{697.8}F(n).\cos 1.09h_o.\sin 1.42\alpha.\cos\beta$$
$$=0.0503F(n).\cos 1.09h_o.\sin 1.42\alpha.\cos\beta\qquad(17)$$

where, h_o — average height angle of the sun at noon in the period of calculation.

$F(n)=1-(0.8n+0.02n_L)$.

$A(h_o,\alpha,n,\beta)$ — correcting value, cal/cm².min.

α — the gradient of slope.

β — the azimuth of slope direction to calculating part.

n — the average total cloud amount in a month.

n_L — the average low cloud amount in a month.

The equation to calculate the average daily flux density of scattered radiation on each part of the canal can be derived as the following:

$$\bar{D}'_{\beta\alpha i}\begin{cases}=\dfrac{\bar{D}_\alpha}{2}[1+\cos(\alpha_a+\alpha_b)] & \text{(slope surface of canal)}\\ =\dfrac{\bar{D}_o}{2}(\cos\alpha_a+\cos\alpha_b) & \text{(bottom of canal)}\end{cases}\qquad(18)$$
$$+0.0503F(n).\cos 1.09h_o.\sin 1.42\alpha.\cos\beta$$

From (18), the calculating equation of the monthly summary amount of scattered radiation at each part of the canal can be found easily using:

$$D_{\beta\alpha}\begin{cases}=\dfrac{D_o}{2}[1+\cos(\alpha_a+\alpha_b)] & \text{(slope surface of canal)}\\ =\dfrac{D_o}{2}(\cos\alpha_a+\cos\alpha_b) & \text{(bottom of canal)}\end{cases}$$
$$+0.07243t.F(n).\cos 1.09h_o.\sin 1.42\alpha.\cos\beta\qquad(19)$$

where, t — is the number of days in a month.

5. Calculating the Total Radiant Amount on Each Part of the Canal

Total radiant amount Q is the sum of the directly reaching gradiant amount and scattered radiant amount D, that is:

$$Q = S + D\qquad(20)$$

The monthly sum of total radiation on each part of the canal:

$$Q'_{\beta\alpha} = S'_{\beta\alpha} + D_{\beta\alpha}\qquad(21)$$

The monthly sum of total radiation on the horizontal ground:

$$Q'=S_o + D_o\qquad(22)$$

In a long period the sum of the total radiation is the accumulation of the total monthly amount of total radiation for every month in the period.

6. Determination of the Value K_d for Each Part of the Canal

From the beginning of calculating the frozen index to the day when its maximum value appears, with the following equations (21) and (22), separately calculating the total radiant amount on each part of the canal and horizontal ground, day after day, then accumulating them separately, the total radiant sum $\Sigma Q_{\beta\alpha}$ and ΣQ can be obtained on each part of the canal and horizontal ground in the frozen period. In the period the increment of accumulating temperature on each part of the canal corresponding to the horizontal ground surface is:

$$\Delta F_{\beta\alpha}=\frac{\Sigma Q_{\beta\alpha}-\Sigma Q}{\beta}.a_s\qquad(23)$$

where, β — thermal diffusive coefficient determined by average wind velocity (Zhu Baifang and Wang Tondsheng, 1976), unit. Kcal/m².h.°C.

a_s — thermal absorbing coefficient, taking 0.65 for concrete surface.

Therefore, the degree of sunshine and sunshade is considered by formulation, the value K_d of the revised coefficient of the frozen depth at each part of the canal can be computed as:

$$K_d=\frac{H_{\beta\alpha}}{H_o}=\frac{a.\sqrt{F_{\beta\alpha}}}{a.\sqrt{F_o}}=\sqrt{\frac{F_o-\Delta F_{\beta\alpha}}{F_o}}=\sqrt{1-\frac{(\Sigma Q_{\beta\alpha}-\Sigma Q).a_s}{F_o.\beta}}\qquad(24)$$

where, F_o — frozen index.

$H_{\beta\alpha}, H_o$ — the value of frozen depth of each part of canal section and ground surface.

For example, in Yingchuan frost-heave testing field, its geographical latitude is 38.4872, height above sea level (H) is 1.113 km, the strike of canals in the field are different in E-W, NE45°, N-S, NW45°, the size of the canals in the cross section all are 3.10 m in bottom width, 1.845 m in canal depth, 1:1.35 in slope ratio of side slope. According to the analysis of atmospheric data obtained in the last 30 years, the average frozen index is 666.7°C day, the average frozen depth is 105 cm, the frozen period is from Nov. 20 to Mar. 13, the average wind velocity in the freezing period is 1.84m/s.

On the basis of the calculating method described above, we can get the value K_d at each part of the canal, as shown in the table.

REFERENCES

Fu Baopu, (1983) Atmosphere in Mountains, Science Press, 2-65.

Gao Guodong and Lu Yurong, (1982) Balance of radiation and balance of heat on ground surface in China, Science Press, 9-36.

G.W. Partridge and C.M.R. Platt, (1976) Developments in atmospheric science, 5, radiative processes in meteorology and climatology, Elsevier Scientific Publishing Company, Amsterdam-Oxford-New York, 37-41.

Li Zhanqing and Weng Duming, (198.) The distribution and computing model of the diffused.

radiation on slopes, Acta Meteorological Sinica, Vol.46, No.3, 349-356.
Zhu Baifang and Wang Tongsheng, (1976) The temperature stress and temperature controlment of hydraulic concrete structures, Water Resources and Electric Power Press, 28-35.

SIMILARITY ANALYSIS OF MODELING TEST OF FROZEN SOIL UNDER LOAD

Li Dongqing Zhu Linnan

State Key Laboratory of Frozen Soil Engineering
Lanzhou Institute of Glaciology and Geocryology
Chinese Academy of Sciences

The article is based on the principle of similarity theory , analyzed the static question of thawed and frozen soil on similarity analysis systematically , derived the similar conditions of mechanics which modeling test of frozen soil under load must be satisfied with ;and on the basis of the conditions , we propose a approximate method of modeling test of freezing and thawing settle ment under load.

INTRODUCTION

According to the similarity analysis of modeling test of frozen soil without load(Zhu Linnan etc. 1993) ,we can write the following similar criteria of thawing and freezing modeling test without load :

$$\frac{\lambda Tt}{ql^2} \quad \text{and} \quad \frac{D\theta t}{\triangle \theta l^2}$$

where ($q = L\rho_w(\theta_0 - \theta_u + \triangle\theta)$), in which θ_u,$\triangle\theta$, θ_0 respectively are the unfrozen water content , water content of migration , and initial water content . L is the potential heat of phase change . ρ_w is the density of water , λ is the thermol conductivity of soil , D is the diffusive coefficient , t is time , l is the geometric length . In order to study the interaction between engineering building and basement soil , and the engineering stability . the article , on the basis of conclusions above , applied the similarity theory to draw the similar conditions of mechanics of modeling test of frozen soil under load , at two angles of dimensional and equational analyses , and we proposed a concrete applied method of modeling test of freezing–thawing settlement .

SIMILARITY ANALYSIS

This paragraph applied the exponental method of the dimensional analysis (Xu Ting 1982) to derive the static similarity criteria of the question of unfrozen and frozen soil and construct the similar relations . Although the stress and displacement in thawing–freezing soil are not linearly proportional to the external load , In this case , the stress σ has a relation to the load P (supposed , here only is a concentrating force P) , the basement dimensions and thickness l of soil layer , elastic coefficients E and μ , and volume weight γ . therefor , the stress in the soil can be written as :

$$\sigma = f\ (\ P,\ l,\ E,\ \mu,\ \gamma\ ) \qquad (1)$$

According to the theory of dimension , when the physical quantity y is a function of physical quantities x_1, x_2, x_3, ..., x_n , the dimension 〔y〕 of y is equal to the multiplication of dimensions 〔x_i〕 of x_1, x_2, x_3, ..., x_n. thus , if

$$y = f(x_1, x_2, x_3, \ldots, x_n)$$

and then

$$[y] = [x_1]^{a_1} \cdot [x_2]^{a_2} \cdot \ldots \cdot [x_n]^{a_n}$$

therefor , the dimension of the stress σ can be written as

$$[\sigma] = [P]^a \cdot [l]^b \cdot [E]^c \cdot [\mu]^d \cdot [\gamma]^e \qquad (2)$$

where , a ,b ,c ,d ,e are unknown exponental constants . from the dimensional table (MLT) (Xu Ting 1982) of quality , length , and time , we find all the dimensions of physical quantities above and put them into the formula (2), we can obtain

$$[ML^{-1}T^{-2}] = [MLT^{-2}]^a \cdot [L]^b \cdot [ML^{-1}T^{-2}]^c \cdot [M^0L^0T^0]^d \cdot [ML^{-2}T^{-2}]^e$$

Making a comparision between same dimensions of two sides of the above formula , we can obtain

$$a = 1-c-e, \quad b = 2c+3e-2$$

we introduce them into (2) and rewrite it as

$$\left[\frac{\sigma l^2}{P}\right]=\left[\frac{El^2}{P}\right]^e\cdot\left[\frac{\gamma l^3}{P}\right]^e\cdot[\mu]^d \qquad (3)$$

We respectively regard $\frac{\sigma l^2}{P}$, $\frac{El^2}{P}$, $\frac{\gamma l}{E}$ (from $\frac{El^2}{P}$ and $\frac{\gamma l^3}{P}$) ,μ as a quantity, according to equation(3) and taking $c=e=d=1$, we can write their functional relationship (4) , and then (4) is a dimensionless expression of the formula (1)

$$\left(\frac{\sigma l^2}{P}\right)=F\left(\frac{El^2}{P},\frac{\gamma l}{E},\mu\right) \qquad (4)$$

letting $\pi_1=\frac{\sigma l^2}{P},\pi_2=\frac{El^2}{P},\pi_3=\frac{\gamma l}{E},\pi_4=\mu$

thus (4) is rewritten as

$$\pi_1=F(\pi_2,\pi_3,\pi_4) \qquad (5)$$

This is the equation of similar criteria of the nonlinear thawing–freezing soil , where π_2, π_3, π_4 are determinational criteria .

We supposed above, there is only a concentrating force . if there are a linear load q , a areal p and a moment m , we also consider them as factors influenced on the stress , and introduce them into (1) . thus , we can arrive at similar criteria comprised of them , which is to say , the criterion $\pi_2=\frac{El^2}{P}$ is respectively inverted into :

$$\frac{El}{q}\ ,\ \frac{El^3}{m}\ ,\ \frac{E}{p} \qquad (6)$$

MODEL DESIGN

According to the paragraph two, mechanic similar criteria are:

$$\pi_1=\frac{\sigma l^2}{P},\pi_2=\frac{El^2}{P},\pi_3=\frac{\gamma l}{E},\pi_4=\mu$$

When designing model, the model must be satisfied with similar criteria of determination:

$$\pi_2'=\pi_2\ ,\ \pi_3'=\pi_3\ ,\ \pi_4'=\pi_4$$

in other words, the following criteria are equal to 1

$$\frac{c_E c_l^2}{c_P}=1\ ,\ \frac{c_\gamma c_l}{c_E}=1\ ,\ \text{and}\ c_\mu=1$$

According to the factors of the conditions of adding load, test field, workmanship of making model, etc., we take $c_l=19.1$, in order to satisfy $\pi_2'=\pi_2$. in terms of the references(An Weidong 1990; Zhu Yuanlin and Carbee 1984): tests results between the relations of the stress–strain curve and initial elastic module E of frozen soil and temperature T , we choose the case in which the soil of model and prototype have the same conditions of water content and temperature change, thus, the initial and conditions of modeling test without external load (Zhu Linnan etc. 1993) are satisfied, in this case, we regard $E'=E$, $\mu'=\mu$, then $\pi_4'=\pi_4$ is also satisfied.

From $\pi_2'=\pi_2$, we arrive at $c_P=c_E c_l^2=19.1^2$, thus, the concentrating force (to pile basement) on model, $P'=\frac{P}{c_l^2}=\frac{1}{19.1^2}P$; and according to (4) , we arrive at the areal load(to buildings) $p'=p$, the line load (to long basement) $q'=\frac{q}{c_l}=\frac{1}{19.1}q$.

From $\pi_3'=\pi_3$, we arrive at $c_\gamma=\frac{c_E}{c_l}=\frac{1}{19.1}$, thus, the volume weight on the model $\gamma'=c_l\gamma=19.1\gamma$.

According to the equation (5) of similar criteria, it is impossible to satisfy $\pi_3'=\pi_3$, because we can't find the material, the volume weight of which is 19.1 times as weight as that of natural soil, but other characters (for example E, μ, etc.,) are unchanged. we known, in the procedure of thawing–freezing and heaving of soil, the weight can't be omitted ,which is regarded as the key control factor caused the settlement of thawing. in order to satisfy the similar relations between the gravitational stresses of the model and prototype, we can approximately regard the partial gravity of the model diminished when the length scale of the model is diminishing as a additional stress of a external load. at the same time, according to the result of similarity analysis of thawing–freezing heat and mass migration, we write the similar ratioes of temperature , moisture, geometry and time:

$$c_T=1\ ,\ c_\theta=1\ ,\ c_l=19.1\ ,\ c_t=c_l^2=19.1^2=365.$$

THAWING–FREEZING MODELING TEST OF SETTLEMENT UNDER LOAD

To state the application of similarity theory and modeling test in the frozen soil, at first we use the calculation of thawing settlement to state the principle of above those paragraphs. as far as the soil of basement, whether it is thawing settlement of frozen soil or settlement of unfrozen soil, the soil body gives birth to two kinds of stresses: one is the gravitational stress; the second is the additional stress within basement, resulted from the external load. so far as undisturbanced or unfrozen natural soil, it have experienced prolonged geologic eras, and have fully consolidated under the gravity, in this case, only the additional stress under the external load gives birth to the compression and consolidation of soil body; and in the frozen soil, since there is ice , its characters of physics, mechanics and thermology are obviously not the same these

of unfrozen soil, with the result that although there is not any external load on the frozen soil(exactly speaking, under a finny load), the thawing soil body also yields a consolidation and settlement. thus, when solving the thawing settlement of frozen soil, at first we should calculate the additional stress of basement soil under the external load.

According to the theory of elastic mechanics (Xu Zhilun 1978) and geotechnics (Qian Jiahuan 1988), under a uniform load, as far as a rectangular and circle basement, below the central point, the additional stress of arbitrary point can be written as the formula

$$\sigma_z = K_z p \qquad (7)$$

where p is the uniform areal load of the bottom of basement, K_z is the additional stress coefficient relative to the dimensions of basement, depth(z) and their proportional dimensions, under the conditions whitch the dimensions of basement and the thickness of soil layer are satisfied with the similar proportion of geometry, the additional stress coefficient of the basement of model and prototype are equal, $K_z = K_z'$. in this case, according to the conditions of mechanic similarity $c_p = c_E = 1$, then, $c_{\sigma_z} = 1$. that is to say, to the satisfaction of the conditions of mechanic similarity, the additional stress in the model and prototype soil are both equal.

We have known the additional stress σ_z , then according to references and documents(An Weidong etc. 1990 and Tsytovich, N.A. 1973) , under uniform load, the thawing–settlement of frozen soil can be expressed as

$$S = A_0 \bar{H} + a\sigma_z \bar{H} \qquad (8)$$

Here A_0 is the thawing settlement coefficient; σ_z is the average additional stress of thawing compression layer; a is the thawing compression coefficient; $\bar{H}$ is the thickness of thawing compression layer.

Obviously, if the model has the same initial conditions of soil moisture and temperature change as the prototype, then A_0 and a are unchanged, at the same time, the condition of mechanic similarity is satisfied, that is to say, $C_{\sigma_z} = 1$, $c_{\bar{H}} = c_l$, thus $c_S = c_l$.

Therefor, when the external load is satisfied with the similar condition of mechanics, the ratio of the main settlement values of model soil and prototype soil is equal to the geometric proportion.

As far as the settlement value of the nonuniform frozen soil under load, we can use the method of geotechnics(Qian Jiahuan 1988) to write:

$$S = \sum_{i=1}^{n} S_i = \sum_{i=1}^{n} A_{0i} \bar{H}_i + \sum_{i=1}^{n} a_i p_i \bar{H}_i \qquad (9)$$

Since the procedure of analog simulation is the same as the uniform soil, here we do not state it in detail.

CONCLUSIONS

Under the conditions content with similarities of heat and mass migration , we added the following similar conditions of mechanics , that is :

$$\frac{EI^2}{P} \ , \ \frac{\gamma l}{E} \ , \text{and } \mu \ ,$$

are three similar unchanged quantities

(1)The linear load(q) ,the moment (m) ,and the areal load (p) of the prototype and the model should be satisfied with :

$$\frac{EI}{q} \ , \ \frac{EI^3}{m} \ , \ \frac{E}{p}$$

(2)The stresses and the displacements of the prototype and the model have the following relations:

$$\begin{cases} \sigma' = \sigma \\ S' = c_l S \end{cases}$$

In which ,c_l is the geometric scale between the prototype and the model , σ' and S' are the stress and the displacement of the model , σ and S are the stress and the displacement of the prototype .

These conditions above , gave the practicable theoretical proofs of experiments in order better to study the interaction between engineering buildings and basement soil , and the engineering stability. at same time , according to these similar conditions , we proposed a concrete applied method of modeling test of freezing–thawing .

REFERENCES

Zhu Linnan and Li Dongqing(1993) , Similarity analysis of modeling test without load, Journal of Glaciology and Geocryology 15(1) ,189–192.

Xu Ting(1982) , Similarity Theory and Modeling Test, Agromachinery Press of China, 34–62, Pecking.

An Weidong etc.(1990) , Interaction Among Temperature, Moisture and Stress Fields in Frozen Soil, Lan Zhou University Press, 244–246, Lan Zhou.

Xu Zhilun (1978) , Mechanics of Elasticity, Higher Education Press, 105–108 , Pecking.

Qian Jiahuan (1988) , Mechanica of Soil, He Hai University Press, 53–69, Pecking.

Zhu YuanLin and Carbee ,D.L.(1984), Uniaxial compressive strength of frozen silt under constant deformation ,Cold Region Science Technology , Vol.a, No.1 , pp.3–15.

Tsytovich , N.A.(1973) Mechanics of Frozen Soils. High Education Press, Moscow, 250–276.

A COMPOSITE MODEL OF MULTIPLE ACTIONS FOR FORMING PATTERNED GROUND

Li Guangpan and Gao Min

Lanzhou Institute of Glaciology and Geocryology,
Chinese Academy of Science, Lanzhou 730000,China

This paper points out that the patterned ground is a spatial ordered structure which naturally exists and is called a "dissipative structure" in the branch of nonequilibrium thermodynamics. During freezing and thawing, the soil-water system is in a state far from equilibrium and the ordered convection in non-equilibrium is formed at critical conditions because of the various actions in dynamics such as the buoyancy, the gravity, the force of migratory water caused by frozen field, the diffusion, and the surface tension, etc. The continuous actions of convection change the combination between soil particles and slightly depict spatially structural patterns of convection in ground. Each convective action alone is very weak. However their effects are enhanced when frost heave and desiccative shrink are superimposed on the processes of ordered convection. And these processes repeat again and again, finally resulting in the formation of macroscopic visible patterned ground.

INTRODUCTION

The regular polygons in permafrost ground and in periglacial environments or near water bodies in cold regions has attracted geoscientists for a century. Recently, mathematicians and physicists have also undertaken this study and have made the research range be expanded and the research content be deepened. The research includes (1) the existence of polygonal net and its characteristics (Guo Dongxin, 1990, Li Shude, 1990); (2) the environmental conditions for the formation of patterned ground, the property of polygons and its regularity (Troy L. Pewé, 1969); (3) the frozen polygons appeared again in laboratory (Edwin J. Chamberlain et al., 1979); (4) the origin and the formation mechanism of polygons (R.J. Ray, 1983); (5) Climate and environmental change information recorded by polygons (Wang Baolai, 1991).

R.J. Ray and W.B. Krantz reviewed the history of formative mechanism research on patterned ground and evaluated the theses such as the frost cracking, the desiccative and shrinking cracking and the Rayleigh convection. The crack theses have not gripped the basic problem--where the regularity originates from? R.J. Ray and others proposed their Rayleigh convection model and pointed out that Rayleigh convection is the cause for the formation of patterned ground. Through Linear stability analysis they obtained the critical Rayleigh number and the ratios of the width of polygon to the depth of seasonal frozen layer (W/L), which is 3.18 for polygon and 2.7 for parallel stripes. But they did not clearly show the process from convection cells to patterned ground and only emphasized the undulatory pattern forming by convective action at the interface between the seasonal thawed layer and permafrost. Though the physical process of this model is very simple, it is still of significant meaning.

In this paper, the stresses are payed to the formative mechanism of patterned ground using modern physics theories and a composite model of multiple actions is put forward.

THE THEORETICAL BASIS OF THE COMPOSITE MODEL FOR MULTIPLE ACTIONS

The main thermodynamic processes in ground are the heat transfer, the migration of particles and water and the convection of water. Although these processes belong to the category of nonequilibrium, but it can be determined with quasi-equilibrium when the temperature gradient ($\frac{\partial T}{\partial r}$) or the concentration gradient of particles ($\frac{\partial M}{\partial r}$) is not large. By adopting the principle of successive stable state and the Stephen boundary condition, we can solve equations of thermal conduction and calculate the depth of permafrost, the temperature field of the active layer (G.M. Feldman, 1973) and the temperature field of man-made freezing walls (Gao Min, 1989). But the equilibrium theory of thermodynamics is incapable of solving problems of the patterned ground and strong moisture migration. While the non-equilibrium theory developed recently can play an important role.

The nonequilibrium theory in thermodynamics affirms that there is a kind of macroscopic spacial and temporal ordered structure existing widely in nature, Prigogine called it "dissipative structure". It is different from ordered crystals at a molecular level. Under the conditions when open system is far from equilibrium this ordered configuration of nonequilibrium will appear (for example, if the temperature gradient is large enough). The system exchanges mass and energy with the outside environment, and it can form and keep a certain macroscopic order through the mechanism of nonlinear dynamics and the dissipative process of energy in the system itself. For example, the Benard's pattern (Fig.1) the circle in granite (Fig.2) and the order of Bio-organization. In quantita-

tive research the nonequilibrium theory is based on the mass-balance equations, the equation of momentum conservation, the equation of energy conservation and entropy-balance equation. The relationship of force X and fluxes J in thermodynamics is deduced from these equations:

$$J = LX + \frac{1}{2}\left(\frac{\partial^2 J}{\partial X^2}\right)_0 X^2 + \cdots\cdots$$

where $L = \left(\frac{\partial J}{\partial X}\right)_0$

When the system is far from thermodynamic equilibrium i.e. the force of thermodynamics is not weak, the high power of X can not be neglected and the equation is a nonlinear partial differential equation. The main work of this theory is to analyse its stability. For example, Benard's pattern, starting from mass-balance equation, momentum conservation and energy conservation and adopting the method of linear stable analyses, the Rayleigh number is derived:

$$R_c = \frac{27}{4}\pi^4 = 657.51$$

$$R = \frac{g\alpha(T_0 - T_d)d^3}{\gamma k}$$

When $R > R_c$, the Benard's pattern can be produced.

Another school of thought of nonequilibrium in thermodynamics is synergetics founded by H. Haken (H. Haken, 1982; Jin Baishun, 1982). It studies the system which is constituted by a lot of subsystems. Under certain conditions the macroscopic ordered state will be formed coordinately by the interaction and cooperation of the subsystem. The parameters describing the macroscopic order degree of the system are called order parameters. Through analyzing the stability of equations of order parameters for various processes, the results and evolutionary processes at the critical state can be obtained.

ACTUAL EVIDENCES AND THEIR CHARACTERS

There were many data of patterned ground in the literature about permafrost and periglacial environments. We selected some photos as are example, the polygons in natural environments are shown in Fig.3, 4 and 5, the frozen polygons of simulating tests in laboratory are shown in Fig.6. Though there are a few photos, they are enough to identify the existence of the patterned ground.

The photos obviously show that the patterns are very regular. The patterns are generally hexagons or other polygons or paralled stripes, the shape mainly depends on environmental conditions. According to literature, these patterns are formed on seashores and lakesides or at the drying lake bottoms or in regions which have had rich water historically. These areas not only are severely cold but also have warm seasons. It is a miracle for the desert field to have such regular patterns. It is obvious that these patterns are not man-made, so they are called self-organization patterns. It is undoubtful that the reasons for their formation are the opening of the system or the unbalanced temperature and water content. This coincides with the formation conditions of the macroscopic ordered configuration in nonequilibrium and nonlinear thermodynamics. Therefore, we need not feel puzzled by this phenomenon, it is just a dissipative structure existing in nature.

SOME MAIN TYPES OF ORDERED CONVECTIONS

Soil is a complex mixture mainly made of particles of silicate minerals, water and void. There are many physical and chemical actions between soil and water. Soil influences the frozen threshold and conductibility of water, and the surface soil particles can absorb water. The freezing and thawing of water can compress or loosen the soil-body. Compared with soil, water is a very active factor. Because the bulk of water can move (convection), the water molecule can diffuse and water phase change can occur. Thus various phenomenons of the water-soil system have strong relation to the water actions.

The types of water convections in the soil-water system are different in dynamics because it is caused by different acting forces under different conditions. But ordered convections in physics have a common point which is the nonequilibrium phase change (second phase change) and the mathematical models are similar. When the temperature gradient is larger and the system exceeds the critical state, the regular structure of convection would occur mainly by the action of buoyancy-gravity. That is only one kind of the ordered convections. Similar to that in R.J. Ray's literature, when the frozen ground is thawing, it is assumed that the ground surface is at or near 277°K and the interface between frozen and thawing ground is at 273°K. According to the character of water, the density of upper water is large and the gravity is larger than buoyancy, the upper water will tend to sink. The density of lower water is small and tends to rise. But it cannot move in both opposite directions at the same place and time. Under the influence of other factors (such as permeability) the water movement would appear in a regular distribution (Rayleigh convection). As shown in Fig.7(a), the neighboring water flows of the convection circle have an opposite direction. According to analysis of Bernard's pattern, hexagonal convections should be in the form shown in Fig.7(b). The striped pattern of convection is shown is Fig.7(c).

The convection patterns can also appear in freezing process. The frozen polygon shown in Fig.6 was formed in a horizontal direction in laboratory, this study showed increased permability in a vertical direction during freezing and thawing (Edwin J. et al., 1979). These results make known the existence of ordered convection. It isn't doubted that during the freezing period, the soil-water system is in a nonequilibrium state and may be in a state of strong nonequilibrium. It had been known for a long time that water migrates to the freezing front (Kinosita seiiti, 1985; N.A. Cytovich, 1973). No matter what the mechanism of migration is, we can think that a kind of forces acts on the water in the thawing region with direction to the freezing front. In literature (Li Guangpan, 1982) it is calculated that the value of binding energy of ice is larger than that of water. Binding energy takes a negative sign, so the potential energy of water is higher than that of ice. From the water of high temperature to the water near the freezing point and then to the ice, the potential energy forms a varying potential field. According to the relationship of potential ϕ and force F,

$F=-K\frac{d\phi}{dL}$, the force should point to the ice surface. Under the action of this force, the water migrates to the freezing front and accumulates there and as a result the water increases there. Taking the downward freezing from the ground surface to underground in winter as a example, first, the water migrates to the freezing front, and after water far from the freezing front had migrated, the water migration becomes difficult. The water content of the freezing front may be larger than that at the bottom, the diffusion from top to bottom will appear. At the same time the gravity is a downward force, therefore the feedback system of dynamics will be formed. These factors as a whole constitute the basic conditions for the forming of a macroscopic ordered structure and the basic conditions are proved by the theory of nonequilibrium thermodynamics. Under the influences of other factors, ordered convection will be formed.

The third kind of ordered convections in soil is caused by surface tension. In laboratory test were conducted by heating the thin liquid layer with a thickness of 50 micron and a hexagnol pattern was also observed. The ordered and dried cracking polygon at the bottom of pools could appear in the field after the pools dried up in summer. In the evaporating process of the soil-water system, the water rises along the capillary because of the action of surface tension. This leads to a change of water content at various soil layers. Accompanied by the downward gravity action, it constitutes a feedback system of dynamics in nonlinear and nonequilibrium states and the ordered convection therefore appears. The actual cases could be very complex. Such as the decreasing of surface temperature during the night, the buoyancy of water is smaller than gravity which may lead to an increasing downward force.

At present the theoretical analyses are to assess critical conditions for the formation of ordered patterns, that is to analyse the stability of stable state solution for the differential equations and to find the critical conditions of losing stability. What kind of realistic macroscopic structure will appear is relative to the boundary conditions and the realistic dynamic processes, and it is very difficult to calculate. If the principle of synergetics is utilized and the consider that we patterns in the nonequilibrium system are relative to synergic consistency of the subsystems, then it is easy to explain the reason to the formation of hexagonal nets of the water convection. The water molecules link in the tetrahedral structure that belongs to the hexagonal system (Fig. 8). The molecules of laminary silicate are also joined by hexagonal nets (Fig.9). These hexagons in the subsystem may be relative to the hexagonal in the soil-water system in a certain way, just as the snow-flake is always hexagonal.

A COMPOSITE MODEL OF MULTIPLE ACTIONS

First, the multiple and composite actions mean that the action of formed patterned ground not only is the ordered convection but also must be accompanied by other processes of physical actions. Second, the ordered convections of water are caused by buoyancy or by the actional force of freezing field or the surface tension as mentioned-above. When the soil-water system is far from equilibrium, the ordered convection of water is the origin of the formation of patterned ground, but its not the sole reason. Before the ordered convection appeared, the water distribution can be regarded as nearly homogeneous (at least it is true at the same layer), the water distribution becomes nonuniform after the convection started. In Fig.7(b), the water flow in the boundary of the hexagon centralized more and joined the strips. Though the water flow in the centre of the hexagon is also centralised, it is only an isolated region and the action of water flow is not stronger than that at the boundary. The water flow slightly scours out the soil. In general, the convection not only exists in transient, but continues for a time and is repeated many times. The results of prolonged action make the combinations between particles in soil became relaxed and the structural patterns of nonuniform distribution of water are slightly carved in the soil body. But this action is very weak, the obvious and macroscopic patterns can not appear. When other actions or processes superimpose on the above action in the soil-water system, the original and cutting traits can be enhanced. The superimposing action may be the freezing or the dry shrinkage. During the freezing period the ordered convection and phase change in the equilibrium (ice up) are simultaneously. In places where the water flow is centralized there is a lot of ice. The volume of ice expanded the distance between particles of soil there. The large voids can contain a lot of water. When environmental conditions do not change basically, the convection of water will appear at the same place the next year (next freezing period). The more the non-uniformity of water, the more water in the boundary. Year after year, this process cycles several times to form more large cracks, the macroscopic ordered pattern then appears. The freezing force may be large and then soil body can be sunk in thawing. Through several cyclical processes of freezing and thawing the rock underground can be moved to the ground surface. In the drying processes, the soil body gradually loses water content and will shrink. The shrinking and the ordered convection are also in progress simultaneously. The water greatly influences the soil body in the boundary of the convection pattern, therefore the combinative force between particles of soil is relatively weak. So in shrinking processes it is easy to form the tiny cracks in the boundary. According to the principle of fracture mechanics, once the cracks appeared, it can be developed quickly. The cracks developed along the boundary of convective patterns can form the ordered patterns in the macrocosm. The above-mentioned, the buoyancy-gravity, the acting force of freezing-diffusion and gravity or the surface tension-gravity etc. caused various types of ordered convections, these convections and frost heave or the dried shrinking superimpose on each other and repeat their action on the soil system, these actions repeat again and again and finally the ordered ground patterns in the macrocosm are formed. That is the composite model of multiple actions.

ACKNOWLEDGEMENTS

The works of Prof. Cheng Guodong, Associate Prof. Guo Dongxin and Mr. Li Shude helped us to put forward this model. Mr. Guo Dongxin and Mr. Li Shude and Ph. D. Zhao Xiufeng provided photos for this paper. The authors wish to acknowledge their support here.

REFERENCES

Edwin J. Chamberlain and Anthony J. Gow (1979) Effect of Freezing and Thawing on the Permeability and Structure of Soils; Engineering Geology Vol.13, 73-92.

G.M. Feldman (1973) The Calculation Method of Temperature Field on Frozen Ground (in Russian)

Guo Dongxin, (1990) The Permafrost of China, Gansu Education Press.

Gao Min, (1989) Mathematical Model of the Variation of Freezing Wall with Double Circle of Freezing Pipes and its Numeral Calculation; Proceedings of the Third Chinese Conference on Permafrost, 395-399.

H. Haken, (1983) Synergetics and its Recent Realms of Application; Nature Journal Vol.6, No.6, 1983, 403-410 (in Chinese)

Jin Baishun, Zhang Jiyue and Guo Zhian, (1982) Synergetics-A New Subject; Nature Journal Vol.5, No.3, 1982, 189-195.

Kinosita Seiiti, (1985) The Physics of Frozen Ground (in Japanese)

Li Guangpen and Gao Min, (1982) Study on the Calculating Method for Bound Water; Soils Vol.14, No.1, 20-24.

Li Rusheng, (1986) Non-equilibrium Thermodynamics and Dissipative Structure; Qinghua University Press.

Li Shude and He Yixian, (1990) Features of Permafrost in the west Kunlun Mountains; Proceedings of Fourth National Conference on Glaciology and Geocryology (selection), 1-8.

N.A. Cytorich (1973) The Mechanics of Frozen Ground (in Russian).

Ray R.J., W.B. Krantz et al., (1983) A Model for Sorted Patterned Ground Regularity; Journal of Glaciology, Vol.29, No.102, 317-337.

Ray R.J., W.B. Krantz et al., (1983) A Mathematical Model for Patterned Ground: Sorted Polygons and Stripes and Underwater Polygons.

Troy L. Pèwè (1969) The Periglacial Environment, Montreal, McGill-Queen's University Press.

Wang Baolai, (1991) Some Advances in Periglacial Environment Studies: Journal of Glaciology and Geocryology, Vol.13, No.3, 273-280.

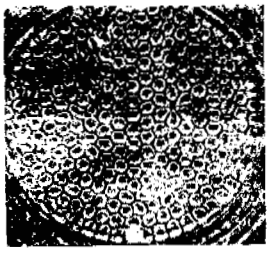

Fig.1 Benard's pattern

Fig.2 The circle in granite

Fig.3 Grassy circle caused by frost heave in Qinghai-Xizang Plateau (photo taken by Guo Dongxing)

Fig.4 Patterned frozen ground in the Aksaygin Lake (photo taken by Li Shude)

Fig.5 Sorted frozen polygon in Qinghai-Xizang Plateau (photo taken by Zhao Xiufeng)

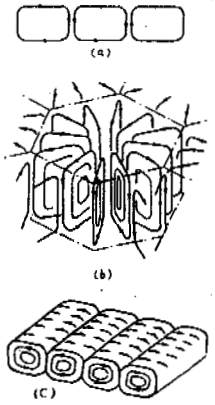

Fig.7 Schematic drawing of the circle of water convection in soil

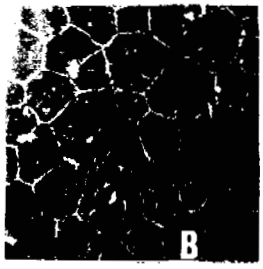

Fig.6 Frozen polygon appeared again in lab. (photo selected from Literature of Edwin J. Chamberlain et al. 1979)

Fig.8 Schematic drawing of hexagona cell (The combination of water molecules is a tetrahedral arrangement and belongs to a hexagonal system)

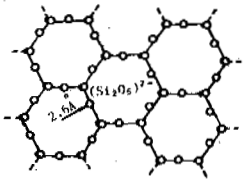

Fig.9 Schematic drawing of microstructure of laminary silicat

CONSOLIDATION OF DEEP LAYERFROZEN SOILS IN TRIAXIAL TESTS

Li Kun Wang Changsheng Chen Xiangsheng

Central Coal Mining Research Institute, China

Before triaxial shear test, the results of the deep layer frozen soil tests are greatly effected by the consolidation or non-consolidation of the sample. The paper qives the preliminary conclusions of the consolidated and non-consolidated samples, and Comparison belween the consolidated samples before and after freezing. According to these resuots, the authors propose thet before the triaxial test the samples should be tested with hydrostatic pressure consolidation, so that the earth pressure is molded as much as possible after the sample reached the original density, so thar the test results are more reliable. Clayey soil samples should be consolidated before freezing and samdy soil samples should be consolidated after freezing.

INTRODUCTION

The method of artificially freezing ground has been widely used in sinking shaft engineering in soft and friable soil layer regions. Under ground the freezing wall is in a three dimensional stress state.In order to understand frozen soil characteristics in a three dimensional stress state it is necessary for frozen samples at different depth to be taken for mechanical test. As soon as the samples are taken out of the ground, the volume will expand as the three dimensional pressure disappears, the unit weight will decrease with the volume expansion. Generally speaking, the frozem soil triaxial shear strength increases with the unit weight increasing. If a sample can not recover its original unit weight, the triaxial shear strength will be lower than the "real" strength. This is more evident when the original sample is replaced by a remolded sample. It is improbable that remolded samples containing air can be avoided, the original structure of these samples has been disrupted. Due to the air content, the triaxial strength of the remolded samples is lower, it can not reflect the real strength.

The deeper the soil layer is, the larger the geostatic pressure and unit weight are. If the samples are not consolidated, the error between the triaxial strength of the remolded sample and the "real" strength will increase. The above mentioned tests are different from those in the shallow layer.

To reduce the error between ground samples and remolded samples, consolidation tests should be conducted, so that the original pressure state can be molded and the unit weight can be as close as possible to the original. Hydrostatic pressure (P) of consolidation tests is usually calculated with the heavy liquid theory, i.e.:

$$P = 0.13\,H \qquad (1)$$

where, P — lateral earth pressure; MPa

H — depth of sample; m

Another method to attain the value of P is to measure the lateral earth pressure with a pressure transducer, the method is more expensive and takes more time. In these tests the anthors found the consolidated hydrostatic value by calculatiog with Formula (1).

PRELIMINARY RESULTS OF THE TEST AND COMPARISON

Sample size: diameter $\varphi = 61.8$mm, height h = 150mm, Natural unit weight:$r = 19.012 KN/m^3$, Water content:W = 32.03%, Soil type: clay.

The tests were conducted on the FS-1 triaxial sheer (creep) machine, the machine was made in Beijing Research Institute of Mine Construction. The samples were taken from Jining, Shandong Province, The samples were frozen clay and the depth of the samples was 170 m. The tests were conducted under the following three conditions:

(1) Freezing-unconsolidated (FUC) triaxial shear test;

(2) Freezing before consolidation (FC) with exhausted and undrained triaxial shear test;

(3) Consolidation before freezing with exhausted and undrained (CF) triaxial shear test.

Thetriaxial shear testswere conducted respectively for conditions (1) FUC, the samples were frozen at −30°C for 48 hours, then were stabilized at the appropriate test temperature −10°C for 48 hours; (2) FC, the first two steps of sample preparation are the same as in (1), after this the samples were consolidated under constant pressure; (3) CF, the samples were consolidated at room temperature, then were frozen at the test temperature under constant pressure for 48 hours.

The consolidation time depends on the arrival of the principal consolidation point, during tests the consolidation condition of the

specimen was demonstrated by the liquid volume entering the pressure cell under consolidation pressure, The relationsthip between the liquid volume (△L) entering the pressure cell and time is shown in Figure 1. The principal consolidation point and principal consolidation time can be obtained from Figure 1.

It can be seen from Figure 1 that the regularity of the two consolidation curves is almost the same or Similar Curves 1 and 2 indicate consolidations under conditions (1) and (2) respectively. The volume changes of the two curves are different. Curve 2 is below curve 1, thisshows that the volume compression of curve 2 is more than that of curve 1, but the difference is very small, about 2–5 ml, the principal consolidation time is close as well. After the principal

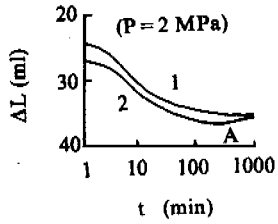

Fig.1 Clay consolidation curve
(1——consolidation after frozen)
(2——frozen after consolidation)
(start from A)

consolidation point of the curve 2 appears for 1–2 hours, the sample was frozen under constant pressure at the temperature of −10°C. From A the curve starts to bend upwards, it shows that the liquid is squeezed out from the pressure cell, and indicates that the sample was frozen and the volume also expanded. Curve 2 is below curve 1, the unit weight of sample CF is slightly larger than that of sample FC. If we want to obtain the failure curve of frozen soil in triaxial shear tests, 2–3 Mohr's circles are usually needed. To attain the goal there are several types of loading. In tests a group of Mohr's circles are obtained with changing confined pressure. Each sample was tested under three different confined pressures, the middle one of the three confined pressures is the pressure born by the sample under ground. Under conditions FUC, FC and CF, the triaxial shear test results are plotted in Figure 2.

From Figure 2 it is clear that the difference of the test results is due to different test conditions. This difference is reflected mainly in the cohesion C of the frozen clay, the angle of internal friction hardly changes with the test conditions. The cohesion C is of the folliwing rule: $C_{CF} > C_{FC} > C_{FUC}$. In the artificial freezing sinking engineering, the earth is frozen under earth pressure, however the condition CF is similar, so that triaxial test result is clise to the real value under this condition. The condition FC and FUC don't conform with the condition of the artificial freezing earth layers, there is a significant difference between the test result and the real value.

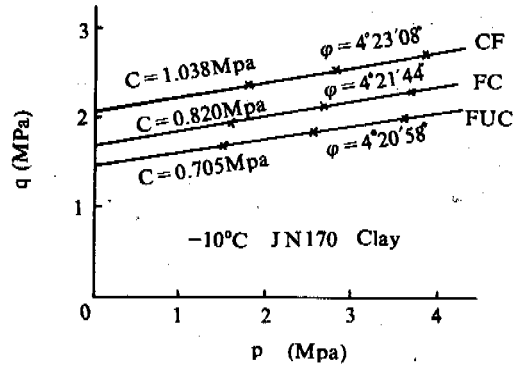

Fig.2 Triaxial shear yield line of frozen clay

C_{CF} reaches a maximum value under three conditions, one of the main reasons is the unit weight under this condition. From Figure 1 it can be seen that the unit weight of sample FC is less than that of sample CF.

In triaxial shear tests the difference of the test conditions affects only the cohesion C. with the Drucker–Prager law it doesn't affect the value of β, but affect the value of K_f, i.e.:

$$K_f = \frac{\sqrt{3}C\cos\varphi}{\sqrt{3+\sin^2\varphi}} \tag{2}$$

$$\beta = \frac{\sqrt{3}\sin\varphi}{\sqrt{3+\sin^2\varphi}} \tag{3}$$

Drucker—— Prager law is

$$\beta I_1 + \sqrt{I_2} = K_f \tag{4}$$

where I_1 is the first invariant of the stress, I_2 is the second invariant of the stress, β is a parameter, K_f is a yield value.

From Equation 4 it can be seen that the difference of the test conditions affect directly the yield value.

Recently, triaxial shear tests were conducted in frozen clay from (No.305) Chen Si Lou Mine, the clay lay at a depth of 305 m, through the test comparisons the tendency was found to be the same as those mentioned above.

In addition, the difference of the test conditions affects the relationshipof stress–strain as well, however an essential change doesn't occur, only the constants differ.

SUGGESTIONS

From above it is known that the yield values of the triaxial shear strength change with the test conditions. When the frozen soil was measured in the laboratory, the testing conditions (including stress state, freezing pattern, water content, etc.) in situ should be simulated as much as possible, so that more reliable data in accordance with the in situ testing are obtained, which can bemore

dependably applied to engineering. The condition CF accords well with the test circumstances of the ground sample, but the condition FC and FUC have a large difference, for this rsason it can be deduced that the other two conditions are not quite in accord with the real circumstances. Therefore, for the triaxial shear strength of frozen soils in deeper qround, the test conditions should be considered. The most suitable condition is the condition CF.

For flow sand in ground layer the condition CF can not reflect the real value, if the test is conducted under the condition CF the water will be squeezed out from the sample, therefore the test results will be affected. So, the authors suggest that for sand samples, freezing should be prior to consolidation, in case the test results lose their true value.

This paper gives only the preliminary test results, and provides the information for scientiffic discussion.

The authors hope that the triaxial shear test can be perfected and more unified.

REFERENCES

ChengXiangsheng, 1988, Mechanical Characteristics of Artificial Frozen Clays Under Triaxial Stress Condition, Ground Freezing 88, pp 173–179.

Huang Wenxi, 1983, Engineering Properties of Soil

PERMAFROST AND PERIGLACIAL LANDFORMS IN KEKEXILI AREA OF QINGHAI PROVINCE

Li Shude and Li Shijie

Lanzhou Institute of Glaciology and Geocryology,
Chinese Academy of Sciences

Kekexili area is located in the hinterland of Qinghai-Xizang Plateau, where the mean elevation is more than 5000 m. Climate is arid and cold, the freezing period is as long as eight months, and mean annual air temperature ranges from -4.1°C to -1.0°C. Mid-low latitude, high elevation permafrost is special to China, the formation of permafrost is controlled by the height, the thickness changes from 1 m to 128.5 m and much more in rock mountains. The geological tectonics and surface water body induced taliks, permafrost was formed during the late glaciation and neoglaciation, and periglacial landforms are widely distributed in this area.

1. PERMAFROST

The Qinghai-Xizang Plateau is called the third pole of the globe and is famous for its lofty heights, special geological and geomorphological conditions and natural environment. Permafrost, is a product of the natural environment evolution during the forming process of the plateau, and is widely distributed. Climate and the natural environment have brought about various changes with the uprise of the plateau.

Kekexili area, with mean elevation of 5000 m, is located in the hinterland of the Qinghai-Xizang Plateau, where the climate is arid and cold and terrain is lofty. The height ranges from the maximum peak Bukaleike summit of 6860 m (also called Xinqing summit) to the lowest site in the south piedmont of Kunlun mountains, transcending Bekaleike mountain to Hongshui River bend, where elevation is 4200 m.

The studied area extends northward, to the main ridge of mid-Kunlun mountain, southwards to the Geladantong glaciers in Tanggula Mountains, east as far as the Qinghai-Xizang highway, and westward to the boundary of three provinces or regions: Qinghai, Xizang and Xinjiang (Fig.1). The area is approximately 0.83 million km^2.

Kekexili is the most intact area of preserved plateau surface on the plateau and also is the most developed area for permafrost. The cold and arid environment and thermal conditions provide a good condition for the formation and development of periglacial geomorphologics and permafrost.

1.1 Distribution, Temperature and Thickness of Permafrost

This area is more than 500 km long from south to north, about 400 km wide from east to west. Permafrost is continuously distributed and occupies about 90 per cent of the investigated area, and permafrost can be subdivided into five zones from north to south.

(1) Ice, snow and perennially frozen rock in the lofty mountains of Kunlun ridge, where there are many modern glaciers, and the mean annual ground temperature is below -3.5°C. The thickness of permafrost exceeds 120 m and approaches 400 m in the rock mountains.

(2) Permafrost zone within the drainage basin of the high plain within Chumer River on the south piedmont of Kunlun mountains, where, the mean annual ground temperature ranges from -1.2°C to -3.5°C and permafrost is from 40 to 100 m thick.

(3) Permafrost zone in hills and high mountains (more than 5000 m) such as, Kekexili hill, Wulanwula, Wuerkewula, Dongbule, Fenghuo Shan and Wudaoliang, where mean annual ground temperature is -1.4 to -4.0°C, and permafrost is 36 m to 120 m thick. Ground ice is a well developed periglacial form and appears widely.

(4) Permafrost zone in the expanse of the valley and basin in Tuotuo River, where mean annual ground temperature changes from zero degrees to -1.0°C and permafrost is 1 m to 50 m in thickness. There are fluvial and permeable taliks occurring within the zone.

(5) Perennially frozen zone in lofty mountains of Geladandong in Tanggula ranges, where the height is more than 5000 m, mean annual ground temperature ranges from -1.7°C to -4.5°C. There are a lot of modern glaciers and well developed ground ice. The thickness of permafrost changes from 10 m to 128.5 m and reaches 300 m on mountain rocks (see Table 1).

1.2 Ground Ice and Cryotexture

Ground ice forms an important but variable cryotexture of frozen ground and occurs regularly in the upper layer of permafrost in this area, such as the density, network and layer cryotexture, and layer cryotexture of them is common. The variable ice layer is from a few millimeters to several meters thick, alternately occurs in

the upper layer of permafrost, ice layer with the level bedding regularly develops in the lacustrine sediments of Chumerhe high plain, and changes from a few centimetres to tens of centimetres (Zhou Youwu, 1981). The ice layer, 10 to 12 cm thick was found at the depth of 20.6 m in the lacustrine sediments near No.68 maintenace station of Qinghai-Xizang highway. The volumetric ice content of permafrost approximates 30 to 50 per cent. The ground ice can be subdivided into three types in this area, by their formation conditions and distribution features. That is cemented, segregated, buried glacier ice and fissure ice.

1.3 The Formation and Development of Taliks

The causes of the formation of taliks in this area are complex. The formation and evolution and characteristics of taliks are controlled by the climate, environment, geological tectonics and hydrogeologic and surface cover conditions. Geological tectonics is an underground factor that always influences on taliks. Based on the predominant factors determining the appearance and existence of taliks, the taliks in this area can be divided into three classifications as follows:

1.3.1 Tectonical talik

This type of talik is related to the tectonical faulting and magmatism, it is formed when heat ground water arises along the fault zones and brings about heat influences around the stratum. It often occurs in the faults in the south of Kunlun Mountain ridge. For example, there are a lot of hot springs in the south pediment of Buhadaban Peak (temperatures up to 90°C), it is estimated that the talik extends more than 200 m from south to north; others, such as, the talik extending from Tanyang Lake to Hongshui River.

1.3.2 Talik of surface water

This type of talik was formed due to the thermal influences of surface water bodies on permafrost, it is also subdivided into fluvial and lacustrine taliks by the category of water body and the features of talik. For perennial rivers,the river surface is frozen during winter but river water still flows. The heat transmission and insulation from the water body causes linear talik to form in the beds and laterals of rivers. There are fluvial taliks under Tuotuo River, Tongtian River and Buqu River, and the one in Tuotuo River is as wide as 875 m, and is the largest one on the plateau (Qiu Guoqing, 1982; Shang Jianyi, 1982 and Guo Dongxin, 1982).

1.3.3 Permeable and radiation talik

The formation of this type of talik is a result of atmosphere precipitation permeation and solar radiation. Such as those in the terrace with sandy sediments on the north bank of Tuotuo River, crescent dune near Wuxijin lake and in bare gravel surface in the valley of Buqu River.

The presence of the taliks mentioned above causes the integrity and stability of permafrost to be damaged, the continuity, temperature and thickness of permafrost to be disturbed and complicated.

1.4 The Development History of Permafrost

Many data (geologic, geographic, paleontological palso-glaciers and palao-preglacial) have shown that the mean height of the plateau was about 2000 m in early Pleistocene, 3000 m in mid-Pleistocene and 4000 m in late Pleistocene.

Evidence of glaciation in the high plain of Chumer River, and involution layers in lacustrine sandy clay in Kunlun Shan pass, dating to about the early Pleistocene, indicated the glacial and preglacial environment existed on the plateau in mid-Pleistocene, when permafrost was expansive. After glaciation of mid Pleistocene, air temperature rose and deglaciation commenced. Air temperature at that time was higher by 11°C than at the present, in Qingshuihe area, permafrost has been disappearing mostly, with the exception of the high mountains. The air temperature decreased again in the beginning of the late Pleistocene when the glaciers advanced, for example, the Zhufeng glaciation. The second or third glaciation had occurred in Kunlun and Tanggula Mountains. Although we found no evidence of Pleistocene glacier advancing in Kekexili area, it is a fact that periglacial environment covered this area at that time. As a result, permafrost expanded, other evidence for this are sand wedges in the No.2 terrace of Tuotuo River (dating 23500±1200 ^{14}C B.P.), and sand and gravel wedges were also found in the No.2 terrace of Chumer River, Gangqiqu, Mazhangcuoqing, Tongtian River and Buqu River. About 3000-1500 year ago (Zhou han cold stage) neoglaciation commenced on the plateau. The ground was refrozen and coincided with the perennially frozen layer formed during the late Pleistocene. The hole in Xidatan indicates that the permafrost layer and underlain humus 4.4 m thick were formed during neoglaciation: on the No.1 terrace of Nachitan, involution developed in the upper layer of sandy soil with charcoal fragments which gives a date of 4910±100 ^{14}C years B.P. indicating it as the north lower boundary of permafrost during neoglaciation (Pu Qingyu, 1982).

1.5 Cooling Soil

There is a special soil occurring in the dried and seasonal lakes of this area. A grey or grey white salinized soil, underlying the silt and sandy clay of the lacustrine or fluviolacustine facies, with 30-40 percent moisture content and high salt content, measurements show that it will freeze at temperatures below -4°C — -7°C.

2. PERIGLACIAL LANDFORMS

Due to the circulation of freezing and thawing a lot of cryogenetical phenomena were formed in the active layer and upper part of permafrost in the expansive permafrost region. The development and movable process of periglacial landforms are mainly controlled by the exogonic force, whose property is related to the special height and geological-geographical factors in this area. Based on the dominant action forming the varied periglacial landforms, which can be divided into seven classifications including more than 70 forms which are presented as follow (Fig.1).

2.1 Frost Mounds

Both perennial and seasonal frost mounds develop in this area. Such as those in the basin of Kunlun Mountain pass, in the headwater of Yema River and in the gorge and divide between Gangqiqu and Mazhang Cuoqin. The famous perennial frost mound in the basin of Kunlun Mountain pass, is up to 18 m high, 140 m long, and 45 m wide. There are two depression from the mound

Map of Periglacial Landforms in Kekexili Area

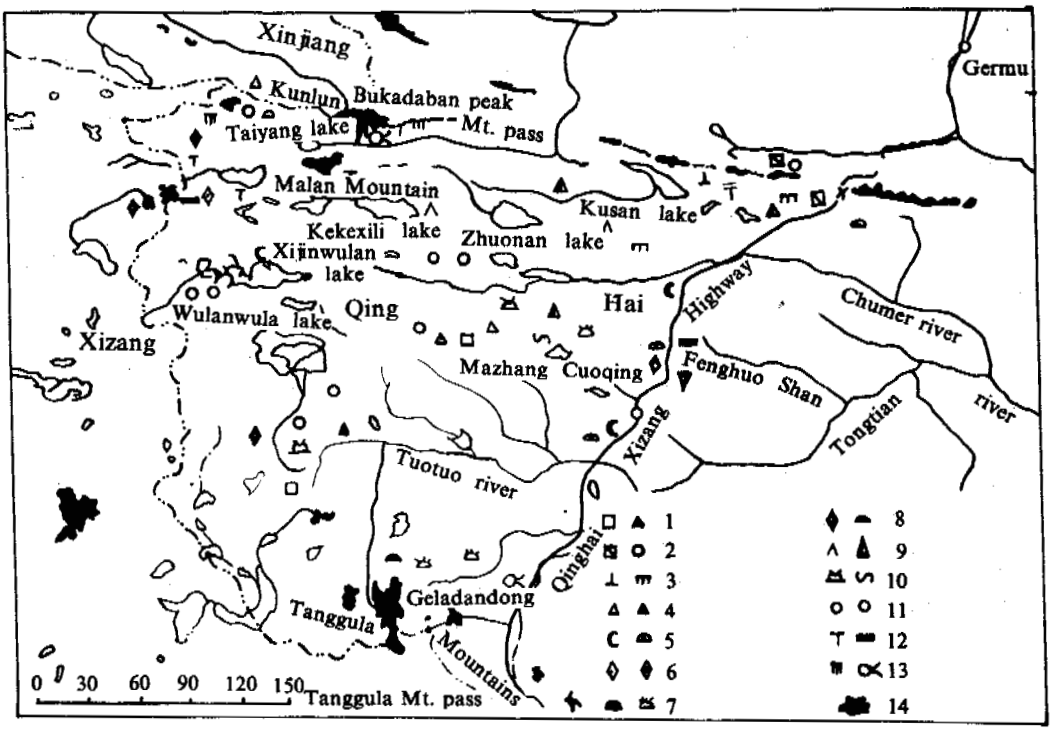

1. rock streams block field; 2. block slope rock glaciers; 3. periglacial pillar periglacial loess; 4. debris cone icing; 5. sand dune solifluction tongue; 6. macro sorted circles micro sorted circles; 7. frost mound earth hummocks; 8. patterned ground palsas; 9. frost block wedge shaped body; 10. explosive frost mound involution; 11. settlement lake settlement depression; 12. glaciofluvial terrace massive ice; 13. periglacial castle hot spring; 14. glacier.

General Table of the Seasonal Thawing Depth and the Temperature and Thickness of Permafrost in Kekexili Area, Qinghai Province

Site	Latitude (N°)	Elevation (m)	MAAT (°C)	MAGT (°C)	Thickness of permafrost	Seasonal thaw depth (M)
Kunlun Shan	35°40'	4800-5000	below -3.5	-2.8 — -3.5	75-100	1.5
Chumer River	35°20'	4480-4500	-6.2	-1.2	40	2-3
Wudaoliang	35°15'	4610	-6.5	-1.4	36-60	3-3.2
Fenghuo Shan	34°20'	4700-5100	-6.6	-2.0 — -4.0	60-120	1-2
Tuotuo River	33°50'	4500-4700	-4.4	0.0 — -1.0	1-50	0.8-6
Tongtian River	33°30'	4500-4600	-4.4	-0.3 — -1.0	25	1-4
Tanggula Mt.	32°57'	4900-5300	-6.4	—	10-120	1-3
Tangquanguo	32°40'	5000	below -6.4	—	128.5	2.8
Zhuonan Lake Area	35°18'	4800	about -6.5	—	74.8	2.4

subsidence occurring in the north and south sides of the mound enclosed by a soil ridge, which is more than 10 m high. Groundwater overflows on the top of the mound to form the seasonal icing which is 1.5-20 m high.

2.2 Earth Hummocks

These dome shaped hummocks were formed by the air circulation of frequent freezing and thawing, small plastic mounds are usually covered with grass 20 to 40 cm in diameter and 10-30 cm high.

2.3 Rockglaciers

It is a special geomorphological form in the cold permafrost region, it is also called a movable permafrost body, and consists of clastic debris, breccai and ground ice. Such as the rockglacier in Kunlun Mountain which is unique to China (Cui Zhijiu, 1981).

2.4 Settlement Depressions or Lakes

The landforms in the handwater of Chumer River, near Xinxing Lake and between Xijinwulan Lake and Yonghong Lake are surface disturbances resulting from disruptions of the thermal equilibrium of underlying permafrost due to the variation of surface conditions.

2.5 Periglacial Loess and Sand Dunes

With a lofty and expansive terrain, cold and arid climate and the effects from violently aerological west wind currents make this area become one of the areas with maximum wind speed within the plateau or in China*

The loess deposited under the periglacial environment is called periglacial loess, it widely occurs in pediment, terraces and valleys. Sand dunes, crescent dunes also occur widely in the north side of Xijinwulan Lake and along Qinghai-Xizang highway, and impedes on the highway.

2.6 Frost Jacking of Stones

A lot of frost jacking of stones are often discovered in this area. Some of them stand in great numbers like trees in a forest on the slope. Such as those on the slope on the bank of Kekexili Lake, where sandstone and slate are widely distributed.

*Information from investigation for Kekexili.

REFERENCES

Guo Dongxin and Li Shude, (1982) The formation and history of massive ground ice in Fenghuo Shan on Qinghai-Xizang Plateau. Proceedings of Conference on Glaciology and Geocryology (Geocryology), Science Press.

Pu Qingyu, (1982) History of permafrost along Qinghai-Xizang highway. Proceedings of Conference on Glaciology and Geocryology (Geocryology), Science Press.

Shang Jianyi, (1982) The development features of permafrost along Qinghai-Xizang highway. Proceedings of Conference on Glaciology and Geocryology (Geocryology), Science Press.

Cui Zhijiu, (1983) Discussion on rockglacier in Kunlun Mountains. Proceedings of Second National Conference on Glaciology and Geocryology, Gansu People's Press.

REGIONAL FEATURES OF PERMAFROST IN MAHAN MOUNTAIN AND THEIR RELATIONSHIP TO THE ENVIRONMENT*

Li Zuofu, Li Shude and Wang Yinxue

Lanzhou Institute of Glaciology and Geocryology,
Chinese Academy of Sciences

Drilling and ground temperature measurements at some sites in the study area demenstrated that the presence of permafrost within the loess plateau in China is an irrefutable fact. Permafrost distribution is sporadic and island, varying in extent from tens of square metres to $1.5 \times 10^5 m^2$ and in thickness from about 3 or 5 m to 30 m. Sporadic permafrost was first discovered in China. A key to permafrost occurrence is high elevation, through 2 range of above 3500 m, the spatial distribution of permafrost areas is complicated by the local conditions.

STUDY AREA

Mahan Mountain, (35°45'N and 103°45'—104°00'E) 3670.4 m above sea level, located about 40 km south of the city of Lanzhou, is the highest point within the loess plateau. The summit is a planation surface formed in the Pliocene epoch (Liu and Li, 1991) and has a generally subdued relief. There are scattered rock outcrops and poorly developed Quaternary sediments including remnant blocks formed by frost weathering.

The climate of Mahan Mountain is subhumid and cold although it is located in the expanse and arid loess plateau due to the lofty height and air temperature abruptly decreasing with the increase of height. Mean annual air temperature and precipitation are -2.3°C and 494 mm (observed in 1961, after by Re Binghui, 1981). The freezing duration is as long as seven months. Especially lapse rate of air temperature in winter (from December to February) is only 0.3°C/100 m, less than the normal value, based on the relative statistics between air temperature and height at 24 weather stations near the study area.

PERMAFROST DISTRIBUTION

In this area, mean air temperature is -2.3°C yearly and 9.2°C in July, the difference between the ground and air temperature is 2.8°C (observation in 1991). Permafrost was found in Oct. 1985. Therefore, four sections, including 12 sites, where holes and pits were dug were selected for the programs of the investigation of permafrost distribution and measurement of ground temperature in 1991. At least, eight of them have been identified to have existing permafrost (Fig.1).

Of the four sections, Section A (termed Xiaohutan), 3560 m above sea level, an area of approximately 0.5 km^2, situated on the north facing slope of Mahan Mountain, is an elliptical hollow with poorly drained and well developed hummocks. In winter it is free of snow pile, only thin snow fills in the trenches of the earch hummocks. Four holes were drilled on the bottom of the hollow in July and September 1991 to obtain information on perennially frozen ground and bedrock and to install thermometers for monitoring ground temperature. The results (Fig.2) indicate that permafrost occurs on the bottom of the hollow varying in extent of about $1.5 \times 10^5 m^2$, almost coincident with the occurrence of the well developed earth hummocks in thickness from about 5 m on the edge and 30 m in the centre of the hollow. The depth of the active layer is 1.5 m on the edge and 1.2 m in the centre of the hollow. No permafrost occurs on the slope around the hollow, where the depth of seasonal freezing varies from 3.5 m to 4.0 m.

Section B, adjacent to Xiaohutan, situated on the back well of the paleo-cirques of Douling trench. Three holes were drilled on the solifluction sediment and nivation hollow. Of the three holes, the first was selected in a nivation hollow with well developed earth hummocks and solifluction. Prevailing north westerly winter wind accumulated a thick snow cover (thickness; 40-50 cm), near the surface soil moisture was very high, the depth of seasonal freezing was 2.5 m. The ground temperature at a depth of 5.1m was 0.8°C during early July to early August. No permafrost exists in this site. The second and third were all selected on the solifluction tougues with an average gradient of 12°. There is no redistribution of snow in winter, the depth of snow varies only from 10 cm to 15 cm. Although they have a steeper gradient and are well drained, near the surface soil moisture in summer is very high. As a result, the maximum depth of seasonal freezing reaches to 4.0 m. the ground temperature at a depth of 3.5 m was from -0.1°C to -0.2°C during early July to

*The project supported by National Natural Science Foundation of China.

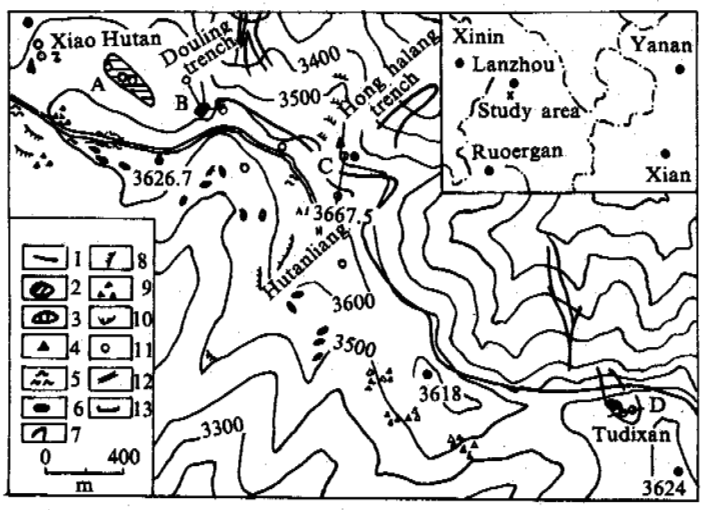

Fig.1 The map of permafrost and periglacial landforms in Mahan Mountain
1. Bush upper limit; 2. Island permafrost; 3. Sporadic permafrost (amplified); 4. Icing; 5. Earth hummocks; 6. Nivation hollow; 7. Glacial deposits; 8. Solifluction terrace; 9. Block fields; 10. Cirque; 11. Boreholes and pits; 12. Roads; 13. Investigation section.

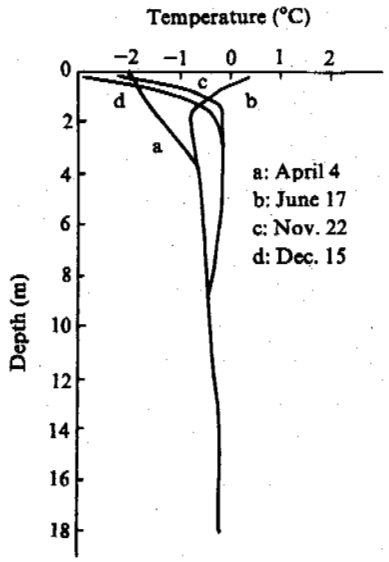

Fig.2 Ground temperature envelopes at island permafrost in Xiaohutan

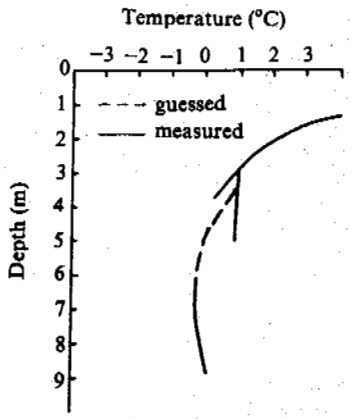

Fig.3 Ground temperature curve of sporadic permafrost in bedrock

early August and up to 1.2°C until late Sept. There was also no permafrost in these sites. However, permafrost was found between these sites in October 1985, where a 1.2-m-thick layer of clay with debris overlying dolomitite with developed fissures in which ground ice, primarily in the form of fissure ice up to 2 m thick (average thickness being from 5 to 12 cm), was encountered at a depth of 8 m below ground surface (Li Shude, 1986). Based on the above mentioned and hydrochemical analysis of ice samples taken at the depth of 8 m below the ground surface, permafrost exists at the bedrock in this site (Fig.3).

Section C, from Honghalang trench to the summit. At Hutanliang, one hole was drilled at a modern nivation hollow at 3640 m elevation on a scattered meadow, with coarse grained material and a snow patch 0.3-0.4 m thick. Although meltwater from patches of snow accumulated in the hollow flows near the hole, the soil moisture in late Autumn is low owing to the steeper gradient (gradient of 15 to 20°), the maximum depth of seasonal freezing was 3.2 m, the ground temperature at a depth of 3.6 m was 0.1°C in early July and increased to 2.2°C in early August; At 3520 m elevation on the solifluction tongue at the bottom of Douling trench has an average

gradient of 3° to 5°. Vegetation consists of alpine azalea and cryptomeria up to 50 cm high with scattered growth. Because the surface runoff from the upper slope flows around the solifluction tongue there was no organic layer but soil moisture was very high or the soil remained essentially saturated through the thawing season. The runoff has no thermal affect on the change of soil temperature. Ground temperature at a depth of 3.5 m was -0.2°C from early July to late October. The maximum depth of seasonal thawing occurs until mid-December (depth; 2.0 m). At this time, however, the ground temperature at a depth of 3.5 m was -0.1°C (Fig.4). It is estimated that permafrost is about 3.0 m in thickness and a few tens of square metres in extent.

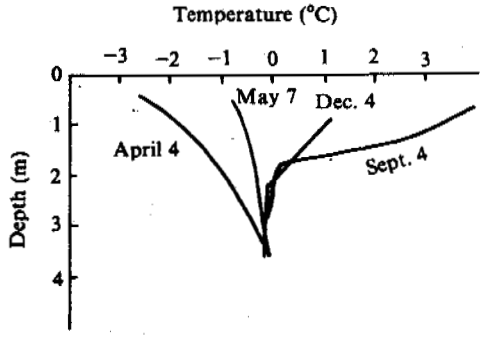

Fig.4 Ground temperature curve of sporadic permafrost at Honghalang trench

Section D, situated at a paleo-cirque with subdued terrain in Tudixian at 3520 m elevation, and plant cover consists of an alpine meadow. Local swamp or solifluction tongues with well developed hummocks also occur at these sites. Snow cover in winter varies from 10 cm to 20 cm in thickness, two holes were drilled at the swamp and the no swamp solifluction in July 1991, respectively, to contrast the freeze and thaw process at different microterrain units, but the measurement results of ground temperature are different between them.

The distance between them is only 30 m, one at the swamp solifluction tongue with permafrost (Fig.5) and at the other with none.

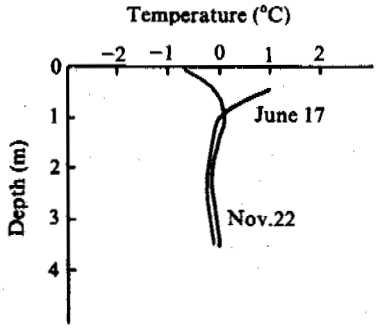

Fig.5 Ground temperature curve of sporadic permafrost at swamp solifluction tongue in cirque of Tudixian

The above mentioned permafrost distribution in this area is quite complex.

TYPES OF PERMAFROST

Alpine permafrost in Mahan Mountain can also be subdivided into island and sporadic permafrost. The former is similar to those in other regions of China, the mean annual ground temperature is between -0.2°C and -0.3°C. The ground temperature gradient profile is almost zero, so, it is warm permafrost which usually is susceptible to the environmental changes but it still exists within the loess plateau with an arid or semi-arid climate in mid-latitude regions and is about 30 m in thickness. The depth of annual zero amplitude was encountered at a depth of 12 m below the ground surface. The thickness of the active layer and the depth of annual zero amplitude are all lower than those in other alpine permafrost regions of China. These are largely due to the original layer near the surface (thickness; 30 to 40 cm) which contains much more moisture, and acts as an insulating cover, just as those above Klune Lake (Harris, 1987), partly due to the presence of supra-permafrost water in the hollow. In addition, massive ice and ice-rich soil developed in the upper layer of permafrost which retards permafrost degradation. As a result, it can be preserved in the loess plateau as seen at present.

The sporadic permafrost was first suggested by Gorbunov (1978) who found perennially frozen bodies, that occur in the debris and clastic sediments and exist for a few years in the mid-Asian mountains, its occurrence has been not reported in China. So it is unique, that one of them was encountered in bedrock with fissures, it has a thickness of about 10 m, and its mean annual ground temperature approximates zero, the depth of seasonal thawing probably exceeds 4 m, and mean annual air temperature is below 0°C. The reason for scattered distribution appears to be that it is located near the lower limit of alpine permafrost and in thermal equilibrium with the present surface temperature or alternatively may represent remnant permafrost degrading in response to an increase of surface temperature to above 0°C. Especially snow patches insulate the ground from the cold in winter, so that no permafrost occurs in the sites mentioned above.

Other sites with permafrost are at solifluction deposits at Honghalong trench and swamp solifluction tongue at the cirque of Dudixian, which have zero gradient in ground temperature profile and mean annual ground temperature is above 0°C. Permafrost is about 2 m to 3 m in thickness. They may be largely a function of local conditions. For example, there is thin snow cover and much moisture for fine grained soil in summer in these cases. They may be in thermal equilibrium with the local surface temperature, so that sporadic permafrost only exists in the microterrain.

GROUND ICE

Up to now, epigenentic ground ice has been not found in the study area, although some researchers think the sediments at Douling trench to be rock glaciers. Syngenetic ground ice, however, including fissure ice in bedrock, and segeretion ice, is controlled by local geological and geomorphological conditions. Fissure ice in bedrock develops on the summit or

sections along the ridge. For example, those encountered in the exposure dug at the backwall of the cirque of Douling trench. Hydrochemical composition for the ice sample taken in a depth of 8 m below surface is different from those of groundwater from the solifluction tongues, icing and snow samples taken around the site. Tritium content of 11.63 TU indicates that the fissure ice was formed before the 1950's (Li Zuofu and Li Shude, 1986). In addition, fissure ice in bedrock occurred on a mining exposure in early July and was preserved until late July 1991. Ice stalactite formed at a man-made cave in the summit and was preserved until late August. Duration is as long as eight months.

Segeregated ice mainly develops in the micro-terrain with thickly fine grained soil. So in this area, Xihuotan is an unique site where segregated ice develops. Borehole data shows the vertical variability of ground ice content. Total ice volume decreases from values of more than 90 percent at depths of 1.2-1.7 m below surface to 45-55 per cent at depths of 1.7-3.5 m, and frozen sediment at depths of 3.7-4.2 m containing no visible needle ice. They may be classified in terms of the field observation and have a relationship to enclosing sediments.

Lens ice or an ice layer with silty particles 50 cm thick. Grey silty particles were apparently in suspension within the ice, roughly 3-7 per cent by volume, lens with uniform coarse crystal size was similar to columnar. Vertically oriented and elongated crystal structure is perpendicular to the overlying sediment; Layer ice occurs at a depth of 1.7 m below the surface, the total thickness is 2.0 m (each layer being 1-2 cm thick) layer cryotexture and short columnar ice crystals. When it was melted the core looks whorled.

MAIN FACTORS EFFECTING PERMAFROST

High Elevation

Permafrost found in this area existed at the lowest heights of above 3500 m and at the highest elevation of 3620 m (on the north facing slope), which were determined by many investigations in the site. Especially, the reconnaissance study of permafrost distribution in detail and measurement of ground temperature which was carried out in 1991. Through a range of the heights, one site has permafrost but another will have none, even though they are only a few meters apart. Meanwhile, on the north facing slope permafrost occurs at lower heights, but no permafrost exists at higher elevations. Thus, the high elevation is a key factor to determine whether permafrost occurs or not, through the range of this height, regional factors have a great deal of effect on the occurrence, temperature, and thickness of permafrost and ground ice.

Facing Slope

From statistics, within the alpine permafrost region in the Northern Hemisphere, the lower boundary of permafrost on the south facing slope is high, 300-400 m more than that on the north facing slope (Qiu, Huang and Li, 1982). Based on the difference between the south and north facing slope mentioned above. The 3600 m height appears to be a critical one for permafrost occurrence in this area from the geographic location, mountain height and cryogenic phenomena developed on the north facing slope and on the summit. Through a range of the elevation, steep relief on the north facing slope is advantageous to the blocking of the cold current in winter, so that cold duration becomes much longer on the north facing slope than that on the south facing slope. In summer, it makes a vertical current develop, so that on the north facing slope cloud cover increases, and incoming radiation reduces, which are also advantageous to the decrease of mean annual surface temperature, meanwhile, it is much wetter on the north facing slope. For example, there is alpine azalea up to above 3600 m above sea level, and only on the alpine steppe on the south facing slope. These differences between them have a great effect to thermal interchange between the air and the ground. There is no possibility of existing permafrost on the south facing slope in this area.

Terrain and Soil

As mentioned above, the loosened sediments in study area are thin and overlies the coarse debris 0.3-1.0 m thick. Thus, under the same conditions, the thickness of fine grained soil is very important for the absence or presence of permafrost, in the sites with a thin layer of fine grained soil. Permeation from water makes heat in soil quickly migrate downwards, so that the rate of thawing of the soil would be fast, owing to suitable permeability and steeper gradient.

Measurements of ground temperature at the various sites near Hutanliang show that isogeotherms of 3.2°C at a depth of 1.2 m occurred on July 15 at the site with coarse debris. But at the sites with fine grained soil it occurs at a depth of 0.5 m until late September and has never been at the depth of 1.2 m annually. This variation was largely due to the difference in the thickness of fine grained soil with time as the water permeates through the fine grained layer to the coarse debris.

In addition, island permafrost exists in Xiaohutan and its active layer varies from 1.2 m to 1.5 m in thickness. The reason for this is probably partly due to organic rich muck and poor drainage in summer and partly due to the cooling of the snow cover in trenches of hummocks to the ground surface in winter. Thus, under the same conditions, the thickness of fine grained soil in the study area appears to be the major factor controlling the absence or presence of permafrost.

Snow Cover

Snow cover influences the heat transfer between the air and the ground, and, hence, affects the distribution of permafrost, due to redistribution of snow cover by wind. The snow cover at the study area exhibits considerable spatial variation in depth. Some snow patches 30-50 cm thick persist on the nivation hollows through winter to reduce winter heat loss. The hollows have relatively thick loosened deposits, but a thin snow cover filled in the trenches of earth hummocks remains for a long time, most of the area studied is exposed to wind. Thus the effect of the snow cover to ground surface is both insulating and cooling in this area. Insulating; insulation of snow cover to ground surface is with a relation to heat circles in soil, because the area studied is in the range of 3500-3650 m elevation which is a critical height for permafrost to exist and which has violent heat circles in soil. Therefore, snow cover insulates the ground from the winter cold. For example, on the back wall of the cirque in Douling trench, a snow patch on the hollow was

50 cm thick, the depth of seasonal freezing was about 2.5 m. But snow cover on the solifluction tongue varies from 15 to 20 cm in thickness. The depth of seasonal freezing was about 3.5 m to 4.0 m, observed at Xiaohutan on December 15, 1991 showed that the temperature at noon was 2.0°C in ground surface, -0.6°C in snow surface and -1.6°C under snow; and that temperature in afternoon was -10°C in ground surface and -13.2°C under snow.

In addition, snow patches on the north facing slope cause the thawing data to be postponed for 20 days. It appears that the snow cover acts as a cooling cover when it is thinner than 20 cm and as an insulating cover when thicker than 30 cm.

In summary, on the north facing slope in Mahan Mountain the occurrence of permafrost is complicated by the general influences of soil microterrain, and gradient, and the alternative action from insulating and cooling of snow cover to the ground.

REFERENCES

Re Binghui, (1981) A study on Quaternary glacier and periglacier in mountains near Lanzhou, Journal of Glaciology and Geocryology, Vol.3(1).

Liu Yun and Li Jijun, (1991) Late Quaternary glacier and environment in Mahan Mountains, The Quaternary Glacier and Environment of Western China, Science Press, Beijing, China.

Li Shude, (1986) Permafrost was found in Mahan Mountain near Lanzhou, Journal of Glaciology and Geocryology, Vol.8(4).

Li Zuofu and Li Shude, (1986) Permafrost on the loess plateau in China, Geographical Knowledge, No.9.

Qiu Guoqing, Huang Yizhi and Li Zuofu, (1982) Features of permafrost in Tianshan of China, Proceeding: 2nd National Permafrost Conference, Gansu Press, p.21-29.

Gorbunov, A.P., (1978) Proceedings Third International Conference on Permafrost, Vol.1, p.349-353.

Harris, S.A., (1978) Arctic, Vol.40, No.3, p.179-183.

A SOLUTION FOR THE ICING HEAVE OF FOUNDATIONS IN PERMAFROST REGIONS BY LOWERING THE GROUND WATER TABLE

Liu Shifeng and Zou Xinqing

The Institute of Forestry Design of Da Hinggan Ling

The frost heave of foundations is one of the most important problems damaging buildings in permafrost regions. From many years of surveying the damage to the buildings in Da Hinggan Ling region, particularly in dealing wity the heave of foundation of residential buildings in Gulian mining area, we propose a method of lowering the ground water table to solve the frost heave of foundations in permafrost regions and to obtain some results. Through two years of observation it was found to be effective.

ANALYSIS OF FEASIBILITY

Based on the freezing principle, the frost heave that occurs in soil must be qualified with three conditions: 1) susceptible soil, 2) preliminary water contentand externally supplied water, 3) optimum freezing conditions and time. The frost heave can be resisted by the weakening of one of the three conditions, so that the frost damage is protected.

When the soil properties are constant, the amount of water content is one of the basic factors affecting the frost heave. In a closed system, the water capacity determines the frost susceptibility. In an open system, the externally supplied water can greatly raise the susceptibility of soil, although the preliminary water content is small. Both the water content of soil and externally supplied water are related to ground water. There is rarely rain in the developing permafrost area in Da Hinggan Ling. The surface soil begins to freeze from October to April, the water supplied from the surface is replaced gradually by ground water. The groundwater table affects directly the water content and the supplied water during soil freezing. As a result, the frost susceptibility of soil is decided. The more shallow the ground water table, the lower the frost heave. Thus it is feasible to decrease the frost heave by lowering the ground water table.

SPECIFIC IMPLEMENTS

After the structure of the foundation of the four residential buildings is Gulian mining area were completed, a water zone welled from the foundations in October that year and ice formed later. The exit was frozen in the middle of December, and an icing formed about 60m ling in size, 20m wide and 1.2m in average height. When the surface ice was dug out, a column of cinfined ground water was spread which reached to 0.6m high and its flux was 15t / h. The coater column changed into welling water after half an hour, and its flux was 6t / h. The icing expanded continuously with time, andthe girds ofthe foundations might of been damaged at any time. In order to determine an optimum solving method, we investigated the hydrogeological condition.

REGIONAL PHYSIOGEOGRAPHICAL CONDITION AND GEOLOGYAND GEOMORPHOLOGY

The area is located on the north slope of Da Hinggan Ling, where it experiences a continental climate in a temperal frigid zore, and altitiude is 440—600m. The summer is short and hot and the winter is long and cold. The annual air temperature is −5°C, the minimum air temperature is −49°C, and the maximum air temperature is 36.8°C.

The residential buildings were built on the low ridge and gentle slope. The topography declines from northeast to southwest. There are geomorphology units of denudated accumulation and frozen soil periglacial forms which are in the expression of icing in winters which forms swamps after thawing in summer. There is no obvious welling water, and streams exist. The lithological character of the stratum is simple. The ground surface is clayey sand and loam with stones formed of Quaternary slope wash and deluvium. The bedrock is tuffy gravel rock on the granite is variscian.

REGIONAL HYDROGEOLOGY

Owing to the artificial influences and the destruction of vegetation, the permafrost in the upper fringe of the low ridge decreases, but there is permafrost in most parts of the area. Therefore, the classification and motion of the ground water is limited by permafrost. Based on this, the ground water is divided into two types: superpermafrost water and subpermafrost water.

The superpermafrost water which is affected greatly by different seasons is stored in the pores of the Quaternary unconsolidated layer and in the pores and crevasse of strong weathering gravel. After the seasonally frost soil thaws, the water is directly supplied from the rain and the melted water from ice and snow.

The subpermafrost water is stored in the pores and cevasse of bedrock. The result of hydrogeological exploration illustrated that the crevasse of bedrock is developed and provides the conditions for the storing and flow of water. The subpermafrost water posses a confined character, because the freezing layer is a water-resisting layer. Moreover, because there is no permafrost in some areas, and a hydraulic relation exists between the two layers. Analyzing the figures of the contours of the water table and the isoline of the degree of mineralization, the main part of the two layers of groundwater are drained away to Gulian River, another part to the ground surface from springs and forms icings in the winter.

The distribution of ground water is homogeneous due to the uneven distribution of clay content. Some run off channels form where the clay content is small and the water is rich. Most of the channels have a linear distribution from south to north. So that distribution of ground water has the character of linear enrichment.

SOLVING METHOD

Based on the hydrogeological conditionsand analysis of various factors, the reason that the icing forms in the foundation is the linear enrichment of the ground water due to the unevenly distributed clay content. The amount of the run-off of the ground water is large and confined. At the same time, the excavation of the foundation of the residential buildings changes the layer into a weak belt. This provides the drainage condition for the ground water that directly flows to the basel pit. The superpermafrost water is supplied continuously from the subpermafrost water because of the hydraulic connection between the two layers of groundwater.After the temperature becomes negative, the icing gets larger and larger.

In view of this situation, we proposed a treatment method of lowering the ground water table. In July of the next year, an unwatering hole was excavated which was about 15m apart from the icing. The beginning diameter of the hole was 420mm, the end diameter was 180mm and its depth was 120m. From the exploration results, the distribution of the ground water along the depth is mainly pore phreatic water of the Quaternary unconsolidated layer above 3m, pore and crevasse water in the weathering layer from 7m to 10m and ground water in the bedrock crevasse and tectonic crevasse from 70m to 90m. The ground water began to be withdrawn 12 hours each day on the 13th of August. The amount of welling water was 33 tons each hour. A recording of the unwatering is listed in Table 1 and the coresponding figures are shown in Figure 1. The sketch figure of lowering the ground water table is shown in Figure 2. Three months later, a linear withdrawing hopper formed that was 300m from south to north and 100m from east to west. The decreased depth in the center was 25m.

It was found during the withdrawing that phreatic water in the pores of the Quaternary unconsolidated layer was rich in Septmber. and October. and the ground water in the pores and crevasse of the weathering layer between 7m and 10m became the main supply after November. The large hopper formed around the residential

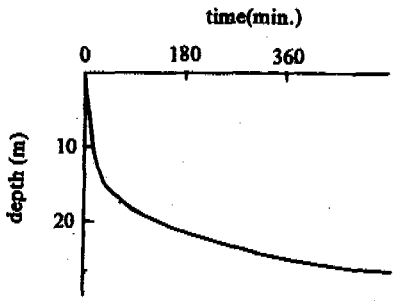

Fig. 1 The process of the lowering depth of ground water table with time

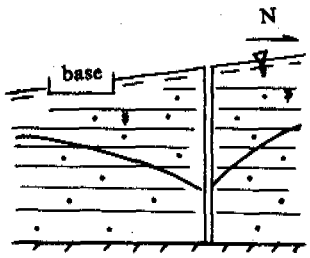

Fig.2 The scheme diagram of the loweringground water table

Table 1 Record of withdrawing

lasting time(min.)	ground water level(m)
0.0	0.0
6.0	8.26
20.0	14.28
40.0	15.80
60.0	16.90
120.0	19.40
180.0	21.08
360.0	24.80
540.0	26.31

buildings was controlled effectively by drainage of ground water and by cutting the supply water of the icing, so that the icing didn't form. At the same time, due to the decrease of the ground water in the soil and the water content reduction from 17–24% to about 12%, the frost heaving greatly decreased.

EFFECTS AND PROBLEMS

Since the foundation of the residential building in Gulian mining area was treated by withdrawing, there has not occurred any welling water and icing. Therefore, the engineering geological conditions in the area, located on the footslope that easily causes frost heave, are greatly improved. The susceptibility of the frost heave of the foundations decreases clearly and the safety of the residential buildings is ensured. Because the method is a radical treatment, the effect is stable.

Higher expense is the disadvantage of the method. But after making the well better, it becomes a tubular well to supply water for boilers and for drinking.

CONCLUSIONS

Through treating the frost heave of foundations in DaHinggan Ling and other regions, it is considered that the frost heave caused by the rich groundand surface water can be solved ty artificially lowering the ground water table. The extent of the lowered ground water table should be in the state that the water content of soil in the range of the capillarity is less or slightly higher than that of the initial frost heaving. In general, the ground water table is 2m lower than the frost depth. Through many contrast tests, it is known that lowering the ground water table should begin a month before the soil freezing, which is from the beginning to the middle of September in Da Hinggan Ling region. Therefore, there is enough time to decrease the water content after the fround water table is lowered, the small water content is ensured when the soil freezes and the seasonally frozen soil freezes, which runs from the middle of December. to January.

The problem that is has a higher expense is solved by using the withdrawn water for boilers. Therefore, a well can be used for many aspects. It not only treats the frost heave of foundations, but also keeps the water supply. The cost of the well will be decreased and a good economic benefit is obtained.

REFERENCES

Tong Changjiang and Guan Fennian (1985) Frost Heave of Soil and Prevention of the Frost Damage to Building. Published by Hydroelectricity.

Jin Junde (1988) IceLake and Protection Information on Forestry Science ane Technology (Translated Proceedings), Vol. 10.

Yang Rongtian and Lin Fentong, 1986 Hydrogeology and Engineering Geology in Permafrost Regions, Published by Northeast Forestry University.

THE GEOGRAPHIC SOUTHERN BOUNDARY OF PERMAFROST IN THE NORTHEAST OF CHINA

Lu Guowei[1], Wang Binlin[1] and Guo Dongxing[2]

[1]Da Hinggan Ling Institute of Forestation, Inner Mongolia
[2]Lanzhou Institute of Glaciology and Geocryology,
Chinese Academy of Sciences

Permafrost has wide distribution on the Hulunbeier Plateau and the Songleng plain, and in the forest regions of the Da Hinggan Ling and Xiao Hinggan Ling ranges, in the northeast of China. It's geographic southern boundary has been decided, based on the abundant data obtained. The southern boundary distribution of permafrost is characterized by the integrated influences of geographical latitudes and regional natural conditions. However, the southern permafrost boundary has been moving northward because of the serious destruction of natural flora due to the frequent human activity during the last century. The only relative stable northward-movement of the boundary occurs in the permafrost regions inside forest areas where the frozen ground is in a natural environment with most favourable forest restoration.

HISTORIC OUTLINE OF THE DIVISION OF THE SOUTHERN PERMAFROST BOUNDARY

The frozen ground in the northeast of China, has a total area of 38 to $39 \times 10^4 km^2$. The formation, distribution and development are influenced by the geographic latitudes and regional natural conditions, and is the southern extension of permafrost on the high latitude Euroasian continent. It can be divided into three types, namely: large-sheet, island-melting, and island permafrost, with latitude variations and accordign to the continuity of its distribution (Table 1). In the island permafrost zone, it develops better in lower lands than on slopes and it hardly exists on mountain tops. This shows that the regional natural conditions have a significant influence. There are very sparse distributions or no distribution of permafrost in the area of the southern boundary (Zhou Youwu et al., 1981).

Scientists have tried to decide the southern boundary of permafrost in the Da Hinggan Ling and Xiao Hinggan Ling ranges since the 19th century. For instance, A.ϕ. Migandolf (1864), M.N. Shumkin (1940), and others have given the southern boundaries in the geographical map of permafrost zones in the northern hemisphere, of which six boundaries were outlined through the Da Hinggan Ling and Xiao Hinggan Ling ranges with a range of latitude from 44° to 52°N (Fig. 1), which have important differences from the real situation in these regions.

After investigations of frozen ground in these regions, Chinese geologists, e.g. Xing Kuide and Ren Qijia (1956), indicated that the southern boundary of permafrost in the two ranges traces through Artika, Huduke and Tato Aili in Mongolia into Nan Hingan, Buteha Qi, south Paligen, Dedu and Shajindi of Dulu River in China, and then crosses the Heilong Jiang River into the former Soviet Union (Fig.1). This

Table 1. Distribution Types and the Characteristics of the Frozen Ground

Type of permafrost zone	Division characteristics	Continuity (%)	Coefficient of interruption
Large-sheet permafrost	Large-sheet continuous	65-75	0.65-0.75
Island-melting permafrost	Locally continuous	50-65	0.50-0.65
	Discontinuous	40-50	0.40-0.50
Island permafrost zone	Island	20-40	0.20-0.40
	Sparse island	5-20	0.05-0.20
	Very sparse island	<5	<0.05

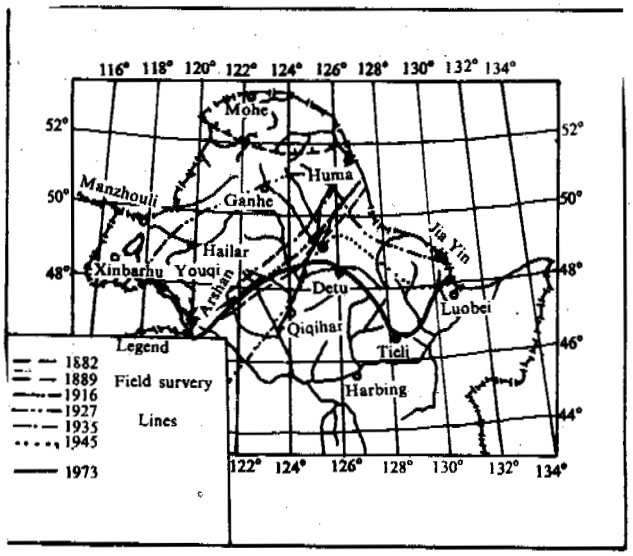

Fig.1 The Historic Outline Diagram of the Southern Permafrost Boundary in Da and Xiao Hinggan Ling

boundary corresponds to the annual average 0°C isotherm or to the January mean atmospheric temperature -24°C isotherm (Xin Dekui, et al., 1959), which is significant as a reference, as well as showing the slight difference from the actual situation.

In the areas of Jiayin, Detu, Arshan and Xinbarhu Youqi, dozens of separate field surveys were carried out during Sept.-Nov. 1973 and during May-July 1974. The studies included meteorology, hydrology, geology, geomorphology, soil, paleobiology, botany, geocryology, glaciology, and periglaciology. At the present time the southern boundary of permafrost has been initially based on the large amount of information obtained in the above mentioned expeditions. It has also been adjusted after two further expeditions to the areas of the Da Hinggan Ling and Xiao Hinggan Ling ranges, Hulunbeir grassland, Changbaishan Mountains and Huang Gangling territory, etc. These expeditions were carried out with practical research in mind, to study the long boundary of 1300 km and complex variations of natural conditions, as well as the need to understand the basic features of permafrost distribution and fluctuation tendencies of the southern boundary in the last century.

THE BASIC CHARACTERISTICS OF THE DISTRIBUTION OF THE SOUTHERN PERMAFROST BOUNDARY

Since the Late Quaternary, the permafrost distribution has been expanding and shrinking as a result of climatic changes in the Ice Ages and Interglacial period. For example, during the Guxiangtun cold period of the Late Pleistocene (7-1x10⁴years B.P.-Wisconsin Ice Age), the permafrost expanded southward in the Da Hinggan Ling and Xiao Hinggan Ling ranges and has been proven to be close to the average present annual average isotherm of 7-8°C along the boundary linked with Aohan Qi, Ganqika and Shuangliao, to the south of Xila Mulun River, and extended eastwardly to Panshi, Huinan, Dunghua, etc. After that, in the warm period of the Holocene (1-0.3x10⁴years B.P.), the permafrost retreated northward to Jinling and Gangyuan on the north part of the Da Hinggan Ling range, and to the north side of Yilihuli Mountains. The permafrost at present was formed in the Neo-Ice Age, 3000 years B.P., which was a result of the expansion of the remnant permafrost and the restoration of frozen ground in the melting areas, as well as climate colling (Guo Dongxin, et al., 1981). These factors demonstrate that the southern permafrost boundaries have advanced southward and retreated northward several times due to climate changes since the permafrost formation in the Late Pleistocene (Fig.2).

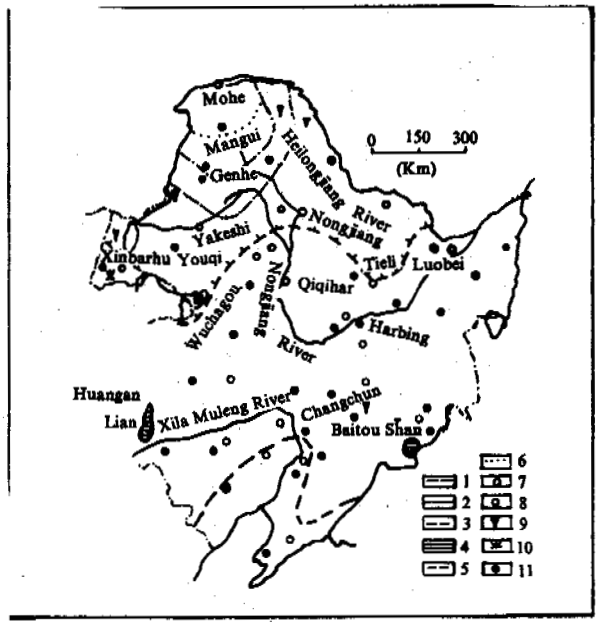

Fig.2 The Historic Evolutional Giagram of the Southern Permafrost Boundary in the Northeast of China Since Late Quaternary Period

1. The southern boundary of large-sheet continuous permafrost now;
2. The southern boundary of island-melting permafrost now;
3. The southern boundary of island permafrost now;
4. The high-mountainous permafrost now;
5. The southern boundary of permafrost in the Late Pleistocene;
6. The southern boundary of permafrost in the holocene high-temperature period;
7. Rhinoceros tichorhmus fossil site;
8. Mammoth fossil site;
9. Fossil ice wedge;
10. Hemiaric grassland;
11. County.

The western section of the southern permafrost boundary in the northeast of China is composed of southern boundaries of island melting permafrost, in Arshan Mountains, and in the island permafrost on the east slope of the Da Hinggan Ling range and on the Hulunbeier Plateau. It was shown, after the expeditions, that the permafrost is sparsely distributed to the north side of Xingbarhu, Youqi, and Zuoqi regions, and no permafrost develops in the region between Kelulun and Wurson Rivers, on the island perma-

frost of Hulanbeier Plateau. Therefore, the southern boundary of permafrost east of Mongolia crosses the upper course of Kelu River, and should reach the boundary (Number 34) in the Hulunbeier Plateau of China through Ba.Yangwula and through Xinbarhu Youqi and Zuoqi along the Halaha River and come invertedly into the Arshan Mountainous region. But, because the relief of the Arshan Mountains (above 700-1200 m) is higher than the surrounding areas, the climate is very cold, the frozen ground is more developed and shows the vertical regional change. The lower limit of the frozen ground links with the southern boundary of frozen ground in the Hulunbeier Plateau, as well as being to the south of Arshan Mountains and the eastern slope of Da Hinggan Ling. That is to say, it extends from the Halaha River, the Arshan Mountains, Wuchagou, through to Chaihe, Namu, and to the north of the Songlong Plateau.

The middle section of the southern permafrost boundary in the northeast of China is composed of the southern boundaries of the northern permafrost in the Songlong Plateau. The altitude is lower (200-400 meters), and has a plain relief. The soil is fertile and there is a river running through the region. The permafrost and the natural flora have a closely interdependent relationship. In the last decade the lumber and agricultural production ranges have expanded and have caused the southern boundary of permafrost to cross south of the Longjian River and has developed to the south of Xiao Hinggan Ling. The boundary also extends from the eastern slope forest district into this district. The range is from the north of Chaihe, Nanmu, Aronqi, through Laochai, Detu, etc., then into the southern mountainous regions of Xiao Hinggan Ling.

The eastern section of the southern permafrost boundary, in the northeast of China, is composed of the southern boundaries of the low mountains and hill regions of Xiao Hinggan Ling through to the southern permafrost boundary of Da Hinggan Ling. It has shrunk northward by two latitudes more than that of the southern section of Da Hinggan Ling. But, because the relief of the southern section of Xiao Hinggan Ling is higher (above 400-700 meters), the southern permafrost boundary in the north of Songleng Plain extends to the southeast. It also extends to the southern section of Xiao Hinggan Ling, crosses the Qing Heishan Mountains, Hei Longjian River and into the former Soviet Union. That is to say, the region is from the south of Detu, Qingan, Tianshan, Nancha, through the south of Jia Yin River, to the opposite shore of the Hei Longjian River to the Buleya Mountains.

Because of the factors stated above, the southern permafrost boundary in the northeast of China is about 1300 kilometers long, it has a western distribution and is under the influence of global climate, flora, relief, human activity, etc. Generally speaking, the western amplitude of the southern boundary is the range of the annual average isotherm between 0 to -1.0°C, the middle section is in accordance with the isotherm 0°C, and the eastern section crosses between the isotherm 0 to 1.0°C.

THE RECENT CHANGING TREND OF THE SOUTHERN PERMAFROST BOUNDARY

In the last century, the change of the southern permafrost boundary of Da Hinggan Ling and Xiao Hinggan Ling has had a close relationship with the frequent human activities and the increasingly warm climate. According to the statistics of Han Sen and others (1987), since the last century the global mean atmospheric temperature has risen 0.5°C every year, from 1880 to 1940. From 1940 to 1965 it decreased by 0.2°C and from 1965 to 1980 it rose by 0.3°C. From the observational data it was found that 1981, 1987, 1988 and 1990 were the four warmest years, with a progressive rise in temperature (Li Peiji, 1991). This is in accordance with the meteorologic observation data obtained from Sheng Yang and Harbin since 1906. In the last century, disregarding the decreasing fluctuation trend in the atmospheric temperature in 1969, generally speaking there has been a warming trend (Zhu Kezheng, 1972). Thus, because of the warming trend of the global climate and the frequent human activity, such as, the expanded range of agricultural reclamation, excessive grazing on grasslands, large scale lumbering, etc., there has been a profound influence on the soil, flora, climate, water conditions, etc., of the region. These factors have caused the northward trend of the southern permafrost boundary in the last century.

The Hulanbeier Plateau is one of the semi-arid regions in China. Because of the 8-9 months of dry wind from Mongolia the region is semi-arid for long periods. For example, from 1958 to 1962 the annual mean rainfall was 308.3 mm, in Xinbarhu Xiqi. From 1963 to 1980 it was 220.5 mm. From 1980 to present, the yearly rainfall has had a decreasing trend (in 1981 it was only 141.5 mm). This seriously influences the growth of grass, particularly in Kerlun, Saihatala, Hanwula and in southwestern regions. The aridity is very serious and because of the excessive grazing the grassland regression and the desertization phenomenon is increasing. Thus, in the permafrost of the low ground and in the moist zone, the temperature has risen (0 to 0.5°C) and the permafrost thickness has decreased (5 to 10 m) and the permafrost has gradually vanished. The southern permafrost boundary has shrunk from the semi-arid regions to the semi-moist forests of the north and the east. Therefore, the long term aridity is one of the main causes of the northward movement of the southern permafrost boundary in this region.

The Songleng Plain and the Hulunbeier Plateau extends to the south of Da Hinggan Ling, the area is about $17 \times 10^4 km^2$. The region has a temperate and semi-moist continental monsoon climate. The rainfall can be as high as 400-500 mm. From 1841 until 1897, in this region, the Qing Government had three policies, no reclaiming, no hunting and no lumbering, so the natural forest environment was maintained. From 1897 until 1945 there was a large influx of immigrants from inner districts, the Binzhou Railway was constructed, and destructive lumbering was carried out in this region. These factors caused the lumbering range between Qiqihar and Nongjian county to be expanded and the natural flora was destroyed. As well, the natural covering action on the permafrost layer vanished causing the seasonal freezing and thawing depth to increase. The very sparse island permafrost started to shrink and vanish. In a few decades the southern permafrost boundary of the region retreated northward more than two latitudinal degrees.

The southern permafrost boundary in the southern section of Da Hinggan Ling has been relatively more stabilized in recent times, more so than that of the Hulunbeier Plateau and the Songleng Plain. The main reason for this is the

controlling and influencing factors of the altitude height. Thus, to some extent, the distribution of frozen ground abides by the law of vertical zone properties. For instance, the lowest altitude height of the permafrost distribution is about 800 m in the Artaishan Mountains of Da Hinggan Ling, and there is also biennial frozen ground on the slope bottom with a thick clayey soil layer in Wuchagou and Bailan. With an increase in the altitude, the climate of the region gets colder and the frozen ground develops better, the frozen ground area is 40 to 50% of the total area of the region. The mean annual ground temperature of the frozen ground is -0.5 to -1.0°C. The thickness of the frozen ground is more than 20 to 30 m. Xinan Larix gmelini is the main wood seed of the forest flora, which is advantageous because the natural regeneration is above 90% (Lu Guowei, 1989). We can assert that, under the construction policies of forestry the forest area will be gradually increased in China. To have the optimum natural environment, the rate of the northward movement of permafrost must decrease and the southern permafrost boundary must be stabilized.

REFERENCES

Guo Dongxin, et al., (1981) The Permafrost Historic Evolution and Formation Period in the Northeast of China Since Late Pleistocene, Glaciology and Geocryology, Vol.3, No.4.

Li Peiji, (1991) Greenhouse Effect and Climate Change, Glaciology and Geocryology, Vol.13, No.3.

Lu Guowei, (1989) Xinan Pine Vegetation and Variation of the Ecological Environment of Permafrost in Northeast China, The Proceedings of the Third Chinese Conference on Permafrost, The Press of Sciences.

Xin Dekui et al., (1959) The Geological Knowledge About the Permafrost Distribution in the Northeast of China, No.10.

Zhou Youwu, et al., (1980) Permafrost and Ice Edge Geomorphology, the Natural Geography of China (Geomorphology) The Press of Sciences.

Zhu Kezheng, (1972) The Preliminary Study on the Recent Five Thousand Year Chinese Climatic Fluctuation, Zhu Kezheng Monograph, The Press of Sciences.

ROAD DESIGN AND RENOVATIONS OF THE NORTH SLOPE IN DA HINGGAN LING

Luo Weiquan

Design House of Management Forest Bureau,
Eer Guna Lift, Inner
Mongolia Autonomous Region, China

Research and practice have been carried out for many years to determine a method of selecting the road line, renovation against frost heave and thaw settlement, determination of embankment height, foundation depth for bridge culverts, foundation type, and preventing pingoes and icings. These methods have been used in recent constructions of roads in cities and towns, especially in the design and construction of concrete pavement in sections with massive ice, measures are taken to choose a reasonable embankment height, dredging, paving soil material, protecting the natural environment and berm, enhancing the strength of the pavement layer and base course, and to ensure that the 12 m width of concrete road is safe for transportation in cities and towns.

INTRODUCTION

Mengui Forest Bureau is on the north slope of Da Hinggan Ling, the climate is frigid and the yearly average temperature is below -5°C. The extreme temperature is -54°C and the frost season is as long as 8 months of the year. Permafrost has an extensive distribution and is from several meters to around 100 m, but the large riverbed is talik. The Quaternary covering layer is composed of stones with loam gravel, cobble soil and peat loam stratum. The surface vegetation is mainly a heavy growth of eriophorum tussock, and swamp ground is distributed in the basin and wide valley of the region. The largest depth of seasonal thawing is from 0.5 m (peat section) to 3.2 m (cobble and gravel, stone section). The permafrost includes a large amount of ground ice. More than 350 km of road and 200 bridge culverts were constructed from 1960 to 1983, and most have some extent of frost damage. The damage is mainly shown in the non-uniform subsidence of the roadbed, wrenching and inclination of bridges and culverts, pingo and ice erosion of the road and the formation of potholes in the spring. This causes the ecological equilibrium to be destroyed as the buildings do not adapt to the natural environment of frozen soil, as well as the causes of unreasonable design and construction. In general, in several months or years, deformation or destruction of the buildings occur. Roads change their original line and culverts have to be renovated. The light damage needs to be repaired and prevented and the cost of repairing 180 km of road is more than two million Reminbi Yuan a year.

ROAD DESIGN AND RENOVATION OF FROST DAMAGE

Roads and bridge culverts in the north slope of Da Hinggan Ling suffer damage due to the large amount of ground ice in the permafrost, plentiful surface water and groundwater, suitable freezing conditions, and loam stones with stronger frost heave sensitivity, etc. Road designs and methods for renovating the frost damage should take into account the above mentioned factors. For the north slope region of Da Hinggan Ling, the renovations of frost damage should stress the aspects of drainage water, heat preservation and the filling soil used in the past. Combined with choosing the line, design and renovation can often be more effective.

Choosing the Line

The north slope of Da Hinggan Ling is mainly a hilly land of middle-low mountains. The road often crosses the basin and valley. When choosing the line in the permafrost region with these natural conditions, the basic design principles are: sufficient filling and little excavation, selecting a high site and avoiding low sites. The line in the hills should have a higher site, and cross from the top of the low pitch in front of the mountain, and a sun exposed site is preferable. When built along the river valley, a high terrace and river talik should be chosen. Based on selecting the line and investigation, poor geological sections should be avoided when possible. The line should cross the embankment in the upper front of the massive ice section or in the lower part of the thaw slumping body. The possibility of changing hydrogeological conditions in the road should be prevented in the regions where ground water exists, surface water should be dredged and the roadbed periphery should be kept dry. Design and construction should protect the natural environment of permafrost and the ecological equilibrium. Designs of bridge culverts, except for the flood table area with the largest flow amount, jammed height of pingo and icing and foundation handling should be considered. In recent years, the above mentioned principles have been used when choosing the

line and design and the frost damage of roads has greatly decreased.

Roadbed Engineering

Filling height of embankment: A large amount of investigations and testing have shown that the minimum filling height of the embankment in the region of the north slope of Da Hinggan Ling is determined by using the following experience equation:

$$H = h_1 + h_c \quad (1)$$

where H — embankment height (m)
h_1 — dry soil thickness of embankment (m) in general h_1=0.6 m
h_c — dangerous capillary height of roadbed soil (m)

The relative soil types and degrees of compaction are given in Table 1.

THE MEASURES OF WATER DRAINAGE AND STOPPAGE

A water stoppage ditch, water drainage ditch and retaining wall are often used to drain surface water in road engineering. A blank ditch and water penetration ditch are used to drain ground water or decrease the ground water table. The drainage ditch should be kept a definite distance from the slopefoot of the roadbed. The distance can not be less than 1.5-2.0m in general conditions and the drainage ditch must be consolidated to prevent penetration and to have enough vertical gradient. A tapered gutter to preserve heat should be set up to avoid pingo and icing from forming. When the ground water table is higher an insulating layer should be set up to insulate the ground water (see Fig.1)

Table 1. Dangerous capillary height of types of roadbed soil (m)

Soil type	Compacted soil approaching optimun water content	Soil of air dried and compacted	Soil of non-compacted
Sand	0.10	0.20	0.20 — 0.60
Sandy loam	0.20	0.30	0.30 — 0.60
Silt	0.50	1.0 — 1.20	0.80 — 1.50
Loam	0.40	0.80	1.50 — 2.00
Clay	0.40	0.80	1.50 — 2.00

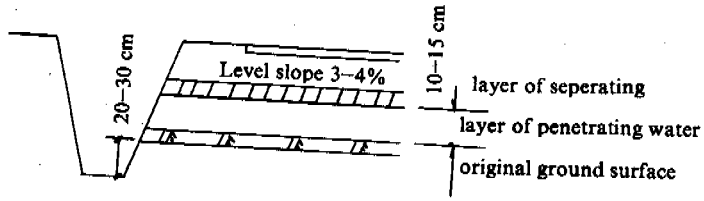

Fig.1 Insulating layer structure of roadbed

ROADBED WITH FROST HEAVE AND THAW SETTLEMENT

The handling of roadbeds with frost heave in the north slope of Da Hinggan Ling often uses the method of changing the soil, gravel soil, cobble gravel and medium coarse sand are often used instead of frost heave soil, the replacement soil should be less than 80% of the maximum depth of freezing. The road after the soil has been changed must meet the demands of strength and water insulation. The heat preservation method is chiefly used in the sections with massive ice, eriophorum tussock at the location can be used as the heat preservation material. One layer is paved in the original surface and berm with heat preservation is constructed (Fig. 2).

Except for increasing the height of the roadbed (minimum value is 1.2 m), the measure of draining insulating water is used in the concrete road in the town of Mengui. Three layers of soil are used as a cushion in the bottom of the pavement, and underneath, 15 cm of soil material is added. This method not only enhances the action but also quickly diffuses water so that thaw settlement cannot be produced in the sections of massive ice (Fig.3). It is also considered important in protecting the natural surface beside roadbed. The ground surface within the range of 10-15 m of the roadbed can not have its general condition destroyed. Zheng Yang road was constructed with this method and basically no changes have occurred from 1987 to present.

PINGO AND ICING PREVENTION

Except for the naturally forming pingoes and icings, pingoes icings and some small rising pingoes are caused by the changing movement law of ground water after the road construction on the northern slope zone of Da Hinggan Ling.

The drainage ditch and freezing ditch are generally installed above the embankment to block and drain ground water, meanwhile enough field accumulated ice remained for the embankment or blank ditch for penetrating water, to decrease the pressure and heat preservation, are

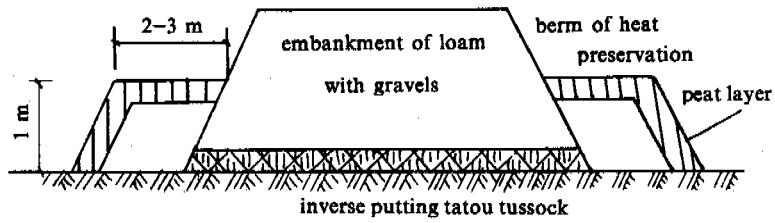

Fig.2 The section of heat preservation embankment

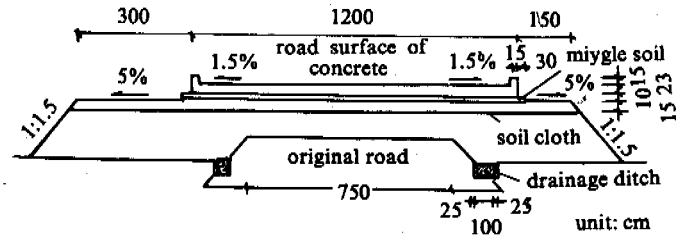

Fig.3 Sketch map of cross section on concrete roadbed in Mengui

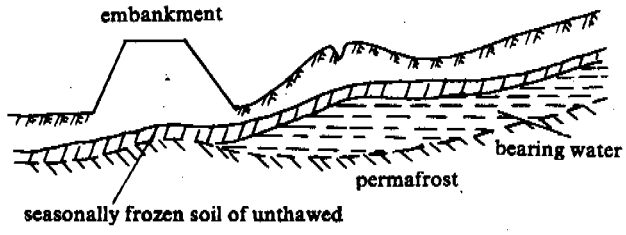

Fig.4 A sketch map of a pingo

installed in the upper part of the embankment to divert ground water to the lower part of the embankment. Engineering renovations at many sites show the effect of the blank ditch for penetrating water, decreasing pressure and heat preservation is very good. Success or failure of this measure depends on the heat preservation and drainage conditions.

Bridge Culvert Engineering

Most of the bridge culverts were provisional wood structures and have been changed to concrete structures to meet road standards. Frost damage of the bridge culvert is mainly shown to be an upfreezing of objects causing subsidence and wrenching inclination. A deep foundation is used for the pit foundation. For meeting the design demand for the bridge pile of roads its embedded depth H is determined by the following equation:

$$H = \frac{2\pi rh\sigma_T - P}{2\pi r\tau_f}$$

where r – pile radius (cm)
h – maximum thaw depth (cm)
σ_T – tangential frost heaving force (kPa)
τ_f – normal frost heaving forces (kPa)
P – surcharge load (kN)

The expanding column foundation of reinforced concrete exploded short pile and pilot pile are used in shallow foundations. Practice shows that the effect of preventing frost heave with pilot pile foundation is better. One layer of heat preservation needs to be paved, as well as the sand cushion under the foundation, in order to prevent heat transfer of the foundation and the prevention of frost heave of the foundation is enhanced, as with soil changing the chemical addition is used to enhance the hydrophobicity of the subsoil.

CONCLUSION

To summarize that mentioned above, the preventative steps against frost damage and comprehensive renovation of damages are used with the location conditions for a better effectiveness.

1. The main methods of protecting the roadbed stability are that the environment in the permafrost region should be protected, and the embankment height should meet the critical height.
2. Effective drainage, the better form of drainage ditch is with a shallow width and multiple dams.
3. Choosing coarse soil for constructing the road and using soil material to quicken the water drainage and enhance the roadbed.
4. Reasonably choosing the line and construction method ensures roadbed stability in permafrost regions.

PRACTICE OF REINFORCED CONCRETE STRIP FOUNDATION IN PERMAFROST REGIONS

Men Zhaohe

Amuer Design House Forestry Bureau, Management Bureau of Da Hinggan Ling, Heilongjiang, China

In Amuer permafrost region, various of building foundation, for example, rubble foundation, rubble-sand pad foundation, concrete foundation with sand pad, pile foundation, and reinforced concrete strip foundation have been used. It is proved that the former three types of foundations are not appropriate to be built in permafrost region. The designing principal of reinfore concrete strip foundation permits the foundation ground to thaw, that is the frost state of foundation ground is unconsiderable. The mechanical properties, such as, bend, shear, tension and deformation, can be completely contributed. According to various frost heaving soil and the depth of maximum thawing plate, the depth of sand pad and the section size of base (mainly the height of base) are designed and calculated. Meanwhile, by adopting relevant technical measurements, sufficient rididity and strength of the structure of base and upper soil are assured, so as to resist various stress and uneven settlement of frozen ground foundation during frost heaving and thawing.

INTRODUCTION

Amuer Forestry Bureau is located in the north of Da Hinggan Ling, about 52°15'-53°34'N, 122°39'-124°14'E. The total area of the region is 5556.06 km². It belongs to a hilly region and the altitude is 800-1000 m. Permafrost has an extensive distribution and the largest thickness of permafrost is about 50-80 m. The yearly average temperature is -3.8 — -6.3°C, the freezing index is 3810 day °C. The extreme lowest temperature is -49.7°C, the highest temperature is 35°C. The average ground temperature is -1.0°C — -4.2°C. The winter is as long as 7 months and the summer is about 5 months. The yearly precipitation is 597.70 mm. The maximum depth of accumulating snow is 36 cm. The seasonally thawed depth is 1.0 m in the permafrost region with vegetation.

REINFORCED CONCRETE STRIP FOUNDATION

According to the observation of base in the past, the causes of fissures and deformation are due to three aspects.

1) The foundation is not stable, and the deformation of freezing and thawing is not uniform.

2) The rigidity of the base is not strong enough to prevent various stresses from deformation in the frozen soil foundation, such as bending stress, tensile stress, shear stress, etc.

3) The foundation type and embedded depth are not reasonable.

The three aspects are analyzed as follows:

1. Design Principle of Frozen Soil Subgrade

The subgrade is designed without considering the depth of frozen soil under the foundation and the effects of the freezing state of the subsoil and the effects of gradual thaw. Then based on the engineering information, corresponding measures are taken such as reinforcement and trying to restrengthen and restabilize the destroyed frozen soil subgrade. If the subgrade has normal or strong thaw settlement, fissures for settlement and girds are set up to reinforce the integral rigidity of the building in the sand cushion in designed thickness under the bottom of foundation. The calculated thickness of the sand cushion is based on the following formula:

$$\sigma_E + \sigma_C < [R] \tag{1}$$

where σ_E — additional stress of sand cushion bottom (kg/cm²)

σ_C — self-weight stress of sand cushion bottom (kg/cm²)

$[R]$ — bearing allowance of soft layer at cushion bottom (kg/cm²)

2. Design of Foundation Rigidity

In order to increase and reinforce the rigidity of the foundation, the following steps are taken:

1) Material with the best mechanical properties is chosen for the foundation to reinforce the concrete.

2) The strip foundation is chosen because the pressure of the subsoil is small and uniform and the thickness of the bearing stratum can be decreased for this foundation type.

3) The foundation sectional shape chosen is the inverse "T" shape or the "I" shape section which have a large bending rigidity.

4) Checking the calculation of wall ridigity.

The height of the concrete foundation (h) is changed into the height of the brick bonding body H_o, and is the following:

$$H_o = 0.9h\sqrt[3]{E_n/E} \tag{2}$$

After the converted height is calculated, the integral rigidity of the wall is accounted for according to L/H<2.5-3 (allowance value). Its integral rigidity is adequate, the foundation height is adjusted and other steps are taken.

3. Design of Embedded Depth of Base

The embedded depth of the foundation is one of the factors that destroy buildings in the processes of frost heave and subsidence deformation of the permafrost subsoils. Before the type of foundation is determined, the importance of a sand cushion must be considered, especially in subsoil foundations that have normal or strong thaw settlement. Then according to the subsidence value and the bearing capacity of the subsoil, the subsidence value is calculated and the value is less than the allowence limit value. Lastly, the reasonable embedded depth of the base is calculated.

PRACTICAL DESIGN EXAMPLE

Two buildings were built in 1984 and 1985. One building was located in a permafrost region, the another was located in a sporadic permafrost region. Both had strip foundations of reinforced concrete and sand cushions.

1. Survey Conclusions of Teaching Building of A Special High School

(1) Depth of the seasonal thaw was 3.5 m, frost heave was produced during freezing, subsidence was produced after thawing.

(2) Ice layers exist prosperly in the permafrost layer and thaw settlements of different degrees were produced.

2. Design of Base

2.1 Steps of construction

According to the profile of engineering geology (Fig.1), there are many ice layers in the subgrade, non-uniform subsidence is produced when the foundation soil thaws, the level length is 76 meters and the height difference of the building is large. So two subsidence fissures are installed and a gird is installed in the upper layer of every unit to insure the rigidity of each unit.

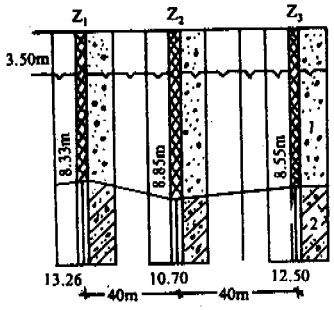

Fig.1 Geological profile

1. Gravel soil, massive cryogenic texture. 0-2.0 m, frozen soil with ice coefficient of thaw settlement amount is 2.6 cm, 2.0-4.8 m, rich ice frozen soil. A_o=6.2%, 4.8-8.55 m, there are many layers which its thickness is 1-2 m, the thickest one is 30 cm, average A_o=7.0%, 3.8-8.55 m, frozen soil R=60T/m², thaw soil R=25 T/m².

2. Day, massive cryogenic texture. A_o=1%, bearing capacity of frozen soil R=35 T/m², thaw soil R=18 T/m².

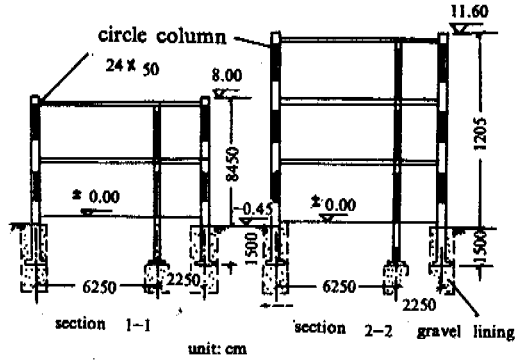

Fig.2 Profile and confined layer

2.2 Design and calculation

The foundation type used was a reinforced concrete strip foundation and a sand cushion is installed under it. According to the geological profile, the embedded depth of the foundation is determined to be 0.5 m. The section size and reinforcement are shown in Fig.2. The calculated load is the back force of the subgrade. So reinforcement quality is gained by the double reinforcement and the foundation height is 1.5 m.

2.3 Checking calculations

The width of the foundation is calculated according to Equation (3)

$$P = (N + G)/B \leq [R] \qquad (3)$$

where N — outside foundation static and dynamic bearing load every meter;
G — total weight of the soil in the upper foundation, average unit weight is 2 T/m³;
N — load of calculated unit;
R — bearing capacity of sand cushion, R=25 T/m².

then:

$N_F = G_F + P_F = 14.88 + 1.28 = 17$J/m (static load and dynamic load)

$N_S = 10.05 + 0.64 = 11$ T/m

by Equation(3):

$$P_F = (N_F + G_F)/B_F = 17.2\text{T/m} < 25\ \text{T/m}^2$$

pressure of foundation bottom:

$$P_S = (11+3)/1.0 = 14\text{T/m}^2 < 25\ \text{T/m}^2$$

This shows that the width of the foundation is correctly designed.

According to equation(3):

$$H_o = 0.9h^2\sqrt{E_n/E}$$

where E_n — Young's modulus of reinforced concrete 2.6×10^5kg/cm;
E — Young's modulus of brick bonding body 15.4×10^3kg/cm;

Conventional height of the bonding body H_o is 3.46 m.

thus, H_F=15.51 m, H_S=11.91 m (Fig.2). L_F=22 m, L_S=27 m, then:

$$L_F/H_F=1.42<[L/H]=2.5$$

$$L_S/H_S=2.26<2.5$$

So, this shows that the height of the foundation is correctly designed and meets the demands of rigidity of the wall body.

3. Design and Calculation of Subgrade

(1) Thickness of sand cushion: the material of the sand cushion is natural mingled sand stones, the unit weight is 1.8 T/m³, and the bearing capacity is R=2.5 T/m². The section of the sand cushion is shown in Fig.2.

The self-weight stress in the bottom of the sand cushion is:

$$\sigma_c = \nu_1 D + \nu_2 H = 5.7 \text{ T/m}^2$$

self-weight stress in the bottom of foundation:

$$\sigma_c' = \nu_1 D = 3 \text{ T/m}^2$$

Additional stress in the bottom of the sand cushion:

$$Z_F = \{B_F(P_F-\sigma_c')\}/(B_F+2Htg30°)=6\tau/m^2$$

$$Z_S = \{B_S(P_S-\sigma_c')\}/(B_S+2Htg30°)=4\tau/m^2$$

Substituting the results into equation (1)

$$\sigma Z_F+\sigma_c=11.7 \text{ T/m}^2<[R]=25 \text{ T/m}^2$$

$$\sigma Z_S+\sigma_c=9.7 \text{ T/m}^2<[R]=25 \text{ T/m}^2$$

where [R] — bearing allowence of soft soil under the sand cushion (Fig.2).

This shows that the thickness of the sand cushion is correctly designed.

(2) Calculation of derformation and subsidence: According to Equation (4), the thickness of the bearing stratum is calculated as follows:

$$\sigma_E / \sigma_c \leq 0.2 \qquad (4)$$

Results of calculation are listed in Table 1.

According to Equation (5), the subsidence amount is calculated.

$$S=PB_i\sum_{i=1}^{n}\frac{\beta_i}{E_c}(K_i-K_{i-1}) \qquad (5)$$

where E_c--deformation modulus of compressed soil 40 (kg/cm²)

β_i--relative coefficient, β=0.742

Values of K is listed in Table 2, then subsidence amount of compression are given:

S_F'=5.30 cm (first unit)

S_S'=3.30 cm (second unit)

The amount of thaw settlement is shown in Fig. 1. The average coefficient of thaw settlement A=7%, the subsidence amounts are:

S_F''=23.1 cm

S_S''=17.5 cm

the total subsidence amounts are:

S_F=28.4 cm

S_S=20.8 cm

Table 2. Settlement coefficient K

Depth of bearing layer	B_F=120 cm		B_S=100 cm	
	h/B_F	K_F	h/B_S	K_S
0.0 m	0.0	0.0	0.0	0.0
1.5 m	1.25	0.92	1.50	1.04
4.0 m			4.0	1.65
4.8 m	4.0	1.65		

Because of the rigidity of the first unit wall D/H=1.42<2.5, we can consider the wall body has uniform subsidence, but the second unit has subsidence on an inclination.

Table 1. Calculation of the thickness of bearing stratum

Depth (m)	B_F=120 cm		First unit 1(1') point		B_S=100 cm		Second unit 2(2') point	
	h/B_F	K_o	$\sigma_E=1.42K_o$	$\sigma_c=0.3+yh$	h/B_F	K_o	$\sigma_z=1.1K_o$	$\sigma_c=0.3+yh$
1.5	1.25	0.46	0.65	0.57	1.5	0.4	0.44	0.57
3.0	2.5	0.26	0.37	0.84	3.0	0.21	0.23	0.84
4.0	3.33	0.19	0.27	1.02	4.0	0.16	0.18	1.02
4.8	4	0.16	0.23	1.16	4.8	0.13	0.14	1.16

thus: $\Delta s = z' = 28.4 - 20.4 = 7.6$ cm

$$P = \Delta s / Ls = 7.6/2700 < 0.003 = [f] = 0.003$$

This shows that Δs value is not more than the allowance value. In fact, the teaching building of the special high school has been used for eight years, and the teaching building of the primary school in the Forestry Bureau has been used for six years, and there are no fissures and deformation in either.

CONCLUSIONS

According to the exploration of the above mentioned theory, practical examples of design and practics, it is feasible for strip foundations of reinforced concrete to be used in permafrost regions. This is due to its special advantages:

(1) Integral rigidity is very large. It has a harmonious capacity to the stresses in the deformation process of nonuniform frost heave and thaw settlement of frozen soil subgrade.

(2) Economic cost.

(3) It is easily built and is not confined by technical conditions.

(4) It is not confined by the subgrade condition.

So, application of strip foundations of reinforced concrete in permafrost regions has certain practical significante.

REFERENCES

Tong Changjiang and Guan Fengnan, (1983) Frost heave of soil and prevention of frost damage of building, Publishing House of Hydroelectricity.

Subgrade and foundation, Publishing House of Industry of Construction in China.

Research and Design in Forestry, (1977) Yakeshi Institute of Forestry, Neimen Province.

A MICROSTRUCTURE DAMAGE THEORY OF CREEP IN FROZEN SOIL

Miao Tiande[1,2], Wei Xuexia [2], Zhang Changqing[1]

[1]State Key Laboratory of Frozen Soil Engineering, LIGG,CAS,China
[2]Lanzhou Universitv

In the paper damage mechanics was used into mechanics of frozen soil to study the infer relation between creep deformation and it change of microstructure. Based on a series of creep test of frozen soil, and also observated its change of microstructure by "Duplication–electronmicroscope" method. We consider that the sticky force of ice remained in frozen soil, the degree of directional of mineral grain and the area damage (include the production of microcrackle and its later extension control) the whole creep process. So analysis in theory, we start at the basic equations of continuum mechanics, introduce the ice content in frozen soil. The factor of damage area and the factor of area occupied by directional mineral grains as the three internal variables which characterize the change of microstructure of frozen soil.

INTRODUCTION

Creep is one of the most important mechanical behavior of frozen soil. Since 1930, when Tsytovich (1930) published the first paper on the subject, many investigations have been reported. Several theories to explain creep in frozen soil were forwarded,most of these studies were based on the macroscopic tests. However, because the complexity of the microstruction changes, and sensitity to tempreture, these very facts make it very difficult to study the creep mechanics at microscopic level.

In 1967, S. S. Vyalov(ACFEL,1952) reported his first observation of the microstructure changes of frozen soil in creep process. He used "area" and "orientation" factors —— to characterize the microchanges. This might be the initial considerration of microstructure damage in studying behavior of frozen soil. Since then, no significant progress was made in the area. there isn't any related published work in china.

In past few decades damage mechanics as one of the disciplines of solid mechanics was been firmly founded, and has been successfully applied in many scientific fields. In light of the damage mechanics, we have studied the relationship between creep deformation and the microstructure changes of frozen soil. Limited by the paper length, only part of theoretical analysis is given in this paper. Experements results will be reported in separate paper.

Through a series of creep tests and microstructure obvervation by so called "duplication–eletromicroscope" technique, we found that the cohesive force created by ice, the orientalization of soil grains, and the creatation with its late extension of microcrack control the whole process of creep in frozen soil. Starting from these basic points, we developed a 3–dimensional damage theory for the creep deformation in reference to the principles of continuum mechanics and the frame of damage mechanics.

A detailed analysis has been made for the case of uniaxial compression, a prediction equation for the long–term strength has been derived. The theoretical curves correlate with the corresponding test ones.

BASIC EQUATIONS OF CONTINUUM DAMAGE MECHANICS

when we treat frozen soil as a continuum medium, the following equilibrium and thermodynamic restrictions should be satisfied:

$$\frac{\partial \rho}{\partial t} + (\rho v_k)_{,k} = 0 \qquad \text{Conservation of mass} \qquad (2\text{–}1)$$

$$\sigma_{kl,l} + \rho(f_k - \dot{v}_k) = 0 \qquad \text{Balance of momenta} \qquad (2\text{–}2)$$

$$\sigma_{kl} = \sigma_{lk} \qquad \text{Balence of moment of momentum} \qquad (2\text{–}3)$$

$$\rho\dot{e} - \sigma_{kl} d_{lk} - q_{k,k} = 0 \qquad \text{Conservation of energy} \qquad (2\text{–}4)$$

$$\rho\dot{\eta} - (q_k / \theta)_{,k} \geqslant 0 \qquad \text{Principle of entropy} \qquad (2\text{–}5)$$

where

ρ—— the mass density;
v_k—— the component of displacement velocity, k = 1,2,3;
σ_{kl}—— the component of stress tensor;
f_k—— the component of the body force per unit mass;
d_{kl}—— the component of strain velocity tensor;
q_k—— the component of the heat vector per unit area;
e—— the internal energy density per unit mass;
η—— the entropy density;
θ—— the absolute temperature.

In addition, $(\dot{}) = \frac{d}{dt}(\ )$ indicates the differentiation with respect to time t.

Introducing the free–energy function

$$\varphi = e - \theta\eta \qquad (2-6)$$

and thinking φ is the function of elastic strainε^{e}_{kl}, temperature θ and internal damage variables α_i

$$\varphi = \varphi(\varepsilon^{e}_{kl}, \theta, \alpha_i) \qquad (2-7)$$

Substituting (2–6), (2–7) into (2–5), and using (2–4), we obtain

$$-\rho\left(\frac{\partial\varphi}{\partial\theta} + \eta\right)\dot{\theta} + \left(\sigma_{kl} - \rho\frac{\partial\varphi}{\partial\varepsilon^{e}_{kl}}\right)\dot{\varepsilon}^{e}_{lk} + \sigma_{kl}\dot{\varepsilon}^{p}_{lk}$$
$$-\rho\frac{\partial\varphi}{\partial\alpha_i}\dot{\alpha}_i + \frac{1}{\theta}q_k\theta_{,k} \geqslant 0 \qquad (2-8)$$

Here we use

$$\dot{\varepsilon}_{kl} = d_{kl} = \dot{\varepsilon}^{e}_{kl} + \dot{\varepsilon}^{p}_{kl} \qquad (2-9)$$

where ε^{p}_{lk} is the plastic strain.

Because φ, η , $\sigma_{kl}$and $q_k$are independent of $\dot{\theta}$,$\dot{\varepsilon}^{e}_{lk}$ and $\dot{\theta}_{,k}$, the inequality (2–8) can't be maintained unless:

$$\left.\begin{aligned} q_k &= 0 \\ \eta &= -\frac{\partial\varphi}{\partial\theta} \\ \sigma_{kl} &= \rho\frac{\partial\varphi}{\partial\varepsilon^{e}_{kl}} \end{aligned}\right\} \qquad (2-10)$$

and

$$\sigma_{kl}\dot{\varepsilon}^{p}_{lk} - \rho\frac{\partial\varphi}{\partial\alpha_i}\dot{\alpha}_i \geqslant 0 \qquad (2-11)$$

Assuming

$$A_i = -\rho\frac{\partial\varphi}{\partial\alpha_i} \qquad (2-12)$$

(2–11) becomes

$$\sigma_{kl}\dot{\varepsilon}^{p}_{lk} + A_i\dot{\alpha}_i \geqslant 0 \qquad (2-13)$$

One of the methods to handle (2–13) is to choose a functional dissipativepotential,

$$F = F(\sigma_{kl}, A_i) \qquad (2-14)$$

The hypersurface expressed by (2–14) should be convex, this leads to

$$\left.\begin{aligned} \dot{\varepsilon}^{p}_{kl} &= \lambda\frac{\partial F}{\partial\sigma_{kl}} \\ \dot{\alpha}_i &= \lambda\frac{\partial F}{\partial A_i} \end{aligned}\right\} \qquad (2-15)$$

where λ is a scolar factor.

(2–15) gives the evolution equations of the plastic strain ε^{p}_{lk} and the internal damage variables α_i.

INTERNAL VARIABLES DESCRIBING THE MICROSTRUCTURE DAMAGE

By the method of "duplication–eletronmicroscope", the microstructure of frozen soil has been observed at different creep stages. Examining result of our observation and refering to Vyalov's work, we chose three internal variables which are most important to characterize the microstructure change in the creep process.

1) The cohesive force of ice in frozen soil plays a key role in the deformation of frozen soil. So we choose

$$\xi^{(i)} = \frac{\rho^{(i)}}{\rho} \qquad (3-1)$$

to be one of the internal damage variables.

Where:

ρ—— the mass density of frozen soil;

$\rho^{(i)}$—— the mass of ice in unit volume of frozen soil.

Following Vyalov's work, we introduce

$$\omega = 1 - \psi_\omega = 1 - \frac{A_\omega}{A_0} \qquad (3-2)$$

the factor of damaged area.

$$\Omega = 1 - \psi_\Omega = 1 - \frac{A_\Omega}{A_0} \qquad (3-3)$$

the factor of oriented area of mineral grain

as the other two internal damage variables, where ω defines the area damaged by the microcack and its extension, while Ω represents the area occupied by the oriented grains.

A_ω—— the effective area on which force acts;

A_Ω—— the area which mineral grain are not orientalized;

A_0—— the initinal area.

Let $\alpha_1 = \xi^{(i)}$, $\alpha_2 = \Omega$, $\alpha_3 = \omega$, then $\alpha_i (i = 1,2,3)$ are the internal damage variables, and $A_i (i = 1,2,3)$ which mentioned before, are the corresponding thermodynamic force of α_i.

A YIELD CRITERION FOR SOIL / ROCK

A yield criterion suitable for soil / rock is suggested. The criterion can be expressed by genernal stress components with advantage of that it has asingle expression, and it coincides with Coulomb yield criterion at thespecial stress condition——pure compression and pure stretch. It's yieldfunction G is expressed as

$$G = \bar{\sigma} + hJ_3' / \bar{\sigma}^3 + \alpha J_1 - H \qquad (4-1)$$

where

$$\left.\begin{aligned} \bar{\sigma} &= \sqrt{3J_2'} \\ J_3' &= |S_{ij}| \\ h &= \frac{81c\sin\phi\cos\phi}{9 - (\sin\phi)^2} \\ H &= \frac{18c\cos\phi}{9 - (\sin\phi)^2} \end{aligned}\right\}.$$

α is a material constant which characterize the compression behavior.

PARTICULAR EXPRESSION OF THE DAMAGE EVOLUTION EQUATIONS

The function of dissipative potential F is usually composed of two parts: one part $F_1(G)$ is to express the effect of viscoplasticity, while the other part $F_2(x)$ relates to effect of internal stress x, x is the strength of x .

Bacause the viscous flow occours before the plastic deformation, thus

$$F = F_1(G(\sigma - X))H(G(\sigma - X)) + F_2(\bar{X}) \qquad (5-1)$$

where H( ) is Heariside unit function.

F_1 and F_2 adaptable extensively to creep deformation is powerfunction:

$$F_1(G) = \frac{N}{n+1}\left(\frac{G}{N}\right)^{n+1} \qquad (5-2)$$

$$F_2(\bar{X}) = \frac{M}{m+1}\left(\frac{\bar{X}}{M}\right)^{m+1} \qquad (5-3)$$

where N, M, n, m are all constants depending on temperature.

There are some additional assumptions:

1) The cohesion C of frozen soil depends on $\xi^{(i)}$and ω (based on test), we simply assume,

$$C = C_0(1-\omega)\frac{\xi_0^{(i)}}{b+1}\left(\frac{\xi^{(i)}}{\xi_0^{(i)}}\right)^{b+1} \qquad (5-4)$$

where

C_0—— the initial value of C;

$\xi_0^{(i)}$—— the original ice content;

b —— a material constant dependent on temperature.

2) The orientation factor Ω leads frozen soil to be anisotropic, which relates to vector x of the center of yield hypersurface $x = x(\Omega)$, also causes change of the friction angle ϕ, thus

$$\phi = \phi(\Omega) = \phi(\bar{X}) \qquad (5-5)$$

3) The effect of the thermodynamic pressure π on F can be contained in the yield function G by the following equation:

$$G = \bar{\sigma} + \alpha(J_1 - \pi) + kJ_3'/\bar{\sigma}^3 - H \qquad (5-6)$$

4) to simplify the calculations, we suggest particular functions of thethermodynamic forces A_i with α_i by

$$\left.\begin{aligned} &\pi = \pi(\xi^{(i)}, \omega) \\ &A = \bar{X}(\Omega) \\ &B = -\beta\left(\frac{C}{C_0}\right)(1-\omega)Sign(\omega) \end{aligned}\right\} \qquad (5-7)$$

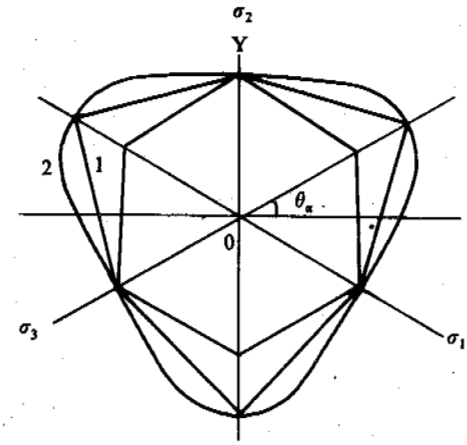

Fig.1 Forms of yield criterions on π plane
1. Coulomb yield criterion
2. The suggested yieldcriterion

where β is a material constant.

substituting (5–1)–(5–7) into (2–15), we arrived at a set of 3–D damage evolution equations:

$$\dot{\varepsilon}_{kl}^{p} = \{\lambda\left(\frac{G}{N}\right)^{n}[\frac{3}{2}(1-3k\bar{\sigma}^{-4}J_3')\bar{\sigma}^{-1}S_{kl} + (\alpha + \frac{k}{9}\bar{\sigma}^{-1})\delta_{kl} + k(2 - \delta_{kl})\bar{\sigma}^{-3}(j_3')\bar{k}_{\bar{l}}]\}^{1}\sigma \to \sigma - X \qquad (5-8)$$

where $(j_3)_{kl}$indicates the algebraic complement of $J'_3.(\ )_{kl}$ indicates that not plus with k, l, and $(\ )_{\sigma\to\sigma-x}$shows σ is all displaced by σ–x in every expression.

$$\dot{\xi}^{(i)} = \{\lambda\left(\frac{G}{N}\right)^{n}[-\alpha + (\frac{\partial h}{\partial \xi^{(i)}}J_3'/\bar{\sigma}^3 - \frac{\partial H}{\partial \xi^{(i)}})\frac{\partial \xi^{(i)}}{\partial \pi} + (\frac{\partial h}{\partial \omega}J_3'/\bar{\sigma}^3 - \frac{\partial H}{\partial \omega})\frac{\partial \omega}{\partial \pi}]\}_{\sigma\to\sigma-X} \qquad (5-9)$$

where

$$\left.\begin{aligned} \frac{\partial h}{\partial \xi^{(i)}} &= \frac{81C_0 sin\phi cos\phi}{9 - sin^2\phi}(1-\omega)\left(\frac{\xi^{(i)}}{\xi_0^{(i)}}\right)^{b} \\ \frac{\partial H}{\partial \xi^{(i)}} &= \frac{18C_0 Cos\phi}{9 - sin^2\phi}(1-\omega)\left(\frac{\xi^{(i)}}{\xi_0^{(i)}}\right)^{b} \\ \frac{\partial h}{\partial \omega} &= -\frac{81C_0 sin\phi cos\phi}{9 - sin^2\phi}\frac{\xi^{(i)}{}_0}{b+1}\left(\frac{\xi^{(i)}}{\xi_0^{(i)}}b + 1\right. \\ \frac{\partial H}{\partial \omega} &= -\frac{18C_0 cos\phi}{9 - sin^2\phi}\frac{\xi^{(i)}{}_0}{b+1}\left(\frac{\xi^{(i)}}{\xi_0^{(i)}}\right)^{b+1} \end{aligned}\right\} \qquad (5-10)$$

$$\dot{\omega} = \{\frac{\lambda}{C}\left(\frac{G}{N}\right)^{n}(kJ_3'(\bar{\sigma}^{-3} - H)\frac{\partial C}{\partial B}\}_{\sigma\to\sigma-X} \qquad (5-11)$$

$$\frac{\partial C}{\partial B} = -\frac{C_0}{2\beta}\frac{Sign(\omega)}{(1-\omega)} \qquad (5-12)$$

$$\dot{\Omega} = -\dot{\varepsilon}_{kl}^{p}\frac{X_{dkl}}{\bar{x}} + \{\lambda\left(\frac{G}{N}\right)^{n}\frac{\partial G}{\partial \phi}\frac{\partial \phi(\bar{X})}{\partial \bar{X}}\}_{\sigma\to\sigma-X} \qquad (5-13)$$

where

$$\frac{\partial G}{\partial \phi} = J_3' \bar{\sigma}^{-3} \frac{\partial h}{\partial \phi} - \frac{\partial H}{\partial \phi} \qquad (5-14)$$

As the creep developes, x is absolutely relaxed, so the effect of $F_2(x)$ is neglected in (5–13).

THE CASE OF UNIAXIAL COMPRESSION

If $\sigma_{33} = -\sigma$ and all other $\sigma_{kl} = 0$, then (5–8)–(5–14) degenerate to one dimensional for which

$$\dot{\varepsilon}^p = -\lambda(1-\alpha)\{\frac{1}{N}[(1-\alpha)(\sigma - X) - \alpha\pi - T_c]\}^n \qquad (6-1)$$

$$T_c = \frac{6C_0 \cos\phi}{3 - \sin\phi}(1-\omega)\frac{\xi_0^{(i)}}{b+1}\left(\frac{\xi^{(i)}}{\xi_0^{(i)}}\right)^{b+1} \qquad (6-2)$$

$$\dot{\xi}^{(i)} = \dot{\varepsilon}^p\{\frac{\alpha}{1-\alpha} + \frac{1}{1-\alpha}(\frac{2}{27}\frac{\partial h}{\partial \xi^{(i)}} + \frac{\partial H}{\partial \xi^{(i)}})\frac{\partial \xi^{(i)}}{\partial \pi} + \frac{1}{1-\alpha}(\frac{2}{27}\frac{\partial h}{\partial \omega} + \frac{\partial H}{\partial \omega})\frac{\partial \omega}{\partial \pi}\} \qquad (6-3)$$

The expression of $\frac{\partial h}{\partial \xi^{(i)}}, \frac{\partial H}{\partial \xi^{(i)}}, \frac{\partial h}{\partial \omega}, and \frac{\partial H}{\partial \omega}$ are given by (5–10),and $\pi(\xi^{(i)}, \omega)$ will be determined in lateranalysis.

$$\left.\begin{aligned} |\dot{\omega}| &= -T_c' \frac{\dot{\varepsilon}^p}{1-\omega}, (\dot{\varepsilon}^p < 0) \\ T_c' &= \frac{3C_0}{\beta(1-\alpha)}\frac{Cos\phi}{3 - Sin\phi} \end{aligned}\right\} \qquad (6-4)$$

$$\dot{\Omega} = -\dot{\varepsilon}^p(\frac{2}{3} - \frac{1}{1-\alpha}\frac{\partial G}{\partial \phi}\frac{\partial \phi(x)}{\partial x}) \qquad (6-5)$$

where

$$\frac{\partial G}{\partial \phi} = -6C\frac{1 - 3Sin\phi}{(3 - Sin\phi)^2} \qquad (6-5)_2$$

$\phi = \phi(x)$ is also to be determined.

The Particular Evolution Laws

In order to simplify the calculation, we divide the entire process of nondecline creep deformation into five phases(shown as Fig.2). In every phase the creep curve are imitated by a simple function.

At the first phase the response is absolute elasticity, that is

$$\varepsilon = \varepsilon^e = \frac{-\sigma}{E} \qquad (6-6)$$

where E is the elasticity modolus.

In addition, we consider that there is no change of the internal friction angle ϕ in each phase, but ϕ could be different for different phases.

a) phase 1:

$$-\varepsilon^p = C_1 - C_2(t - T^*)^2, (0 \leqslant t \leqslant t_1 \leqslant t^*) \qquad (6-7)$$

$$\phi = \phi_1 = Const. \qquad (6-8)$$

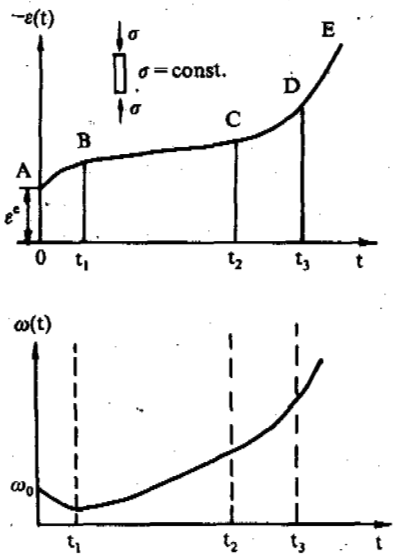

Fig.2 The variation of ε(t) and ω(t) in the whole creep process

The significance of t^* is given later, C_1, $C_2 > 0$, are all constant. Substituting (6–7) and (6–8) into (6–4), we get

$$\omega = 2C_2 T_c' \quad \phi_1 \frac{(t - t^*)}{(1-\omega)} \qquad (6-9)$$

where $T'_c \quad \phi_1$indicates that ϕ is replaced bv $\phi_1$in $(6-4)_2$.
Integrating (6–9), we obtain

$$(1-\omega)^2 - (1-\omega_0)^2 = -2T_c'\phi_1(t^2 - 2t^* t) \qquad (6-10)$$

$\omega_o$is the initial factor of damage area. An intevesting result from (6–10) is that ω is reduced when time t is increasing, it characterizesthe "harding" phenomenon at phase 1.

b) phase 2:

$$-\varepsilon^p = C_3 t + C_4, (t_1 \leqslant t \leqslant t_2) \qquad (6-11)$$

$$\phi = \phi_2 = Const. \qquad (6-12)$$

Similarly, we have

$$(1-\omega)^2 - (1-\omega_1)^2 = -2C_3 T_{c\,\phi_2}'(t - t_1) \qquad (6-13)$$

Substituting (6–11) into (6–1), we get

$$|\varepsilon^p| = C_3 = \left(\frac{\sigma - \sigma_0}{N_1}\right)^n \qquad (6-14)$$

$$N_1 = \frac{N}{1-\alpha}(\frac{1}{\lambda(1-\alpha)})^{\frac{1}{n}} \qquad (6-15)$$

(6–14) is just the famous Bingham–Shvtov equation, its widely adaptality to ice and frozen soil was proved by some direct tests.

From (6–14),one can see that

$C_3 = 0$ when $\sigma = \sigma_0$, we have a decline creep;

$C_3 > 0$ when $\sigma > \sigma_0$, the creep is nondecline.

Thus we consider σ is the long-term strength of frozen soil, while t^* is the shortest time when the rate of plastic strain becomes zero. For a certain material and t^* are all constants.

c) phase 3 ($t_2 < t < t_3$)

$$-\varepsilon^p = C_5 t^2 + C_6, (t_2 \leqslant t \leqslant t_3) \qquad (6-16)$$

$$\dot{\phi} = \dot{\phi}_3 = Const. \qquad (6-17)$$

$$(1-\omega)^2 - (1-\omega_2)^2 = -2C_5 T_c^{\prime} \dot{\phi}_3 (t^2 - t_2^2) \qquad (6-18)$$

where $\omega_2 = \omega(t_2)$.

d)phase 4 ($t > t_3$)

$$-\varepsilon^p = C_7 t^4 + C_8 \qquad (6 \geqslant t_3) \qquad (6-19)$$

$$\dot{\phi} = \dot{\phi}_4 = Const. \qquad (6-20)$$

$$(1-\omega)^2 - (1-\omega_3)^2 = -2C_7 T_c^{\prime} \dot{\phi}_4 (t^4 - t_3^4) \qquad (6-21)$$

where $\omega_3 = \omega(t_3)$.

Considering smoothness of creep curves, the continue conditions at each t_i($i = 1,2,3$) must be satisfied.

$$\varepsilon^p(t_i^+) = \varepsilon^p(t_i^-) \qquad (6-22)$$

$$\dot{\varepsilon}^p(t_i^+) = \dot{\varepsilon}^p(t_i^-) \qquad (6-23)$$

The variation of $\omega(t)$ in the whole creep process is shown as Fig.2.

Material Constants $\triangle_i$($i = 1,2,3$)

$\omega_i = \omega(t_i)$ ($i = 1,2,3$) corresponding to the time when one phase transit to another is determined by temperature, but not related to the level of load, therefore, $\omega_i = \omega(t_i)$ are material constants. Substituting it into (6–12), (6–14) and (6–20), we get

$$C_2(t_1^2 - 2t^* t_1) = \triangle_1 \qquad (6-24)$$

$$C_3(t_2 - t_1) = \triangle_2 \qquad (6-25)$$

$$C_5(t_3^2 - t_2^2) = \triangle_3 \qquad (6-26)$$

$\triangle_i$ is also material constants only depending on temperature. One can see that $\triangle_i$ is equal to the increment of plastic deformation at every corresponding phase.

The Equation of Long-Term Strength

By substituting (6–14) to (6–25), and letting $t_2 = t_p$, the long-termstrength equation is obtained as

$$\sigma = \sigma_0 + N_1 \left(\frac{\triangle_2}{t_p - t_1}\right)^{\frac{1}{n}} \qquad (6-27)$$

If $\sigma_0 = 0$, $t_1 = 0$, $1/n = \alpha$, $N_1^n \triangle_2 = T^*$, then (6–27) degenerates to the long-term strength equation given by S. S. Vyalov

$$\sigma = \left(\frac{T_p}{T^*}\right)^{-\alpha} \qquad (6-28)$$

which have been extensively used in cold engineering.

Predicting The Creep Curves and Comparing to Test Data

Material constants $\triangle_i$ and t^* can be fixed from a nondecline creep curve done by test. N_1, n and have to be determined by three test curves with different load level each. After that we can predict the creep behavior at any load level.

Fig.3 shows a comparison of the predicted curves with the test ones at temperature of −5℃. A good agreement exists between the two types of curves.

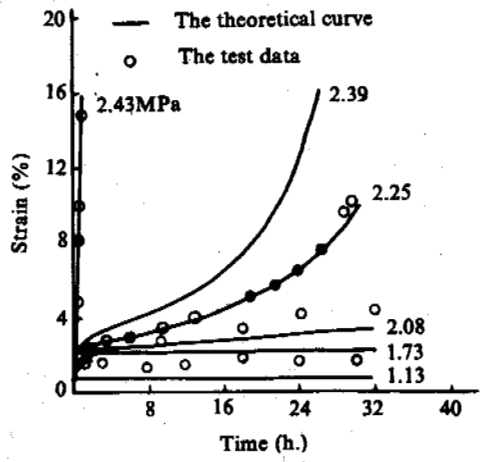

Fig.3 Comparison of calculated strain with test data

REFERENCES

Tsytovich,N.A.(1930):"Permafrost as a base structures. material of the permanent Commiossion for the study of the Nature Productive Force of the USSR",(1980):USSR Academy of Sciences Press.

ACFEL(1952):"Investigation of description classification and strength properties of frozen soils".Vol. 1 and 2.USA arctic Construction and Frost Effects Laboratory (ACFEL)Technical Report 40,AD721745 and AD721746.

Vialov,S.S.(1978),Rheological principles of soil mechanics. Higher Education Publisher.

Wu Hongyao(1990),Damage Mechanics .

Tstovich N.A.(1973), The Mechanics of Frozen Soil, Higher Education Publisher.

THE PALEOCLIMATE CHARACTERISTICS IN XINJIANG SINCE THE LATE PLEISTOCENE

Pan Anding

Department of Geography, Lanzhou University, Lanzhou 730000, China

This paper advances the arguments on the correspondence of cold–wet or warm–dry periods under the special geographical environment of Xinjiang since the late Quaternary. Evidence is cited and approached from various aspects, the paper points out that the monsoon was the main factor in forming the combination of warm–wet and cold–dry periods in eastern China. With the typical continental climate, Xinjiang had a contrary combination of temperature and humidity since the late Quaternary. The author does not deny the possibility that some short periods of warm–humid or cold–dry climate existed in Xinjiang since the late Pleistocene. But the correspondence of cold–wet or warm–dry should be the main features of climatic type in Xinjiang, the special arid region.

INTRODUCTION

Under the domains of monsoon climate, the combination of dry with cold or warm with wet climate is common knowledge in eastern China, in the past and present. But it is not so in Xinjiang. The cold glacial epochs were not extremely dry and the warm interglacial epochs were not wet since the late Pleistocene. On the other hand, in line with the sandards of the aridity index in the natural divisions of China, there almost are no humid areas in Xinjiang. Picea schrenkiana forest belt is located in the greatest precipitation belt of Tianshan Mountain and represents the most humid environment of Xinjiang with a yearly precipitation of about 400–800 mm. While this tree species should be included in xerophilous undoubtedly by the standards in eastern China, and often is used as the representative of a dry–cold environment of a glacial epoch in paleoclimatic research. For this reason, humid, the word used in this paper, is just a comparative concept under the special situation of an arid area, which is different from the humid climate of eastern China. But this relatively humidity benefits the conservation of soil moisture and the decrement of evapo–transpiration, and causes the great difference of ecological environment in the extremely dry region.

CHARACTERISTICS OF SPORO–POLLEN ASSEMBLAGES

There were a series of stronger temperature dropping epochs and remarkable high temperature epochs since the late Quaternary in northern Xinjiang, based on the analysis and computation of sporo–pollen identification results and ^{14}C dating. The characteristics of sporo–pollen assemblages in the cold periods were similar with that of the surface samples from various grasslands. In which there were variety of mesophilous herbs such as Gramineae, Labiatae, Alhagi, Ranunculaceae, etc. Still more pollen of hygrophytes or hydrophytes Typha, Acorus, Sparganiaceae, Cyperaceae, etc. could be found and the pollen of Salix, Ulmus, and Rosaceae appeared occasionally in some samples. It reflected the climatic environment with low temperature and humidity, which was favorable to form Grasslands and Marshlands, at the same time, the altitude of forest belt of picea was lower so that the conifer pollen often added to the deposits at the foot of the mountains. The climate conditions then was more humid and colder than present. In the hot period, the content of xerophte pollen as Chenopodiaceae III and IV, Ephedra, Artemisia, etc. rose abruptly, which often reached to the highest value in each of the cores or sections, taking the ZK–024 drilling in Balikun Lake as an example. The sporo–pollen assemblages were divided by visual and computer inspection into six zones (Fig 1). Zone I (89.05–65.09 m) is the zone of Chenopodiaceae–Cuperassaceae–Gramineae, that reflected the cold–wet climate of grasslands or grassy marshlands. And from 74.63 to 79.01 is a special cold–wet stage with a higher sporo–pollen influx. Zone II (65.09–23.49 m) is the zone of chenopodiaceae–Artemisia–Alhagi–Ephedra. The vegetation belongs to deserts–grassland, the climate was becoming warm and dry. This zone can be further divided to two warm–dry and a cold–wet stages. Thje third zone (23.49–10.76 m) is that of Chenopodiaceae–Rosaceae–Gramineae. The ancient environment recovered to grassland in the cold–wet climate, the sporo–pollen influx increased to the highest point. The forth zone (10.76–7.84 m), Chenopodiaceae–Leguminosae–Acorns Zone, reflected the flora of shrub–grasslands in the cold–wet climate. Zone V (7.84–2.96 m) is Chenopodiaceae–Artemisia–Ephedra zone, the assemblages are similar to the modern desert in a warm–dry climate, and the sporo–pollen influx is low here. Zone VI (2.96–0.75 m) is Chenopodiaceae–Artemisia–Gramineae Zone, which can be further divided into two parts. The lower part has some pollen of shrubs and trees, Such as Picea, Betula, Cupressaceae etc., and rep-

resents the slightly cold and wet climate. The higher pollen percentage of Ephedra, Artemisia and Gramineae in the upper part reflected the desert environment of warm–dry climate. The whole section shows four cold–wet and four warm–dry climatic epochs. Each cold–wet stage shown by sporo–pollen assemblages and influx corresponds to the fresh or slight salutes water layer provided by mussel–shrimp analysis, and the warm–dry stage to the salt water layer. The paleo–ecologic environment evolution reflected the paleo–climate changes. When the arid region entered a cold–wet stage, the lower air temperature dropped the evaporation power so that the relative humidity rose, and the vegetation did well. The sporo–pollen assemblage represented flora in a great variety,the sporo–pollen influx was raised to a higher point, and the percentage of xerophyte and salt herb decreased in the assemblages at those times. When the arid region returned to the warm–dry or hot dry climate,the plant's growing was blocked,the sporo–pollen assemblages displayed the dry features and the influx in lower values because of the higher temperature, the stronger evaporating power and the less effective precipitation. Then the percentages of Xerophyte and salt herb increased. The characteristics of sporo–pollen assemblages corresponded to that of surface samples from the general or driest deserts.

PARTICULARS OF THE PALEOCLIMATE IN XINJIANG

The correlation of warm–dry and cold wet climate seems contrary to the traditional ideas on cold–dry stages in glacial epochs and warm–wet stages in interglacial epochs. In this connections the author makes the following approaches:

1) The research on the climate of Xinjiang had showed clearly, that the relative humidity is smaller even though there is more water–vapor content in the air, if the air temperature is higher (Chen Hanyao,1963). Table 1 shows the contradictory situation in Urumqi as an example. The water–Vapor content of the air Urumqi in July is 5.6 times and the water–vapor pressure is 7.4 times as much as those in January. The relative humidity in July is 40 percent lower than that in January, for the mean monthly temperature in july is 39°C higher than that in January. The statistical data on the monthly relative humidity reported (Chen Hanyao, 1963), that the relative humidities were higher in winter than in summer in all of the meteorological observation stations of Xinjiang. The lower relative humidity in high–temperature periods increases the evaporation power and transpiration, hastens the vanishing of surface water and soil moisture content, and restricts the growing of mesophyte.

Table 2 shows that the increasing water–vapor pressure caused a variation of the precipitation, which rises by a greater proportion in eastern China. In Xinjiang, however, the water–vapor pressure in Urumqi is greater by 640 percent in July than in January, but the precipitation increased only 150 percent in the same period; the water–vapor pressure in Turpan, where it is hotter and dryer, is greater by 710 percent in July than in January;nevertheless, the precipitation, is increased only by 50 percent. The facts illustrated the increment of water–vapor to a great extent in hot periods. But the strong evaporation power at the same time,however, counteracted the effect of water–vapor greatly, and made the little difference in precipitation between summer and winter become more slight. Thus it can be seen that the dry environment is not followed by cold but by a hot stage at the present time.

2) We can see the similar situation from the research on the climate periodicity in Xinjiang (Zhang Jacheng,1974) that around 1970 could be taken for a transition in periodic variation. Table 3 shows the extreme minimum temperature that took place in the cold period before 1970, and the extreme maximum temperature in the warm period after 1970, which reflected the feature of the periodicity. In the warm period, the precipitation decreased by 7.4–16.4 percent, evaporation increased by 1.6–49.9 percent. The evaporation–precipitation ratio shows the air became dryer in the warm period.

3) The archaeological evidence. The 1,000–year cold period from the end of the Yin Dynasty to the beginning of the Zhou Dynasty (about 1,000 B.C) had been divided on the base of the phonology and historical records (Zhu Kezhen,1973). and was provided and received by many scholars. Xinjiang was also in a cold environment in 3,000–2,000 B.P. Li Guangli, a general of Han Dynasty,attacked the Xiongnu (Hun) at Tianshan Mountain with thirty thousand cavalry in the autumu of 99 B.C. General Li ordered the soldiers to take big pieces of ice as a beverage in the assault. It is thus shown that the weather was cold. Now the lake water can not ice up to such a thickness, even on Tianshan Mountain a height to 1,000–2,000 meters in the autumn. The chief of Xiongnu went on a punitive expedition for Wusun, the ancient Kazakh, in the winter of 72 B.C. Being caught in heavy snow with depths to 240 cm, the personal and domestic animals died in large numbers. This period was named the New Ice–epoch (Wang Qingtai,1981). At that time, the lakes had larger areas in the Tarim Basin and there were many hydrographic nets around it. The famous Silk Road was rather brisk at 2,000 B.P. According to the narratives in the Shan HAi Classic and the Annotations on the Water Classic, the books on ancient Chinese Geography, there were 8 rivers distributed over the east, the south, and the north which flowed into Luobubo Lake. Based on the American satellite photographs and the textual criticism(Zhou Tingru,1978), the area of Luobubo Lake was indeed larger during the former Qin Dynasty and Han Dynasty. Which confirms the records in the ancient books. Some researchers (Yang Huairen,1981) considered the stiuation which "did not accord with the common law of dry glacial epoch", reflected " the size of the lakes and the rivers in Tarim Basin were not absolutely dominated by the dry or humid period". The author thought that stiuation is just another piece of evidence for the coexistence of cold and wet climates.

4) The formation and development of most interior lakes in the northwest of China related to the Quaternary glacial action. Each glacial action made up a depositional cycle together with the relevant new deposition. When the glacier had the strongest action, the lake was provided with the highest water level, the largest area, and the thickest deposition layer. The contraction of the lake surface and the thinning of the deposition layer was accompanied with the recession of the glacial action. The relationship between cold climate and precipitation was also reflected therefrom.

5) The evidence of annual rings of trees. The restrictive factor of the naturally survived trees is not temperature but moisture in Xinjiang. In the dryer years, the photosynthesis was weakened and the cell division of cambium was restrained, thus the annual rings

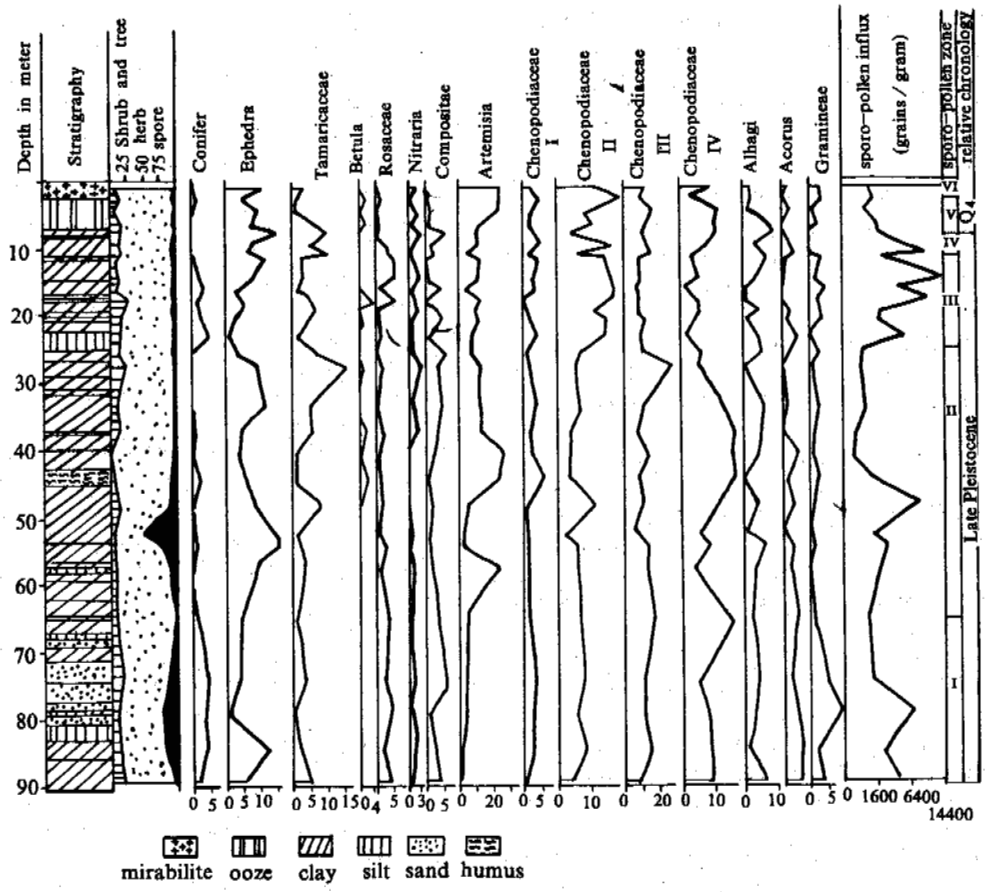

Fig.1 Sporo-pollen percentage diagram,Balikun Lake Core ZK-024

were narrow. The annual rings widened at the year with more humidity.

6) The research results on mean wind-field and the transported vapor quantity in the atmosphere above China showed (Qi Chengyu,1986),the compound quantity of the whole atmosphere above China comes from three annual air flows. The vapor carried by the southwestly airflow from the Indian Ocean and the Bay of Bengal made the greatest contribution. We can see from the 5,500 meter uper-air charts, the thermodynamic action of the Qinghai-Xizang Plateau was strengthened in summer, it then intensified the wet monsoon, which carried a great quantity of vapor and made the precipitation increase largely in the area which was effected by the monsoon in summer. The motion height of the wet monsoon, however, is only about 3,500 meters (Xia Xuncheng.1985), little of it could go over the Qinghai-Xizang plateau of 5,000 meters in mean height. In the northwest of the plateau, the upward air current from the surface of the plateau comes down and the subsidence heating effect caused the air to be dryer in summer.

Xinjiang could not get enough moisture to form plentiful summer rainfall as a conclusion.There was hardly any change in the swelling state of the Qinghai-Xizang Plateau since the late Quaternary.It is deducible that the great moisture increase were not able to make a significant influence to Xinjiang in the warm interglacial epoch.

In summary, the high temperature was bound to cause aridity, and only low temperatures enable the humid climate trend. The correspondence between dry and warm or humid and cold periods has been a general law in Xinjiang since the late Pleistocene.

ON THE FORMING MECHANISM OF THE COLD-WET OR HOT-DRY CLIMATES

Xinjiang is located at the middle-latitudes, the movement of the planetary frontal zone does not constitute the most important influence on its humidity and precipitation for many resons, which was greatly different from the situation in eastern China, where the main cause of the greater rainfalls in the warm period was the southwest monsoon. The beginning and the end of the rainy season and the motion of the rain-band were also closely related to the advance and retreat of the summer monsoon there. The research on 18,000 B.P. climagraph showed that the precipitation decreased 20 percent in the northern hemisphere in the glacial epochs (Yang Huairen,1981). But this decrement was not homogeneous everywhere.In China, this situation might find expression in the eastern part with the monsoon climate.Xinjiang was not affected by the

Table 1 A comparison of the monthly mean temperature and humidity between January and July at Urumqi,Xinjiang

Times	Jan.	Jul.
Water content in the air (g / cm^2)	0.49	2.77
Water–vapour pressure (hpa)	1.6	11.8
Precipitation (mm)	8.7	21.5
Temperature (°C)	−15.4	23.5
Evaporation (mm)	10.1	357.1
Relative humidity (%)	78	38

monsoon, so the increment and decrement of the precipitation caused by the monsoon had hardly any effect on Xinjaing. Merely the increment and decrement of evaporation in the global sea–surface might cause the variation of the water–vapor transpiration volume in the prevailing westerly jet stream above Xinjiang.But the scale of this variation, as illustrated by the facts cited in table 1, was minor, compared with the change scale of the temperature and evaporation power in the arid area. Therefore the warm interglacial epoch could not bring about the humid environment. On the other hand, the cyclone actrivities were enhanced in the middle latitude areas,and the depression of the dew point in upper–air dropped greatly during the glacial epoch, which enabled the water vapor to saturate easily and contribute to the formation of precipitation. Though the water vapor in the air current decreased to some extent, the precipitation did not decrease distinctly.

Fig.2 shows the relationship between the saturation vapor pressure (Ew) and the air temperature. The lower the temperature, the smaller the satuation vapor pressure, which decreses by the index rate. When the temperature decreses from 0°C to −10°C , Ew decreases from 6.1 hpa to 2.61 hpa; and when the temperature deceases from 30°C to 20°C, Ew deceases from 42.4hpa to 22.9hpa. It is the same in a decrease by 10 °C, but the Ew value decreased with heat is over five times as much as with cold. Thus it can be seen that the lower temperature greatly contributed to the condensation and precipitation, not dryness. Because of the great disparity of water vapor content between summer and winter, the promotive effect of

Table 2 A comparison of mean monthly vapour pressure and precipitation of the typical months of winter and summer between eastern and western China

Place name	Harbin	Peking	Nanjing	Chengdu	Yaxian	Taibei	Urumqi	Turpan
Meanmonthly vapour(Jan) Pressure (hpa) (Jul)	1.1 21.0	1.9 25.4	5.3 30.6	7.2 27.8	18.3 32.0	10.9 21.6	1.6 11.8	1.8 14.5
Mean monthly (Jan) precipitation (mm)(Jul)	3.7 160.7	3.0 192.5	30.9 183.6	5.9 235.5	7.2 142.9	87.8 227.5	8.7 21.5	1.5 2.3
Themultiple of vapourpressure of Jul / Jan	19.1	13.4	5.8	3.9	1.8	2.0	7.4	8.1
The multiple of precipitation of Jul / Jan	43.4	64.2	5.9	39.9	19.8	2.6	2.5	1.5
The increment of precipitation in July (mm)	157.0	189.5	152.7	229.6	135.7	139.7	12.8	0.8

* The data cited from Zhang Jacheng et al, 1985

* The data cited from Zhang Jacheng et al, 1885

Table 3 A comparison of climatic fluctuation in some regions of northern Xinjiang within thirty years

place / climate periods	Dabancheng cold	Dabancheng warm	Urumqi cold	Urumqi warm	Paotai cold	Paotai warm	Mucsuowan cold	Mucsuowan warm	Buole cold	Buole warm
the years when the extreme temperature happened	1969	1973	1951–1977		1956	1974	1969	1975	1960	1974
mean annual precipitation (mm)	67	52	293	249	150	128	127	106	194	170
decrement of precipitaion in warm periods(%)		7.4		15.0		14.7		16.4		12.4
mean annual evaporation (mm)	2700	2745	1508	2262	1802	1865	1894	2003	1534	1592
increment of evaporation in warm periods(%)		1.6		49.9		3.5		5.8		3.9
mean annual evaporation–precipitaion ratio	40.6	44.6	5.1	9.1	12.0	14.5	15.0	18.9	7.9	9.4
increment of E–P ratio in warm period(%)		10.0		78.4		20.0		26.0		19.4
predipitaion anomaly percentage in the year when the extreme temperature appeared(%)	3	−23	−13	−42	19	−55	20	−13	46	−44

* The data were sorted out from the records of surface observation

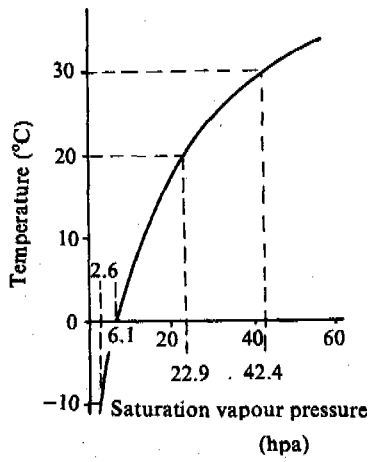

Fig.2 A diagram of interrelation curve of saturation vapour pressure with respect to water and temperature

low temperature to humidity is concealed in eastern China. But in Xinjiang, with an exceedingly low content and smaller changing ratio of water vapor, the humid effect of low temperature can manifest itself. It can be seen from the research results on the advance and retreat of ancient glaciers. It was provided by the research on the glaciology that the development of glaciers must have two of main conditions.

One is low temperature, and the other is precipitation. The glacier is unable to advance by a wide margin if it is in low temperaturee but the accumulated snow is insufficient. It is provided by the research on the relationship between the ten-years periodic climate fluctuation of China in the last eighty years and the process of glacial advance or recession on the Mount Qomolangma and Tianshan Mountain, that the scale and moving speed of the glacier could increase only in the periods when cold corresponded with humidity. Therefore, the periods when the ancient galciers advanced by a big margin should be the cold–wet environment.

CONCLUSIONS AND DISCUSSIONS

In summary, under the special geographical environment of

Xinjiang, the correspondence of a cold–wet or warm–dry period is the general climatic law in the arid region since the late Pleistocene. Though the vapor concentration of the upper air current was less in cold periods, the relative humidity near the ground was higher than that in warm periods.

The interior arid region got dryer and dryer as a result of the Qinghai–Xizang Plateau getting higher since the late Pleistocene. Humidity, the word used in this paper is just a comparative concept. The vegetative cover rate was lower regardless of the dry inter–glacial epoch or humid glacial epoch. It is for this reson that duststorms or sandstorms were able to be formed in any epoch in the arid region. In the warm inter–glacials, the higher vapor concentration of the upper air current makes the tiny dusts into the condensation nucleus and drops back to the ground with the rains despite the fact that the rainfall still cannot contend with the strong evaporation power. On the other hand, the vapor concentration of upper air currents was lower in cold periods. The dusats, failed to collect vapor to form raindrops drifted with the air current eastward to the monsoon region, then condensed and dropped to form loess deposition.

The author does not deny the possibility that some short periods of warm–humid or cold–dry climate existed in Xinjiang since the late Peistocene. But the correspondence of cold–wet or warm–dry periods should be the main features of climatic type in Xinjiang, the special arid region.

ACKNOWLEDGMENTS

I would like to thank Dr. Zhang Xuewen, the Senior Engineer of Xinjiang Meteology Service, for helpful suggestios and critiques of the manuscript.

REFERENCES

Chen Hanyao et al (1963) Xinjiang Climate and The Relationship between It and The Agriculture, Science Press, Beijiang,pp. 62–118.

Qi Chengyu et al (1986) The General Expression of Chinese Climate, Science press, Beijiang, p.34.

Wang Qingtai (1981) Ancient Glaciers at The Head of Urumqi River, Tian shan, Journal of Glaciology and Cryopedology, Vol.3, Secial Issue.

Xia Xuncheng and Fan Zili (1985) On The Environment and Climatic Changes in Luobubo Region, Collected Papers on Quaternary Research in Xinjiang, Xinjiang Press, Urumqi, 8–26.

Yang Huairen and Xu Xin (1981) The Influence of Quaternary Ice–Age Climate on The Loess and Desert, Selected Papers on Quaternary and Glacial Geology of Xinjiang, Xinjiang Press,pp.6–18.

Yang Huairen and Xu Xin (1981) The Physical Evolution of China in Quaternary, Geography Science and Technical Information, Nanjiang University Press,pp. 4–6.

Zhang Jiacheng et al (1974) Preliminary Approach of The Climate Changes of China, Science Bulletin, 4.

Zhang Jiacheng and Lin Zhiguang (1985) The Climate of China, Shanghai Science and Technical Press, Shanghai, 178,579–588.

Zhou Tingru (1978) On The Remove of The Luobunor Lake, Journal of Beijing Normal University, 3.

Zhu Kezhen (1973) Premary Research on The Climate Changes of China in Recent 5,000 Years, Science Sinica.

THE INTRODUCTION OF APPLICATION METHODS FOR CT IN FROZEN SOIL EXPERIMENTAL RESEARCH

Pu Yibin

State Key Laboratory of Frozen Soil Engineering
LIGG,CAS,China

This paper introduces the basic theory and method for experimenting with frozen soil samples nondestructively, quantitatively and dynamically using CT (Computer Tomograph). Accurately observing the digital images inside the samples in experiments, we can find a new technique for studying frozen soil in engineering.

THE SIGNIFICANCE OF INTACT QUANTITATIVE EXAMINATION SAMPLES

Along with intensively developing scientific study, computer technology has beeen widely applied to analyse experimental processes for many experimental equipment. On the other hand, intact examination of frozen soil and other samples is a very efficacious method in theoretical studying and engineering applications in different environments (temperature, pressure, composition of samples and their changes). We hope to find some way of connecting the two fuctions of reflecting the physical shape and properties of materials in experiments. The CT equipment is an efficacious method. Using data analysis, We can find the regularity inside exchange samples, and get new theorys for engineering applications.

THE THEORY OF CT EXAMINATION

"CT" is the abbreviation for the computer tomography. It uses X rays to penetrate the object slice which is revolving. Detectors gather the X-rays which have been attenuated from the object. The computer gets this information, does A / D transformation and calculates according to algorithms. Then the absorbed coefficient μ, which corresponds, with the physical properties of everypoint of the object, is quantitively displayed as data images and the instructions are dynamically analysed, quantitatively and dynamically. Because the samples are not damaged in the whole process, the samples can be examined many times for every slices, the images can be recorded, processed and analyzed. CT is ordinarily used to examine the human body, but it also can be used to check non-metallic materials. With some improvements, the instrument may become an efficient examination tool for samles. The principle schematic diagram below shows the system.

THE TECHNOLOGY INDEX OF CT

Different material has different absorbing coefficient μ of X-ray. The image of scanning and reconstruction shows quantitative μ maps. Professor Housfield has given a definition of CT count, air is −1000, water is 0. The biggest examinable material

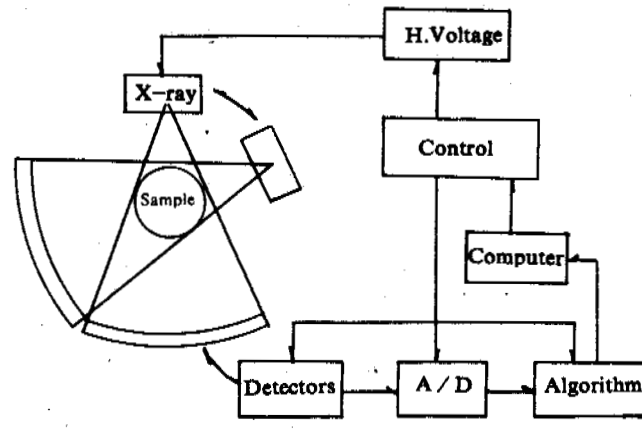

Dig.1 CT system working schemitic diagram

density is about 4 grem / cm^3, and a count of 3000. This density measurement range can fully check every non-metallic material. The CT count caculation contents linear equation:

$$CT = \frac{\mu_o - \mu_w}{\mu_w} \times 1000$$

In the equation, CT-CT count, μ_o-the X-ray absorbing coefficient

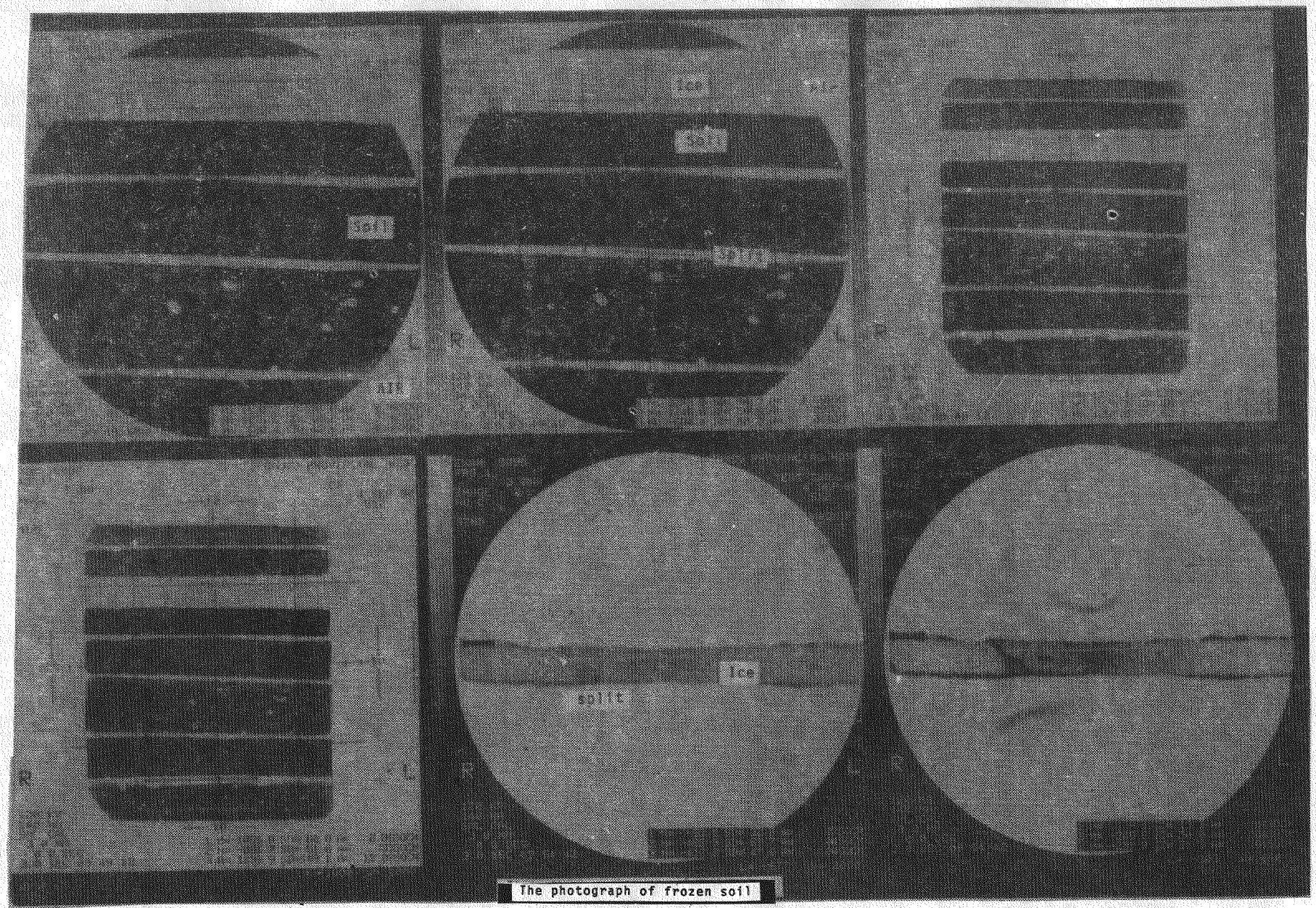

Photo 1. The image of layer sample

of examined object, μ_w–the X–ray absorbing coefficient of pure water.

In 20 years of development , there are 5 designed types of CT. The equipment of our laboratory may complete examination of a slice within 5–10 seconds, the diameter of the sample extends to 42 cm, It has 523 detectors, 576 pulse exposures for a slice. The detected data is calculated by computer. Spatial resolution reaches 0.8 × 0.8 mm and smaller linear objects and 0.065 mm diameter metal point can also be found. The density contrast resolution reaches to 0.5%. Since calibrating has been done by using standard polyethylene phantom, which has the same shape as samples, the CT counts have absolute quantitative significance, more accurate ray and display data. The images would be enhanced, distinguished and compared with other data. So we shall get better results of experiments.

THE EXAMINING METHOD OF SAMPLES

Adding some equipment to the common CT, making some sample containers and models which comply with experiment standardization, using programmed software for data calibrating in the scanning process, making the apparatus of pressure and temperature inside the sample container for examining construction changes in different environmental conditions, pre–burying some physical quality materials, we can analyse temperature and stress field in samples according to the changes of form position. We also can use new software to display 3 dimensional images and to analyse sample quality more clearly. Combining physical principles and other techniques, we may design many efficient experiments depending on the purpose, and so that extensive research may be done.

THE SIMPLE EXAMPLE

The photo 1 is an image which shows the layers of a sample. It indicates that there is great difference of CT data among ice, water, air, and soil. The split of ice appears very clearly. In the different areas, the statistical data shows the expansion or contraction of the samples. The position change of image point reflects movement of the matter in the examining process. The display control of the images is very useful for spectators to distinguish different materials.

Because the examination study of CT is just beginning, the new method is only introduced so that it may be of use in future scientific studies.

" Preliminary Data for Permafrost Thermal Regime and its Correlation Meteorological Parameters near the Spanish Antarctic Station"

M. Ramos. Department of Physic. UAH. 28871- Alcalá de Henares. Spain.

During 1991/92 Antarctic summer a turbulent atmospheric parameters measuring device was installed near the Spanish Antarctic Station (SAS), in order to register the exchanged energy flux between the soil and the low atmosphere.

Temporal evolution of permafrost was also registered using several temperature probes.

Base on the energy exchanged flux data and the movement of the free boundary in permafrost. We will study the permafrost evolution as function as the energy change in the soil/atmosphere surface.

INTRODUCTION.

Soil thermal evolution in cold regions where permafrost exists depends on the energy exchange between soil surface and low atmosphere and this will be a boundary condition in the heat and mass transfer process in the permafrost active layer. This frost and thaw processes could generate different geomorphy surface structures which can be quantified.

In the study area, Livington (South Setlhand Island. Antarctica) see figure 1 where the Spanish Antarctic Station is, the active layer of permafrost is about 0.7 to 1.0 m. deep Hall (1992).

The aim of this study is to measure, using the aerodynamic method Dyer (1974), Cancillo (1991) with a two levels micro meteorological tower the energy flux exchanges between soil and low atmosphere in different turbulents regimes in 1991/92 summer polar conditions.

The measured flux energy exchange in the soil/atmosphere will be use as a condition in the heat transfer permafrost problem Sorbjan (1989).

Theoretical thermal evolution of the permafrost active layer study will be compared with experimental thermal distribution data measured with several thermal probes Ramos (1993).

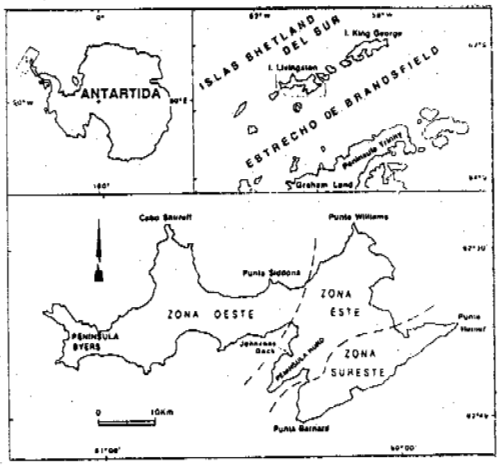

Figure 1
Experimental area.

EXPERIMENTAL METHOD.

Characteristic parameters, of the turbulent atmospheric flux in atmospheric surface layer, air speed, temperature, relative humidity are ramdon function of space and time. Any soil/atmosphere energy exchange model has restriction and there is not exact solution to the problem.

To study thermal evolution in permafrost a necessary condition is to know the energy exchange flux in soil/atmosphere interface. And it will define boundary conditions in the heat mass transfer permafrost process.

The most important energy exchange flux between soil and the lower atmospheric layer, are:

- The soil (as a grey body) visible radiation absorption.
- Soil/sky infrared radiation exchange.
- Air/soil sensible heat flux.
- Air/soil latent heat flux (less important) Lunardini (1981).

A two levels micro meteorological tower was designed and installed near SAS in the Antarctic 1991/92 summer to measure wind speed, temperature, relative humidity, incident and reflected radiation into the soil. So base on this and using the aerodynamic method we studied the soil/atmosphere energy flux evolution.

The tower was equipped with two common anemometers (180, 560 cm. height) and three thermocouples for temperatures measuring (90, 180, 560 cm. height). Data was registered every minute and average value was stored every thirty minutes. Local air temperatures were also measured (0, 5, 10, 20 cm. height) at the same rate.

Figures show the evolution of following parameters in a typical day:

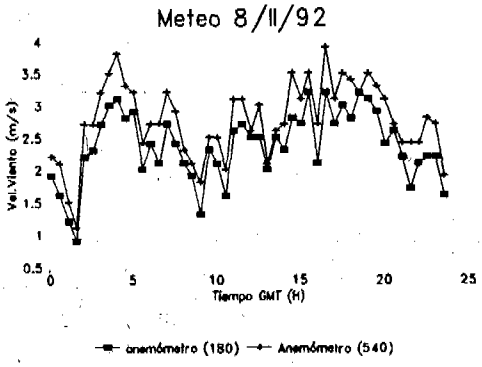

Figure 2.- wind speed evolution in both levels.

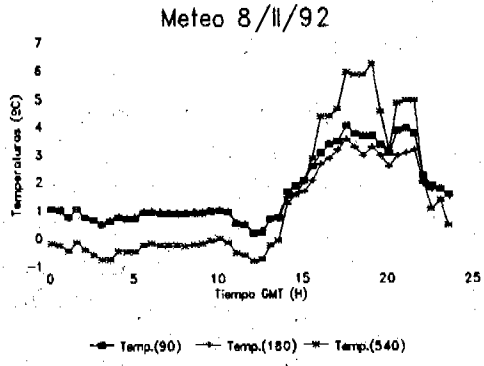

Figure 3.- Daily tower temperatures evolution.

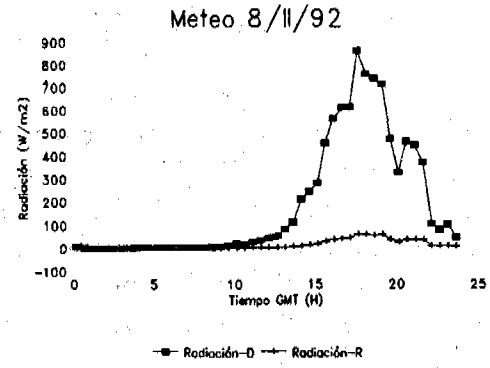

Figure 4.- Incident and reflected visible radiation.

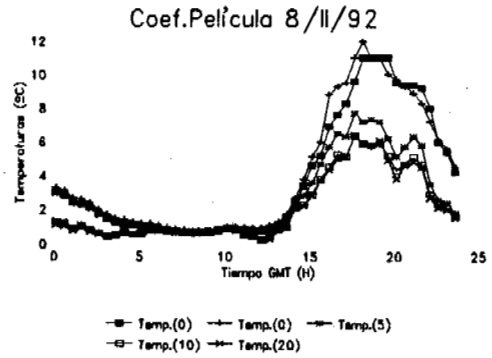

Figure 5.- Daily temperatures of the close to soil layer.

With data acquired and using aerodynamic method we will find out sensible and latent heat flux evolution in soil/atmosphere boundary.

Thermal distribution in the permafrost active layer was measured at different deeps (between 0 to 1 m.). Steady-state analyze of the thermal evolution measures will allow us to study the fluxes inside soil and its correlation with the soil/atmosphere exchanged energy flux balance.

Figures 6 and 7 show typical daily evolution on two of the group of five temperature probes used in our measuring system.

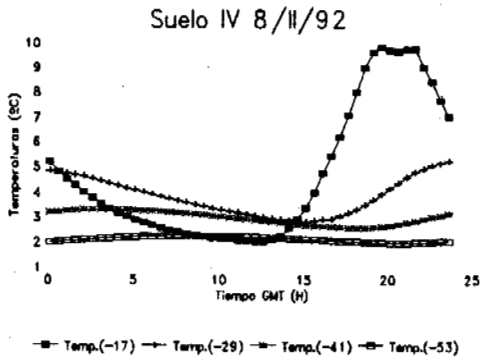

Figure 6.- Daily active permafrost layer evolution in prove IV.

Data analysis will allow to find out soil roughness. So, thermal difusivity, could be obtained using thermal distribution in the soil and the quasiestacionary method for sine wave propagation.

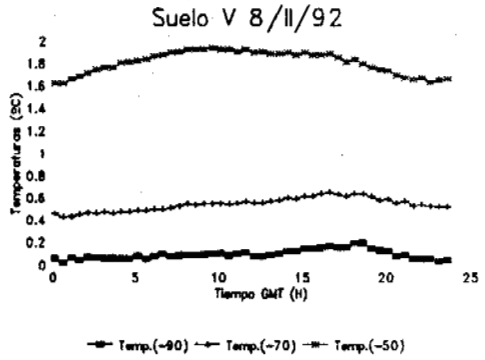

Figure 7.- Daily active permafrost layer evolution in probe V.

CONCLUSIONS.

1.- Aerodynamics method is suitable for studiing turbulent flux balance in the low atmospheric layer.
2.- Thermal spatial evolution in permafrost is suitable for analyzing the active permafrost behavior and its correlation with the surface energy fluxes.

REFERENCES.

Cancillo. M,L; " Estudio e los flujos de energía en la capa límite de superficie ". Tesis. Unv. Extremadura. (1991).

Dyer, A.J; " A Review of Flux Profile Relationships ". Boundary Layer Meteor. 7, pp 363-372. (1974).

Hall. K,L " Mechanical Weathering on Livinston Island South Shetland Islands, Antarctica". Recent Progress in Antarctica Earth Science. 757-762. (1992).

Lunardini, V.J; " Heat Transfer in Could Climates ". New York. VNR. (1981).

Ramos, M; "An Exact Solution for the Finite Stefan Problem with Temperature-dependent thermal Conductivity and Specific Heat". Int. J. Refrig. Vol 16, nº 5 (1993).

Sorbjan, Z; " Structure of the atmospheric Boundary Layer". Prentice Hall (1989).

AN EXPERIMENTAL STUDY OF CANAL LINING PREVENTED FROM FROST DAMAGE AND SEEPAGE

Ren Zhizhong

Northwest Hydrotechnical Science Research Institute
Yangling Town, China

This paper presents the observation results during the two freezing periods of 1985–1987 for an experimental canal with a length of 400m and the operation investigations from 1988–1991 for the lined canal with a length of 49.8 Km. The results show that the canal should adapt, limit or partly eliminate the frost heave and cut off seepage loss. For the canal section types, the best structural type of lining slabs is the trapezoid with an arc at the down slope angle. The best material type of lining is the concrete slab combined with a layer of plastic film. The better structural types of lining slabs are the concrete slabs with 18 and 10 cm thick, the "Π" shape concrete slab (6 cm thick), the 6 cm thick asphalt concrete slab, and the cast–in–site ribbed concrete slab (8 cm thick, 20cm rib height).

INTRODUCTION

In Dongying of Shangdong province, an arterial canal was built with a 49.8 Km length, 16.5–11.0 m bed width, 3 m depth, 1:1.5 slope coefficient, 2 m water depth, 1:7000 in water slope ratio, 35 m^3/s in design flow capacity. In order to find reasonable types of materials and structures for canal linings which can be prevent frost damage and seepage, a length of the arterial canal, when constructed, was used as an experimental canal with a length of more than 400 m. In the area, the mean annual air temperature is about 12.2°C, the days of mean daily air temperature below 0°C are about 76–87 days. The negative surface temperature indices are 250–350°C day. The frozen depth is about 55 cm. More than 80% of the area distributed under the canal bed is composed of sandy loam with the ground water table ranging from 0.7 to 1.9 m. Fine and loam particle content in the sandy loam is about 68.6–87.7%. The capillary water is up to 1.7–1.9 m. The dry density and plastic limit water content are 1.4–1.5 g/cm^3 and 17.2–20.3%.

DESIGN PRINCIPLE

From a technical and economical point of view and due to strong frost damage in the area, the experimental canal design principle was that the structural type of canal lining should adapt, eliminate and limit partly the frost heave, and cut off seepage loss.

From the design principle, the structural types of canal linings consisted of:

(A). (1) Prefabricated slab (8–10 cm thick) and a layer of plastic film (0.2 mm thick), (2) "Π" shape prefabricated concrete slab (6 cm thick) and plastic film;

(B). Cast–in–situ ribbed concrete slab (8 cm thick, 20 cm rib height) and plastic film;

(C). 6 cm thick asphalt concrete slab;

(D). Prefabricated concrete slab (8 cm thick) and sealed subsoil (40–60 cm thick) with plastic film;

(E). (1) Prefabricated concrete slab and plastic film, (2) prefabricated reinforced concrete slab and plastic film (the two types are widely used in canals).

OBSERVATION AND RESULTS

After the experimental canal was built, systematic observations were conducted from 1985 to 1987. The distribution of observation points along the canal section is as shown in Fig.1. The main results are decribed as follows:

In the two freezing periods of 1985–1987, the lowest and highest air temperatures were −16.4°C, −20.4°C and −12.6°C, −19.4°C, the lowest and highest mean daily air temperatures were −12°C, −10.3°C and −11°C, −8.5°C, and the negative surface temperature indices were 282.2°day and 141.4°C day, respectively. The distribution property of ground temperature and frozen depth are shown in Tab.1, and Fig.2. It is clear that the lowest ground temperature was −6.8°C and the maximum frozen depths was 83 cm for structure A. The ground water table underlying the canal bed was about 1 m in 1986, and 0.1–0.5 m in 1987. The subsoil water content was about 27–35% for the shaded slope and bottom, and about 20–25% for the sun exposed slope.

The maximum frost heave amount of the observation points is shown in Tab.2. The greatest and the lowest displacement were 200 mm and 29 mm respectively for structure E and D.

The structures of A, B, C and D had been operated well during 1988–1991. They could effectively prevent the canal from frost damage and seepage after undergoing several freezing–thawing cycles, except for a small crack on the shaded slope for C structure (see Fig.3). But E type of lining slab suffered from frost damage. The damage circumstance are shown in Fig.4, 5, and 6.

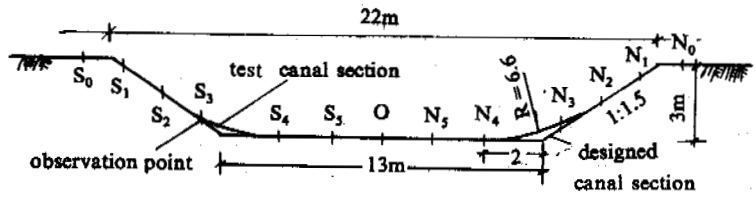

Fig.1 Distribution of observation points along canal section

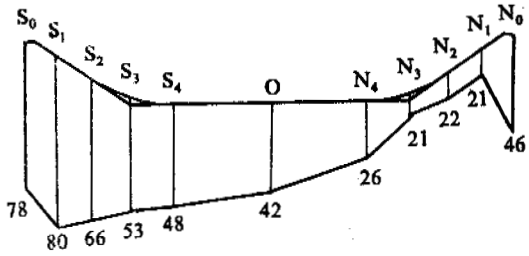

Fig.2 Distribution of frozen depth in A structure

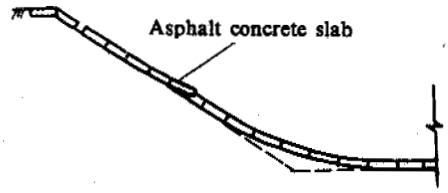

Fig.3 Sliding circumstance of test section

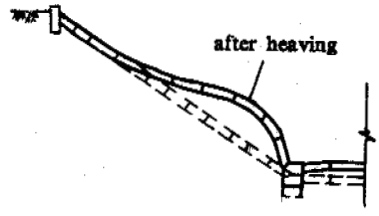

Fig.4 Frost heave circumstance in structure E

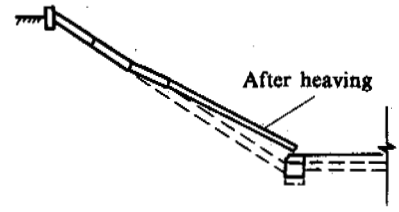

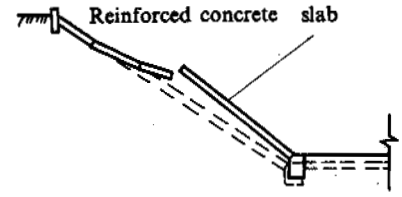

Fig.5 Frost heave stagger in structure E

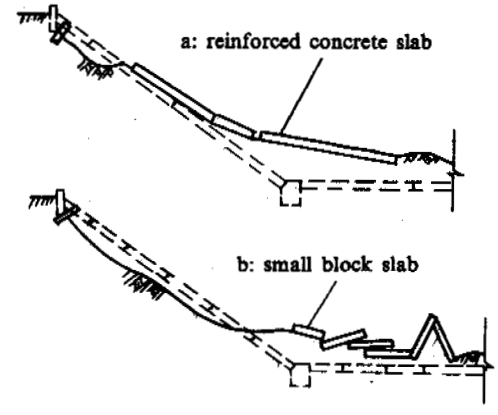

Fig.6 Slide and collaps in structure E

Table 1. Maximum frost depth (cm) and lowest ground temperature (°C) at 10 cm depth under slab

No	section	Π slab		8 cm slab		sealed slab		asphalt concrete slab	
		1986	1987	1986	1987	1986	1987	1986	1987
S_0	ground temp.			−6.8	−4.8				
	frozen depth			73	53				
S_1	ground temp.	−5.8	−5.0	−6.8	−6.5		−6.0		−5.2
	frozen depth	77	59	83	58	50*	50	77	53
S_2	ground temp.	−4.4	−4.0	−6.8	−6.2		−5.8		−5.0
	frozen depth	54	44	65	52	50*	45	72	55
S_3	ground temp.	−3.6	−2.9	−4.2	−3.8		−3.8		−3.6
	frozen depth	53	37	56	34	50*	44	62	38
S_4	ground temp.	−3.2	–	−4.0	–				
	frozen depth	49		49		50*			
O	ground temp.	−2.0	–	−2.8	–				
	frozen depth	40		42		47	39		
N_4	ground temp.	−1.2	–	−1.4	–				
	frozen depth	29		28		31			
N_3	ground temp.	−0.6	−1.0	−0.8	−1.5		−1.2		−1.4
	frozen depth	21	21	14	21	20	18	14	18
N_2	ground temp.	−0.6	−0.5	−0.6	−1.0		−1.2		−0.5
	frozen depth	23	19	19	18	21	18	20	20
N_1	ground temp.	−1.0	−0.3	−0.6	−1.3		−2.2		−1.2
	frozen depth	22	21	11	21	23	21	17	20
N_0	ground temp.			−4.9	−2.8				
	frozen depth			48	41				

* The maximum depth measured is 50 cm.

RESULT ANALYSIS

Subsoil Frost Heave Property

Because the frost heave amount is from 5 to 10 cm, according to <The Design Specification for Antifrost Heave in Canal System Engineering> (SL23–91), the subsoil engineering classification of frost heave belongs to the III class.

Frost Damage Types for Different Canal Section Shapes

Because of the restraint of the down–slope angle to the frost heave displacement, the displacement failure often occureed in the centre ot the bed for narrow canal, and the displacement drack occurs near the down–slope angle for the wide bed canals.

The trapezoid canal with an arc at the down–slope angle, compared with trapezoid section canal, it has some sepcial advantages, such as eliminating the restraint at the down–slope angle, decreasing the inequable frost heave, better anti–heave capacity, better hydraulic properties and low cost. Therefore in strong frost heave and high ground water table areas, it is the best canal section shape.

Effective Methods of Preventing Canals from Frost Damage

The methods to prevent canals from damage are as follows:

(1) In order to adapt canal to the displacement of freezing–thawing, the trapezoid section canal with an arc at the down–slope angle and bed can be selected.

(2) For materials, the structure consisting of a concrete slab and plastic film is the best one. It combines the advantages of both concrete and plastic film.

(3) Through the contrast of structure and cost analysis, the better structural types of lining slabs are arranged as A(1), A(2), C, and B. For D, if the construction problem can be solved, it is also a better one. For the structures of A(2) and B (see Fig.7), because of the effect of air insulation between slabs, and films and ribs around the slab, frost damage is reduced. In addition, using link expansion joints, concrete slab failure is avoided.

Design of Frozen Depth and Calculation of Frost Heave Amount

The relationships between negative temperature index of the concrete slab and of the air and frozen depth are shown in Fig.8. The subsoil frost heave properties and corresponding structures are determined by the maximum value of frozen depth. The calculation method is described as follows:

Design of frozen depth

S_1observation point for A(1) structure:

$$h_1 = 34.45 + 4.28\sqrt{T_{a1}} \quad (1)$$

S_1observation point for A(2) structure:

$$h_1 = 45.72 + 3.32\sqrt{T_{a1}} \quad (2)$$

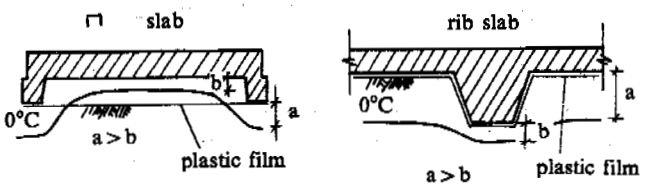

Fig.7 Local effect of structure

where $h_1$is frozen depth (mm), $T_{a1}$is surface negative temperature index of lining slab (°C day). For A(1):

$$T_{a1} = -3.09 + 0.67T_b, \quad r = 0.999. \quad (3)$$

For A(2):

$$T_{a1} = -2.97 + 0.55T_b, \quad r = 0.999. \quad (4)$$

$T_b$is daily lowest negative air temperative index (°C day), r is regression coefficient.

Frost heave amount (the displacement of lining slab)

S_1observation point for A(1):

$$\delta_1 = -1.73 + 0.15 + (h_1 \cdot W_1), \quad r = 0.97 \quad (5)$$

S_1obervation point for A(2):

$$\delta_1 = 1.04 + 0.13 + (h_1 \cdot W_1), \quad r = 0.84 \quad (6)$$

Table 2. Maximum frost heave amount of observation point (mm)

No.	year	structure E	10 cm slab	II slab	8 cm slab	seal slab	asphalt slab	structure B
S'_1	86	12.5	0.83	19.0	13.0	3.0	12.0	6.7
	87			−20.0	27.0	23.0	15.0	
S'_3	86	33.3	12.5	58.0	31.9	4.0	32.0	39.1
	87			44.0	41.0	43.0	60.0	
S'_5	86	48–200	46.6	78	69	14	45	77.4
	87			47	51	79	83	
S'_7	86	37.4	58.2	54.0	69	16	72	68.2
	87					20.0	53	
S'_9	86	30.8	53.2	63	73	29	101	70.1
	87						36	
S'_{11}	86			60.0	70.0	22.0	74.0	
N'_{11}	86			57	76	7.0	62.0	
N'_9	86	37.4	9.2	61.0	64.0	18.0	4.0	44.1
N'_7	86	25.8	4.2	7.0	29.0	2.0	6.0	3.3
N'_6	87			−13.0	−16	−18	−26	
N'_5	86	−5.0	5.0	2.0	6.0	8.0	9.0	0.83
	87			7.0	−10	8.0	−10	
N'_3	86	−1.7	8.3	7.0	2.0	4.0	6.0	−0.83
	87			3.0	−6.0	−14.0	5.0	
N'_1	86	1.7	6.7	14.0	6.0	0	5	0
	87			4.0	5.0	−7	−5	

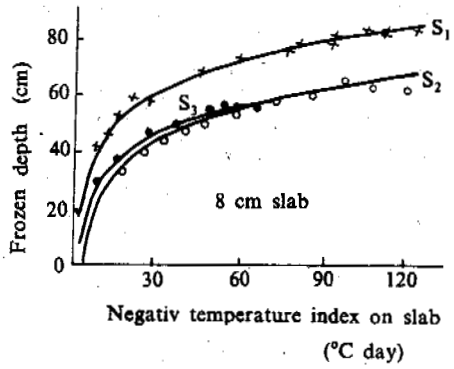

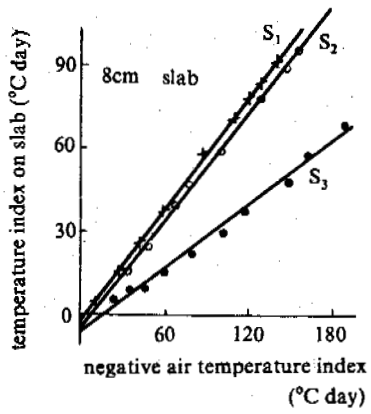

Fig.8 Relationships between the frozen depth and negative temperature index on concrete slab and of the air

where $\delta_1$is frost heave amount (cm), $W_1$is soil water content at S_1point (mean value of 100cm soil depth).

REFERENCES

Thritovize, H.A., 1985, Mechanics of Frozen Soil, Publishing House of Science.

Mathematical Research Institute, 1977, Chinese Academy of Science, Common Mathematic Statistics Methods, Publishing House of Science.

THE IMPACT OF SALT TYPE ON DEFORMATION OF FROZEN SALINE SOILS

Roman L.T.[1],Alifanova A.A.[1], Zhang Changqing[2]

[1]Department of Geology, Moscow State University, Russia
[2]State KeyLaboratoryof Frozen Soil Engineering,
LIGG,CAS,China

This paper contains data on long-term deformation of frozen soils contaminated with solium chloride and magnesiam and sodium salphates. The results show that testing of samples with similar physical properties which differ only is salt content gives a family of creep curves.Relative deformation increases proportionally to salt content rise and the time necessary to achieve the same magnitude of deformation reduces. Thus, higher salt content accelerates creep. The impact of salt content on deformation is identical to the effect of time.This reduces the time required for deformation analysis and to apply salt-time analogy to predict long-term deformation of frozen saline soils based on shorter experiments.

It is generally recognized that salts present in soil water reduce strength of frozen soils and increasedeformation since during dissolution salt ions dissociate into anions and cations thus contributing to water coherence. The freezing point of soil water drops and the amount of unfrozen waterincreases. The above processes depend on the quantity of dissociated ions which, in turn, is affected by the chemical composition of salts and theirconcentration.Hence, the extent to which salts affect strength and deformation of frozen soils depends on the same parameters, i.e., salts somposition and pore solutionconcentration.

Soilsgenerally contain a complex of salts and it is difficult to identify the effect of each salt type. The concentration of pore solution is unstable and varies with moisture content. That is why to assess the impact of salt type on soil strength and deformation total salt content is most commonly used which is the ratio between salt and dry salt masses. The experimental evidence available establishes only relationship between mechanical properties of saline soils and total soil content. Such an approach does not permit investigators to establish the nature of impact of salt type on the strength and deformation of frozen soils andobtainreliable quantitative values for design characteristics.

Only purposeful investigations based on extensive experimental evidence can eliminate this gap. This paper contains data on long-term deformation of frozen soils contaminated with sodium chloride andmagnesium and sodium sulphates.

Tests and data processing were carried out following salt-time analogy method. The validity of time analogymethods to predict long-term deformation of frozen soils, including saline, has been demonstrated before (Roman,1987,1990). Frozen saline loam has been tested for uniaxial compression under isothermal conditions. The test samples were 89.8–92.5 mm high and 44.8–45 mm in diameter. Major physical properties were assumed to be constant. Given below are theirmean values: frozen soil density = 2.0 g/cm^3; soil particle density = 2.71 g/cm^3; moisture content = 30%. The salts were NaCl, Na2SO4 and MgSO4 and salt content = 0.2, 0.4, 0.6, 0.8, 1.0, 1.5%.Three tests were conducted for each salt content case. Mean deformation values were used in the analysis of test data.

The results show that testing of samples with similar physical properties whichdiffer only in salt content gives a family of creep curves. Fig. 1 shows such a family of MgSO4 frozen loam. Itfollows from Fig. 1 that relative deformation increases proportionally to salt content rise and the time necessary to achieve the same magnitude of deformation reduces.

Thus, higher salt content accelerates creep. The impact of salt content on deformation is identical to the effect of time.This reduces time required for deformation analysis andapply salt-time analogy to predict long-term deformation of frozen saline soils based on shorter experiments.

Both the results of short-term experiments and expected values of long-term deformation modulus yielded by salt-time analogy were analysed to determine the impact of salts on frozen saline soil deformation. Themajor task of such an approach is to define transmission coefficient, i.e., correlation between times $t_1$and $t_2$during which similar deformations offrozen saline soils are achieved for each given salinity.

Creep test data permit one to define transmission coefficient through time-dependent compliance which is a relative deformation-stress Relation ($J_t=\varepsilon_t/\sigma$). A family of curves J_t–lnt is plotted for each series of isometric constant-stress tests. Here salt content is the only factor which accelerates compliance. The rest physical properties of samples remain stable. According to time-analogy theory(Urzhumtsev,1982) determination of transmission coefficient is much easier when compliance curves of such a family are similar. Our investigations revelled that compliance curves of saline soils are observed if stress is attributed to the area

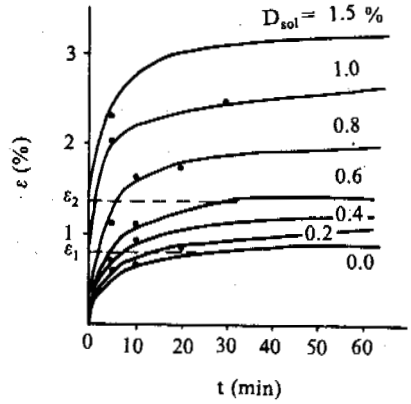

Fig. 1. Creep curve family for frozen loam with different MgSO4 content. Uniaxial compression test.Stress = 1.26 MPa, temperature = −3℃ ($\rho = 2.0$ g / cm^3; $\rho_s = 2.71$ g / cm^3; $W_a = 0.3$).

occupied by solid components (soil particles and ice) instead of the cross−section area of the sample. With accuracy acceptable for practical purposes this area (F_k) can be assumed to be proportional to the content of solid components in volume unit of soil (k) which can be easily calculated provided basic physical properties are known (soil particle density, ρ_s; dry soil density, ρ_d; ice, ρ_i; totalmoisture, $W_a$and unfrozen water content, W_{uf}

$$K = \rho_d [\frac{1}{\rho_s} - \frac{(W_a - W_{uf})}{\rho_i}] \quad (1)$$

With this assumptiontaken into account the area occupied by solid components (F_k) will be $F_k = F K$ and stress attributed to this area $\sigma_k = \sigma / K$. Here compliance is the relationshipbetween the relative settlement at a given instant of time t (ε_t) and stress σ_k, $J_{kt} = \varepsilon_t / \sigma_k$(where F is area and σ is stress attributed to the sample cross−section).

The obtained creep curve families for saline loam are shown on Fig.2. It follows from Fig.2 that compliance of loam contaminatedwith NaCl is several timeshigherthan for $Na_2SO_4$and $MgSO_4$, all other things beingequal.

The effects of the two latter salts on the compliance differ slightly. The transmission coefficient is also salt−dependent. NaCl has a more pronounced effect on the transmissioncoefficient increase with increasing salinity than two other salts. These examples also illustrate the applicability of salt−time analogy for the prediction of long−term deformation of saline frozen soils based on short−term experiments. Table 1 shows values of the long−term deformation modulus for tested soils.

The analysisof thechemical properties of salts of the tested samples shows that the essential differencebetween them is in the number of ions which dissociate into cations.and anions upon dissolution which in turn affect the freezing point of the soil water.Raul's equation with Vant−Goff's correction factor(Glinka,1976) can be used to assess the impact of a salt on the freezing point (T_{bf}) since solutions are weak

$$T_{bf} = 1.86\ m\ i \quad (2)$$

Table 1 Long−term deformation modulus (50 years) of frozen saline loam, MPa

Soil	Salt	T, ℃	Salt content, Dsol,%							
			0.0	0.2	0.4	0.6	0.7	0.8	1.0	1.5
Loam $\rho = 2$g / cm^3	NaCl	−5	16	12	10	6.5	5.8	–	4.2	3.5
$\rho_s = 2.71$ g / cm^3	$NaSO_4$	−3	49.5	44.8	33	24.5	–	18.2	13.5	10.3
		−7	244	190	181	134	–	90	67	55
$W_a = 0.3$	$MgSO_4$	−3	22	19	16	12	–	10	7.5	7
		−5	49.5	35	30	22	–	18	12	9.5
		−7	242	164	148	116	–	90	60	49.5

where m is mole−mass solution strength equal to $K_s \times 1000 / M$ ($K_s$is the pore solution strength, $K_s = D_{sol} / D_{sol} + W_a$; M is mole mass) and i is isotonic coefficient.

Our experiments revealed(Roman,1992) that i can be taken as 2 for salt soil solutions formed byunivalent metals and monobasic acids. For salt solutions formed by bivalent metals and monobasic acids i approaches 3. Should soils be contaminated with several salts the freezing point is definded as the sum of temperatures at which freezing starts. These temperatures depend on the effect of each salt and the particle surface energy.

Table 2 showssalt− and salt−content−dependent freezing points of soil water for loamy sand. They agree well with test data(Roman,1992).

The analysis of the test data shows that the form of the relation− ship between the transmission coefficient and the freezing point is similar to that of Villiams−Landall−Ferry equation(Ferry,1963) derived from time−− and tempe− rature−−dependent consolidation rate

$$ln\alpha_{D_{sol}} = \frac{C_1 (T_{bf} - T_{bf_0})}{C_2 + (T_{bf} - T_{bf_0})} \quad (3)$$

where $T_{bf}$is the freezing point of saline soil, $T_{bf_0}$is the freezing point of a salt−free soil and $C_1$and $C_2$are constants derived from the test data.

The freezing point of soil water is an important parameter of frozen soils, particularly saline. Frozen soil temperature − freezing pointratio (T / T_b) is a homological temperature which together with stress−instantenous strength (σ / σ_q) determines gomological row of changes in deformation properties. The above is supported by experiments. Fig.3 shows compliance of saline frozen soil σ / σ_qration for the same time period vs. homological temperature.

Experimental compliance data are close despite the fact that salts differ, broad range of salt content (between 0 and 1.5%) and temperature (−3, −5 and −7℃). This fact indicates that homologous temperature is a parameter common for physical properties of saline soils which affects their load de− formation rate.

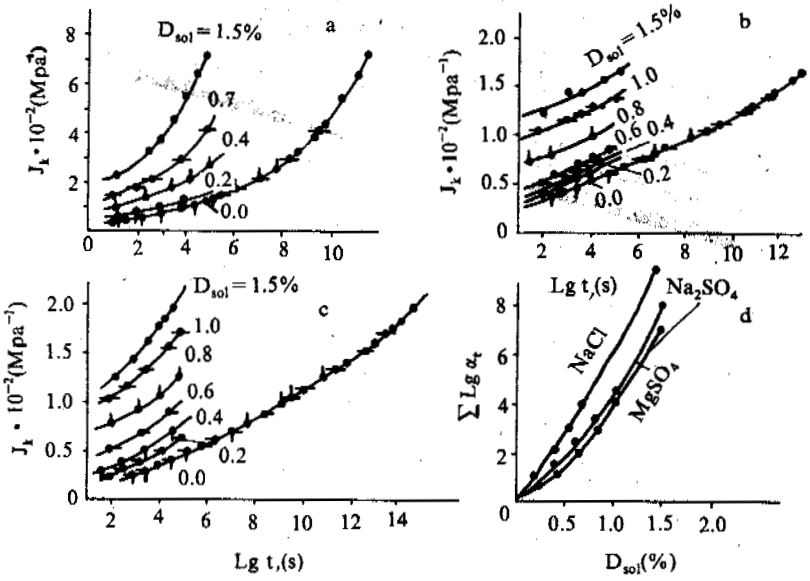

Fig. 2. $J_k$vs lgt_c. Uniaxial compression test data for loam with different salt content. Temperature = −5℃; a − NaCl; b = $NaSO_4$; c − $MgSO_4$; d − $\sum lg\alpha_t$vs (D_{sol}).

Table 2 Freezing point of loamy sand
(ρ = 2 ; ρ_s = 2.71 ; Wa = 0.3)

Salt \ D_{sol}%	0.0	0.2	0.4	0.6	0.7	0.8	1.0	1.5
$MgSO_4$	−0.2	−0.4	−0.6	−0.8	–	−1.0	−1.2	−1.68
Na_2SO_2	−0.2	−0.41	−0.61	−0.81	–	−1.01	−1.21	−1.7
NaCl	−0.2	−0.68	−1.08	–	−1.61	–	−2.21	−3.21

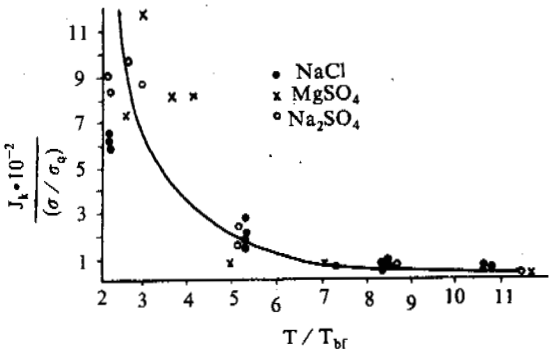

Fig. 3. $J_k\sigma / \sigma_q$ vs $T / T_{bf}$for frozen loam contaminated with different salts (salt content between 0 and 1.5%, temperature = −3, −5, −7℃), time = 8 h.

REFERENCES

Glinka N.L.,1976, General Chemistry.Chemistry Publishing House, Moscow,p.712.

Roman L.T.,1987, Frozen peat as foundation soil of engineering structures.Science Publishing House,Moscow.p.229

Roman L.T., Kuleshov Yu.V.,1990, Prediction of long−term deformation of saline soils with time analogies. In: Frozen Saline Soils As Foundation of Engineering Structures. Science Publishing House, Moscow.p.73−83.

Roman L.T., Artyushina V.I., Ivanova L.G.,1992, Relationship between frozen saline soil strength and soil water freezing point. Moscow State University Publishing House,Moscow.

Urzhumtsev Yu.S.,1982, Prediction of long−term resistance of polymeric meterials.Sciences Publishing House,Moscow.p.221

Ferry G.,1963, Visco−elastic properties of polymers.Literature Publishing house, Moscow.p.535.

GEOPHYSICAL METHODS OF CRYOLOGY ECOLOGICAL MONITORING

B.M. Sedov, Yu.Ya. Vashchilov
North–East Interdisciplinary Research Institute, Russia Academy of Sciences, Magadan

Geocryological wells are peculiar as they can be drilled without muds, and so–called "dry" drilling allows to avoid thawing of rock. There are some difficulties in making geophysical investigations of such wells due to impossibility to use electrical logs. But this can be easily done by using a series of radiactive methods, seismic log and caliper log, which allows to take into account the effect of change in a well diameter. The series of radiactive methods includes gamma–log, gamma–gamma density log, neutron gamma–log and X–ray radiometric log. The combination of all these methods allows to make lithological division of the section to distinguish ice including very thin ice interbed, to determine the total ice content. Seismic log method also allows to investigate the space between wells and to make sounding of well–surface rock mass. The sounding can be made to obtain three dimensional seismic geocryological models.

Cryology zone depth to 20–30 m is permanently effected by season temperature variation. Human activity influences this part of section and this can cause the damage of the natural temperature regime. When rocks containing ice and water are higher or lower than 0°C, cryology ecological situation changes. The major monitoring objects of cryological ecological situation in cryozone can be divided into two groups according to the rate of the influence on the temperature regime of the rocks.The first group is connected with warmth addition which cause the temperature increases till 0°C. In contrast, in the second group the temperature decreases to degrees below zero. In the first case ice thaws out in frozen rocks, in the second case water freezes. The process of transition of temperature to degrees above or below zero is accompanied by an abrupt change in some physical and mechanical properties of rocks.

The sharp change in seismic electrical properties of friable and fractured rocks, which contain water and ice, are the most interesting for geophysical methods. This allows to use electrical and seismic methods of geophysical investigation to determine physical condition of frozen or thaw rocks, to find out their location in manydimensional space including time coordinate.

In north–east Asia the geophysical methods of geocryology ecological condition monitoring is used to do the following: to identify taliks and to watch their development during the exploitation of dambs and during the filling of water collecting areas; to discover the places of water leakage; for open and underground mining of natural resources; to search for abandoned mines, for agricultural works; for engineering–geocryological investigation; for prediction of possible change in geocryological condition and for some other purposes. The human influence is accompanied by the rock temperature decrease which cause increase in permafrost thickness or the beginning of permafrost. For instance, when ground dambs are being built, there is natural freezing or artificial cooling of their bodies; when show is removed from aerodromes and roads this is accompanied by drop in annual average rock temperature; the permafrost appears in the places of taliks of drained lakes, which are used for haymowing.

As compared with other geophysical investigations geophysical methods of cryology ecological monitoring have some advantages, mainly, they don't have additional influence on the temperature regime change. For instance, the study of temperature regime of perennial rock warming, up to its thawing out in the well's walls at some depth. To restore temperature regime it takes much time during which it is impossible to distinguish between the studied cryological changes and the influence of drilling.

When wells are used during a long period of time they need to be properly equipped to be always in the working condition.

The practical use of geophysical methods of cryology ecological monitoring in cryologyzone evidences its effectiveness. It helps to make detailed and rapid investigations, it may be more economical than other methods.

PERMAFROST IN THE SELENGE RIVER BASIN (ON THE MONGOLIAN TERRITORY)

A.SHARKHUU

Institute of Geography and Geocryology, Mongolian Academy of Sciences, Ulaanbaatu,210620, Mongolia

In this paper, the basic results of permafrost investigation in the Selenge River are considered, including a territory of more than 300,000 Km^2. The study of the thermal region in the rock and ground, depending on different natural factors, serves as a scientific methodical basis for discovering qualitative and quantitative parameters of permafrost conditions. On the basis of this analysis and field research small scale permafrost map has been complied of the Selenge River Basin, in which basic parameters of permafrost distribution, thickness, temperature and composition are shown.

INTRODUCTION

The zone of permafrost occurrence embraces all the territory of the Selenge River Basin which is a basic economical region of Mongolia. The circumstances required a comprehensive study of permafrost in the given region.

The first summarized characteristics of Mongolian permafrost were determined by N.Longid(1969), G.F.Gravis (1974) and N.Sharkhuu (1975). In the last 20 years, permafrost investigations have been concentrated by the author in the Selenge River Basin. As a result all materials obtained were generalized and compiled into a number of large and middle scale geocryological maps of industrial areas, and a small scale map of this Basin (1978,1982,1989).

The main purpose of this paper was to discover the general and regional regularities of permafrost occurrence on the basis of analysis of the changing ground temperature regime depending on various factors of natural conditions.

NATURAL CONDITIONS

The Selenge River Basin is situated in the central part of Mongolia and is surrounded by the high ridges(2,000–3,500 m) of the Hubsugul, Hangai and Hentei mountains from the west, south and east. Between these mountains is the Orhon–Selenge middle–low mountain depression.

The basin has a sharp continental climate. Mean annual air temperature changes from −22°C to −30°C in January and from 12°C to 18°C in July. The mean annual value is from −6°C in the high mountains to 3°C in the depression.

A large part of the Hubsugul and Hentei areas is characterized by a taiga zone and the Hangai area – by a forest steppe zone. Forest coverage occurs predominantly on the north facing slopes of the mountains. Only the south part of the Orhon–Selenge depression is characteristic of a steppe zone.

GROUND TEMPERATURE REGIME

An important indicator of the ground temperature regime is the mean annual ground temperature at the level of zero annual amplitude. The penetration depth of zero annual amplitude temperatures in a large part of the given territory is about 10–15 m. However it decreases to 5–10 m at the swamp sites of valleys and watersheds and reaches to 15–30 m in the sand – pebbles deposits and in the fissuring solid rocks.

The analysis of the permafrost map sections of this basin has given the quantitative characteristics of general regularities in the changing of mean annual ground temperatures. In particular, the mean annual ground temperature by the mountain altitudinal belt decreases about 0.4–0.6°C for each 100 m rise above the absolute surface height, and by the latitudinal zonation it increases 0.9–1.0°C for each 100 kilometers moved from north to south (N. Sharkhuu, 1975).

The regional regularities in the changing of ground temperature regime have been studied in the sites of geocryological investigations such as the sites of the Hatgal, Erdenet, Ulaanbaatar and other areas. On the basis of approximate calculations and factor analysis carried out by using data of geothermal measurements in more than 450, boreholes with depths from 10 m to 200 m, the author established a number of quantitative parameters of changing mean annual ground temperature depending on basic factors of natural conditions.As on ground composition and moisture, slope aspect, vegetation and snow cover, rain infiltration water and other factors. Therefore, the mean annual ground temperature in the Selenge River Basin changed within the large ranges of plus 6°C to minus 8°C, including the predominant ground temperature of the

magnitude of plus 2°C to minus 2°C.

The value of geothermal gradient at depths exceeding the layers of yearly temperature fluctuations ranges from 1°C to 3°C for every 100 m. The geothermal gradient in the transition from valleys to watersheds under similar geological and geographical conditions decreased by almost 1.5–2.0 times. Therefore, the gradient on the watersheds and slope of mountains averages 0.01–0.02 deg / m and in the valley bottoms it is 0.02–0.03 deg / m. Consistent with this, the thickest permafrost is observed at the mountain uplands and the relative cancellation of permafrost thickness is characteristic of the valley bottoms.

PERMAFROST FEATURES

Permafrost is determined by the features of it's occurrence, thickness, temperature, cryogenic structure and evolution history. These features are closely connected with ground temperature.Especially occurrence, thickness and temperature of permafrost which have a direct relationship not only between each other and but with general and regional regularities in the changing of ground temperature regime(Geocryological Conditions of The Mongolian People's Republic, 1974).

As the result of the above established regularities, the author compiled, in 1982, an engineering geocryological map of the Selenge River Basin on the scale 1:1,000,000. On a generalized basis, this map had been made the permafrost map or the map of geocryological regionalization of this territory on the scale 1:6,000,000, in which are shown only interrelation indicators of occurrence, thickness and temperature of permafrost. (see figure...). This map has three geocryological sections, which is a sufficiently illustrated altitudinal belt of permafrost occurrence. Besides, more generalized characteristics of latitudinal zonation and the altitudinal belt of permafrost occurrence in the Selenge River Basin is presented in summary table 1.

The permafrost map of this Basin is divided into the following geocryological two zones and five areas, in particular : the areas of continuous (>85%) and discontinuous (50–85%) permafrost are characteristic of the zone with predominant permafrost and the areas of widespread (10–50%) and rare spread (1–10%) island permafrost and sporadic permafrost are characteristic of the zone with predominant seasonal freezing (or thawed grounds.) As well the map is subdivided into ten geocryological sub areas (or sites), distinguished by the magnitude qradations of occurrence and mean annual temperature of permafrost sequences.

The above represented map and table shows clearly that the occurrence, thickness and temperature of permafrost are submitted to general regularities or to latitudinal zonation and the altitudinal belt of natural landshafts. So according to the latitudinal belt, with a rise of absolute hight of the earth's surface in the mountains of the Alpine type and in the mountain taiga and forest steppe zone of the Selenge River Basin there is a regular increase in the continuity and thickness of permafrost and decrease in temperature. The latitudinal zonation of permafrost occurrence is characteristic of the steppe and forest steppe zone of this Basin.

The territory of the Selenge River Basin is characterized by unextended permafrost. Therefore, the depth of seasonal ground thawing or thickness of the active layer corresponds to the

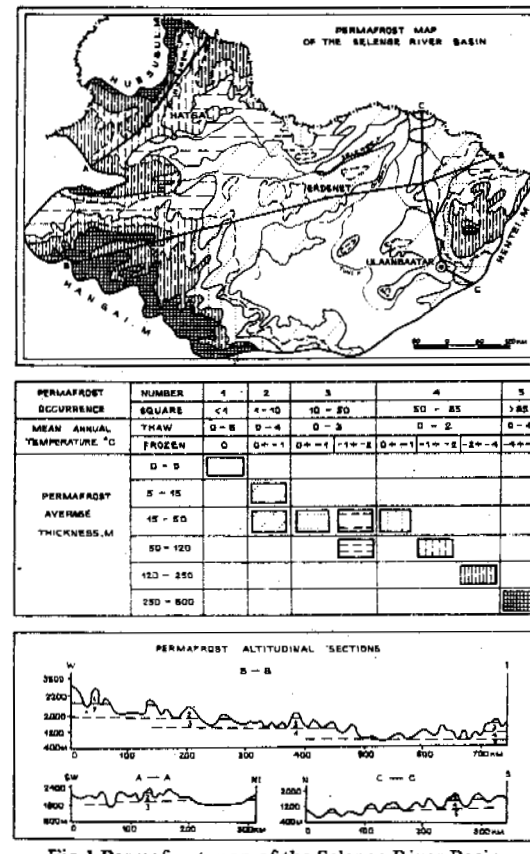

Fig.1 Permafrost map of the Selenge River Basin

permafrost table or to the upper boundary of the permafrost sequence. The average thickness of seasonally thawing or active layers is about 2–3 m.

An important feature of permafrost is the cryogenic structure of permafrost sequence characterized mainly by freezing type,cryogenic texture and ice content of rock and ground. In general, overwhelming masses of permafrost sequence in the zone with predominant permafrost are confined to solid rocks and in the zone with predominant seasonal freezing which is confined to loose deposits or grounds.

Epigenetic frozen solid (magmatic, sedimentary and metamorphic) rock have inherited cryogenic texture, which corresponds to the character of rock fracturing and to the type of underground water, in particular ice is arranged in rock fissures, fractures and joint chacks. They are characterized by cold rocks. However, in the upper (0.5–3.0 m) layers of the rock weathering zone, the ice content is 3–10%, until the depth of 20–30 m — 2–5% and lower than 100–150 m it is less than 0.5%.

Predominantly epigenetic and partically syngenetic frozen loose (alluvial, lacustrine, glacial and their mixed) deposits have cryogenic or ice connection which depends on facial, cryotexture and ice content of loose deposits. In most cases loamy frozen ground has layered and netting cryotexture, sandy frozen ground–massive cryotexture and gravelly frozen ground – ring visible cryotexture. One may approximately account that permafrost with massive and ring cryotextures has a poorly (5–15%) ice con-

Table 1. Characteristics of the latitudinal zonation and altitudinal belt of the permafrost occurrence

permafrost occurrence number	areas of	altitudinal belt and latitudinal zonation	areas	permafrost occurrence
1	continuous permafrost	golets and mountain meadow belt of alpine type	17.6	on golets and meadows of mountains
2	discontinuous permafrost	mountain taiga,meadow and steppe beltof taiga and foreststeppe zone	85.6	on all type of landshaft
3	widespread is lands of permafrost	mountain forest and steppe belt of forest steppe zone	64.5	in valley bottoms and on north–facing slopes of mountains
4	rarespread lands of permafrost	mountain–forest–steppe belt of forest steppe zone	93.1	
5	sporadic permafrost	mountain steppe belt of steppe zone	75.5	on swamp sites of valleys
1–5	island permafrost	forest steppe zone	336.3	in valley bottoms and on north–facing slopes of mountains

tent, permafrost with netting cryotexture – a greatly (20–40%) ice content. In general, the Selenge River is characterized relatively by poorly and middle ice content loose deposits with predominant of massive texture. Lacastrine and lacusrine alluvial deposits are usually related to the more ice content permafrost.

At present, a stability of permafrost evolution is characteristic of all the territory of the Selenge River Basin. Relic permafrost has not discovered here. However, on some local sites of the basin degradation and agradation tendencies of permafrost evolution are noted, which have only local characteristics. In particular, the permafrost agradation is noted only on some sites situated in the taiga zone of the Hentei mountainous region. The permafrost degradation is observed comparatively often in some local sites located in the other territories of the Basin. The noted aggradation and degradation of permafrost in the Selenge River Basin is closely connected with a large dynamic evolution of relatively high temperature (minus 0–1°) and low ice content (about 8–15%) permafrost sequences, which is characteristic of territory in the southern fringe zone of permafrost occurrence. Especially the large dynamic evolution of permafrost predominantly in the direction of degradation is rapidly manifested under economic development of new territories in the Basin.

PERMAFROST ASSESSMENT

The degree of complicated permafrost conditions of the Selenge River Basin may be divided into three geocryological regions:

1. The region of continuous and discontinuous permafrost is characterized by complicated permafrost conditions for economic development of territory caused by widespread comparatively low temperature (minus 1–4°C), large ice content (about 10–40%) and the thickest (100–200 m and more) permafrost sequences.

2. The region of widespread and rare spread island permafrost is characterized by middle complicated permafrost conditions for economic development. The main cause of difficulties for economic development is a large dynamic evolution of high temperature (minus 0–1°C) permafrost sequences.

3. The region of sporadic permafrost is characterized by no complicated permafrost conditions for economic development because the ice content of permafrost sequences is practically absent.

CONCLUSIONS

The most rational method of geocryological investigation for studying the occurrence, thickness, dynamic and other indicators of permafrost may be based on the discovery of general and regional regularities in the formation of the ground temperature regime.

A compilation of permafrost maps on small scales is advisable to carry out a united (table form) legend determined by the interdependent characteristics of occurrence, thickness and temperature of permafrost i.e. as in the compilation of the permafrost map of the Selenge River Basin.

Further investigations, especially on the dynamic evolution of

permafrost in the Selenge River Basin situated in the southern fringe zone of permafrost occurence, are presented for scientific and practical interest for geocryologists and other specialists. They may be at a high scientific level, and carried out only under close collaboration with scientists–geocryolists from interested countries who are adhering members of the International Permafrost Association.

REFERENCES

Geocryological Conditions of The Mongolian People's Republic, 1974, Transactions of Joined Soviet–Mongolian Scientific–Research Expedition; Vol.10, Moscow, pp30–48,74–91.

Sharkhuu, N., Lubsandagva D. and Zhamsran S., 1975, Basic Features of Permafrost in Mongolia, Ulaanbaatar, pp22–66,90–103.

Sharkhuu N., 1982, Engineering Geocryological Conditions of The Selenge River Basin, In Proceedings: Materials of VIII–th Conference of Young Scientists and Aspirants on Geocryology of Geologic Department of Moscow State University by M.V. Lomonosov.

Sharkhuu N., 1989, Geocryological Conditions on Territory of Hubsugul Phosphorit Deposits, In Bulletin of Mongolian Academy of Sciences, 4, Ulaanbaatar.

DEFORMATION OF THAWING DISPERSED LARGE DETRITAL ROCKS OF CRYOLITE ZONE

Shesternyov D.M.

Institute of Permafrost, Chita

The paper is concerned with the composition and structure peculiarities of large detrital rocks of cryolite zone. Classification diagram on basic structures of large detrital rocks has been suggested, which is put into the basis of analysis of deformation changes of thawing dispersed large detrital rocks of cryolite zone. It has been established, that for large detrital rocks with contact cryogenic textures and frame structures cryogenic textures have greater influence on thawing coefficient values than ice saturation (total moisture) of rocks as a whole, and the curves of thawing coefficient variations of different genesis rocks are identical.

An intensive national-economic exploitation of cryolite zone of platform and mountain folded regions of Russia and other countries is being done during the last decades. According to our calculations the cryolite zone in these regions on the depth of annual temperature variations consists of 80-90% of seasonally and perennially frozen large detrital rocks (LD). LD are considered to be the rocks which contain more than 10% of detrital rocks and minerals, the diameter of which is more than 2 mm.

Comparatively few papers are devoted to the study of deformation of thawing LD. (Vedernikov, 1959; Tsytovich, Kronik, 1973; Ushkalov, 1974; Votyakov, 1975; Vyalov, 1979; Davidenko, 1981; Ziandirov, Kilbergenov, 1987; et al). In these works some regularities of thawing coefficient variations (A_o) and compression coefficient variations (a) for LD with different genesis, composition, structure and properties are shown, the methods of field and laboratory investigations are offered; correlation-regression LD models of regional importance are built. However, though the authors have made a great contribution to the study of thawing LD deformations it should be noted that some problems in their works have been paid little attention to. The main of them is the absence of profound investigations on the influence lithogene structures (L S L D) and cryogenic textures (C T L D) on deformations of thawing LD. But satisfactory solution of the problem could not have been solved because profound research into structure and cryotexture formation in LD has not yet been done. That is why we had to pay great attention to the solution of this problem when studying the deformation of thawing LD.

Using methodical approach offered by V.I. Osipov (1985) and taking into account the peculiarities of LD composition and structure we shall treat the LD structure in regard to space distribution, interrelation, size and geometrical form of LD-forming granulometric elements and their groups (Table).

Classification of Structures of LD.

Class	Group	Subgroup	
$50>K_v\geq10$ Frameless	Mixed (LD particles, sand, dust and clay particles) $90>K_v\geq10$	Sand, clay	Episodically contact $10\leq K_v<30$
			Locally contact $30\leq K_v<50$
		Unfully contact $50\leq K_v<70$	Sand, clay
		Fully contact $70\leq K_v<90$	
$90>K_v\geq50$ Frame	Simple (only LD particles) $K_v\geq90$	Fully contact (all LD particles have active contacts)	
		Unfully contact (not all LD particles have active contacts)	

Notes: K_v - volume composition of LD particles

Presented classification made it possible, in our opinion, to generalize without logical contradictions the results of the research into the cryogenic LD structure (Shesternyov, 1986; Shesternyov, Jadrishenskv, 1990).

The experimental study of LD deformations was carried out in field conditions. A_o and "a" coefficient were determined by the method of a

"hot stamp of an area of 5000 cm in pits and shafts up to 10 m in depth. At the same time detailed description of the distribution of large-detrital particles in LD was performed, the interrelation of definite L S L D and C T L D types was revealed, identification of the latter with the A_o and "a" coefficient values was done. The regularities of ice inclusion distribution in a finely-dispersed LD component and the character of ice covering of large detrital particles were paid attention to. The research was done by the author since 1976 to 1986 under B.A. Kydryavtsev and E.D. Ershov at the geocryology chair of the Moscow State University, then by the author himself or under his direct guidance at the hydrogeology and engineering geology chair of the Chits Politechnical Institute, and since 1986 up to now in the laboratory of engineering cryogeodynamics of the Chita Department of the Permafrost Institute of the Russian Academy of Sciences Siberian Department.

The processing of the data obtained has been done in two stages. At the first stage the analysis of the change of granulometric LI composition of different genesis was performed and their influence on litho- and cryogenic LD structures was established. At the second stage standard values $\overline{W}_{tot}$, $\overline{\rho}_c$, $\overline{\rho}$ (total moisture, density of LD skeleton and LD density in natural state), A and "a" were established for rocks with different L S L D and C T L D.

It made possible to establish the following:

1) Dispersity increase in the series sand-sandy loam-loam, for one subgroup of LD structures with LD particle content, practically always leads to the increase of values W_{tot};

2) LD particle content increase with one and the same finely dispersed component type reduces W_{tot} and increase $\overline{\rho}$, $\overline{\rho}_c$ (there is no considerable difference between W_{tot}, $\overline{\rho}$ and $\overline{\rho}_c$ for the frame LD structures, irrespective of the FC dispersity increase, but we could not say the same about the range of their variation series).

Clearly, the changes of P M P (physico-mechanical properties) of large detrital rocks, L S L D and C T L D affect in a definite way the formation of A and "a" coefficient values. Thus, for example, in layer 3 (Fig.1a), gravel-pebble LD with sandy FC is characterized by frame and unfully contact L S L D.

Similar L S L D types are typical for separate levels of gravelpebble LD, the sections of them are shown in Fig.1b and 1c. But C T L D and W_{tot} differ greatly from each other in every concrete case. Contact-fully crust-massive C T L D (W_{tot}=0.20-0.18) are developed in the range from 4.0 to 6.0 m (Fig.1a), contact-unfully crust-massive C T L D (W_{tot}=0.12-0.08)—in the range from 6.0 to 8.0 m. In the first case the ice crust thickness on the contacts between rock debris equals 1-2 mm, in the second — 2-3 mm. In the process of thawing heat settlement of rocks A_o with less values W_{tot} were 1.5-2.0 times higher than in the rocks with greater values W_{tot}. It shows that the possibility to evaluate A_o according to W_{tot} changes, even in the quantitative respect, is rather problematic for LD. That the above-mentioned

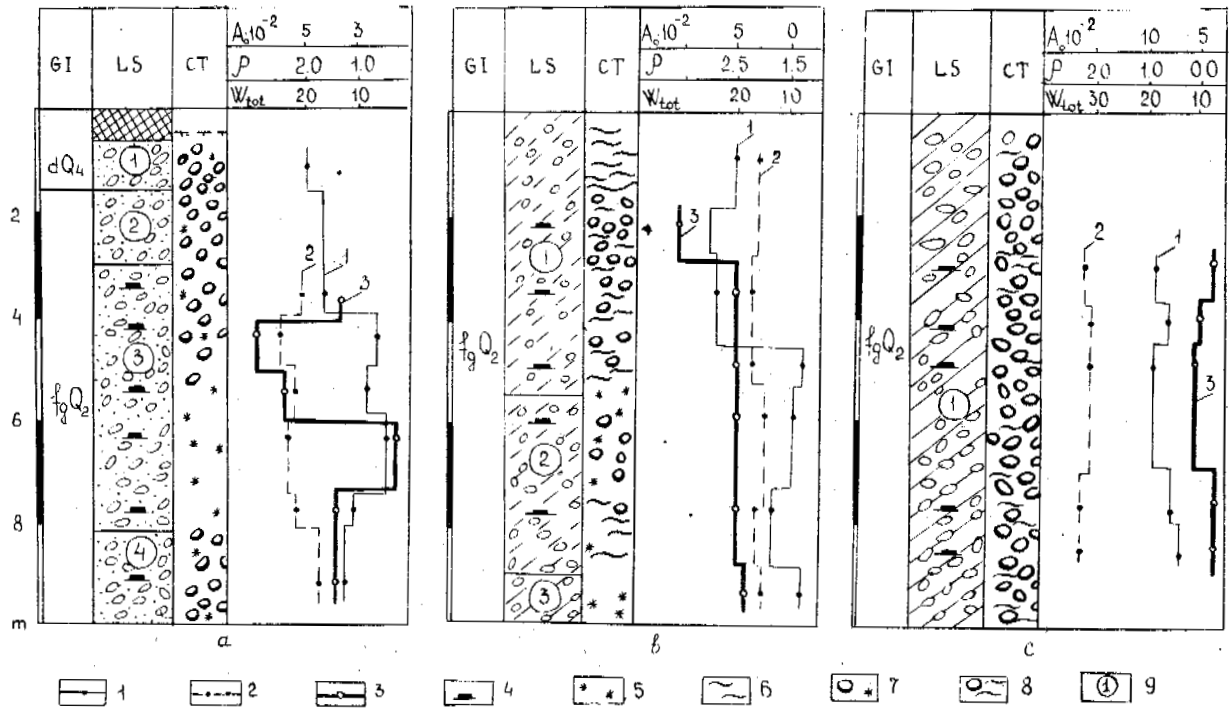

Fig.1 Changes of cryogenic textures, total moisture and thawing coefficient of fluvioglacial Middle Pleistocene dispersed large detrital rocks of Udokan. Conditional symbols: Changes in the rocks profile: 1-total moisture (W_{tot}), 2-density (ρ), 3-thawing coefficient (A_o) of rocks, 4-depth of determining thawing rocks deformations using the method of a "hot stamp". Cryotextures: 5-massive, 6-lentiform-stratified, 7-contact-crust-massive, 8-contact-crust-lentiform, 9-number of a rock lithologic layer: GI-geological index, LS-lithologic structure, CT-cryotexture. (Other notes to Fig.1 are to be found in the text).

example is not the only one is seen from the data in Fig.1b and Fig.1c. In Fig.1b contact-crust-lentiform C T L D are developed along the soil profile of gravelpebble LD with loamy FC (layer 1), and they differ only in the thickness of ice crust on rock debris. In the rock profile from 9.0 and down and from 3.0 to 4.0 the ice crust thickness on large detrital particles equals 1-2 mm, in a layer between these depth the ice crust thickness on rock debris hardly average 1 mm, but on the contacts between them it equals 1-3 mm. That is why A_o values are higher in LD with the same C T L D types but with lower values of their W_{tot}.

Geologo-genetic and regional peculiarities of formation greatly influence deformation values of thawing large detrital rocks of cryolite zone. $\bar{A}_o$ dependence on large detrital particles content ($\bar{K}_v$) for large detrital rocks of different genesis is shown in Fig.2.

There were not less than 5 separate definitions when calculating $\bar{A}_o$ and W_{tot} in every case. Generalized curves were obtained for LD of different genesis with sandy (Fig.2a), sandy loam (Fig.2b) and loamy (Fig.2c) finely dispersed components. It follows from the dependences indicated in the figure that when $\bar{K}_v$ content in LD increases from 0.1 to 0.9, $\bar{A}_o$ values decreases. In the first part of the segment $\bar{K}_v$=0.1-0.5, the rate of the decrease is the highest for all LD genetic types and increases with the increase of FC dispersity. Its largest values are typical for alluvial, fluviolacial and diluvial-soliflual LD deposits; i.e. deposits

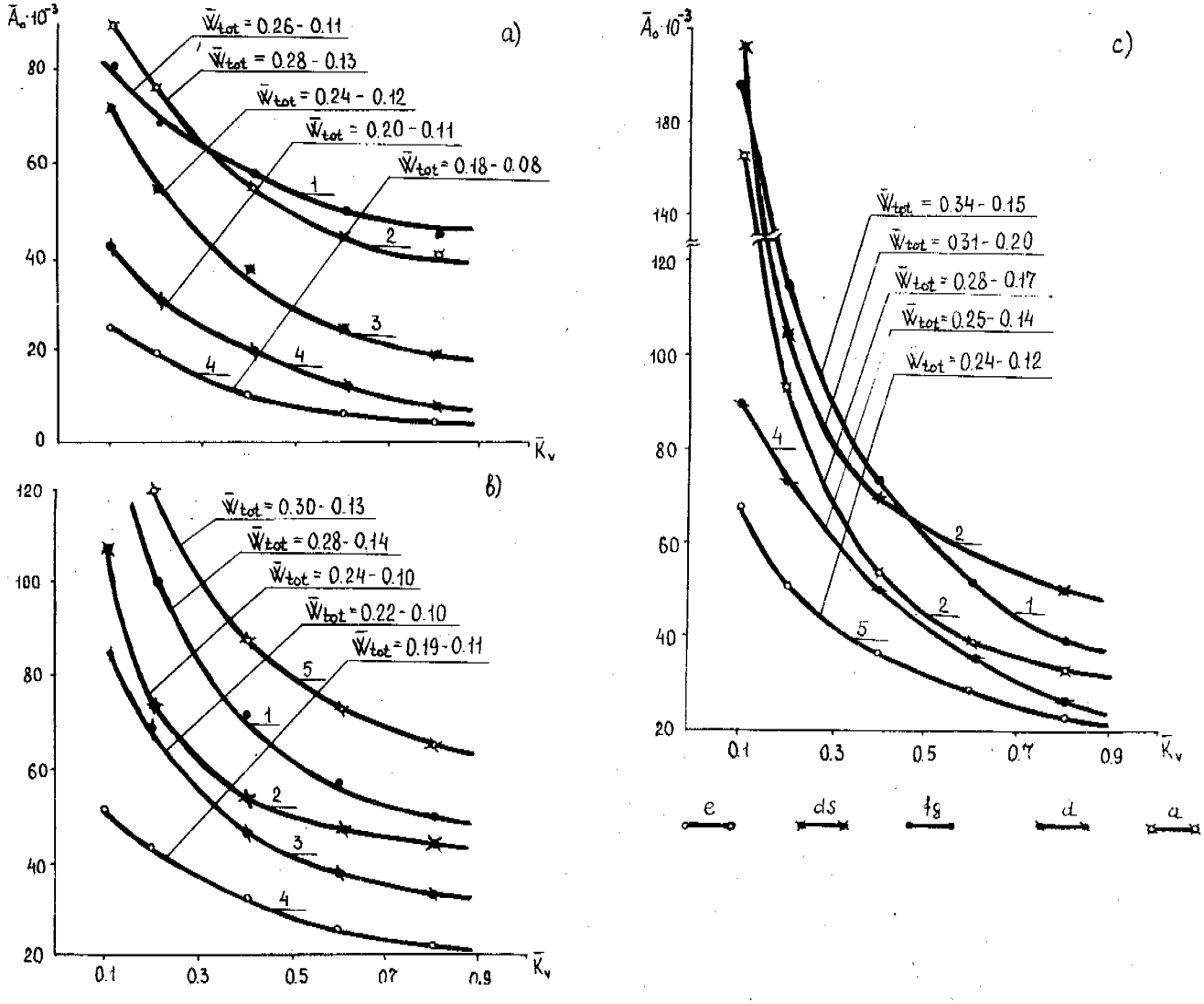

Fig.2 Standard thawing coefficient value changes ($\bar{A}_o$) of different genesis large detrital rocks for separate regions of Russia. Conditional symbols: 1-Udokan range, 2-Vitim-Patom plateau, 3-Stanovoy range, 4-Chulman hollow, 5-Chita-Ingoda Hollow; e,ds, fg, a -correspondingly LD of eluvial, diluvial-soliflual, fluvio-glacial, diluvial and alluvial genesis, W_{tot}=24-10 - standard values of total moisture (the first number - when K_v=0.55-0.15, the second - when K_v=0.85-0.90).

that are characterized by comparatively high values W_{tot}, great variations of C T L D, weak lithification or good roundness of large detrital particles, its least values are typical for eluvial and diluvial LD. An exception is eluvial LD having been formed in weathering granites of Stanovoy range, the variation range W_{tot} (Fig.2a) is similar to variation range W_{tot} for diluvial-soliflual LD deposits with loamy FC (Fig.2b). In the segment of $\overline{K}_v$ from 0.5 to 0.9 the rate of $\overline{A}_o$ changes drastically. But differentiation of its values for LD of different genesis is practically invariable. Here the $\overline{W}_{tot}$ influence on the rate of $\overline{A}_o$ changes reduces drastically, because though W_{tot} values are practically the same for LD of different genesis, the differences between $\overline{A}_o$ are rather great. In this connection our hypothesis about the predominant influence of the distribution character of ice inclusions (C T L D) over W_{tot} on $\overline{A}_o$ changes becomes, in our opinion, more evident.

Thus, based on the results of this study, it is concluded that:

-in the segment of changes of K_v content from 0.5 to 0.9 lithogene structures and cryogenic textures of LD have predominant influence on A_o value;

-the largest A_o values and the highest rate of their decreasing with the K_v increase from 0.1 to 0.9 are typical for alluvial, fluvio-glacial and diluvial-soliflual LD deposits.

-changes of $A_o=f(W_{tot}, K_v, K_{fc})$ in the segment K_v=0.1-0.9 irrespective of LD genesis and FC type are descibed by the following equationt:

$$A_o = W_{tot} \cdot K_{FC} / (n_1 K_v + n_2 K_{FC})$$

where n_1, n_2 - empirical coefficient; $K_{FC}=1-K_v$, i,e K_{FC} - volume composition FC in LD.

The results of the research are tested and put into practice in desigining and constructing of large mining complexes of Eastern Siberia.

REFERENCES

Davidenko V.P., (1981) Classification of Complexity of Permafrost-Engineering-Geological Conditions on the Basis of Setting Evaluation in Frozen Large Detrital Grounds Thawing (on the example of central districts in the Magadan region). In the book "Thawing Grounds as Structure Foundations". -M.: Nedra, pp.72-92.

Osipov V.I., (1985) Concept "Ground Structure" in Engineering Geology. In the Journ. Eng. Geology, No.3, -M. Nauka, pp.4-20.

Shesternyov D.M., (1986) On the Problem of Classification of Large Detrital Rock Cryogenic Textures. In the book: Eng. Geol. Investigations in the Permafrost Region. Blagoveshchensk, pp.331-333.

Shesteryov D.M., Yadrishchensky G.E., (1990) Rock Structure and Properties of Udokan Cryolite Zone. Novosibirsk.: Nauka, p.126.

Tsytovich N.A., Kronik Ya. A., (1973) Physical and Mechanical Properties of Frozen and Thawing Large Detrital Grounds. In the book: II International Permafrost Conference. Rep. and inform., Vol.4, Yakutsk, pp.52-62.

Ushkalov V.P., (1974) Building Properties of Perennially Frozen Basis and Quick Methods of their Determining. Novosibirsk: Nauks, p.84.

Vedernikov L.E., (1959) Research into Frozen Large Detrital Grounds. Proceedings of All-Union Research Institute-Magadan, Vol.13, pp.43-267.

Votyakov I.N., (1975) Physicomechanical Properties of Frozen and Thawing Grounds in Yakutia. Novosibirsk: Nauka, p.176.

Vyalov S.S., (1979) Engineering Problems in Geocryological Investigations on sites of BAM, In the book "Engineering Permafrostology" M.: Nauka, pp.149-156.

Ziangirov R.S., Kilbergenov R.G., (1987) Deformability Evaluation of Large detrital Grounds. Engineering Geology, No.3, M.: Nauka, pp.107-109.

PALSA FORMATION IN THE DAISETSU MOUNTAINS, JAPAN

Toshio SONE[1] and Nobuyuki TAKAHASHI[2]

[1]Institute of Low Temperature Science,
Hokkaido University, Sapporo, 060, Japan
[2]Hokkai-Gakuen University, Sapporo, 062, Japan

Palsas and peat plateaus, in different stages of development, exist in a mire (1,720m a.s.l.) in the Daisetsu Mountains (43°37' N). They consist of peat cover about 1m thick and permafrost core of sand and silt. Many segregated ice lenses were visible in the silt layer. The permafrost base is at a depth of 5m. Ground temperature observations in the palsa indicates that temperature is in equilibrium with the present climate, and that permafrost can develop under present climatic conditions. On the basis of two tephra layers in the peat, the palsa was initiated to heave in around A.D.1830.

INTRODUCTION

Palsas and peat plateaus are common features in many permafrost regions. According to the definition of palsas, they are peaty permafrost mound possessing core of alteration layers of segregated ice and peat or mineral soil material (N.R.C.C.,1988). They are considered to be the only reliable indicator of the discontinuous permafrost (Brown,1974). However, palsas or palsa-like mounds are recently reported also in continuous permafrost (Washburn, 1983a).

In Japan, palsas were first discovered in 1986 and their forms,sizes and distributions were reported (Takahashi and Sone, 1988;Sone et al.,1988). The authors attempted to measure the ground temperature profiles of a palsa and investigated its internal structures by drilling. In this paper, we describe the results and discuss the type and age of palsas in the Daisetsu Mountains.

ENVIRONMENTAL SETTINGS OF THE DAISETSU MOUNTAINS

The Daisetsu Mountains are located in central Hokkaido, northern Japan. They are composed of Pleistocene pyroclastic or lava plateaus with several younger strato-volcanoes. Many kinds of periglacial phenomena and landforms, such as earth hummocks, sorted polygons, block fields and slopes, and frost crack polygons have been reported. Discontinuous permafrost is distributed mainly of the windward bare ground above 1650 m (Sone,1992). Palsas were discovered in a mire. They indicate geomorphologicaly the existence of permafrost at around the lower limit of permafrost in the Daisetsu Mountains.

The mire at the south of Mt.Hiraga-take is located at an altitude of 1720 m(43°36'54"N, 142°54'06"E), on a broad pass of the lava plateau between Mt.Chubetsu-dake and Mt.Hakuun-dake (Figure 1). The length of the mire is about 650m from east to west, and 350m from north to south. The surrounding vegetation of the mire is *Pinus pumila* community. The mire is characterized by palsas, peat plateaus and string bogs. In the Daisetsu Mountains, palsas and peat plateaus develop only in this mire.

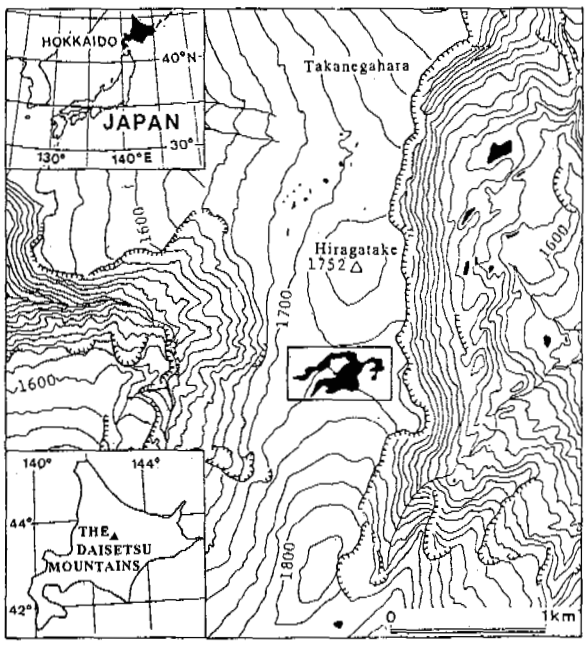

Figure 1 Location of the palsa mire in the Daisetsu Mountains

The elevation of the timber line around the mire is about 1,500 - 1,600m a.s.l. The mean annual air temperature, and the freezing and thawing indexes at the mire are estimated to be -2.0°C, 2,000°C days and 1,500°C days respectively (Sone,1992).

PALSAS AND PEAT PLATEAUS IN THE MIRE AT THE SOUTH OF MT.HIRAGATAKE

About twenty palsas and peat plateaus exist at this location with sizes ranging from 4 to 80 m in diameter and from 0.2 to 1 m in height. Their plan figure is generally circular or elliptic. Most are peat plateaus in morphological classification, and mineral-cored palsas in structural classification. These are characterized by flat upper surface and relatively steep side slopes, sometimes accompanied with ponds just around them(Figure 2). Permafrost is observed only under the palsas in the mire. Severe westerly winds in winter sweep away the snow deposit of the ground surface, and the snow depth of the mire is less than 1m. The top of palsas is often exposed partly during a whole winter season (Takahashi and Sone,1988).

For an investigation of internal structures and monitoring the ground temperature, a palsa was chosen. Palsa B, named by Takahashi and Sone(1988), is 80cm high and 10m long, elongated in north-south direction. The palsa is composed of a peat layer of 60 - 110cm thick underlain by silty sand and gravel layer. The permafrost table is about 70cm deep and was nearly parallel to the palsa's surface in late September. The permafrost table is nearly coincident with the boundary between the peat and the silty sand and gravel layers. The snow cover thickness was measured as much as 40 - 60 cm deep on the east and west side of palsa on 29th December, 1986. However, the snow was less than 40 cm deep on the top of palsa B, and some parts of palsa were exposed. A small pond on the south part of palsa indicates that part of this feature has begun to decay.

BORING CORE ANALYSIS OF PALSA B

Drilling of the top of the palsa was attempted in late June, 1988 and 1989. Core samples with a diameter of 4.5 cm were collected from the ground surface to a depth of 423 cm for analysis of stratigraphy, water content, bulk density and ignition loss in 1988. The depth of permafrost base was observed to be 500 cm in 1989.

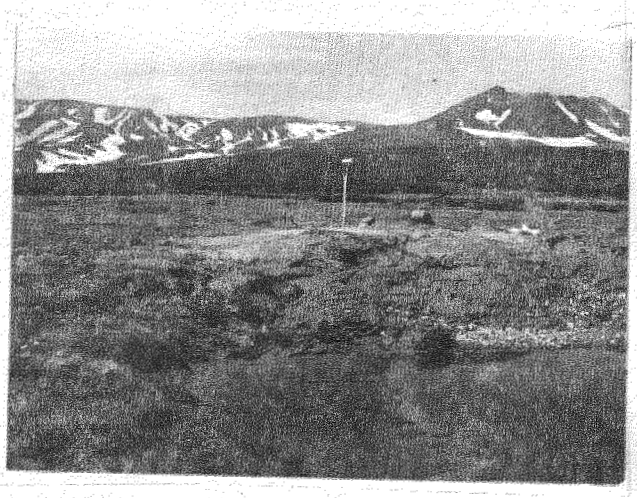

Figure 2 Palsa B in the Daisetsu Mountains

Figure 3 shows the internal structure of palsa B. It's top was peat with a thickness of 80 cm, the lower part of which contained sand and gravel. The peat layer was underlain by sand and gravel with a silty matrix (80 - 170 cm). At the depth of 150 cm, a thin ice lens was visible. The sand and gravel layer was underlain by silt with sand and gravel (170 - 220 cm). Thin ice lenses (1 - 2 mm) were found in this silt layer. This silt layer was underlain by sand and gravel with silty matrix (220 - 250 cm). From the depth of 250 cm, silt layer extended to the bottom of the core sample. This lower silt layer includes alternations of ice-lenses and frozen soil layers indicating rhythmic ice-lens formation. The thickness of the ice-lenses in this silt was 1 - 3 cm. These ice layers were concentrated in the lower part at the depth of 320 cm from the ground surface.

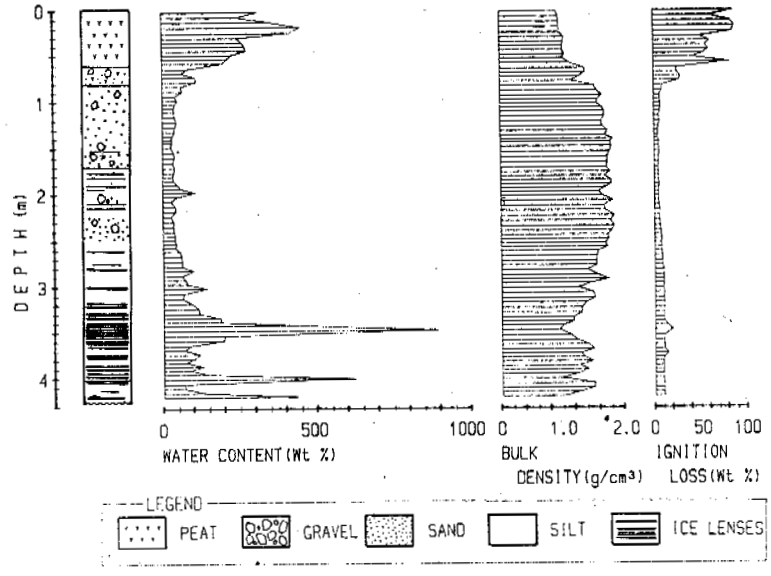

Figure 3 Water content, bulk density and ignition loss of the boring core of palsa B

Core samples were transported to a low temperature laboratory in frozen state. Each sample was cut and sectioned with thickness of 3 - 7 cm. In analysis of bulk density, each sectioned sample was weighed in air and in kerosene at -10°C in the laboratory. After drying for 2 hours at a temperature of 110 °C, the air-dried weight was measured. The results of the analyses are also shown in Figure 3.

The water content of the upper peat layer was more than 200 %, while those of the mineral layers down to 2.6 m were lower than 110 %. The high water content of the upper peat layer, does not, however, indicate the richness of ice. Since organic materials are lighter than the mineral ones, the former show higher water content of a percentage dry weight basis. In fact, high ignition loss of the peat layer indicates a high organic content in the upper peat layer than the lower part of the core. The bulk density of the peat layer was lower than 1.0, while that of mineral layers until 2.6 m deep from the ground surface was higher than 1.5.

Water content in the lower silt layer was variable, partly very high and partly low: 438.3 %, 891.2 % and 624.8 % at depths of 341-34 5 cm, 345-351.5 cm and 398.5-404. 5 cm respectively, while 60 %, 63.9 % and 69.4 % at depths of 285.5-291 cm, 310.5-361 cm and 367-371.5 cm respectively. The bulk density was also variable in the lower silt layer.

A high percentage of water content and relatively low bulk density suggest that the mineral samples are rich in ice lenses. Silt is usually very frost-susceptible. In fact, the ice lenses or layers develop mostly in silt layers, especially in the lower silt layer below the depth of 320 cm, where they consist of pure ice.

These ice-lens layers are surely formed not by ice injection but by ice segregation, because they are parallel to the freezing surface and alternate with frozen silt layers.

THERMAL REGIME IN PALSA B

The authors carried out a continuous monitoring of ground temperature at the top of palsa B, where the ground surface is often exposed in winter. As a result, nearly year-round ground temperature data were obtained.

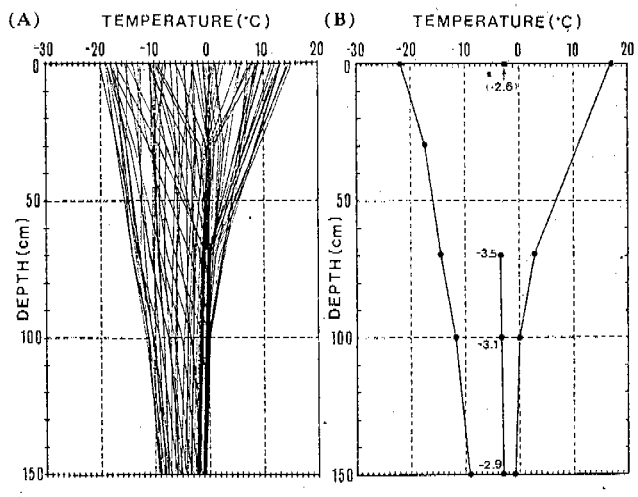

Figure 4 (A) Every five day profiles of mean daily ground temperature (B) Maximum, minimum and mean ground temperatures at palsa B from September 1987 to September 1988

On palsa B, the temperature sensors (Pt 100) were inserted in another bore hole at the depths of 0 cm, 30 cm, 70 cm, 100 cm and 150 cm. Ground temperature records were obtained at every two-hour interval from September 14, 1987 to September 21, 1988 except for 10 days in June. Figure 4A shows every five day profiles of mean daily ground temperature for this duration. The temperature ranges and mean values of mean daily ground temperatures at each position of palsa are indicated in Figure 4B.

The seasonal fluctuation of air temperature affected the ground temperature variation at each position. From October to December in 1987, the ground temperatures of the palsa at depths of 70,100 and 150 cm were nearly constant, and very close to the freezing point; these periods should correspond to the "zero curtain" at each depth. The ground temperature remained below 0°C at below a depth of 150 cm. The depth of the permafrost table is estimated to be 105 cm on the basis of Figure 4B. The temperature measurement of palsa indicates that the temperature of the upper portion on the ground is adjusted to the present climate, and that permafrost can develop at sites with thin snow cover, even under present climatic conditions in the mire.

The thermal properties of peat contribute to the preservation of permafrost (Brown and Péwé, 1973). The annual mean ground temperatures are calculated to be -3.5 °C, -3.1 and -2.9 at 70 cm, 100cm and 150 cm deep respectively (Figure 4B). The mean annual temperature of the ground surface of palsa is calculated as to be -2.6°C, while the mean annual temperature of the ground at depths of 70, 100 and 150 cm are lower than that of the ground surface. This fact reveals that the thermal properties of peat affect the temperature profiles at this site.

TYPE AND AGE OF PALSA FORMATION

Washburn (1983b) proposed that palsas comprise two different forms: one is an aggravation form due to frost heaving by growth of ice; the other is degradation form due to the disintegration of an extensive peaty deposit. The two types of palsas are difficult to identify by shape (Washburn, 1983b). While the degradational type indicates thermokarst processes, the aggradational one indicates the growth of permafrost underneath.

On the basis of the comparisons of air photos taken in 1955, 1966, 1971, 1978 and 1982, the changes in size and areal extent of palsas and peat plateaus during the period of 1955-82 were examined (Takahashi and Sone, 1988). Their total area was reduced by 36 % over 27 years. However, there are several palsas that were hardly reduced.

On the contrary, a palsa appeared on the photograph taken after 1971. It was not visible on the photographs taken in 1955 and1966. This indicates that the palsa grew after 1971. In addition, another palsa, which was discovered in the field survey, seems to be in an early stage of development. Hence, some palsas seem to be in the growth stage.

While string bogs around the palsa develop in harmony with the present slope direction, traced on the string bogs remain on the surface on palsa B. Therefore, the palsa began to grow after the string bogs were formed. This shows that the palsa was upheaved recently by permafrost aggradation, because there is no permafrost underneath the string bogs, developing at lower places than surroundings. The palsa contains the segregated ice layers in the lower silt layer, and the ground temperature profiles of the palsa indicate that at least the upper part of the palsa was affected the present seasonal alternations of air temperature. Therefore, ice-lens layers of palsa can be formed under present climatic conditions.

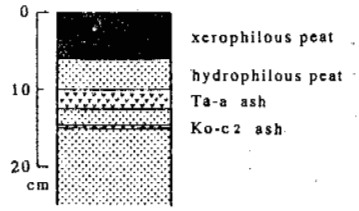

Figure 5 Columnar section of surfacial peat layer of palsa B

The peat layer in palsa B consists of two types of peat; xerophilous peat in the upper part and hydrophilous peat in the lower part (Figure 5). Two tephra (volcanic ash) layers are embedded in the peat layer at depths of10.0-12.5 cm and 14.0-15.0 cm from the surface. These layers are "Tarumai-a ash (Ta-a) and "Komagatake-c2 ash" (Ko-c2), deposited in A.D.1739 and A.D.1694 respectively (Endo et al.,1989). The boundary between the xerophilous and hydrophilous peat is at a depth of 6 cm from the surface. On the basis of the rate of peat accumulation between the tephra layers, the hydrophilous peat ceased to accumulate in A.D.1829. The change from the hydrophilous to the xerophilous peat indicates an environmental change from wet conditions to dry conditions at the site. Therefore, it is considered that the upheaval of palsa began in around A.D.1830.

The authors conclude that some palsas and peat plateaus have been formed under present climatic conditions associated with permafrost aggradation in the Daisetsu Mountains.

A considerable thickness of peat is required for palsa formation at this location, because the thermal properties of peat contribute to the formation of a palsa (Zoltai and Tarnocai,1971). According to Seppälä (1988), the minimum thickness of insulating peat layer, needed for palsa formation in a region with a mean annual air temperature of -2.0°C, is about 40 cm. In the mire, a peat cover of more than 60 cm thick is necessary for the growth and persistence of palsa (Takahashi,1990). The ^{14}C age of the peat samples at 40 cm below Ko-c1 layer (A.D.1694), was measured at 4,520±130 B.P.(NUTA-455) (Takahashi et al.,1988). The mean rate of peat accumulation in the mire is calculated to be about 0.1 mm/year. The thickness of the peat of palsa is 80 cm. According to the mean rate of peat accumulation, 6,000 years are required to accumulate the peat thicker than 60cm, in the thermal condition for peat growing is constant. The peat accumulation in the mire of the Daisetsu Mountains began around 7,000B.P. (Takahashi, 1990). The beginning of the palsa formation in this mire, therefore, is calculated to be after 1,000 B.P., though more data are required for the reconstruction of the developmental history of palsas and peat plateaus in the mire.

From a view of the internal structure, palsas and peat plateaus in this location are not easy to grow in their early stage of development. Because frost-susceptible silt, in which ice-lenses grow effectively, is under 2.5 m deep from the ground surface, the palsas and peat plateaus do not begin to heave until freezing penetrates to the silt layer.

ACKNOWLEDGMENTS

The authors wish to thank Professors M. Fukuda and Y.Ono (Hokkaido University) and Dr.M.Sumita (GEOMAR, Kiel University) for their suggestions and her instructions on tephra layers. They are also indebted to Mr.Y.Watanabe (Photographer), Mr.N.Yasuda (Curator, Sounkyo Museum), Mr.H.Daimaru, Mr.T.Sato, Mr.H.Muto, Mr. K.Yoshikawa, Mr.D.Nagaoka, Mr.D.Ogawa, Mr.S.Ishimaru, Mr.A.Ozawa (graduate students, Hokkaido University, at that time) for their encouragements and assistances in the field.

REFERENCES

Brown, R.J.E.(1974) Some aspect of airphoto interpretation of permafrost in Canada. National Research Council of Canada, Division of Building Research, Technical Paper, 409, 20p.

Brown, R.J.E. and Péwé, T.L. (1973) Distribution of permafrost in north America and its relationship to the environment:A review,.1963-1973. Permafrost North American Contribution, Second International Permafrost Conference, Yakutsk, USSR, National Academy of Science Publication 2115, 71-100.

Endo, K., Sumita, M. and Uno, R. (1989) Late-Holocene tephra sequences in eastern Hokkaido and their source volcanoes. Journal of Geography, 98, 506-510.

National Research Council of Canada (1988) Glossary of permafrost and related ground-ice terms, Technical Memorandum No.142, p.156.

Seppälä M. (1988) Palsas and related forms. In "Advances in periglacial geomorphology" edited by Clark M.J., 247-278, John Wiley & Sons Ltd.

Sone, T.(1992) Permafrost environment of the Daisetsu Mountains, Hokkaido, Japan. P.P.P., 3, 235-240.

Sone, T., Takahashi, N. and Fukuda, M. (1988) Alpine permafrost occurrence at Mt.Taisetsu, central Hokkaido, in northern Japan. Permafrost; Proceedings vol.1, Fifth International Conference on Permafrost in Trondheim, Norway, August 1988, Tapir Publishers, Trondheim, 253-258.

Takahashi N. (1990) Environmental-geomorphological study on the Holocene mire development in the Daisetsuzan Mountains, central Hokkaido, northern Japan. Environ.Sci., Hokkaido University, 13(1), 93-156.

Takahashi, N. and Sone, T. (1988) Palsas in the Daisetsuzan Mountains, central Hokkaido, Japan. Geographical Review of Japan, 61, 665-684.

Takahashi, N., Nakamura,T., Sone, T. and Igarashi, Y. (1988) ^{14}C dates around the bottom of peat layer in the bogs on the Daisetsuzan Mountains, central Hokkaido, Japan. The Quaternary Research, 27, 39-41.

Washburn, A.L. (1983a)Palsas and continuous permafrost. Permafrost, Forth Intern. Conf. Proc., Nat. Acad. Press, Washington, D.C., 1372-1377.

Washburn, A.L. (1983b) What is a palsa ?. Akad. Wiss. Gottingen Abh., Math.-Phys. Kl. Folge 3, 35, 34-47.

Zoltai, S.C. and Tarnocai, C. (1971) Property of a wooden palsa in northern Manitoba. Arctic and Alpine Research, 3, 115-129.

A STUDY ON CHARACTERISTICS OF ICE-DAMAGE AND PRVENTION OF HYDRAULIC PROJECTS IN NORTH CHINA

Su Sheng kui and Zhang Tiehua

Tianjin Water Resources and Conservancy Bureau

Based on investigation and analysis, this paper introduces the characteristics of ice damage, the effect of ice damage on hydraulic projects, the counter measure and design for preventing ice damage, and some obtained results in the North China. These presentations could contribute to a reference of assuring a safe operation and design of hydraulic projects.

INTRODUCTION

The North China is about 0.32 million square killometers in area. It is close to the Bohai sea on the east, near by Taihang mountain on the west, attained to Yellow river on the south and against the Inner Mongolia plateau on the north. It belongs to the semi-dry monsoon climate of temperate zone. In winter, the slanting north wind runs currently, and along seashore, river and reservoir etc, the hydraulic projects have suffered from serious ice damage and brought about certain effect on the living of people.

In North China, Northeast and Northwest area, there are different degree processes of freezing-thawing in water areas of river, reserviors etc. in winter. In Northeast area, there are a longer freeze and a thicker ice layer, such as, the thickness of ice layer is 1.8--2.8m in Heilongjiang river and the freeze is 180 days or so. The characteristic of ice damage is that the damage of frozen soil is more serious than that of the running ice. Northwest area has a shorter freeze because of the effect of alpine air flow, so the period of running ice is longer before freezing. The characteristic of ice damage is that the damage of running ice is more serious than that of frozen soil. In region of North China, the freeze is about 120 days. Thickness of ice layer is 0.3-0.5m and the maximum thickness of ice layer is 1.2m. The characteristic is double damages of frozen soil and running ice. The characteristic shows that the ice damage in North China is more serious than that in Northeast and Northwest area.

Tianjin is a typical region of ice damage in North china . Because of affections of dynamic, static and frictional force etc produced by ice layer and running ice during the process of freezing-thawing in winter, the hydraulic project along river and seashore etc. suffered from serious damage.

According to records of Feb. and March in 1936, 1947,1957,1969 and 1977, the coast of Bohai sea bay on the northern region was formed continuous ice layer. This caused many facilities (e.g. ship and platform of petroleum etc.) suffered from serious damage.

In water areas of river, canal and reservior etc, because of ice resistance produced during the process of ice growing, there are affection of static ice pressure after ice tha wing and affection of dynamic lash and friction when ice thawing. particularly, there is an affection of obstruction during the period of running ice in spring. So, these actions will bring violent hit to base pier of bridge and agueduct and result in serious loss of projects.

In short, the damage of ice and hydraulic projects are fairly serious in winter in North China. Therefore, we must investigate and analyze seriousiy conditions, sum up these experiences and take efficient measures to ensure a safe operation of hydraulic project.

THE EFFECT OF ICE DAMAGE IN WINTER

The Obstruction of Canal and Trashrack Produced by Ice

Along hydraulic project line, there are trashracks, which are composed of steel belts weldded and has a interval of 7-8cm between belts, in the front pool of every pump station. Since the thin ice is unsteady and broken easily in early winter, so, these broken ices flow to the front of trashrack with water and mass to form a ice stack besides a fraction of broken ice into front pool through trashrack. Meanwhile, the bottom of ice stack dives with rivers and nestles closely against trashrack. This results in the reduction of flow section and decrease of water level. So, it often causes accident of cutting off water when water level of the front pool drops down to critical submerged water level of the flow entrace. When ice laver of canal thawes in the yearly middle of Febrary, there will be many running ice of different size massing in front of trashrack. In this stage, since the body of running ice is thickness in size, softer in tex-

ture and bigger in buoyancy, so they do not dive generally and not bring about the the phenomenon of ice stack also. But when they meet the pile of grass in front of trashrack, they will form a "mixture of ice–grass". This will not only result in reduction of flow, but also form an ice–dam in front of trashrack. During proecss of the running ice advancing in open canal in spring, if there is ice stack to resist flow in front of the backward siphon tunnel. This will cause increase of water level of upoer reaches and form ice flood.

Damage Under Static Ice Pressure of Contionuous Close Ice Cover

In early winter, the ice cover becomes more stable with the change of air temperature in day and night, the expansion of ice cover takes on periodic change. Meanwhile, the static ice pressure also increases with increase of expansion. vice versa, In thawing stage of ice, the expansion of ice layer increases continuously with gradual increase of air temperature. The value of static ice pressure which put itself brokenness of ice layer as a maximum limit relates with thickness of ice layer, boundary conditions, allowable deformation and rigidity. That is, the thicker the ice layer, the bigger the boundary rigidity, the shorter the affecting span, and the higher the air temperature, the bigger the static ice pressure. Otherwise, it is oppsite. So, the damages of different degrees occur on the bank–wall of front pool, both side slopes of canal, slope of reservior and wall of anti–wave along Yinluan line.

Since the slope of canal or reservior is pushed by the static ice pressure or ice layre, so, the slope which has slope of 1:3 and uneven surface can be damaged. Its law of damage is that slope protection which has slope protection built by laying stones is damaged and surface of dyke without slope protection is damaged. Position of damage generally occurs onto sun slope or corner of dyke. In thawing stage of ice layer, the temperature is different at day and night. At night, the ice layer contracts forming continuous or discontinuous crack, then is filled with water forming a new continuous ice layer. From 8 to 14 o'clock on the next day, with the increase of air tempreature, the ice layer expands and climbs up intermittently along sun slope of dyke. As a result of climbing, the push force of climbing ice is produced. This push force can bring about serious damage to the wall of anti–wave or sub–cofferdam. For cutting off passageway which the ice layer climbed up, the thawing zone was cleared out by artificial way to protect the wall of anti–wave, but the cost of artificial clearing needs 6000 Yuan every year.

Because of continuous action of static ice pressure of ice layer, the front pool of pump station often suffered from damaged. Such as the front pools of pump station in Yinluan project which are composed of two side upright walls of pump room and canal of entering water, the damaged place was mainly on the two side upright walls of sheet pile of reinforced concrete. Under static ice pressure, the expansion joint of sheet pile wall was moved 3–5cm. On the contact place of ice layer and the side wall, the epidermis of concrete fell off and had a devoloping rate of 1–2mm every year.

COUNTERMEASURE FOR AVOIDING ICE DAMAGE

Take the project of Diverting Water from Luan River to Tianjin(DWLT project)as an example. In order to enssure a normal operation of water transport in winter, electric heat conducting pipe, high water pressure pipe and high air pressure pipe were set up on edges of sluice gate respectively. It was confirmed that before a continuous ice layer was formed,it was effective to disturb the freezing water surface not to form a frozen area by successive passes of electricity, warter and air, except for a greater consumption of power. Once the ice layer was formed, it would be very difficult to melt the ice using the method.

According to various features in DWLT project, the following methods were proved to be effective.

Countermeasure for Preventing Runing Ice From Blocking up Canal and Trashrack.

The failure of ice layer is the reason that the trashrack is blocked up in early winter. Therefore, one of the following three methods may be effective: avoiding freezing in front of trashrack; transporting water at a speed of less than 0.67m / s, at which ice layer can't be broken; transporting water normally afer temporary stop in order to form a continuous ice layer.

The key to prevent trashrack from blocked up is to avoid the formation of ice–grass mixture in front of the trashrack in spring. In order to clear out the ice–grass mixture, the grass grown in winter in front of the trashrack has to be cleared out. As long as no grass exists, the runing ice floaded on water would melt with the warming of climate in spring.

In the aspect of the blocked up siphon with runing ice, after observation for ten siphons, only the siphon in Beijn drainage river was blocked up in 1984. It is considered that the solution is to renew the iceproof pier at the entrace of tunnel. Meanwhile, trashrack should be settled within 10m outside the entrace of tunnel. The trashrack should be able to intercept the runing ice which has a width of a quater of the width of tunnel, resist the punching of runing ice, and split runing ice.

Countermeasure for Preventing The Ice Damage on Slopes of Canal and Reservior Cofferdam

The slopes of canal and reservior cofferdam, where the sun shines heavily on the North, are pushed off by ice layer. According to observation of ground coffer in the North China, the limit of slope without slope protection is 1:5, that is, when the slope is greater than 1:5, the slope would be pushed off. The slope which has a siope of 1:2 was most heavily pushed off by ice layer, and a mound was pushed up by about 1–2m.

The limit of slope, which has a smooth–faced stone lining is 1:3. The slope which has a slope of more than 1:3, an uneven surface or a unsteady base, would be suffered from failure in different degrees. Therefore, in the future design, slope protection must be accepted, and it is better to use reinforced concrete or concerte slope protection rather than stone. Fabric filter layer beneath the slope protection is the best. The surface of slope protection should be smooth as possible as it could be. Considering the unhindered climbing up of the interface between ice layer and slope protection, safe slope should be adapted. Is possible, slippy coating can be painted on the surface of lining or slope protection, so that the ice layer can climb easily. This is an effective measure to reduce the slope protections of canal and reservior cofferdam.

If anti–wave wall, sub–cofferdam and other constructions are set up on the top of the cofferdam, the capacity to resist the compressive strength of ice layer must be calculated. The acting point should be checked at 1 / 3 or 1 / 2 of the height of the wall. This is an effective measure to controll the anti–wave wall on the slope protections of canal and reservior cofferdam not to be damaged by the compressing stress of static ice layer.

Countermeasure for Reducing the Static Ice Pressure in the Front Pool of Pump Station

After continuous ice layer is formed in the front pool in winter, the static ice pressure would be acting from stable stage to melting stage. The ice pressure is defined as the combined stress of the compressive strength of the maximum thickness of ice layer. If the side wall has a greater stability and rigidity, the ice pressure is stated in accordance with the fracture or heave of ice layre. If the capacity to resist static ice pressure is lower, the ice pressure on the side slope wall is stated in accordance with its deformation or unsteady.

Su shengkui's formula is recommended for the calculation of static ice pressure. Based on icefield stability thoery, the calculating method for static ice pressure is illustrated as follows:

Combining practice with the concept of lever stability in the mechanics of material, authors proposed the icefield stability thoery in accordance with the research of the maximum horizontal pressure on hydraulic buildings at the moment that the ice layer becomes unsteady. Basic assumptions are as follows:

Ice layer is elastic and istropic material, and its stress–strain behaviour is satisfied with Hooke's law.

The compressing stress reaches to its maximum value at the moment that the ice layer changes to unsteady.

Connection between ice layer and building is regarded as hinged joiht.

Based on above assumptions, before the compressed lever is out of stability, the differential eqution of the bending deformation of the lever in the axial direction is:

$$EIY''P_kY = 0 \qquad (1)$$

where: p_k:static ice pressure(T / m^2);

Y:vertical deformation of ice layer(shown in Fig.1);

EI:rigidity of ice layer.

Solving the above equation with a hinged joint boundary coundary condition, we obtain:

$$P_k = \frac{\pi^2 EI}{l^2} \qquad (2)$$

Where, l is the distance from building to the opposite bank of ice layer. Generally, the value of l is selected as 15 times of the net width in calculation, but it should not be greater than 150m.

If the thickness of ice layer h and the calculating width of the extruding of ice on building b are obtained, equation (2) can be transformed to:

$$P_k = \frac{\pi^2 Ebh^3}{12l^2} \qquad (3)$$

Where, l: the distance from front pool to opposite side wall; E: elastic modulus of ice, 88–98 (T / m^2); b:1.0m; h:thichness of ice layer (m).

In order to diminish the action of static ice pressure on the side wall in the front pool of Yinluan Pump Station, it turns out to be effective that water is pumped from bottom by dive pump and sprayed out from a guiding pipe on the surface of front pool, so that a artificial spring is formed, which keeps water from freezing and a voids the action of static ice pressure. This kind of method is used in a few hydraulic buildings, to eliminate the action of ice pressure, for instance, Erwangzhuang reservior, canal and front pool, At the same time, the natural surounding around pump station is improved.

CONCLUSION

In short, the prevention of ice damage for a long water transport is an important subject to ensure safe operation in winter. After transporting water of 8 winters, it is proved that the original design is still not perfect. In addition to popularize above successful countermeasures, management and scientific research should be devoloped; field observation carried out; better combined measure studied; and true operation run, so as to ensure absolute safty of transportion of water in winter.

REFERENCE

Su Shengkui, 1980. Action of Ice Load on Hydraulic Buildings. Water Transportion Engineering, No 5.

Xu Bomen, 1985. Inflate Pressure and Calculation of Ice Layer in Reservior. Hydraulic Electric Technique. No 15.

Su–Shengkui, 1980. Problems of Analysis and Design of Anti–ice Damage in Yongdinxin River. Hydraulic and Electric Technique. No6.

Snib, B, 1982. Load and Effect of Water Wave, Ice and Ship on Hydraulic buildings. Haihe River Water Cconservancy (Supplement). No1.

Xu–Jianfeng and Xu Caihua, 1986. Ice Damage and Prevention in Yollow River. China Water Conservancy. No3.

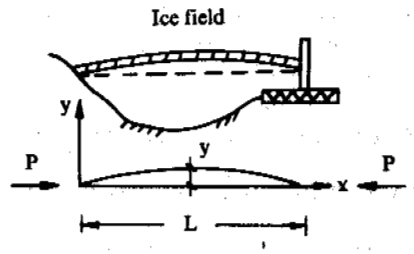

Fig.1 Ice field calculation sketch

THE LATEST PLEISTOCENE CRYOMERE IN THE REGION OF "KOPJES" AND THE BIG MESETAS, PATAGONIA, ARGENTINA

Dario Trombotto[1] & Bernd Stein[2]

[1] Centro Nacional Patagónico (Cenpat), Boulevard Brown 3000, 9120 Puerto Madryn, Ch., Argentina.
[2] Universität Bamberg, Physische Geographie, Am Kranen 1 D-8600 Bamberg, Germany.

In the northern area of South Patagonia, near the 46° S. L. and at different sites we find clear cryogenic structures that prove the activity of freezing and thawing of the latest cryomere during the Pleistocene in Patagonia. The profiles show ice wedge-casts. At the flanking sides of the "Pampa del Castillo" the head penetrates into the Tertiary forming droplike subhorizontal involutions. An intermediate clay-layer could indicate a possible interstadial. Paleoclimatic and sedimentary indicators express conditions of coldness which are ameliorating towards the Holocene Age and a predominantly dry environment with a strong participation of the wind.

INTRODUCTION

The paleoclimatic reconstruction of the Quaternary Patagonia, or the Neogene, has brought up many questions and different hypothesis. The idea of enormous glaciations during the big cryomeres contrasts with rather restricted glaciations near the Cordillera or minor local "glacioblastos" (GROEBER, 1950, etc) associated to the big mesetas or Patagonian mountains of over 2000 m a.s.l. The Patagonian glaciation helped to explain theories about the origin and dispersion of the famous "Rodados Patagónicos" and certain hypothesis on geomorphology. Until now it is generally assumed that the glaciation covered mainly the "Cordillera Austral" reaching partly into the extense Patagonian area. In some cases the glaciations approached 70° W.L. but it is only near 52° S.L. where they reach the Atlantic Ocean (CALDENIUS, 1932, etc). Step by step new information has been achieved and some cold periods in the past have already been documented. Geochronometric datings told as about old glacials towards the limit of the Messinian/Tortonian (MERCER, 1985).

During all these years the past geocryology of the area has been neglected. CALDENIUS (1940) holds that the fluvial deposits of the formation of the "Rodados Patagónicos", embedded with fine sediments or a kind of "loess", were influenced by solifluction and he underlines an important denudation cycle in East Patagonia. CZAJKA (1955) mentions rests of structures caused by thermal contraction during the Pleistocene at the "Pampa del Castillo" and on the "Rodados Patagónicos". He supposes that permafrost must have reached at least the mouth of the river Rio Negro. Ice wedge-casts were placed at SE of the locality "Las Heras" (CORTE, 1982). The important cold periods however, left their traces of freezing and thawing through the course of time. During the Quaternary cryomeres and possibly even earlier the biggest part if not the whole area was covered by permafrost.

Periglacial phenomena imprinted their marks during the Pliocene-Pleistocene when the "Rodados Patagónicos" (short RP) were depositing and also a posteriori. It analyses indicators of the Late Glacial and proves relevant climato-stratigraphical changes of the environmental conditions of selected sites before the arid or semiarid conditons of Patagonia today.

STUDY AREA

The study area corresponds to the typical Patagonian landscape: big mesetas , such as "Pampa del Castillo" (fig. 1) which have been classified into different levels according to their height and degree of erosion. Apart from

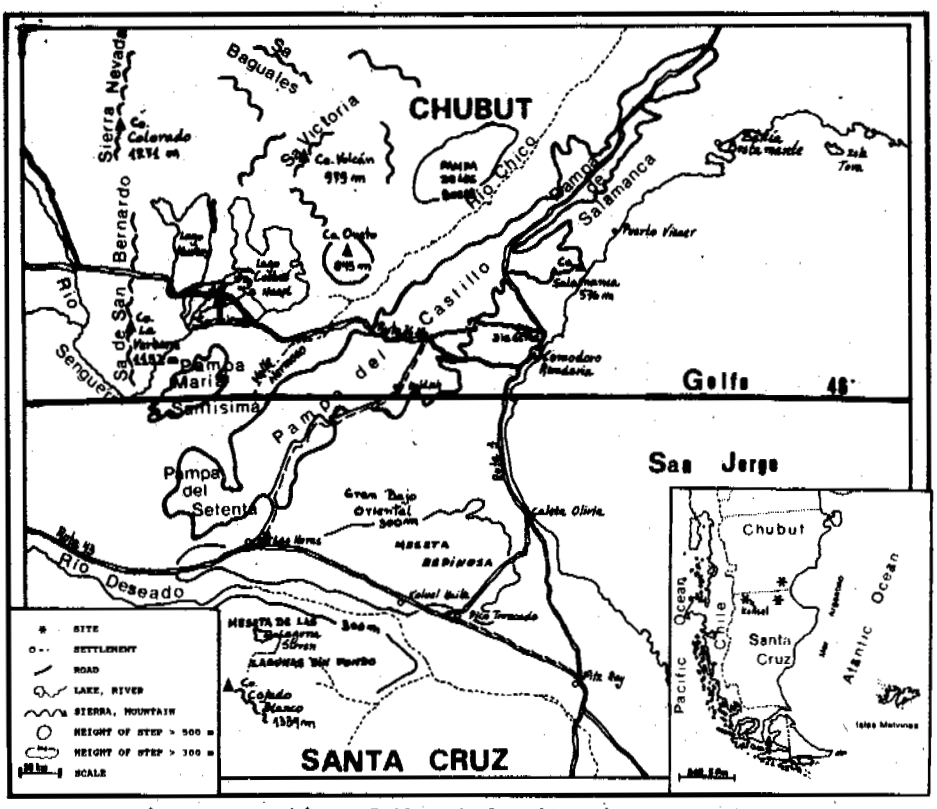

Fig. 1: Location of the study sites in Patagonia

the continental mesetas and approaching the coast we find mesetas of marine origin. The mesetas, surrounded by bad lands, generally dry valleys and "bajos", together with mountains, table-tops or "kopjes" and of course frequent and different Neogene basaltic layers constitute the Patagonian table land of the study area.

The analysed profiles are situated at three characteristic sites close to the 46 0 S.L. (fig. 1) where excellent examples of ice wedge-casts together with other characteristics of a periglacial paleoenvironment are found. The sites are :"Holdich", "Kensel" and "Las Heras". The first site is located in the SE of Chubut and related to the flanking sides of the geoform called "Pampa del Castillo" (appr. 700 m a.s.l.). Site "Kensel", near "Cerro Kensel", is located in the NW of Sta. Cruz (appr. 720 m a.s.l.), east of the "Meseta del Genguel" on the nat. road no 40. The third site is located in the NE of Sta. Cruz, at a height of 350 m a.s.l., near the settlement "Las Heras". Here the level of terraces is lower than at site "Holdich". According to TROLL and PAFFEN (1969) the climate belongs to zone III, e.g. cool temperate, type No 12: steppe climate: semidesertic and desertic climate.

The absolute min. temp. registered in Sarmiento is -33° C (incomplete data). The absolute min. temp. for Perito Moreno is -17,5° C and the mean annual precipitation is 116 mm (CABRERA, 1976). Towards the Southern Andes cool temperatures and their influence gain more and more importance.

The study area is characterized by luvic yermosols in two typical layers. The upper layer consists of sand and silt mixed with gravel (RP)) of a greyish-brown colour. Below we find a thin chestnut-coloured clay-layer.

The vegetation belongs to the "provincia patagonica" (CABRERA, 1976). Thorny plants and species that grow in form of "cushions" adapted to an arid and windy environment prevail.

Geologically the study area belongs to "Chubut extraandino", north of the "Nesocraton del Deseado". WINDHAUSEN (1924) carried out a very important geological and topographical investigation in the area of " golfo San Jorge". Quarternary geology and stratigraphy however, are relatively unknown.

In the whole study area a deposition of evaporites on top of the RP, volcanic ashes and eolian sediments which were retransported and then modified by fluvial, cryogenic and sedimentary agents, can be observed.

METHODOLOGY

During the expedition different study transsects in EW and NS direction were traced in order to investigate the Neogene stratigraphy and draw geomorphological conclusions. We made profiles at different sites which represented cryogenic phenomena of the past in and exemplary way and also proved to be related to those levels exposed to paleoclimatic changes. The profiles were layed out along roads, in quarries or excavations of waste deposits. Whenever this was impossible drillings and excavations were made. For our analyses we applied classical methods as well as visual and tactile characteristics. Representative samples of important layers and levels were taken. In the laboratory mainly granulometric analyses and analyses of carbonates were realized and where possible the sand-quartz grain surface textures were analysed in order to support the paleoenvironmental genesis.

DISCUSSION AND RESULTS

At site "Holdich" we found pseudomorphs of ice wedges (fig. 1) which penetrate up to 90 cm into the marine Oligocene at the flanking sides of the "Pampa del Castillo". The interior of the ice wedge contains 7% silt, 9% clay and over 84% fine and medium sand. The ice wedges were filled and later on covered and protected by the head which reaches a thickness of over 1 m. This deposit (sediments > -2 phi) is composed mainly of fine sand (41%), appr. 13% of silt and 17% of clay. It does not contain $CaCO_3$ and is rich in RP. At the inferior part of the head a clay layer (49%), with a thickness of 10-15 cm can be identified. This layer displays a polyhedral structure, clay skins, 37% sand and 14% silt, a strong carbonatic reaction and a content of gypsum.

Site "Holdich" is evidently influenced by solifluction. The head penetrates in some cases into the Tertiary forming droplike subhorizontal involutions. Solifluction can be identified with the help of the following pattern: 1- general characteristics of the deposit with sorting of certain levels and a special orientation of the clasts; 2- continuity of the covering layer even on the slope and spatial distribution of the deposit; 3- geomorphology of the area with characteristic soft relief and 4- textural characteristics of the quartz grains.

The eolian origin of the sediments can be verified through quartz grain surface texture analyses with SEM. The abundance (over 25%) of textures with high relief, angular outline, conchoideal fractures of different size, striations, parallel steps and arch-shaped steps are due to cryogenic phenomena which added to the inherited textures, probably related to interstitial material of the RP. Inside the casts, the quartz grains show eolization and a higher frequency of chemical textures due to different environmental characteristics and the age of the sediments.

Near "Cerro Kensel" the pseudomorphs very frequently appear in form of polygons (with sides over 1 m) along the road. The sediments of the casts are of a darker colour than the host material. They are rich in fine and medium sand (37% / 30%) and contain 15% clay and 10% silt. The RP appear in the filling as well as in the host material and on the surface. The host material contains $CaCO_3$ (appr. 50%), very much clay (55%) and silt (19%) and contrasts with the filling because of its lighter colour.

Site "Las Heras" is an example of the characteristic succession and the lithologic model described for Pto. Madryn in Northern Patagonia (TROMBOTTO, 1992). The upper layer consists of sand and silt of a greyish-brown colour. Its thickness varies between 10 and 20 cm depending on human influence. This layer covers another layer of brown sand with a thickness of 10-15 cm, polyhedral structure and clay skins. Below these two layers we find ice wedge casts with a depth of up to 70 cm. The pseudomorphs penetrate a sandy, calcareous layer with RP. A transversal cut reveals the characteristic polygonal structure. Just as in the case of site "Kensel" there is a contrast between the colour of the host material which is less dark, sandy (44%) with $CaCO_3$ (27%; 10 yr 7/3 - 8/3) and the filling of the structure which is darker and only slightly calcareous (10 yr 4/2-5/3). At site "Las Heras" the sediments of the filling are composed of medium sand mainly (52%), with 14% clay and 6% silt. At the lowest part of the profile we find again RP impregnated with $CaCO_3$, displaying a "nougat structure" (50 cm) and subsequently forming "columns" and subhorizontal structures as well as "windows" (TROMBOTTO, 1992). These last carbonatic deposits, or "tosca" clearly prove the relation between structures and the subsuperficial water drainage and the wash-out of sediments and minerals.

The sediments of the fillings of the

pseudomorphs at the three sites mentioned can be very well compared. Analysing the granulometric cumulative curves, we obtain a Qd between 2.1 and 2.5 phi, e.g. fine sand tending towards medium. The STD values (2-2.5) indicate a poor sorting of the material. While site "Holdich" displays an extremely leptokurtic curve, the other two sites, very similarly, indicate leptokurtic curves. The symmetry of the frequency curves gives us values of 0.3-0.6 in all cases. For "Kensel" and "Las Heras" we obtain exactly the same values. The peak in sand may be due to the transport of colloids during the pedogenesis.

Comparing "Holdich" and "Las Heras" we find a remarkable continuity and similarity with the difference that "Holdich" is strongly affected by solifluction and influenced by its geomorphological position. Solifluction must have participated in the decarbonization of the deposit.

CONCLUSIONS

In this first attempt and based on the investigation of characteristic sites we dare a paleoclimatic and sedimentary reconstruction of the area near the 46° S.L in Southern Patagonia. For this purpose we developed the following general pattern of the paleoenvironment:

1· The ice wedge casts we found represent the latest glacial and probably the coldest period of the Late Glacial appr. 20.000 years ago. The existence of those structures required permafrost and a mean annual temp. of at least 14° C below the present temp.

2· Some casts are filled with solifluction eolian material. A paleoenvironment of this kind would indicate still cold, but slightly more temperate conditions and aridity or semiaridity.

3· A warm impulse allowed the creation of the clay level through pedogenesis for which we suppose a min. mean annual temp. of 5° C and a mean annual precipitation of 250 mm. This moment might be related to an interstadial.

4· A posteriori this clay layer is covered by solifluction which again is related to a cold impulse and a semiarid paleoenvironment.

5· Finally the predominating climate during the Holocene was cool temperate and dry; conditions which hardly allow a pedogenesis and which are generally valid until today.

ACKNOWLEDGEMENTS

We would like to thank Dr. Frank Schäbitz (University of Bamberg, Germany) very much for the chance of participating in the expedition and sharing with him a month of adventures all over Patagonia which enabled us to realize this study. We are indebted to ALUAR, Puerto Madryn for offering us its laboratories, to IHEM-CONICET, Mendoza for its cooperation with the SEM and we are especially grateful to Sabine Herfert for the translation.

REFERENCES

Cabrera, A. (1976). Regiones Fitogeográficas Argentinas. Enciclopedia Argentina de Agricultura y Jardinería, Tomo II, 1, 85 pp., Buenos Aires.

Caldenius, C. (1932). Las Glaciaciones Cuaternarias en la Patagonia y Tierra del Fuego. Geografiska Annaler, Häft 1-2, 1-164.

---(1940). The Tehuelche or Patagonian Shingle-Formation. Geografiska Annaler, 160-181.

Corte, A. (1982). Geocriología general y aplicada. Revista del Instituto de Ciencias Geológicas, Universidad Nacional de Jujuy, Nr. 5: 1-33 ps.

Czajka, W. (1955). Rezente und pleistozäne Verbreitung und Typen des periglazialen Denudationszyklus in Argentinien. Acta Geographica 14, Nr. 10, 121-140, Helsinki.

Groeber, P. (1950). Quartäre Vereisung Nordpatagoniens. Sonderdrück der Zeitschrift "Südamerika", 6 pp., Buenos Aires.

Mercer, J.H. (1985). Las Variaciones Glaciales del Antiguo Cenozoico en Sudamérica al Sur del Ecuador. Acta Geocriogénica, Nr. 3, 86-206, Mendoza.

Troll, C. und Paffen, KH. (1969). Karte der Jahreszeiten-Klimate der Erde. Erdkunde, Band XVIII, 28 pp.

Trombotto, D. (1992). The Cryomere Penfordd, Patagonia. International Workshop: "Permafrost and Periglacial Environments in Mountain Areas", 33 pp., Calgary.

Windhausen, A. (1924). Líneas Generales de la Constitución Geológica de la Región Situada al Oeste del Golfo de San Jorge. Boletín de la Academia Nacional de Ciencias, Tomo XXVII, 3, 167-320, Córdoba.

SEASONAL FREEZING AND THAWING GROUNDS OF MONGOLIA

D. Tumurbaatar

Institute of Geography and Geocryology, Mongolian Academy of Sciences

The seasonal freezing and thawing grounds of Mongolia are subdivided into three regions: the first is a seasonally thawed ground region, the ground thaw depth in the loam is 1.8-2.8 m and in the loamy sand with gravel is 2.8-3.6 m. That thaw begins from June and continues until October; the second is seasonally thawed and frozen ground region, the depth of seasonally thawed and frozen ground is 2.6-2.8 m in the loam and 3.5-4.5 m in the loamy sand with gravel. Ground frost begins from the middle of October and continues until April. The third is ground freezing region, permafrost does not occur here. Ground is frozen seasonally. Depth of frozen ground is 1.7-2.5 m in the loam and 2.5-3.2 m in the loamy sand with gravel. Ground freezing is from the beginning of November to March.

INTRODUCTION

The seasonally freezing embraces all of the territory of Mongolia. The first summary of Mongolian seasonally freezing was given by P.I. Gukov (1961), N. Longid (1969), S.I. Zabolotnuc (1974) and D. Tumurbaatar (1975).

In the last 25 years, seasonally freezing investigations have been concentrated by the author in the territory of Mongolia. All materials were generalized and complied into large and small scale seasonally frozen and thawed ground maps of Mongolia (1977, 1985).

In some industrial areas maps were compiled of large and middle scale seasonally frozen and thawed ground (1971, 1976, 1989).

The main purpose of this report is the discovery of the general and regional regularities in the seasonal freezing and thawing of ground, of changing of temperature and composition of ground and natural conditions.

NATURAL CONDITIONS

Mongolia is situated in Central Asia, from the sea, to the border of the Russian Republic in the north and China in the south. The southwestern and western part of the territory is composed of the Altai, Khangai and Khubsugul mountains in the eastern-Khentei mountains, the eastern-north-Khingane mountains, the eastern and south-steppe and Gobi desert.

Mongolia is on the whole a mountainous country with an average absolute height of 1580 metres above sea level. The lowest point is the basin of Khukh-Nuur in the east, which lies at an altitude of 560 metres above sea level and the highest point within the Republic is Khyiten in the Mongolian-Altai, which stands at 4374 metres.

Average air temperature of the coldest month-January is -30°C in the north of Mongolia and -14°C in the south. The value of the warmest month-July is 12°C in the north and 24°C in the south. Average annual air temperature in the south part of country is -5.2°C and in the north 4°C.

Mongolia has a sharp continental climate and these conditions promoted the development of permafrost in 15% of the territory and the deepening of seasonally freezing ground on the whole.

THE THAWING OF GROUND IN MONGOLIA

The main permafrost regions are in the Khangai, Khubsugul, Khentei and Mongol-Altai mountain territories and are characteristically seasonal grounds.

The predominant absolute altitude of Khubsugul mountains country ranges from 2000 to 3460 m (a.s.l.). But absolute altitude in the Darkhat depression ranges from 1500 to 1800 m (a.s.l.). At Dood Tsagan Nuur in the Darkhadin depression on the left bank of the Shishkid river, the depth of seasonal thawing is 1.3-2.3 m in the loamy lake grounds, 1.5-2.5 m in the loamy sand, and 2.6-3.3 m in the sand. In the beginning of the valley, in Sharga at the river, it is 3.3-3.5 m in the gravelly ground with sandy fill.

Seasonally thawing of ground in the north-facing slope of the mountain is 2.3 m in the loamy sand. On the south bank of Khubsugul lake is situated the city of Khatgal (1650-1700 m a.s.l.), in which seasonal thawing is -3.2 — 3.5m in the gravel ground with loamy fill.

The above research materials shows that the depth of seasonally thawed ground ranges from 1.3 m to 4.0 m in Khubsugul mountain territories.

Deepest ground thaw is 3.3-3.5 m in the sand and gravel. Shallowest thaw of ground is observed to be 1.3-2.3 m in clay and loam.

The river-heads Sharga and Tes are located on the lake plateau of the Khandai mountain region. Here the depth of the seasonal thawing is 2.2-3.1 m in the boulders with sandy fill.

The depth of the seasonal thawing ground on

the Tarbagatai range at the altitude of 3000-3200 m (a.s.l.) is 0.9-2.3 m in the loam and loamy sand ground, and at the height of 2000-2300 m a.s.l. it is 2.8-3.8 m in the same type of ground.

In the lake hollow, Terkhiin Tsagaan Nuur, the seasonal thaw of ground is 1.6 m on the hidrolaccolite in the loam.

Seasonally thawed ground (Northern Khangai range) in the region of Shiluustei at the altitude of 2200 m a.s.l. is 3.8-4.5 m in the loamy sand and sand with gravel, in the settlement Bajan Oboo somon near the lake valley (country) Tsagaan Nuur (1935 m a.s.l.) it is 1.7 m in the loam, in the center of the settlement Galuut somon it is 3.5 m in the sand with gravel, and in the center of the settlement Bajanbylag somon (2200 m a.s.l.) it is 4.2 m in the sand with gravel.

The above mentioned data shows the depth of seasonally thawing changed from 0.9-4.5 m, in the Khangai mountain country.

The smallest thaw located on north-facing slope and lake and river valleys is 0.9-2.3 m in the clay and loam, the deepest thaw on south-facing slope is 3.5-4.5 m in the sand with gravel ground. Absolute altitude of Khentei mountainous country is 1500-2000 m.

In Bajanzurkh somon and Nalaikh, located in the south-west part of Khentei mountains, the seasonal thaw is 2.6-2.8 m in loam and 3.0-3.5 m in sand.

In the southern part of Khentei range, in the region of the settlement Mangunmorit somon, the seasonal thawing ground is 2.8-3.2 m in loam with gravel.

The absolute altitude 1620-1730 m in local-lowlands, marshlands and hollows, and the seasonal thaw is 1.2-2.3 m in the loam and locally is 2.3-2.8 m. In the eastern part of Khentei range, in the region of Batshereet on the north facing slopes, the depth of thaw is 3.0 m in low moisture (7-13%) sand with gravel.

The smallest depth of thaw in Khentei Mountain region is 0.6-1.3 m and occurs in the areas of the north-facing slopes, marshland, wet sand with thick continuous moss cover and water shed.

The deepest thaw (3.5-4.5 m) occurs in the areas of the south-facing slopes and of the discontinuous permafrost zone and water shed. As well as in the river deposits with the sand, loamy sand pebbles and gravels.

Altai mountainous region is situated in the west edge of Mongolia, and the absolute altitude of Altai mountain is from 3000 m to 3474 m. There is continuous and discontinuous permafrost in the region.

The valley "Khonghor ulen" located between the Altai mountainous region is situated at the absolute altitude of 2420 m and the seasonal thawing of ground is 2.6 m in the gravels or gravelly sand. And near to lake "Tsagaan Nuur" which is at the absolute altitude of 2100 m the thawing depth in the clay and loam is 1.8-2.2 m, and in the sandy ground is 2.8-3.0 m. Near "Tsenghel" somon at the absolute height of 2150 m, the thawing depth of sandy ground is 4.3 m. Lake "Tolbo" is at 2100 m and the thawing of muddy loam ground near the lake "Noghoon" is 2.8-3.0 m.

On the north facing slopes of the Altai mountainous region the thawing of broken stone ground is 3.0-3.8 m and on the south facing slopes the thawing of the same ground is 3.5-4.5 m.

The conclusion is that the thawing of the lake mid clay and loamy ground in the valley bottoms between the mountains of the Altai mountains region is 1.8-2.2 m, and in the sandy ground is 2.8-3.0 m.

Thawing of gravel and sandy ground on the south facing slopes of mountains is 3.5-4.5 m. And the thawing of north facing slopes of mountains in the same ground is 3.0-3.5 m.

It was easier to reveal the altitudinal regularities in the changing seasonal thawing ground than to reveal the latitudinal regularities. The deepest thawing of ground in loam is 2.8 m and in sand is 4.8 m under 1000 m height from the latitude of 48 in Mongolia.

At the absolute altitude of 1700-2300 m in Khanghai, Altai, Khubsugul and Khentei mountainous region the deepest seasonal thawing is from 2.0 m in loam and to 4.5 m in sand. At the heights of 2300-3000 m the thawing depth decreases 1.5 m in loam, 3.5 m in sand and at the heights above 3000 m it is 1.0 m in loam and 2.0 m in sand. In the direction from south to north the thawing depth of ground decreased. For example: the thawing depth of ground near Ghalut somon situated in front side of Khangai mountains ridge is 2.5 m in loam and 3.5 m in sand. But 500 km to the north in the Tsagaan lake valley of Khubsugul province the depth of thawing is 2.0 m in sand and 1.3 m in loam (Fig.1).

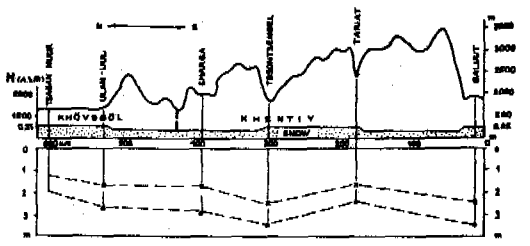

Fig.1 The change of the depth of seasonal thawing in loam (x) and sands (o) in Khangay-Khöysgöl mountain regions of Mongolia

THE SEASONAL FREEZING OF GROUND

The south part of Mongolia is predominated by the steppe and Gobi semidesert zone.

The seasonal freezing of ground in this zone is tightly connected with the natural complex. In the southern part of Mongolia the precipitation is low annually, 40-100 mm, snow cover is thin 3-5 cm, and is cold in winter and warm in summer.

The seasonal freezing ground consists generally of clay, loam, loamy sand, gravel, sand and different solid rocks of the Tertiary and Quaternary period.

In the southernmost point of Mongolia, Zamin Uud, the amplitude of surface temperature is 21-22°C, mean annual ground temperature is 6-7°C, ground moisture is 8-12%, depth of seasonal freezing is 2.3-2.4 m in loam, and 2.4-2.5 m in sandy ground. To the north near Sain Shand, moisture of sandy ground is 10-15%, mean annual ground temperature is 4.5-5.0°C, and depth of ground freezing is 2.2-2.4 m in loam and 2.4-2.6 m in sand (Table 1).

Near Dalanzadghad the mean annual ground temperature is 7-8°C, and depth of freezing is 1.7-2.1 m in loam and 2.2-2.4 m in sand.

Table 1. Depth of seasonally freezing ground of Mongolia

Populated area (settlement)	Mean annual ground temperature (°C)	Amplitude oscillation of temperature of ground surface	Moisture of ground	Composition of lithology of the ground	Depth of seasonal frozen ground
		Southern part of Mongolia			
Dalanzadghad	8.0	18.6	10.0	loam	2.0
Zamiin Uud	7.1	21.5	8.0	sand	2.5
Sain Shand	6.2	20.9	9.0	sand	2.6
Mandalgobi	5.0	18.6	5.2	loamy sand	2.5
		Central part of Mongolia			
Bajan	1.6	19.9	16.0	loamy sand	3.4
Choir	3.1	20.0	15.3	loamy sand	3.0
Tsetserleg	2.8	15.9	14.9	loamy sand	3.4
Ulaanbaatar	0.6	25.0	18.0	loamy sand	3.7
		Northern part of Mongolia			
Kharaa	2.1	22.8	16.5	sand	2.8
Erdenet	1.0	15.8	13.4	loamy sand	3.0
Bulghan	1.6	19.3	20.0	loamy sand	2.9
Ulaantolgoi	1.8	16.0	19.7	loamy sand	2.5

The conclusion is that the seasonal freezing of ground in the southern part of Mongolia begins from the beginning of November and is completely frozen at the end of February. The thaw of seasonal freezing ground begins from second week of March and ends in April.

The ground freezing in the southern part of Mongolia is 1.7-2.4 m in loam and 2.4-2.6 m in sandy ground.

Examples of the ground seasonal freezing of steppe and mountainous steppe zone of the central part of Mongolia can be seen in the regions near to Bajan somon, Ulaanbaatar, Tsetserleg, Bajanhonghor and Arcaykher.

Bajan somon in the Central province is situated in the steppe zone which is 90 km to the south of Ulaanbaatar.

The main structure of seasonal thawing and freezing ground are deluvium break stone and gravel, lacustrine loam and sandy loam.

The fluctuation of surface temperature is 10.1-14.2°C and the mean annual ground temperature is 0.8-1.9°C, and the ground moisture content is 3-15%. Ground freezing is 2.7-4.5 m in loam and 3.5-3.9 m in the sandy ground.

The ground freezing near Ulaanbaatar occurs in the proluvial and alluvial sands with gravels, and deluvial loamy sands with broken stones.

The fluctuation of surface temperature is 20-25°C, mean annual ground temperature is 0.5-2.5°C, ground moisture is 6-20%, and the depth of seasonal freezing of ground in the gravel ground with sand in the river and lake valley is 2.6-3.3 m.

The depth of ground freezing in the back sides of the mountains in loamy sand with broken stones is 4.2-4.8 m. The fluctuation of surface temperature near Arvaikher town is 15-18°C, mean annual ground temperature is 0.3-2.0°C, ground moisture is 5-10% and the depth of freezing of ground is 2.2-3.2 m in sandy ground and 2.5-2.9m in loamy ground. The freezing of ground is from the end of October until the beginning of April.

The seasonal freezing of ground near Bajanhonghor town is 2.9 m in loam and clay, and 3.4m in sand and loamy sand. The depth of seasonal freezing of ground near Tsetserleg town is 2.9 m in clay and loam, and 3.4 m in sand and loamy sand. The seasonal freezing of ground in the central part of Mongolia is from the end of October until the beginning of April. The mean annual ground temperature is 0.3-1.0°C in the loamy sand with deluvial broken stones in the back sides of mountains, and 2.0-2.5°C in the alluvial sand and loamy sand with gravel. The depth of seasonal freezing of ground is 4.0-4.8m in the back sides and 3.5-4.0 m in the front sides of mountains, and 2.6-3.3 m in the river and lake valleys. It's possible to determine the seasonal freezing of ground of the northern part of Mongolia or the region of Orhon and Selenga on the basis of the studied materials obtained in the territories of Selenga, Bulghan and Khubsugul provinces.

The state farm of Zun Khara is situated 120 km to the north of Ulaanbaatar. Here the seasonal freezing of ground begins from the first ten days of November and finishes at the end of April. The mean annual ground temperature is 1.5-2.1°C, depth of seasonal freezing is 3.2-3.4 m in clay and loam and 3.6 m in sand and loamy sand of Khara and Shara river valleys (Table 1).

The depth of sandy ground freezing in the east-north facing slope of the mountain near Darkhan city is 4.0-4.3 m, the smallest freezing was 1.7 m in the loamy ground with 16-25% moisture near the high bottomland of Khara river valley.

The depth of freezing ground in the valley near Erdenet hill (1240 m) is 2.3 m in lake sand with moisture of 25%, and is 3.5-3.7 m in light loamy sand on west facing slope of Erdenet hill (1300 m a.s.l.). Ground freezing is 3.9 m in the north facing slope of Erdenet hill (1450 m a.s.l.).

The seasonal freezing of ground in the Khanghal river basin begins in the beginning of November and finishes at the end of April. There is sand with loamy fill and with moisture of 15-20%, mean annual ground temperature is

3.0-3.2°C, and depth of seasonal freezing is 2.4-2.7 m.

The mean annual ground temperature of the loam and loamy sand with broken stems on the south facing slopes of mountains is 2.5-3.0°C, moisture is 9-11%, and depth of seasonal freezing is 2.3-3.7 m. And on the facing slopes of the mountains the moisture is 10-12% in the loam and loamy sand, it is mean annual temperature is 0.5-1.0°C, and the ground freezing is 3.7-4.0 m deep.

Near Bulghan town (1220 m a.s.l.) the ground freezing begins from the beginning of November and finishes at end of April. Mean annual ground temperature is 1.6°C and it is seasonal freezing is 3.2 m deep. In Murun town, which is situated in the northeast point, the seasonal freezing of ground begins after October 20, and finishes at the end of April. It's seasonal freezing is 3.9 m deep.

The conclusions taken from the above mentioned evidence shows that there is a fluctuation of 1.7-4.0 m in the seasonal freezing of ground in the Orkhon-Selengha region.

The depth of seasonal freezing in the ground increases from the south to the north until reaching the central region (Ulaanbaatar). And it confirms fully the conclusions of Russian scientist S.I. Zabolotnik who discovered that according to the natural regularities there is a reduction in the Orkhon-Selengha region.

The changes of the thickness of seasonal freezing is tightly connected with the factors of the rise in the winter duration in the direction of the north and the increase of absolute altitude of the earth and also the influence of snow cover.

Beside these factors it is also connected with other factors of freezing lake ground structure, moisture and temperature. Under the increasing absolute altitude from 900-1000 m in Dalanzadghad to 1200-1700 m in Ulaanbaatar the mean annual ground temperature reduces slowly from 6.7°C in Dalanzadghad to 0°C in Ulaanbaatar. But the thickness of snow cover does not change.

On this condition the depth of ground freezing is increasing from south to north.

The surface absolute altitude is reducing from Ulaanbaatar to the border from 850 m to 600 m, and the thickness of snow cover increases.

And snow cover reduces the depth of seasonal freezing by 0.2-0.7 m. Therefore the thickness of seasonal freezing in the northern part of the Orkhon-Selengha region is 0.8-1.4 m less than the region of Ulaanbaatar city (Fig.2).

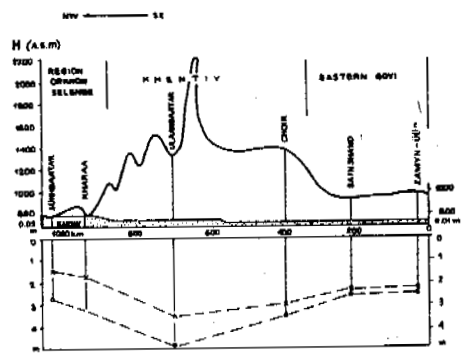

Fig.2 The change of the depth of seasonal freezing in loam (x) and sand (o) in central Mongolia

THE REGIONALIZATION OF THE SEASONAL FREEZING AND THAWING GROUND

The seasonal freezing and thawing ground of Mongolia is subdivided into three regions (Fig. 3):

1. Region of seasonally thawed ground. The distribution of permafrost is continuous. Ground thaw in the loam is 1.8-2.8 m and in the loamy sand with gravel is 2.8-3.6 m. That thaw begins from beginning of May and finishes in October.

2. Region of seasonally thawed and frozen ground. The distribution of permafrost is discontinuous. The region of seasonal thawing and freezing grounds are subdivided into subregions:

a. Subregion: Depth of seasonally thawed and frozen ground is 2.8-3.4 m in the loam and loamy sand and 3.5-4.5 m in the sand with gravel.

b. Subregion: Depth of seasonally thawed and frozen ground is 2.6-2.9 m in the loam and loamy sand and 2.9-3.5 m in the sand with gravel. Ground frost begins from middle of October and finishes at the end of April.

3. Region of seasonal frozen ground. Permafrost does not occur here. The region of seasonal freezing grounds are subdivided into two subregions:

a. Subregion: Depth of seasonally frozen ground is 2.5-2.7 m in the loam and loamy sand and 2.8-3.2 m in the sand with gravel.

b. Subregion: Depth of seasonally frozen ground is 1.7-2.1 m in the loam and loamy sand and 2.4-2.5 m in the sand with gravel.

CONCLUSIONS

The territory of Mongolia on the whole has seasonal freezing and thaw.

The depth of seasonal thawing in loam is 1.8-2.8 m and in gravel is 3.6-4.6 m. The depth of seasonally freezing in loam is 2.6-3.2 m and in sand with gravel is 2.8-4.5 m.

REFERENCES

Brown R.J.E., Permafrost in Canada, University of Toronto Press, 234p.

Zabolotnick S.I. (1975) Seasonal freezing and thawing grounds. Geocryological conditions of the Mongolian People's Republic. The joint Soviet-Mongolian scientific-research geological expedition, transations, Vol.10, pp.49-73. (Text in russian).

Zhou Youwu, Qiu Guoqing and Guo Dongxin (1991) Quaternary permafrost in China, Quaternary Science Reviews, Vol.10, pp.511-517.

Longid H. (1969) Permafrost of Mongolia. (Text in Mongolian).

Tumurbaatar D. (1975) Seasonal freezing and thawing grounds of the Mongolian, Academy of Sciences pp.39-74. (Text in Mongolian).

Tumurbaatar D. (1983) Classification of seasonally freezing and thawing grounds, Geographic problems of Mongolia, Vol.23, pp.25-29.

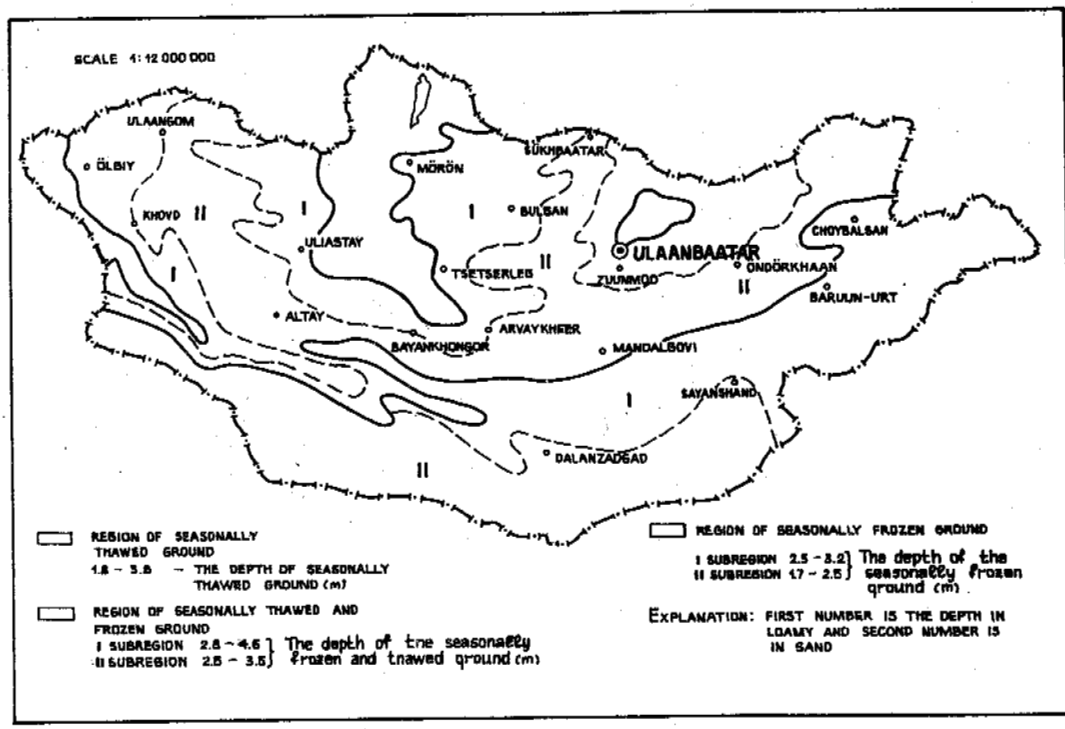

Fig.3 Map of region of seasonal freezing and thawing ground of Mongolia

HIGHWALL STABILITY IN STRIP MINES IN PERMAFROST

Jalal Vakili

Ninyo & Moore
9272 Jeronimo Road, Suite 123A
Irvine, California 92718 USA

The instability of highwall slopes, exposed to thawing, in surface coal mines in permafrost regions is described. Remedial measures are proposed to prevent shallow as well as deep slope failures in these regions. A practical design configuration, which involves introduction of a wide bench at the bottom of the permafrost layer, is proposed to mitigate highwall instabilities.

INTRODUCTION

Coals, ranging in age from carboniferous to tertiary, are found in many areas of permafrost regions. Although predominantly lignite and subbituminous in rank, the range is complete from lignite to anthracite. Reserves of strippable coal in Alaska, for example, are considered as 5 billion tons subbituminous and 2 billion tons bituminous coals. Reserves for this area include 120 billion tons of inferred resources and probably more than 1.5 trillion tons of estimated reserves (Hammond 1976). The coal is mined at present by the strip mining method. Draglines and scrapers are primarily used to remove the overburden. Coal seams are mined using front-end loaders, shovels, and trucks, or easy miners.

In designing large excavated slopes in strip mines, the most important decision of the engineer is the selection of a slope angle. The purpose of the geotechnical study of the slope is to ensure reasonable stability of the slope in the most economical way. Because the rock mass composing each highwall slope is unique, there are no standard solutions for slope stability analysis. A practical solution is formulated from the basic geology data, engineering properties of soil and rock, geometry of the slope, the ground water and environmental observations.

This paper describes the factors affecting cut slope stability in permafrost regions and the alternatives available for improving the stability of slopes.

FACTORS AFFECTING STABILITY OF SLOPES

Overburden Characteristics

The overburden of coal beds, in permafrost regions of Alaska, and particularly the strata between the coal beds, consists largely of poorly consolidated sandstone and claystone with pebbly layers (Wahrhaftig 1954). The response of cut slopes in frozen ground is directly related to the nature of the soil and the distribution of ground ice. It is difficult to determine the conditions from a site investigation program alone, and a clear picture of the anticipated response may not emerge until actual ground ice conditions are exposed during mining operations.

Mining Method

Strip mining usually is accomplished by removing the overburden from a strip across one dimension of the deposit. A parallel strip is then excavated usually in the opposite direction and the overburden is placed into the strip previously mined. This cycle is repeated as long as the deposit allows. The pit configuration is determined essentially by considering all the important factors: i.e. terrain, ratios, overburden, shape of deposit, thickness of seam, production requirement, and equipment available. Where the overburden is well over average thickness, or is of such a nature that is has a low angle of repose, the longer reach and other characteristics of dragline may make it the cheapest stripping unit in the long run (Bhattacharyya, 1982).

If the coal is pitching, as is in the anthracite region, the dragline makes it possible to operate by casting, work deeper down the pitch at a lower cost, and in some instances, to recover the coal without the necessity of men or equipment entering the pit.

Method of mining determines the height and angle of highwall and spoil slopes, bench width, location and specifications of equipment. Dragline exerts extra load on the highwall and contributes to the overall instability of slopes, and can often generate shallow failures in the surface alluvium and thawed rocks.

MECHANISM OF SLOPE FAILURE

Once the factors affecting slope stability are evaluated, it will be necessary to develop a model that represents the particular conditions found within the pit. For the selected model, the shear resistance will be calculated along the potential failure surface that would be necessary to bring the material enclosed by the slope profile and the failure surface to the point where the movement is about to occur, as shown on Figure 1. If the calculated shear resistance at limiting equilibrium is less than the available shear strength, the slope will be stable. The comparison of the available and computed shear resistances is carried out by means of an index known as the factor of safety. In mathematical terms:

$$F = \frac{\tau_f}{\tau}$$

where:
- F = factor of safety
- τ_f = $c + \sigma \tan \phi$ = shear strength along some shear surface
- τ = equilibrium shear stress along the same shear surface
- c = cohesion
- σ = normal stress
- ϕ = angle of internal friction

To determine the effective normal stress σ and the shear stress τ along the failure surface, various analysis methods are used, i.e. method of slices for circular arc analysis (Bishop 1955).

The analysis of failure in permafrost ground requires the specification of the in-situ shear strength of frozen ground. The strength of frozen ground develops from cohesion, interparticle friction, and particle interlocking, much as in unfrozen soils. Cohesive forces are attributed to adhesion between soil particles and the ice in the soil voids and to surface forces between particles.

The strength of frozen soil decreases with duration of load application and exposure to the atmosphere (Vyalov 1959). Therefore, long-term estimates of permafrost soils strength are needed in order to be able to apply classical methods of analysis such as method of slices (McRoberts, 1974b). When a frozen soil is subjected to a load, it will respond with an instantaneous deformation and a time- and temperature-dependent deformation called creep. At low solid concentrations (ice-rich soil) the strength may approximate that for ice and the long-term strength will be very small since ice creeps under extremely small stresses. At high solid concentrations (ice-poor soils) interparticle friction and dilatancy play a major part in determining the soil strength. The great difference in strength between frozen and unfrozen soil is derived from added cohesion due to the ice component and the creep effects of ice. Ice-poor ground exposed to thawing will lose its cohesive bonding and long-term strength of this kind of soil can be deduced from triaxial testing of unfrozen soils. In coal mines, when overburden is removed, the highwall slope and the pit bottom will be exposed to thawing. Permafrost material will, therefore, lose their cohesive strength which may result in highwall slope failures. Failures may be in the form of a shallow slope face failure or a deep-seated overall slope failure.

Two kinds of shallow face failures are common in permafrost terrain:

If permafrost soils are not sufficiently ice-rich, a thawed layer begins to form on the steeply inclined cut slope. This thaws to some critical depth, at which time the face failure starts by development of a skin flow in the thawed layer which exhibits characteristics of a viscous fluid in its downslope motion, as shown on Figure 2. Skin flow has been reported by many investigators (McRoberts 1973).

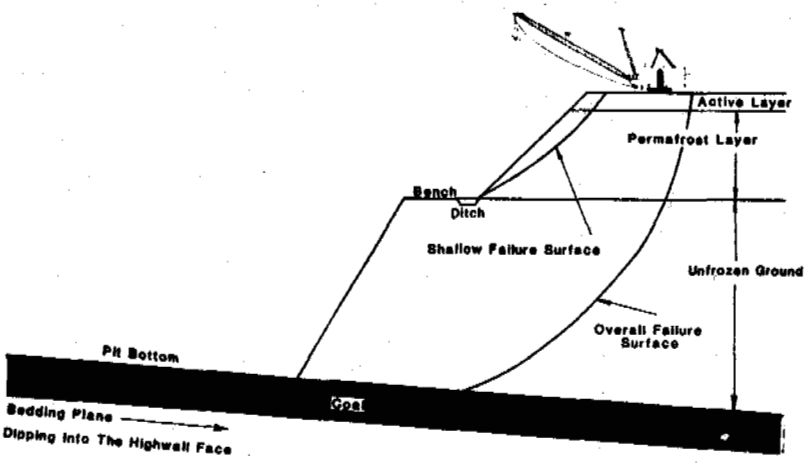

FIGURE 1 - PROPOSED HIGHWALL MODEL FOR PERMAFROST REGION

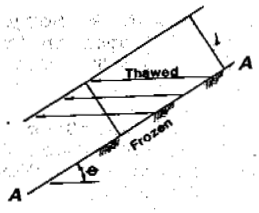

FIGURE 2 - SKIN FLOW

Less thaw-susceptible soils can be subject to rapid desiccation and after undermining by melting ice, may fail as a fall failure. It simply involves the downward movement of detached blocks falling under the influence of gravity as shown on Figure 3 (McRoberts 1973; 1974a).

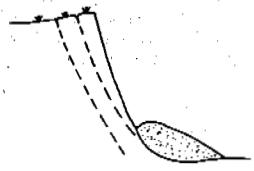

FIGURE 3 - FALL FAILURE

Three types of deep-seated overall slope failure have been encountered in permafrost terrain.

Block slides involve the movement of a large block that has moved out and down with a varying degree of back tilting. These types of slide are common where glacio fluvial sands and gravels overlie glaciolacustrine silts and clays. Slumps along bedding plane could involve large areas, as shown on Figure 4. Detailed observations of block slides are given by (McRoberts 1973, 1974b, and Isaacs 1972).

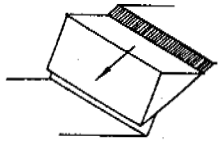

FIGURE 4 - BLOCK SLIDE

Rotational slides usually occur in completely thawed soil. These failures are similar to the classical circular type of failure common in clays in more temperate regions as shown on Figure 5 (McRoberts 1973).

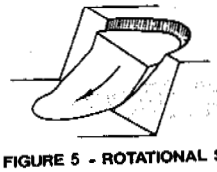

FIGURE 5 - ROTATIONAL SLIDE

The third type of slide of icy permafrost slopes is creep movement along the beddings (McRoberts, 1975a). Creep movement might be initiated by a warming up but not thawing of frozen ground (Figure 6) caused by removing the insulating vegetation cover, or by changing stress levels from additional load applied from equipment, or stress relief from cutting the slope. If such a process occurs, one result may be long-term creep rupture of the frozen soil, which would result in a failure form like block slides. The creep strength of frozen soils is defined as the stress level, after a finite time, at which rupture, instability leading to rupture, or extremely large deformations without rupture occur, and can be determined by tests on undisturbed permafrost soil samples.

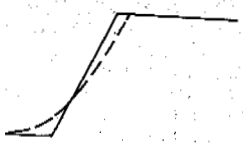

$$\dot{\varepsilon}_o = A\sigma_o^n + B\sigma_o^n$$

Mc ROBERTS CREEP MODEL

$\dot{\varepsilon}_o$ = SHEAR STRAIN RATE

σ_o = SHEAR STRESS

A, B, n, n PARAMETERS TO BE DETERMINED EXPERIMENTALLY

FIGURE 6 - CREEP MOVEMENT

REMEDIAL MEASURES TO PREVENT SLOPE FAILURE

The feature complicating the design of cuts in permafrost soils is the instability that may occur when exposed frozen soils are allowed to thaw. If the soil is fine-grained and ice-rich, ablation processes can generate substantial rates of surficial failures. The magnitude of the movements produced by actively retreating cuts is substantial and could be deliberately induced to speed stripping process.

The performance of actual cuts in permafrost soils has been studied by several authors (Pufahl 1975, McPhail 1976). Experience to date suggests that the following design configurations are appropriate:

- Cuts in frozen ice-poor soil, or bedrock
  - Cuts in soil and bedrock which are stable upon thaw can be designed so that the slope angle is compatible with the unfrozen properties.
- Cuts in ice-wedge terrain
  - If a cut in terrain in which the ground-ice condition exists as a matrix of ice-wedge in ice-poor mineral soil, the most suitable design depends on local conditions. Steep cuts are usually desirable because fewer ice wedges are encountered.
- Cuts in ice-rich permafrost
  - Various design configurations can be considered for cuts in which the ground-ice conditions are horizontally continuous. Because it can be difficult to prevent degradation, the design of ice-rich cuts in warm permafrost must necessarily allow for some thaw in the ice-rich soil. Introducing highwall benches will prevent thawed material from moving into the pit as shown on Figure 1. An alternative method for improving slope stability, in this case, is to operate stripping operations during winter time when the ambient temperature is below freezing point and there is no danger of thawing.

To reduce the danger of along-bedding slides, the strip mining operation should be planned so that all bedding planes on which sliding could take place would dip into the highwall face as shown on Figure 1.

When the mining depth is more than the depth of permafrost layer, it is recommended to introduce a bench in the highwall slope at the bottom of the permafrost layer, as shown on Figure 1. The lower slope of the highwall is not frozen and will not thaw, so there is a scarce possibility of instability of the lower slope. Additional water from thawing permafrost and ice wedges should be collected at the toe of the upper slope by introducing a drainage ditch as shown on Figure 1. A wide bench will help to improve the overall stability of the slope and prevent the thawed material of the permafrost layer from moving into the pit. To prevent face failure in the upper slope after thawing, the slope angle should be designed on the basis of frictional strength of the thawed permafrost materials only.

Finally, in no other area of slope stability design do construction activities offer such an important influence as in permafrost terrain. Inappropriate construction activities, such as premature removal of topsoil or overburden, may disrupt slope stability and should be avoided by careful advance planning of mining methods and mining sequences.

REFERENCES

Bhattacharyya, K. K., J. Vakili, S. Y. Chi, 1982, "Geotechnical Considerations for the Design of Highwall and Spoil Slopes in Lignite Mines," Proc. Mini Symposium, "Lignite Mining and Stability, Sept. 1982, Honolulu, Hawaii.

Bishop, A. W., 1955, "The Use of Slip Circle in the Stability Analysis of Slopes", Geotechnique, 5, 1, pp. 7-17.

Hammond, S., G. R. Martin, and R. G. Schaff, 1976, "Biennial Report 1974-75," Division of Geological and Geophysical Surveys, State of Alaska.

Isaacs, R. M. and J. A. Code, 1972, "Problems in Engineering Geology Related to Pipeline Construction". National Res. Counc. Tech. Mem. 104 pp. 147-179.

McPhail, J. F., W. B. McMullen, and A. W. Murfitt, 1976, "Yukon River to Prudhoe Bay:" Lessons in Arctic Design and Construction, Civ. Eng. (N.Y.), 46(2): 78-82.

McRoberts, E. C., 1973, "The Stability of Slopes in Permafrost," unpublished Ph.D. thesis, University of Alberta, Edmonton.

McRoberts, E. C. and N. R. Morgenstern, 1974a, "The Stability of Thawing Slopes," Can. Geotech. J., 11:447-469.

McRoberts, E. C. and N. R. Morgenstern, 1974b, "The Stability of Slopes in Frozen Soil," Mackenzie Valley, N.W.T., Can. Geotech. J., 11:554-573.

McRoberts, E. C., 1975a, "Some Aspects of a Simple Secondary Creep Model for Deformations in Permafrost Slopes, Can. Geotech., J., 12:98-105.

Pufahl, D. E., 1975, "The Stability of Thawing Slopes," unpublished Ph.D. thesis, University of Alberta, Edmonton.

Vyalov, S. S., 1959, "The Strength and Creep of Frozen Soils and Calculations for Ice-Soil Retaining Structures," U.S. Army Cold Reg. Res. Eng. Lab. Trans. 76, Hanover, N.H.

Wahrhaftig, Clyde and J. H. Birman, 1954, "Stripping - Coal Deposits on Lower Lignite Creek, Nenana Coal Field, Alaska," Geological Survey Circular 310.

DESTRUCTION AND REHABILITATION OF SHAFT LINING USED IN FROZEN SHAFT

Wang Changsheng and Liu Rihui

Beijing Research Institute of Mine Construction,
Central Coal Mining Research Institute
Beijing, 100013, China

In recent years, the shaft linings of more than 10 shafts sunk with freezing method in China coal mine were destructed in varying degrees; the regions of destruction occurrence are mainly in Huaibei, Xuzhou and Datun coal mine districts,and the major expressions of shaft lining destructions are peeling and coming off of shaft lining concrete and crooked reinforcing bars,thus leading to short-term stop production of mines and seriously menacing the security of mines. In this paper ,the process of shaft lining destruction of these shafts is expounded and a simple analysis is made of the reason of shaft lining destructions. In accordance with shaft lining destructions, rehabilitations of these shafts have been carried out many times by mine construction departments. The state of the rehabilitations is also given briefly in this paper.

BRIEF ACCOUNT FOR DESTRUCTION OF SHAFT LINING IN FROZEN SHAFT AND EMERGENCY TREATMENT

Since 1955 when freezing method for sinking shaft was adopted first in China, more than 320 shafts have been sunk, totalling to 50 km. In China freezing method has already become a major special shaft sinking method in unstable water-bearing strata. After 1987, the accidents of peeling and coming off of shaft lining concrete occurred , early or late, in 17 shafts sunk with the freezing method in Huaibei & Datun coalfields, China. In some shafts, there were water flowing into shaft, carrying sand with it, thus menacing the security of mine production. The mine had no alternative but to stop production to make emergency treatment. This paper briefly describes the destruction and rehabilitations of Linhuan Colliery auxiliary shaft, Haizi Colliery auxiliary shaft and Zhangshuanglou Colliery auxiliary shaft.

Linhuan Colliery Auxiliary Shaft

The coal annual output of the mine was designed as 1.8 million tons.The mine was handed over and put into production in 1985. The auxiliary shaft of the mine is 508.7 m in net depth and 7.2 m in net diameter. Freezing method was adopted in overburden and double-wall reinforced concrete lining was used with the outer wall and inner wall being 450 mm and 900 mm thick respectively.The outer wall was closely integrated with the inner wall. The design strength grade of concrete is 40MPa and the actual cube strength is generally 50MPa or so with the maximum value being 59.5 MPa, so concrete is very good in quality and is an excellent product.

In April, 1987, there happened severe burst sound from inside the shaft and then some scraps of concrete dropped from the shaft, the whole process lasted for half an hour.

Inspection after the sound stopped showed that there was severe circumferencial peeling off around shaft at the depth of 241 m , the destruction surface was smooth, and gravel was cut off into a plane, with peeling-off depth being 200-250 mm and height being 500-1500 mm. The reinforced bars was revealed and bent under force. There were several seepages in the shaft. Afterwards, it was also found that cracks appeared in hoist tower with the longitudinal cracks in the lead and some cracks looked like the character ∧ with a dip angle of 50-60° . There were altogether 14 cracks(Fig.1).

The method for emergency treatment is that three lines of 18# channel steel rings are used every one meter. 5# channel steel lagging is employed between the ring and shaft lining.There is iron wedge for tightening between the lagging and shaft lining. 22 pieces of 180 N/m rail are placed longitudinally around each circle for reinforcing the rings.Rails are connected to the rings with clips and then gunite is used for reinforcement.

Auxiliary Shaft of Haizi Colliery

The design annual output of Haizi Colliery is 1.5 mt. The mine was handed over and put into production in 1987. The Auxiliary shaft of the mine has a net diameter of 7.2 m.Freezing method for sinking shaft was adopted in overburden and compound lining was used with its thickness being 1100 to 1400 mm. Where the destruction of shaft happened, triple-wall lining was used. The outer wall is 400 mm thick and is made of pre-cast concrete blocks. The middle and inner walls are 300 mm and 700 mm thick respectively and are consisted of in-situ concrete with a plastic plate placed in between. The concrete grade of lining is designed as 40MPa and concrete quality was rated as an product up to the mark.

An overall inspection of lining was made in September, 1987.It was found from the inspection

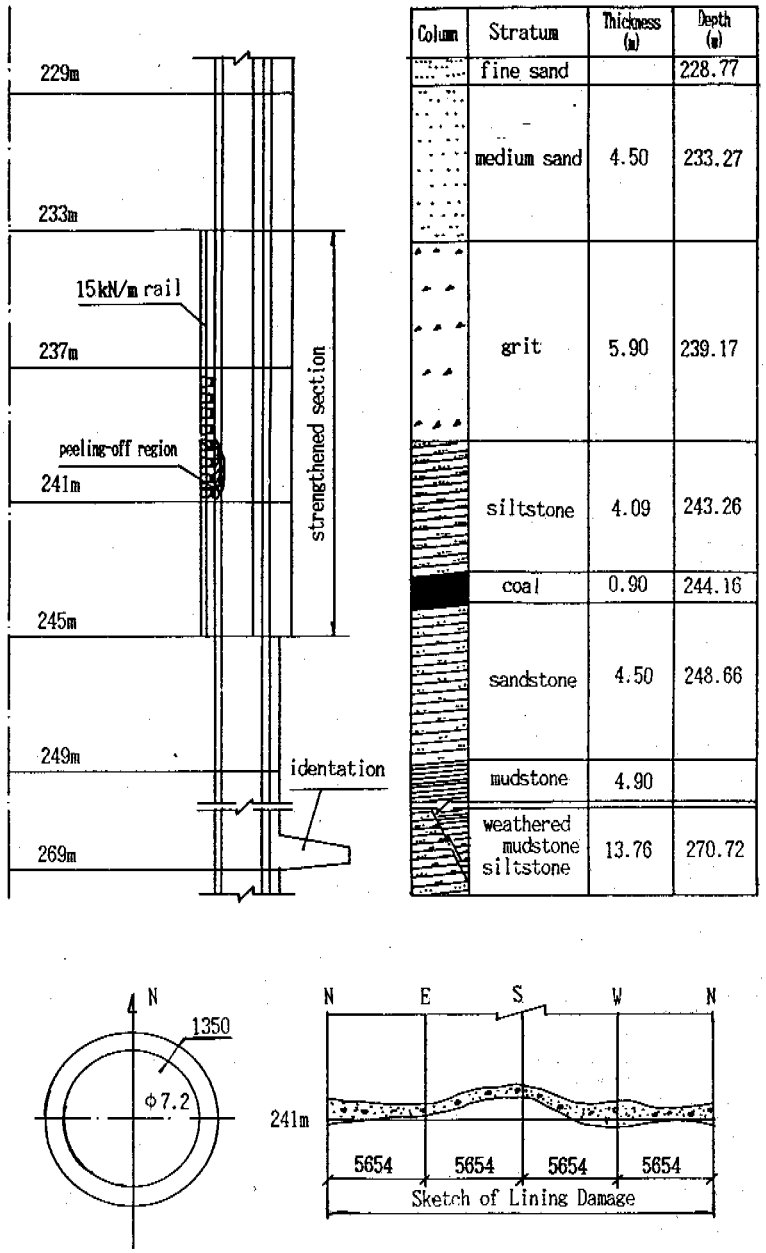

Fig.1 Strengthening scheme chart of Linhuan Colliery auxiliary shaft

that ruptures of concrete were observed in two places of shaft. The upper place of rupture is 232.8 m deep in the direction of NE with a circumference of about 7.5 m and a maximum height of 0. 5 m. The lower place of rupture is located in 237.5m depth in the direction of NW with a circumference of about 7 m and a maximum height of 1 m. The strata in which the shaft lining ruptures happened are clay , fine sand and water-bearing sediments of the Quarternary Period, and are about 6 m from weathered zone. At destructive part, 9 reinforced bars in the direction of NW could be revealed. Also there was a seepage of water. The emergency treatment of this shaft was same as that of Linhuan Colliery auxiliary shaft.

Zhangshuanglou Colliery Auxiliary Shaft

The mine was designed to have a annual output of 1.2 mt and put into production in 1986. The net diameter of the mine's auxiliary shaft is 6.5 m; depth, 565.7 m; overburden thickness, 242 m; freezing depth, 315 m. Double-wall lining was adopted with the outer and inner reinforced concrete walls being 600 mm thick each. A layer of compressible polystyrene plastic sheet 20-40 mm thick was filled between the shaft wall and the outer lining at the vertical depth of 200-248 m.

In the late July of 1987, partial rupture of shaft lining was noticed at the vertical depth of 229-230 m. The circumference of the rupture is 15 m; height, 0.5-1.3m; peeling-off depth, 250 mm. According to above-mentioned experiences for shaft consolidation, 18# channel ring was applied and connected to each other longitudinally by rails. And the shotcrete 150-200 mm thick is used for further consolidation. In August the rupture at the last burst region at the vertical depth of 225-229 m happened again with the height of the rupture being about 6 m. Exposed vertical bars were bent. A circumferencial bar in the direction of NE lost contact with shaft lining. There began water leakage out of lining. The shaft was in very imminent danger. The following day, the water-make having a sand content of 0.8 ‰ reached 15.5 m^3 /hr. Later the water-make was increased to 47.7 m^3 /hr, 60.5 m^3 /hr and 66.5 m^3 /hr, and the sand content was increased to 7‰. At that time, the following measures were taken: lessening the diameter of the reinforcing ring, increasing channel dimension, forcing to hang the ring on the shaft and to set up form, and placing concrete as soon as possible. Not until the first ten-day period of September did the whole emergency work end. Cement grouting for water control had caused water-make at destruction section of shaft reduced to 0.2 m^3 /hr (Fig.2).

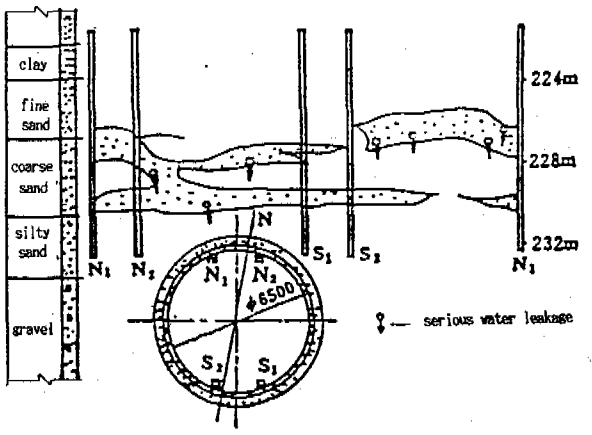

Fig.2 Sketch of shaft lining damage of Zhangshuanglou Colliery auxiliary shaft

MECHANISM OF DESTRUCTION OF LINING IN FROZEN SHAFT

Surface Subsidence Resulted in Shaft Suffering Vertical Compressive Force

There are no clear and definite explanation at present on the reason why the pseudo-mining surface subsidence phenomenon of these mines took place, the reason why the accidents of peeling-off of shaft emerged, and whether there was a connection on contributing factor between the former and the latter. But it may be preliminarily thought that the phenomenon of sudden rupture and peeling-off of shaft is a dynamic phenomena induced in mine engineering activity. This showed that large amount of elastic latent energy has accumulated in the peeling-off destructive part of the shaft and revealed itself in the form of sudden release when the energy exceeds the ultimate load-bearing capacity of lining, resulting in the destruction of shaft lining.

17 shafts the lining of which have suffered partial destruction are scattered over Huaibei, Xuzhou and Datun coal mine areas. There was one layer of bottom water-bearing formation in all strata through which the shafts pass. The formation, 10-20 m in thickness, has direct contact with coal formation. Dewatering during development of mines makes the water table of the Quarternary bottom aquifer decreasing continuously, generally to 50-120 m. This causes surface obvious subsidence, e.g. 408mm of subsidence in Zhangshuanglou Colliery industrial plane and 277mm of subsidence in Linhuan Colliery industrial plane. Thus the aquifer was compressed under the gravity of overlain strata at the same time as the confined water head dropped, resulting in surrounding formation producing friction force on shaft itself and subsiding simultaneously. The shafts, being rigid body and uncompressible, therefore destructs. Computations showed the friction force is 30-40 MPa.

Effects of Temperature Stress on Lining Destruction

In recent years, it was generally in summer that shaft lining destruction happened many times. Temperature stress had some influence on this. In summer the lining temperature increased; linear expansion took place; the restraining of surrounding strata makes shaft lining subjected to compressive force (Su 1991) .The force can be calculated in the following formulum:

$$\sigma_z^t = -E\alpha\Delta T\left(1-\frac{\mathrm{ch}\beta Z'}{\mathrm{ch}\beta H_s}\right)$$

Where

E --- Young's Modulus of shaft lining;

α --- temperature linear expansion coefficient of lining material;

Z'--- longitudinal coordinate, $Z'=0$ at the border between overburden and base rock;
Ha--- lining height above the border;
β --- coefficient, $\beta=\sqrt{\frac{C}{\delta E}}$,
C --- proportional coefficient between lining surface shear stress and lining displacement;
δ --- lining thickness.

Above calculation values show that why shaft lining destruction happens mostly in summer is mainly because of additional compressive force arising from temperature increase in summer.

BACK GROUTING

For above-mentioned destructed frozen shaft, we have, inside shaft, adopted such methods for emergency treatment as hanging channel rings on shaft with vertical rail reinforcing and grouting inside shaft for control of water etc., but the problem has not been solved fundamentally. The shafts still continued to subside, causing shaft installations twisted and making production unable to conduct properly.The choices for solving it are placing a lay of in-situ lining inside shaft or consolidating formations behind shaft lining thus transforming their structure from loose state to half-consolidated or consolidated state, the ultimate aim of which is making shaft itself bearing capacity greater than external forces and keeping shaft stable. The latter choice is used to strengthen formations behind shaft lining at present.

Surface Grouting Plan

Boreholes are put down around the shaft lining destruction from the ground surface away from the shaft by means of the directional drilling. This method, not having an effect on the production of mine, is an effective and good measure. But owing to some reason, this plan is still in preparatory stage.

Back Grouting Inside Shaft

The purpose of back grouting inside shaft is strengthening the shaft lining in the vicinity of the border between base rock and overburden; forming a ring of grout diaphram wall of some thickness surrounding the shaft and shaping a water-absent and pressure-absent consolidated region, in order to share vertical pressure and horizontal strata pressure which the shaft bear; blocking up and consolidating original lining cracks and fissures,controlling water-make,water-drenching and water seepage, increasing the entirety and stability of shaft, and so preventing deformative destruction from further developing and happening again (Zeng 1991).

Take Haizi Colliery as an example. Grouting began with weatherig zoon in base rock. Every layer of boreholes were put down from bottom to top. Grouting was mainly in the cracked region and in the formation of grit gravel and medium to fine sand of Quarternary Water-bearing strata. For the sake of construction, the first row of boreholes were arranged in weathered base rock.As grout is liable to diffuse upwards,it is possible not only to build a good basis at the bottom, to block the border surface between the base rock and the overburden,and also to prevent later grout from diffusing downwards.

Grouting Effect

Over 1000 t concrete was injected in the main shaft and auxiliary shaft of Haizi Colliery. The thickness of grout diaphram and water-absent and pressure-absent consolidated region are all greater than 2 m. Basicly there exists no water in cracked region of lining after grouting. During one year following grouting, measurements made through displacement and strain indicators showed that there was little changes in displacement, especially in radial displacement, so that by means of back grouting , the displacement at ruptured part of shaft has been got an effective control.

CONCLUSIONS

Although lining cracking has got controlled effectively after treatment, it is not able to be eradicated. Various kinds of shaft lining structure have been adopted in the construction of frozen shafts in China (Yu & Wang 1988). When the strata which the shafts pass contain grit gravel formation in the lower part, it is preferable to adopt flexible shaft lining structure. Placing a layer of bitumen sliding sheet between the outer and inner wall,having an advantage of being flexible and seepage-resistent, helps to reduce the effect of strata subsidence on interneal lining and to change uneven loading condition of internal lining.

REFERENCES

Su Lifan (1991) Damage of lining in frozen shaft and reason analysis. Mine Construction Technology No.1,33-37.

Yu Xiang and Wang Changsheng (1988)Structure and stress analysis of seepage resistant linings in shafts sunk with the freezing method. Nottingham: 5th Int. Symp.of Ground Freezing, Vol.1,311-318.

Zeng Rongxiu (1991) A new technique for backwall injection for water-bearing sand shaft, World Coal Technology No.9, 3-6.

PRESSURE INFLUENCE ON PORE CHARACTERISTIC OF FROZEN SOILS

Wang Jiacheng[1], Xu Xiaozu[1], Deng Yousheng[1] and Zhang Lixing[1]
IU.P. Lebedenko[2] and E.M. Chuvilin[2]

[1]State Key Laboratory of Frozen Soil Engineering, LIGG, AS
[2]Faculty of Geology, Moscow State University

By using a Poresizer we determined the pore characteristic of saturated frozen Neimong clay under the conditions of constant temperature and pressure and of constant pressure and temperature gradient. Results show that when the temperature is the same, the total pore volume and the amount of greater pore size of frozen soils are the minimum under the atmospheric environment, and the maximum under the vacuum condition and increases with increasing air pressure under the environment of air pressure higher than the atmospheric pressure. When the air pressure is the same, the total pore volume of frozen soils increases with decreasing temperature and the structures in frozen soils change from big ice strips to the small.

INTRODUCTION

The pore characteristic of soils before and after freezing is of great significance for physico-mechanical properties and cryogenetic structure and for mass transfer in soils. Chuvilin, E.M. and Lebedenko, IU.P. (1988) described the formation and classification of cryogenetic structures of frozen soils. Viyalov, S.S. and Chuitoviqi N.A. (1953) pointed out that there is higher pressibility for the frozen soil with higher temperature under overburden pressure so as to decrease porosity and to move texture elements. Wang Jiacheng (1989) studied the physical process and cryogenetic structure during soil freezing. All of the description mentioned above are of great significance for the understanding of pore characteristic changes during soil freezing. So far, there is little information about the pore characteristic of frozen soils under overburden pressure or atmospheric pressures. By using the porometer, we determined the porosity of frozen soils under overburden pressure and atmospheric pressures. The purpose of this paper is to present the test results.

TEST PRINCIPLE AND METHOD

The sample used in the test is Neimongolia Clay. Its grained size composition and physical properties are shown in Table 1.

The test conditions can be divided into two groups: one is pressure loaded on the sample, including atmosphere and vacuum. The sample is quickly frozen and the temperature kept constant. In other words, the influence of water migration during soil freezing is negligible. Another is pressure loaded on one end of the sample and the temperature is kept different at both ends of the soil column. i.e., the sample is frozen slightly and water migration and ice segregation occurred.

Sample preparation is as follows:

For the first group, the saturated clay ball with a diameter of 5 cm is put into a container made of stainless steel. Nitrogen is filled into the container or air extracted from the container (vacuum) and then the pressure is kept constant for about two hours. Afterwards the container with the sample is put into a low temperature circulation bath to let the sample quickly freeze for four hours. Finally, the sample is

Table 1. Physical properties of clay

Sample name	Grained size composition >0.05	0.05-0.002	<0.002	limit, %	limit, %	Gravity	Spe. Surf. area m^2/g
Clay	2.1	50.8	47.1	32.8	20.4	2.73	28

taken out of the container and air dried at zero degree centigrade and the porosity is determined at the side and the center locations, respectively. The test conditions are shown in Table 2. For the second group, the saturated clay is compacted into a soil box made of plexiglass with a size of 15 cm in diameter and 5 cm in height. The atmospheric condition is kept at the top of the sample with different values of 0, -600 mmHg and 0.2 MPa, respectively. The temperature at both ends of the sample is kept at 0 and -4 degree centigrade, respectively and the sample is frozen from the bottom upward. After 3 days of testing, the sample is taken out of the soil box and air dried and the porosity is determined.

RESULTS AND ANALYSIS

Pore Characteristic of Frozen Soil Under Constant Temperature and Pressure and Quick Freezing Conditions

From Table 2 it can be seen that there is a great change in porous volume before and after testing under non-pressure condition. The fact of the increasing of porous volume in the sample after freezing indicates swelling occurs in the sample due to phase change of water. The fact of porous volume in the center of the sample greater than that in the sides indicates that water migrates from the side to the center during sample freezing. If the temperature keeps at -30 degree centigrade, we can see that the total porous volume increases with the increase of the atmospheric pressure no matter where the sample is located and is greater in the side than in the center. But the total porous volume is the maximum and greater in the side, too, under vacuum condition. This means that the pressure gradient is the main mechanism for the change of the porous characteristic in soils. If the atmospheric pressure is kept at 8 MPa, we can see that the total porous volume of the sample increases with the decrease of temperature. It implies that frost heave is the essential mechanism for the change of porous volume. The changing regularity of the porosity under different temperature and pressure conditions is the same as that of the total porous volume. The pressure not only changes the total porous volume but also changes the composition of porous diameter. With the increase of pressure or in the vacuum condition, the number of large porous diameter is increased, but small porous diameter decreased.

Figures 1 and 2 show the distribution curves of porous diameter of samples under different temperature and pressure conditions, respectively. From Figures 1 and 2 it can be seen that the content of porous diameter greater than 0.03 μm of the sample before freezing occupies only 3%. But as a result of freezing and pressure, the content of porous diameter in the range from 0.03 μm to 10 μm is increased from 1% to 15% and that of diameter greater than 10 μm increased to about 20%. The changes of the pore characteristic under the action of the pressure mentioned above induce the recombination and re-orientation of the structural elements of soils and result in the difference of micro-cryogenetic structures of frozen soils.

Photos 1 to 6 show the micro-cryogenetic structures of frozen soils under different temperature and pressure conditions. From those photos it can be seen that when temperature is kept at -30°C and there is no pressure loaded on the sample, the quasi-layered and network cryogenetic structure is formed under the conditions of multi-direction freezing. With an increase in pressure, the range of quasi-network structure is shrunk from the side to the center of the sample and the branchy structure is

Table 2. Porous characteristic of soils frozen under constant temperature and pressure conditions

No.	Total porous volume, ml/g	Specif. surf. area, m^2/g	Porosity %	Cont. of poro. dia. <0.03, %	Place*	Temp. °C	Pressure MPa
10-1	0.2091	11.785	31.75	72	c	-30	0
10-2	0.2057	15.369		75	s		
5-1	0.1802	14.454	26.48	84	c	-30	4
5-2	0.2047	13.589	30.55	73	s		
6-1	0.2094	11.861	35.31	70	c	-30	8
6-2	0.2282	12.426	36.27	65	s		
7-1	0.2058	12.330	34.91	71	c	-10	8
7-2	0.1947	12.755	32.01	76	s		
8-1	0.1896	16.782	32.14	92	c	-5	8
8-2	0.2352	12.145	37.89		s		
15-1	0.2320	14.638	36.06	66	c	-30	11.5
15-2	0.2385	14.418	37.65	62	s		
9-1	0.2393	14.677	38.93	69	c	-30	-600 mmHg
9-2	0.3888	12.972	48.12	42	s		
12-1	0.3297	21.211	40.51	63	c	-5	-600mmHg
	0.1776	12.980	32.66	97		20	0

*where c – center; s – side.

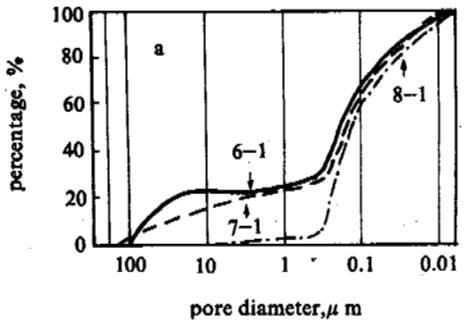

Fig.1 Pore size distribution curves under different atmospheric pressure conditions

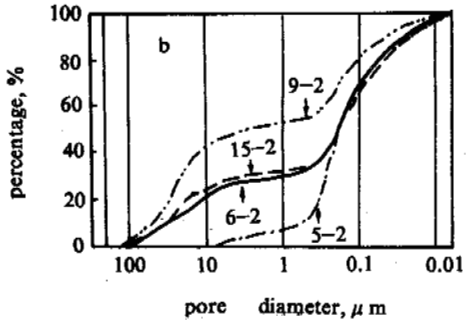

Fig.2 Pore size distribution curves under different temperature conditions

formed instead of the quasi-network. When pressure is kept at 8 MPa, the cryogenetic structure changes from the network structure to the branch gradually and the network changes from big to small and ice straps from thick to thin with the increase of freezing speed.

Photo 1 X P=0 T=-30°C

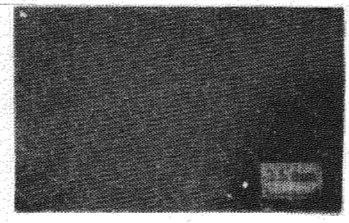

Photo 2 X P=4MPa T=-30°C

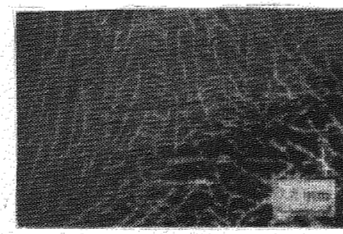

Photo 3 X P=8MPa T=-30°C

Photo 4 X P=11.5MPa T=-30°C

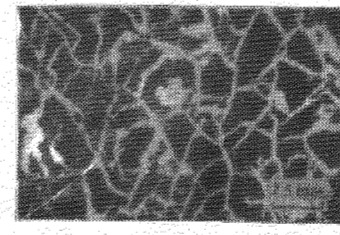

Photo 5 X P=8MPa T=-10°C

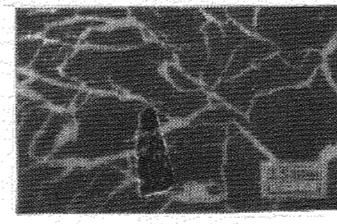

Photo 6 X P=8MPa T=-5°C

Pore Characteristic of Freezing Soil Under Temperature gradient and Constant Pressure

Table 3 shows the determined result of the pore characteristic of soils under unidirectional freezing conditions. It is shown that the pore characteristic along the soil profile is changed after testing due to water migration and ice segregation. If there is an overburden pressure, the total porous volume and the amount of porous diameter greater than 0.03 μm are increased in the ice segregated zone and decreased in the dehydrated zone after testing.

In the case of vacuum condition, the porous profile is still controlled by water migration and ice segregation. The overburden pressure can reduce the differences of total porous volume and diameter distribution of porous profile, but the vacuum environment can enlarge the differences. The cryogenetic structure is mainly in the shape of horizontal layers. When the overburden pressure exists, many vertical

Table 3. Porous characteristic of soils frozen under unidirectional pressure conditions

No.	Total porous volume, ml/g	Specif. surf. area, m^2/g	Porosity %	Cont. of poro. dia. <0.03, %	Place	Temp. °C	Pressure MPa
3-1	0.1838	14.285	29.02	90	0-1 cm	0	
3-2	0.1756	16.543	26.34	97	2-3 cm		0
3-3	0.1985	14.851	52.00	85	3-4	-4	
14-1	0.1727	13.775	27.32	95	top	0	
14-2	0.1754	14.397	29.98	97	middle		0.2
14-3	0.1779	15.566	32.12	98	bottom	-4	
1-1	0.2121	16.291	36.31	64	0-1 cm	0	
1-2	0.2076	17.181	36.95	81	1-2 cm		
1-3	0.2187	16.864	36.28	73	2-3 cm		-600mmHg
1-4	0.1940	17.141	33.70	86	3-4 cm	-4	
1-5	0.1940	15.282	35.28	90	4-5 cm		
	0.1776	12.980	32.66	97		20	0

fissures occur in the profile and the network structure is formed.

CONCLUSIONS

1. Porous characteristic of soils frozen under constant temperature and pressure conditions is controlled by the temperature and pressure. When the temperature is the same, the atmospheric pressure gradient is the main mechanism for the formation of the porous characteristic. The total porous volume increases with the increasing of atmospheric pressure. When the atmospheric pressure is the same, frost heave is the main mechanism for the formation of the porous characteristic. The total porous volume increases with the decreasing of temperature.

2. Water migration and ice segregation are the main mechanism for the formation of the porous characteristic of freezing soils. When there exists overburden pressure, the differences of the porous characteristic in freezing soils become less because of densification.

3. Under vacuum condition, the total porous volume and the amount of greater porous diameter are greater than those in the conditions with overburden pressure.

4. The cryogenetic structure of frozen soil is influenced by temperature and pressure. In the case of multidirection freezing, the network structure gradually changes to a branchy structure with the increasing of atmospheric pressure. In the case of unidirection freezing with overburden pressure, the vertical ice straps increase along the direction of the temperature gradient.

REFERENCES

Chuitoviqi, H.A., (1986) Mechanics of Frozen Soils, Translated by Zhu Yuanlin et al.

Chuvilin, E.M. and O.M. Yazulin, (1988) Frozen Soil Macro- and Microtexture Formation, Proceedings of 5th International Conference on Permafrost, 320-323.

Lebedenko, IU.P. and L.V. Shevchenko, (1988) Cryogenic deformation in fine grained soils. Proceedings of 5th International Conference on Permafrost, 396-400.

Wang Jiacheng and Liu Jimin, (1989) Physical Process and Cryogenetic Structure of Freezing Soils, Proceedings of 3rd National Conference on Frozen Ground, Press of Sciences, 78-84.

PERMAFROST CHANGE FOR ASPHALT PAVEMENT ALONG QINGHAI-XIZANG HIGHWAY

Wang Shaoling and Mi Haizhen

Lanzhou Institute of Glaciology and Geocryology,
Chinese Academy of Sciences

Due to the thermal absorption of black asphalt road surface, 60% of the man-made table of permafrost under roadbed has been decreasing. The formation of the thaw core and uncoincidently frozen ground in the vertical profile accelerates differential settlement of the roadbed and damage of road surfaces. Besides the above mentioned, either types of frozen ground tend to change, or perennially frozen ground disappears completely under some of the roadbeds.

Qinghai-Xizang highway with asphalt pavement has been used for 7 to 15 years, differental settlement appears in most of the roadbeds within the permafrost region and damage of roadbed heavily influences transportation. There are many reasons for the damage of roadbeds, in which the thaw settlement of permafrost is the most important.

The authors worked in the study area from June to August of 1991. 380 holes at the roadbed and at natural sites were drilled to contrast the permafrost changes at sites between natural and man-made conditions.

1. A CONTRACTED LENGTH OF HIGHWAY THROUGH THE PERMAFROST REGION

The investigation along the highway in the 1970's showed that the northern boundary of island permafrost was at K 2877+600 of Xidatan and the southern boundary of continuous permafrost was at K 3424, north of Anduo. From Anduo southwards to No.125 highway maintenance station, permafrost occupies 20 per cent of the length of 90 km of the highway within the island permafrost region. Exploratory data for this time demonstrated that the southern and northern boundary of permafrost have been changing indeed, especially the southern boundary of continuous permafrost which has moved northwards 16 km. Within the island permafrost south of Anduo, permafrost was only found in the roadbed at an accumulated length of 2 km. The length of highway through the permafrost region at present that has been contracted is about 18 km.

2. TYPE OF FROZEN GROUND UNDER THE ROADBED

Under natural conditions, with the exception of a few sections, frozen ground is mostly coincided in the vertical profile for both laterals of the highway within island permafrost and it all coincided within the continuous permafrost region. The holes on the roadbed from Xidatan to Anduo (K 2880 to K 3424) indicate that the type of frozen ground under roadbed is different from that under natural conditions. Frozen ground under the roadbed all discoincided within the island permafrost region, and most of them also discoincided.

2.1 Coincided Frozen Ground

The man-made table of coincided permafrost under the roadbed is 2.8 to 4.2 m deep, this depth is close to or less than that under natural conditions. Ice layer with soil or ice-rich soil occurs below the table of permafrost, it is distributed on the hills with high elevation (Table 1). Where mean annual air temperature is below -6.0°C, the depth of seasonal freezing under the roadbed exceeds or equals the depth of seasonal thawing each year. Frozen ground is coincided in addition. Coincided permafrost also appears in the low roadbed (height <50 cm). The destroyed asphalt pavement section, where asphalt pavement zero fill cut sections, and subgrades of part of culvert are coincided permafrost it is estimated that distribution length of coincided permafrost approximates to 80 km, occupying 15 percent of the roadbed within the permafrost region.

2.2 Discoincided Frozen Ground

With the exception of the above mentioned and taliks, 70 per cent of the roadbed along the highway is discoincided permafrost which is distributed generally in the high plain, intermontain basin and valley, where mean annual air temperature ranges from -4.4°C to -6.0°C. Under the roadbed the thawing depth is in excess of the freezing depth each year. The man-made table of permafrost goes downwards year by year, which induces the frozen ground in vertical profile to become discoincided. As a result, the thaw core

Table 1. Mileage and distribution section of coincided frozen ground under roadbed along Qinghai-Xizang highway

Section	Road mileage	Length (km)
Kunlun Shan	K 2893-2904	11
Kekexili Shan	K 3009-3020	11
Qusuihenan Shan	K 3035-3037	2
Fenghuo Shan	K 3064-3080	16
Kanxinlin	K 3171-3176	5
Tanggula Shan	K 3316-3348	32
Total length		77

was formed between the seasonal frozen layer and the man-made table of permafrost whose depth changes from 4.5 m to 10.1 m. The thickness of thaw core changes from 0.2 m to 6.6 m, most of them are 0.5 to 2.0 m. The development of thaw core is related to the constraction duration of the asphalt road, properties of filled soil, water content and type of permafrost under road. The section, which spends shorter constraction time, has more coarse grained soil and less water content, has a thicher thaw core.

3. CAUSES OF THE THAW CORE FORMATION AND ITS HARMFULNESS

3.1 Causes of Formation

Since the asphalt pavement has been constructed, the thermal condition under the roadbed has changed obviously due to the specific solar radiation and thermal balance conditions on the plateau and thermal absorption of the black road surface. Contrasting with the natural conditions, the difference between mean annual surface temperature on the asphalt pavement and mean annual air temperature is 6°C, which induces the frozen ground in the roadbed to thaw 20-30 days earlier and freezes 20 days later. Annual thermal input on the road surface exceeds output within the areas with a mean annual air temperature of more than -6°C. In the above area, the depths of the seasonal freezing and thawing are 4.2-4.5 m and 4.5-6.0 m, respectively; and the layer of seasonal freezing disappears completely during the period between early July to late August. The heat during August to October enters into the roadbed and is accumulated, which induces the man-made table of permafrost to go downwards, causes the frozen ground to discoincide in the vertical profile and finally makes the thaw core form.

In recent decades there has been a trend of climate warming on Qinghai-Xizang Plateau, which is advantageous to the formation of thaw core.

3.2 Harmfulness

In the forming process of thaw core differential settlement of roadbeds developed gradually and finally induces the damage of road surface. The harmfulness of thaw core to the highway is different due to differences of the type of frozen ground and the lighologic distribution.

(1) In the road section of Xidatan, because the roadbed is filled with coarse grained soil with little ice and water content although there is a thick thaw core, the total settlement and deformation are still little.

(2) Large total settlements and serious damage of road surfaces emerge in the roadbed filled with lacustrine sediment or fine grained soil with an ice layer with soil and ice-rich soil. Such as those in the basin of Kunlun Shan, in both banks of Qingshui River and on the north facing slope of Kekexili. After the thaw core in the roadbed is condensed repeatedly, the thickness of the thaw core increases slowly with the development of the man-made table of permafrost. So it is difficult for the roadbed to attain stability.

(3) The man-made table of permafrost under the roadbed is like a pan in which water is accumulated perennially. The water accumulation makes the man-made table of permafrost go downwards and the heat balance system in the roadbed become sophisticated. On the other hand this also causes a hidden problem in that an expansion mound emerges in the road surface in which water flows continually into the thaw core and pressure water forms in the thaw core. At present, most of thaw cores under road along Qinghai-Xizang highway is forming and developing, and it would spend a long time for them to be relatively steady.

4. PERMAFROST CHANGES UNDER THE ROADBED

In recent decades, degradation of permafrost within the Qinghai-Xizang Plateau is under way with world wide warming, esp. in the margin of the plateau with island permafrost. The regional degradation, the economic activity and some technical factors aggravate permafrost degradation under the roadbed. There are apparent indications that permafrost degradates and changes from quantity to quality in some sites where vegetation has been removed and with many water pits. Such as in both sides of the roadbed.

4.1 Permafrost Disappears and Talik Expands

There are various talik salong the highway. However, since the asphalt pavement was constructed, the thaw core under the roadbed has expanded step by step to form a thaw passage of a few kilometers long and which finally approaches each other. As a result, closed taliks form in some roadbeds. Comparing survey data in 1991 to what was obtained formerly shows that the extent of closed taliks under the asphalt pavement has become larger than that under the original sandy roadbed. The reasons are that thin frozen ground and high ground temperature develop in the warm permafrost area nearby taliks and in the valley basin and that the thin permafrost under the roadbed has disppeared and becomes closed talik as the asphalt pavement has been operated for years. For example, frozen ground with ice-rich content was found under the road in the west side of Yamer River (K 3104 +600 to K 311+266) in the early 1980's and at present, most of it has become talik. The frozen ground with a large rich ice content under the roadbed from the south bank of Tuotuo River to Kaxinling (K 3154+150 to K 3159+550) in the early 1980's, has also disappeared. A similar event took place in the north bank of Tuotuo River, Budong Quan and the valley of Buqu River.

Apparent changes in permafrost also occurred in both sides of Xiushui River and Beilu River.

Exploratory data for railways in the 1970's demonstrated that permafrost develops in terrace and high flood plains with the exception of the river bed on the No.1 terrace of Beilu River. The permafrost was 12.8 m thick and continuous (No.1 hydrogeological team of Qinghai Province). The changes are as follows:

In Xushui River permafrost was not found at two of the 18 m deep coreholes on the roadbed of both sides of bridge; but, permafrost of 8.1 m thick only occurs on the high flood plain.

Permafrost was also not found at two corehole of 15 m and 18 m depths on the roadbed of both sides of the bridge in Beilu River, it is 9.5 m thick in the high flood plain.

The above facts show that thin permafrost under the roadbed has thawed completely because of asphalt pavement influence on it. However, permafrost develops under natural conditions such as in high flood plains.

4.2 Types Change of Frozen Ground Under Roadbed

Under natural conditions, ground ice is distributed widely within depths of 1 to 2 m below the table of permafrost and decreases gradually with the increasing of depth. At present, the depth of most of the man-made table of permafrost under the roadbed along the highway is 1-3 m lower than that of natural ones. The table of permafrost decreases gradually to induce ground ice near the table to thaw partly or completely. By comparsion of statistics (study group of Qinghai-Xizang highway, 1983). The proportion of frozen ground with high ice content has decreased under the roadbed along the highway (Table 2). The type of frozen ground below the man-made table of permafrost appears to change in some sections of the roadbed, there is a trend that ground ice content is getting smaller, which is advantageous for roadbed stability.

Many engineerings along the highway have demonstrated that the influences of human activity and technical factors on the permafrost environment exceed the influence of climate warming, esp. the degeneration under the roadbed within warm permafrost areas which transforms from qualitative to quantitative. Many deformations are not reversible. Damage of permafrost environment in the both sides of the highway may have serious consequences. After the asphalt pavement was constructed it is inevitable that permafrost under roadbeds thaws year by year by adding to the height of roadbed within most areas where mean annual air temperature is above -6°C. In order to gain an ideal effect, general methods, such as to make alterations of the material and colour and the property of heat absorption of the roadbed, to improve on the insulation in the roadbed and the drainage in both sides of roadbed and to protect the permafrost environment, must be adopted for the renovation projects along the highway.

REFERENCES

Wang Jiachen, Wang Shaoling and Qiu Guoqing, (1979) Permafrost along the Qinghai-Xizang highway, Journal of Geography, 34(1): p.18-32.

Study Group of Qinghai-Xizang Highway, (1983) Distribution laws of frozen ground with high ice content along Qinghai-Xizang highway, Proceedings of Second National Conference on Geocryology, Gansu People's Press: 43-51.

Table 2. Type change of frozen ground with high ice content north of Tanggula Pass

Section	Kunlun Shan	High plain of Chumer He	Kekexili	Fenghuo Shan	Basin of Tuotuo He	Kanxinlin	Basin of Tongtian He	Section of the north facing slope of Tanggula Shan
Percentage amount in 1979	46.6	52.9	68.2	61.5	19.7	50.4	24.7	38.5
Percentage amount in 1991	39.7	50.8	43.7	32.3	16.5	41.8	21.5	36.7
Decreased percent	6.9	2.1	24.5	29.2	3.2	8.6	3.2	1.8

A STUDY ON PREVENTING FROST HEAVE OF THE SHAFT-TYPE ENERGY DISSIPATOR

Wang Shirong

Water Conservancy Bureau of Panjin City,
Liao Nin Province, China

In the seasonal frost ground area the breakages of traditional open-type energy dissipator by frost heave are very widespread and serious. The new shaft-type energy dissipator was adopted. The complex problem of frost damage was solved satisfactorily by means of its overall arrangement and construction (no need of special measures to prevent frost heave). The overall arrangement is quite a new type and made of shaft (including shaft dissipating force) and tunnel. The shaft and the tunnel adopt a thin-wall structure of a cross-section of circular, arch, egg-shaped or U-shaped, these shapes are advantage to equalize and to decay the force of frost heave. This type is simple, convenience, economic and safe in structure. It is a new-important way to prevent frost damage in middle and small hydraulic engineering.

INTRODUCTION

Many open-type fall-water structure (including steep gradient) of hydraulic constructure of irrigation channel were destroyed by frost damage because its foundation are not at same level, high or low, and the amount and the force of frost heave are non-uniform. One side of the open-type retaining wall was filled with soil, so it was easily toppled down and broken up by horizontal force of frost heave. The open-type energy dissipator, which was built out of traditional shaft-spillway, has same weakness of not preventing frost heave. In recently ten years, the engineers and techniciance of water conservancy project set up creatively the shaft-type energy dissipator in entrance (instead of the open-type energy dissipator out of the traditional shaft-spillway). For widely used in water conservancy project, it gains good results (Wang Shirong, 1990).

THE BASICALLY ARRANGING TYPES OF THE SHAFT-TYPE ENERGY DISSIPATOR

We research the shaft-type energy dissipators in over 200 places of Heilongjiang, Jilin, Liaonin, Shuanxi Province and Inner Mongolia Autonomous Region. There are a lot of types, but basic type was shown in Fig.1, the direction of water to be flow in entrance changes down to the shaft dissipating energy to consume energy, the horizontal tunnel is lower to form as a pool decaing force so that the bottom current consume energy. In engineering practice, the dissipating energy with shaft is main, sometimes a supplementary means is to set up barrier or baffle decaing force for dissipating water energy. The shaft-type energy dissipator is widely used in the sluice gate with falling differentia, the culvert, the emissary of small reservoir and the spillway besides.

THE STUDY ON FROST HEAVE OF THE SHAFT-TYPE ENERGY DISSIPATOR

We made investigations on the shaft-type energy dissipator to prevent frost heave in over 200 places. From 1984 to now the experimental study of the shaft-type energy dissipator was carried out in Laboratory of Heilongjiang Hydraulic Training School (especial experiments on the ratio of dissipating energy and on frost heave) and the outdoor observations were went on in experimental field (the author took part in the experiments and the outdoor investigations). A lot of scientific data was gained. The cross-section of shaft-type energy dissipator is circular, and the cross-section of the horizontal tunnal has complexly curvilineal shapes, such as circular, arch, egg-shaped and "U"-shaped (Wang Shirong, 1990). The horizontal stress, the tangential stress and the normal stress of frost were influenced by shapes of structure, therefore the concrete calculation of these stresses is complex. Because the geologic condition is not the same in different region, so it greatly influences on frost heave, therefore it is difficult to calculate the stresses and the amount of frost heave with a united-constant formula. For this reason, the calculating method was not detailed here. In engineering pratice, experiments of the shaft-type energy dissipator show that the characters of preventing frost heave are as follows:

The Overall Arrangement to be Rigorous is Convenient to Prevent Frost Heave

In comparison with traditional shaft-spillway, the open-type energy dissipator out of shaft was superseded, the combination of energy dissipation of shaft with dissipating energy of the bottom current in tunnel was taken and longitudinal length was decreased. The shaft-type fall-water structure has only a shaft with little cross-section to decay force (in Fig.1),

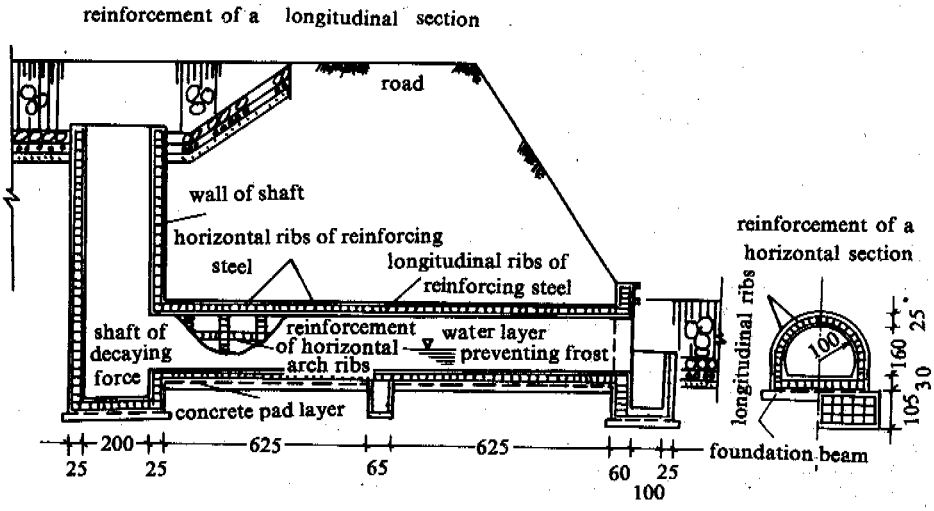

Fig.1 Liuhe fall water structure of Mulan County in Heilongjiang Province

this shaft replaces open-type multi-pools decaing force of multistage fall-water structure and thus the longitudinal length of the fall-water structure was reduced to half in comparison with the traditional multistage fall-water structure. It has many advantage, such as, the flat area is little, the parts of structure is a few, the frozen part and frozen area are little, the overall arrangement is concentrated and simple, so it is convenient to prevent frost heave (Wang Shirong, 1990).

It is Advantages to Prevent Frost Heave that the Foundations are in One Level

It is well stable and advantageous to prevent frost heave that the foundation of the entrance and the outlet of the shaft-type energy dissipator are in one level. When the foundations are in one level, the soil is uniform, the water content is the same and the amount and the stress of frost heave are uniform. It is convenient to keep temperature with water to prevent frost heave for whole foundation and to eliminate damage of normal stress from the foundation. Because the shaft and the horizontal tunnel are burried in soil, the frost depth is shallow and the stress and the amount of frost heave are little.

The Entrance of Water Adopts the Shaft to Antistress of Frost Heave

In Fig.2, the wall of shaft is circular symmetry to bear the force of frost heave, horizontal stress is equal in magnitude and is opposite in direction, the forces transmited through the circle of shaft are equilibrated. The soil around the cylinder of shaft is in state of circular stress, the hard frozen soil was compressed by himself and offsets the force of frost heave. Actually the soil around the cylinder of shaft is not frozen immediately, but one layer by one, the first layer is frozen to form frozen soil ring, it offsets the force formed by next frozen layer.

In other words, the cylindric frozen wall in every layer offsets the force of frost heave in near layer, the concrete shaft can not be directly damaged by frost heave.

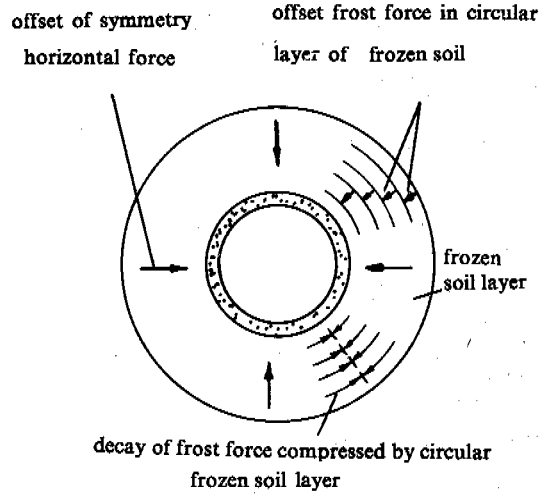

Fig.2 Schematic drawing of the equilibrium or the decay of frost force in shaft circle of shaft-type energy dissipator

The Horizontal Tunnel adopts Advantageous Structure for Offseting and Decaing Force of Frost Heave

The horizontal tunnel in the shaft-type energy dissipator adopts advantageous structure for preventing frost heave, such as cross-section of circular, arch, egg-shaped and U-shaped. Fig.3 shows the arch-shaped horizontal tunnel in the shaft-type energy dissipator. In arch action, earth of arch way is in state to bear arch-shaped stress, the arch-shaped hard frozen soil was compressed by each other and to offset force formed by frozen soil. Therefore the frost force does not directly acts the arch way. Actually the frozen depth of soil around the arch is not very thick, but arch soil is frozen layer by layer, first frozen layer formed the frozen arch wall to offset the frost force formed by next layer. The bilateral surface of arch is symmetry to bear horizontal force of frost heave, its magnitude is equal and the direction is oppsite, these forces keep in

equilibrium through arch which has good character of compressive resistance. The tangential force of frost heave in a side of arch slips along the angularly curved surface and decays. It keeps the temperature of foundation with water to prevent frost and to dispel the damage of normal force in the foundation. As the same, horizontal tunnel in the shaft-type energy dissipator has a cross-section circular shape, egg-shaped or U-shaped etc., all of shapes has above advantages to keep in equilibrium of frost force or to decay frost force.

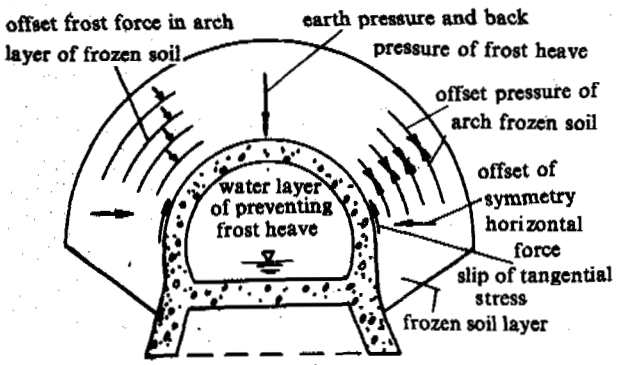

Fig.3 Schematic drawing of the equilibrium or the decay of frost force in horizontal arch of shaft-type energy dissipator

CONCLUSIONS

It makes known the advantages to prevent frost heave with the shaft-type energy dissipator through the theoretical study and the engineering application for ten years. Its overall arrangement is scientific rationality. The main part is a cylinder of shaft, and the horizontal tunnel adopts thin-wall structure of a cross-section of circular, arch, egg-shaped or U-shaped shapes. These shapes have advantages to bear force equilibrium. This structure economizes the engineering amount and its application is safe reliability for long period. The style of dissipating water energy has creative characters. The shaft to dissipate energy is main and combines with dissipating energy of barrier, baffle and the bottom current in tunnel. The vertical arrangement made up multirepeated, synthetic consumed energy, although the space of dissipating energy is little, but the effect of dissipating water energy is good. This type of the shaft-type energy dissipator has developmental future.

REFERENCES

Wang Shirong, (1990) An application of composite construction energy dissipator to small hydraulic engineering in seasonally frost regions, (Journal of Glaciology and Geocryology) Vol.12, No.1.

Wang Shirong, (1990) Analysis of preventing freezing property with shaft-type energy dissipator, (Journal of Engineering and Permafrost), 1990 No.2.

Wang Shirong, (1990) Developmental symmarization of the engineering of the fall-water structure in China, (Society of Heilongjiang Hydraulic Training School), 1990 No.4.

FIELD EXPERIMENT RESEARCH OF WATER AND HEAT TRANSFER WITHIN FREEZING AND THAWING SILT LOAM UNDER FIXED GROUNDWATER LEVELS

Wang Yi, Gao Weiyue, Zhang Lianghui

Water Resources Research Institute of Inner Mongolia, Huhhot,Inner Mongolia, 010020, China

In order to research the accumulating and declining law of water content within the active layer of frozen soil in the Hetao Irrigation Area of Inner Mongolia, the heat and water transfer experiments were carried out in the site. The results show that the frozen depth is less than the depth where the ground temperature is °C. During freezing period, the water content at the same depth changes in "S" form with a increasing time and insreases fast and slow in earlier and later periods respectively. Change curve of water content has a obvious peak value. During thawing period, the thawing speed is from slow to fast with decreasing groundwater levels. The dissipating curve of water content is shown in opposite "S" form.

INTRODUCTION

The Hetao Irrigation Area of Inner Mogolia is a seasonally frozen area. Before frozen, the groundwater level is high and the water content is large. After the soil has thawed out, sowing can not be done on time because of a large amount of water in the soil. So it is very important to research the water and heat transfer laws of frozen–thawing soil under different groundwater levels for irrigation area management and agriculture production.

A lot of research work about water and heat transfer in freezing soil has been made (Xu Xuezu, 1991),which mainly include the influences of soil texture, temperature gradient and freezing speed on water transfer, large part of the experiments were made in laboratories. There was a little information on the field experiment. Fukuda (1985), Kuntsson(1985) respectively published field observation results of frost heave under constant and unconstant groundwater levels,Gao Weiyue (1989) gave forth field observing information about groundwater inflow during freezing period.Until now we have not seen more detailed information about time and space changes of groundwater accumulation during thawing period and especially about the process of water dissipating within frozen soil layer during thawing period.

In order to investigate laws of water and heat transfer in the Hetao Irrigation Area during frozen–thawing period, the experiments of water content accumulation and dissipating during frozen–thawing period were carried out from Nov. 1991 to Apr. 1992.

EXPERIMENT METHODS

Experiment site is located in Linhe City, in the middle of Hetao Irriation Area. The experiment soil is silt loam with the following physical properties,(see Tab.1).

Welded by using 4 mm thick steel plate, the measuring buckets of 1 m^2 in opening area are installed into the natural soil under three fixed groundwater level i.e. 1.5 m, 2.0 m and 2.5 m. The soil is put into the buckets. A layer of sand filter of 30 cm thick is put under the bottom of the soil column. The top of the bucket is at the same level as the natural ground surface.

Table 1. Experiment soil physical properties

Gravity	Dry unit weight	Saturated water content	Total salt content	Grain	Size(mm)
	(g/cm^3)	(%)	(g / 100g soil)	>0.005	<0.005
2.71	1.36	30.6	0.69	89.5	10.5

In order to get homogeneous soil column samples as far as possible, the experiment soil is selected carefully and sieved to remove the impurity. After being mixed fully and calculated by using the same dry unit weight (1.36 g/cm^3) , the weighted wet soil is put into bucket in each working layer of 20 cm thick.

During freezing and thawing period, the water content of soil is measured with the neutron moisture meter. Soil temperature is measured with thermometers and phreatic water supply is also measured.

EXPERIMENT RESULTS AND ANALYSIS

Soil Freezing and Thawing

According to the observing information, the soil begin to freeze downward on November 20 each year and the maximum frozen depth is 110 cm, which happens in February of next year.

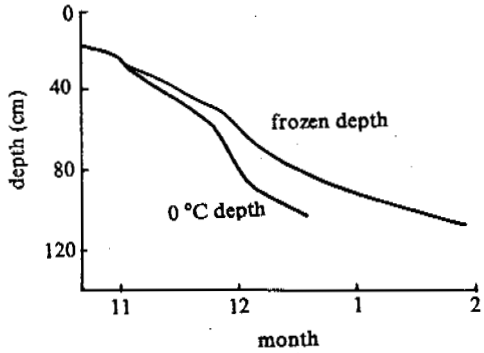

Fig.1 Frozen depth 0°C depth vs. elapsed time

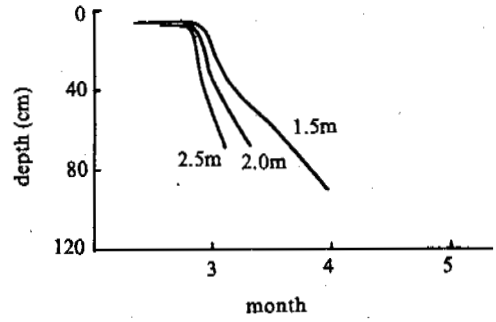

Fig.2 Thawing depth vs. elapsed time under different groundwater levels

From March 10, the frozen soil thaws downward from the ground surface and upwards from the frozen soil bottom and the thawing soil reaches together on the end of April.

Soil freezing

In Fig.1, the change curves of frozen depth with changing time and the depth where the ground temperature is o °C are drawn. At the beginning of freezing from Nov.20 to Dec. 5, the soil surface is frozen at night and thawed on day. So a thin frozen soil layer is formed within the surface temperature decreases steadily below 0°C and the frozen soil layer thickens downward. This period is called as the steady freezing period.

During freezing period, the 0°C soil depth is larger than frozen soil depth. The deeper the depth is, the larger the distance between them is. The reasons are: first, the surface energy of soil grain acts on the water of soil; second with the increase of frozen depth, the groundwater with salt flows continuously towards frozen layers and the salt content of unfrozen water will be concentrated; so the belt of more salt concentration is formed in the moist belt of frozen front. The salt in the concentrated belt moves up with the unfrozen water and at the same time moves down because of the concentration gradient. The results are, with the freezing front moving downward, there are more and more salt concentration at the frozen front and the frozen temperature becomes low and low.This is a reason that frozen depth is gradually less than soil depth at o°C. The second reason is that the soil temperature is not the same at different depth. The deeper the soil layer is, the higher the soil temperature is and the smaller the temperature change is.

Soil thawing

During thawing in spring, freezing and thawing of soil surface take place alternately on day and at night. Affected by North Mongolia and Siberia cold current, there is also intermittence freezing–thawing. A unsteady thawing layer of 20–30 cm thick is formed in the soil surface. At this time, the temperature at the bottom of the frozen layer begins rising and the temperature of the whole frozen layer is almost the same. This period is not steady. When the temperature is higher than 0°C, the frozen soil layer thaws grasually and this period is steady. Seen in Fig.2, the thawing speed is not the same at different water level. The thawing speed is slow at the high groundwater level. This shows that in high groundwater level, the water accumulation quantity within frozen layer is large and the ice crystal almost occupies whole soil pores; in low groundwater level, water accumulation quantity is less and ice crystal occupies part of soil pores. During thawing period, when groundwater is high, the thawing water within the top of soil makes heat energy go down to frozen soil, this is called the infiltrating thaw. When the groundwater is low, the thawing water affected by gravity seeps down along the pores. At the same time the thawing water releases heat to heat the low frozen soil and widen the water route.

From the above experiment data, the thawing ways are not the same at the different water levels. The way at high groundwater level is that in energy transferring and the thawing speed is slow. The way at low groundwater levels is that in energy and medium transferring and the thawing speed is fast.

Water Accumulation within Frozen Layers

As the soil is freezing, the freezing front moves down gradually. The curves of the water content within different soil layers are in "S" form. At the beginning, the water content increases fast and later the water content increases slowly and finally water content does not change (see Fig.3).

The water accumulation within the soil layer has two sources. One is the water content within frozen layers moving upwards from the bottom with higher temperature to top of layer with lower temperature. The other is the groundwater moving from unfrozen soil to frozen soil. At the beginning of the freezing, the groundwater moves from the unfrozen layer to the frozen layer. The water routes within the soil are unblocked. With the freezing time increasing, the freezing front moves downward a certain distance, at frozen layer, water routes are blocked gradually by ice crystal. The groundwater moves to frozen layer less and less. Therefore, at the beginning, the water content accumulation mainly depends on the groundwater transfer. The speed of water accumulation is fast. Later, the water content transfer mainly depends on unfrozen water within the soil. The water content rises from the low layer with high temperature to top layer with low temperature and the speed is slow. Thus the "s" shape of water accumulation within frozen soil is formed.

Fig.4 is the sections of moisture content at different time and different water levels. In Fig.4, the water content accumulation within frozen layers has obviously peak value. With pushing down,

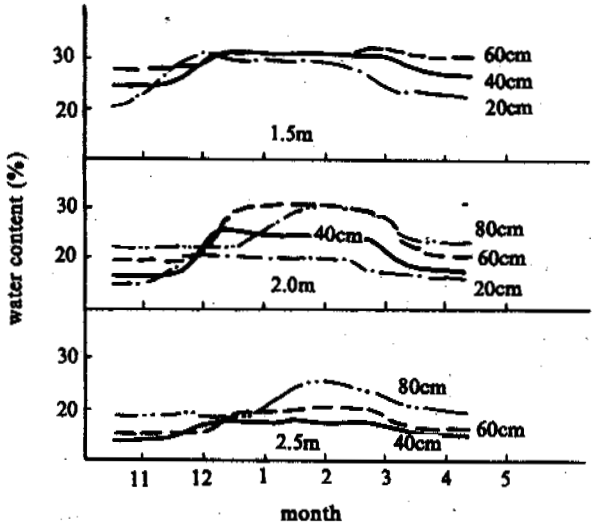

Fig.3 Water content given layers vs. elapsed time during freezing and thawing

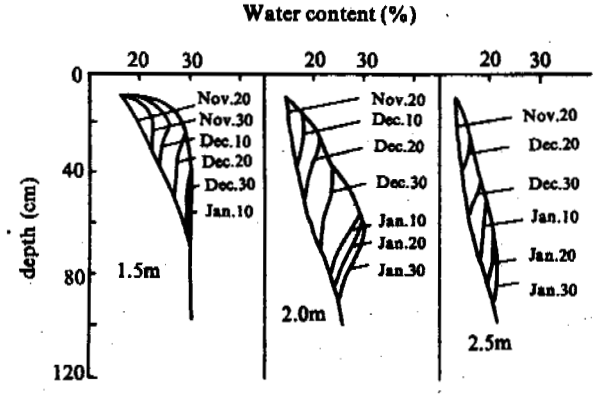

Fig.4 Water content profiles under different grounwater levels during freezing

the peak value increases and the peak value location shifts down. The peak value gets the biggest value when the frozen period ends.

The location of the biggest moisture content is not the same at different water levels. When the groundwater level is low, the location of the biggest value moves down and the value becomes small. This is the result affected by seasonal frozen depth and original moisture content.

Water Content Dissipating whthin Thawing Layer

When the daily average temperature rises above 0°C, the ground surface and the bottom of the frozen layer begin to thaw.The water content within thawing layers dissipating gradually.In Fig.3,the curve of thawing water disspating with the time at different layer are shawn in reverse "S". This can be explained as follows: The thawing water within thawing layer (layer a) transmits heat to low frozen (layer b).The result is that layer b thaws.Ice within layer b transform into water.The layer volume decreases nine percent and vacuum is formed (Wang Jiacheng, 1992). Because of the vacuum soak, surplus water content within layer a moves downward to layer b. Later, the frozen–thawing border surface shifts down.The water content dissipating within layer a depends on vaporization and gravity seepage.From above,it can be seen at the beginning of thaw, the water shifting mainly depends on vacuum soak and the speed is fast; Later, the thawing water shifting mainly depends on vaporization and gravity seepage and the speed is slow.

The moisture content sections at different water levels and date are drawn in Fig.5. As can be seen., the water content dissipating are not the same at the different water levels. When the groundwater level is 1.5 m, the water content within lower frozen soil layer does not change obviously and the groundwater level dose not rise obviously. When the groundwater level is 2.0m and 2.5m,from the thaw beginning the groundwater rises and water

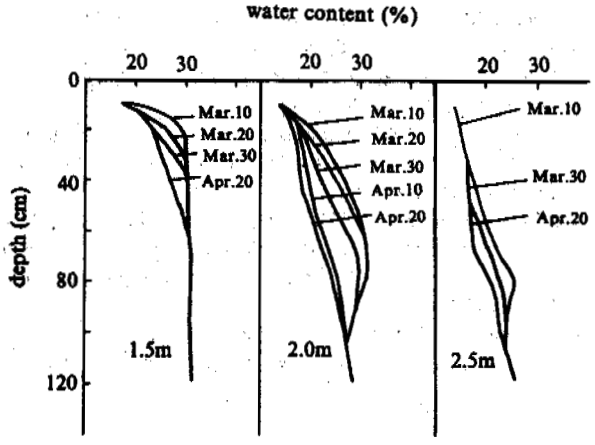

Fig.5 Water content profiles under different groundwater levels during thawing

content within lower frozen soil layer decrease. This shaws that the surplus thawing water dissipating at high groundwater level mainly depends on the vaporization. When the groundwater level is low ,the dissipating of the thawing water mainly depends on the vaporization and soak.That is ,when the groundwater level is high, the form of the thawing is in energy transmitting;when the level is low, the form of the thawing is in enenrgy and medium transmitting.

CONCLUSION

The temperature decreases along the soil depth and the salt concentration at the freezing front make the frozen depth be smaller than the depth where the soil temperature is 0°C.The deeper the layer is ,the longer two distance is.

The thawing speeds are not the same at different groundwater

levels. When the groundwater level is high, the form of the thawing is in energy transmitting and the speed is slow. When the water level is deep, the form of the thawing is in energy and medium transmitting and the speed is fast.

During freezing period, the curve of the water content within each frozen layers is in "S" shape. At the early period, the water accumulation mainly depends on outside water source and increase fast.Later it depends on inside unfrozen water and increase slow. The curve of water content along the different depths has the obvious peak value. The deeper the water level is, the bigger the peak value is and the location of the peak value shift down.

The dissipating curve of the water content within thawing layers is in reverse "S" shape. At the early period, the dissipating mainly depends on the vacuum soak and speed is fast. Later, it depends on vaporization and gravity seepage and speed is slow.

REFERENCES

Fukuda,M. and Nakagawa,S.(1985) Numerical Analysis of Frost Heaving Based on The Coupled Heat and Water Flow Model, Proc. of 4th Intern'l. Sympo.on Ground Freezing.71–75

Gao Weiyue and et al. (1989) The Observing of Groundwater Inflow during Freezing Period, Journal of Glaciology and Geocryology, Vol.14, No.2, 137.

Knutsson,S., et al. (1985) Analysis of Large Scale Laboratory and in Situ, Frost Heave Tests, Proc.of 4th Intern'l Sympo. on Groud Freezing, 65–70.

Wang Jiacheng and et al. (1992) Experimental Study on Conditions for Ice Formation of Saturated Sand in Freezing and Thawing Cycles, Journal of Glaciology and Geocryology, Vol.14, No.2.101–106.

Xu Xuezu and et al. (1991) Experiment Research of Water Transfer Within Frozen Soil, Science Publication House, Beijing.

THE EFFECTS OF GOLD MINING ON THE PERMAFROST ENVIRONMENT, WUMA MINING AREA, INNER MONGOLIA OF CHINA

Wang Yingxue & Tong Boliang

Lanzhou Institute of Glaciology & Geocryology,
Chinese Academy of Sciences, Lanzhou, China

It is found that mining is the main factor which caused the changes of the permafrost environment. After mining, the area of forest decreased, the soil layer was reversed and the fertility decreased, the ground surface and ground temperature and water content in the soil layer decreased, all of which resulted in the increase of the seasonally thaw depth, the deterioration of permafrost, the disappearance of swamp and a tendency of aridness and desertification, and finally affected the ecosystem and caused the vegetation to be in an inversion succession. We suggest that the mining and environmental administration must be considered at the same time and propose some suggestions about recovery and administration of the environment after mining.

INTRODUCTION

Wuma mining area is situated on the northwest slope of Da Hinggan Ling dominated by permafrost. Topography of the region is mainly low ridges with an altitude of about 450 m and a relative undulation of 200-400 m. The mining area is located between the Yilijiqi River valley, which is one branch of the Eerguna River, and Lajigan valley. The width of the valley is 100 m to 800 m. In the lower terraces and low-lying land there is seasonal running water and the region is heavily swampy. The mining site had been mined and the vegetation has been destroyed. Today, the site is prevalent with successional forest which are scattered in the virgin forest. The vegetation is mainly Pumila, Betula dehuricaea, Salix hypoda and Populus devidiana etc. Except for some sand dunes and bore-holes, the ground is covered by forest and herbaceous whose canopy density is 60-90%. Eriophorum vaginatum and Carex are exuberant in marsh-land. The depth of Carex layer is 0.1-0.3 m.

Because of its high latitude location and the high barometric influences of Siberia and Mongolia, the mining region is the coldest in China. From the correlation analysis of 10 years of information (1977-1988) of Eergunayouqi meteorological station and the observed information in Wuma mining area in warm seasons, the mean annual air temperature in Wuma mining area is -4.4°C, and the coldest temperature is -46.2°C. The frozen period is about seven months and the thaw index is 1829.3 (°C.d). The total radiation in warm season (May-Sept.) is only 59.7-67.4 kcal/cm^2. The annual precipitation is 400-500 mm among which 70-90% of it is from June to September. The depth of snow cover is about 20 cm.

The region belongs to a fault-block valley of Mesozoic age. Granite of the Haixi period forms the bedrock and appears on the tops of the ridges (Guo Dongxin, 1981). Quaternary desposits are widely distributed. The depth of the unconsolidated layer of Quaternary sediments is 4-9 m. The lithology of them is mainly humus soil and sandy clay. In the valley, the upper 0.9 m is black and grey humus soil and peat, the lower part is greyish-yellow sandy clay, gravel-sand and weathering layer (Fig.1).

From the information of physical prospecting in this region and the information of the adjacent regions of Gulian (Guo Dongxin, 1981) and Eluosi which have the same latitude of the

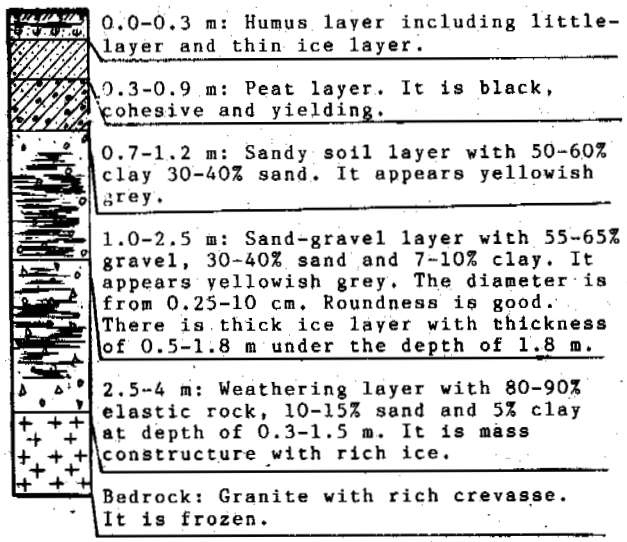

Fig.1 The Bar-graph of Lithologic Characteristics in Wuma mining Area

study area, we estimated that the depth of permafrost in this region is 50-80 m. The maximum

is about 100 m. The temperature of the depth of zero annual amplitude is -1.0 — 1.5°C. The observed temperature at a depth of 2.5 m is -3.0 and 0.8°C in swamp and non-swamp sites respectively. The seasonal thaw depth is 0.3-0.9 m and 0.5-1.0 m in the eastern footslope and swamp respectively, which is the minimum in the region, 0.8-1.0 m in the front of the diluvial fan, 1.2-2.0 m in the eastern slope and 2.5-3.5 m in the western slope. Eastern and western slopes are respectively 1.2-2.0 m and 2.5-3.5 m.

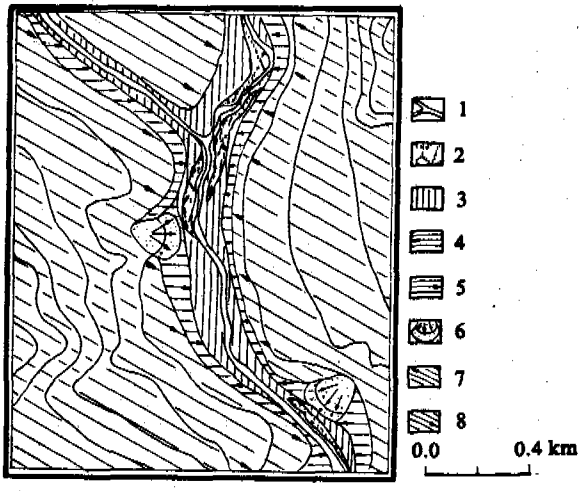

Fig.2 The Distribution of the Maximum Seasonal Thaw Depth in Wuma Mining Area, Chinese Mongolia
1 — River talik; 2 — Swamp (0.5-1.0 m);
3 — Alluvial flat (1.3-2.0 m);
4 — Western footslope (1.3-0.9 m);
5 — Eastern footslope (0.3-0.9 m);
6 — Front of diluvial fan (0.8-1.0 m);
7 — Middle part of eastern slope (2.5-3.5m);
8 — Middle part eastern slope (1.2-2.0 m).

Thick layered ground ice is well-developed in Wuma Mining area. In swamp, the thickness of ground ice is 0.3-0.5 m within the depth of 0.5-1.0 m. In same section, there is massive ground ice whose thickness is between 0.5 and 0.8 m and the length is more than 100 meters stretched along the valley of the region at the depth of 1.8 m under the first terrace of the western bank of Yilijiqi River from a mining cross section of the western side of Wuma mining area. In the ice there are thin clay layers between pure ice layers which form a layered structure. From the abandoned pits ground ice is also found which appears to be pingoes with diameters of about 2-4 m.

THE EFFECTS OF MINING ON THE PERMAFROST ENVIRONMENT

Wuma mining area is about 300 m wide and 20000 m long. Around the area there are nine other mining areas. All of them are strip-mining, mechanized mining has destroyed large amount of vegetation and the layer of soil.

The mining includes two periods of pre-stripping and mine-choosing. The pre-stripping means to strip forest, the layer of herbaceous plants, bryophyta, humus and peat before the next years' mining. In the process of layer-to-layer mining, we monitored air temperature, water content, ground and ground surface temperatures in different geographical positions in stripped and un-stripped sites. The results are as following.

(1) After trees, herbaceous and bryophta covers are stripped, a lot of water appears on the ground surface. One year after the stripping, water content in the frozen layer reduced abruptly in comparison with the un-stripped site (Fig.3). The water contents of humus and peat decreased 50% and the content of sand-loam decreased 30-40%. The main reason is that the ground accepts a large amount of radiation directly. In the stripped site, the radiation intensity increased more than 100 times in comparison with natural sites only in the moss covered site and non-moss covered site, the difference of temperature at the depth of 20 cm is 11-15°C (The Branch of Siberia Institute of Permafrost, Russian Academy of Sciences, 1988).

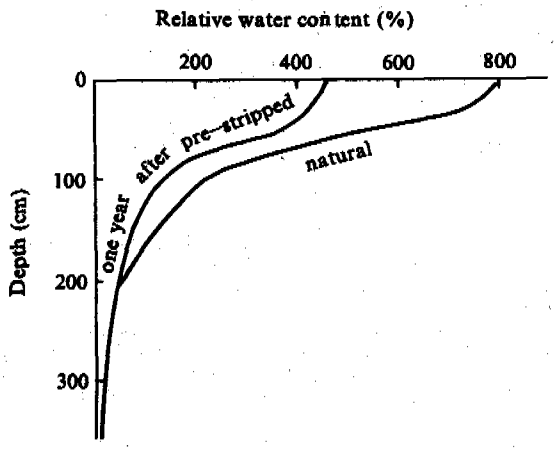

Fig.3 The comparison of water content of frozen ground in pre-stripped

From the observed information of stripped and un-stripped sites during July (one year after the stripping) and un-stripped sites in Wuma mining area to August of 1990 (Table 1), we found that one year after the stripping, the air temperature, ground surface and ground temperatures and daily ground surface temperature ranges in stripped sites have increased obviously in contrast with un-stripped sites.

It is evident that the vegetation and peat have a strong protection effect on the permafrost. When they are removed, the layer of sand-gravel is exposed and has a higher temperature, simutaneously, the water on the ground surface and in soil and the water from the thawed ground ice discharge easily, which had made soil drier and swamp disappear.

(2) Thaw depth increased after the vegetation cover was removed. The contrast observation between stripped and un-stripped sites indicates that the thaw-depth in stripped sites is 2-3 times more than un-stripped sites one year after the stripping (Fig.4). This is caused by the decrease of water content in soil and heat used for evaporation, and the disappearance of swamp.

(3) Environmental changes after mining. Before mining, the forest in mining sites must

Table 1. The contrast of temperature between stripped and un-stripped sites in 1990 (°C)

Site	Month	Daily air temp.	Daily ground surf. temp.	Daily ranges of ground surf. temp.	Ground temp. depth of 2.5 m
un-stripped	7	16.4	15.9	18.0	-3
	8	14.8	14.6	8.7	-2.4
Stripped	7	17.6	22.3	29.2	-0.8
	8	15.2	18.3	18.3	-0.6

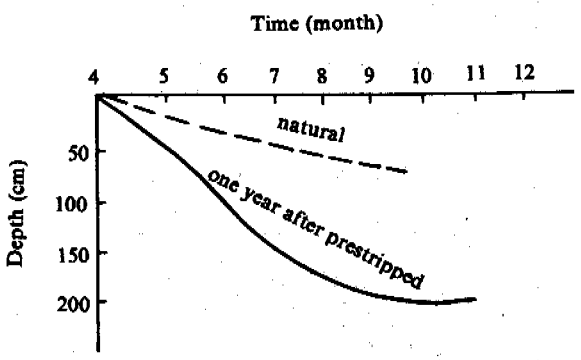

Fig.4 The comparison of thaw depth between stripped and un-stripped sites one year after the stripping in Wuma mining area

be cut or buried, but the forest around the mining sites was destroyed differently. In the main mining sites forest was destroyed completely, all of this made 80% of the forest destroyed around the river valley area.

(4) Vegetation succeeds slowly. Owing to the destruction of vegetation and soil layer, the environment has changed greatly. In some places forest has been destroyed forever or has been made to be in a reversed succession. No vegetation is in the main mining sites two years after mining. Only in both sides adjacent to the main mining sites is there green moss and some patches of grass growing there.

The gold mining history in the region can be divided into two periods, the first is from Ming and Qin Dynasty to the beginning of the 1940's. The second is from 1988 to present. There is 80 years between the two periods. From field investigation the destroyed forest in the first period has not recovered completely considering that mining in the first period was manual and ore deposit came from boreholes, the destruction of vegetation is mainly man-made. Thus, the vegetation is in the process of recovering. The pine recovery is slow, but the birch is rapid. The difference between virgin forest and successional forest is obvious. The diameter of virgin forest is 40-60 cm, but the successional forest is 10-20 cm. The area of abandoned boreholes is now mostly occupied by flats and sand dunes, only very sparse vegetation has grown there. It is evident that when the vegetation is destroyed, the recovery is very slow. It needs more than 100 years for the succession to reach its climax. But the modern mining technology destroyed vegetation severely which may be never recovered or recvoered for a very long time.

As permafrost and vegetation depend on each other in permafrost regions, the vegetation recovery is very slow in permafrost regions, which affect the steady state of permafrost. But the destruction of vegetation is one of the main factors to cause the changes of environment.

Because of severe destruction to the environment in the process of mining we must take some measures to decrease the degree of destruction. We suggest that, first, we must do our best to reduce the destruction of ground surface and natural landscape; second, rationally desposit the used ore body and reduce its cover in the natural surface; third, pre-store the organic soil layer and replace the layer after mining; fourth, plant trees on the mining sites after mining.

REFERENCES

Gu Dongxin and Wang Shaoling, (1981) Division of Permafrost Regions in Da Hinggan Ling Northeast of China (in Chinese). Journal of Glaciology and Geocryology, 3(3), p.1-9.

The Branch of Siberian Institute of Permafrost, Russian Academy of Sciences, (1988) General Geocryology, p.280-283, (in Russian).

RECENT DISCOVERY OF PERIGLACIAL PHENOMENA ON TU WEI BA SHAN (BROKEN TAIL HILL) IN ZHALAINOER,INNER MONGOLIA

Wang Zhenyi[1] and Lin Yipu[2]

[1]Department of Geology and Surveying Zhalainoer Administration of the Ministry of Power Industry of P.R.C. in China
[2]Institution of Paleontology and Paleoanthropology of Academia Sinica, Beijing,China

Since 1957,two terms —"WANG SHAN Solifeuction" and "ZHALAINOER Solifluction" were coined and their tentative age corresponding to "Riss" and "Wurm" subglacial in Europe respectly by Prof. Pei Wenchung, being discussed continually by scholars who interested in periglacial phenomena.This paper deals with a new find of solifluction showing on broken tail hill which may be comparable to that of "WANG SHAN Solifluction". Beside, damage caused by freeze are to be reported.

INTRODUCTION

Solifluction (literlly "soil flow"), a term first proposed by J. G. Andersson(1906) while studying periglacial phenomema on Bear Island, is definitely one of the most significant processes of soil movement in periglacial areas.

Zhalainoer,(N.49°20′, E.117°35′) is one of the famous periglacial areas in China. Since 1957, two terms ––WANG SHAN Solifluction and ZHALAINOER Solifluction were coined and their tentative age, the former corresponding to Riss the latter corresponding to Wurm by Prof. Pei Wenchung while studying the periglacial phenomena in Zhalainoer, Manchouli, Inner Mongolia.

The age of WANG SHAN Solifluction is one of the debateing focus among scholars who interest in studying the periglacial phenomena in Zhalainoer . The former author (Wang) discovered recently a solifluction on TU WEI BA SHAN (Broken Tail Hill),it may be comparable to that of WANG SHAN Solifluction, therefore, the authors wish to report the new find, and discuss its age.

Broken Tail Hill(Tu Wei Ba Shan in chinese) is a littee solitary promontory situating onto East–North of Zhalainoer station, being not far away from the open–pit of Ling Chuan coal mine in Zhalainoer, a well–studied locus studying WANG SHAN Solifluction and ZhALAINOER Solifluction.

A few years ago, a program of paving tube across throught that Hill was carried out, in the course of digging a series of outcrops were revealed,and some fossil bones were collected by the workes.The former author Wang, as a senior engineer, went to the spot investigating after he heard without hesitate.

GEOLOGICAL COLUMN OF BROKEN TAIL HILL

The Visible Layers seen

The visible layers from the outcrops of the sections on broken tail hill are as folliwings, from top to bottom:

1) The layer of silt–sands thickness1–2 M

There were several fossil skulls of Bos primigenius and Coelodonta antiqitatisunearthed from the lower portions of this layer.

2) The layer of involuted structures

thickness 2–3 M

Involutions (cryoturbations, Ger. Taschenboden) are major periglacial features of periglacial phenomena, they are characterized by bedding distortion and interpenetration of different layers. It may be explaned as resulting from the squeezing of moist, plastic layers between rigid parts of soil. Before 1957, both geologists and freshmen saw the involutions already, but could say no more than "I dondt known". Instead, Prof. pei came here and saw them, he was excited by reminiscenting of the involutions which he saw previously when he was studing the periglacial phenomena in French. "It seems to me that I meet an acquaintance again, certainly, he must be called Solifluction," said Prof. Pei.

3)The Layer of Gravels thickness unknown

This gravels may be the remains of sediments of ancient river.

4)The white sands–stone layer

thickness unknown

DISCUSSION OF THE SOLIFLUCTION

As visualized catographically by K.Kaiser, cryoturbations (involution) are widespread in the periglacial areas,particularly in Siberia. Zhalainoer situates in the permafrost area of eastern Mongolian Plain being in the neighbourhood of East Siberia, it is not strange that cryoturbations always occur, the question arise that what's age of WANG SHAN Solifluction? and what's the age of the new find of Solifluction on broken tail hill?are they both in

the same subglacial stage?

"Yes, They are both of Wurm subglacial stage". After studing, The authors give such answer.

The age of WANG SHAN Solifluction was to be presumptively Riss subglacial stage, it is under the circumstance without any C–14 dating; However, up to present, there are two C–14 daings particularly for WANG SHAN Solifluction:

1) 28,900 1,300 years before present (PV–172); and

2) 33,760 1,700 years before present (PV–170).

Hence, the authors answer that both WANG SHAN and TU WEI BA SHAN Solifluctions are of Wurm subglacial stage.

For years, the authors studied WANG SHAN Solifluation thoroughly, in the Upper Pleistocene geological column, from top to boffom, there are 8 datings for it, they are:

1) 3,080 ± 80 (PV–201).....540 M
2) 5,270 ± 80 (PV–167)..... > 540 M
3) 6,710 ± 200 (PV–ZK–825)..... > 540 M
4) 7,070 ± 200 (PV–166)..... > 540 M
5) 11,460 ± 230(PV–15).....535–536 M
6) 11,600 ± 130 (PV–171)
7) 28,900 ± 1,300 (PV–172).....538 M
8) 33,760 ± 1,700 (PV–170).....538 M

This is the standard section seen in the openpit of Ling Chuan coal mine. Both WANG SHAN and TU WEI BA SHAN Solifluction might be comparable to that of the Solifluction occures in the level above sea water 538 M , therefore . their ages are of 28,900 ± 1,300 years before present.

REFERENCES

Tage Nilssov (1982) , The Pleistocene Geoligy and Life in the Quaternary Ice Age. PP.45–48.

UNIAXIAL STRESS RELAXATION OF FROZEN LOESS

Wu Ziwang, Ma Wei, Chang Xiaoxiao and Sheng Zhongyan

State-Key Laboratory of Frozen Soil Engineering, Lanzhou Institute of Glaciology and Geocryology, Chinese Academy of Sciences, China

This paper analyses and discusses the relaxation law and affect factors of loess under constant strain conditions. It was found that the larger the inital stress or higher temperature was, the stronger the stress relaxation was. Its relaxation equation is:

$$\sigma(t) = A(\theta)\varepsilon_0^m(t+1)^{-\zeta}$$

Meanwhile, this paper introduces a new method of determining viscose coefficient η of frozen soil: $\eta=T_r.G$.

INTRODUCTION

Since ice and unfrozen water are present in frozen soil the frozen soils have very obvious rheological behavior. Under loading, in this type of soil there will simultaneously take place deformation (creep), stress weakness (relaxation) and strength reduction (Thritovize, 1985). The strength reduction is due to the production of the rheological process of stress relaxation in frozen soil. So the important factors affecting the strength of frozen soil are re-direction of mineral grains and ice and stress relaxation. In view of this problem, a large amount of tests were done. This paper discusses and analyzes the studied results of stress relaxation of frozen loess under an uniaxial stress state.

SAMPLES AND THEIR PREPARATION

In the Lanzhou loess sample the size was 101x 200 mm; the water content was 14-15%; the dry unit weight was 1.72-1.78 g/cm^3; the test temperatures were -2, -5, and -10°C, and its precision was 0.1°C. All of the tests were done on a MTS-810 Vibrational Tri-axial Experimental Mechine. The basic physical parameters are shown Table 1:

EXPERIMENTAL RESULTS AND ANALYSES

1. Relation of Stress-Strain

Through tests, the curves of instantaneous stress-strain were obtained under different temperatures (Fig.1). From Fig.1, we can know instantaneous strength and failure strain of frozen loess under different temperatures (Table 2).

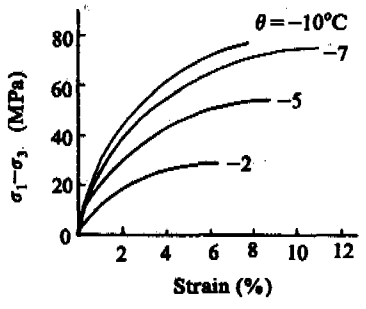

Fig.1 Stress-strain curves of frozen loess

Table 1. Physical parameters of sample

Soil name	Composition of grain size (%)				Gravity	Liquid limit (%)	Plastic limit (%)
	>0.1	0.1-0.05	0.05-0.005	<0.005			
Lanzhou loess	1.7	5.4	58.6	34.3	2.7	24.6	17.7

Table 2. Instantaneous compressive strength and failure strain*

Temperature (°C)	-2	-5	-7	-10
σ_f (MPa)	2.914	5.776	7.727	8.003
ε_f (%)	6.32	9.18	11.5	8.63

*Load rate was 12.5 MPa/min, Failure time was 1 min.

2. Relaxation Law

Through tests, we obtained the relaxation curves shown in Fig.2. From the top downwards, the constant strain of each curve is respectively 7%, 4%, and 3%. It is seen that relaxation process obviously has two stages: the strong relaxation stage and the slow relaxation stage. The first stage is the main relaxation stage, it is about 30-40% of the initial value or higher, and this process generally is completed within 1-2 hr.

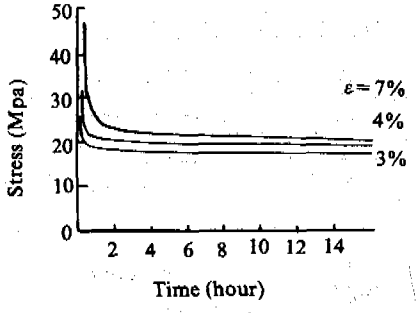

Fig.2 Relaxation curves of frozen loess (-5°C)

From Fig.2, it is seen that different constant strains are closely related to the corresponding initial stress. The initial stress increases with an increase of constant strain. With an increase of constant strain, the initial stress will be close to the instantaneous strength, and the stress relaxation will become strong. We define the relaxation degree S as:

$$S = \frac{\sigma_o - \sigma_\infty}{\sigma_f} \qquad (1)$$

Where σ_o is initial stress; σ_∞ is stable stress; σ_f is instantaneous strength. Fig.3 are the curves of S vs. initial strain ε_o. This relation can be described by eq.(2):

$$S = A\varepsilon_o^{\frac{1}{6}} + B \qquad (2)$$

Where A=2.174, B=-0.6029.

3. Effect of Temperature on Stress Relaxation of Frozen Soil

We know that the lower the temperature of frozen soil, the bigger its strength is. Our relaxation tests also reflect this phenomen on (shown in Fig.4 and Fig.5). Both initial stress and relaxation stress increase gradually with a decrease of temperature.

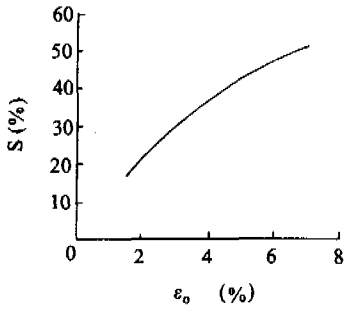

Fig.3 Change of relaxation degree vs. constant strain (-5°C)

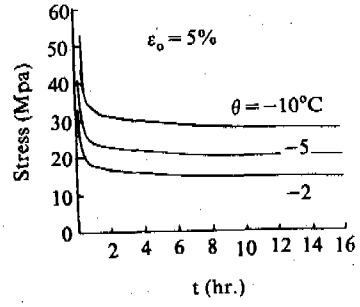

Fig.4 Under different temperatures, curves of stress relaxation of frozen loess

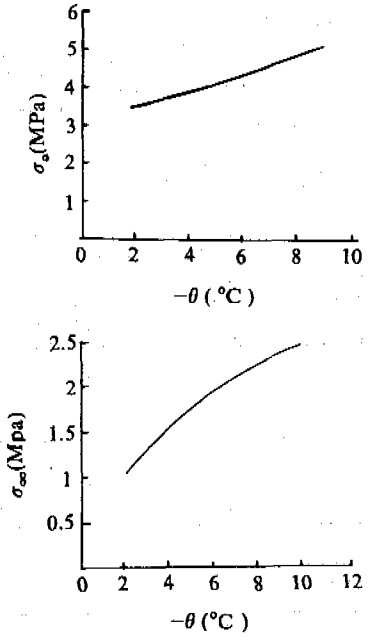

Fig.5 The relation between stress and temperature

Strength of frozen soil is affected obviously by temperature, so is the degree of stress relaxation of frozen soil (Fig.6). The relaxation degree reduces obviously with a decrease of temperature.

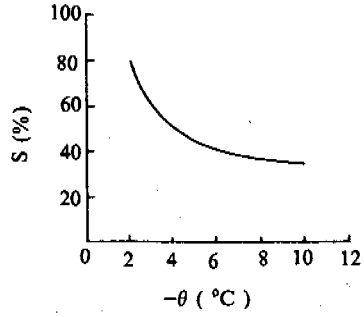

Fig.6 The relation between relaxation degree and temperature

Through synthesizing the above-mentioned problems, we may obtain the following equation of stress relaxation:

$$\sigma(t) = A(\theta)\varepsilon_o^m (t+1)^{-\zeta} \qquad (3)$$

Where $\sigma(t)$ is stress at an arbitrary time (MPa); ε_o is constant strain; t is time (hr.); θ is temperature; m and ζ are test parameters, m=0.46, ζ=0.3; $A=(B|\theta|+C)^2$, B and C are parameters, B=0.1115, C=3.473. From eq.(3), we may predict the later conditions of stress relaxation (For instance 50 years), this is shown in Table 3:

4. The Intrinsic Parameter--Relaxation Time

We know that relaxation is the redistributional results of elastic and plastic deformation. According to the viewpoint of statistical physics, the relaxation is the statistical equilibrium in the physical system, it indicates that the microcosmic value of the system state approaches gradually its own equilibrium value. Maxwell described this process by eq.(4) (Vyalov, C.C., 1987).

$$\sigma(t) = \sigma_o e^{\frac{-t}{T_r}} \qquad (4)$$

Afterwards, eq.(4) is corrected by Shividof (1890) (Vyalov, C.C., 1987):

$$\sigma(t) = \sigma_\infty + [\sigma_o - \sigma_\infty] e^{\frac{-t}{T_r}} \qquad (5)$$

Where relaxation time is one of important rheological parameters, from eq.(4), when $t=T_r$, $\sigma(t)=\sigma_o/e$, namely, when time t comes up to relaxation time T_r, stress will attenuate to 1/e of initial stress σ_o. In accordance to its physical essence, the relaxation time accords with the so-called molecular settlement time of the instantaneous equilibrium principle. In other words, the relaxation time T_r determines the "activity" of materials. The smaller T_r value, the more materials approach a liquid state to a greater extent; Conversely, the greater T_r value, the more materials approach a solid state.

From eq.(5), we may obtain:

$$\dot{\sigma}(t)|_{t=o} = -\frac{\sigma_o - \sigma_\infty}{T_r} \qquad (6)$$

So, through Fig.7, we may determined T_r value of our tests.

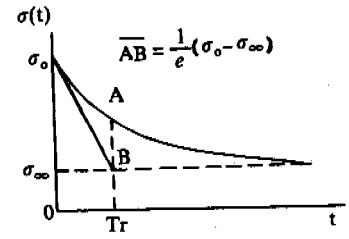

Fig.7 Schematic drawing of relaxation curve

From Fig.3, it is seen that T_r increases gradually with the decrease of temperature, in other words, the bigger T_r the smaller strength of relaxation (shown in Fig.8). So, the relaxation time can also reflect the stable degree of frozen soil to a certain extent.

We know that frozen soil is a rheologic body, the viscosity factor η is one of factors evaluated in the rheologic body, but it is difficult to obtain parameter η. The relaxation time provides a very good condition for us to determine η. Since $T_r=\eta/G$, once we obtain shearing modulus G through tests, it is easy to obtain $\eta=T_rG$.

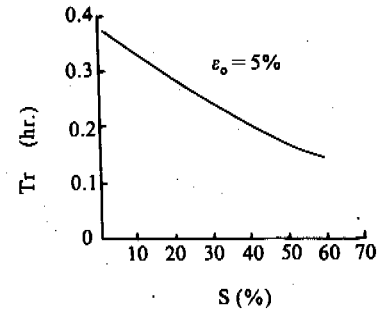

.Fig.8 The relation between relaxation time and relaxation degree

Table 3. The conditions of stress relaxation at 50 years

θ(°C)	-2			-5			-10		
ε_o(%)	2	4	6	2	4	6	2	4	6
σ_{50}(MPa)	0.04406	0.06335	0.07634	0.05477	0.07534	0.09079	0.07097	0.09762	0.11764

CONCLUSIONS

1) Under the same condition, the bigger the constant strain or the higher the temperature, the stronger the stress relaxation of frozen soil.

2) The relaxation law of frozen loess can be described by the following equation:

$$\sigma(t) = A(\theta)\varepsilon_0^m(t + 1)^{-\zeta}$$

3) Once we know the shearing modulus of frozen soil, it is easy to obtain its viscosity factor from relaxation tests..

REFERENCES

Thritovize, H.A., (1985) Mechanics of frozen soil, Publishing House of Sciences, pp.127-135.

Vyalov, C.C., (1987) The rheologic principle of soil mechanics, Publishing House of Sciences, pp.130-137.

APPLICATIONS OF DATA BASE TECHNOLOGY IN FROZEN SOIL RESEARCH

Xia Zhiying

Lanzhou Institute of Glaciology and Geocryology,
Chinese Academy of Sciences, Lanzhou 730000,China

The paper analyzes in detail the features of the permafrost data, states the methodes of how to process them, and classifies the data into several types. Furthermore, the data was handled according to the theory of standardization and theory of a relational data base, and developed a data base system suitable for the characters of permafrost data and practical application. The system is mainly composed of the following three parts. The first is information acquisition and systematic design of the data base system, the second is retrieval of data, the third is output of information and its technical utilities. Tests show that the system is very effective for registering, management and technical manipulation. Therefore it possesses important practical values.

1. INTRODUCTION

Data base technology which concerns data sharing is an important branch of computer sciences and is the core of information systems, its application has expanded in geoscience research in recent years in 1983, a conference on geographic information systems was held by the geoscience department of the Chinese Academy of Sciences and the developing centre of geographic information systems was established soon afterwards. In 1988, the glaciology and geocryology data base centre (WDC-D) was set up in China by the organization of World data Base Centre (WDC) and the works of data standardization and system development were gradually carried out. Based on the research done by the author in recent years on data arrangement, evaluation and standardizing, especially for the data or materials collected along the Qinghai-Xizang highway, the author provides a method for establishing the data base application system of permafrost environment and forecast of Qinghai-Xizang Plateau. This paper discusses some problems related to establishing a frozen soil data base, and it is possible for the data base to cover gradually all the permafrost regions in China. The model development methods (Pan Jinping, 1985) and principles are adopted in the system development according to different software developing periods to establish an information system of permafrost environments and forecast with completed functions and perfect properties.

2. THE RESEARCH CONTENTS OF GEOCRYOLOGY AND ITS PRESENT DATA MANAGEMENT

The requirement analysis for any software before developed is of important meaning, so it is necessary to discuss the research contents, data types and the applicable management of data and so on.

Geocryology is both an independent discipline and an inter-discipline science. It studies the cryosphere, its spacial and temporal development, its relationship with the lithosphere, hydrosphere and human economic activities etc.

Geocryology emphasizes the freeze-thaw processes of soil or rock, including (1) The thermodynamic condition in the freeze-thaw processes; (2) The physical and physiochemistry processes occurring in freezing and thawing soil; (3) The frozen soil and its components, its structure, its state and properties; (4) The geographical phonemena and processes of frozen soil and their determining conditions.

From the development viewpoint, geocryology stresses several points. The first is the synthesis research which is based on amounts of reliable information. The second is the transition from qualitative to quantitative analysis. The third is the transition from static description to dynamic forecast, etc. All the above features ask for scientific data management and treatment which in turn are needed to rule out the data collecting regularity to determine the collecting range, quantity, accuracy, time periods and means, to establish a unified data management system-the data base system, to increase the data utilization ratio and decrease the unnecessary repetition in investigational work and to find a suitable mathematical tool for quantitating the qualitative information and for transforming them into numerical, comparable, and measureable values (Cheng Guodong, 1988).

The data in permafrost research covers a wide range and is the foundation for the establishment of a data base system. But the data administration work has been in a manual period for a long time and the data is so dispersed, non unifiedly formulated and nonstandardizing that establishment of permafrost data base has to be in our agenda. The more important thing is that no relationship has been founded among the data. The data base system is designed to

solve this problem of backwardly data management by adopting the data base administration techniques. Then the data can be recorded, and stored in a normalized manner and data-sharing can be realized.

3. THE INCLUDED DATA

The data of frozen soil can be classified into the following types:

3.1. The Permafrost Environment and Forecast

1. The classification of frozen soil: Permafrost (predominantly continuous permafrost and isolated permafrost), taliks, seasonal frozen ground, instantaneous frozen ground, little ice, saturated ice and rich ice frost soil.
2. The permafrost distribution: Da-Xiao Hinggan Ling, Qinghai-Xizang Plateau, Qilian Mts. Altay Mts., Hengduan Mts., Himalaya Mts., latitudinal zonality, vertical zonality, the depth of the upper and base table of the permafrost, permafrost thickness, the depth of seasonally frozen ground, the depth of seasonal thawing, the area of permafrost and seasonally frozen ground, the maps of permafrost, engineerign geology and profiles etc.
3. Observation and experimental data: The mean annual ground temperature, the distribution characteristics of temperature, the ground temperature and its gradient, meteorological materials, the melting areas under buildings, the temperature and deformation under hydrological engineerings water content, unit weight, plastic yield point and flowing point, grain-size analysis, thermophysical coefficients (soil specific heat, thermal conductivity, thermal diffusivity, unfrozen water content etc.), permafrost hydrophysical properties (hydraulie conductivity, coefficients of soil infiltration, etc.), the mechanical properties (compressed strength, shear strength, soil bearing capacity, the thaw setterment coefficient, frost heaving forces etc.).
4. Drill-hole materials: profile, legend, lithological properties, frozen structure, volumetric ice content, boundary of frost soil types, geological boundary, fault, geological age, etc.
5. Periglacial phonemena: Pingo, ice core, frost heaving mounds, solifluction, thermokarst slumpings and settlements, thermokarst lakes, block fields, etc.
6. Hydrology and geology features: The ground water level, ground water temperature, water chemical properties, etc.

3.2. The Physical, Chemical and Mechanical Properties of Permafrost

1. The physical properties of frozen soil;
2. The chemical properties of frozen soil;
3. The thermology properties of frozen soil;
4. The heat-mass transformation in frost-thaw processes;
5. The frost soil strength and deformation properties;
6. Frost heaving and frost heaving forces;
7. The compressed properties in thawing process.

3.3. Engineering Geocryology

1. The engineering geology condition of permafrost;
2. The temperature field of frozen foundations;
3. Simulated engineering tests of frozen ground;
4. Road construction;
5. Irrigation works;
6. Energy resource engineering;
7. Industry and civil buildings;
8. Underground engineering;
9. Agriculture engineering;
10. The protection principles and measures for frost disaster.

4. THE GUIDING IDEOLOGY IN THE SYSTEM DESIGN

The frozen ground data base system is the sub-system of glaciology and geocryology data centre mainly used in data gathering, storing and managing for providing data service for frozen ground research, engineering construction, agriculture and forestry production. It also provides a data exchange either internationally or internally. The system design does not pay much attention to its common utilizations but stresses the integroty, security and reliability so as to satisfy the needs of frozen ground research or related departments. The normalized relational record adopted in the system can decreases the data redundancy, keep the unanimity of data, improve the storage quality and guarantee the inquiry velocity of the system (Yao Qingda, 1987). The foxbase plus relationship data base administration system is used in software compiling and it can deal with all the materials in Chinese and foreign languages simultaneously because of its Chinese character treatment function.

5. THE FUNCTIONS OF THE SYSTEM

5.1. Input and Storage Functions

The collected data and written materials of various types, will be recorded stored into the computer system in a normalized relationship by the necessary formulating and stardardilizing (C.J. Data 1983). Now there are two input means: one is the manual method for manual observation data, the other is the automatic input means for automatic collecting data. It is realized by controlling and transforming programmes with a middle link consisting of a PC-1500 computer and a Rs232C data transmitting connected hardware.

5.2. Inquiry Function

The search or inquiry of data files, data records and data types can be divided into a main search and sub-search. For increasing the inquiry velocity, the system set up the orderde files of different maincodes and makes the speed of high frequency inquiry increase. The corresponding application programmes are programmed by a controlling language and inquiry language of the data base system.

5.3. Data Maintenance Function

That is the process of adding new data records, deleting useless data files or data records and changing the logic records or a certain item of the data.

5.4. The Statistical Function of Data

It is the information statistics according to different practical needs. Such as: the mean temperatures in a fortnight, month and year, the materials of different drill-holes meterological and experimental data, etc. The corresponding report forms can be outputed.

5.5. The Functions of Numerical Calculation and

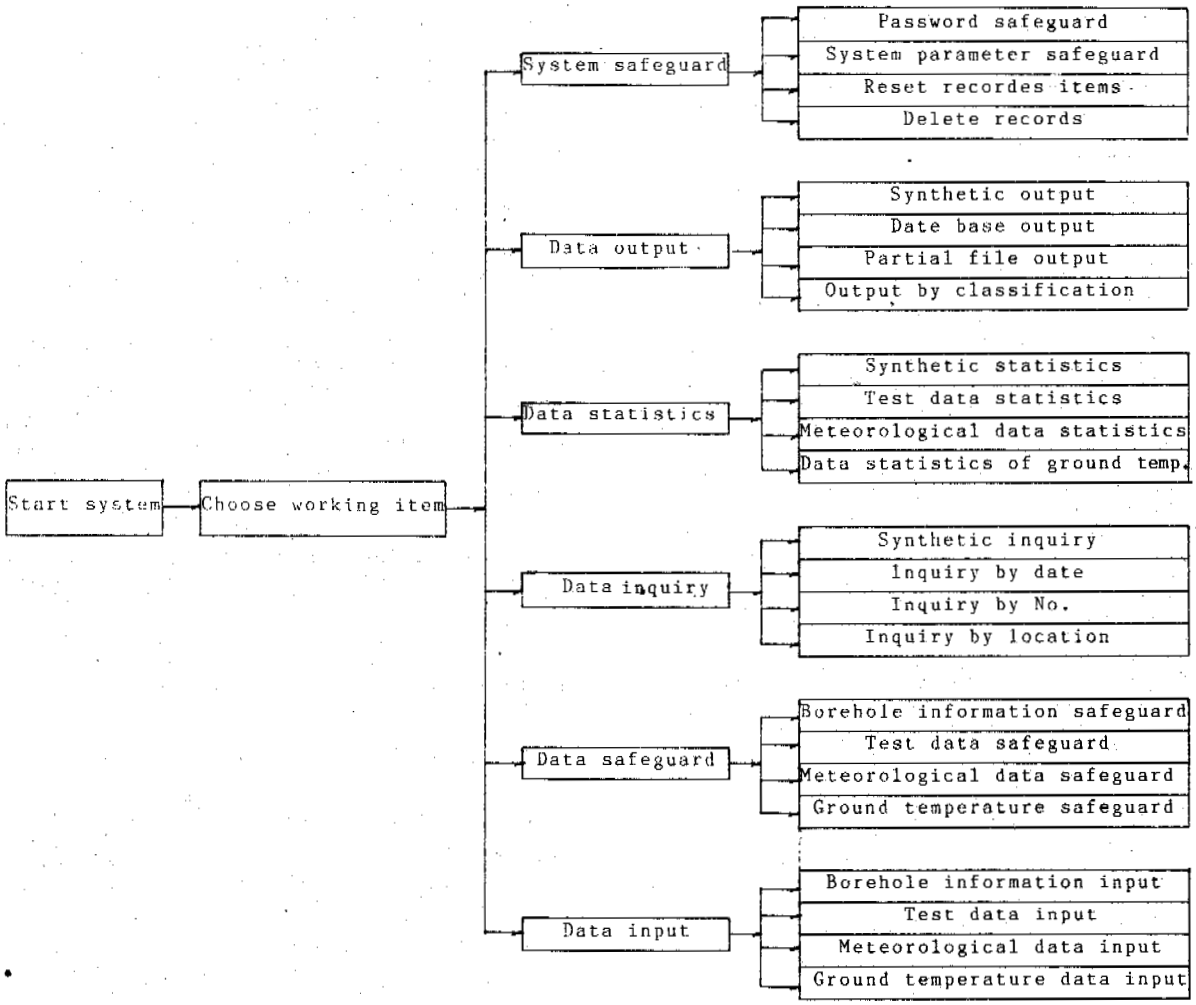

Fig.1 System appearance

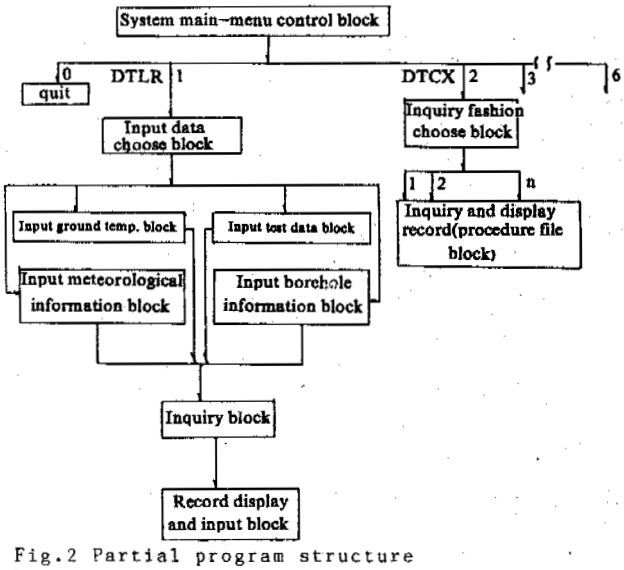

Fig.2 Partial program structure

Graphing

It is the function of choosing data based on different application models to calculate, for example, the numerical calculation of natural and man-made upper table of the permafrost and the temperature gradient, etc. Simple figures can be drawn.

5.6. Providing Various Data Services

The system provides operating instructions and other services like inquiry, coping, data unloading, etc.

5.7. The Measures of System Maintenance and Security

The system has security characters of different security classifications to guarantee each user operates the data base system within the limits of authority. When necessary, it can reset recorded items so as to protect the security, independence, reliability and integrity of the system.

6. THE OUTLINE OF THE SYSTEM AND ITS PROGRAM STRUCTURE

The outline of the system is the operation flow diagram appearing in the system design and data exchanging (see Fig.1). It is the foundation of the program design and the guide of operation. A part of the structure of the systems program is presented in Fig.2. The structural program design method used in programming and program design can be seen from it. It is unnecessary to divide the module in detail for this can make the system dispatch too frequently and decrease the operating speed of the system under foxbase. When the controlling flow logic is clear, less modules are divided, when complex, more modules are divided. In that way, the maintenance and operating speed of the system are both considered at the same time (Sa Shixuan, Wang Shan, 1983).

7. CONCLUSIONS

Based on detailed analysis of the various data of frozen ground, this paper concentrates on the establishment of the frozen ground data base system, which is suitable for frozen ground research, engineering construction in permafrost regions and the data exchange either internationally or internally. It also presents the basic function and system constitution the system can realize. The following problems are discussed or solved:

1. The system design based on microcomputer hardware;
2. Realized normalized storage and management of data;
3. Realized data-sharing and eliminating the phenomena of personal occupied materials;
4. Avoiding the data loss caused by manual data management;
5. Providing reliable, integrated data or material about frozen ground for the World Data Centre (WDC);
6. It is convenient for the user because the data statistic, analysis, calculation and the outputing of results and simple figures are all realized on computer;
7. The data compilation and changing can be carried out at any time.

It should be pointed out that this system is non a perfected application system especially in the normalized data research for there is no unified formulation and normalized principle.

Applied in the frozen ground data base system domestically or from abroad, the author can only carry out the basic system development work based on the various materials gathered mainly along Qinghai-Xizang highway. It needs great improvement and recommendations and suggestions are welcome. We'll benefit from them by being able to establish a more perfected information system of permafrost environment and forecasting.

REFERENCES

Cheng Guodong (1988) A review and prospect for the regional permafrost researches in China. Journal of Glaciology and Geocryology, Vol.10, No.3.

C.J. Data (1986) An introduction to base systems, Vol.I, II.

Pan Jinping (1985) Software Development Technique, Shanghai Science Publisher.

Sa Shixuan, Wang Shan (1983) Concept on Data Base System, High Education Publisher.

Yao Qingda (1987) Data Base and Application, Science Publisher.

FROST HEAVE PROPERTIES OF NONSATURATED COMPACTED COHESIVE SOIL AND ITS APPLICATION IN WINTER CONSTRUCTION OF CORE DAMS

Xie Yingqi and Wang Jianguo

Heilongjiang Hydraulic Research Institute

The authors introduce the frost heave regularity of nonsaturated compacted cohesive soil and evaluate quantitatively the influence of the saturated degree and density on the frost heave. Meanwhile, we have an idea that the compacted soil with the low saturated degree and high density could be used to make the impervious barrier which would be safe in the winter without insulation in seasonal frozen regions. The practical engineering method is given, and in addition, the formula of estimating the needed time of melting the frozen layer thoroughly will be mentioned in the method of thermal equilibrium.

INTRODUCTION

In order to solve engineering problems in the seasonal frozen regions, we regard the impervious barrier of cohesive soil which is built to last the winter under freezing without insulation, allow no external water recharge, pass a freezing and melting cycle and meeting the physical and mechanical index that is the penetration coefficient, compressibility coefficient and shearing coefficient, etc. So we studied the unrestrained frost heave regularity of nonsaturated compacted cohesive soil under a confined system, with one directional freezing, no additional load, as well as the changing situation of soil permeability (Paggy, 1980) and shearing strength after one freeze-thaw cycle.

THE TEST CONDITIONS AND METHODS

The unidirectional frost heave instrument was operated in the low temperature laboratory.

The sample tube is 130 mm in inner diameter at the top, 120 mm at the bottom in 1/20, internal wall taper 200 mm in height.

The sample's temperature along the depth each 30 mm was measured by one or two thermocouples which were made from copper.

The freezing temperature at the top was -20°C, and at the bottom it was +2°C. The melting temperature at the top was +15°C — +20°C, and at the bottom was +6°C — +10°C.

The amount of heave was determined by dial gauge or LVDT-10 displacement gauge.

Four kinds of soil were used in the test. The analysis results are listed in Table 1.

The samples were prepared by a compactive method and were 170 mm in height, 150 mm in controlled frozen depth, and 20 mm in the base of the warm soil layer.

EXPERIMENTAL RESULTS AND DISCUSSIONS

Some of the measured parameters in Table 2 clearly show that the amount of frost heave increases with the decrease of dry unit weight.

Fig.1, Fig.2 and Fig.3 show the curves of the frost heave amount (Δh), frozen depth (H_m) vs. elapsed time. Based on these figures, we can see: When the degree of saturation is constant, the amount of frost heave will reduce with the enlargement of dry unit weight. From Fig.4, the Δh-W curve with parameter ρ_d, we can see that when the water content (W) is constant, the amount of frost heave will increase with the enlargement of the dry unit weight. So the contradictions between the amounts of frost heave reduction with the enlargement of dry unit weight and frost heave increasing with the enlargement of the soil skeleton differences of density in some references (Orouf, 1980) reflected the practical conditions respectively.

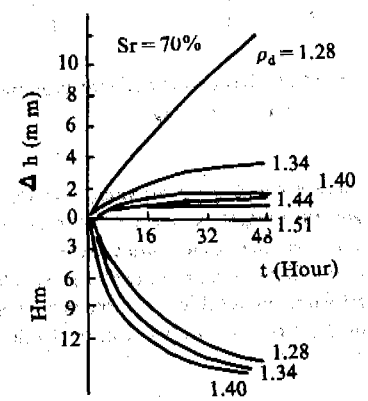

Fig.1 The test result of Δh-H_m-t when S_r equals to 70%

General soil mechanics mentioned:

$$W = \frac{S_r(G\rho_s - \rho_d)}{G\rho_d} \quad (1)$$

Table 1. The analysing results of soil for the test

Samples collecting site	Percentage of following size (mm) by weight (%)			W_P %	W_L %	I_P	Specific gravity g/cm³	Classification
	>0.05	0.05-0.005	<0.005					
Wanjia, Harbin, Heilongjiang Province	16.4	64.0	20.0	21.5	34.6	13.1	2.69	CI
Geibahe, Wuchang County, Heilongjiang Province	16.0	63.0	21.0	23.0	35.0	12.0	2.66	CI
Linxong County Heilongjiang Province	11.0	50.0	39.0	23.5	43.4	19.9	2.71	CI
Charseng Reservior Jilin Province	27.0	42.0	31.0	21.7	38.8	17.1	2.71	CI

Table 2. The results of test data

Test Item Results Number	Saturation S_r(%)	Water content W (%)	Dry unit weight (g/cm³)		The maximum frost heave amount (mm)	Frost heave ratio (%)	Note
F—IV—1	70	17.8	1.89	1.60	-0.27	-0.2	
2	70	20.2	1.83	1.52	0.71	0.5	
3	70	22.7	1.77	1.44	1.20	0.8	
4	70	24.1	1.74	1.40	1.55	1.0	
5	70	26.3	1.69	1.34	3.53	2.4	
6	70	28.6	1.65	1.28	12.23	8.9	
F—III—1	80	17.8	1.97	1.63	1.12	0.7	
2	80	20.2	1.92	1.60	0.95	0.6	
3	80	22.7	1.87	1.52	2.17	1.4	
4	80	24.1	1.85	1.49	6.07	4.0	
5	80	26.3	1.81	1.43	9.98	6.7	
6	80	28.6	1.76	1.37	14.28	9.5	
F —V—1	90	17.8	2.06	1.75	0.58	0.4	
2	90	20.2	2.02	1.68	1.20	0.8	
3	90	22.7	1.96	1.60	3.44	2.3	
4	90	24.1	1.94	1.56	8.40	5.6	
5	90	26.3	1.90	1.50	9.08	6.1	
6	90	28.6	1.87	1.45	13.96	9.3	

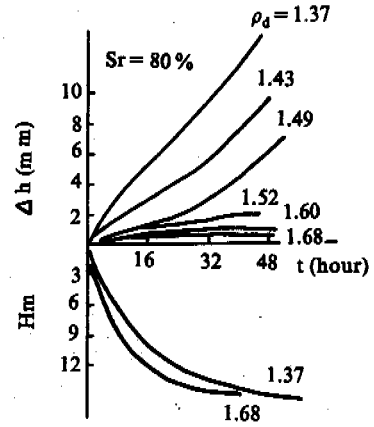

Fig.2 The test result of Δh-H_m-t when S_r equals to 80%

In equation (1), the enlargement of ρ_d will result in the reduction of W when S_r is a constant. Under the circumstances that other conditions weren't changable, the absorbed water content of soil was relative to the surface energy of particles.

The reduction of water content means the reduction of migrated water content which provided for the phase change and ice gathering and produced heave. From the macroscopic scale, the amount of frost heave will decrease with the enlargement of ρ_d. Generally speaking, the amount of frost heave would increase with the rising of ρ_d and the frost heave property of soil was directly relative to the degree of saturation in soil.

On the other hand, the property of the compacted warm soil can be known as: When the work of compaction was a constants, the dry unit weight was the function of water content (see Fig.5). On the contrary, when the work of compaction was not constant, a different dry unit weight could

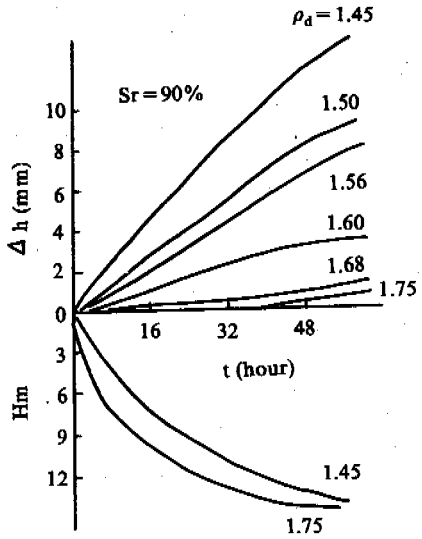

Fig.3 The test result of Δh-H_m-t when S_r equals to 90%

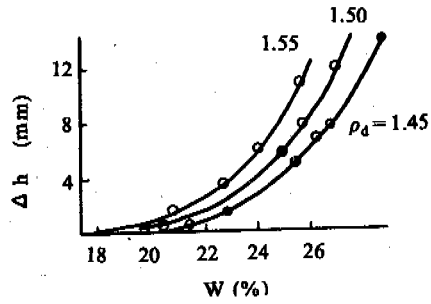

Fig.4 The curves of ρ_d-Δh-W function

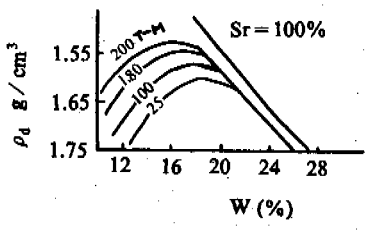

Fig.5 The curves of compacted warm soil

be obtained in the same water content or a different water content could be obtained in the same dry unit weight. So we consider: it is very necessary to apply the degree of saturation related to the dry unit weight and water content as the controlled index in the discussion on the frost heave properties of nonsaturated compacted soil.

According to Fig.1, 2, and 3, we can see: that the dry unit weight effected differently the degree of the amount of frost heave. If their density values which acted obviously on the frost heave ability under the different degrees of saturation were shown in a mathematical equation, it would be:

$$\rho_{di} = S_r + 0.7 \qquad (2)$$

where, ρ_{di} – the density value which acted obviously on the frost heave ability, unit: g/cm;
S_r – the degree of saturation which was listed in decimals.

Fig.6 was the curve of the frost heave ratio with dry unit weight with a parameter ρ_d. They are a group of approximate logarithmic curves which met at the point of the horizontal axis S_r=70%. According to the suggestion of some data that non-frost heave soil was $\eta \leq 1\%$, the critical dry unit weight value of the frost and non-heave soil was:

S_r=70% ρ_d<1.45
S_r=80% ρ_d<1.55
S_r=90% ρ_d<1.65

or

$$\rho_d' = S_r + 0.75 \qquad (3)$$

where, ρ_d' – the critical dry unit weight value of the frost and non-heave soil, unit: g/cm³;
S_r – the degree of saturation which was listed in decimals.

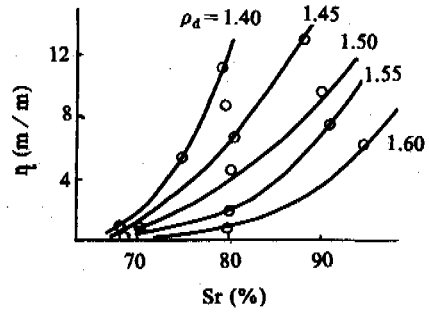

Fig.6 The curves of ρ_d-η-S_r function

Compared with the series of curves i.e. Δh-H_m-t, we can know that when the degree of saturation was one of the constants, the frost depth increased quickly with the enlargement of ρ_d. When ρ_d was one of the constants, the frost depth increased slowly with the enlargement of S_r.

Table 3 and Table 4 were the permeability and shearing strength of warm soil and the soil after a freezing melting cycle. We know that after the nonsaturated compacted cohesive soil passed a freezing-melting cycle, its permeability increased the semi-quantity scale, but its cohesion and angle of internal friction didn't change obviously.

In order to make the layer of frozen ground melt completely in the following year when the temperature is warmer and rebuilding begins, the needed melting time should be evaluated.

In Fig.7, H_m was the total frozen depth in the cold season and H_t was the new filled warm soil depth after the rise in temperature. Based on practical engineering demands, the following

Table 3. The permeability and shearing strength of warm soil

ρ_d (g/cm³)	K (cm/sec)	Shearing strength C (kg/cm²)	Shearing strength φ (°)	Note
1.75		1.86	32.5	non-permeability
1.70	5.9×10^{-7}	0.90	16.5	in test
1.65	3.5×10^{-7}	0.89	13.0	
1.60	2.8×10^{-7}	0.79	7.5	
1.55		0.74	4.0	

Table 4. The permeability and shearing strength of frost boil soil

ρ_d (g/cm³)	K (cm/sec)	Shearing strength C (kg/cm²)	Shearing strength φ (°)	Note
1.75	8.7×10^{-6}	1.65	22.0	
1.70	6.5×10^{-6}	1.31	14.5	
1.65	5.5×10^{-6}	1.07	13.5	
1.60	5.4×10^{-6}	0.83	8.5	
1.55	4.7×10^{-6}	0.60	5.5	

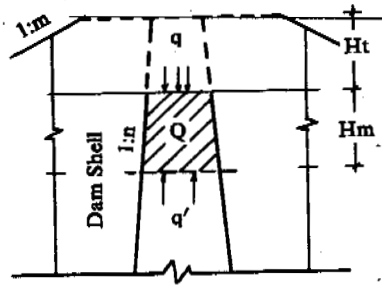

Fig.7 The ideograph of calculating the shawing time in frozen layer

simple evaluation method is suggested.

If the cold quantity inside the frozen layer height H in one unit area was Q, the quantity of heat inside the frozen layer transferred through the new filled warm layer in one unit time and area was q, the quantity of underground thermal heat in one unit time and area was q' and the time needed in melting all the frozen layer was τ, the thermal equilibrium equation is:

$$Q = (q + q')\tau \tag{4}$$

Because the melted layer depth produced by underground thermal heat in the seasonal frozen ground made up about one-tenth, so we could continue to assume: q'=0.1Q. The equation 4 could be simplified as:

$$0.9Q = q\tau \tag{5}$$

and

$$Q=H_M(C_v|t_{cp}^-|+L\cdot\rho_d\cdot W\cdot i) \tag{6}$$

where, C_v — the volume specific heat of frozen ground;
t_{cp}^- — the coverage minus temperature of frozen ground;
L — the latent heat of water phase;
ρ_d — dry unit weight of frozen layer;
W — water content of frozen layer;
i — relative ice content.

$$q = \frac{\lambda\cdot t_{cp}^+}{\frac{H_t}{2}} \tag{7}$$

where, λ — heat transfer coefficient;
t_{cp}^+ — average air temperature during melting.

After Equations (6) and (7) were put into Equation (5) the time needed to melt the frozen layer is as follows:

$$\tau = \frac{0.45H_t\cdot H_M(C_v|t_{cp}^-|+L\cdot\rho_d\cdot W\cdot i)}{\lambda\cdot t_{cp}^+} \tag{8}$$

Under the condition of natural air temperature, the cohesive soil was compacted in the optimum water content and its relative ice content must be less than 1. In order to consider safety and simplify the calculation, we can assume that i=1.0, so Equation 8 can be written:

$$\tau = \frac{0.45H_t\cdot H_M(C_v|t_{cp}^-|L\cdot\rho_d\cdot W)}{\lambda\cdot t_{cp}^+} \tag{9}$$

Equation (9) was the function that we referred to evaluate melting time of the frozen layer. Using Equation (9), we can also know that from the rebuilding to the beginning of the next cold season, the new filled warm layer maximum depth without residual frozen layers inside the impervious barrier should be:

$$H_{tmax} = \frac{\lambda t_{cp}^{+} \cdot \tau}{0.45 H_M (C_v |t_{cp}^{-}| + L \cdot \rho_d \cdot W)} \qquad (10)$$

The value in Equation (10) was a known number and its maximum value was the continual time of plus temperature on a daily average in the seasonally frozen ground region.

CONCLUSION

The regularity of frost heave in compacted soil obviously showed that: when soil was saturated in the special conditions, the frost heave ratio would reduce with the enlargement of dry unit weight. When the dry unit weight reached a critical value, the compacted soil which froze without heave, i.e. frost heave ratio $\eta \leq 1\%$ could be reached. In order to obtain the soil, at first, degree of saturation S_r was solved according to the designed dry weight and corresponding optimum water content and then the critical dry unit weight ρ_d^1 needed for freezing without the heave could be arrived at in Equation 3. If the compacted soil was made to reach ρ_d^0 and S_r was kept at one constant, the water content should be decreased. Equation 9 can be used to evaluate the melting time of the frozen layer and determine a suitable time for rebuilding.

REFERENCES

C.A. Peggy and V.K. Horsler, (1980) The Engineering Property of Compacted Cohesive in the State of Saturated and Frost Boil Recycline, Beijing Water Conservancy Science and Technology, Complimentary Issue.

B.O. Orouf, et al., (1980) The Frost Heave of Soil and the Application on Building Structure, Translated by Li Yongsheng.

OBSERVATION AND RESEARCH OF SORTED CIRCLES IN EMPTY CIRQUE AT THE HEAD OF URUMQI RIVER, TIAN SHAN, CHINA

Xiong Heigang[1] Liu Gengnian[2] and Cui Zhiju[2]

[1]Department of Geography, Xinjiang University, Xinjiang, China
[2]Departmint of Geography, Beijing University, Beijing, China

The features of the sorted circles have been analysised with the form of the sorted circle, grain size, water content, frost heave stone sirting, fabric and reference to wooden stakes inserted vertically into the ground. The results show that the sorting degree becomes much better; the influence of frostheave decreases gradually; and the center of sorted circles was covered by vegetation increasingly from the upper to lower sorted circles. Moreover, the general tendency of the frostheave is central frostheave > internal gutter frostheave > gutter frostheave in a sorted circle.

THE STUDY AREA

The Urumqi river rises on the north slope of the Kalawchen ridge, Tian Shan and is about 150 Km long. Precipitous mountain peaks, 4,000—4,400 m in altitude, are covered by snow and glaciers. Snow line is 3,950—4,200 m above sea level. The empty cirque is approximately 3,820—3,950 m (a.s.l) with an area of 1.5 Km^2, located in the north of the river head, and is facing south—east (Fig 1). In the empty cirque many sorted circles, sorted stripes, sorted nets and sorted polygons developed, almost including all the classifications of sorted forms given by Washburn (1979) The sorted circles, with different diameters and forms, are a typical case among them. Since the place, altitude and developing time are different, developmental degrees of sorted circles have an obvious diversity. For recounting conveniently, the sorted circles distributed in three different elevations, 3,820, 3,880 and 3,950 m, were called lower; middle and upper sorted circles separatly. The conditions of sorted circles are shown in Table 1.

STONE STATISTICS

Since sorted circles of different developmental stages undergo different sorting degree has diversity. Generally, of three principal characteristics of stone can use to decided the sorting and developmental degrees. First, ratio ($P = Dr / Dc$) of mean size of gutter stone (Dr) and central stone (Dc) The bigger P is, the better the sorting and developmental degree are. Second, variance (S) to mean (X) ratio ($F = S / 100 \times X$) of stone size in the centre of sorted circle. The F is regarded as the parameter of the represented sorting degree. The bigger its value is, the worse the sorting degrees are. Third, percentage ($Q = A / 100 \times 100$) of numbers of gutter stone (A) which ab face is tangent with sorted circles. The bigger Q is, the more mature and sorted the sorted circles are. All the parameters were counted from one hundred stones.

Statistical data(Table 2) shows that the ratio (P), increased from 2.5 to 12.5, the percentage (Q) rose by 17 percent and the variance to mean size ratio (F) of central stone decreased nearly one time, three results of the stone statistics suggested that sorting and developmental degree increase gradually from upper to lower sorted circles.

The developmental degree of sorted circles is a sequence of changes gradually along the matrixal source region in the same place. If the sorted circles are near the source region, their developmental degree is worse. Conversely, if they are far from the source region the degree is better. In middle sorted circles. We measured the forms and stone sizes of sorted circle from the edge of the talus to the centre of the cirque on a line (Table 3). The ratio (P) far from the talus, is more ten times than that of it near the talus. Moreover, the height between the centre and gutter of sorted circles decrease and the microcircles, soil polygons appear on the centre of sorted circles gradually with the distance increased. These also prove that the sorting and developmental degree of sorted circles much better gradually. From a review of field evidence and physical logistics it has been deduced that the place, which is far from the talus,has a comparatively smooth surface and fineness of high content, so it can contain much water, and is influenced by frost– thaw easily, implying that the developing rate of sorted circles is fast.

OBSERVATION OF FROST-HEAVE

In the summer of 1990 wooden stakes were used to set up observational posts in lower and middle sorted circles. Three different methods were used to measure frost heave. First, 15 wooden stakes 3.5 cm in diameter and 25 cm long were completely driven into different positions of a sorted circle (Fig 2), observing the frost heave of different positions with stakes of the same diameter and length.Second, 6 wooden stakes 25 cm long and 1×1— 5×6 cm in diameter were placed in the centres of 6 sorted circles with a similar

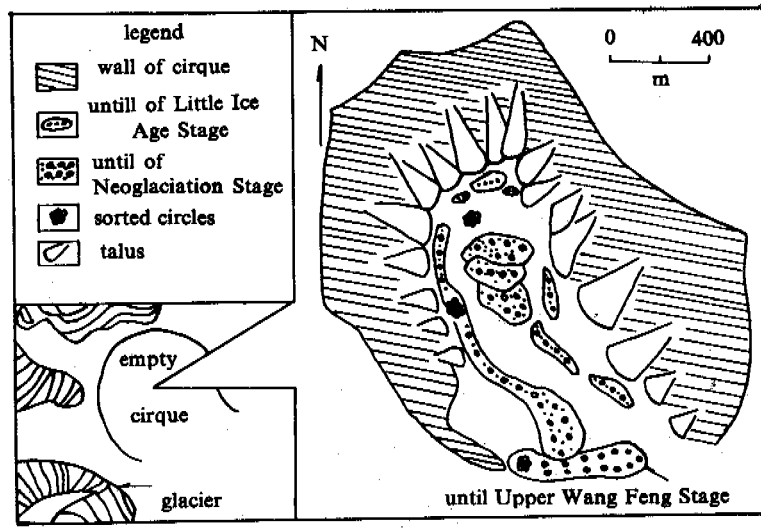

Fig.1 Index map of sorted circles in empty cirque

Table 1 . Conditions of the different sorted circles in empty cirque

	altitude (m)	till age * in place	diameter (m)	form	place	central condition
upper sorted circles	3,950	16th—19th centurics	1—5	like a steamed bread	back of empty cirque	no vegetation
middle sorted circles	3,880	2,000—3,500 B.P	2—5	slightly high centre	middle of empty cirque	no vegetation
lower sorted circle	3,820	10,000—20,000 B.P	1—3	higher gutter	mouth of empty cirque	covered by vegetation

* after Cui Zhiju 1981. Wang Qingtai 1981.

scale, trying to find out the function of frost heave to the wooden stakes with the same length but different diameter.Third, 8 wooden stakes 3.5 cm in diameter and 5—40 cm long were separately driven to the centres of 8 sorted circles with the similar scales, in order to understand the condition and influence of frost heave to the wooden stakes of different depths and the development of sorted circles. Generally, the layer 40 cm beneath the ground surface acts very strongly, so the longest wooden stake selected was 40 cm. The accuracy of the survey was to 1 mm or better.

For discussing the frost heave relationship between the centre

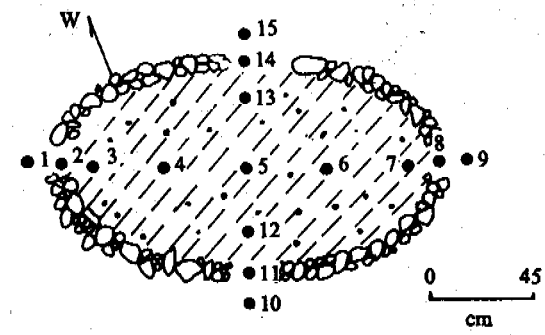

Fig.2 Position and numbers of wooden stake in sorted circle

Table 2 . Statistical parameters of stone of sorted circle in three different places

	F	P	Q	Altitude
upper sorted circles	5.57	2.5	49	3,950
middle sorted circles	4.96	6.0	60	3,880
lower sorted circles	2.82	12.5	66	3,820

and gutter in a sorted circle,the observational data which was gathered by the first method, were divided into 4 groups: (1).Central stakes;(2).Internal gutter stakes; (3).Outside gutter stakes;(4).Gutter stakes (Table 4). The data shows that action of the central stakes was strong and that of the gutter stakes was weak. The mean heave of the central stakes was 2.65 times than that of the gutter stakes in the first observational cycle(July 6,1990 —August 20, 1990) and 1.3 times in the second observational cycle (August 20, 1990— — August 14, 1991). The general tendency of mean heave of the stakes was central stakes > internal gutter stakes > outside gutter stakes > gutter stakes. This reflected fully that the frost heave decreased from the centre to the gutter of sorted circles. There was also great diversity among the action of every side of the sorted circle. The fastest rising stakes were on the west side and the slowest rising stakes were on the south side(Table 4). The mean heave of the former was 2.15 times and 1. 83 times than that of latter, separately in two oberational cycles. This difference may be related to the water content and grain size of different parts of the sorted circle.

The heave of the wooden stakes for the period 1990—1991 ranged from 33 mm, for 5× 5 cm in diameter, to 67 mm, for 1 × 1 cm in diameter (Table 5). This suggested that wooden stakes with the least diameter rose quickly in the centre of the sorted circle. It coincides with the condition that the small stones rise to the ground surface quickly in the process of freeze–thaw sorting.But the tendency of frost heave is not clear, this may be related to the maturity and inaction of lower sorted circles.

The heave of the stake 20 cm long was 122 mm and stake 40 cm long was 45 mm from August 20,1990 to August 14, 1991. The former is more 2.7 times than the latter. The surface layer above 25 cm acted strongly. Three stakes, 5, 10 and 15 cm long rose out completely and lay down on the ground surface in the field observation of August 14,1991. This is consistent with the conclusion that the frost heave of the surface is stronger than that of depth, which was also achieved in research of other regions(Wang Xiyao,1982, Cuitoweiqi,1985).

The ground surface was easily influenced by changes of the outside environment. In early summer the ground surface began to thaw, and the highest frequency of frost–thaw appeared in June. The stakes were pushed upward with ground surface freezing. When the ground thawed from the surface downward, the stakes failed to return fully to their prefreezing position, to produce a net of upward heave of the stakes. Repetitive freeze–thaw cycles result in a gradual upward movement of the stake. There was still freezing in the depths of the sorted circles at this time. In summer the thick active layer was caused by high temperature, precipitation and lower frequency of freeze–thaw. If the material in the depths move upward, it must overcome the gravity and cohesive forces of mud in the upper layer, In September the frequency of freeze– thaw increased. There are still very strong influences of freeze–thaw in the ground surface, the stakes in the surface layer rise quickly.The con-

Table 3. Changes of sorted circle with an increased distance from talus in middle sorted circles

numbers	distance from talus(m)	diameter (m)	P	height between centre and gutter (m)	condition of centre
1	5.0	5.25	0.32	25	
2	9.5	4.5	0.6	20	
3	14.5	5.6	0.79	17	
4	18.0	3.2	1.41	13	soil polygons
5	21.5	3.6	1.14	10	microcircles and polygons
6	24.5	2.8	1.57	0	microcircles and polygons
7	26.5	2.5	3.44	0	microcircles and polygons

Table 4. Heave of wooden stakes in different positions and sides of lower sorted circle

	central stakes (4,5,6)	internal gutter stakes (3,7,12,13)	outside gutter stakes (1,9,10,15)	gutter stakes (2,8,11,14)	north stakes (7,8,9)	east stakes (10,11,12)	south stakes (1,2,3)	west stakes (13,14,15)
July 6,1990	0	0	0	0	0	0	0	0
August 20,1990	5.3mm	4.0mm	4.8mm	2.0mm	4.3mm	3.7mm	2.0mm	4.3mm
August 14,1991	39.2mm	37.0mm	29.5mm	30.0mm	37.8mm		23.5mm	43.0mm

Table 5. Heave of wooden stakes with different diameter in lower sorted circles

	Diameter of stakes					
	1×1	2×2	3×3	4×4	5×5	6×6
July 6,1990	0	0	0	0	0	0
August 20,1990	2mm	5mm	5mm	10mm	4mm	3mm
August 14,1991	67mm	38mm	36mm	47mm	33mm	41mm

Table 6. Heave of wooden stakes with different length in middle sorted circles

	lenght of stakes (cm).							
	5	10	15	20	25	30	35	40
July 6,1990	0	0	0	0	0	0	0	0
August 20,1990	20mm	47mm	26mm	13mm	8mm	7mm	4mm	1mm
August 14,1991	*	*	*	122mm	81mm	39mm	30mm	45mm

* stake rose out completely and lay down on the ground

dition is similar with that of June.In autumn temperature decreases, the active layer begins 0double freezing1from both surface and bottom. Conditions of frost heave are very complicated and the frost–pull theory and frost–push theory are used to explain the frost heave of stones by downward freezing which can not be directly applied to upward freezing by reversing signs, because the vertical direction of ground surface easily influenced by the outside environment is higher than that of depth.

Comparing the data of lower sorted circles, the heave of wooden stake in middle sorted corcles is a markedly larger. From August 20, 1990 to August 14, 1991, the heave of stakes, with the same lengths, diameters and at the same position in middle sorted circles, is 3 times than that of stake in lower sorted circles.

CONCLUSION

From the upper to lower sorted circles (from infant stage to old stage) the sorting degree becomes much better; the influence of frostheave decreases gradually; the centre of sorted circles was covered by vegetation increasingly; and forms of sorted circles change from the high to low centre. Preliminary conclusions of their features and developmental backgrond which have been drawn from field and laboratory analysis is in Table 7.

Wooden stakes with small diameter heave higher than that of ones with a large diameter in the same period. Furthmore, the frost heave of surface is stronger than that of depth. The strongest active layer is above 25 cm from the surface. In the same place the general

Table 7. Feature of sorted circle in different developmental stages at empty cirque

	develop-mental stage	sorting degree	condition of frost heave	condition of circle centre	glacial stage in place
upper sorted circles	infant	lower	very strong frostheave	small sorted circles	Little Ice Age
middle sorted circles	mature	medium	strong frost heave	small sorted circles and polygons	Neo-glaci-ation
lower sorted circles	old	higher	weak frost heave	no small sorted-circles	upper Wang Fen

tendency of the frost heave is central frost heave > internal gutter frost heave > gutter frost heave in a sorted circle. The maturity and sorting degree of sorted circles increase along with the increase of distance of the material source region.

Finally, additional data and research are necessary on the developmental time, microclimate changes in different heights which control the developmental degree of sorted circles.

ACKNOWLEDGMENT

Financial assistance for this study was provides by the National Natural Science Foundation of China and Science Foudation of Tian Shan Station, Prof. Liu Chaohai(LanZhou Institute of Glaciology and Cryopedology, Academia Sinica) supplied various help with our work.

REFERENCE

Cui Zhijiu,1981. On the glacial cirque at the head of Urumqi River, Tian Shan, Journal of Glaciology and Cryopedology,Vol. 3, Special Issue.pp 57—63 (in Chinese), Cuitoweiqi,H.A, 1985, The mechanics of frozen ground, Sciences Press, Beijing. pp 80-99(in Chinese).

Mackay,J.R.1984, The frost heave of stones in the active layer above permafrost with downward and upward freezin,Arctic and Alpine Research, Vol, 6,N0. 4, pp439—446.

Wang Jingtai,1981,Ancient glaciers at the head of Urumqi River, Tian Shian, Journal of Glaciaology and Cryopedology, Vol.3, Special Issue pp 24—35 (in Chinese).

Wang Xiiao, 1982, Frost heave and its distribution in different layers influenced by shallow ground water,Journal of Glaciology and Cryopedology, Vol. 4, No.2, pp55—62(in Chinese).

Washburn,A.L, 1979,Geocryology,Edward Arnold, pp22— 277.

STUDY AND DEVELOPMENT OF THE TECHNIQUES AGAINST FROST DAMAGE OF HYDRAULIC STRUCTURES

Bomeng Xu Anguo Li Lijun Shao

Information System of Antifrost Techniques of Hydraulic Structures of China,74 Beian Road, Changchun City,China

The progress of the study on the techniques against frost damage of hydraulic struc--tures in China is introduced in the aspects of foundation soil heaving,frost heaving force and the design measures against frost damage, The remaining problems to be solved are simply discussed and the study direction and tasks in the future are also presented.

key words: Hydraulic stucture, frost damage, frost heave prevention and treatment.

INTRODUCTION

Our country has a vast territory, quite a large part of which is in the cold zone of the Northern Hemisphere. The area of frozen soil in our country is 68.6% of the whole territory, in which the seasonally frozen soil with frost depth more than 0.5m--46.3% , the permafrost--22.3% . In these regions, not only a few hydraulic structures were severely damaged by the freezing and thawing action. The investigation data indicated that in Lishu and seven other irrigation districts of the province of Jiling, 71.4% of the irrigation canal structures were damaged by the frost action; in the Chahayang irrigation dostrict there were 93 structures damag--ed in the 112 investigated structures; the canal lining in the different regions were also damaged to a certain extent (Xu Shaoxin, 1986). Therefore, it is necessary to study the various problems concerned with soil frost and ice action.

DEVELOPMENT OF THE RESEARCH WORK

On the whole, the research work in this field in China may be divided into three development stages as follows(Xu Bomeng,1988).

The first stage approximately ran through the 1950's. In this stage, the research work was developed mainly around the influence of soil frost and the physical and mechanical properties and earth filling techniques in winter. In the early 1950's, a number of laboratory and in-site tests of the earth filling methods, earth fill qualities in winter were,carried out and thawing subsidence characteristics of frozen soil cakes and their filling bodies in water were studied. These test results had application in the waterti--ght blankets of Longfunshan and other reservoirs in the province of Heilongjiang, which initiated a precedent of utilizing frozen soils in hydraulic construction in cold regions. At the same time,the previous Shengyang Hydraulic Research Institute of Ministry of Water Resources had compiled and publi--shed "Construction of Roller Earth Dam in Winter"

The second stage was approximately from the early 1960's to the mid-1970's. The research on frozen soil developed mainly with the focuson the hydraulic structures destroyed by the heave of foundation soil. Some efficious measures against frost damage were sommarized. At the same time,the investigation of ice injury and observation of ice pressure were carried out, the law of ice pressure formation and calculating method were studied.

The third stage was from the mid-1970's to pvesent. It is the stage that the study of preven--tion and treatment of freeze damage of hydraulic stuctures and canal lining and soil freezing were quickly developed. Since 1977, the "Cooperation Group of Research on Antifrost Technigues of Hydr--aulic Structures" and "Informatin System of Anti--frost Techniques of Hydraulic Structures" were established. They held eleven academic exchange and more than thirty symposiums, on which over 500 papers were presented about the investigation and summary of freeze damage and its prevention and the treatment techniques of hydraulic stuctures, soil heaving and its action to the stuctures were presented. Forty volumes of the Jounal "Engineering and Frozen Soil",fifty volumes of the Journal "Watertight Techniques of Canal" have been published. The "Experimental Method of frozen soil", the "Design Standard of Anti-Frost-heaving of Canal System Structures", the writings "Prevention and Treatment of Freeze Damage of Hydr--aulic Structures", "Watertight of Canal" and the "Collecting Drawings of Canal System Structures in Seasonally Frozen Soil Regions" have been printed. At present, the "Standard of Hydraulic Structures Design Against Ice and Frost Heave" is in compilation. Besides, not quite a few foreign useful references have also been translated into Chinese.

RESEARCH ACHIEVEMENT

The primary achievements are as follows:

1. The Freezing and Thawing Properties of Soils and Earth Dam Filling in Winter

The test indicated that the stable freezing temperature of clay is lower than 0℃ and its minimum supercooling temperature may reach -5℃, at this time,the clay is still in a plastic condition, consequently, can be filled and compacted with increasing speed. The clay core of the earth dam of Qinghe reservoir was constructed in winter, the compacted density under an air temperature of -12℃ reached 1.68g/cm^3, satisfying the design requirement.The tests of the effect of soil freezing and thawing on the filled soil properties indicated that controlling the moisture of filled soil to be near or lower than the plastic limit can assure the quality, and avoid the effect of freezing and thawing action. As a result of the soil being separated by the ice in the course of freezing, the compressibility increases, whereas the shear strength decreases(Wang Liang,1983). These results mentioned above have been applied in the clay cores of Qinghe and Dahofong reservoirs and the earth-rock coffendam with weathering sand of Baishan Hydroelectric Station and have a good efficiency.

2. Characteristics of Crumbling, Sinking and Consolidation of Frozen Soils and Their Filled Bodies in Water and Application in the Watertight Blanket of Earth Dams

The test results demonstrated that the frozen soil, when puts into water, thaws and crumbles into small pieces from layer to layer and drops down. The crumbled amount within several hours is over 80% in weight. By the action of the dead weight and seepage pressure, the density of soil pieces accumulation gradually increases, appoaching the natural density of the soil within a short time. This indicates that the properties of frozen clayer soils crumbling in water can be used to form a good watertight blanket. These results have been applied in several reservoirs of HeilongJiang province and have had good results.

3.Moisture Migration and Frost Heave

Observations indicate that the distribution of the frost heaving amount along the depth is not uniform with different forms. The limit of the depth of the water table influencing on the moisture migration and frost heaving may be evaluated by the capillary lift of soil. The hydraulic structures are usually located at the sites with higher water tables. Under the condition of an open system, frost heaving of ground is great. According to the observations,in Heilongjiang and Jiling provinces, having greater frost depth of ground, the maximum heaving reached 55cm and 43cm,respectively, consequently the hydraulic structures were damaged to a larger extent.

With a number of laboratory test and in-situ observations, the design values of frost depth and heaving and their calculation methods are presented.

4. Frost Heaving Force of Soil

The observations for years in severl field test sites indicate that the tangential frost heaving force mainly occurs at a certain range of the upper frost depth; the maximum value is brought about at the time of the frost depth being about 70-80% of its maximum, The main factors affecting tangential frost heaving force are the heave of soil and roughness of pile surface.

The design values of tangential frost force for pile with even surface are presented: 20~40kPa for the soil with weak heaving susceptibility, 40~80kPa for the soil with medium heaving susceptibility, 80~150kPa for the strongly heaving soil.

The value of horizontal frost heaving force acting on the retaining wall under bi-direction freezing of the back-filling soil behind the walls is associated with the frost susceptibility of the soil and the allowable deformation of the wall.The horizontal heaving force follows an increase of the depth from the ground surface and has the maximum in a certain height from the wall bottom.

Based on the in-situ observation data, the distribution of horizontal heaving force along the depth in triangle or trapezoid form has been derived, having the maximum value of about 50~100kPa for weakly heaving soils, 100~150kPa for mid-heaving soils and 150~200kPa for strongly heaving soils(Sui Tieling,1990).

The vertical frost heaving force is dependant upon the heaving susceptibility of soil and heaving constraint, and also associated with the bottom area embedded depth and allowable deformation of the foundation(Xu Shaoxin,1989). The larger the bottom area, the lower the heaving force caused by the surrounding soil to the foundation; the deeper the foundation, the smaller the freezing layer of soil beneath the foundation and the heaving force.

5.Mechanism of Frost Damage of Canal Linings.

The frost heave amount at each position of the canal is mainly dependant upon the moisture condition of foundation soil. The canals with different runs have different frost depths and heaving amounts. The lower part and bottom of the canal the heave amount is great, reversely, at the top part of the canal slope the heaving is small. The frost depth, heaving amount, and allowable displacement of the canal linning are the govering parameters for canal design to prevet frost damage (Li Anguo,1987).

THE MEASURES AGAINST FROST DAMAGE

Based on the research results,quite a few effective methods against frost damage have been provided and have created a considerable amoant of economic and societal benefits in practice.

1.Thermal insulation

The one these methods is using a water layer. If possible, a certain depth of water above the bottom plate of the structure in winter can keep the foundation soil unfrozen. The depth of water may be considered to be equal to 0.6 times that of the soil frost depth of the corresponding site. Another method is placing a layer of rigid foamed plastic plate with a certain thickneess beneath the foundation, lining slabs of canal or on the back of retaining wall. The third method is to make the concrete foundation plate hollow, using the air in the cavity pocket to insolate heat.

2. Replacement of soil

The non-frost-heaving material of sand and gravel is used to replace the frost susceptible soils. The particles smaller than 0.05 mm in the replacement meterial do not exceed 10% in weight. The replacement thickness usually is 0.75~1.0 of the frost dept and dependent on the distribution of the horizontal frost heaving force along the depth for retaining walls. Also, the impermeable meterial is used and embedded into the foundation soil to interrupt moisture migration and eliminate frost heaving.

3.Structurl measures

Different structural types that are effectual in preventing frost damage are applied: such as the sluice type called the word "-":the sluice with foundation in the form of reversed placing box or reversed arch self anchoring piles involving the pile with the expanded foundation plate, the pile with exploding-expanding ends, and the pile with bottom beam; the wall consisting of precast hollow boxes filled with non-frost heaving material of sand gravel, etc; the buttress retaining wall with the buttress spans not exceeding the maximum frost depth and the retaining structure with anchored slabs, etc. For the canal linings, the structural measures involve flexible structures, such as the embedded membrane lining and asphalt concrete lining; the rigid structures, such as concrete slab, concrete slab with beam, concretc slab in the form of "∩", wide-shallow concretc channel, arc concrete channel, small water trough of "U" type(Li Anguo,1987); reasonable arrangement of deformation seams filled with flexible seal material such as polyvinyl chloride ointment or tar plastic daub.

4.The other measures

The other measures involve evasive methods, such as making the channel alignment to evade the location with soil susceptive to frost heaving; adopting the canal in fill or cut-and-fill as possible; adopting the tube the or overhead water trouhg to transfer water; compaction of clay or clayey loam foundation soil to increase its den-sity; strengthening the waterproofing of canal and surface drainage; limiting the date of the canal being out of operation prior to 5~10 days of the initial date of the cold season; the date of water running through canal in spring not being prior to the end of cold season; strengthening the main-tenance of the structures, etc.

FUTURE DIRECTIONS AND RESPONSIBILITIES

Over the years, gratifying achievements of pro-tecting hydraulic structure and canal lining from frost damage have been made. Very many questions, however, need to be resolved. The study direction and responsibilitiey in the future are mainly:

1.Intensive studies on the law of soil frost heav and technigues of preventing frost damage, the characteristics of frost and frost heaving of canals, the methods for prediction, classification standards of frost heaving for the foundation soils.

2.Studying the formation and developing mecha-nisms of frost heaving forces to select reasonable measures of preventing frost damage.

3.Perfecting measuring instruments and methods of temperature, stress etc. used in laboratory and in site, draving unitive test operation rules to increase the accuracy of test data.

4.Studying new materials, new structures and mechanized construction techniques to reduce work cost and quarantee construction quality.

5.To sommarize further the experiences in pre-venting frost damage, spreading presented results, making them real productive forces.

REFERENCE

1.Li Anguo and Han Shujian, 1987, Brief Intro-duction of Antifrost Technique of Canal Lining. Engineering & Frozen Soil, NO 4 .

2.Sui Tieling, Na Wenjie and Li Dazuo, 1990, Distribution of Horizontal Heaving Force on Test Retaining Wall. Proc.4th Nat. Conf on Glaciology and Geocryology(selection).

3.Wang Siyao, 1982, Frost Heave and Its Distri-bution in Different Layers Influenced by Shallow Groundwater,Journal of Glaciology and Cryopedology, Vol, NO 2.

4.Wang Liang, Xu Bomeng and Wu Zhijin, 1983, Property of Soil Freezing-Thaving and Earth Dam Construction in Winter, Proc 4th Int. Conf. on Permafrost.

5.Xu Bomeng etc, 1990, Prevention and Control of Frost Damage of Hydraulic Structures, Jiling Science and Technology Publishing House, China.

6.Xu Bomeng,1988, Study on Prevention and Control Technique of Hydraulic Engineering in Northeast Region, Engineering and Frozen Soil,No.1.

7.Xu Shaoxin,1987, Review of the Study on Frozen Soil in Hydraulic Engineering of Our Courtry, Engineering and Frozen Soil, No.4.

8.Xu Shaoxin, 1989, Frost Heaving Force on Foundations in Seasonal Frozen Ground Region, Proc. 3rd Chinese Conf. Permafrost (selection).

9.Zhu Dafu and Lin Suxing,1986, A Frost Heave Classification of Canal Base-Soil with Concrete Lining and the Measures Against Frost Damage, Journal of Glaciology and Geocryology, Vol.8, No.3.

10.Zhu Qiang,1990, Quantitative Study on Basic Relation between Frost Heave of Canal Base-Soil, Egineering and Frozen Soil, No.1.

UNFROZEN WATER CONTENT IN MULTI-CRYSTAL ICE

Xu Xiaozu[1], Zhang Lixin[1], Deng Yousheng[1], Wang Jiacheng[1]
IU.P.Lebedenko[2]and E.M.Chuvilin[2]
[1]State Key Laboratory of Frozen Soil Engineering, IGGAS,PRC
[2]Geology Faculty of Moscow State University, Russia

An artificially large crystal ice was smashed and divided into four groups with the grain sizes of >10, 7–3, 3–1, and <1mm, respectively. The unfrozen water content of multi-crystal ice was determined by the nuclear magnetic resonance technique and by calorimeter. Four factors influencing the unfrozen water content in multi-crystal ice, including grain size of ice, interfaces between crystals, freezing speed and air content in water, were investigated. Results show that the unfrozen water content increases with decreasing of grain size of ice. The unfrozen water content between interfaces of ice–water–ice is greater than that of ice–water–air. By using deaerated water and a quick freezing, we can obtain greater multi-crystal of ice than the undeaerated water and a lower unfrozen water content if other conditions are the same.

INTRODUCTION

The basic difference between frozen and unfrozen soils is that ice exists in frozen soils. The ice content and its property in frozen soils are of great significance for physical and mechanical properties of frozen soils. And the ice content and its property depend on the unfrozen water content in ice to a large extent. A lot of previous work has been done on unfrozen water content in frozen soils (M.Anderson et. al.,1974, A.R.Tice et. al.,1978, E.D.Ershov, 1979), but seldom dealt with unfrozen water content in multi-crystal ice. Xu Xiaozu determined the unfrozen water content in ice made by distilled water (1987), but didn't describle the changing regularity of unfrozen water content in multi-crystal ice.

SAMPLE PREPARATION

To obtain multi-crystal ice with different grain sizes, it is necessary to prepare large crystal ice first. Therefore, we pour distilled water into a plexiglass container with the size of 15 cm in diameter and 25 cm high. The temperature at the water surface is kept at zero or slightly below zero degrees centigrade. The side of the container is surrounded by insulation material. Water is gradually frozen from the top downwards. Usually, after one week of freezing the ice thickness may reach to about 10 cm and the diameter of the ice crystal is larger than 10 mm. Taking one sample from this massive ice as the sample with a grain size of larger than 10 mm. After that the massive ice is smashed and sieved and divided into three groups with a grain size of less than 1 mm, 1 to 3 mm and 3 to 7 mm, respectively. Each group of multi-crystal ice is divided into two subgroups. One subgroup is emerged in distilled water of zero degrees centigrade and quick frozen again to create ice–water–ice interfaces between ice crystals, and the other subgroup is kept without distilled water to create ice–water–air interfaces.

To investigate the influence of freezing speed and air content in water on the unfrozen water content in multi-crystal ice, two other samples are prepared. One sample is made with water from the previous determined sample with the grain size of the ice crystal being larger than 10 mm and another sample made from deaerated water and both of them are frozen with a high speed. All of the samples mentioned above are frozen at minus 20 degrees centigrade for 5 hours and are determined by the nuclear magnetic resonance technique in a warming cycle and by a calorimeter.

RESULTS AND ANALYSIS

As a kind of grained material, ice crystals, like soil particles, can absorb a certain amount of unfrozen water under the condition of the temperature being below zero degrees centigade because of the existence of free energy at the surface of particles. Figure 1 shows the curves of unfrozen water content vs. temperature for the ice crystals with the different grain sizes mentioned above. It can be seen from figure 1 that the unfrozen water content increases with decreasing of temperature in the power form. From figur 1–a it can be seen that if the temperature is the same, the unfrozen water content of multi-crystals of ice changes with the grain size of ice crystal and can be divided into three groups: the minimum a grain size is larger than 10 mm, the middle grain size is from 1 to 7 mm and the maximum grain size is less than 1 mm. The difference of frozen water content curves for ice grain size less than 7 mm is not great because of the difference of ice grain size being less after water is filled and being quickly frozen. From figure 1–b it can be seen that under the conditions of ice–water–air interface and quick freezing the changing regularity of unfrozen water content with temperature is the same as shown in figure 1–a, but the maximum of unfrozen water content for the case of IWA is less.

The curves in figure 1 can be expressed by the regressive equations shown in table 1. From table 1 it can be seen that the related coefficients are greater than 0.94.

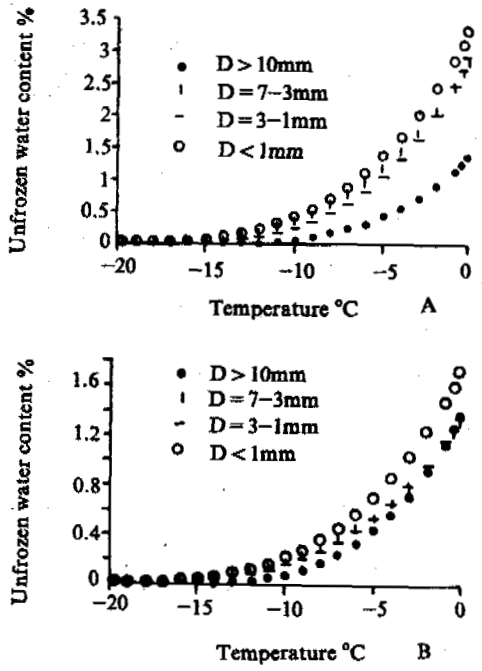

Fig.1 Unfrozen water content in multicrystal ice with different grain sizes vs. temperature (A–for the IWI case and B–for the IWA case)

Figure 2 shows the curves of unfrozen water content vs. temperature for multi–crystal ice with grain size less than 7 mm and interface of ice–water–ice and ice–water–air respectively. From figure 2 it can be seen that if temperature is the same, the unfrozen water content of multi–crystalice with interface of ice–water–ice is higher than that with interface of ice–water–air. There is no much difference for different grain sizes.

Figure 3 shows the curves of unfrozen water content vs. temperature for samples of grain size larger than 10 mm and deaerated and undeaerated distilled water being quickly frozen. From figure 3 it can be seen that if the temperature is the same, the unfrozen water content of the sample made by undeaerated distilled water being quickly frozen is much greater than that of the sample with grain sizez greater than 10 mm. It indicates the freezing rate has a great influence on the unfrozen water content. Microscope observation on the thin section indicates that the freezing rate influeces the grain size of ice crystals. The higher the freezing rate, the less the ice crystals is and the less the ice crystal, the higher the unfrozen water content. Compared with the unfrozen water content of the deaerated sample, the unfrozen water content of the undeaerated sample is higher even if the freezing condition is the same. Microscope observation indicates that the grain size of the deaerated sample is greater than that of the undeaerated sample.

CONCLUSIONS

The unfrozen water content of multi–crystal ice is controlled by the grain size and the interface between ice crystals. If other

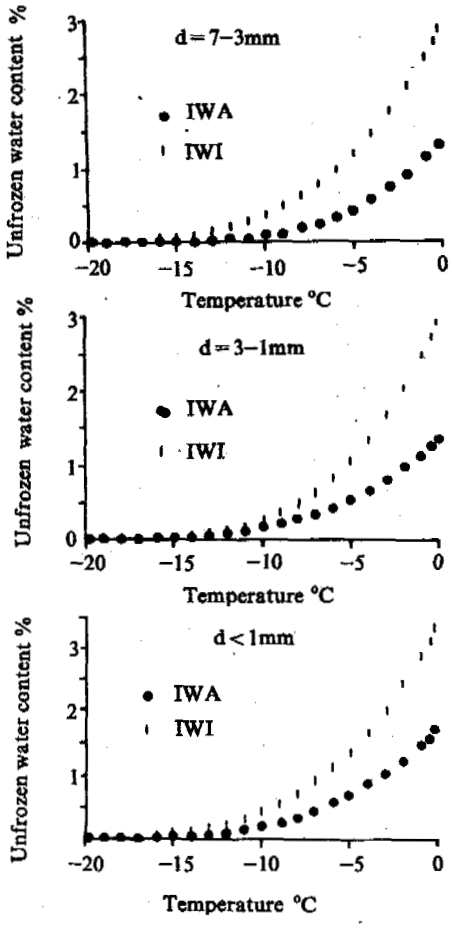

Fig.2 Unfrozen water content of multicrystal ice with different interfaces

Table 1 Regressive equation of unfrozen water content of multi–crystal ice

grain size,mm	regressive equation	coefficient A	coefficient B	related coefficient	Number of point
>10	$Y=(AX+B)^4$	−0.05498	1.0895	0.9418	11
3–7		−0.04259	1.0723	0.9772	14
3–7 *		−0.05224	1.3045	0.9965	15
1–3		−0.04568	1.0838	0.9837	11
1–3 *		−0.05967	1.3170	0.9989	14
<1		−0.04675	1.1505	0.9976	15
< 1 *		−0.05445	1.3582	0.9989	14
refreeze		−0.05503	1.3725	0.9995	15
vacuum		−0.05565	1.3696	0.9989	12

Where Y – unfrozen water content,%; X – absolute value of temperature, °C; A and B– constants; * – ice–water–ice interface.

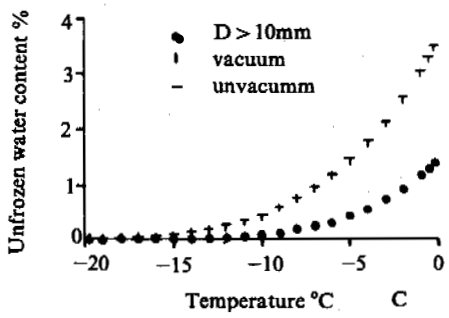

Fig.3 Unfrozen water content in multicrystal ice with deaerated and undeaerated water quickly frozen

conditions are the same, the unfrozen water content of multi–crystal ice increases with decreasing grain size and with increasing ice content.

The freezing rate and air content in the sample are the important factos for the grain size of ice crystal formation. If other conditions are the same, grain size of ice crystals decreases with an increase in the freezing rate and air content.

The maximum of unfrozen water content for IWI and IWA interface is less than 3.5 and 1.5 %, respectively.

ACKNOWLEDGEMENTS

The authors wish to express their thanks to senior engineer, Tao Zhaoxiang and Mr. Gu Tongxin for their determination by calorimeter. This work is very important for calibration of unfrozen water content taken from NMR.

REFERENCES

Anderson,D.M., Tice, A.R. and Banin A., 1974, The water–ice composition of clay / water system, CRREL Research Report 322, pp.10.

Tice, A.R., Burrows,C.M. and Anderson, D.M., 1978, Phase composition measurements on soil at very high water contents by the pulsed nuclear magnetic resonance technique, reprinted from Moisture and frost–related soil properties, Transportation Research Board, National Academy of Sciences, p11–14.

Xu Xiaozu, Oliphant, J.L. and Tice,A.R., 1987, Factors affecting water migration in frozen soils, CRREL Rport 87–9,pp16.

Ershov,A.D., 1979, Water phase composition of frozen soils, Moscow University Publishing House, pp189.

THE THAW SETTLEMENT OF RAILWAY FOUNDATIONS IN PERMAFROST SWAMP REGIONS

Yang Hairong[1] Liu Tieliang[1] and Guan Zhifu[2]

[1]Northwestern Institute, Railway Ministry Academia, China
[2]Gingwu Department of Railway Bureau in Harbin, China

In the permafrost swamp areas of northeast China, thaw settlement is one of the main causes of damage to railway foundations, which are very difficult to repair. Since the establishment of the line, sucessive reparative measures have been taken, but they have not been effective and the damages continue to worsen. Through observation and analysis of thaw settlement of railway foundations, in the permafrost swamp regions in China, a summary of the theoretical and synthetic countermeasures is given to prevent thaw settlement using industrial material for water insulation.

SURVEY OF NATURAL GEOGRAPHY

The permafrost region of Da Hinggan Ling is located in the eastern fringe of Nei Meng Gu and in the northwest of Heilongjiang. The winter is frigid and long, with the period of negative temperatures continuing for around 7-8 months, the summer is short. The highest temperature is about 36°C, in the north, the extreme lowest temperature is -52.3°C. The yearly average temperature is -2 — -6.2°C, the yearly precipitation is 450-550 mm, and the yearly evaportion is about 820 mm (Deer Buer). The altitude is between 500-1300 m, and the relative difference in elevation is generally less than 300 m. This region is one of the main distribution areas of permafrost in China and swamp land has an extensive distribution. The railway length crossing the permafrost region is about 530 km. Geological phenomena, such as pingo, icing, massive ice, etc., make railway construction and operation very difficult.

According to observation and analysis of preventing settlement in the railway foundation in the past, new methods of keeping ground water and surface water from penetrating into the railway foundation have been researched and the evolutional tendency of settlement deformation in the railway foundation can be forecasted (Yuan Haiyi, 1987).

THE LOW EFFECTIVENESS OF REPAIRMENTS

The problem of settlement in the railway foundation in permafrost regions mainly occurs in swamp sections with poor drainage. In the past, other than the step of controlling the height of the embankment, the synthetic methods of constructing a berm in one or two sides of the foundation and the installation of a ladder shaped drainage ditch 20 m from the slope bottom were used (Fig.1).

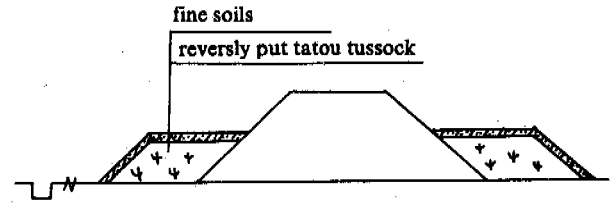

Fig.1 Diagram of Embankment Berm

1. Roadbed Berm

Berms installed in the foot of the slope of the roadbed are most often used to prevent thaw settlement of the roadbed in permafrost regions. According to statistics, new berms were constructed to prevent thaw settlement in swamp regions from 1974 to 1990, and the extended distance is as long as 126.7 km. Through observation, it has been shown that berms installed in settlement sections are effective at first, but with time, settlement damage continuously appears in parts of the roadbed. The causes of the thaw settlement and the ineffectiveness of berm are analyzed as follows:

(1) Effect of surface water: Because of poor drainage in the drainage ditch or in the area around the slope bottom of the roadbed, ground water and surface water accumulates in the slope bottom of the berm which causes heat to successively penetrate into the base of the roadbed. This causes non-uniform deformation of the roadbed and parts of the permafrost thaw under the base of the roadbed. Successive heavy rains are one of the direct causes of fast settlement in the roadbed.

(2) Effect of ground water (suprapermafrost water). In sections with ground water, when the drainage ditch cannot prevent surface water from successively supplied ground water, surface water penetrates into the ground and flows into the roadbed from the drainage ditch causing the berm

to lose its effectivity.

(3) Effect of berm without enough length. Joints are set up at the heavy settlement sections of the roadbed berm but are not set up at slight settlement sections in the berm of the road bed so they are often not connected properly.

(4) Effect of ballast puddle ditch. The ballast in the upper layer of permafrost below the roadbed forms a deep potshaped ballast puddle ditch which is advantageous for the accumulation of ground water. Based on investigations, ballast puddle ditches can be as deep as 2 m. If the ballast puddle ditch is not dealt with, even if berm is constructed on one or two sides of the raodbed, seasonal precipitation penetrates into the base of the roadbed through the ballast puddle ditch causing the permafrost below the base to thaw and causing roadbed settlement.

(5) Effect of the filling material used in berm. Tatou tussock that grows locally is often used as filling material for berm in the northeast of China. But due to a lack of water the tatou tussock dies and rots, thus causing a biochemical reaction which causes the temperature of the frozen soil to rise along with the rotting process. Meanwhile, its effect on the heat preservation and insulation heat gradually decreases with time (Table 1). With time, the migration becomes dense, its effect of protecting against heat gradually worsens, so after the berm is constructed the effect of preventing roadbed settlement gradually decreases.

Table 1. Change table of the coefficient thermal conductivity of tatou tussock

Yearly limit	Grass of original place	Grass of berm after 2 years	Grass of berm after 10 years
Coefficient thermal conductivity w/mk	0.1663	0.2745	0.5358

(6) Effect of berm with enough height. The purpose of constructing berm is to decrease the amplitude of the upper boundary in the slope foot of the roadbed to keep the surface and ground water from penetrating into the roadbed base. So the rule of providing the berm with the proper height and filled with tatou tussock or peat cannot be less than 1.0 m. But in practice, some berm do not have the above mentioned stipulated height.

2. Drainage Ditch

(1) The distance of the drainage ditch far from the slope foot of the roadbed. The main reason for this was to keep the natural surface near the slopefoot from being destroyed by the digging of the drainage ditch and to prevent water from flowing into the frozen soil around the ditch which would cause thawing and affect the stability of the roadbed. Practice verifies that the distance of the drainage ditch from the slopefoot should be 10 m. Drainage ditches should conduct prevention treatment, if not, even if the drainage ditch is far from the roadbed, a large amount of settlement occurs in the roadbed.

(2) Shape of the drainage ditch. A conventional ladder shaped section is continually used in drainage ditches in frozen soil regions. There are many problems with this form, such as it is difficult to construct, it doesn't have effective slope prevention and it is easily blocked. The Gongwu Department of Railways, based on many years of practical research, used a new shape for drainage ditches, an inverse "T" shape used on the heave section. The self buried principle was used for the purpose of protecting the slope of the ditch in areas where thaw and collapse occur in the frozen soil region.

INDUSTRIAL MATERIAL USED FOR INSULATION AND WATER PREVENTION IN ROADBED SETTLEMENT RENOVATIONS

Renovations are a basic step for preventing surface and ground water from penetrating into the base of the roadbed and for preventing settlement of roadbeds in permafrost regions. In recent years, railway departments have used intricate methods of renovation, by burying industrial material for preventing water penetration into one side of the upper reaches of the roadbed and for preventing ground water from flowing into the roadbed. Based on the depth of ground water, the embedded depth of the water prevention material is divided into shallow and deep embedded depth.

1. Shallow depth: in the area with more plentiful surface water and shallower ground water (less than 1 m), when it is difficult for one side of the upper reaches of the roadbed to vertically drain water, a large amount of surface and ground water may cross the roadbed and flow downwards causing the roadbed to seriously subside. In that condition, the measure of dredging and burying industrial material for insulating against ground and surface water penetrating into the roadbed is taken. For example, in some roadbeds in the northeast, the height at the center of the embankment is 1.5-1.7 m, the roadbed has a large amount of subsidence every year from surface water and shallow ground water crossing the embankment from the upper side of the line. Thus, other than the constructed berm in the section, a two layered polystyrene foam slab is paved at the bottom of the berm, and a one layered chloroprene rubber slab is paved under that. The two kinds of slabs are vertically buried to a certain depth under the ground water table 2.0 m from the slopefoot of the other side of the berm and standard berm is constructed (Fig.2).

After the water insulation industrial material is set up in the section, ground and surface water could not flow and penetrate into the roadbed, but a large amount of water accumulated in the berm slopefoot at the side of the upper roadbed. In order to eliminate harmful accumulating water on the roadbed or to prevent damage in the nearby roadbed section without water insulation, a new culvert is constructed in the lowest area of the roadbed so that water accumulation in the slopefoot of the berm quickly drains and makes the base of the nearby embankment in a long-term dry state.

In the low embankment, when the depth of the ballast puddle ditch is more than 1 m, one layer of soil material to prevent water penetration should be paved under the roadbed to prevent the damage from roadbed subsidence and for protecting against potholes that allow rain to

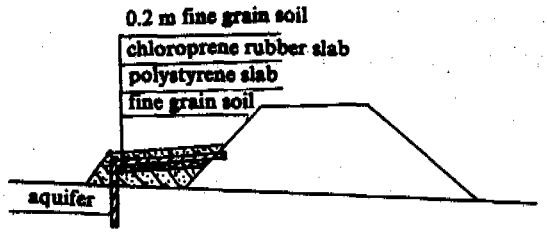

Fig.2 Diagram of a buried shallow shaped insulating water slab

penetrate into the embankment and the base through the ballast puddle ditch.

2. Deep depth: when the depth of the ground water is deeper or themokarst lakes exist near the roadbed, because the water penetrates into the roadbed base and produces a large amount of subsidence, the treatment method of using deeply buried water insulating industrial material is used. An example is that there exist several thermokarst lakes which are 7 m from the slope-foot of the roadbed which has a height of 3-4 m, in order to prevent damage from a large number of subsidences caused by the lake water pentrating into the roadbed, water insulating industrial material is buried in one side above the roadbed. The ground water bearing bed is dug away and a chloroprene rubber slab is vertically buried, with the largest buried depth being 4 m, then soil is refilled to the surface to form a "water stoppage wall", meanwhile the surface water between the slopefoot of the embankment and the water stoppage wall is prevented from penetrating into the roadbed and this prevents subsidence of the roadbed. On the other hand, a drainage ditch is constructed and the original drainage ditch is renovated in the upper side of the thermokarst lake so that the surface water supplying the thermokarst lake is cut off. Before renovation, there is a little water flow in the original drainage ditch and in the nearby roadbed. After renovation a large amount of water flow obviously accumulates in the ditch and drains away through the bearing culvert. After the above mentioned section is renevated by dredging and water insulation, the final results are being observed at present.

DEVELOPMENT TREND OF SUBSIDENCE DAMAGE OF ROADBEDS IN THE FUTURE

Since the last century, permafrost in undeveloped regions in Da Hinggan Ling of China is in the stage of degeneration due to the gradual warming of the climate. In fact, not only the climate has the trend of warming in Da Hinggan Ling region, but the permafrost as well, which has produced regional degeneration in the south and southwest regions, these regions have not been influenced by human activity in the last ten years according to observations. The existing animal and plant life have been greatly changed by permafrost degeneration, so the plant coenosium and animal type that originally existed in the region have seriously changed.

In the southern regions with permafrost degeneration not effected by human activity (such as the upper reaches of the Nanwen river and Hala river), latch, pinus sylvestris, etc., which is suited to a permafrost environment have obviously decreased. Aagiospermous forest, fallow and herbaceous vegetation which are suited to extensively distributed talik environment are increasing. Meanwhile the animal life which is found in permafrost regions has been significantly changed (Shi Yafeng, 1986).

Because the global climate is rapidly becoming warmer the southern boundary of permafrost will vanish from the Da Hinggan Ling region in China by the year 2030. The degenerative process of permafrost in this region will also be further aggravated by the increasing development and construction taking place. This process will happen very quickly so that in the next ten years the original composition and cryogenic texture of the frozen soil layer will be seriously changed. The bearing capacity of permafrost and thawing soil will be obviously decreased after the temperature rises, the deformation capacity will quickly increase and thaw settlement action will also increase. Meanwhile a large number of engineering buildings will be destroyed by many deformations. In railway roadbeds in permafrost swamp regions there will be produced lasting, undepleated and large scale thaw settlement so the question of thaw settlement in roadbeds which is originally difficult to renovate will become more intricate. How this situation will be handled can not be determined at present.

REFERENCES

Shi Yafeng,(1986) Big Changes in Climate and Environment will Appear in Whole Earth, Scientific Newspaper, 3.29.

Yuan Haiyi, (1987) Definating Permafrost in Da Hinggan Ling Region, Proceedings of the Third Chinese Conference on Permafrost, Publishing House of Science.

THAW-CONSOLIDATION OF UNSATURATED FROZEN SOIL

Yang Lifeng, Xu Bomeng and Lu Xingliang

Research Iistitute of Water Conservancy Committee of Songhua-Liao Rive Basin, China

In recent years, we have conducted research on the thaw-consolidation of unsaturated frozen soils. Taking loam obtained from the right tank of Heilong River as an example, the research results are discussed. The results indicate that the saturation of frozen soils has an important effect on their thaw-consloidation properties. Consequently, the quantitative evaluation of thaw-consolidation of frozen soil should be determinde in terms of its saturation. For unsaturated frozen soils, thaw-consolidation properties will be affected not only by their moisture content, but also by dry densities. Comprehensive effect of the both factors on thaw-consolidation properties would not be the same as that of saturated frozen soils. Based on the test data, the equations of calculating thaw-consolidation coefficients of frozen soils are presented.

INTRODUCTION

The construction experience in cold regions tells us that in frozen ground, expecially in permafrost zones, thaw-consolidation of frozen foundation soil is the main cause of the engineering structure settlement, even damage. Thus, in years of study, the principles and features of thaw-consilidation of frozen soil is one of the most important research areas.

The previous investigations(Wu Ziwang 1981,Cheng Xiaobo 1981, Zhu Yuanlin 1982 and Tong Changjiang 1985 et al.) show that thaw-consolidation of frozen soils were mostly evaluated by the moisture content. Strictly speaking, it is suitable only for the saturated frozen soil but not for unsaturated frozen soil. To correctly evaluate the thaw-consolidation properties of unsaturated frozen soils, taking loam as an example, we have conducted experimental research and obtained the special law which describes the multiple influence of dry density and moisture content on the thaw-consolidation of unsaturated frozen soils.

TEST CONDITIONS

Experiments were carried out on the frozen soil thaw-compression meter. The soil samples consisting of medium-loam and heavy-loam were obtained from the right bank of Heilong River. To bring to light the law of thaw-consolidation properties of frozen soils, besides a few experiments made undisturbed frozen soil samples, we mainly carried out simulated tests with the soils taken from in-site. Firstly, soil samples were prepared to have different dry densities and moisture contents, then frozen in single direction. The samples were 2.5cm high with diameter of 6.4cm. The preload on the samples was 0.01MPa. The thaw-consolidation deformation was directly measured with a micrometer.

ANALYSIS OF TEST RESULTS

The magnitude of thaw-consolidation is directly governed by the decrease in porosity, which is related to the dry density and moisture content.

When frozen soil is in saturated condition, the moisture and dry density or porosity have a quantitative relatyion as follows(Yin Zhijian,1980)

$$\frac{Gr_d w}{r_w G - r_d} = 1 \qquad (1)$$

or

$$Gw = e \qquad (2)$$

where G is specific gravity of the soil grain; W, $r_d$and e are the saturated moisture content, dry density and porosity of frozen soil, respectively;$r_w$is the density of pure water at 4°C.

Therefore. the saturated moisture content may be taken to characterize the magnitude of the void ratio, the reverse is ture. Thus the general effect of saturated moisture content and dry density (or porosity) on the frozen soil thaw-consolidation may be termed as single effect of moisture content or dry density, namely, thaw-consolidation coefficient A_o (relative thaw-consolidation quantity expressed as a percentage) may be expressed as follows.

$$A_o = f_1 (w) \qquad (3)$$

or

$$A_o = f_2 (r_d) \qquad (4)$$

However, when frozen soil is in an unsaturated condition, there is not a definite quantitative relation between moisture content and dry density (or void ratio). Thus, depending upon the conditions of dry density and moisture content, the thaw-consolidation characteristics of unsaturated frozen soils will be not the

same as that of saturated frozen soil. Based on the testdata, the thaw–consolidation characteristics of unsaturated frozen soil are discussed.

The Relation of Thaw–Consolidation Coefficient to Dry Density and Moisture Content

The test results indicate that thaw–consolidation characteristics of frozen soils depends upon both dry density and moisture content, the test data is ploted in Fig.1. The general tendency is that with either of dry density or moisture content changing, variation of thaw–consolidation coefficient would take place, which is obvi-

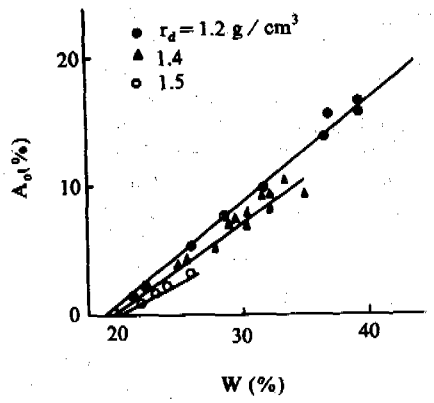

Fig.1 Relationship of A_o with $r_d$and w
(heavy silty loam, W_p = 17%)

ously different from the thaw–consolidation characteristics of saturated frozen soils.Simultaneously, the thaw–consolidation coefficient decreases with dry density increasing and moisture content decreasing.

It is not difficult to understand the phenomena mentioned above. It is well kmownthat in geotechnique, dry density and void ratio are the two indexs describing the density of soil. The high density of soil shows the intervals of soil grains being small, and certainly,the relative displacement between soil grains in the thaw–consolidation process would be small, Thus, the thaw–consolidation coefficient is in inverse proportion to dry density. Besides, in the process of soil freezing, the compactive action on the soil grains formed by the ice crystals strengthens as moisture content increases. Such action to thaw–consolidation can not be caught up by the dead weight. Thus, even if two samples have the same dry density, while their moisture contents are different, the thaw–consolidation coefficient for the two samples will be not the same. In this condition the higher the moisture the greater the thaw–consolidation coefficient is.

Besides, it can also be seen from fig.1 that under unsaturated conditions, the initial moisture content of frozen soil thaw–consolidation w_o is not a definite value as it is under saturated conditions. At this time, it varies as dry density changes although the range of such variation is smaller. The research concerned on the initial thaw–consolidation moisture content of frozen soil indicates that the initial thaw–consolidation moisture content is close to the plastic limit w_p of the soil. The data in fig.1 show that there is a similar conclusion obtained by the author of using unsaturated soil. Thereby, in practice, when the initial thaw–consolidation moisture content is unknown, it may be replaceed with w_p.

The objective existance of the initial thaw–consolidation moisture content means that only the part of the natural moisture content over the initial thaw–consolidation moisture content is the efficient moisture causing the thaw–consolidation process of frozen soil. Thus, in general, this part of moisture is called the efficient thaw–consolidation moisture content W_e (Zhu Yuanlin 1982), namely

$$W_e = w - w_o \tag{5}$$

The efficient thaw–consolidation moisture content essentially reveals the effect of moisture content on thaw–consolidation characteristics.

The Law of Combined Effect of Dry Density and Moisture on the Thaw–Consolidation Property of Frozen Soil

In summary, in order to reflect the combined effect of dry density and moisture content on the thaw–consolidation property of frozen soil, the test data were arranged, taking $R=W_e / r_d$ as a variable and replacing the initial thaw–consolidation moisture content by plastic limit. The results are shown in fig.2. It is illustrated in this fig. That there exists a good linear relation between the thaw–consolidation coefficient of heavy loam and variable. It is demonstrated from this that taking $R = W_e / r_d$ as a variable can really reflect the inherent law of the combined effect of dry density and moisture content on the thaw–consolidation coefficient. By analyzing with the test square method, the optimum probable value of the thaw–consolidation coefficient A_o of frozen heavy silty loam can be obtained as follows

$$A_o = 0.97\left(\frac{W - W_p}{r_d} - 0.02\right) \tag{6}$$

(Coefficient of correlation r = 0.98)

Similarly, using the above mentioned method, the relation of thaw–consolidation coefficient of medium loam to its dry density and moisture content can also be obtained as follows

$$A_o = 1.1\left(\frac{W - W_p}{r_d} - 0.0039\right) \tag{7}$$

(Coefficient of correlation r = 0.99)

It can be seen from above two formulas that while $A_o = 0$, $(W-W_p) / r_d$ is a constant, namely

$$(W-W_p) / r_d = B \tag{8}$$

In other words, under unsaturated conditions, when the relation between moisture content and dry density is satisfied, the thaw–consolidation phenomenon would not occur. In formula (8), B is the parameter concerned with soil properties.

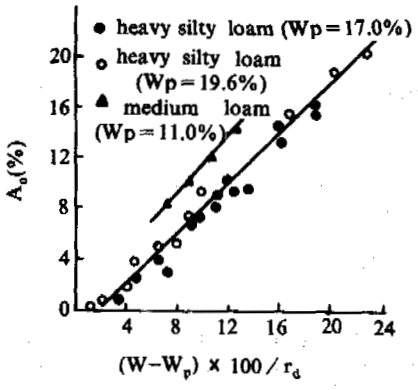

Fig.2 Variation of A_o vs. $(w-w_p) / r_d$

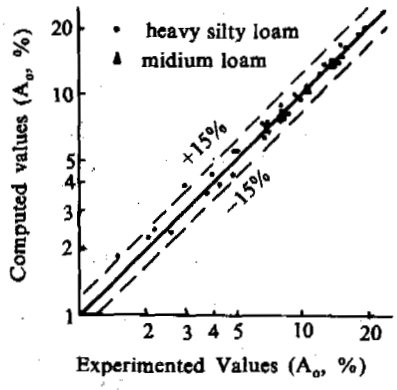

Fig.3 Comparision of computed and tested values of A_o

Verifying and Discussing

While putting the computed values of formulas (6) and (7) to be compared with corresponding test values(Fig.3), as will be readily seen, both of them coincide well. Most of the relative errors between computed and test values do not exceeds 15%.

Having formula (8) simply changed, we asn obtain

$$W_o = W_p + Br_d \qquad (9)$$

which verifies the above related analysis that under unsaturated conditions the initial thaw–consolidation moisture content of frozen soil is in direct propertion to dry density.

In existing information, the combined effect of dry density and moisture content on thaw–consolidation of frozen soils is not considered, the belief being that either of then may be used to express thaw–consolidation characteristics of frozen soils. As a consequence, two formulas considered to be equivalent were derived from dry density and moisture content, correspondingly. Both experiments and computations indicate that only under saturated conditions can the two formulas be equivalent and unitive, that is to say, what is expressed by them is the thaw–consolidation properties in a given condition of saturated soil. Therefore, they are not suitable for unsaturated soils. Whereas, formulas (6) and (7) have unitedly reflected the multiple effect of dry density and moisture content on thaw–consolidation properties of frozen soil, eliminating calculated deviations from using different formulas.

CONCLUSION

The following conclusions are obtained from this investigation:

1. Under unsaturated conditions, the thaw–consolidation properties of frozen soils depend upon the combinative effect of dry density and density and moisture content, the law of which is

$$A_o = A\left(\frac{W - W_p}{r_d} B\right)$$

where A and B are parameters concerned with soil properties.

2.Under unsaturated condition, the initial thaw–consolidation moisture content, plastic limit and dry density satisfy following relationship

$$W_o = W_p + Br_d$$

3.The calculated values obtained by the formulas in this paper coincide well with the experimental results, the relative deviation between them does not exceed 15% in general.

4.Through the study of thaw–consolidation properties of unsaturated frozen soils, it is indicated that the method used in this study has generality without being limitted by soil properties. It may also give as a reference to the thaw–consolidation properties of seasonally frozen soil.

REFERENCES

Wu Ziwang etal, 1981, Preliminary studyof thawing–sinking characte–ristics of frozen soils, Professional Papers of Lanzhou Institute of Cryopedology, Chinese Academy of Sciences No.2, Science Press, Beijing.

Chen Xiaobo, 1981, The thawing–sinking and compression characteristics of frozen soils of Muli region, Qilian mountains, Professional Papers of Lanzhou Institute of Cryopedoligy, Chinese Academy of Sciences, No.2, Science Press, Beijing.

Tong Changjiang, 1985, Thaw–consolidation behavior of seasonally frozen ground, Fourth Int. Symp. on Ground Freezing,pp.159–163.

Yin Zhijian et al, 1980, Geotechnics and Foundation, Pub.Constructional Industry,Beijing,China.

Zhu Yuanlin et al, 1982, The thawing–sinking of frozen soils, Proceedings of Chinese Society of Glaciology and Geocryology Conference (Selection, Geo–cryology), Science Press, Beijing, China.

NOTCHED CHARPY BAR IMPACT TEST ON FROZEN SOIL

Yu Qihao Zhu Yuanlin

State Key Laboratory of Frozen Soil Engineering, LIGG, CAS,China

A series of notched Charpy bar impact tests were conducted on remolded frozen Lanzhou fine sand, Lanzhou silt and Wuxi silty clay under different temperature, water content, dry density. The results show that the absorbed energy in fracture of frozen soil increases with decreasing temperature, increasing water content and dry density. The tradional impact test method of fracture mechanics was firstly used in the field of frozen soil mechanics in this study. The regularity and rationality of the testing results show that this attempt is practical. Further more, this work makes a good foundation for future research work in the field.

INTRODUCTION

In permafrost regions many engineering were in progress, such as making foundations of buildings, highway and bridges, water conservancy projects and exploring minerals and so on. None of them has no relationship with excavating of frozen soil. In this case, some problems about the excavating strength of frozen soil were involved. For lacking of expermental data and theoritical guid, engineers could not design the machines effectively and economicaly to process the frozen soil (Zhang S. X., 1992). So the study on such problem is of great significiance for the designing of the excavating method of frozen soil in various projects.

There are only a few materials about the cutting and impacting penetration strength of frozen soil. The earliest studies started in 1950s. The institute of exploring mineral in USSR applied a standard cut with a simple section (flat wedge) to study on the cutting strength of frozen soil (H. A. Cuitocich, 1985). At the same time, the institute of road in USSR adopted a standard impacting head to study on the strength of frozen soil. In recent period, with the needs of projects, Zhang Zhaoxiang (zhang S.X., 1992) from Beijing Agriculture Engineering University did a deep research on the process and speciality of the impacting penetration with self-designed quick triaxis experiment plate and auto-impacting penetrator. Meanwhile he did some experiments on the cutting strength of frozen soil. In the same period, Wang Shuwen (Wang S.W., 1989) studied on the relations among the impacting penetration index, impacting penetration resistance and the various influencing factors and has got some good results. In addition, Ladanyi (Ladanyi, 1976) has also done some experiments on impacting penetration of frozen soil at different impacting speed.

The purpose of this study is to investigate the effect of temperature, water content and drydensity on the fracture absorbed energy of remolded frozen Lanzhou sand, Lanzhou silt and Wuxi clay. The test progrom was as follows: 1) the samples with same dry density (sand and silt are 1.5g / cm^3,clay is 1.4g / cm^3) and different water content (sand and silt from 8.9 to 18%, clay from 23.3 to 28.8%) were tested at three different temperature −5, −10, −15°C, respectively. 2) with same water content (sand and silt are 10%, clay is 27.7%) and different dry density (sand and silt are 1.4 to 1.55g / cm^3, clay is 1.3 to 1.45g / cm^3), the samples were also tested at three differert temperature −5, −10, −15°C.

SAMPLES AND THERE PREPARATION

The materials used in this study was remolded Lanzhou sand, Lanzhou silt and Wuxi clay. There main physical properities are as Table 1, Table 2, and Figure 1.

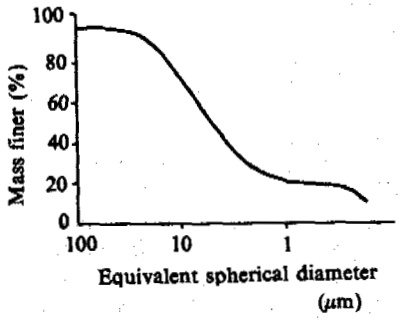

Fig.1 Cumulative mass percent finer vs. diameter of Wuxi clay

Table 1. Physical Parameter of Silt

Soil	Composition of grain size(%)				Gravity	Liquid limit	Plastic limit
name	>0.1	0.1–0.05	0.05–0.005	<0.005		(%)	(%)
Lanzhou loess	1.7	5.4	58.6	34.3	2.7	24.6	17.7

Table 2. Physical parameter of Lanzhou sand

Grain size(mm)	>0.5	0.5–0.25	0.25–0.1	<0.1
Content(%)	0.2	15.2	73.9	9.3

INSTRUMENTS AND TEST PRINCIPLES

The impacting test machine, auto-recordor, electric rammer were used in this test.

The amount of energy absorbed by the notched Charpy bar can be measured by the machine as shown in Figure 2. Diagram shows that impact hammer W dropping from height h1, impacting sample at C and rising to maximum final height h2. Energy absorbed by sample, related to height difference h2–h1, is recorded on dial D.

The testing soils are first dealed with according to testing requirements, then they are made to samples with models and be frozen quickly. The ready-made samples are cuboid shape with its height as 50mm, width as 70mm and length as 225mm and in the middle part of the samples bottom there is a notch which is 8mm in height and 45C in angle.

RESULTS AND DISCUSSION

The Influence of Temperature

When the temperature changes, the cementing ice, unfrozen water content and the strength of ice will also change. These changings influent on the absorbed energy of sample. In the range of testing temperature. The cementing ice and unfrozen water content is much more stronger than that of the strength of ice. The Boltzman law of thermodynamics theory thinks that the number of active molecules with active energy U can be expressed as:

$$N = N_0 e^{-\frac{U}{KT}} \qquad (1)$$

where k is a boltzman constant, T is the absolute temperature,N is number of active molecules.

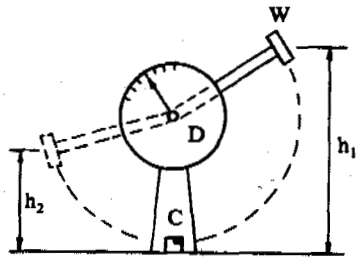

Fig.2 The Principle of impact machine

The above formula shows that the value of N goes down e.g. the number of active molecules decreases with decreasing of temperature. In frozen soils, it presents the decreasing of unfrozen water content or increasing of cementing ice content. As what Cuitovich described, the speciality of ice is that the linking action of hydrogen atoms is very weak. But the activity of hydrogen atoms becomes weaker with decreasing of temperature. This results in more strengthenning of ice structure. Of couse, this situstion makes the absorbed energy increase. (Fig.3, Fig.4, Fig.5)

Based on the data from three kinds of soils in the range of test temperature, a regression equation can be used to describe the relation between the absorbed energy and temperature.

$$CVN = A(\theta / \theta_0) + B \qquad (2)$$

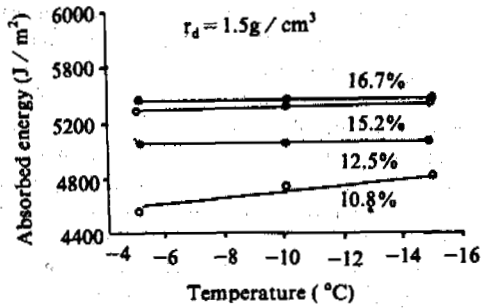

Fig.3 The absorbed energy vs. temperature with different water content

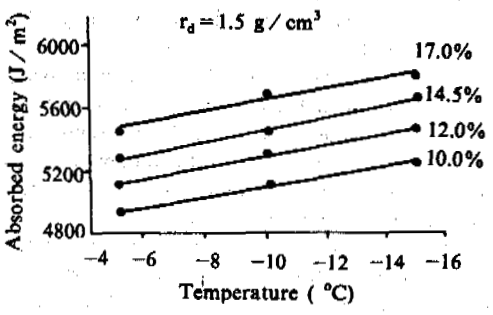

Fig.4 The absorbed energy vs. temperature with different water content

where CVN is the absorbed energy, A and B are parameters, θ is minus temperature (°C), θ_0 is a reference temperature (−1°C)

The Influence of Water Content

The influence of water content on impacting test is similar to that of temperature. The cementing ice content increases with increasing of water content under the same conditions. This makes the pores become more and more smaller. The strength of the samples increases. In terms of the absorbed energy, it also increases with the increasing of water content (Fig.6, Fig.7, Fig.8). But the trends are different for different types of soils. The results can be described respectively as follows:

for sand:

$$CVN = (C \cdot W + D) \qquad (3)$$

for silt:

$$CVN = W / (E \cdot W + F) \qquad (4)$$

for clay:

$$CVN = G\,\mathrm{Log}W + H \qquad (5)$$

where, CVN is the absorbed energy, W is the water content, C, D, E, F, G, and H are test parameters.

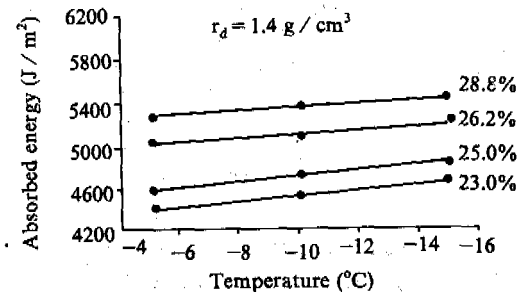

Fig.5 The absorbed energy vs. temperature with different water content

The Influence of Dry Density

With increasing of dry density, the distance between soil grains becomes shorter. The connecting surface and cementing ice content increase. This results in the increasing of the linking strength among soil grains. So the absorbed energy increases with increasing of soil dry density. The data show that the frictional angle of sand starts to influent on its strength at critical dry density. And its strength increases quickly when the dry density gets over this critical value (Chamberlain, 1972).

In the same general trend, there are different laws about the absorbed energy changing corresponding to sand, silt, and clay respectively because of internal reasons (Fig.9, Fig.10, Fig.11). Under the conditions of same water content and dry density, the changing scale of absorbed energy of sand is 12% higher than that of silt. Inparticularly, the curveof the absorbed energy changing with the dry density of silt is clearly different from that of sand and clay. It increases slowly in non−linear type when the dry density is

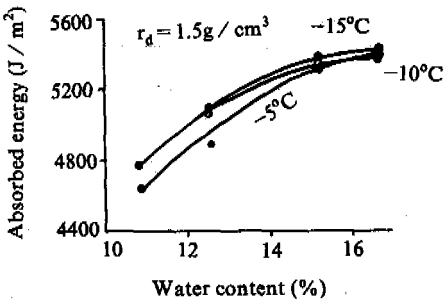

Fig.6 The absorbed energy vs. water content (sand)

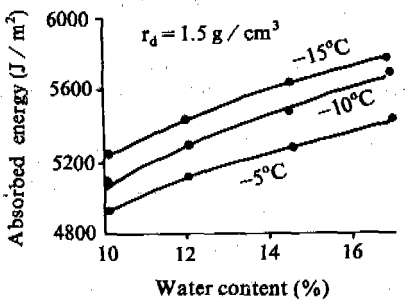

Fig.7 The absorbed energy vs. water content (silt)

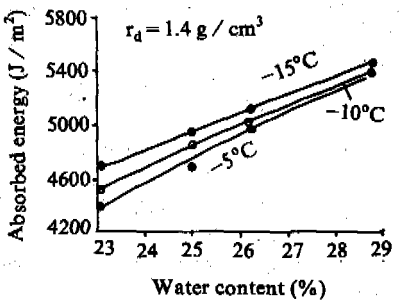

Fig.8 The absorbed energy vs. water content (clay)

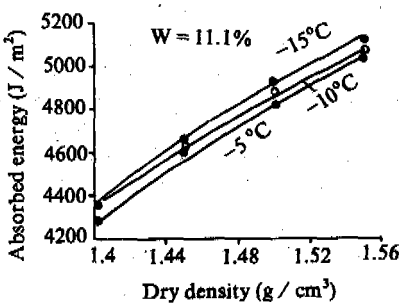

Fig.9 The absorbed energy vs. dry density (sand)

lower than 1.45g / $cm^3$and increases fast in similar linear type when the dry density is higher than 1.45g / cm^3. The grains of clay are very small and their ratio surface is very big. It's difficult for the grains to connect well each other. Its absorbed energy is mainly from the amount of cementing ice. The internal frictional force has little effect on the absorbed energy. Its changing law likes that of sand.

We work out three equations as follows:

for sand:

$$CVN=(K \cdot r_d+L)^{1/4} \qquad (6)$$

for silt:

$$CVN=\sqrt{\frac{1}{(M \cdot r_d+N)}} \qquad (7)$$

for clay:

$$CVN=R \cdot \mathrm{Sin}(r_d)+S \qquad (8)$$

where, $r_d$is dry density (g / cm^3);K,L,M,N,R, and S are test parameters.

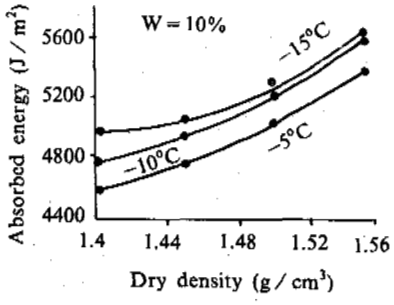

Fig.10 The absorbed energy vs. dry density (silt)

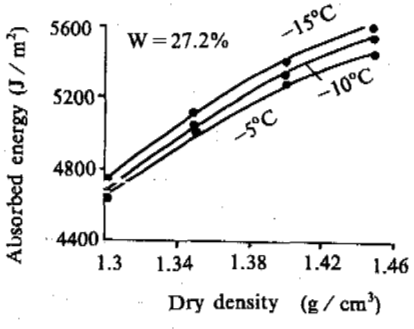

Fig.11 The absorbed energy vs. dry density (clay)

CNCLUSIONS

With the traditional notched Charpy bar impact test in fracture mechanics, the value CVN of frozen soil were firstly investigated. It shows that the results are resonable and this method can be used in the study of frozen soil, and the methods and theories in fracture mechanics can be completely introduced into the field of frozen soil mechanics.

Following with the decreasing in temperature, the value CVN increases continuously. The CVN changing range of sand is not great. But the range of silt and clay is bigger than sand .

With increasing of water content, the absorbed energy also increases in non-linear for the three types of soils. The send is biggest in changing range and at the point of 15% it obviously has an inflection point. The changing range of silt and clay is relatively smooth and there are not inflection points.

Following the increasing of dry density, the CVN value also has a similar case as the former. Under the same conditions, the changing range of CVN value of sand is usually greater than that of silt by 12%. Moreover, there is a inflection point on the curve of CVN VS. dry density at the dry density 1.45g / cm^3. Before this point the value of CVN increases slowly, and after increases fast.

REFERENCE

Zhang Shaoxiang, 1992, The Mechanics Characteristics and there relations of Instantaneous Strength of Impacting Penetration and Cutting, Ph. D paper, Beijing Agriculture Engineering University. P3–16.

Cuitovich,H.A., 1985, Frozen Soil Mechanics, Science Press, Beijing. P464.

Ladanyi,B., 1976, Use of the Static Penetration Test in Soils, Cana. Geotech. J. Vol.13, No.13.

Chamberlain, 1972, The Mechanical Behavior of Frozen Earth Maperialsunder High Pressure Triaxial Test Conditions. P76–78.

Wang Shuweng, 1989, Study on the Technology of Field Testing of Frozen Soil Strength, M.D. paper, Beijing Agriculture Engineering University.P3–48.

PERMAFROST CHARACTERISTICS AND THE EXPLOITATION AND UTILIZATION OF GROUND WATER IN HANJIAYUAN, DA HINGGAN LING, CHINA

Yuan Haiyi and Liu Xuekui

Heilongjiang Institute of Forestry design, Heilongjiang Province

Many geological and engineering geological investigations and designs have been done in the Heilongjiang area, Da Hinggan Ling. The investigations indicated that the permafrost in Hanjiayuan area is deteriorating rapidly. This results in the change of the hydrogeological conditions and poses new problems in the areas of utilizing and exploiting ground water.

INTRODUCTION

Hanjiayuan area (125°39'00"—125°51'13"E, 52°0'6"-52°5'12"N) is located in Huma county, Heilongjiang Province. The area is about 32 km². In order to select the optimum schemes for constructing Hanjiayuan Forest Bureau, our institute undertook many hydrogeological and engineering geological investigations, physical prospecting and designs from 1985 to 1992, and has done detailed research on the permafrost characteristics and the exploitation and utilization of ground water. The research provided scientific information for constructing Hanjiayuan Forest Bureau, frost damage prevention and reasonable exploitation and utilization of ground water resources.

DISTRIBUTION OF THE CHARACTERISTICS OF PERMAFROST IN HANJIAYUAN AREA

Hanjiayuan area lies on the eastern slope of Da Hinggan Ling. The mean annual air temperature in the area is -2.6°C, the maximum air temperature is 38°C and the minimum air temperature is -48°C. The area includes the Weileigeng River and its branches, which include the inflow and outflow rivers, Changqingou River, Jinjiagou River, Laohuibaogou River and Xinhuibagou River.

Weileigeng River originates in the northern slope of Yilihule mountain and crosses Fuxili from the west to east, through Hanjiayuan, and finally reaches the Huma River. The width of the river bed is 50-90 m, the river depth is 0.5-2.0 m, and the maximum discharge is 229.42 ton/s. The rivers in this area are controlled by different factors.

The area is in the intermontane valleys. The vegetation on the mountains are Larixgemlinii, Betula sylvestris, Populus davidiana, etc. In the valleys, shrubs and gress are exuberant. Some regions have been cultivated.

The distribution of permafrost is controlled by climate, hydrology, geology and geomorphology, and presents a special rule on the low ridges. Granite is distributed widely. High forests are exhuberant. In local areas, the bedrock is bare. Because of the increase of global temperature, permafrost has deteriorated on the footslopes and little remains (Guo Dongxin, 1981). In the valley areas around the drainage and branches of the Weileigeng River, the topography is flat and there are a lot of tussock hummocks. In this area, permafrost is well developed and in the local bare areas there are taliks (Fig.1).

HYDROLOGICAL CHARACTERISTICS

The hydrological conditions in this area are controlled by geology, geomorphology, hydrology, geological texture, and permafrost. The structural system belongs to a latitudinal structure belt of Yilihuli, the anticlinorium of Jiagedaqi and the southern edge of the weileigeng rise. From the results of physical prospecting, there are two structure lines in this area. One is the main structure line along Weileigeng River from west to east, and the other is along the out flow tributary of Weileigeng and Jingjiagou River. The two lines belong to a compression structure belt (see Fig.2).

Quaternary deposits are simple. There is only granite of the Variscan period from the Neopaleozoic era. The granite mainly consists of diorit granite, andesite granite, biotite granite, etc., which is distributed in the low rolling ridges and forms the bedrock of Quaternary deposits. Quaternary deposits are mainly distributed in the valley area. The lithology is course sand, middle sand and gravel. The characteristics of hydrology are controlled by geology, geomorphology, hydrology, geological structures and permafrost. The characteristics are listed below:

1. The Types of Ground Water

There are two types of ground water: Water in

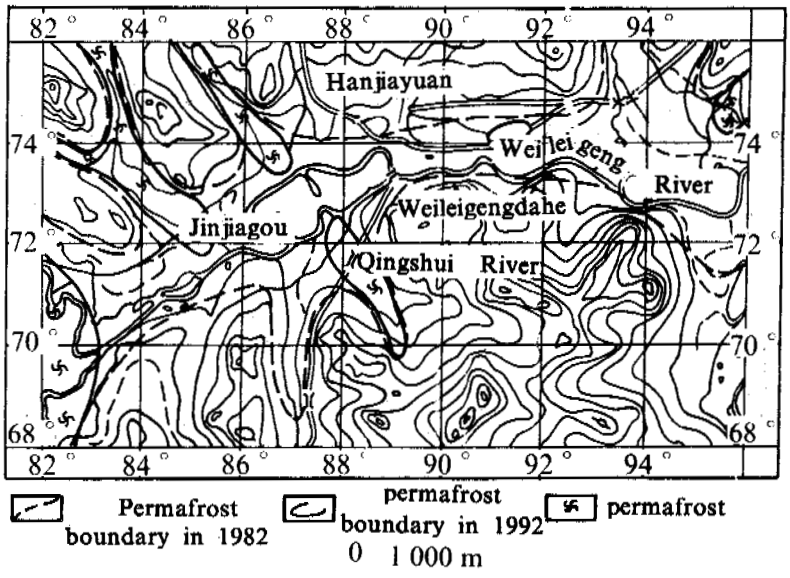

Fig.1 The distribution of permafrost

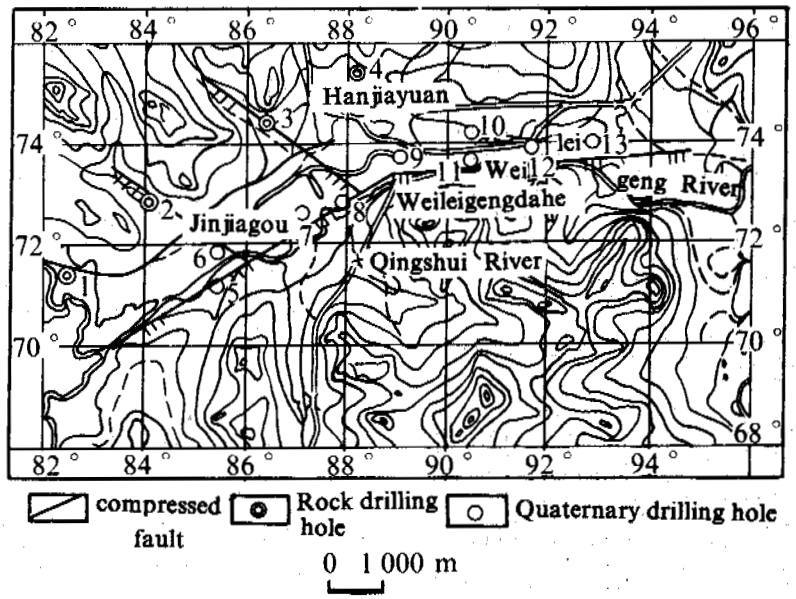

Fig.2 Geological texture

rock fractures and in pores of the Quaternary deposits. The water in the rock fractures is controlled by an expression structure, the quality is not rich. The water in pores (phreatic water) is influenced by permafrost. It only occurs in local areas (taliks) of the Weileigeng River. This branch is frozen, because the Quaternary layer is thin, therefore,there is no phreatic water in the Quaternary layer.

2. The Quality of Ground Water

The type of water in rock fractures is HCO_3-Ca-Na and HCO_3-Ca-Mg, pH>7, the mineralization degree is 0.428g/1, and the water hardness is 5.42 H. The types of water in the Quaternary pores is HCO_3-Ca, HCO_3-SO -CaMg, ph<7. The mineralization is 0.428g/1, and the water hardness is 5.88H. It belongs to low mineralized water.

3. The Supply of Ground Water

The supply of water in rock fractures is mainly from precipitation. It penetrates into the weathering fractures and texture fractures. Because it is limited by the conditions of topography (the lolling and slope degree). Phreatic water in the pores of the Quaternary deposits occurs only, like convexity, in some parts of the drainage area of Weileigeng River. The supply condition is complex. The quality of the vertical supply is less, because of the lesser area of water accumulation. It is mainly the horizontal supply from the rock fractures.

4. The State of Ground Water

From 1987-1992's observation information in low water periods, the phreatic water in the pores of the Quaternary deposits reach the maximum in July, and minimum at the end of April. The time of the two extreme values is close. This is another characteristic of this area.

EXPLOITATION AND UTILIZATION OF GROUND WATER

As described above, our institute has undertaken many hydrogeological and engineering geological investigations and designs, and many boreholes have been drilled for this purpose. In order to see the situation clearly, representative boreholes were chosen and renumbered. The details are presented in Table 1 and 2.

As mentioned above, the hydrogeological conditions in this area are controlled by geology, geomorphology, geological structure and permafrost. The authors of this paper consider that the factors of geology, geomorphology and geological structure are comparatively constant and their drainages are not obvious. But the deterioration of permafrost is rapidly changing.

In the region, permafrost was distributed in Weileigeng River and its branch valleys before 1982. Thus, in the region, there was no phreatic

Table 1. Groundwater in rock fractures

Hole No.	Welling water (t/d)	Decreased depth (m)	Penetrating coefficient (m/d)	Chemical types	Mineralization (g/l)	PH	Thickness of aquifer (m)
1	107.39	41.84	0.0578	H-C-M	0.106	7.4	75
2	120.53	47.60	0.051	H-C-N	0.160	7.5	59
3	68.60	49.35	0.02	H-N	0.201	8.0	75.77
4	126.23	16.10	0.10	H-C-N	0.3188	7.8	81.80

Table 2. Phreatic water in pores of Quaternary deposits

Hole No.	Welling water (t/d)	Decreased depth (m)	Penetrating coefficient (m/d)	Chemical types	Mineralization (g/l)	PH	Thickness of aquifer (m)
5	737.16	0.450	62245	H-C-N	0.101	6.0	3.3
6	737.16	0.500	575.93	H-N-C	0.081	6.5	2.75
7	681.7	0.410	417.43	H-C-M	0.073	6.3	4.00
	902.97	1.200	326.86	H-C-M	0.128	6.3	3.15
8	853.79	0.3	1079.99	HS-CM	0.087	6.2	2.65
9	485.48	0.15	926.24	H-C-N	0.088	6.4	2.59
	566.44	0.8	457.6	H-C	0.103	6.4	2.0
10	6888.3	0.15	1473.42	H-C	0.161	6.8	2.68
	628.91	1.35	301.72	HS-CM	0.295	6.6	2.37
11	737.16	0.52	604.72	H-C-M	0.089	7.1	2.57
12	566.44	0.19	875.87	H-N-C	0.070	6.4	3.05
	1054.08	0.64	679.52	HS-CN	0.137	6.2	2.95
13	793.14	0.29	1046.31	H-C-M	0.123	6.9	2.60
	723.00	0.58	723.89	HS-NC	0.229	6.8	2.05

water in the pores of the Quaternary deposits. Only water in rock fractures existed (including weathering and structural fractures). There was subpermafrost water supplied horizontally by the water in rock fractures below the Quaternary deposits. The water was quality water with no pollution.

With the lapse of time, permafrost in this region is deteriorating rapidly, which makes the hydrogeological conditions change rapidly as well. The porous water that previously did not exist, now increases in the pores of the Quaternary deposits and is becoming the water supply resource. The water not only comes from the horizontal supply but also from vertical supply. It can accept vertical supply directly from atmospheric precipitation. The supply resource expands further. At present, the permafrost in the drainage area of Weileigeng River and in the branch areas, is becoming taliks. At the same time, the water pollution in the local area becomes intensive. This situation will

cause new problems for exploiting and utilizing the ground water in this region.

1. Water in rock fractures is not rich. The amount of water in boreholes is 100 t/d. It has a good quality and is not polluted. It basically belongs to calcium bicarbonate water and can be used as drinking water in small residential areas and should be supplied by pipes. The optimum depth of the well is 120 m, but the well mouth needs to be well covered.

2. Phreatic water in the pores of the Quaternary deposits is rich. The welling water in a single borehole is up to 1000 t/d. But the drainage area is small, the thickness of the aquifer is thin and not suitable for the storage of large amounts of water. From this, it can be used as a water resource for large or middle scale industry. A large mouthed well and penetrating channels can be used to exploit the ground water.

3. The increased area of gold mining has increased the number of inhabitants, which has destroyed the original state of phreatic water in the pores of the Quaternary deposits, and has increased the degree of pollution. The situation appears to be worsening and due to this, the water in the pores of the Quaternary deposits is not suitable for drinking water in the eastern part of Jinjiagou, but is suitable for industrial use.

4. Ground water in the western part of Jinjiagou is not polluted. The area has not been exploited at present. The water in the Quaternary deposits can be used as drinking water, but a protection belt must be established to prevent pollution. It can be exploited with a large mouthed well and penetrating channel.

RAPID DETERIORATION OF PERMAFROST

The authors of the paper "The Deteriorating Permafrost in Da Hinggan Ling" (Yuan Haiyi, 1989), generally described the deterioration. Through field tests, we verified that when plant life is destroyed, the deterioration speed of permafrost increases. The main reason is that the air temperature becomes increasingly warmer. From the information of Mehe meteorological station, the air temperature was -5°C from 1957 to 1970, and -4.4°C from 1971-1985. From the information of Huma meteorological station, the air temperature was -2.68°C in 1985, and -2.01°C in 1987. The rising air temperature, in addition to human activity, makes the permafrost deteriorate rapidly.

Hanjiayuan area, Weileigeng River and its branches are the gold enrichment zones. The mechanized mining and local mining are growing rapidly. As gold mining is developing quickly, it causes the prospering and development of highways, sideroads and farming. All of these factors cause the deterioration of permafrost. We can say with certainty, that the permafrost in the area of Hanjiayuan will deteriorate further following the construction of Hanjiayuan Bureau, and subsequent damage of vegetation.

From the information of 1982's investigation, the drainage areas of Weileigeng River and its branches were almost all occpied by permafrost and there was local sporadic permafrost.

1985 and 1987's investigation information indicated that the permafrost in the drainage of Weileigeng River and its branches, had deteriorated on a large scale. Only in local areas was there permafrost.

1992's investigation information illustrates that the remaining permafrost in the valleys of Weileigeng River and in some branch areas, has completely disappeared.

The lowered permafrost base also represents the permafrost in its deteriorating process. From 1982's survey, the permafrost base was more than 5 m (drilled into the weathering layer), 1987's surveyed results indicated that the base had risen to 3.8 m, and only in local areas was 5 m (near Jingjiagou area). According to this, the permafrost in Hanjiayuan area in Da Hinggan Ling is gradually disappearing at an accelerating rate.

REFERENCES

Guan Wuanjun, (1983) Trees in China, Forestry Publishing House of China, 929pp.

Guo Dongxin, (1981) Permafrost zonation of the Daxing Anling Range, Northeast China, Journal of Glaciology and Geocryology, 3(3), 1-9.

Yuan Haiyi, (1989) Degrading permafrost in Daxing Anling Range. In: Proceedings of the Third Chinese Conference on Frozen Ground, Science Press of China, Beijing, 54-58.

Zhang Wuanru, (1986) Forestry and soils of China. Science Press of China, Beijing, 96pp.

SEASONALLY FROZEN GROUND AND ITS BEHAVIOR ON FROST HEAVE IN THE YUMENZHEN REGION, GANSU PROVINCE, CHINA*

Yue Hansen and Qiu Guoqing

Lanzhou Institute of Glaciology and Geocryology,
Academia Sinica, Lanzhou 730000, China

The field observations in the Yumenzhen region, Gansu Province during 1985-1986 showed that the behavior of the seasonally freezing and frost heaving of ground was controlled by the local climatic conditions, geological and hydro-geological conditions. Under similar climatic conditions with a mean annual air temperature of 6.9°C and a freezing period lasting about 125 to 135 days, the grounds composed of well-drained bed rock and gravels didn't have any obvious frost heaving. The fine-graded soils had a strong-heaved with a ratio of frost heaving $\eta>6\%$ as the buried depth of ground water $Z<1.5$ m when Z equals to 1.5 to 2 m, $\eta=3-6\%$; and as $Z>2.5$ m, the η of fine-graded soils might be as low as <1%. Based on the field observations, a map showing the difference in frost heaving of ground was suggested.

INTRODUCTION

The uneven frost heaving of ground is the main reason for damage to structures in seasonally frozen regions. To survey and research the formation conditions and development processes of frost heaving in Yumenzhen region, investigations of the natural conditions and frost hazards, the stated observations in seasonally freezing and frost-heaving processes were carried out from late Autumn, 1985 to early spring, 1986. Regional division mapping of seasonal freezing was undertaken in order to illustrate the characteristics of the frost heaving of soil on the basis of the analysis of the developing conditions and the differentiation of seasonally frozen ground. The authors hope that all of the information can be the basis for the general regional planning and the controlling of frost damage in the civil engineerings of this region.

GENERAL PHYSICAL GEOGRAPHICAL FEATURES

The researched area is located in the middle reach of Sule River, in western Gansu Province, between longitude, 96°52' — 97°15'E, latitude 40°15' — 40°30'N. The area is comprised of mainly the Changma Pluvial Fan and the Fine-graded soil Plain. Its eastern and northern part is bordered by Mt. Hanxiashan and Mt. Yenmabeishan (1450-1650 m a.s.l.) respectively. Generally the terrain slopes slightly from southeast to northwest. Yumenzhen stands on the middle-lower part of Changma Pluvial Fan, 1530 m a.s.l. The front part of the Pluvial Fan stands at 1440 m a.s.l. The gentle Fine-graded Soil Plain lies at about 1400 m a.s.l. According to the observation of the Yumenzhen Meteorological Station, the annual mean air temperature is 6.9°C, the annual precipitation 61.8 mm and the mean annual evaporation is about 3000 mm.

The very thick gravel layer of the Quaternary System was deposited extensively in Changma Basin, filled by sand with a fine content of 7.2%. The subaerial layer, about 15 cm in thickness, contains a great deal of silt and clay. In the Fine-graded soil Plain, the lacustrine stratum is composed of the clayey sand and sandy clay alternately. The present eolian sand is found in a partial area on the verge of the Fine-graded Soil Plain.

Due to the incessant recharging of melt water from Mt. Qilianshan, there is abundant ground water including artesian water within Quaternary loose deposits in this region. The buried depth of ground water varies from 100 m or more at the upper part of the pluvial fan to 5-10 m by its margin, then, less than 3 m in the Fine-graded soil Plain. The ground water increases gradually in mineralization and deteriorates from south to north. Saline soils are widespreaded in the plain. The bedrock hills, lacking recharged water, are poor in ground water.

The main agricultural area in this region is the Fine-graded Soil Plain with wide-ranging farmlands and criss-crossing channels. The phenomena associated with deformation and destruction of houses, channels and roads, due to uneven frost heaving, could be seen frequently in the plain.

THE GENERAL CONDITION OF SEASONALLY FROZEN GROUND

This area posseses an arid continental climate with a warm summer and cold winter. The mean monthly air temperature from Nov. to Feb. of the next year is below 0°C, the lowest mean monthly air temperature is -10.5°C in Jan. The freezing

*This project is supported by the National Natural Science Foundation of China, the Natural Science Foundation of Gansu Province and the Gansu Provincial General Company on Agricultural Exploitation.

Table 1. Major parameters and characteristic indexes at various sites

Observation site	Yumenzhen Meteorological Station	Nantan Huanghua	Team 16 Huanghua	Team 17 Huanghua	Team 8 Yenma	Team 4 Yenma	Team 20 Yenma	Baishuei-duan
A	Clayey soil	Clayey soil	Clayey soil	Clayey soil	Clayey soil	Clayey soil	Clayey soil	Clayey soil
B	8.48	29.03	20.75	31.53	37.79	14.62	26.88	27.42
C	13	1.08	2.52	1.62	0.4	>4	1.18	1.72
D		1.29	1.50	1.09	1.07	1.55	1.28	1.40
E		1.58	0.85	3.70	0.65	0.55	6.78	0.21
F	113	63	101.8	83	78.5	99	69	75
G	0	7.4	0.8	13	24.7	0	5.2	11.2
H	113	55.6	101	70	53.8	89	68.8	63.8
I	0	13.31	0.79	18.57	45.91	0	8.15	17.55
J	End of Oct.	Mid. Oct.	Mid. Oct.	Mid. Oct.	Mid. Oct.	Mid. Oct.	Mid. Oct.	Mid. Oct.
K	Nov. 22	Nov.25	Nov.20	Nov.20	Nov.20	Nov.25	Nov.25	Nov.20
L		Dec. 8	Nov.23	Dec.13	Nov.23		Dec.28	Nov.20
M	Feb.18	Mar.10	Mar.20	Mar.15	Mar.1	Mar.5	Mar.15	Mar.10
N		Mar.10	Nov.30	Mar.15	Mar.10		Mar.15	Mar.10
O	Apr.6		Apr.15	Apr.25	Apr.25	Apr.15	Apr.20	Apr.25

A: Lithological character;
B: Water content before freezing;
C: Buried depth of ground water;
D: Dry unit weight;
E: Salt content;
F: Thickness of frozen ground;
G: Total amount of frost heaving;
H: Freezing penetrating depth;
I: Frost heaving ratio;
J: Beginning of unstable freezing;
K: Beginning of stable freezing
L: Beginning of stable frost heaving;
M: Time when freezing front reaches maximum depth;
N: Time when maximum frost heaving occurs;
O: Time when ground thawed out thoroughly.

Table 2. Temperature at Yumenzhen and Yenma Farm (1974-1976)[1), 2)]

Site	Month / Item	Jan.	Feb.	Mar.	Apr.	May	June	July	Aug.	Sept.	Oct.	Nov.	Dec.	Mean annual value
Yumenzhen	A	-9.5	-8.0	0.3	8.9	15.4	19.3	21.3	20.2	14.9	6.8	-2.7	-11.7	6.5
	B	-8.8	-5.2	-1.1	6.3	18.2	22.8	24.9	24.2	18.4	9.0	1.3	-9.2	8.1
Yenma	A	-11.5	-8.5	-1.7	7.3	14.8	19.3	20.9	19.6	13.7	5.2	-3.6	-13.9	5.2
	B	-7.1	-5.0	-1.3	3.8	10.3	16.6	19.7	18.9	14.4	6.8	-0.7	-6.7	5.8

A: Mean monthy value of air temperature;
B: Mean monthy value of ground temperature at the depth of 5 cm.
1) Depth of ground water table 11.2 m at Yumenzhen, 1.4 m at Yenma Farm;
2) The Yumenzhen Meterological Station, 1984, the analysis and division of the climatic data for agriculture, Yumen City, Gansu Province, Unpublished.

period lasts about 125 to 135 days. The ground beings to freeze in the middle of October. The maximum freezing depth of the ground occurred in late February. The thorough thawing period occurred from the middle of April to early May. The frozen period of the ground is as long as six to seven months. Generally, the freezing process in the north begins earlier than in the south while the thawing process is to the contrary.

The different combination of the geological, and geographical conditions leads to a great difference in the development process of the seasonally frozen layer in the time to reach the maximum frozen depth and to be melted thoroughly (Table 1). The thickness of the active layer changed largely at various sites, 113 cm in Yumenzhen, 101 to 60 cm in the Fine-graded Soil Plain. The formation and development of frost heaving of the soil was dramatically different in the region. On the pluvial fan there was no obvious frost heaving. On the Fine-graded Soil Plain at various sections, along with different buried depths of ground water, frost heaving of the soil occurred in different degrees, weak frost heaving when the buried depth of ground water was deeper; strong frost heaving when shallower. Table 2 also shows that the distribution of the frost heaving along the depth was greatly changeable at various sections in this region.

THE GEOGRAPHICAL DIFFERENTIATION LAW OF THE DEVELOPMENT OF SEASONALLY FROZEN GROUND

There are many complex natural geological and geographical factors influencing the formation, development and disappearance of the seasonally frozen ground. They can be grouped as follows: 1) The composition (grain size, mineral and chemical composition), texture, and buried condition of the rock and soil; 2) The initial water content before freezing in deposits and its distribution along the depth, the buried depth and their dynamics as well as chemical composition and salt content of ground water; 3) The thermal region of soil layer (Cudlevcev V.A. 1978), the geographical differentiation of the development of seasonally frozen ground is governed by the combination of the rock (or soil), water, and temperature.

The Differentiation Resultant from Geomorphic Units

The landform is the most important factor resulting in geographical differentiation. In regards to the above, the researched area can be divided into 4 parts: Changma Pluvial Fan, Fine-graded Soil Plain, Mt. Yenmabeishan and Mt. Hanxishan. These geomorphic units are different in water-heat condition, lithological characters, supply and drainage of the ground surface water, and buried depth and flow of the ground water, governing the difference and combination of soil, water and temperature in time and space, leading to the differences in development of the seasonally frozen ground.

As shown in Table 2, because the mean monthly air temperature at Yumenzhen was higher than that at Yenma Farm, the freezing of the ground surface at Yumenzhen started later than at Yenma Farm; but thawing was earlier. From south to north, along with the gradual change of the geomorphic position, the air condition, features of the soil, and buried depth of ground water, as well as, the developing conditions of the seasonally frozen ground, change correspondingly. on the Changma Pluvial Fan, the arid ground composed of gravels and sands with the deeper buried depth of ground water didn't have any obvious frost heaving under natural conditions during the observation period, while on the Fine-graded Soil Plain, under natural conditions the moist fine-graded soils with a shallower buried depth of ground water exhibited frost heaving to a certain degree. In Nantan, team 16, team 8, team 20 were examples (Table 1). In Mt. Yenmabeishan and Mt. Hanxiashan, the ground composed of well-drained bed rock with a poor water supply didn't have any frost heaving.

The Differentiations Resultant from the Buried Depth of Ground Water

In the Fine-graded Soil Plain with similar climatic conditions, the buried depth of ground water is the difinitive factor; determining the structure and chemical composition of soil, responsible for the magnitude and distribution of moisture content and thermal regime of the soil profile, leading to geographical differentiation of seasonally frozen ground. As shown in Table 1, the soil tended to densify with the increasing buried depth of ground water. Under such a natural condition, the soil moisture mainly originated from the recharge of ground water. So, water content and its distribution along the soil profile will be logically in relation to the buried depth of ground water. As shown in Table 1, the water content and salt content in the ground tended to decrease with the increasing buried depth of ground water. The buried depth of ground water was also influenced by the development situation of vegetation directly. Therefore, it was the buried depth of ground water that determined the presence and change of the various factors influencing, the freezing-thawing conditions, and that governed the different development situation of seasonally frozen ground.

The influence of buried depth of ground water on the ground temperature

The development of seasonally frozen ground is closely related to the ground temperature. The ground water, as a natural heat source, is greatly influences the soil temperature during the frozen period. As shown in Table 2, during the period from November to February of 1974 to 1976, the temperature at the depth of 5 cm at Yenma Farm was observed to be higher than that in Yumenzhen, although the air temperature was higher in the latter. This might result from the fact that the table of ground water was buried as deep as 11.2 m in the latter while 1.4 m in the former. A lower ground temperature, of course, would lead to a deeper penetration of the freezing process, as a result, the thickness of the seasonally frozen ground was observed to be 113 cm at the Yumenzhen and 99 cm at the Yenma Farm.

The effect of buried depth of ground water on the freezing process and freezing penetration

Due to the different buried depths of ground water, there was great difference in the freezing process and freezing penetration depth of soil on the various sections. Generally, the maximum freezing depth of soil would occur earlier at those places with a shallower buried depth of ground water, while the time for the soil to completely thaw was opposite. Also, the maximum freezing depth of soil would decrease

with the buried depth of ground water decreasing. For example, the soil at Team 8 of Yenma Farm where the table of ground water was bured at a depth of 0.4 m reached the maximum freezing depth of 53.8 cm on Mar. 1, thawed thoroughly after Apr. 25; at Team 20 where the buried depth of ground water water was 1.18 m, it reached the maximum freezing depth of 63.8 cm on Mar. 15, thawed thoroughly on Apr. 20; at Team 16 where the buried depth of ground water was 2.52 m, it reached the maximum freezing depth of 101 cm on Mar. 20, thawed thoroughly on Apr. 15 (Fig.1).

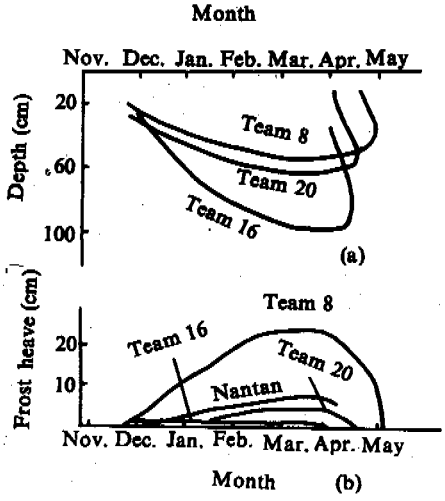

Fig.1 Dependence of freezing depth (a) and frost heave (b) on buried depth of ground water

The effect of the buried depth of ground water on the frost heaving

The process, magnitude and distribution of the frost heaving along the soil profile varied with the buried depth of ground water. Generally, as the buried depth of ground water gradually increased, the maximum frost heaving of soil occurred earlier; the total frost heaving magnitude decreased (Table 1).

In order to analyze the quantitative relationship between the frost heaving and the buried depth of ground water, the statistical quations were used, as shown below,

$$h = 41.35\ e^{-0.016z} \qquad (1)$$

$$\eta = 94.05\ e^{-0.019z}$$

where: h, Frost heaving magnitude (cm);
η, Frost heaving ratio (%);
z, Buried depth of ground water (cm).

The correlation coefficient is -0.995 for Equ.(1) and -0.997 for Equ.(2).

The Effect of Human activity

The effects of human activity were in the areas of the irrigation of farmland, the supply and drainage of water by engineering, and in changing the soil-water-temperature situation of ground greatly. Generally, the irrigation of farmland and the leakage from canals made the water content in the ground increase, impelling the frost heave especially. In the areas of Team 17 and Beishueiduan, because of the effect of canals and irrigation, the frost heaving ratio of soil increased by 14.24% and 13.97% respectively in comparison with that of the soil under natural conditions. According to investigation on Changma Pluvial fan, the surface layer containing a large fine content and a little water didn't have obvious frost heaving under natural conditions; however, where affected by the leakage of canals, the frost heaving ratio can be as high as 20% or more.

DIVISION AND CLASSIFICATION OF FROST HEAVING OF GROUND

To reflect the engineering geological conditions of seasonally frozen ground overall in this region for the general planning of civil engineering and canals to be constructed, and for the prevention and solution of the engineering from frost damage, it is necessary to classify the seasonally frozen ground in accordance with the frost heaving behaviour of soil.

Division Principle

The division was based on the comprehensive analysis of the natural factors affecting the development of seasonally frozen ground and of the natural processes, mainly to reflect the frost heaving of seasonally frozen ground under natural conditions. Considering the natural conditions and researched degree, the division may be divided into two orders.

(1) First order: Seasonally frozen ground area. According to geomorphic units, this region may be divided into: 1) Mt. Yenmabeishan seasonally frozen ground area, 2) Mt. Hanxishan seasonally frozen ground area, 3) Changma Pluvial Fan seasonally frozen ground area, and 4) the Fine-graded Soil Plain seasonally frozen ground area.

(2) Second order: Frost heaving section. Based on difference of rock (or soil) preperties, and hydro-geological conditions and mainly the buried depth of ground water, the seasonally frozen ground areas were subdivided into frost heaving sections in accordance with classification of ground foundation by frost heaving susceptibility. Due to the randomness of human activity, the frost heaving susceptibility of the ground near arterial canals was marked qualitatively.

The division of frost heaving of ground is shown in Fig.2.

Frost Heave Classification

The classification of frost heave in seasonally frozen ground is an important basic problem in Geocryology. So far, due to the complexity of the question, there is no overall reliable method to evaluate comprehensively the frost heaving susceptibility of soil foundation. Considering the aim and task of this project, the authors put forward the frost heaving classification for natural frozen ground in this region.

The principal guiding thought to classify the frost heaving susceptibility of frozen ground in this region is that the suggested classification should be able to reflect the actual situation of seasonally frozen ground under the natural conditions of this region and to harmonize it with the existing related

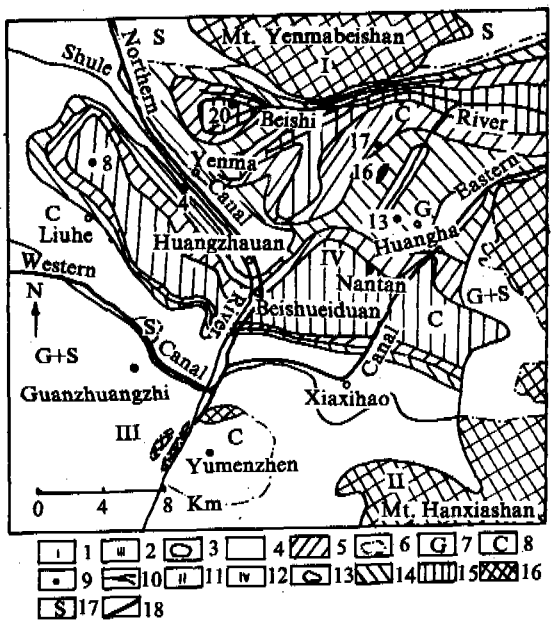

Fig.2 Division of seasonally frozen ground surrounding Yumenzhen

1. Mt. Yenmabeishan seasonally frozen ground area;
2. Changma Pluvial Fan seasonally frozen ground area;
3. Boundary of seasonally frozen ground area;
4. Unfrost-heaving section;
5. Frost-heaving section;
6. Boundary of rock and soil;
7. Gravelly soil;
8. Clayey soil;
9. Observation site;
10. River;
11. Mt. Hanxiashan seasonally frozen ground area;
12. Fine-grade soil Plain seasonally frozen ground area;
13. Boundary of frost heaving section;
14. Weak-frost heaving section;
15. Strong-frost heaving section;
16. Bedrock; 17. Sandy soil; 18. Arterial canal.

classification. Based on the fact that the buried depth of ground water and the soil character are the major factors determining the behavior of soils in frost heaving, the classification is suggested as shown in Table 3.

Table 3. Classification of foundation soils by frost heaving susceptibility

Soil	Buried depth of ground water Z(m)	Frost heaving ratio (%)	Class
Bedrock Gravel Sand	Not consided		Unfrost-heaving
Clayey soil	$Z \geq 2.5$	$\eta \leq 1$	Unfrost-heaving
	$2.5 > Z \geq 2$	$1 < \eta \leq 3$	Weak-frost heaving
	$2 > Z \geq 1.5$	$3 < \eta \leq 6$	Frost heaving
	$Z < 1.5$	$\eta > 6$	Strong-frost heaving

ACKNOWLEDGEMENTS

The authors would like to express their gratitude to Mr. Yin Rongfa, the manager of the Gansu Provicial general Company on Agricultural Exploitation, and his colleagues for their help in field works and to Prof. Cheng Guodong, Zhou Youwu and Chen Xiabai for their valuable suggestions with this paper.

REFERENCE

Cudlevcev, V.A. et al. (1978) General Geocryology, 2nd Press, Moscow University Press, p.185-230.

CULVERT ENGINEERING IN THE PERMAFROST REGION ON QINGHAI-XIZANG PLATEAU

Zhang Jinzhao and Yao Cuiqin

The First Survey and Design Institute of Highways,
The Ministry of Communications, Xian, China

This paper mainly introduces the engineering environment and characteristics of culvert engineering in the permafrost region of Qinghai-Xizang Plateau. Based on the investigation of the effects and state of culverts and the long term observation of representative culverts in the permafrost region of Qinghai-Xizang highway, and by analyzing the damage of culvert engineering and renovating the Qinghai-Xizang highway design by taking into consideration previous examples of construction, the principles of damage protection and engineering measures of culverts are given with regard to the different aspects of design, construction and maintenace. This paper can be used as reference in the areas of design, construction and maintenance of highways.

THE ENVIRONMENT AND CHARACTERISTICS OF CULVERT ENGINEERING

A part of Qinghai-Xizang highway passes through a continuous permafrost region of 520 km, the height above sea level is more than 4500 m. Heat thaw lakes and ponds are spread throughout the region, ground ice is very developed, the superpermafrost water is rich, thaw settlement, frost heave, frostchurning and other disadvantageous geologic phenomena in engineering commonly exist.

It is high and cold and the oxygen content in air is only 50% of that in the interior. The annual mean air temperature is low (about -3.0 to -6.0°C), the freezing period is more than 7-8 months of the year. Even in warm season, minus air temperatures often occur in evening. The amount of annual precipitation is 250-400 mm, it is concentrated between June and September and occurs in the solid forms of snow and hail.

Hundreds of culverts have been created in the permafrost region with a total length of 520 km along Qinghai-Xizang highway. The operating states of the culverts were carefully investigated in October, 1990. The results showed that serious damage occurred in 15% of all culverts, middle level damage occurred in 21.1% and little or no damage occurred in 63.5% of the culverts. The easily and very seriously damaged sections are the inlet buildings and culvert bottom linnings. These two types of damage make up more than 86% of all damaged culverts.

CULVERT ENGINEERING DAMAGE TYPE

The main types of culvert damage in the permafrost region of Qinghai-Xizang highway are (1) cracking and settlement of the culvert terrace, (2) cracking, breakage and settlement of the bottom lining of the culvert, (3) seepage through the bottom lining of the culvert, (4) cracking, slope and settlement of the inlet and outlet walls and flank walls of the culvert, (5) damage of the lining on the inlet and outlet and the wall to cut off water, (6) the collapse of the inlet and outlet of the culvert. The main reasons causing the damages are the changes of the permafrost table and the repeated freezing-thawing effects of the seasonal active layer.

THE PRINCIPLES TO PREVENT AND TREAT DAMAGE IN CULVERT ENGINEERING

In addition to the factors of general displacement, effective stress is closely related to the temperature acting on the permafrost and the culvert base stability affected by water latent heat must be considered for base designs in permafrost regions. Simultaneously, the corresponding engineering countermeasures to keep the demanded thermal regime during culvert construction and operation must be taken. This is a basic principle for preventing frost damage in culverts in permafrost regions.

Geothermal Characteristics

The geothermal regimes of the base of the typical culvert along Qinghai-Xizang highway were investigated, as shown in Figures 1 and 2. The figures show that at 0.5 m depth the maximum ground temperature of the culvert mouth is higher by 4-5°C than that of the culvert centre. But the difference of the temperatures is only about 1°C at 2.0 m depth between the body and mouth. Figures 3 and 4 also show the same regulation that the permafrost table beneath the culvert mouth is 1.0 m deeper than beneath the culvert centre. This indicates that (1) the air temperature effect on the culvert inlet and outlet is greater than on the culvert body, (2) the air temperature effect on the upper layer is greater than that on the deep layer, (3) in the culvert design, the base depth at the inlet and outlet of the culvert should be 0.5-1.0 m more than at the culvert centre, otherwise other

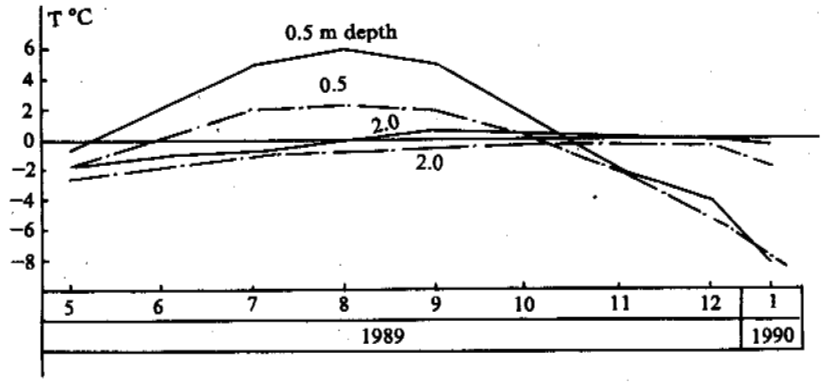

Fig.1 Ground temperature curves below the mouth and centre of culvert
——— ground temperature curves below culvert mouth;
—·—·—· ground temperature curves below culvert centre.

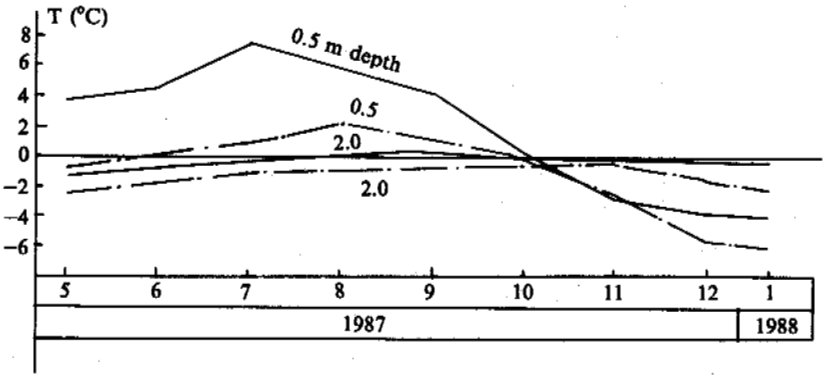

Fig.2 Ground temperature curves below the mouth and centre of culvert
——— Ground temperature curves below culvert mouth;
—·—·—· ground temperature curves below culvert centre.

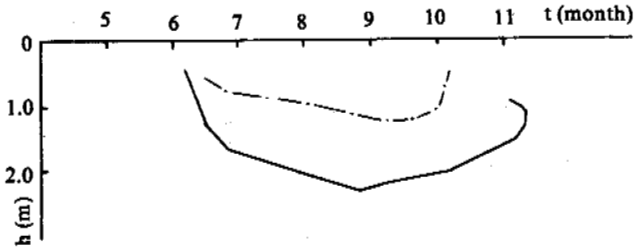

Fig.3 Curves of zero temperature below the mouth and centre of culvert
——— below culvert mouth;
—·—·— below culvert centre.

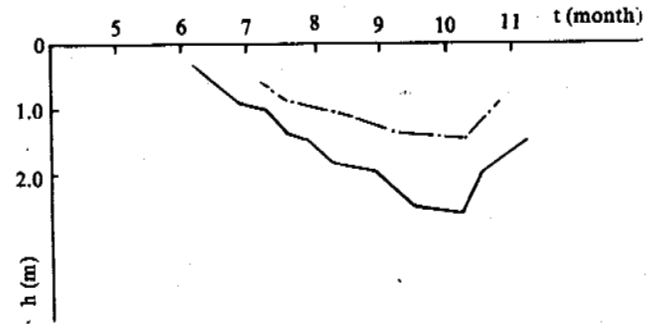

Fig.4 Curves of zero temperature below the mouth and centre of culvert
——— below culvert mouth;
—·—·— below culvert centre.

engineering countermeasures should be taken, (4) after understanding the base geothermal regimes during the operation of the culvert, reasonable culvert engineering design can be determined.

Culvert Design

Design principle

Based on the structural types and construction characteristics of culvert engineering and engineering geological and hydrological conditions in the area, two kinds of design principles can be taken. a) One is the principal of maintaining the frozen condition, i.e. the base of the culvert beneath a certain depth is kept in a frozen state during the operation of the culvert. b) Another is the principal of allowing thaw, i.e. the base of the culvert between certain depths is allowed to thaw during the operation of the culvert, the principle is only adapted to the weak thaw settlement soil and non-thaw settlement soil.

The depth of the refilled soil is closely related to the engineering cost and the effective prevention of frost damage. It is determined by the means of the structural type, the degree of allowed deformation, soil type and ice content of base soil. The two following design principles should be mainly considered.

(A) Frost heave deformation of base soil should be controlled in the range of allowed deformation of culvert engineering after being refilled.

(B) During thawing the bearing capacity of refilled soil and active layer of permafrost must satisfy the design requests, the thaw settlement amount must also satisfy the engineering requests.

In order to reduce the vertical and horizontal frost heave force, sand-gravel soil must be filled in the base bottom and around the base. Simultaneously, asphalt 1 cm in thickness should be filled into the positions where base touches the embankment. The expansion joint should be also filled with rubber asphalt that has a large deformation at low temperatures.

Because a large settlement amount in culvert engineering is allowed, it is effective to set a settlement joint to prevent and treat culvert engineering cracks caused by inhomogeneous settlement. After building the culvert the natural permafrost table beneath the culvert centre will again rise beneath the inlet and outlet of the culvert and will again descend, as shown in Table 1. In order to get a reasonable design for culverts in technique and cost, it is better to build the culvert base in sections, the sections base depths are determined by different permafrost tables.

Table 1. A comparison between man-made table and natural permafrost table

No.	Pile No.	Man-made table (m)			Natural permafrost table (m)
		Left	Centre	Right	
1	K157+373	1.68	0.65	0.83	1.75-2.10
2	K279+370	2.45	1.50	2.15	2.05-2.10
3	K287+166	2.23	1.41	1.73	1.60
4	K337+170	1.75	1.35	2.05	1.80-2.45

Choosing the structural type

In a permafrost area, the culvert structural type is the technical key to assuring the engineering quality and a lower engineering cost.

Based on design priciple I, rapid construction is the main condition to select the culvert structure. And for design priciple II, the strength and the ability of adapted deformation can be taken as the main conditions to select the culvert structure. From the investigation of the state of the culverts and the long term observation of typical culverts along Qinghai-Xizang highway, the culverts with a cover slab made with reinforced concrete, the framework structure culverts with a cover slab made with reinforced concrete, the culvert box of reinforced concrete and the culvert tube made with tin-plated alloy steel are good structural types in permafrost areas. For the culvert with a cover slab made of reinforced concrete, based on the different base conditions, different structural types can be chosen, for example, the concrete base of a strip type, concrete base in sections, etc.

Buried depth of base

The following value can be used to determined the depth.

A) For design priciple I. The base depth should be 2/3-3/4 times the depth of the natural permafrost table. The base depth at the transition section from the body to the inlet and outlet must be deeper by 0.4 m than the depth of culvert body. The base depth at the inlet and outlet must be 0.25 m beneath the natural permafrost table.

B) For design priciple II. The base depth at the culvert body can be determined by the calculation of thaw settlement. The base depths of the body and the inlet and outlet must be greater than 1.00 m and 1.25 m respectively.

The above methods are only adopted to the base of the culvert with a cover slab made of reinforced concrete.

Culvert Construction

Culvert construction in permafrost areas have many special demands besides the general demand of culvert construction.

Construction season

The cold seasons after Oct. and before May are the better construction seasons for the culverts designed with the principle of permafrost protection.

For the culvert design based on the principal of allowing thaw, the warm season from June to Sept. is the better construction season; otherwise, special designs and countermeasures must be taken.

Construction method

Because the base depth is shallower and the section of construction is scattered, the open excavation method should be taken in culvert construction. But the method has the technical problems that the labour conditions are difficult, the efficiency is low and the water-heat state of the permafrost is disturbed greatly. For resolving the disadvantageous problems, the method of demolition and rapid excavation is adapted to the permafrost along Qinghai-Xizang highway.

Notes on construction

(A) In warm season construction, the base pit can not be allowed to be exposed for long periods. The exposure time was not longer than 15 days and the construction time for whole culvert project was not longer than 50 days.

(B) After excavated, if the whole or part of the base is built on the ice and soil-content ice layer, the design must be changed and the base depth must be adjusted.

(C) Water, snow and high-water-content soil in the base pits must be cleared up due to its large latent heat.

(D) The artificial disturbance of permafrost must be reduced as much as possible.

(E) Before excavation, all material used in the base construction must be prepared.

Culvert Maintenance

Preventing damages in culverts

(A) The connected section between the culvert and the pavement must be checked frequently. If damages are discovered, relevant maintenance and repair countermeasures must be taken.

(B) A culvert platform base bears the load of the culvert and vehicles. The deformation, displacement, cracking and settlement of the base should not be allowed but when occurring should be treated quickly.

(C) The effect of water on the permafrost base and culvert is great, the unblocked culvert must be maintained and cleared when blockage occurs.

(D) Cracking and expansion joints must be checked to prevent water permeation.

CONCLUSIONS

Two kinds of design principles of culvert engineering can be taken. One is the principle of maintaining the frozen condition. Another is the principle of allowing thaw. The two priciples only adapt to the weak and non thaw settlement soil. Otherwise other countermeasure must be taken.

In the permafrost area, the selected structural type of culvert is very important for the quality and cost of engineering. The culvert with a cover slab made with reinforced concrete, the framework structure culvert with a cover slab made with reinforced concrete, the culvert box made with reinforced concrete and the culvert tube made with tin-plated alloy steel are good structural types in permafrost areas.

The observation and analysis for typical sections along Qinghai-Xizang highway show that the air temperature effect on the shallow layer is greater than the deep layer. In the culvert design, the base buried depths at the inlet and outlet of the culvert should be more than 0.5-1.0 m than that of the culvert centre.

The cold seasons after Oct. and before May are the better construction seasons for the principle of maintaining the frozen condition. For the principle of allowing thaw, the warm season from June to Sept. is the better construction season.

NUMERICAL ANALYSIS OF TEMPERATURE AND STRESS ON THE CANAL SUBSOIL DURING FREEZING

Zhang Zhao[1,2] and Wu Ziwang[1]

[1]State Key Laboratory of Frozen Soil Engineering, LIGG,AS,China
[2]The First Survey Design Institute, Lanzhou, Ministry of Railway of China

This paper presents the numerical simulation analysis of two-demensional nonlinear mathematical model for the heat transfer in the saturated canal subsoil using the finite differences mothed. Elements divided based on the different isothermers at different moment, are used to calculate the stress of the freezing canal subsoil by the finite elements method of plane strain problem. The following main conclusion are obtained: The maximum values of stresses and deformations on the surface of the canal linning occur at bottom and down slop; The stresses decrease with the increase of depth under the canal bottom and down slop; And the stresses value cyclically decrease and increase with the increase of depth on two sides slop of the canal because of the binding force of boundary. Finally, if the surface deformation of canal lining is restricted to zero, the restrictive stresses of lining must reach up to $0.5\times 10^5 N/m^2$. The calculated result correspond relatively well with the measured results of similar condition in site.

INTRODUCTION

When the subsoil water freezes due to low air temperature in winter, the subsoil volume will expand. The increment of volume expansion will be much more considerable expecially for saturated subsoil in open system. While subsoil freezes and thus induces volume expansion, the total expansion of subsoil will be confined partially by the presence of canal lining. When the increment of valume expansion is more than the allowable deformation of canal lining, the damage of canal lining will happen. Therefore, the changes of temperature and moisture field are the basic reason of emerging frost heave and frost heave force. In this paper, the distribution of two-dimensional unstable temperature field on the canal subsoil was obtained by the numerical analysis of the finite difference mothed. Based on the analysis results, the analysis method of finite elements about plane strain problem were carried out to caculate the frost heave force. The close relationship between elastic modulus of frozen soil and minus temperature was taker into consideration.

THE STRESS DISTRIBUTION OF CANAL SUBSOIL

The Determination of Temperature Distribution

The mathematic model to determin the temperature distribution was based on the bad engineering geologic condition; i.e. the groundwater table is about 1.73–2.0m; The canal water is supplied to groundwater when canal operating in summer; The subsoil frezzing begins when the canal operation stop in Nov. So the simulation calculation of saturated subsoil in open system were considered. Assuming the canal to be unlimited long, homogeneous subsoil, no transport of water and heat by evaporation and no other potential energy, taking a vertical section, therefore, this process can be described as two-dimensional parabolical partial nonlinear differential equation. For the definite problem, finite differences by caculation were made, the differential equation were differenced by Crank-Nicholson method. Finally the problem were solved by means of IBM-PC with self-compiled program.

Mechanics Model and Calculation Method

In the certain condition of temperature and moisture, while frost heave is partially by the canal lining, heave pressure will act on canal lining. When the frost heave pressure is greater than the allowable deformation strength of canal lining, the damage deformation of canal lining will occur. The finite element method analysis to calculate the stress distribution in freezing subsoil is shown below.

Taking a vertical section as a XOY coordinate plane, canal long direction as Z coordinate axis, it is obvious that the stress, strain and deformation on the section are only the function of x and y. This is a plane strain problem. Analysis will be performed under the following conditions.

1). The boundary force on the upper boundary of canal is the weight of canal lining and the freezing force between canal lining and subsoil in the vertical direction of canal lining. The lower boundary is back-up roll.

2). The subsoil is homogenous and isotropic frozen and unfrozen soil.

3). Frost heave occurs in the direction of heat flow by 100%.

4). The defromation in the direction of x on the right and left boundary are zero.

Elements

As zhu Qiang (1988) pointed out, when the freezing depth reaches the one-thirds to two-thirds of maximum freezing depth, frost heave force rapidly increases, in the last period, it will be leap

increasing until the frozen depth reaches the maximum value. i.e. The appearance of maximum frost heave force is corresponding with the stable stage of maximum freezing depth. Therefore, based on the configuration of isotherm line at 1760 hour obtained by finite differences analysis, the caculating range can be decided triangle element as showed in Fig.1.

Elastic Modulus and Poisson's Ratio

The experimental research (Wu Ziwang, 1983) indicated that the relationship between elastic modulus of frozen soil and minus temerature can be described as following empirical formula,

$$E = a + b|t|^m \tag{1}$$

where, m is a constant with less than 1, generally taking 0.6. a and b are experimental constants related with soil type , for loess generally taking 100 and 500.

In calculation, the temperature of subsoil are from −10°C at top to 0°C at lower position. Therefore, taking the average of triangle element into formula (1), the different elastic modulus of triangle element of frozen soil can be obtained. Poisson's ration of frozen and unfrozen soil is 0.3 and 0.4 respectively.

Nodal External Load

In the calculation of finite elements method, external force were transmitted at element nodes. Therefore, all kinds of load must be considered at element node. In this analysis, there are two kinds of load. One is concentrated load. Another is distributed load.

The equivalent node load of distributed boundary force , as shown Fig.1, induced by dead load of lining and freezing force acted on the boundary, 1–2, 2–3, ..., 18–19, of the upper boundary elements, 2,4, ..., 18, 20,..23. based on the experimental result of the relationship between leap anti–stretch strength of lining material in contact with frozen soil and temperature (Wang Jianjuen, 1986)*, and long period strength is about one–thirds leap strength (Wu Ziwang, 1981), the freezing force will be taking $3.4\times10^4 N/m^2$ in this calculation. Taking 0.07 m thick of lining and $2.0\times10^4 N/m^3$ density of lining, the dead load of lining will be carried out. Therefore, using virtual displacement priciple, the equivalent node load will be:

$$(P_1)^e=(X_i^e\ Y_i^e\ X_j^e\ Y_j^e\ X_m^e\ Y_m^e)=\frac{P_1}{2}tl(0\ 1\ 0\ 1\ 0\ 0)^T \tag{2}$$

$$(P_2)^e=(X_i^e\ Y_i^e\ X_j^e\ Y_j^e\ X_m^e\ Y_m^e)$$

$$=\frac{P_2}{2}tl(sin(x)cox(x)sin(x)cos(x)00)^T \tag{3}$$

$$(P)^e=(P_1)^e+(P_2)^e \tag{4}$$

where, P_1 is dead load of lining, taking $0.02 Kg/cm^3$; P_2 is freezing force, taking $0.34 Kg/cm^2$; l is the thick of element, taking one unit.

The node load of distributed volume force, for each homogenous element, can be written as:

$$Q_y = q_r t A \tag{5}$$

where A is area of element, q is specific gravity of element.

Based on dead froce equivalent priciple and virtual work principle, the node load of distributed volume force can be expressed as load vector type. i.e.

$$(P)^e=\frac{1}{3}(Q_xQ_yQ_xQ_yQ_xQ_y)^T=\frac{1}{3}(0Q_y0Q_y0Q_y) \tag{6}$$

The node load caused by initial strain expreeses the load caused by frost heave ratio in the heat flow direction. The research shows (Zhu Qiang, et. al. 1988) that, in the condition of high ground water table, the frost heave will be occured in the whole freezing layer and frost heave ratio increases with the increasing of depth. The experimental research (Chen Xiaobai, 1983) also shows this requlation, and in the load pressure condition, the frost heave will be confined especially in low freezing ratio condition.

The freezing ratio on the typical position of canal section obtained from temperature field analysis is shown in Tab.1. Based on the background condition and distributed force, the frost heave ratio for each freezing layer can be obtained as shown in Fig.2. Therefore, taking this as initial strain, the node load can be determined.

Assumpting initial strain of anyone element is (ε_0), the equation for calculating stress is become,

$$(\sigma)=(D)[(\varepsilon)-(\varepsilon_0)]=(D)(B)(\delta)^e-(D)(\varepsilon_0) \tag{7}$$

Taking equation (7) into following equation:

$$(F)^e=tA(B)^T(\sigma) \tag{8}$$

The node force of element will be written as :

$$(F)^e=(K)(\delta)^e-(B)^T(D)tA(\varepsilon_0) \tag{9}$$

Based on the relationship between the node force and the node displacement,

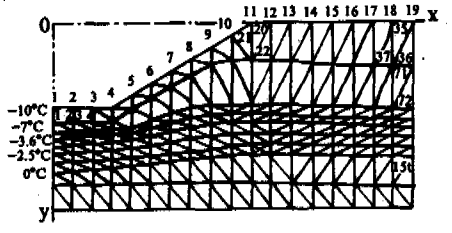

Fig.1 The diagram of elements decided

* Wang Jianjun, (1986). The finite element calculation for the canal lining structure in seasonal frost.

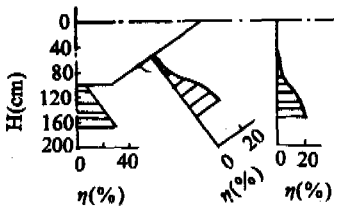

Fig.2 The frost heave ratio of canal section

Table 1. The freezing ratio on the typical position

layers	bottom	slop	embankmen
1	2.983	3.255	3.527
2	1.140	2.418	3.696
3	1.462	2.155	2.849
4	1.190	1.795	2.400
5	0.987	1.508	2.030
6	0.583	0.843	1.102
7	0.335	0.558	0.782

$$(F)_e=(K)(\delta)^e \tag{10}$$

and changing the second item of equation (9) into minus one, which is the node force caused by initial strain, the node load caused by initial strain can be written as:

$$(R)^e_{\varepsilon_0}=(B^T)(D)(\varepsilon_0)tA \tag{11}$$

where,

$$(B)=\frac{1}{2A}\begin{bmatrix} b_i & 0 & b_j & 0 & b_m & 0 \\ 0 & C_i & 0 & C_j & 0 & C_m \\ C_i & b_i & C_j & b_j & C_m & b_m \end{bmatrix}=(B_iB_jB_m) \tag{12}$$

$a_i=x_jy_m-x_my_j$, $a_j=x_my_i-x_iy_m$,
$a_m=x_iy_j-x_jy_i$, $b_i=y_j-y_m$,
$b_j=y_m-y_i$, $b_m=y_i-y_j$,
$c_i=x_m-x_j$, $c_j=x_j-x_m$,
$c_m=x_j-x_i$.

$$A=\frac{1}{2}\begin{bmatrix} 1 & x_i & y_i \\ 1 & x_j & y_j \\ 1 & x_m & y_m \end{bmatrix} \tag{13}$$

$$D=\frac{E(1-\mu)}{(1+\mu)(1-2\mu)}\begin{bmatrix} 1 & \frac{\mu}{(1-\mu)} & 0 \\ \frac{1}{(1-\mu)} & 1 & 0 \\ 0 & 0 & \frac{(1-2\mu)}{2(1-\mu)} \end{bmatrix} \tag{14}$$

taking equation (12), (14) into equation (11), the following eqation can be obtained.

$$(R)^e_{\varepsilon_0}=A_0\begin{bmatrix} b_i & \beta b_i & \gamma c_i \\ \beta c_i & c_i & \gamma b_i \\ b_j & \beta b_j & \gamma c_j \\ \beta c_j & c_j & \gamma b_j \\ b_m & \beta b_m & \gamma c_m \\ \beta c_m & c_m & \gamma b_m \end{bmatrix} \tag{15}$$

where,

$$A_0=\frac{E(1-\mu)t}{2(1+\mu)(1-2\mu)},$$

$$\beta=\frac{\mu}{(1-\mu)} \qquad \gamma=\frac{1-2\mu}{2(1-\mu)} \tag{16}$$

Finally, based on the relationship between displacement and strain,

$$(\varepsilon)=(B)(\delta)^e \tag{17}$$

and the equation (15), the node load caused by frost heave ratio can be obtained.

Therefore, according to accumulation principle of force, the node load can be expressed as following equation.

$$F=Q+P+R \tag{18}$$

The node equlibrium equation and general rigid matrix, the node forces and the node loads of each element must be in equilibrium state. Based on the equilibrium condition of each node in direction of x and y, the equilibrium equation for each node can be set up.

$$\sum_i U_i=x_i; \quad \sum_i V_i=y_i \tag{19}$$

where, $\sum_i$: summing for the all elements in circle of node. Using the matrix pattern, it can be expressed as:

$$\sum_i P_i=F_i \tag{20}$$

Taking equation (11) into above equation, the node equilibrium equation expressed by node displacement can be obtained.

$$[K]\,\delta = F \tag{21}$$

where, [K] is general rigid matrix, δ is row vector of displacement, F is row vector of load.

For the n–th node, the equilibrium equation (21) will be the linear algebraic coupled equation of 2n–th rank. Resolving this coupled equation, the node displacement can be obtained. Therefore, the element stress can also be obtained by equation (7).

The Calculating Results

Through different kinds of frost heave ratio and confined condition, the stress distribution along the direction of horizontal and depth, and the displacement distribution on the canal surface have been carried out by means of computer with self–compiled program.

DISCUSSION AND ANALYSIS

When freezing period is 1760 hours, the Fig.3 shows the calculated results. Its regulation is similar with the observated data (see Fig.4), that is the maximum deformation occurs at the bottom and slop down of canal, and the deformation of upper part is small and almost same. But the calculated values of deformation are more than the obervated values because the most disadvantage background condition were considered and the resisting heat effect of linning material were not considered in this calculation. The maximum frost heave force is also at the bottom and down slop of canal. It is why the failure often occurs in these parts. It is given by calculation that the maximum frost heave stresses are $0.9\times 10^5 N/m^2$ and $0.5\times 10^5 N/m^2$ in the horizontal and vertical direction respectively.

Fig.5 is the calculated values of frost heave stresses along depth at the points of A,B,C,D,E. Because of effect of the surface restraining and the dead weight of subsoil, the frost deformation is small on the upper of subsoil, and the stresses on the upper of subsoil is attenuated. With the depth increasing, the effect of frost deformation increases, after it is more than the surface restrain and dead weight, the subsoil stress increases with the depth increasing.

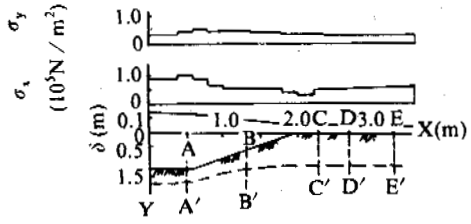

Fig.3 The frozen depth, displacement, and frost heave force at 1760 hour

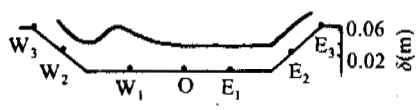

Fig.4 The observated data of displacement

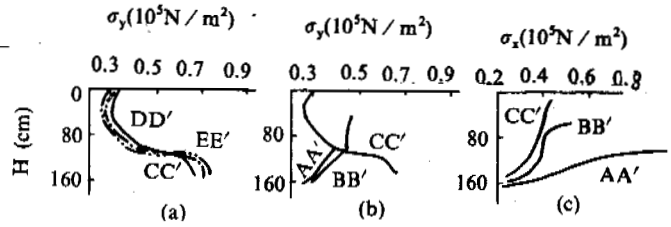

Fig.5 The frost heave force vs. frozen depth

(a), the maximum vertival frost heave forces of different sections

(b), the maximum vertical frost heave forces of different sections

(c), the maximum horizontal frost heave forces of different sections

The calculation also shows that, if the surface deformation of canal lining is restricted to zero, even in the small frost heave ratio condition, the restrictive stresses of lining must reach up to $0.5\times 10^5 N/m^2$.

CONCLUSION

After analysing the freezing regime of canal subsoil, the finite element analysis of the elastic model are used to calculate stress field in this paper. The elastic model is feasible, it is because: (1), when the compress stress range of subsoil is not large, the stress and strain is linear relationship. The loading is small on the canal subsoil so that the plastic deformation characteristics is not obvious for frost subsoil; (2), in the calculation, the elastic modulus is different for different temperature layers, so the calculated precision can be guaranted.

It can be concluded from this study that: (1), The two–dimension temperature field of the canal section is restrained by ground surface temperature, ground temperature, the shape of canal section, water content of subsoil, ground water level and boundary condition. The frozen depth are maximum and minimum at the bottom and the embankment of the canal respectively. (2), The maximum deformation and stress for lining are at the bottom and down slope of the canal. (3), In the conditions of restrains, the frost stresses is attenuated with depth increasing. The larger the restrain is, the stronger the attenuating is. In the conditions of the small and non restrains, the frost stresses display the trend of attenuating–increasing–attenuating with depth increasing. (4), If the surface deformation of canal lining is restricted to zero, the restrictive stresses of lining must reach up to $0.5\times 10^5 N/m^2$.

REFERENCES

Chen Xiaobai, 1983. The effect of freezing rate and overloading compress on the frost heave. The proceeding of Second National Conference of Permafrost. Gansu People's Press. Lanzhou. p223–228.

Zhu Qing,1988. The distribution of seasonally frozen soil along the depth. Journal of Glaciology and Geocryology, 10(1).

Wu Ziwang, 1981. The experimental study of frozen strength between the foundation and frozen soil. Anthology of Glaciology and Geocryology, No.2. Sciense Press, Beijing, p129–139.

Wu Ziwang, 1983. The characteristics of the strength and failure of frozen soil. The proceeding of Second National Conference of Permafrost. Gansu People's Press. Lanzhu. p275–280.

THE RELATIONSHIP BETWEEN THE RAILWAY PROJECT CONSTRUCTION AND ENVIRONMENT PROTECTION IN PERMAFROST AREA

Zheng Qipu

The 3rd Design Institute of Surveying and Investigation
The Ministry of Railway

It has been practically proven that various hazards will occur if the protection to the surrounding environment is ignored during the design, construction and operation of railways. Such as the uneven settlement of roadbed, the frost heaving, cleavage and collapse of house walls, frozen fold of the water-supply pipes, cleavage of bridge pier, cracking of bridge surfaces, cleavage of the side walls in the inlets and outlets tuunels.

THE SIGNIFICANCE OF THE ENVIRONMENTAL PROTECTION IN PERMAFROST AREAS

The Daxinanlin permafrost area in the Northeast of China, is a high latitude zone of permafrost, the climate is severely cold. The soil is in frozen and thawed states with the change of seasonal temperatures. The cold resistant and water-favouring plants are aboundant. The landscape in the permafrost area and the main basic conditions formed the ecological features.

In the permafrost area, the strength increases suddenly when the water in the soil changes into ice. The bearing capacity is almost equal to zero when the ice melts into water. This feature of water in the frozen soil decide whether the frozen soil has a very high bearing capacity as well as deciding if the capacity decreases sharply when the ice melts. The frost heaving and melting settlement of this sort of soil-sand really forms the basic difference of the mechanical properties of frozen soil from other soils due to the water in soil freezing and melting. If there is no freezing and melting of the water in soil, there is no frost hazard of buildings. However, the engineering foundation of various buildings in permafrost areas are buried in the perennial frozen soil layer with different foundations. To protect the stability and prevent deformation of the buildings, the stability of the foundation bearing stratum has to be considered first. In that way, it is necessary to protect the stability of the environment surrounding the perennially frozen soil. How to prevent environmental destuction from the economical activities, not the changes due to the natural conditions and regional climate factors of large periods, will be discussed.

In practice it was proved that the various hazards would occur if the protection of the surrounding environment during the design, construction and operation was ignored. Such as the uneven settlement of roadbeds , the frost heaving, cleavage and collapse of house walls, frozen fold of water-supply pipes, cleavage of bridge piers, cracking of bridge surfaces, cleavage of side walls in inlet and outlet tunnels.

In the design of various buildings of railway projects in permafrost areas, the design principle of foundations of "protecting frozen soil" is often adopted. So we often stress the stability of the temperature field between the contact surface of the bearing stratum and various foundations and frozen soil to prevent the frozen soil from melting within the bearing stratum due to the temperature changes, which leads to the deformation and destruction of buildings. This openion is one-sided as proved in practice. Many building damage are not due to the bad contact position between the bearing stratum and foundation boundary, but due to the incorrect surface position of the buildings location and the lack of protection of the surrounding environment, which leads to environmental changes and building damages.For example, deforestation of the forest and vegetationm surrounding the buildings, grazing and cultivation, over excavating and borrowing soil without a plan, no dewatering ditch arragement, unreasonable cultivation and irrigation. All the above factors will lead to the destruction of the ecological equilibrium. The destruction of the heat equilibrium of permafrost due to the destruction of the ecological equilibrium, will cause the frozen soil to melt, and building damage, etc.

From the above examples, it is pointed out that during construction in permafrost areas, not only the environment protection in surveying, designing and constructing, needs to be payed attention to, but more importantly is to enhance the measurements to protect the environment during construction and operation. Some buildings suffered damage in the first ten years of operation. The reason was ignoring the environmental protection during operation. So it is very important to protect the environment surroundings during construction in permafrost areas.

THE RELATIONSHIP BETWEEN ENVIRONMENTAL PROTECTION AND THE RAILWAY PROJECT CONSTRUCTION

The railway project construction in permafrost area mainly in Da and Xiao Hinggan Ling Mts. includes the line, roadbed, aperture of bridge, tunnuel, house buildings, water supply and water drainage, communication and electric power, etc. For forty or more years, since the 1950's, the 2000 km railway has operated in the permafrost areas of Da and Xiao Hinggan Ling Mts., in the northeast which has led to various building damages, the most serious is caused by breaking driving, the lesser is slow driving by rate limiting. Based on the incomplete statistics of the nine lines in the permafrost area by the Railway Ministry of Harbin, there are 124 hazards only for line roadbeds. So, numbers of people are need to renovate and keep the line open. The cost of renovating, curing and maintenance are several million yuan each year, 6460 working days and 5010 working days are respectively used to do rush reopennings, there were only two working day segments of Tahe and Genghe in 1985. From the investigation information for the 33 stations and 230 buildings only 85 buildings are completely stable, 36.9% in total, 110 buildings suffered hazards to different degrees, 47.8% in total, 35 buildings can not to be used or need rebuilding, 15.3% in total.

Thus it is obvious that during railway operation, hazards to the railway are very serious due to a lack of environment protection. Not only is there an extreme waste in labour power and material resources, but the safety during operation is also affected. Now the relationship between the railway and environmental protection is respectively recounted with examples as follows.

1) Soil excavation surrounding the buildings caves the thawing basin to laterally and vertically, the frozen soil foundation melts, settles and causes damage the buildings.

The old train-check house at the Mongui Station, Yalin line, is located on the 2nd platform of Beirzi river, the foundation type is buried pile with earth fill, and the bearing stratum is within the permafrost layer. Because soil excavation and filling is near the train-check house, forming a man-made pond, holding water and ice-forming for many years. Two years later after its operation, the thawing basin below the bottom of the pond is formed and expands year by year, and causes the frozen soil in the bearing stratum to melt, the foundation settles the walls cleaved and the house has to be rebuilt.

2) Soil excavation in the direction of the groundwater recharge zone of the water resource well in the water-supply house causes the vegetation on the earth surface to be damaged, the seasonal frost depth increased and obstructed the recharge of groundwater, and causes the water amount of the water-resource well to decrease day by day.

The water resource well in the 1st water-supply house of Tahe station in Lailin line is located on the 2nd platform of Humahe river. Because the foundation is only buried 5 m from the earth surface, a shallow well with a diameter of 5.0 m and depth of 6.0 m is designed to accumulate water. The seasonal frost depth is 3.0 meters, and the effective maximum water contained layer is only 2.0 m. The groundwater is mainly recharged by the disappearing river water in the melting area of Humahe river. Because the river recharge zone crosses the embankment, soil excavation is large in two sides of the roadbed when the embankment was filled, the vegetation in the underground water recharge zone is damaged, which led to the decrease in the seasonal frost depth of the recharge zone, obstructed river water recharge to the exploited well through the melted area, and caused the exploited amount of the water-resource well to decrease sharply from 430 m^3 / day in 1968 to 120 m^3 / day in 1972. In 1976, after it had been operated for 4 years, the vegetation on the surface had been exploited and damaged the regrowth grass, and the seasonal frost layer rose, as a result, the groundwater recharged sufficiently, and the aviliable exploitable water supply recovered to 450 m^3 / day.

This example proves that the destruction of the vegetation on the earth surface affects the charges of hydrogeologic environment which leads to the normal exploitation of underground water.

3) During the operation of the building, ineffective heat-proofing and heat-conduction caused the thawing basin of the house to deepen year by year and the water rose on the ground level indoors.

The workers' residence at Genhe station, Yalin line, is located in the foot of the mountain slope of the 2nd platform of Genhe river. The water contained layer with alluvium, buried generally 3.0 – 4.5 m from the ground surface, the groundwater level was higher, the thawing basin of the house deepened year by year. While the outdoor temperature drops, the melting zone below the ground surface indoors gradually reduces, as a result the groundwater below the ground surface was compressed, and poured into the weak places, such as the "fire wall",cooking range, fire pit, vegetable cellar, etc. When there is sufficient groundwater recharge, the groundwater would flow from indoors to outdoors, which formed icings and frost hazards.

4) Bad roadbeds and drainage in stations leads to road cutting accumulating water, pipes in station and water supply and heat protection piples covered with ice, which seriously affected the safety.

The distress line Tingtao Station, Nenlin line, is located at the gentle slope of the 3rd platform, the road cutting is 3.5–4.5 m deep. Because of the inefficient drainage of cutting, the groundwater was exposed and formed ice in midwinter each year, and blocked the drain ditch in the two sides of the cutting, submerged steel rails and seriously affected the use of the distress line.

HOW TO PROTECT THE ENVIRONMENT DURING THE CONSTRUCTION AND OPERATION OF RAILWAY PROJECTS IN PERMAFROST AREAS

It is more difficult and complex to carry out railway project construction in permafrost areas than in general areas. Not only are there some special problems different form the general areas, that need to be considered and handled in investigation, design and construction, but also after constructing, environmental protection during the project operation and management ,must be effective. If not it will be difficult to avoid hazards and damage even the factors were considered very carefully and completely in investigation, design and construction.

Effective environmental protection during the project construction, operation and management, are recommended as

follows.

The Protection of Ecological Environment Surrounding The Buildings

Within the permafrost area of the Da and Xiao Hinggan Line Mts. in the Northeast, the main characteristics of the topography are hills, high and middle high mountains are covered with larch and white brich from the foot to the top of the mountains, which effectively conserve a great quantity of groundwater. There are swamps in the low places of defferent topography from the river vally and basin. The cold resistant and water favouring plants, such as bryophyte and cowberry, grows thickly, which formed the characteristic landscape in this area and is a good heat preservation layer, and created the very beneficial condition for permafrost formation and preservation. The railway crosses the permafrost area. However, the great majority of the foundations of all kinds of buildings in the railway project were adapted to the principle of "preserving frozen soil". So, after the buildings were completed and used, not did only the range of the vegetation destroyed not expanded, but also the vegetation will be recovered and afforested surrounding the buildings. The forestry management should design a planned excavation prohibited area in the two sides along the railway, to form a green protective zone, preserve the permafrost from destruction by economical activities, and to keep the stability of the buildings.

The Drainage Engineering Surrounding Buildings

The water is the "blood" of the environment, it circulates in the all the essential factors of the environment. It is more difficult to search for the water supply resource with a certain amount in the uninterrupted permafrost area. But the water is also the cause of all kinds of building hazards. So the following drainage works must be effectively done operation and management in the construction of the railway buildings.

To prevent the surface water and groundwater from seeping into the roadbed and the foundation bottoms of buildings, prevents the occurance of bad environment geology, such as frost heave, frost mounds, icings, etc.

To prevent all kinds of melted water from seeping into the railway and buildings, so as to prevent melting during the day and freezing during the hight which produces circulative frost hazards.

We Successfully studied and designed the drainage engineering that is applicable for different engineering characters, for example, the drainage ditches in deep road cutting and the outlet of a circular cone body, the drainage ditch with cold and heat preservation in tunnels, and the drainage from shallow water eaves and the burying method of drainage pipes in industrial and residential areas.

Excavation of Soil, Sand and Stone Surrounding of Buildings

Besides the above metioned, the excavation of soil, surrounding the buildings is also forbidden, because it will destroy the ecological environment equilibrium of soil. For example, excavation soil surrounding the buildings will decrease the seasonally frozen depth and cause the permafrost to melt and destroy the stability of the foundation with the principle of "frozen soil preservation". Another example is excavating soil in the slope foot of the roadbed, this will destroy the effective protection of heat preservation and cause the roadbed to settle. When exploiting the disappearing river in the river bed and the unfrozen melt area of the two sides, it is forbidden to excavate soil in the groundwater recharge zone, otherwise the seasonally frozen depth will descend and obstruct the groundwater movement and recharging, and will cause the water resource well to dry up day by day.

Reclaiming Land, Channelling Water and Cultivation in The areas

All kinds of buildings in permafrost areas suffer hazards and damage to different degrees, the reason is the economic activities that aggrevate the adverse natural conditions of permafrost. In other words, after the buildings were completed and operated, the environment protection and management are not effective. The economical activities is the main objective of the environment protection. In permafrost areas production and human activities destroy the ecological equilibrium in permafrost areas to different degrees, strictly speaking. Buildings were constructed for the different objectives of production and human activities. It will be considered in the stability of engineering that how to effectively protect the environment surrounding buildings. To protect the frozen soil from destruction is to protect the stability of buildings. For example, the economical activities will be forbidded, such as reclaiming, and cultivating sruuounding buildings which lead to the destruction of frozen soil.

Monitoring of the lovildings and the changes of the ground temperature fields surrounding the buildings

The monitoring of all buildings and the changes of the ground temperature field surrounding the buildings in permafrost areas is a daily and important convention. It is also effective in forecasting and understanding the stability of the buildings and the trend of changes. In the aspect of the temperature monitoring, two types are involved : one is the monitoring of the stability of the building foundations, another is the monitoring of the ground temperature field surrounding the buildings.

the significance and effection of environmental protection is as follows:

1) To understand the stability of the buildins and the safty service life.

2) To understand the stability of buildings by monitoring the changing trend of ground temperature fields of buildings, to remedy and promptly inact emergency measures if problems are found.

3). Provide the experimence and information by monitoring how to select the safe building sites, how to protect the environment surrounding buildings, and how to decide the foundation type of all buildings and design parameters.

We have monitored the temperature field at different positions, different building sites, different building types and different foundations for forty yeras, and accumulated a wealth of experience. The information is not identical concering the buried position of the monitoring point, the period and frequency of monitoring, the unite, method and equipment used for monitoring. In a word, the design, installation and saftety should be based on the diferent monitoring points and conditions.

REFERENCES

Zheng Qipu, 1986, The Harms on the Railway Project of Glacial Hill and Its Prevention, The Papers of The 5th International Engineering Geology Conference (I.A.E.G.) p1557–1567. Buenou Aires, Argentina.

REGULARITY OF FROST HEAVE OF THE SEASONALLY FROZEN SOIL IN HETAO IRRIGATION AREA, INNER MONGOLIA

Zhou Deyuan

Administration Bureau of Hetao Irrigation Area
Yongji, Inner Mongolia

In Hetao irrigation area, in comparison with three other northern regions in China, the freezing index is not very high, but the level of underground water is higher, the freezing speed is lower, the amount of water migration is large and the action of frost heave is very strong, comprehensive action of moisture and heat results from a strong frost heave. With the theories of gray system and similitude and their methods, a random–determination model is set up, and the regularity of frost heave of seasonally frozen soil is revealed more accurately.

SUMMARY OF THE NATURAL CONDITIONS

Yongji test field for frozen soil is located at the center of Hetao irrigation area, 2.5 km northeast from Linhe suburb. The geographical position is 40°43′ N, 104°44′ E, and 1039.55 meters above sea level. The field belongs to seasonally frozen soil area.

The soil in the irrigation area is sand loam. Size composition analysis and physio–chemistry properties are shown in Table 1.

In the test field, the following observations were arranged: frozen depth, frost amount, amount of water migration, frost heave force (tangential, normal, horizontal), meteorology in a small region, ground temperature and development of underground water, etc.

The observation method and the arranged forms were all done using general methods. An open type steel hoop standard dynamometer was used to measure force, thermalcouples were applied to measure temperatures. The secondary meter is a UJ–33a Volt meter. Other methods were general.

PROCESSES OF FREEZING AND FROST HEAVE OF SEASONALLY FROZEN SOIL

Through observation and test in the Yongji test field for frozen soil from 1987 to 1990, the following processes were revealed, they are frozen depth, water migration, amount of frost heave, and frost heave force. In general, they can be divided as following steps:

1. Unsteady freezing, from early November to the middle of November. The ground temperature fluctuated around 0°C, and there was an alternate change of freezing in the night and thawing during the day. When the temperature was continuously below zero, steady freezing formed.

2. Slow freezing, from late November to the late December. The atomosphere temperature decreases, the increase of the freezing index was not fast, the freezing advance was slow, frozen depths reached to 45 percent of the maximum, and water migration, frost heave amount and frost heave force produced gradually.

3. Quick freezing, from the early January to early February. There was a continous decrease in the atmosphere temperature, the

Table 1. Size composition and physiochemistry properties of sand loam

particle	analysis	%		dry	Specific	Void	liquid	plastic	plastic	Salt
				desity	gravity	ratio	limit	limit	index	content
>0.1	0.1–0.05	0.05–0.005	<0.005	g/cm³	g/cm³	e%	W_p%	W_p%	%	%
10.3	14.8	53	21.9	1.53	2.71	69.5	25	18.5	6.5	0.299

increase of the freezing index was fast with the fast freezing penetration which reached to 98 percent of the maximum value. At the same time, the amount of water migration, frost heave and frost heave force also developed quickly, but the frost heave force declined in the late period due to relaxation.

4. Steady freezing, from middle February to late February. The freezing index increased slowly and the freezing entered into a steady freezing state with the frozen depth slowly reaching its maximum. The amount of water migration and frost heave remained comparitively steady and the frost heave force continued to relax and decrease.

5. Thawing, form the early part of March to late April. The atmosphere temperature increases to zero, the frozen layer begins to thaw quickly. Water migration comes to an end. The amount of frost heave and frost heave force decrease gradually until they vanished.

CHARACTERISTICS OF FREEZING AND FROST HEAVE OF SEASONALLY FROZEN SOIL

Characteristics of Freezing

The freezing index was not very high. The heat flow was greater in the ground. The depth of the annual fluctuation layer was 13.5 meter (Luo Xuepo, 1983), and the average temperature was 10.8°C. The gradient of temperature in the frozen layer was smaller. The average temerature gradient of the frozen layer was 0.096°C / cm in sand loam. Freezing speed was slower. The average freezing speed was 0.96 cm / d in the freezing period of sand loam. Frost depth was not very deep. Its averge value was 103.3 cm in sand loam.

Characteristics of water migration

Variance of the underground water table

When the irrigation area was irrigated in autumn, the underground water table rose to its maximum and the ground surface froze. Before freezing the underground water table was high , then in the freezing period, the ground water table was in the decreasing process, which developed at almost the same spped as the freezing front. The length of the penetration was relatively steady from the beginning to the end and was in the range of capillary action.

Redistribution of water content

In the freezing process, the water in the soil was redistributed, showing that the accumulated area of water gradually moved down and the total tends to enlarge. The water content increased to 7.4 percent in sand loam when it was compared with that before freezing.

Characteristics of Frost Heave

The characteristics of frost heave in the layer of sand loam. It was shown that the amount of frost heave took up 21.2 percent in the upper part, 54.4 percent in the middle part, 23.4 percent in the lower part. The thickness of each part was one-third of the thickness of frozen layer. When the freezing speed was smaller, the supply of water was sufficient, and a stronger frost heave was formed. The average ratio was 8.7 percent.

Characteristics of Frost Heave Force

The development of general tangential frost heave force was parallel with unit tangential frost heave force, and both maximum forces appear at the same time.

Frost heave force increases with the increase of the frost heave. The maximum tangential frost heave force appeared when the amount of frost heave reached to 83 percent of its maximum horizontal frost heave force reached to 98 percent of its maximum values, then they decreased one after another.

The distribution of horizontal frost heave force was not the same along with the height of the wall. The outline of maximum force appeared approximately in a trapezium which used the side of the wall as the bottom. The force was zero at the top of the sample, and was similar in the height of 0.3 and 0.7 height of wall reached to their maximum. The force at the base of wall was 40 percent of the maximum.

THE REGULARITY OF FROST HEAVE OF SEASONALLY FROZEN SOIL

Regularity of Frozen Depth

A linear relationship between frozen depth and the square root of the freezing index was found, as shown in Fig.1. The equation of the relationship is:

$$H_f = a + bF^{0.5}$$

where, a and b are coefficients relating to the soil, and they are −5.3310 and 3.7849, respectively for sand loam.

The frozen depth $H_f$had a power function with the depth of underground water table before freezing, as shown in Fig.2, the following is the equation:

$$H_f = a \cdot Z^b$$

where a and b are coefficients related to soil, 0.0276 and 0.213 for sand loam.

The random-determination model of frozen depth

According to the theory of comprehensive transposition of water and heat (Ding Dewen, 1983) and the method of similitude (Gao Min,1983), through therical analysis and regression, the random-determination model was established as followings:

$$H_f = 3.29\left(\frac{F}{W_0 + 0.26Z^{-1.62}}\right)^{0.445}$$

where, H_f— frozen depth (cm), W_0—water content before refeezing (%), Z—averge value of underground water table in the freezing period (cm).

The Regularity of Water migration

The amount of water migration

It had a linear relation with the freezing index F, which is shown in Fig.3, and the equation is:

$$Q = a + bf$$

where a and b — coefficients related to soil, −0.2531 and 0.0111 for sand loam.

Random-determination model of the amount of water migratio

The theory and method to build the model are similar to the

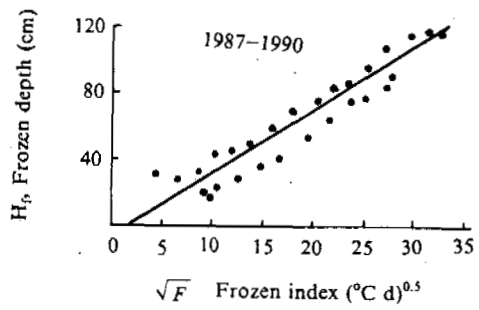

Fig.1 Relationship between frozen depth and freezing index for sand loam

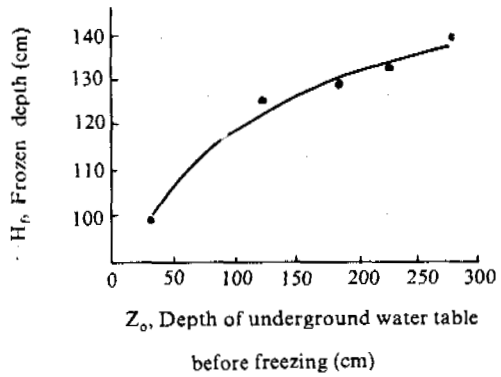

Fig.2 Relationship between frozen depth and the depth of underground water table before freezing

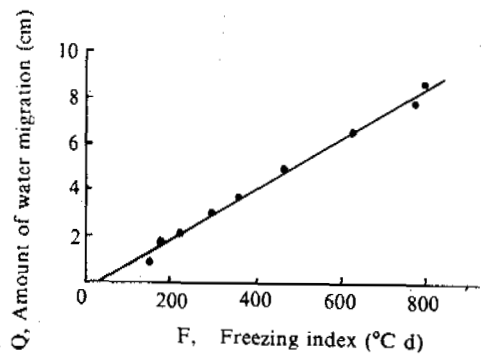

Fig.3 Relationship between water migration and freezing index for sand loam (1989–1990)

frozen depth model. Random–determinancy model of the amount of water migration is as follows:

$$Q = 2.4 \times 10^{-6}\left(\frac{H_f^{2.63}}{Z^{1.90}}\right)$$

where, Q—amount of water migration (%), H_f—frozen depth (cm), Z—average depth of the underground water table in a freezing period.

The Regularity of Frost Heave

The amount of frost heave had a power function with the freezing index F, as shown in Fig.4, and the equation is: $h = a F^b$ where a and b are coefficients related to soil, 0.3347 and 0.850 for sand loam.

The frost heave h had a power function with the depth Z of the underground water table, as shown in Fig.5, and the equation is:

$$h = ae^{-bZo}$$

where a and b are coefficients related to soil, 0.1445 and 0.0020 for sand loam.

Random–determination model of the amount of frost heave

The theory and the method for establishing the model are similar to the above. The random–determination model of the amount of frost heave is:

$$h = -264.25 + 58.55ln[-784 + 324.4(W_0 + 2.4 \times 10^{-6}\frac{H_f^{2.63}}{Z^{1.9}})]$$

where h—amount of frost (cm),. The other symbols are the same as in the previous equations.

The Regularity of Frost Heave Force

The outline of the measured point of tangential frost heave force had a relation with the amount of frost heave, as shown in Fig.6, and the equation is:

$$\tau = a + bh$$

where a and b are coefficients related soil, 0.4858 and 0.0145 for sand loam.

The outline of the measured points of the normal frost heave force showed a linear relation with the amount of frost heave, as shown in Fig.7 and the equation is:

$$\sigma = a\,h^b$$

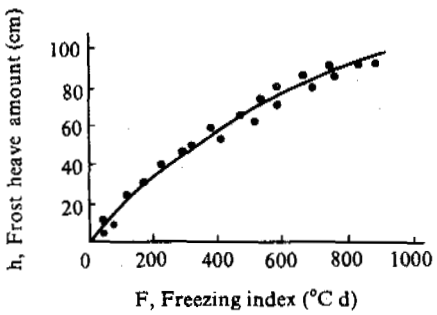

Fig.4 Relationship between frost heave and freezing index

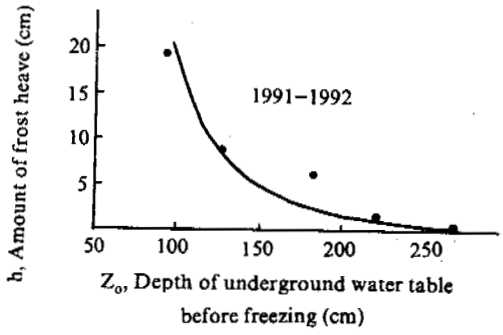

Fig.5 Relationship between water migration and the depth of underground water table before freezing

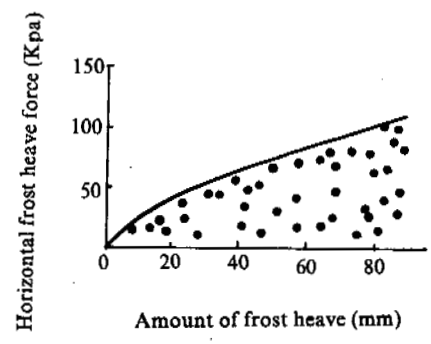

Fig.8 Relationship between horizontal frost force and frost heave (1987–1990)

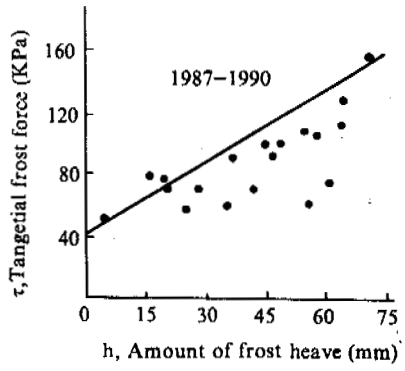

Fig.6 Relationship between tangetial frost force and frost heave

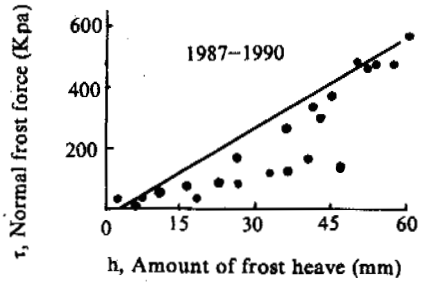

Fig.7 Relationship between normal frost force and frost heave

where a and b are coefficients related to soil, 0.6706 and 0.0546 for sand loam. The outline of the measured points of the horizontal frost heave force had a power function with the frost heave amount h, as shown in Fig.8, and the equation is:

$$\sigma_s = a\,h^b$$

where a and b are coefficients related to soil, 0.6706 and 0.0546 for sand loam.

CONCLUSION

The regularity of frost heave in the area was affected and limited by the conditions of the natural environment and irrigation activity in the Hetao irrigation area, Inner Mongolia. In the area, the freezing index was not very high compared with the three other northern regions in China, but the underground water table was comparitively higher. In the process of freezing, because of the comprehensive action of water and hest transfer, the open type of frost heave was formed with the decrease of freezing speed, the amount of water migration was large, the frozen depth was not very deep, but the frost heave was very strong and the frost heave force was also large. So these cause the intense destruction to ditches and hydraulic engineering buildings.

REFERENCES

Ding Dewen, 1983, Calculation of Frost Depth and Moisture Condition in An Open System. Proceedings of Second National Conference on Permafrost.

Gao Min and Ding Dewen, 1983, Research on The Amount of Free Frost–Heave Soils by Thermodynamic Method, Professional Papers on Permafrost Studies of Qinghai–Xizang Plateau.

Luo Xuepo and Ding Dewen, 1983, Determination of Thermal Regime in Annual Fluctuation Layer of Groud Temperature, Proceedings of Second National Conference on Permafrost.

FOSSIL PERIGLACIAL LANDFORMS IN THE SHENNONGJIA MOUNTAINS, CHINA

Zhou Zhongmin

Changsha Normal University of Water Resources & Electric Power

Two fossil lines of block fields of the Late-Glacial time have been preserved at the elevations of 2800 m and 2900 m in the region of the highest peak of Shennongjia Mountains, and to the northeast at Laojunshan Mountain. The block fields, nivation hollows and cryoplanation terraces differ both in distribution height and in scope within the above mentioned lines, therefore different names are designated for them, i.e. the early Shennongjia periglacial stage and a later one. This is probably related to the cold and dry prairie climate in East China that evolved southward to the riparian basin of the Yangtze River in the late period of the Upper Pleistocene in the year of 18000 B.P. The fossil block field lines represent the geomorphic boundary of the palaeoclimate.

DEFORMATION OF THE FOSSIL PLANATION SURFACE AND THE PROCESS OF THE UPLIFTING STAGES

The area of the Shennongjia Mountains is 3250 km^2. It is the effect of several processes, eg. land formation after the Indo-China movement and subsequent regression, tectonic folding and faulting during the Yanshan movement, and uplifting of the mountains in stages since the Himalaya movement. The long period of planation action resulted in an undulating quasi-plain, that is, the present summit planation surface left over at the highest peak of 3000 m a.s.l. It is equivalent to the ground surface in the Beitai stage, which is also named the Huanghunling stage.

Below the above mentioned fossil geomorphic surface is another broad and flat denudation bench, represented by the Dajiuhu erosion-corrosion quasi-plain of 1800 m. This is the ground surface in the Western Hubei stage. The relevant deposition is the red stratum covering that of the above Cretaceous period. It is equivalent to that of the Tangshian stage and hence belongs to the Miocene Epoch.

Since the first act of the Himalaya movement at the end of the Miocene Epoch, the Western Hubei stage quasi-plain started uplifting to the entirety of 500-600 m. Thereafter a denudation surface of about 1200 m a.s.l. was formed at the foot of the mountain and is called the Mountain Initial stage. This is equivalent to that of the Fenhe stage and belongs to the age of Pliocene (Yang L.K., 1991) to the early Pliestocene.

The second act of the Himalaya movement was from the end of the Pliocene to the beginning of the Quaternary. The Shennongjia Mountains were uplifted by faulting and differential processes, leading to the deformation of the planation surface. The planation surface of the Huanghunling stage was deformed into two benches of 3000 m and 2600 m in elevation; those of the Western Hubei stage were 1800 m and 1500 m; and those of the Mountain Initial stage were 1200 m and 1000 m. The adjacent Yangtze River and the large tributaries originated from the Shennongjia deep undercut, which was around 600 m. The time of the crust uplifting and deep river cutting was named the Three-Gorge stage. Based on the exploration of Huyiatan and Gaojiadian in Yichang city, and to Gulaobei and Luyianchong in Zhijiang county, we discovered that the Lower Pleistocene stratum was mainly a set of fluvial-lacustrine depositions. This suggested that the rivers sharp cutting action mainly occurred after the Middle and Upper Pleistocene, while the terraces developed after the Upper Pleistocene and only took place at the valley slopes below 150 m in altitude. The height of uplifting since the Upper Pleistocene, therefore, accounts for less than one fourth of the total amount in the Quaternary. The Physiographic stage revealed that when compared with the adjacent Yangtze River valley bottom, the Shennongjia Mts. uplifted about 1200 m since the Neogene, and the uplifting height during the Quaternary was as high as 600 m. It is, therefore, concluded that the climatic changes in the highest peak of Shennongjia Mts. since the late period of the Upper Pleistocene of the Quaternary was independent on the crust tectonic uplifting, but dependent on the global climatic oscillations. The up and down fluctuations of the periglacial landforms and the vegetation zone was mainly due to the influence of the East-Asian monsoon circulation changes since the last glaciation in the late period of the Upper Pleistocene.

OUTLINE OF THE PALAEO-CLIMATE ENVIRONMENT BEFORE THE HOLOCENE

Shennongjia has an ancient origin of flora components. It has many tertiary relic plant species. Some examples of such plant species

are given below.

Davidia involucucrata ball, deciduous wood, grows at moist lowlands and valley bottoms between 1100-1600 m a.s.l.

Ginkgo liloba L. grows on hilly land and plains that are below 1000 m in elevation.

Liriodendron L. is the tertiary palaeo-tropical relic species.

The tertiary relic plant species in Shennongjia Mts. are more than ten according to preliminary statistics.

Up to the end of the Neogene and the beginning of the Quaternary, the highest peak might reach 2500 m a.s.l. and two planation benches were distributed at the elevations of 1200 m and 600 m.

During our exploration to the summit of the highest peak from the northern slope, we found neither fossil glacial erosion landforms or fossil moraine. We climbed to the summit from the eastern gully along a large block stream with an elevation of 2500 m at the terminal, what we saw were all of fossil periglacial geomorphogenetic scenery.

CLIMATIC ENVIRONMENT DURING HOLOCENE AND THE PRESENT

In 1984, the author studied the drill core data about the peat layer in Dajiuhu region reported by Zhou Minmin. According to the analyses of the pollen assemblage and ^{14}C dating, Zhou proposed that the vegetation and environment development in Dajiuhu region underwent three stages. (1) Between 12000-8000 years ago, pollens were mainly of Picea, Pinus, Tsuga, Abies, etc. The accompanied broadleaf plants were Quercus, Juglans, Fagus, Betula, Carpinus, Ulmus, etc. (2) Between 8000-3800 years ago, pollens were mainly of Juglans, Fagus, Quercus, Ulmus and Carpinus. About 5000 years ago, Keteleeria davidiana, Tsuga, Podocarpus and other conifer woods increased markedly. (3) From 3800 years ago to the present, pollens were mainly of Quercus, Fagus, Betula, Ulmus, Toxicodendron and Carpinus.

From the first stage, we can see that there were abundant conifers that resembled the present vegetation type at over 2000 m a.s.l. The small amount of peat mingled with the silt clay in profile suggests a dry and humid alteration of the climate. The second stage reflected that the vegetation was dominantly composed of warm and humid favoring plant species. The Tsuga genus is the inherent component in the vertical zonation of subtropical orographic vegetation in China. Fagus, Juglans and Quercus are the major components of the present subtropical orographic evergreen and deciduous broadleaf mixed forest. This suggested that the Keteleeria davidiana, Tsuga, Podocarpus and other broadleaf arbores had their flourishing period around 5000 years ago, ie. the Hypsithermal Interval. Using the present meteorological data of Dajiuhu region, we could deuce that the mean annual air temperature about 5000 years ago was at least 4-3°C higher than at present. The third stage was similar to the present components of vegetation type in Dajiuhu region.

FOSSIL PERIGLACIAL LANDFORMS

Block field: It has a large continuous distribution in Huazhongdin and its periphery area, down to the gentle slope of Feishaiyazhi at 2900 m a.s.. The vertical range of distribution is more than 200 m. The basal volcanic breccia that made up the block field had well developed joints. The frost wedged blocks varied from 0.5-2 m in diameter and were commonly angular in shape. The depth was usually 5 m or so (Photo 1).

The region of the highest peak and, about 20 km to the northeast, at Laojunshan Mt. had a fossil block field line at 2800 m a.s.l. Besides the volcanic breccia in the composition of the block field, there were also dolomite limestone, siliceous limestone and even Silurian green sandstone (Photo 2).

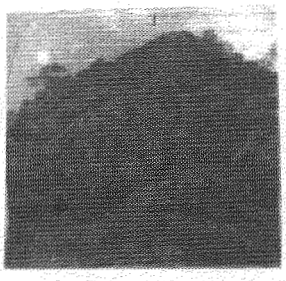

Photo 1. Fossil block field in the late Shennongjia periglacial stage.

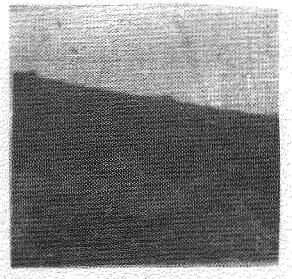

Photo 2. Fossil block field in the early Shennongjia periglacial stage.

Stone fortresses: They are distributed in the areas of Huazhongdin and Feichaiya. Being more than ten metres or even tens of metres high, they look like fortresses at a distance. They are usually composed of green fine diabase in the region of the highest peak (Photo 3). The distinction between periglacial rock bars and rock fortresses is that the former is mainly distributed on slopes with the height being more than width, while the latter stands in block fields with more width than height.

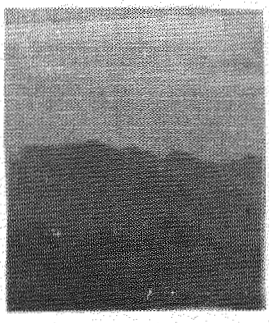

Photo 3. Stone fortress in the late Shennongjia periglacial stage.

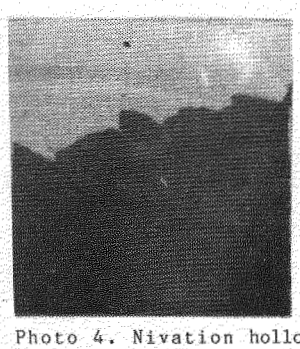

Photo 4. Nivation hollow in the late Shennongjia periglacial stage.

Nivation hollows: One is situated in the vicinity of the fossil block field line at 2900 m a.s.l. in the western side of Huazhongdin peak. It developed in the volcanic breccia and dolomite limestone, and was usually 10-20 m in diameter (Photo 4). The other is near the fossil block field line at 2800 m a.s.l. in the northern slope of Dashennongjia. It developed in the dolomite limestone and was characterized by lacking rock basin and ice threshold and also lacking a complete ledge. In contrast, its

bottom was rather flat and was nearly eight on the flat index. The bottom of the hollow was large and the largest could reach 150 m in diameter. Some of the hollows connected with the flat floor valley (Photo 5).

Flat floor valley: It is a kind of periglacial wide valley. It mainly developed in dolomite limestone on the northern slope of Dashennongjia. There existed nivation hollows in the source area of the flat floor valley. There also survived a fossil rock-bar of 20 m high and fossil frost heaving of about 5 m high on the two sides of the slopes of the flat floor valley. No moraine was found in the valley floor (Photo 6).

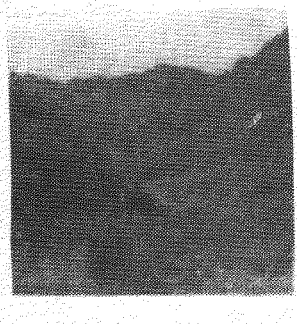

Photo 5. Nivation hollow in the early Shennongjia periglacial stage.

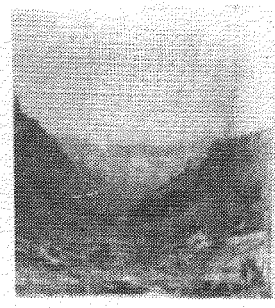

Photo 6. Flat floor valley in the early Shennongjia periglacial stage.

Cryoplanation terrace: There is well developed small bedrock terrace at 2900 m a.s.l. between the southern slope of Huazhongdin and Feichaiyia. The terrace inclines slightly downward and is 50 m in width. It has a veneer of angular debris resulting from frost weathering. There can be seen apparent bedrock steep treads in the background. There can be seen another old cryoplanation terrace, which is 120 m in width, at 2750 m a.s.l. under the above mentioned terrace (Photo 7).

Block slopes: Their distribution is most obvious in elevations of 2800-2600 m. They are accumulations of angular and varying sizes of blocks continuously covering the 30° bedrock slope surfaces. The lithological property of fragments on the block slope on the slopes at 2600 m a.s.l., the block slope, consisting of volcanic breccia fragments, covers the old block slope consisting of dolomite limestone fragments. Different block slopes connected near the toes and thus formed a periglacial debris fan.

Stone streams: Masses of basal volcanic breccia boulders with poor angularity streamed down the gully bed of the Eastern Gully from an elevation of 2850 m to 2500 m. This is a well preserved stone stream, which is 3-5 m in depth and 10 m in width. The boulders are usually 0.5-2 m in diameter and their length axes are parallel to the gully bed. There are Sinarundinaria nitida growing in the fissures of the rocks. There are no protalus rampart developing in the end of the stone stream (Photo 8).

Frost weathering collapsed cliff: It was created under the complex situation consisting of periglacial agents, gravity and water flow action. In the source area of the Eastern Gully at 2850 m a.s.l., the nearly erected collapsed cliff is as high as 30 m.

Photo 7. Cryoplanation terraces during two periglacial processes. The higher terrace has been connected with the strip of land.

Photo 8. Fossil stone stream in the late Shennongjia periglacial stage.

Ice (soil) wedges: One is situated in the source area of the Eastern Gully at 2850 m a.s.l. The other is in the western slope of Huazhongdin peak at 2800 m a.s.l. There are the unclear vertical bedding (Photo 9).

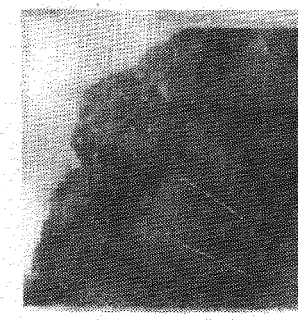

Photo 9. Ice (soil) wedge in the early Shennongjia periglacial stage.

Thin layered loess-like depositions: They can be seen at the foot of mountains, valley slopes or valley bottoms, and are characterized by 0.5 m thick loess-like materials mingled with volcanci breccia, limestone and feldspar quartziferous sandstone debris.

In summary, the distribution of the main fossil periglacial landforms in Shennongjia are shown in Fig.1.

THE SIGNIFICANCE OF FOSSIL PERIGLACIAL LANDFORMS IN SHENNONGJIA

Huazhongdin peak, 3105 m a.s.l., is the second highest peak in the eastern Chinese mainland. It is only lower than Baxiantai (33°56.6'N, 107°46'E, 3767.2 m a.s.l.), the highest peak in Taibaishan of the Qinling Ridge. Its latitude is 2.5° southward of the Qinling Ridge and is situated in the subtropical zone. It is the transitional bridge of the mountain region in the west to the hilly land and plain region in the east. It is more than 1000 m higher than Mt. Huangshan (1841 m a.s.l.) and Mt. Lushan (1426 m a.s.l.).

During the peak of the Last Glaciation at about 18000 B.P., there was a wide distribution of grassland and sparse tree prairie, and loess deposition. It reached southward to Nanjin city, Wuhu Lake to Taihu Lake and the southern area was along the Yangtze River bank, and to Jiujiang city in the west. It belonged to an arid

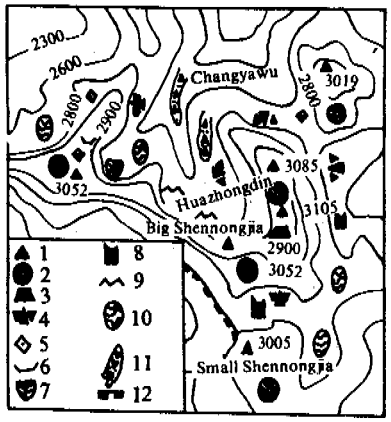

Fig.1 Distribution of fossil periglacial landforms in the highest peak region of the Shennongjia Mts. (1:100000)
1. peak; 2. block field; 3. stone fortress; 4. block slope; 5. nivation hollow; 6. flat floor valley; 7. Ice (soil) wedge; 8. rock bar; 9. cryoplanation terrace; 10. frost weathering collapsed cliff; 11. stone stream; 12. precipice;

and cold climate environment, with the mean annual air temperature being at least 6°C lower than present and even 10-12°C lower during the coldest period. The annual precipitation was 300 mm. The climate didn't favour the development of glacial morphogenetic features but favoured the growth of periglacial morphogenetic features.

In the highest peak of the Shennongjia Mts. and Laojunshan Mt., many kinds of periglacial landforms developed in the early Shennongjia periglacial stage during the late period of the Upper Pleistocene. The fossil block field line (2800 m a.s.l.) was representative and the growth of the flat floor valley was the most obvious feature. A clear fossil block field line was preserved at the altitude of 2900 m in the highest peak of the Shennongjia Mts. The second periglacial process retreated to the summit and the extent shrunk greatly. This can be extrapolated from each single periglacial landform that was greatly less in scope than the former one. The well preserved fossil block field acted as the striking feature of this second periglacial climate.

The Qinling-Taibai Glaciation during the late period of the Upper Pleistocene consisted of two subglaciations (Ma Q.H. and He Y.Q., 1988). There were also two occurrences of periglacial processes during the Late Glacial time in Shennongjia. Whether or not they coincided in chronology needs further precise exploration with age dating. The Quaternary periglacial phenomena in Mt. Huangshan, with a southward latitude and constituted by granite, are not typical, while that in Mt. Lushan are unclear. Thus the fossil periglacial morphogenetic features in Shennongjia are of great value.

Based on the analyses of the physiographic stage, palaeobotany, present vegetation and climate situation, it is evident that all of the Shennongjia Mountains were controlled in a periglacial environment only at the time of the Last Glaciation during the Quaternary, and ended probably before the start of the Holocene.

REFERENCES

Ma Qiuhua and He Yuanqin, (1988) Features of moraine and glacial period on Mt. Taibaishan during Quaternary, (In Chinese), Journal of Glaciology and Geocryology, Vol.10, No.1.

Yang Liankang, (1991) Discovery of relic fluvial pebbles on planation surface in the Three-Gorge section of Changjiang, (In Chinese), Acta Geographica Sinica, 46(3): 373-374.

Zhou Minmin, (1985) Vegetation and its environment in Dajiuhu region of Shennongjia during Holocene, (in Chinese), Thesis of M.S., Inst. of Geography, Academia Sinica.

THE RESEARCH OF POROUS SLAB STRUCTURES FOR PREVENTING FROST DAMAGE OF ROADS

Zhu Yunbing[1] and Guo Zuxin[2]

[1]Yichun Management Department of Roads, Heilongjiang
[2]Harbin College of Building and Engineering

The active mechanisms of porous slab structures are analyzed from two aspects of definite quantity and quality in order that the frost damage of roads can be solved in engineering.

INTRODUCTION

Frost heave and potholes cause serious damage of roads in seasonally frozen soil. Siliceous shale material has an extensive distribution in Heilongjiang. Some properties of siliceous shale material are tested. The soft and low strength siliceous stone cannot be used as a material in the road structure layer, but in order to develop and fully use the resources, mingled material is designed based on the principle of suspension, and the crush rate and the strength are tested. The results show that the compressed elastic modulus of the mixed material is 200-300 MPa and forms a porous slab structure. Because of the low cost and high protection of lime, the mingled material of siliceous stone with a grain size of 20-30 mm is mixed with a soil with a lime content of 10% in the laboratory, and analyzed. The mingled material is called siliceous stone which is used not only in the base of secondary highways but also in the subbase of highways.

PHYSICAL PROPERTIES OF MINGLED MATERIAL

1. Hydraulic Properties

The porosity of the siliceous stone is as high as 35-40% and its pore size is tiny. Table 1 lists the water distribution situation of siliceous stone and lime soil under optimum water content of shaping for mingled material, optimum water content of shaping is about 19% in experiments.

The pore structure of siliceous stone has an excellent water stability (see Fig.1).

Siliceous stone does not expand under water influence. The volume expands after the lime soil absorbs the water and then decreases and vanishes because of the pores of siliceous stone. This can prevent the structures volume from expanding due to frost action produced in the road bed in poor drainage conditions. This is significant for road structures in cold regions.

Table 1. Water content of materials

Type of mingled material	Final water content	Water content of material before mixing	
		Siliceous stone	Lime soil
5:5	19%	23%	16.8%
3:7	19.8%	23.6%	18.5%

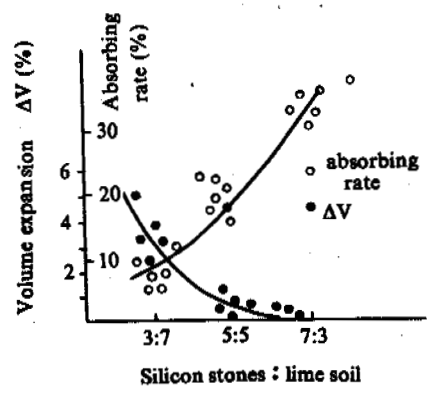

Fig.1 The curves of volume expansion and absorbing rate

2. Freezing Stability

(1) In order to simulate the upper stratum of the road subject to load, samples are tested under the condition of lateral constraint.

(2) After the sample was saturated with water for hours, the sample went through five freeze-thaw cycles.

(3) Freezing temperature was -20°C, for four hours.

The thawing temperature is an ambient one (about 10-15°C), the time for saturation is 2 hours. After the samples are processed by the above mentioned methods, the volume expands and the strength loss is shown in Fig.2. After five freeze-thaw cycles, the mingled material has an fairly good stability.

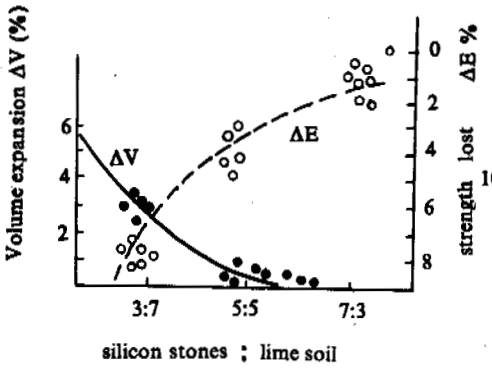

Fig.2 The curves of volume expand and lossing strength

3. Thermal Properties

The coefficient of thermal conductivity for plus and negative temperatures are measured by installing instruments based on the line of heat source principle in a transient state.

Some thermal parameters are given in Table 2. The measuring results show that the thermal conductivity and heat capacity of mingled material are less than that of the base materials. So the property of preventing freezing and heat preservation is very good and it can prevent the freezing thickness of the road surface.

Table 2. Thermal parameters

Material	Parameters	Value	Unit
Asphalt	C_v	473.0	Kcal/m³.°C
	λ_+	0.75	Kcal/m.h.°C
	λ_-	1.03	Kcal/m.h.°C
Siliceous stones mingled material (5:5)	C_v	325.9	Kcal/m³.°C
	$\lambda_\pm$	0.65	Kcal/m.h.°C
Siliceous stones mingled material (3:7)	C_v	352.1	Kcal/m°.°C
	$\lambda_\pm$	1.20	Kcal/m.h.°C
Wet clay	$\bar{W}$	0.28	100%
	Co^T	587.3	Kcal/m°.°C
	Co^{TM}	511.2	Kcal/m.h.°C
	λ_{TM}	1.30	Kcal/m.h.°C
	λ_T	1.05	Kcal/m.h.°C

CONSTRUCTION OF TRIAL ROAD SECTION

Based on the analysis of the ambience, siliceous stone mingled material of two grading proportions are taken for the base course of advanced road surfaces and the trial road sections are constructed.

The surface layer of the original road is 10 cm of asphalt concrete. The base course has two kinds of 50 cm thick lime of semiaridity and stability with steel dregs of fly ash and lime.

In consideration of the heat preservation property of mingled siliceous stone, because it is the base course, its thickness is decreased by 10 cm in the basis of the original design (Fig.3). The structure of the siliceous stone section is calculated in a three-layer system. The design requirement is met in the areas of the downbending value and pull stress.

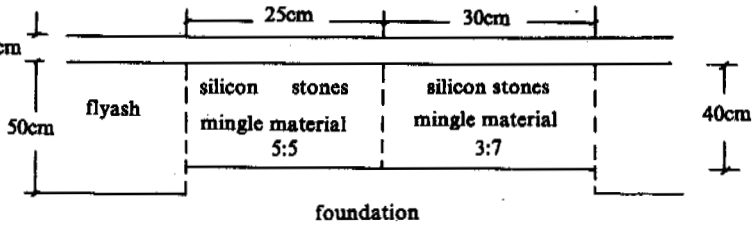

Fig.3 Section of the road surface structure

FIELD TESTING

Frost damage of road structures in the northern regions is mainly displayed by frost heave and potholes.

Based on observation of 45 point datum marks in a trial road section from the beginning of the winter until February, the datum marks changed by 1 cm. Non-uniform frost heave basically did not occur (Table 3). Subsidence deformation and net fissures did not occur until thawing in the spring. The total downbending value is small (see Fig.4, Table 4). It was obvious that the frost-damage prevention method is effective.

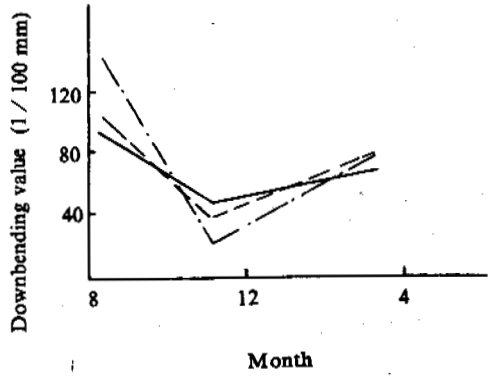

Fig.4 Downbending value vs. time
——— mingled material of siliceous stones;
----- steel dregs;
—.—.— fly ash.

Table 3. Observed frost heave of the porous slab

Structure type	Frost heave (cm)									
	8612		87.1		87.2		87.3		87.4	
	Max	Min	Max	Min	Max	Min	Max	Min	Max	Min
5:5	0.92	0.90	1.10	1.00	1.23	1.21	1.25	1.21	1.24	1.20
3:7	0.93	0.90	1.14	1.00	1.25	1.18	1.25	1.23	1.25	1.23
Steel dregs	0.89	0.89	1.15	1.13	1.30	1.25	8.40	8.01	8.41	8.40
Fly ash	0.91	0.90	1.20	1.13	1.35	1.23	8.71	8.23	8.70	8.53

Table 4. Calculated downbending values

Road section types	Calculated downbending value (1/100) mm				
	End of construction	Autumn end	Decrease	End of spring thaw	Increase
3:7	80	42	46%	66	43%
5:5	85	46	46%	66	43%
Fly ash	143	24	83%	69	187%
Steel dregs	106	40	62%	71	78%

DISCUSSION

Since the trial road was constructed, drilling, sampling and analysis has been taken three times.

The upper drilling profile is the thaw layer, the middle freezing layer and a thaw sublayer. This shows that the thermal property of the road surface structure is so different that the foundation below different road surface structures has a different distribution of temperature and humidity.

Fig.5 shows that humidity is basically identical below a definite depth (e.g. below 220 cm). The identical extent of water migration for different distributions of the temperature field results in an indentical distribution of humidity above the depth. It follows that the humidity of the soil foundation below the base of course of siliceous stone is at a minimum. The adjusted action of the water temperature of the base course of siliceous stone occurs many times. The drilling information in 1988 and 1989 shows that the adjustment action is brought into action more than one or two times.

Siliceous stone mingled material of different graded proportions have a different distribution of the temperature field for different thermal conductivities. Fig.6 shows the results of theoretical calculations and observations, the 0°C isotherm of the base course of siliceous stone mingled material using different grading proportions (3:7, 5:5). Its 0°C isotherm is easily above 30% for heat preservation action of the base course being 50% siliceous stone in the winter.

It is obvious that the negative temperature gradient of the road surface structure of the base course with 50% siliceous stone is less than 30%.

The greater the negative temperature gradient, the smaller is the amount of water migration, and vice versa. The film water of soil frozen at -3 — -5°C is measured in the tests. The heat

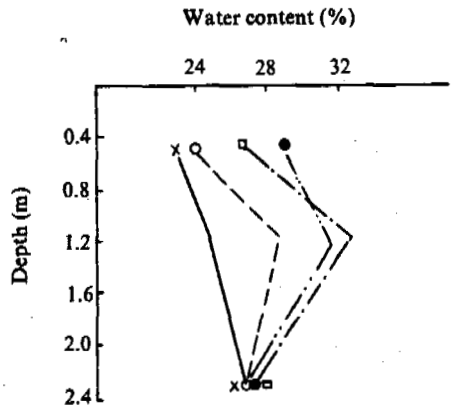

Fig.5 Water content vs. depth
x——5:5 mingled material
o---3:7
—.steel dregs
o—..fly ash

quantity affects the process of the 0°C isotherm developing downwards. So the 0°C isotherm of the road surface structure of the base course with 50% siliceous stone is below 30% in the late stage and the water content of the upper soil layer in the road surface structure of the base course with 30% siliceous stone is greater than 50%.

The total frost heave of the road surface is decreased in the base course of mingled material with the porous and tiny pore siliceous stones adjusting the water temperature of the soil foundation, the soil foundation is kept dryer in the spring and makes the surface structure be able to prevent freezing.

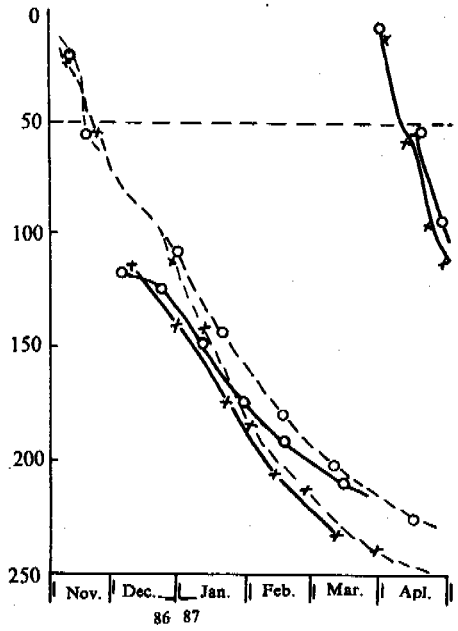

Fig.6 The results of theoretical calculations and observations

——x—— observation A
——o—— observation B
---x--- calculation A
---o--- calculation B

CONCLUSION

Research shows that mingled material of siliceous stone not only adjusts the water temperature but also has effective slab function. It is feasible to design a structure layer of road surface. Resource investigation shows that siliceous shale is not only easily dug but economical. Because of the excellent properties of siliceous stone mingled material, the structure layer of the road surface has the potential to decrease the thickness of the embankment and can reduce the engineering cost. Thus it is of economic significance to use the technique and to develop the material.

DRILLING CHARACTERISTICS OF ENGINEERING GEOLOGY OF PERMAFROST ON DA HINGGAN LING REGION

Zou Xinqing

Da Hinggan Ling Investigation and Design Institute
of Management Bureau, Forestry Ministry of China

Engineering drilling of freezing stone soil was done in the spring and autum seasons, in the north slope of Da Hinggan Ling. The pore sizes were 130–150mm, the length of the jackbit was 150mm, the outblades were 2.0–2.5mm, the main axis pressure was from 800–1200kg when using a low speed and short time, and the circle footage was 0.1–0.2m. The main axis pressure was changed to 600–1000 kg in the soft permafrost stratum and the circle foot age was 0.3–0.6m,through practical investigations it was proven that the above mentioned method met the technical demand and the improved drilling technology can be used in drilling and sampling in engineering geologywith a favourable effect in permafrost regions.

QUESTIONS ASKED

The stratum was of a freezing stone soil in the permafrost region on the north slope of Da Hinggan Ling. The working area of the shallow drilling and pit was large, the efficiency was low and there were many difficulties. When drilling machinery was used, according to the normal technical demand of drilling in the past, the temperature of the frozen ground rose, the ice layer in the freezing stone thawed and even becamedry due to the friction between the drilling rig and the stone soil of the pore wall. Sample taking couldn't present the real condition of the freezing stratum, it was difficult to determine the depth of the permafrost table, measure the water content of the freezing stratum and judge the ice extent and cyogenic texture type. The geotechnical properties of the construction field were misjudged which caused the destruction of buildings in serious cases. The technical drilling demand which is applicable in the permafrost region of Da Hinggan Ling is given in this paper, resulting from extensive research in the last thirty years. It can meet the demand of engineering design and preserve the stability of buildings.

DRILLING TECHNIQUES FOR ENGINEERING GEOLOGY IN THE PERMAFROST REGION

Choice of Drilling Season in The Permafrost Region in The North Slope of Da Hinggan Ling

In general, drilling can be done in any season due to the unique natural environment and climate conditions in the permafrost region. A feasible season must be chosen to ensure the drilling demand of engineering geology in the permafrost region.

In the permafrost region of the north slope of Da Hinggan Ling, the winter is long and the climate is frigid. The daily average temperature is less than 0°C for more than 200 days of the year. Daily low temperature of −30°C has the continuous time of 100–130 days. Daily low temperatures of −40°C occur for 20–30 days. There are heavy rains in the summer and precipitation is concentrated in July, August and November. According to the demands and purposes of engineering it is important to choose a suitable drilling time. Drilling seasons for engineering geology are feasibly chosen in February, March, June and November. The permafrost table can be exactly determined by drilling from July to October. The maximum depth of seasonal freezing can be determined by drilling from the middle of March to the last ten days of April.

Choice of Drillign Pore Size

In order to decrease the thaw outside the undisturbed core of permafrost due to friction heat of the jackbit, the drilling machine type and pore size of the drilling must be suitably chosen. A large number of comparative experiments in the last few years have shown that the effectiveness of the DPP–100–1 type of drilling machine is the best, next is the Xy–100 type. Drilling machines with a large horsepower are suitable for drilling in permafrost regions. According to experiments in drilling in permafrost regions, such as in Gulian, Xilingji, Tuqiang, etc, a 150mm pore size is feasible for a frozen stone stratum, the drilling core is more complete, the soil temperature doesn't change easily and a 130mm pore size can meet the demand of the experiment.

DRILLING FOOTAGE FOR ENGINEERING GEOLOGY

Drilling footage of clear water or slurry is not feasibly used in permafrost regions, dry drilling is preferable. Because of the high stone content in the permafrost stratum of Da Hinggan Ling,

choosing a jackbit of a stiff alloy should meet the following technical demands to gain the best effect.

1. Length of jackbit is 150mm.

2. A k534 type alloyjackbit is selected, with the outblade of the onsideand outside being not less than 2.0–2.5mm.

3. Length of core barrel is 0.6–0.8m.

TECHNIQUE OF DRILLING OPERATION

There is an extensive distribution of frozen stone soil with different ice contents and which is more compacted and soft peat soil with a high ice content in the permafrost region on the north slope of Da Hinggan Ling. The drilling demand is not identical.

Freezing Stone Soil with A Low Ice Content And High Compaction

The volume of the ice content in this soil is small, the general condition is less than 20% of the ice layer is filled in the pores of the stratum and stones, and it is difficult to take ice core in the process of drilling footage. So drilling footage uses a low speed and a middle main axis pressure. If drilling footage uses a high speed and a large pressure, the time is longer and the heat of the drilling rig causes the frozen ground core to thaw. According to experimental data, circle drilling footage is not feasible for more than 2–4 minutes, footage is feasible in the range of 0.1–0.2m. Center pressure of the drilling rig with a 150mm jackbit is feasible in the range of 800–1200kg.

Frozen Soil with A High Ice Content and Soft Peat Stratum

This soil is mainly distributed in the basin and sedimental stratum of the lake facies in Gulian coal mine. Most belongs to a stratified cryogenic texture and the stone content is less. Drilling footage of a middle speed should be chosen, the circle footage should be 0.3–0.6m, and the main axis pressure of the drilling rig can be increased in the drilling footage in the peat stratum. Because of the deeper outblade of the alloy jackbit is pressed into the frozen ground, a higher core ratio is gained when the core sample is drawn in the drilling footage. The main axis pressure should be increased so that the jackbit and core are closely blocked so that a drop in the core can be prevented and the core drawing ratio is improved.

In order to find the destructive causes of the fissures in the hospital of Tuqiang Forestry Bureau in Da Hinggan Ling, drilling was done around the foundation of the building in November, 1984. Using the method of dry drilling, large axis pressure and high speed, the frozen ice core was completely thawed, the core produced heat and no permafrost was found. Using the same method, a second drilling was done with a DPP–100–1 type drilling machine permafrost and the ice layer were still not found in the core of drilling pore. Next, a low speed and middle pressure, with a circle drilling footage of 2–3 minutes was used, and the ice layer and permafrost were found in the core. This shows the importance in choosing the drilling footage parameter in engineering geology drilling in permafrost. Drilling footage with this type of drilling machine should be chosen by the following parameters of drilling footage.

Rotational speeds using the first gear, small–middle throttle, and 40–60 rotations per minute.

Total pressure of the axis center of the drilling bit is 800–1200kg.

Circle drilling footage, in which a 150mm jackbit is used, is 2 minutes for a frozen stone stratum and a quick drawing jackbit. A circle drilling footage, in which a 130mm jackbit is used, is 2–3 minutes for frozen loam, and a circle drilling footage,using a 130mm jackbit, is 3–4 minutes for frozen cobble stratum, but the axis pressure of drilling is more than that of frozeng loam and frozen stone soil.

The length of the core barrel is 0.6–0.8m (being suitable for depths of 0–10m) amd the length of the jackbit is 150mm. Three identical size drillings are prepared, after the first circle end and drawing drilling, and another drilling is needed. Drilling of the first circle can not be continually used until the drilling has cooled.

The above mentioned method of drilling and parameters of drilling footage are very effective in drilling and sampling processes of permafrost engineering geology.

CONCLUSIONS

A large number of experiments in engineering geology drilling in the permafrost regions of Gulian, Xilingji, Tuqiang, etc, show that drilling in different stratums have different parameters for drilling footage. A reasonable pore size, drilling and operational techniques are not only the key factors for excellent effectiveness in engineering geology in permafrost, but are also important factors on which the properties of permafrost can be determined. A satisfactory effect was recieved using a 130mm pore size, 150mm long jackbit, a not less than 2.0–2.5mm outblade of the inside and outside, 800–1200k total pressure of the drilling axis center, circle footage of 0.1–0.2m for frozen stone soil and 0.3–0.6m for frozen soft soil, etc..

ACKNOWLEDGEMENTS

The author wishes to thank Assistant Professor Tong Changjiang and the Lanzhou Institute of Glaciology for permitting this paper to be published.

QUATERNARY GEOLOGY AND GEOCRYOLOGY IN NORTHERN QUEBEC, CANADA

Michel Allard[1] and Jean A. Pilon[2]
[1]Centre d'etudes nordiques, Universite Laval Clement tremblay,
Ministere des transports du Quebec
[2]Geological Survey of Canada

In Nunavik (Northern Quebec) theorical and practical knowledge of periglacial features and permafrost properties has increased tremendously over the last five years. We owe this achievement to a joint task force (governments-universities) set up to carry out a comprehensive research program within the framework of airstrip construction in 14 villages distributed over six degrees of latitude, from the discontinuous to the continuous permafrost zone. Patterned ground types and geocryological facies are closely related to the various types of surficial deposits laid by the Wisconsinan glaciation and, subsequently, by the post-glacial marine inundation and emergence on the coastal fringe of the peninsula. Tundra polygons and low-center mudboils are the dominant periglacial features on glacial landforms such as drumlins and moraines, on glaciofluvial landforms like outwash plains and eskers and on fluvial terraces and raised beaches. Both soil wedges and ice wedges can be found under polygon sides. Soil stripes and gelifluxion lobes occur on slopes. Interstitial ice dominates in these coarse, sandy and gravelly, sediments as revealed in numerous sections, quarries and drill-holes. The dominant periglacial features on the post-glacial marine silty clays are cryogenic mounds and fields of high-center mudboils. In these fine-grained sediments, segregated ice (lenses and reticulated) dominates in warm permafrost (0°C to -2°C) in the southern part of the region. Volumetric ice contents, as measured on cores, are usually 50-60% but they may attain 80% in the upper layers of permafrost. Massive icy beds occur in cold permafrost (-5°C to -6°C) in the northern part of the region and were observed in retrogressive slumps. Ground probing radar and electrical resistivity surveys indicate that such icy beds may be up to 11 m thick. Other features such as palsas in bogs, frost blisters, icings and aggrading permafrost under tidal marshes are also significant in the region. Extensive knowledge of correlations between Quaternary geology, ground patterns and geocryological facies (displayed in table form and illustrated with selected pictures) has made it possible to develop a photo-interpretation key which allows to plot high quality, large scale maps of permafrost conditions prior to decision taking relative to digging, cutting into or moving soil for construction projects (buildings, service and transportation infrastructurs, etc.).

RATIONAL UTILIZATION OF WATER RESOURCES IN PERMAFROST REGIONS, ARTIFICIAL RECHARGE OF GROUNDWATER STORAGE

T.V. Burchak and L.M. Demidyuk
The All-Union Oil & Gas Research Institute, Moscow 125422, Russia

Characteristics of surface and groundwater in permafrost regions are given. It is shown that the most typical resources of ground water are those originating from taliks of river valleys; subpermafrost water of mountain artesian basins; water from structures of limited area or from crevice and creviskarst ground mass and zones of tectonic disturbances. The necessily of due regard for peculiarities of the formation of water resources is marked, and of the surface and subsurface drainage in planning the water resources utilisation and protection from pollution and depletion, and also in designing water-supply systems.

Comparative assessment of surface and groundwater as the source of water supply is given with regard for special requirements depending on severe climatic conditions. Possibility and expediency of wide utilization of groundwater for supply purposes is shown. Possible water intake for various groundwater basins is characterized.

The necessity of researches for non-conventional "Know-how" of water supply is substantiated with regard for permafrost region peculiarities and special requirements of consumers. Particular attention is given to the selection of water supply sources for oil production regions.

Expediency is shown of wide utilization of taliks of river valleys together with artificial recharge of groundwater (ARGW) by:

1) building water storages; 2) widening of river beds; 3) installation of special infiltration facilities; 4) creation of extra negative water pressure in the depression funnel under the river bed; 5) joining a sub-bed-near-bed talik with that of a near-bed one by means of melting the permafrost pillar separating the taliks; 6) enlarging the talik capacity by creation of optimum conditions for melting permafrost ground; 7) taking measures against freezing of the water intake area of the talik.

Principal technical solutions for realization of ARGW method are characterized as well as the design technique of infiltration and vacuum facilities, melting procedure of permafrost pillars, and also the water intake on the whole.

Results of the water supply network selection for an oil production site located in continuous permafrost region are considered.

ICE WEDGE DEVELOPMENT ON SLOPES, FOSHEIM PENINSULA ELLESMERE ISLAND, EASTERN CANADIAN ARCTIC

Antoni G. Lewkowicz
Department of Geography, Erindale College, University of Toronto, Mississauga, Ontario, L5L 1C6, Canada

This paper describes the cryostratigraphy of sites on the Fosheim Peninsula where either multiple ice wedge systems or multiple growth stage ice wedges have been exposed and provides explanations for wedge regrowth.
Seven sites within a 50 km radius of Eureka were examined from 1987-1991. Current cracking activity of wedges was assessed by taking samples across the centres of wedges or in younger growth stages and analysing the tritium content. Rates of wedge growth inferred from this method are between 1 and 5 mm/year. In the headwalls of retrogressive thaw slumps wedge regrowth occurred within former mudflow deposits, but on one low-angled slope, the headwall was in previously undisturbed material and active wedges exhibited secondary and tertiary stages 29 cm and 10 cm high respectively (current active layer of 53 cm). In an exposure beside a recent active-layer detachment slide, four stages of growth were present in an inactive wedge, together with several major layers of segregated ice. The most complex section was at the base of a long slope where colluvial deposits overlay peat. Wedges of at least two and possibly three different ages were present. Wedge 1 was the oldest and grew syngenetically at least partly during the period of peat accumulation which ended at 6460±70 B.P. A secondary vein developed as the surface aggraded further but eventually this became inactive. Wedge 3 may have started epigenetically or syngenetically but existed prior to 540±50 B.P. Since then it has grown syngenetically and is still active. Wedge 4 is the youngest wedge: it was initiated epigenetically after 540±50 B.P. The rate of sedimentation at this site derived from the mean corrected radiocarbon dates is 7 mm/year, but given the standard errors could be between 4-25 mm/year. This surface aggradation is attributed to a combination of slopewash, solifluction and active-layer detachment processes. Although not observed to date, it is presumed that anti-syngenetic wedges exist upslope of this and many of the other sites studied.
There is no evidence of recent cooling within climatic records from Eureka, but the coastal location of this weather station could buffer it from changes that may have occurred further inland. Thus the uppermost growth stages at several of the sites could be the result of changes in the summer climate. However, the degree of active layer change required means that this explanation is very unlikely to be correct for the lower growth stages. Instead, regrowth is attributed to active slope processes which result in colluviation.

LAKES AND PERMAFROST IN THE COLVILLE RIVER DELTA, ALASKA

H. Jesse Walker
Department of Geography, Louisians State University
Baton Rouge, Louisiana, 70803-4105, USA

Lakes in arctic deltas, like lakes in the deltas of lower latitudes; vary greatly in area, depth, shape, seasonal character and formation processes. Lakes in the Colville River Delta on the coastal plain of Northern Alaska provide examples of this variety and reflect the numerous factors, including permafrost, that are involved in arctic lake formation and maintenance.
The delta, only 550 km^2 in area, has innumerable ponds and 641 lakes over 0.0125 km^2 in area; 5 of them over 2 km^2. Lake area (for those larger than 0.0125 km^2) is 96.5 km^2 or 17.5% of the total area of the delta.
The lakes and ponds in the delta include remnants of the well-known oriented lakes that occur over much of the coastal plain, abandoned river channel lakes, terrace flank depression lakes, thermokarst lakes, intra- and inter-dune lakes, intra- and inter-bar lakes, perched lakes, ice shove ponds and ice-wedge polygon ponds. Although some of the delta's lakes are sufficiently deep (over 8 m) so that a thaw bulb exists beneath them, most are less than 2 m deep and freeze to the bottom during winter. These lakes have thin active layers in their bottoms similar to that of the tundra surface. However, the importance of permafrost in lake morphology evidences itself best in relation to shoreline erosion, the eventual breakthrough (tapping) of river to lake and subsequent lake drainage.
Lakes associated with ice-wedge polygons, some of which are perched several meters above normal river level near river banks, frequently drain. Drainage usually occurs on top of an ice wedge that has been cut into by the eroding river leaving the polygon lake dry. A similar process occurs in other lakes (many of which have bottoms well below river level). Once the tundra separating the lake from the river is sufficiently narrowed, breakthrough can occur. After the lake becomes connected with the river its level fluctuates with river stage. During non-flood stages (all but 3-4 weeks per year) the erosional benches, formed along the margins of the lakes as they enlarged due to lake-bank thaw and erosion, are subaerial and thus subjected to the permafrost forming conditions that are typical of the coastal plain. Further, once tapped, lakes become sediment traps for the river's flood water. Such lakes are eventually filled with sediment and the thaw bulb that existed beneath them freezes.

SORTED CIRCLE DYNAMICS: 10 YEARS OF FIELD OBSERVATIONS FROM CENTRAL ALASKA

Walters, James C.
Department of Earth Science, University of Northern Iowa,
Cedar Falls, Iowa 50614, USA

Field studies of sorted circles occurring in the periglacial environment of the Maclaren Summit and High Valley areas of central Alaska have been conducted over a period of 10 years. Repetitive photography and surveys of wooden dowels, metal rods, and marked stones provide information on the surface dynamics of the circles. Excavations provide information on subsurface characteristics. Although much variability was noted in the dynamics of the circles over the study period, some general conclusions can be drawn and inferences can be made within the context of existing models of sorted circle development.

The circles examined in this study are found in low spots in the silty till which blankets the area. These depressions become quite wet in the spring because of snowmelt, rain, and thawing ground ice. Sorted circles have been studied at six sites, three where temporary ponding occurs and three where seasonal wetting but no ponding takes place. Overall, movement of markers in circles was upward and radially outward from the fine-grained centers to the coarse borders. Circles at sites experiencing temporary ponding showed the most activity. Vertical displacements of markers were greatest in circle centers with an average uplift of approximately 1 to 4 cm/yr. Horizontal displacements of markers generally increased from circle centers outward but then decreased as they approached within several centimeters of the coarse borders. Average horizontal movements range from 0.5 to 2.2 cm/yr.

Circle characteristics differ depending on position in the shallow depression in which they occur. Larger circles 1-2 m in diameter are found along the outer margins of a depression. These larger circles are slightly to strongly domelike in their centers, closely spaced, and more oval or even polygonal in plan view. Fine-grained sediment is abundant here and some vegetation exists. Circles in the central portion of a depression are smaller, 0.5-0.1 m in diameter, strongly convex upward, and widely spaced with a stony surface surrounding them. Fines are present only in circle centers, and no vegetation exists. Another common feature in the central area of a depression is a pattern of small stones surrounded in a circular fashion by larger stones. No fines are present on the surface in these features, but excavations reveal plug-like areas of fines beneath their centers.

Long-term monitoring of these sorted circles indicates the diameters of most are becoming smaller. Repeat photography and measurement of circle diameters show the central area of fines decreasing while the border areas are expanding. The fine-grained centers are also becoming coarser. Observations show that coarser material progressively moves up and out away from a circle center to concentrate along the stable border. Fines also move up in a plug-like fashion into the circle center where they dominate the center, but they are slowly removed by deflation, rainwash, sheetwash, etc. Therefore, the diameter of a circle becomes smaller as more stones fill in the circle and the fine-grained sediment becomes separated from its source. If conditions allow for continued activity, a circle will progress to an end point where no fines exist on the surface, and what remains is a pattern of small stones surrounded by larger stones.

AUTHOR INDEX

GENERAL SUBJECT–SENIOR AUTHOR INDEX

ROADS

LIST OF PARTICIPANTS IN VI ICOP

Aguirre-Puente, J.	France	Laboratoire d'Aerothermique du C.N.R.S., Meudon
Akagawa Satoshi	Japan	3-4-17 Etchujima, 3-Chome Koto-Ku, Tokyo 135
Akerman Jonas H. & Ms. Akerman**	Sweden	Department of Physical Geography University of Lund, Solvevgatan 13 S-23362 Lund
Allard, Michel**	Canada	University Laval, Centre D'Etudes Nordiques, Sainte-Foy, Quebec G1K 7P4
An Weidong	Canada	Centre D'Etudes Nordiques, Universite Laval, Quebec G1K 7P4
Anisimova N.P.	Russia	Permafrost Institute, Siberian Branch, Russia Academy of Sciences, 677010, Yakutus, 10
Antonov-Druzhinin V.	Russia	INGEOTES, 626718, Nory Urengoy, Tymen Reg.
Are Felix E.	Russia	Petersburg Institute of Railway Engineers, Moskovsky av., 9, St. Petersburg 190031
Aziz A.	USA	Department of Mechanical Engineering Gonzaga University, Spokane, WA 99258
Balobayev V.T.	Russia	Permafrost Institute, Siberian Branch, Russia Academy of Sciences, 677010, Yakutus, 10
Barry, Roger G.	USA	University of Colorado, CIRES/NSIDC, Boulder Co. 80309-0449
Baulin V.V.	Russia	PNIIIS, Okrujnol PR. 18, 105058 GSP, Moscow
Biggar K.W. & Nil	Canada	Department of Civil Engineering, Royal Military College, Kingston, K7K SLO
Bradley, P.G.	USA	Box 194900, Dept. of Transportation and Public Facilities, Pouch 6900, Anchorage, AK 99510
Brewer M.C.**	USA	U.S. Geological Survey, 4200 University Drive, Anchorage, Alaska, 99508-466
Brown Jerry & Celia Brown*	USA	International Permafrost Association Editorial Committee, P.O. Box 9200, Arlington, Virginia 22219-0200
Cames-Pintaux, Anne-Marie	France	C.N.R.S., Lab. d'Aerothermique, 4, Route Gardes, 92190 Meudon
Carlson Robert & Camille Q. Carlson	USA	Institute of Water Resources, University of Alaska, Fairbanks, AK 99701
Carter, L. David*	USA	U.S. Geological Survey, 4200 University Drive, Anchorage, Alaska 99508-4667
Chang R.V.	Russia	Permafrost Institute, Russian Academy of Sciences, Yakutsk 677018
Chen Fengfeng	China	State Key Laboratory of Frozen Soil Engineering, LIGG, CAS, 730000
Chen Ruijie*	China	State Key Laboratory of Frozen Soil Engineering, LIGG, CAS, 730000
Chen Xiaobai	China	Lanzhou Institute of Glaciology and Geocryology, Chinese Academy of Sciences, Lanzhou 730000
Cheng Guodong*	China	Lanzhou Institute of Glaciology and Geocryology, Chinese Academy of Sciences, Lanzhou 730000
Cheng Youchang	China	Daqing Oil Field Design Academy, 555469
Clark, Michael G.	USA	306 Geology & Geography Building, Knoxville, TENN 37996-1410
Clarke Edwin S. & Alta Clarke	USA	Clarke Engineering Company, 1818 So. University Avenue, Suite 9-Fairbanks, Alaska 99709
Collett, Timothy S.	USA	U.S. Geological Survey, Box 25046, MS-940, Denver Federal Center, Lakewood, Colorado 80225
Corapcioglu M. Yavuz & Carol Y. Wong	USA	Department of Civil Engineering, Texas A&M University, College Station, TX 77843-3136
Cui Guangxin	China	Mining and Technology University, Xuzhou 221008
Cui Jianheng	China	The First Survey and design Institute of Highway, The Ministry of Communications, Xian 710068
Cui Zhijiu	China	Department of Geography, Beijing University, Beijing 100871
Dai Baoguo	China	Heilongjiang Institute of Forestry, Heilongjiang Province, 150040
Dai Huimin	China	Heilongjiang Institute of Highway and Transport, 40 Qingbin Road, Harbin 150080
Dallimore Scott	Canada	Geological Survey of Canada 601 Booth St, Ottawa, K1A OE8

*Participants in the field trip to Lhasa (A-1)
**Participants in the field trip to Tianshan Mountain (A-2)

Deng Nan	China	Chinese Academy of Sciences, Beijing 100864
Deng Yousheng	China	State Key Laboratory of Frozen Soil Engineering, LIGG, CAS, 730000
Devjatkin V.N.	Russia	Institute of Cryosphere of Earth of Russia Academy of Sciences p.b. 1230 Tyumen 625000, Russia Federation
Ding Jingkang	China	Northwest Institute, Chinese Academy of Railway Sciences, Lanzhou
Dramis Francesco	Italy	Department of Geology, Universita di Camerino, Viale Beeti 1, 62032 Camerino
Dubikov G.I.	Russia	Department of Geocryology, Faculty of Geology, Moscow State University, Moscow 119899
Dubina M.M.	Russia	Permafrost Institute, Russian Academy of Sciences, Yakutsk 677018
Esch David	USA	Alaska Dept. of Transportation, Research Engineer, Alaska 2301 Peger Road,
Fedorov A.N.	Russia	Permafrost Institute, Russian Academy of Sciences, Yakutsk 677018
Fedoseeva V.I.	Russia	Permafrost Institute, Russian Academy of Sciences, Yakutsk 677018
Fei Xueliang	China	Xian Highway and Transportation University, Xian
Ferrians, Oscar	USA	U.S. Geological Survey, 4200 University drive, Anchorage, Alaska 99508
Flaate, Kaare & Astrid Flaate	Norway	Norwegian Road Research Laboratory, P.O. Box 6390 Ettertad 0604 Oslo 6
Fortier R. & Brigitte Dufour*	Canada	Centre d'etudes Nordiques, Pavillon F.A. Savard, Universite Lavel, Sainte-Foy, Quebec G1K 7P4
French Hugh M.*	Canada	Dept. of Geography, University of Ottawa, Ottawa, Ontario K1N 6N5
Gamper Barbara*	Switzerland	Eawag, Ste, 8600 DÜbendorf
Gao Weiyue	China	Water Conservancy Research Institute of Inner Mongolia, 010020
Gao Xingwang	China	Lanzhou Institute of Glaciology & Geocryology, Chinese Academy of Sciences, Lanzhou 730000
Garty, Jacob & Garty Rachel*	Israel	Tel-Aviv University, Department of Botany, Tel-Aviv 69978
Gavrilova M.K.	Russia	Permafrost Institute, Siberian Branch, Russian Academy of Sciences, 677010, Yakutus 10
Ge Huanyou	China	Water Resources Bureau of Bayan County, Heilongjiang 151800
Ge Qihua	China	The First Survey and design Institute of Highways, The Ministry of Communication, Xian 710068
Gilichinsky D.A.	Russia	Institute of Soil Science and Photosynthesis of The Russian Academy of Sciences,Pushchino 142292
Gong Wangsheng	China	Chinese Academy of Sciences, Beijing 100864
Gorbunov A.P.	Russia	Permafrost Institute, Siberian Branch, Russian Academy of Sciences, 677010, Yakutus 10
Grechishchev S.E.	Russia	All-Union Research Inst. of Hydrogeology & Eng. Geology, 142452 Zeleny-village, Noginsk District, Moscow Region
Gryc George	USA	U.S. Geological Survey, 345 Middlefield Road, Menlo Park, CA 94025
Gu Zhongwei	China	Lanzhou Institute of Glaciology and Geocryology, Chinese Academy of Sciences, Lanzhou 730000
Guglielmin Mauro	Italy	Istituto di Geologia, Universita degli Studi Di Parma 43100, Parma
Guo Dianxiang	China	Institute of Hydraulics, Shandong Province, 250013
Guo Tingbin	China	The National Natural Science Foundation of China, Academician, Beijing 100083
Guo Xudong	China	Institute of Geologic, CAS, Beijing 634 Box, 100029
Guryanov I.E.	Russia	Permafrost Institute, Siberian Branch, Russian Academy of Sciences, 677010, Yakutus 10
Haeberli W.*	Switzerland	Laboratory of Hydraulics, Hydrology and Glaciology, VAW-ETH Zentrum CH-8092, Zurich
Hall Kevin & Mrs. A.J. Hall	South Africa	Department of geography, University of Natal, P.O. Box 375, 3200 Pietermaritzburg
Hallet, Bernard*	USA	University of Washington, Quaternary Research Center AK-60 Seattle, WA 98195
Han UK**	South Korea	Dept. of Env. Sci., Korea Military Academy, Seoul, Korea 139-799
Harris Charles**	UK	Department of Geology, University of Wales, P.O. Box 914, Cardiff, CF1 3YE
Harris S.A.*& P.R. Harris	Canada	Department of Geography, University of Calgary, Calgary, Alberta, T2N 1N4
He Ping	China	State Key Laboratory of Frozen Soil Engineering, LIGG, CAS, 730000
Heginbottom J.A.	Canada	Geological Survey of Canada, 601 Booth Street, Ottawa K1A 0E8

Hinkel K.M.*	USA	Department of Geograph, Mail Location 131, University Cincinnati, Cincinnati, Ohio 45221-0131
Guo Dongxin*	China	Lanzhou Institute of Glaciology & Geocryology, Chinese Academy of Sciences, Lanzhou 730000
Huneaut, Paul A.	Canada	500 Boul René-Lévesque Ouest, Place Air Canada, Bareau 600 Montreal (Québec) H2Z 1W7
Hinzman, Larry D.	USA	University of Alaska, Water Research Center, Fairbanks, Alaska 99775-1760
Hoelzle M.**	Switzerland	Laboratory of Hydraulics, Hydrology & Glaciology, VAW-ETH Zentrum, CH-8092 Zurich
Horiguchi Kaoru	Japan	The Institute of Low Temperature Science, Hokkaido University, Sapporo 060
Huang Maohuan	China	State Key Laboratory of Frozen Soil Engineering, LIGG, CAS, 730000
Huang Yizhi*	China	Lanzhou Institute of Glaciology & Geocryology, Chinese Academy of Sciences, Lanzhou 730000
Hu Qiheng	China	Chinese Academy of Sciences, Beijing 100864
Iordanescu Mircea	Canada	1800 Monte Sainte-Julie, Varennes, P. Quebec J3X 1S1
Istomin Vladmir A.	Russia	Russia, 142717, Moscow Region, Leninskij Rajon, Razvieka, VNIIGAZ
Jiao Tianbao & Long Jiyun*	China	Yitulihe Branch of Harbin railway Bureau, Heilongjiang 022168
Jia Jianhua	China	The First Survey Design Institute, Lanzhou Branch, Ministry of Railway of China, Lanzhou 730000
Jin Huijun**	China	Lanzhou Institute of Glaciology & Geocryology, Chinese Academy of Sciences, Lanzhou 730000
Jin Naichui	China	Heilongjiang Hydraulic Research Institute, Harbin 150080
Kamensky Rosteslav M.	Russia	Permafrost Institute, Russian Academy of Sciences, Yakutsk 677018
Kane, Douglas L.*	USA	University of Alaska, Fairbanks, Water Research Center, Fairbanks, Alaska 99775-1760
Keller F.*	Switzerland	Laboratory of Hydraulics, Hydrology and Glaciology, ETH Zentrum, CH-8092, Zurich
King Lorenz J.*	Germany	Geographical Institute, Justus Liebig-Universitat, D6300 Giessen
Klimovsky I.V.	Russia	Permafrost Institute, Siberian branch, Russian Academy of Sciences, 677010, Yakutus 10
Koster E.A.**	Netherland	Geographical Institute, University of Utrecht P.O. Box 80. 115, 3508TC Utrecht
Krantz William B. & June Krantz	USA	University of Colorado, Dept. of Chemical Engineering, Campus Box 424, Boulder, Colorado 80309-0424
Kunitskiy V.V.	Russia	Permafrost Institute, Siberian Branch, Russian Academy of Sciences, 677010, Yakutus 10
Kurfurst P.J. & Dana Kurfurst	Canada	Geological Survey of Canada, 601 Booth St. Ottawa, Ontario K1A 0E8
Lachenbruch, Arthur & Edith B. Lachenbruch	USA	345 Middelfield Road, MS/923, Menlo Park, California 94025
Langager, Hans Christian	Denmark	Greenland Field Investigations, Greenland Home Rule Agency 16 Rosenvængets Allé DK-2100 Copenhagen Ø
Lautridou Jean P	France	Centre De Geomorphologie, Ruedes Tilleuls 14000 Caen
Lehmann, Rainer**	Germany	Geographisches Institut, Universitat Heidelberg Im Neuenheimer Feld 348 D/W-6900 Heidelberg
Lewkowicz A.G.	Canada	University of Toronto, Dept. of Geography, Erindale College, Mississauga, Ontario L5L 1C6
Li Anguo	China	Northwest Hydrotechnical Science Research Institute, Yangling Town 712100
Li Dongqing	China	State Key Laboratory of Frozen Soil Engineering, LIGG, CAS, 730000
Li Hao	China	Ningxia Hydrotechnical Science Research Institute, Yinchuan 750001
Li Shijie**	China	Lanzhou Institute of Glaciology & Geocryology, Chinese Academy of Sciences, Lanzhou 730000
Li Shude	China	Lanzhou Institute of Glaciology & Geocryology, Chinese Academy of Sciences, Lanzhou 730000
Li Yi	China	Mining and Technology University, Xuzhou 221008
Li Yusheng	China	Dong Dan San Tiao, No.14, Beijing 100005
Li Zuofu	China	Lanzhou Institute of Glaciology & Geocryology, Chinese Academy of Sciences, Lanzhou 730000
Li Weiguo	China	Heilongjiang Institute of Forestry, Heilongjiang Province, 150040
Liang Fengxian	China	Lanzhou Institute of Glaciology & Geocryology, Chinese Academy of Sciences, Lanzhou 730000
Lin Yipu	China	Bureau of Zhalainoer Coal Mine and Institution of Paleontology and Paleanthropology of Academy Sinica, 021412

Liu Gengnian	China	Department of Geography, Beijing University, Beijing 100871
Liu Hongxu	China	Heilongjiang Province Low Temperature Construction Science Research Institute, Harbin 150080
Liu Xuekui	China	Institute of Forestry Design, Heilongjiang Province, 150080
Lovell, Charles W. & Marry Totten	USA	Purdue University, School of Civil Engineering, West Lafayette, IN 47907
Lu Guowei	China	Da Hingganling Institute of Forestation, Inner Mongolia 022150
Lu Xingliang	China	Bei An Road 74, Changchun 130061
Lunardini Virgil	USA	CRREL, 72 Lyme Road, Hanover NH 03755
Luo Weiquan	China	Design House of Management Forest Bureau, Eer Guna Lift, Inner Mongolia 022363
Ma Chunlin	China	Heilongjiang Institute of Forestry, Heilongjiang Province 150040
Ma Hong	China	Xinjiang Institute of Geography, Chinese Academy of Sciences, Urumqi 830011
Ma Wei	China	State Key Laboratory of Frozen Soil Engineering, LIGG, CAS, 730000
Ma Yijun	China	Institute of Hydraulics, Shandong Province 250013
Ma Zhixue*	China	Lanzhou Institute of Glaciology & Geocryology, Chinese Academy of Sciences, Lanzhou 730000
Mackay, J. Ross	Canada	University of British Columbia, 217-1984 West Mall, Vancouver, B.C. V6T 1W5
Makarov V.I.	Russia	Permafrost Station, Permafrost Institute, Bolishoi Teatr Street, Build. 9, Krasnoyarckiy Krai, Igarka, 663200
Matsuoka Norikazu	Japan	Institute of Geoscience, University of Tsukuba, Ibaraki 305
Matthias Jakob**	Canada	Department of geography, University of british Columbia Vancouver, B.C., V6T 1W5
Melnikov E.S.	Russia	All-Union Research Inst. of Hydrogeology & Eng. Geology, 142452, Zeleny-village, Noginsk District, Moscow Region
Men Zhaohe	China	Amuer Design House Forestry Bureau, Management Bureau of Da Hingganling, 165302, Heilongjiang
Mi Haizheng	China	Lanzhou Institute of Glaciology & Geocryology, Chinese Academy of Sciences, Lanzhou 730000
Na Yunlong	China	Da Hingganling Institute of Prospecting and Design, Ministry of Forestry, 165000
Nakayama Tomoko	Japan	Institute of Low Temperature Science, Hokkaido Univ., Sapporo
Nazarenko Alexander A. & Nazarenko Lydia	Russia	2 Petrousky Streat Yakutsk 677891
Nelson, Frederick & Margaret Wilde*	USA	Rutgers University, Dept. of Geography, Box 5080/Kilmer New Brunswick, New Jersey 08903
Nidowicz Bernard & Ms. Carol Trahim	USA	601 East 57th Place, Anchorage, Alaska, Fairbanks, Alaska AK99517
Ohata Tetsuo	Japan	Institute for Hydrospheric-Atmospheric Sciences, Nagoya University, Chikusa-Ku, Nagoya 464-01
Osterkamp T.E. & J.M. Osterkamp	USA	Geophysical Institute University of Alaska 99517
Outcalt Samuel I.**	USA	2466 Trenton Ct Ann Arbor, M, 48105
Pang Weizhen	China	Consultant (Formerly Central Coal Mining Research Institute), Beijing 100013
Perlstein G.Z.	Russia	Permafrost Institute, Siberian Branch, Russian Academy of Sciences, 677010, Yakutus 10
Péwé Troy L. & Mrs. Péwé	USA	Arizona State University, Department of Geology, Tempe, AZ 85287-1404
Phukan Arvind P.E.	USA	2281 Foxhall Dr Anchorage AK 99504
Ping C.L.	USA	AFES-SALRM 533E. Fireweed St. Palmer, Alaska 99645
Pissart, Albert	Belgium	Université de Liège, Géomorphologie et Géologie du Quaternaire, 7, Place du 20 Aout, 4000 Liége
Prokopieva L.V.	Russia	Permafrost Institute, Siberian Branch, Russian Academy of Sciences, 677010, Yakutus 10
Pu Yibin	China	State Key Laboratory of Frozen Soil Engineering, LIGG, CAS, 730000
Qiao Dianshi	China	Suihua Area Hydraulic Bureau, Heilongjiang 152054
Qiu Guoqing**	China	Lanzhou Institute of Glaciology & Geocryology, Chinese Academy of Sciences, Lanzhou 730000
Romanovski N.N.	Russia	Department of Geocryology, Faculty of Geology, Moscow State University, Moscow 119899
Rooney, James W. & Florence	USA	Rom Consoltants, Inc. 9101 Vorgvard, Anchorage AK 99507
Salnikov P.I.	Russia	Chita Department of Permafrost Institute of Siberian Division of Russian Academy of Sciences
Schmitt Elisabeth*	Germany	Geographisches Institut Di Univ. Giessen Senckenbergstrasse 1, 6300 Giessen

Senneset Kaare & Inger Sofie	Norway	The Norwegian Inst. of Technology, Geotechnical Division, N-7034 Trondheim
Shao Lijun	China	Si Dalin Road 140, Changchun 130012
Sharkhuu N.	Mongolia	Institute of Geography & Geocryology, Mongolian Academy of Sciences,Ulanbartu 21620
Shatz M.M.	Russia	Permafrost Institute, Siberian Branch, Russia Academy of Sciences, 677010, Yakutus 10
Shen Mu	Canada	Genie Civil, Universite Laval, Ste-Foy (Quebec), Quebec G1K 7P4
Shen Yongping**	China	Lanzhou Institute of Glaciology & Geocryology, Chinese Academy of Sciences, Lanzhou 730000
Sheng Yu	China	State Key Laboratory of Frozen Soil Engineering, LIGG, CAS, 730000
Shi Yafeng	China	Lanzhou Institute of Glaciology & Geocryology, Chinese Academy of Sciences, Lanzhou 730000
Shoop, Sally A. & Clayton Morlock	USA	CRREL 73 Lyme RD Hanover, NH 03755-1290
Siegert Christine	Germany	Am Wehr 7, O-8801 Bertsdorf
Slaughter Charles W.**	USA	Land/Water Interactions Research Program Pacific Northwest Research Station, USDA Forest Service, 308 Tanana Drive, Fairbanks, Alaska 99775
Sletten, Ronald S.*	USA	University of Washington, Civil Engineering, Mail Stop FX-10, Seattle, WA 98195
Snegiryev A.M.	Russia	Permafrost Institute, Siberian Branch, Russian Academy of Sciences, 677010, Yakutus 10
Solomatin V.I.	Russia	Faculty of Geography, Moscow State University, Moscow 119899
Sone Toshio**	Japan	Hokkaido University, Institute of Low Temperature Science, Sapporo 060
Soo Sweanum	USA	Department of Civil Engineering and Construction, Bradley University, Peoria, Illinois
Steensboe Jorgen S.	Denmark	Rosenvengets Alle 16-DK 2100 Copenhacen
Sun Jinyue	China	Institute of Crop Germplasm Resources, Chinese Academy of Argriculture Sciences, Beijing 100081
Tang Shuchun	China	Da Qing Oil Field Construction Design Research Institute, 163712
Tao Zhaoxiang	China	State Key Laboratory of Frozen Soil Engineering, LIGG, CAS, 730000
Thomsen Thorkilo	Denmark	Pilestraede 52 P.O. 2128 DK 1015 Copenhagen K
Tilley Philip**	Australia	Dept. of Geography, University of Sydney, NSW 2006 (or 10 Queen ST Mittagong NSW Australia 2575)
Tong Boliang	China	Lanzhou Institute of Glaciology & Geocryology, Chinese Academy of Sciences, Lanzhou 730000
Tong Changjiang	China	Lanzhou Institute of Glaciology & Geocryology, Chinese Academy of Sciences, Lanzhou 730000
Tremblay Clement	Canada	Ministere des Transports du Q., 700, boul. St-cyrille est, 30e etage, Quebec G1R 5H1
Tu Guangzhi	China	Chinese Academy of Sciences, Beijing 100864
Urdea Petru I.	Romania	University of Timisoara, V. Parvan 4, 1900 Timisoara
Uziak Stanislaw	Poland	19 Akadomicka, 20-033 Lublin
Van Everdingen Robert O.	Canada	The Arctic Institute of North America, the University of Calgary, Calgary, Alberta, T2N 1N4
Vandenberghe, Jef**	Netherland	Inst. of Earth Sciences, De Boelelaan 1081 HV Amsterdam
Velikin S.A.	Russia	Permafrost Institute, Russian Academy of Sciences, Yakutsk 677018
Vinson, Ted. S. & Suzanne Vinson	USA	Oregon State University, Dept. of Civil Engineering, Corvallis, Oregon 97331
Vonder Muhll D.S.**	Switzerland	Versuchsanstalt für Wasserbau, Hydrologie und Glaziologie ETH-Zentrum, CH-8092, Zurich
Vyalov Segrey S.	Russia	Scientific and Research Bureau "Geotechnique" Podsosenskg Per., 25, 103062 Moscow
Walker H. Jesse**	USA	Dept. of Geography, Louisians State University, Baton Rouge, LA 70803
Walters James C.	USA	Dept. of Earth Science, University of Northern Iowa, Cedar Falls, IA 50614
Wang Baolai* & Jian Qicen	Canada	Centre d'etudes nordiques, Universite Laval, St-Foy, Quebec G1K 7P4
Wang Changsheng*	China	Central Coal Mining Research Institute, Beijing 100013
Wang Guoshang	China	Lanzhou Institute of Glaciology & Geocryology, Chinese Academy of Sciences, Lanzhou 730000
Wang Huan*	China	Beijing International Convention Center, Beijing
Wang Jiacheng	China	State Key Laboratory of Frozen Soil Engineering, LIGG, CAS, 730000
Wang Jianping	China	Central Coal Mining Research Institute, Beijing 100013

Wang Shangli	China	Lanzhou Institute of Glaciology & Geocryology, Chinese Academy of Sciences, Lanzhou 730000
Wang Shirong	China	Water Conservancy Bureau of Panjin City, Liao Nin Province, 124010
Wang Xinglong	China	Heilongjiang Institute of Highway and Transport, 40 Qingbin Road, Harbin 150080
Wang Yaqing	China	Lanzhou Institute of Glaciology & Geocryology, Chinese Academy of Sciences, Lanzhou 730000
Wang Yi**	China	Water Resources Research Institute of Innef Mongolia Huhhot, Inner Mongolia 010021
Wang Zhanchen	China	Bei An Road 74, Changchun 130061
Wang Zhengyi	China	Bureau of Zhalainoer Coal Mine and Institution of Peleontology and Paleanthropology of Academy Sinica, 021412
Wei Xuexia	China	Department of Mechanics, Lanzhou University, 730000
Woo Ming Ko	Canada	Geography Department, McMaster University, Hamilton, Ontario L8S 4K1
Wu Jingmin	China	The First Survey and Design Institute of Highways, The Ministry of Communication, Xian 710068
Wu Qingbai	China	Lanzhou Institute of Glaciology & Geocryology, Chinese Academy of Sciences, Lanzhou 730000
Wu Ziwang	China	State Key Laboratory of Frozen Soil Engineering, LIGG, CAS, 730000
Xia Zhaojun	Canada	Department of Geography, McMaster University, Hamilton, Ontario L8S 4K1
Xia Zhiying*	China	Lanzhou Institute of Glaciology & Geocryology, Chinese Academy of Sciences, Lanzhou 730000
Xie Yan	China	Lanzhou Institute of Glacciology & Geocryology, Chinese Academy of Sciences, Lanzhou 730000
Xie Yingqi	China	Hei Longjiang Provincial Research Institute of Water Conservancy, 150080
Xue Shiying	China	Chinese Academy of Sciences, Beijing 100864
Xu Zhi Hong	China	Chinese Academy of Sciences, Beijing 100864
Xu Shaoxin	China	Heilongjiang Provincial Research Institute of Water Conservancy, 150080
Xu Xiaozu	China	State Key Laboratory of Frozen Soil Engineering, LIGG, CAS, 730000
Yang Hairong	China	Northwestern Institute, Railway Ministry Academia, Lanzhou 730000
Yang Jinghui	China	Water Conservancy Designing Party, Shuangliao County Jilin Province, 136400
Yang Zhenniang	China	Lanzhou Institute of Glaciology & Geocryology, Chinese Academy of Sciences, Lanzhou 730000
Yen Y.C.	USA	CRREL, Hanover, New Hampshire 03755
Young K.L. & Margaret M.	Canada	Department of Geography, McMaster University, Hamilton, Ontario, L8S 4K1
Yu Qihao	China	State Key Laboratory of Frozen Soil Engineering, LIGG, CAS, 730000
Yu Xiang and Mrs. Yu	China	Central coal Mining Research Institute, He Pingli, Beijing 100013
Zhang Changqing	China	State Key Laboratory of Frozen Soil Engineering, LIGG, CAS, 730000
Zhang Jiazhen	China	Chinese Geography Association, An Ding Men Wai, Da Tun Road No.917, Beijing 100101
Zhang Jie	China	Research Society for Chinese Development of Cold Region, 150010
Zhang Jinzhao	China	The First Survey and design Institute of Highways. The Ministry of Communications, Xian 710068
Zhang Lixin	China	State Key Laboratory of Frozen Soil Engineering, LIGG, CAS, 730000
Zhang Qibin	China	Lanzhou Institute of Glaciology & Geocryology, Chinese Academy of Sciences, Lanzhou 730000
Zhang Zhao	China	The First Survey Design Institute, Ministry of Railway of China, Lanzhou 730000
Zhang Zhaoxiang	China	Beijing Argricultural Engineering University, Beijing 100083
Zhang Hengxuan	China	Chinese Development of Cold Region Research Society, Daoli District, Zhongyi Street 34, Harbin 150010
Zhao Lin**	China	Lanzhou Institute of Glaciology & Geocryology, Chinese Academy of Sciences, Lanzhou 730000
Zhao Xiufeng*	China	Lanzhou Institute of Glaciology & Geocryology, Chinese Academy of Sciences, Lanzhou 730000
Zhao Yutian	China	Institute of Crop Germplasm Resources, Chinese Academy of Argriculture Sciences, Beijing 100081

Zheng Duo	China	Jilin Provincial Institute of Water Conservancy Sciences, Changchun 130022
Zheng Duo	China	Beijing Institute of Geography, Chinese Academy of Sciences, Beijing 100101
Zhou Deyuan	China	Administration Bureau of Hetao Irrigation Area in Yongji, Inner Mongolia 015000
Zhou Youwu	China	Lanzhou Institute of Glaciology & Geocryology, Chinese Academy of Sciences, Lanzhou 730000
Zhou Zhongmin	China	Changsha Hydraulic Electric Power Teachers' College, Changsha 410077
Zhu Jinghu	China	Department of Geography, Harbin Normal University, Harbin 150080
Zhu Linnan	China	State Key Laboratory of Frozen Soil Engineering, LIGG, CAS, 730000
Zhu Qiang	China	Gansu Provincial Research Institute of Water Conservancy, Lanzhou 730000
Zhu Yuanlin	China	State Key Laboratory of Frozen Soil Engineering, LIGG, CAS, 730000